



UNIVERSITAT_{DE}
BARCELONA

**Characterization of the Immune System,
Hematopoietic Stem Cells, and Molecular Biomarkers
in Myelodysplastic Syndromes and Chronic
Myelomonocytic Leukemia: Implications for Improved
Stratification and Treatment**

Juan José Rodríguez-Sevilla



Aquesta tesi doctoral està subjecta a la llicència **Reconeixement 4.0. Espanya de Creative Commons.**

Esta tesis doctoral está sujeta a la licencia **Reconocimiento 4.0. España de Creative Commons.**

This doctoral thesis is licensed under the **Creative Commons Attribution 4.0. Spain License.**

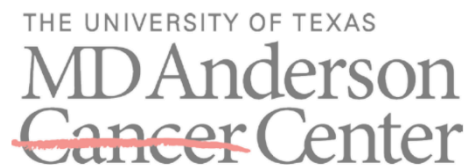


UNIVERSITAT DE
BARCELONA

**Characterization of the Immune System,
Hematopoietic Stem Cells, and Molecular
Biomarkers in Myelodysplastic Syndromes and
Chronic Myelomonocytic Leukemia:
Implications for Improved Stratification and
Treatment**

Doctoral Thesis
Juan José Rodríguez-Sevilla

Doctoral Program
Medicine and Translational Research



Thesis Director

Xavier Calvo González
Hospital del Mar Research Institute

Thesis Tutor

Alberto Álvarez Larrán
Hospital Clinic, Universidad de Barcelona

Barcelona, March 2025

ACKNOWLEDGMENTS

A mi madre Magdalena, por haberme dado todo en la vida.

A mi hermano Tito, por ser mi faro en ella.

A Clara, por hacerme cada día mejor persona.

A mi profe Xavi, por ser una inspiración constante.

A mi padre Juanjo, estoy seguro de que te habría encantado ver esto, pero gracias por sembrar ese "por qué" infinito que me permite disfrutar de la ciencia como un juego de niños.

Juan José Rodríguez-Sevilla

CONTENT

THESIS SUMMARY	VI
ABBREVIATIONS	X
FIGURES & TABLES	XIII
INTRODUCTION.....	1
1. Introduction to Myeloid Neoplasms.....	2
2. Definition of Myelodysplastic Syndromes and Chronic Myelomonocytic Leukemia	3
3. Evolution of the Nosological Classification of Myelodysplastic Syndromes and Chronic Myelomonocytic Leukemia: Rationale for a Unified Analysis in this Doctoral Thesis	4
4. Epidemiology.....	6
4.1 Myelodysplastic Syndromes	6
4.2 Chronic Myelomonocytic Leukemia	6
5. Etiology	6
5.1 Myelodysplastic Syndromes	6
5.2 Chronic Myelomonocytic Leukemia	7
6. Foundations of MDS and CMML Pathogenesis	8
6.1.1 The Hematopoietic Hierarchy: Structure and Dynamics.....	9
6.1.2 HSC Dysregulation in MDS and CMML	11
6.2 Immune Landscape: Tumor Immunity and Immune Escape	15
6.2.1 Bone Marrow Microenvironment and Immune Interactions	15
6.2.2 T Cell Dysregulation in MDS and CMML	16
6.3 The Role of Inflammation in Myeloid Disorders.....	22
6.3.1 Chronic Inflammation: A Driver of Hematopoietic Dysregulation	22

6.3.2 Inflammation and Immune Dysregulation in MDS and CMML	24
6.3.3 Inflammation as a Potential Therapeutic Target in MDS and CMML	26
6.4 Molecular Pathogenesis of MDS And CMML	26
6.4.1 Genetic Landscape and Key Mutations in MDS	27
6.4.2 Genetic Landscape and Key Mutations In CMML	31
6.5 Cytogenetic Landscape of Myelodysplastic Syndromes and Chronic Myelomonocytic Leukemia	33
6.5.1 Cytogenetic Alterations in Myelodysplastic Syndromes	33
6.5.2 Cytogenetic Alterations in CMML.....	35
7. Clinical Manifestations.....	36
8. Diagnosis and Classification of Myelodysplastic Syndromes and Chronic Myelomonocytic Leukemia	36
8.1 Myeloid Continuum in MDS and CMML Pathogenesis: CHIP, CCUS, CMUS and CCMUS.....	39
8.2 Classification of MDS and CMML	41
8.2.1 The FAB Classification	41
8.2.2 The 2001 WHO Classification of Myeloid Neoplasms	42
8.2.3 The 2008 WHO Classification of Myeloid Neoplasms	43
8.2.4 The 2017 WHO Classification of Myeloid Neoplasms	45
8.2.5 The 2022 WHO Classification of Myeloid Neoplasms	47
9 PROGNOSIS	52
9.1 Prognostic Indices for Myelodysplastic Syndromes	52
9.1.1 International Prognostic Scoring System (IPSS).....	52
9.1.2 Revised International Prognostic Scoring System (IPSS-R)	53
9.1.3 WHO Classification-Based Prognostic Scoring System (WPSS)	54

9.1.4 MD Anderson Global Prognostic Scoring System (MPSS) and Low-Risk Prognostic Scoring System (LR-PSS)	54
9.1.6 Molecular International Prognostic Scoring System (IPSS-M) for Myelodysplastic Syndromes.....	55
9.2 Prognostic Indices for CMML.....	58
9.2.1 MD Anderson Prognostic Scoring System (MDAPS)	58
9.2.2 CMML-specific Prognostic Scoring System (CPSS)	58
9.2.3 Groupe Français des Myélodysplasies (GFM) Prognostic Score	59
9.2.4 Mayo Prognostic Model for WHO-defined CMML (Mayo Model).....	60
9.2.5 Mayo Molecular Model (MMM)	61
9.2.6 Molecular CMML-specific Prognostic Scoring System (CPSS-Mol)	61
9.3 Novel Stratification of MDS and CMML and its Clinical Implications	63
9.3.1 HSPC architecture in MDS and CMML.....	63
9.3.2 Immunophenotypically Defined HSPC Hierarchies are predictive of MDS and CMML progression	65
10. Treatment of Myelodysplastic Syndromes and Chronic Myelomonocytic Leukemia67	
10.1.1 Therapies targeting anti-apoptotic proteins.....	70
10.1.2 NEDDylation inhibitors.....	73
10.1.4 Isocitrate dehydrogenase inhibitors	75
10.1.5 Inflammation pathway inhibitors.....	77
10.1.6 Immune Checkpoint Inhibitors and T Cell-Based Therapeutic Strategies.....	79
11. Published Reviews Contributing To The Doctoral Framework	82
First Review	83
Second Review	96
HYPOTHESIS & OBJECTIVES.....	120

METHODS & RESULTS.....	124
First publication	126
Second publication	140
Third publication	179
Fourth publication	217
DISCUSSION	237
CONCLUSIONS	248
REFERENCES.....	250

THESIS SUMMARY

Títol: Caracterització del sistema immunitari, les cèl·lules mare hematopoètiques i els biomarcadors moleculars en les síndromes mielodisplàstiques (SMD) i la leucèmia mielomonocítica crònica (LMMC): Implicacions per a l'estratificació i el tractament.

Introducció:

Les síndromes mielodisplàstiques (SMD) i la leucèmia mielomonocítica crònica (LMMC) són neoplàsies hematològiques clonals caracteritzades per presentar una hematopoesi ineficaç, inflamació crònica i alteracions moleculars complexes. Aquestes patologies també presenten disfunció immunitària, que contribueix a la progressió de la malaltia, l'evasió clonal i la resistència terapèutica. La interacció entre les cèl·lules mare hematopoètiques (HSC), el microambient inflamatori, la disfunció immunitària i les alteracions genètiques subjacents és fonamental per comprendre aquests processos i dissenyar estratègies terapèutiques dirigides.

Hipòtesi:

La progressió i resistència terapèutica en les SMD i la LMMC estan impulsades per mecanismes moleculars, cel·lulars i immunològics que inclouen jerarquies diferenciades de HSC, patrons co-mutacionals i senyalització inflamatòria. Aquestes interaccions afavoreixen l'evolució clonal, la disfunció del microambient medul·lar i la supervivència cel·lular mediada per vies com MCL1 i NF- κ B, configurant noves oportunitats per a l'estratificació de pacients i el disseny de teràpies dirigides.

Aquesta hipòtesi es basa en la premissa que comprendre com la inflamació crònica, les alteracions moleculars i la interacció immunitària afecten les HSC i els seus progenitors permetrà identificar biomarcadors predictius de resposta terapèutica i dissenyar estratègies específiques per superar la resistència, com la inhibició de IL-1 β .

Objectius:

- Analitzar les jerarquies de HSC i el seu impacte en la progressió de les SMD i la LMMC.

- Identificar mecanismes de resistència terapèutica relacionats amb la dependència de MCL1 i la seva associació amb vies com la senyalització de RAS en la LMMC, a més de la resistència a inhibidors de BCL2.
- Avaluar el paper de la inflamació crònica en les dinàmiques cel·lulars, la disfunció hematopoètica i les interaccions entre HSC i el sistema immunitari en les SMD i la LMMC.
- Caracteritzar patrons co-mutacionals en la LMMC per definir subgrups clínicament rellevants i explorar la seva associació amb la progressió de la malaltia, la resposta terapèutica i els resultats clínics.

Mètodes:

- Estudis transcripcionals mitjançant seqüenciació d'ARN unicel·lular (scRNA-seq) i accessibilitat cromatínica unicel·lular (scATAC-seq) van caracteritzar jerarquies cel·lulars i estats moleculars en mostres de pacients amb SMD i LMMC, proporcionant informació clau sobre els mecanismes de diferenciació i resistència.
- Estudis funcionals amb cultius cel·lulars van analitzar els efectes de tractaments específics sobre les HSC i els seus progenitors. Aquests es van complementar amb anàlisis de proteïnes mitjançant citometria de flux i *western blots* per validar les vies implicades en la supervivència cel·lular i la resistència terapèutica. A més, es va utilitzar la imatge multiplex d'immunofluorescència per mapar les interaccions entre cèl·lules al microambient medul·lar, destacant les contribucions del sistema immunitari i els senyals inflamatoris a la progressió clonal.
- Per a l'anàlisi de patrons co-mutacionals en la LMMC, es va desenvolupar una eina computacional basada en models mixtos i l'algoritme de maximització d'expectativa (EM), utilitzant dades de seqüenciació de nova generació (NGS). Aquest enfocament va permetre identificar subgrups definits per perfils genòmics i correlacionar-los amb característiques clíniques i pronòstic.
- Un assaig clínic de fase II va avaluar l'impacte de canakinumab, un inhibidor de IL-1 β , en la inflamació crònica, les interaccions immunitàries i l'hematopoesi en pacients amb SMD de baix risc prèviament tractats.

Resultats principals:

Els estudis transcripcionals en SMD i LMMC van identificar jerarquies de HSC amb un biaix cap a progenitors granulomonocítics (GMP), que depenen de senyals inflamatoris mediat per $\text{TNF}\alpha$ que activen la via de NF- κ B per a la seva supervivència. Aquest biaix es va associar amb la progressió clonal i la resistència a inhibidors de BCL2, identificant configuracions jeràrquiques específiques com a factors clau en la resistència terapèutica.

L'anàlisi de la LMMC va revelar que subpoblacions clonals dependents de MCL1 estan associades funcionalment amb mutacions en RAS. Aquesta interacció potencia la supervivència clonal i la resistència a teràpies convencionals, suggerint un paper rellevant d'aquesta relació en l'evolució de la malaltia.

L'assaig clínic de fase II va mostrar que canakinumab redueix significativament la inflamació crònica i millora l'hematopoesi en pacients amb SMD de baix risc. Les respostes van ser sostingudes, especialment en aquells pacients amb menor complexitat genètica, i es van acompanyar d'una modulació immunològica, evidenciada per la supressió de limfòcits T proinflamatoris i un efecte positiu en l'equilibri del microambient medul·lar.

L'anàlisi de patrons co-mutacionals en la LMMC va permetre identificar subgrups clínics amb perfils de risc diferenciats, associats amb la supervivència global i la progressió clonal. Aquests resultats avalen l'ús de biomarcadors moleculars per personalitzar els tractaments i millorar l'estratificació del risc.

Conclusions:

Aquesta tesi ofereix una visió integrada dels mecanismes que impulsen la progressió i resistència en les SMD i la LMMC. Els resultats subratllen el paper de les jerarquies de HSC, la relació funcional entre MCL1 i RAS en la LMMC, i l'impacte de la inflamació crònica i la disfunció immunitària en la progressió clonal. A més, els resultats de l'assaig clínic amb canakinumab reforcen el potencial de les teràpies dirigides al microambient inflamatori i al sistema immunitari per millorar els resultats clínics en subgrups específics de pacients. Aquest enfocament estableix noves bases per al desenvolupament de tractaments personalitzats més eficaços.

ABBREVIATIONS

Abbreviation	Definition
AML	Acute Myeloid Leukemia
APC	Antigen-Presenting Cell
ASXL1	Additional Sex Combs-Like 1
BAX	BCL2-Associated X Protein
BCL-XL	B-Cell Lymphoma-Extra Large
BCL2	B-Cell Lymphoma 2
BIM	BCL2-Like Protein 11
BM	Bone Marrow
BiTE	Bispecific T Cell Engager
CAR	Chimeric Antigen Receptor
CC	Conventional Cytogenetics
CCUS	Clonal Cytopenia of Undetermined Significance
CD	Cluster of Differentiation
CHIP	Clonal Hematopoiesis of Indeterminate Potential
CLL	Chronic Lymphocytic Leukemia
CLP	Common Lymphoid Progenitor
CMML	Chronic Myelomonocytic Leukemia
CMP	Common Myeloid Progenitor
CN-LOH	Copy Neutral Loss of Heterozygosity
CPSS	CMML-Specific Prognostic Scoring System
CRL	Cullin-RING Ligase
CTLA-4	Cytotoxic T Lymphocyte-Associated Protein 4
CXCL	Chemokine Ligand
DC	Dendritic Cell
DNA	Deoxyribonucleic Acid
DNMT3A	DNA Methyltransferase 3 Alpha
ESA	Erythropoiesis-Stimulating Agents
FAB	French-American-British (classification)
FISH	Fluorescence In Situ Hybridization
FLT3	FMS-like Tyrosine Kinase 3
GATA1	GATA Binding Protein 1
GATA2	GATA Binding Protein 2
GFM	Groupe Français des Myélodysplasies
GMP	Granulocyte-Monocyte Progenitor
HLA	Human Leukocyte Antigen
HMA	Hypomethylating Agent
HRAS	Harvey Rat Sarcoma Virus Oncogene
HSC	Hematopoietic Stem Cell
HPC	Hematopoietic Progenitor Cell
HSPC	Hematopoietic Stem and Progenitor Cell
HUMARA	Human Androgen Receptor X-chromosome Inactivation Assay
Hb	Hemoglobin

Abbreviation	Definition
IDH	Isocitrate Dehydrogenase
IFN-γ	Interferon Gamma
IL	Interleukin
IPSS	International Prognostic Scoring System
IRAK4	Interleukin-1 Receptor-Associated Kinase 4
ISCN	International System for Cytogenomic Nomenclature
JAK	Janus Kinase
LFS	Leukemia-free survival
LMPPs	Lymphoid-Primed Multipotent Progenitors
LT-HSC	Long-Term Hematopoietic Stem Cell
MCL1	Myeloid Cell Leukemia 1
MDS	Myelodysplastic Syndromes
MPN	Myeloproliferative Neoplasm
NEDD8	Neural Precursor Cell Expressed Developmentally Down-Regulated Protein 8
NF-κB	Nuclear Factor kappa-light-chain-enhancer of activated B cells
NGS	Next-Generation Sequencing
NK	Natural Killer
OS	Overall survival
NPM1	Nucleophosmin 1
PD-1	Programmed Death-1
PD-L1	Programmed Death-Ligand 1
PD-L2	Programmed Death Ligand 2
RAEB	Refractory Anemia with Excess Blasts
RAR	Retinoic Acid Receptor
RARS	Refractory Anemia with Ring Sideroblasts
RAS	Rat Sarcoma Virus Oncogene
RCMD	Refractory Cytopenia with Multilineage Dysplasia
TCA	Tricarboxylic Acid Cycle
TCR	T-Cell Receptor
TET2	Tet Methylcytosine Dioxygenase 2
TGF-β	Transforming Growth Factor Beta
TIM-3	T-cell Immunoglobulin and Mucin-Domain Containing-3
TNF-α	Tumor Necrosis Factor Alpha
TP53	Tumor Protein 53
TRIF	TIR-domain-Containing Adapter-Inducing Interferon- γ
WBC	White Blood Cells
WHO	World Health Organization
sAML	Secondary Acute Myeloid Leukemia

FIGURES & TABLES

Figures Index:

Figure 1: Schematic of adult human hematopoiesis.

Figure 2: Distribution of founder mutations in HSPCs in “CMP Pattern” and “GMP Pattern” MDS/CMML patients.

Figure 3: Immune profiles in lower-risk and higher-risk MDS.

Figure 4: Overview of the somatic mutational landscape in MDS and CMML.

Figure 5: Cytogenetic landscape depicting the most common chromosomal alterations in MDS.

Figure 6: Depiction of myelodysplastic features in hematopoiesis.

Figure 7: Clonal evolution across the spectrum of myeloid neoplasms.

Figure 8: Timeline of diagnostic and prognostic milestones in MDS and CMML.

Figure 9: Overview of MDS subtypes according to WHO classifications from 2017 and 2022.

Figure 10: Reclassification of previously diagnosed CMML and monocytosis cases based on the updated WHO 2022 classification.

Figure 11: Kaplan–Meier survival analysis for LFS and OS stratified by IPSS-M risk categories.

Figure 12: Distinct and Recurrent Cellular Hierarchies drive the maintenance and disease progression of MDS and CMML.

Figure 13: Proposed treatment algorithm for lower-risk MDS patients.

Figure 14: Proposed treatment algorithm for higher-risk MDS patients.

Figure 15: Proposed treatment algorithm for CMML.

Figure 16: Mechanisms of action of BCL2 and MCL1 inhibition.

Figure 17: Emerging therapies for MDS and CMML patients following HMA failure.

Tables Index:

Table 1: Prognostic classification of cytogenetic alterations in MDS.

Table 2: Key morphological dysplastic features in MDS and CMML.

Table 3: FAB classification of MDS.

Table 4: The WHO 2001 classification of MDS.

Table 5: The WHO 2008 classification of MDS.

Table 6: The WHO 2017 classification of MDS.

Table 7: The WHO 2022 classification of MDS.

Table 8: The WHO 2022 diagnostic criteria for CMML.

Table 9: IPSS variables and scoring criteria.

Table 10: IPSS-R variables and scoring criteria.

Table 11: WPSS variables and scoring criteria.

Table 12: Adjusted Hazard Ratios and model weights for leukemic transformation or death in MDS patients.

Table 13: CMML-specific Prognostic Scoring System (CPSS).

Table 14: CPSS-Molecular (CPSS-mol).

INTRODUCTION

1. Introduction to Myeloid Neoplasms

Myeloid neoplasms represent a heterogeneous group of clonal hematological disorders originating from a small population of disease-initiating hematopoietic stem cells (HSCs). These aberrant cells demonstrate persistence and expansion during standard therapeutic interventions, significantly driving disease progression and relapse (1). The hallmark of these malignancies is the dysregulated proliferation and aberrant myeloid differentiation, which disrupts normal hematopoiesis and leads to various clinical presentations, including cytopenias, morphological dysplasia, occasionally leukocytosis and organomegaly, and, in more advanced disease stages, transformation to acute myeloid leukemia (AML). The spectrum of myeloid neoplasms encompasses a diverse group of disorders, including myelodysplastic syndromes (MDS) and myelodysplastic/myeloproliferative neoplasms (MDS/MPN), such as chronic myelomonocytic leukemia (CMML). Each disease within this group is characterized by distinct pathological and genetic features (2). Advances in molecular research have uncovered recurrent genetic mutations and aberrant signaling pathways shedding light on the pathophysiology and prognostic landscape of myeloid neoplasms. These molecular and cytogenetic abnormalities are pivotal in classifying disease subtypes, assessing risk, and guiding therapeutic interventions. This introduction explores the biological and clinical complexity of myeloid neoplasms, with a focus on the mechanisms driving their initiation and progression, while addressing the challenges posed by their heterogeneity and treatment resistance.

The clinical and biological diversity of myeloid neoplasms depends on whether there is an excessive proliferation of one or more myeloid lines, an absence or alteration in the maturation of myeloid precursors, or ineffective and/or dysfunctional myelopoiesis. Thus, if myeloid precursors have maturation defects with or without proliferative advantages, they will give rise to AML. Conversely, if myeloid precursors mature effectively, chronic MPNs will develop, and if they mature ineffectively or dysfunctionally, MDS will result. Finally, myeloid neoplasms that present features characteristic of both MDS (morphological dysplasia, cytopenias, risk of evolution to AML) and MPNs (leukocytosis, thrombocytosis, visceromegalies) constitute the group of MDS/MPN neoplasms. CMML is a prominent entity within the MDS/MPN neoplasm group. While monocytosis is essential for diagnosis, additional features such as splenomegaly and bone marrow (BM) dysplasia may also be present, highlighting the dual dysplastic and proliferative nature of the disease. CMML shares molecular and clinical features with both MDS and MPNs, and thus, occupies a unique position within the spectrum of myeloid neoplasms, making it particularly challenging to classify and treat effectively.

The 2022 WHO classification of myeloid neoplasms (3) included the following categories:

- Myeloid precursor lesions
- Myeloproliferative neoplasms
- Mastocytosis
- **Myelodysplastic neoplasms**
- **Myelodysplastic/myeloproliferative neoplasms**
- Acute myeloid leukemia
- Secondary myeloid neoplasms
- Myeloid/lymphoid neoplasms
- Acute leukemias of mixed or ambiguous lineage

Patients with MDS and CMML face limited curative treatment options and continue to experience very poor prognoses (4). Recent years have seen a surge in novel investigational approaches, leading to the identification of new therapeutic targets for both disorders. However, despite promising preclinical and early-phase trial results, the majority of these drugs have not succeeded in phase III trials. The reasons behind these failures are multifaceted, with disease heterogeneity in MDS and CMML emerging as a key factor. This complexity underscores the urgent need for refined stratification systems that can better classify patients based on specific disease biology, facilitating more accurate patient selection and monitoring within clinical trials.

2. Definition of Myelodysplastic Syndromes and Chronic Myelomonocytic Leukemia

MDS represent a diverse group of clonal HSC disorders (5, 6). Hallmarks of MDS include cytopenias, morphological dysplasia affecting one or more hematopoietic lineages, impaired hematopoiesis, and an increased risk of progression to AML (7-9). MDS are most commonly characterized by a hypercellular or normocellular BM; however, hypocellularity is observed in approximately 10–15% of cases (10, 11). CMML, another clonal disorder arising from HSCs, shares features of both myeloproliferative neoplasms (MPNs) and MDS. CMML is characterized by the presence of relative and absolute monocytosis in peripheral blood (PB) accompanied by dysplasia in the BM. Patients frequently present with cytopenias, particularly anemia and thrombocytopenia, and some cases exhibit hepatomegaly and/or splenomegaly. Similar to MDS, CMML has an inherent propensity to evolve into AML (2, 12-15). The overlap in clinical and biological features between MDS and CMML reflects shared yet distinct pathogenic mechanisms, emphasizing their interconnected nature within the broader

spectrum of myeloid neoplasms.

3. Evolution of the Nosological Classification of Myelodysplastic Syndromes and Chronic Myelomonocytic Leukemia: Rationale for a Unified Analysis in this Doctoral Thesis

The term "myelodysplastic syndrome" (MDS) was officially introduced in 1982; however, before its formal adoption, this group of disorders was referred to by several different names (7). Rhoads and Barker introduced the term "refractory anemia" to define cases of anemia unresponsive to therapy (16). A decade later, Hamilton-Patterson described "preleukemic anemia" to characterize refractory anemia cases that later progressed to acute leukemia (17). By 1956, Björkman had further refined the classification with the term "refractory anemia with ring sideroblasts" (18). Subsequently, different terms emphasizing the risk of leukemic evolution were used for these pathologies: preleukemia (19), quiescent acute leukemia (20), and preleukemic syndrome (21) emphasized the potential for leukemic transformation in these disorders. In 1974, Sexauer et al. introduced "subacute myelomonocytic leukemia," (22), while Miescher and Farquet coined the term "chronic myelomonocytic leukemia" (CMML) in the same year (23).

The French-American-British (FAB) group played a pivotal role in shaping modern classifications. In 1976, they coined the term "dysmyelopoietic syndromes" to describe conditions with features overlapping those of acute leukemia but with a more indolent course, typically in elderly patients (24). A 30% BM blast threshold was established to distinguish MDS from AML, with CMML and refractory anemia with excess blasts (RAEB) being the initial subtypes. By 1982, the FAB group expanded this classification to include refractory anemia (RA), refractory anemia with ring sideroblasts (RARS), refractory anemia with excess blasts in transformation (RAEB-T), and CMML (7). These categories were later revised in the World Health Organization (WHO) classifications of 2001 (12), 2008 (25), 2017(14) and 2022(2). Additionally, CMML was reclassified under MDS/MPN due to its overlapping features with both MDS (e.g., cytopenias, dysplasia, risk of AML progression) and MPN (e.g., leukocytosis, splenomegaly, thrombocytosis).

The historical evolution of these classifications highlights the increasing complexity and refinement in understanding MDS and CMML. The FAB and WHO classifications from 2001, 2008, 2017 and 2022 will be reviewed in the section titled "Diagnosis and Classification of Myelodysplastic Syndromes and Chronic Myelomonocytic Leukemia."

As previously discussed, since CMML was classified as a specific subtype of MDS, prognostic scoring systems have been commonly applied across both pathologies. Although specific prognostic indices for CMML were available, they were based on small patient series and were not widely adopted by the scientific community (26, 27). In 2002, the MD Anderson prognostic scoring system (MDAPS) was introduced, representing the first score based on a larger series of 213 CMML patients. However, its application remained limited (28-30). Since 2013, various CMML-specific prognostic indices have emerged, with the CMML-specific prognostic scoring system (CPSS) being the most widely accepted tool for CMML-specific prognostic assessment (31). In 2022, the Revised International Prognostic Scoring System for MDS (IPSS-M) was introduced as a robust and reliable tool that can be applied to both MDS and CMML (32, 33). Unlike previous systems, IPSS-M incorporates a broader range of clinical and molecular data, improving the accuracy of risk stratification by integrating genetic abnormalities alongside traditional factors such as cytopenias and blast percentage. This comprehensive approach has been validated in large patient cohorts, demonstrating its ability to more accurately predict overall survival (OS) and leukemic transformation in both MDS and CMML populations (34, 35).

Given this background, while current classifications distinguish CMML as a separate entity from MDS within the category of MDS/MPN neoplasms, the significant clinical and biological overlap between these two diseases provides a strong rationale for a unified analysis in this doctoral thesis. Both conditions share fundamental pathophysiological mechanisms, including clonal hematopoiesis, inflammatory signaling, and a predisposition to progression into AML, highlighting their interconnected biological continuum. Moreover, therapeutic responses and resistance mechanisms often align, further justifying their joint examination. Importantly, MDS and CMML are frequently grouped together in clinical trials, with shared treatment protocols and outcome measures applied across both patient populations. This shared inclusion in research underscores the practical significance of a combined approach, offering critical translational opportunities to refine therapeutic strategies. By leveraging the overlapping features of these diseases while recognizing their unique characteristics, this thesis aims to advance our understanding of their pathogenesis, prognosis, and treatment, fostering significant progress in the field of myeloid neoplasms.

4. Epidemiology

4.1 Myelodysplastic Syndromes

Myelodysplastic syndromes (MDS) are typically diagnosed in individuals between the ages of 70 and 75, with a higher prevalence observed in men, at an approximate ratio of 2:1 (36, 37). Due to diagnostic complexities and the subtleties associated with MDS, accurately determining its incidence remains challenging. Current estimates suggest an incidence rate of 3–5 cases per 100,000 individuals per year in the general population, rising substantially to at least 20 cases per 100,000 annually in individuals over the age of 70 (36). With the progressive aging of the population, MDS is increasingly relevant in daily clinical practice (36, 38).

4.2 Chronic Myelomonocytic Leukemia

Chronic myelomonocytic leukemia (CMML) is most commonly diagnosed in individuals between the ages of 65 and 75, with a higher prevalence observed in men at a ratio of approximately 1.5–3:1 (31, 39, 40). Accurate data on the incidence of CMML are limited, as epidemiological studies have variably classified it either within the chronic myeloid leukemias or as a subset of MDS (14). Some studies estimate that CMML accounts for around 30% of cases traditionally categorized under MDS (41). While the exact incidence remains uncertain, it is generally approximated at four cases per 100,000 individuals per year (36, 42).

5. Etiology

5.1 Myelodysplastic Syndromes

Primary or de novo MDS arises in the absence of a prior history of chemotherapy or radiotherapy exposure, which distinguishes it from treatment-related myeloid neoplasms (43). The etiology of de novo MDS has been linked to environmental toxins such as benzene, tobacco, ammonia, solvents, and pesticides (43, 44). Additionally, acquired aplastic anemia has been associated with an increased risk of developing MDS (45, 46).

Certain familial syndromes involving germline mutations predispose individuals to MDS or AML. The 2022 WHO classification includes a dedicated chapter on these entities, termed "Myeloid neoplasms associated with germline predisposition" (2). These syndromes can be categorized based on the underlying germline mutation and the presence or absence of non-hematologic disorders:

1. Myeloid neoplasms with germline predisposition without a pre-existing platelet disorder or organ dysfunction: This group includes germline mutations in *CEBPA* and *DDX41*, typically manifesting as MDS or AML without notable systemic dysfunction.
2. Myeloid neoplasms with germline predisposition and pre-existing platelet disorder: Germline mutations in *RUNX1*, *ANKRD26*, or *ETV6* are linked to a history of platelet abnormalities, including altered platelet counts or functional defects in affected individuals.
3. Myeloid neoplasms with germline predisposition and potential organ dysfunction:
 - *GATA2*: Linked to syndromes such as MonoMAC (monocytopenia and mycobacterial infections), familial MDS/AML, and Emberger syndrome (characterized by lymphedema and predisposition to myeloid malignancies).
 - Telomere biology disorders: Germline mutations in *TERC* or *TERT* and dyskeratosis congenita.
 - BM failure syndromes: Conditions like Fanconi anemia, Diamond-Blackfan anemia, Shwachman-Diamond syndrome, and severe congenital neutropenia, typically presenting in childhood.
 - Syndromic associations: MDS linked to germline *GATA1* mutations in Down syndrome, juvenile myelomonocytic leukemia linked to germline *NF1* in neurofibromatosis, and *PTPN11* in Noonan syndrome.

5.2 Chronic Myelomonocytic Leukemia

The etiology of CMML remains poorly understood. However, like MDS, environmental exposures to toxicants such as benzene, tobacco, ammonia, solvents, and pesticides are thought to increase the risk of CMML (47). As highlighted in the case of MDS, when there is a documented history of prior chemotherapy or radiotherapy, the diagnosis shifts to treatment-related CMML, a subset of treatment-related myeloid neoplasms.

The 2017 WHO classification of myeloid neoplasms associated with germline predisposition includes neurofibromatosis (*NF1* mutations) and Noonan syndrome (*PTPN11* mutations) as conditions linked to CMML-like diseases (14). Germline mutations in these genes predispose individuals to juvenile myelomonocytic leukemia (JMML), a pediatric disorder with overlapping clinical and molecular features with CMML (48-50).

In addition to germline mutations, somatic mutations in genes within the RAS-signaling pathway, such as *NF1*, *PTPN11*, *NRAS*, *KRAS*, and *CBL*, are frequently associated with the proliferative forms of CMML. These mutations enhance the sensitivity of hematopoietic

progenitor cells (HPCs), particularly myeloid progenitors to growth factors like granulocyte-macrophage colony-stimulating factor (GM-CSF), promoting autonomous clonal expansion and driving disease progression (51-53). Collectively, these genetic insights underscore the complexity of CMML pathogenesis and highlight the critical role of both germline and somatic mutations in shaping disease biology and progression.

6. Foundations of MDS and CMML Pathogenesis

MDS and CMML are complex hematologic malignancies rooted in the dysregulation of hematopoiesis. Both diseases arise from clonal HSCs that acquire genetic and epigenetic aberrations, resulting in ineffective blood cell production and an elevated risk of progression to AML. The pathogenesis of MDS and CMML arises from a multifactorial interplay of genetic mutations, chronic inflammatory signaling, immune dysregulation, and profound alterations within the BM microenvironment.

Understanding the pathogenesis of these disorders requires a holistic exploration of their foundational elements, including the role of HSCs and their differentiation hierarchies, the role of inflammation and immune system dysfunction, and the molecular alterations that drive clonal evolution. Additionally, the unique features of the BM niche and tumor microenvironment play pivotal roles in shaping disease progression and therapeutic resistance.

In the sections that follow, we delve into the primary components that underpin MDS and CMML pathogenesis. We begin by examining the hierarchical organization of HSCs and their dysregulation in disease, highlighting recent insights into the molecular and functional diversity of these cells. We then explore the critical role of inflammation and immune dysregulation, emphasizing how chronic inflammatory signaling promotes clonal dominance and impairs normal hematopoiesis. This is followed by a detailed analysis of the molecular landscape of MDS and CMML, including the key somatic mutations, cytogenetic aberrations, and epigenetic disruptions that drive these diseases.

By integrating these elements, this comprehensive framework provides a deeper understanding of the complex pathogenesis of MDS and CMML, offering novel insights for better diagnostic and prognostic assessment, and personalized therapeutic strategies.

6.1 Hematopoietic Stem Cells: Hierarchy and Dysregulation

6.1.1 The Hematopoietic Hierarchy: Structure and Dynamics

A comprehensive understanding of MDS and CMML pathogenesis requires an in-depth exploration of hematopoiesis, a tightly regulated process that produces all blood cell types. This process is orchestrated by BM HSCs, which possess the dual abilities of self-renewal and differentiation into downstream progenitor cells (54). Preclinical evidence in animal studies initially characterized the hematopoietic hierarchy as a stepwise, hierarchical differentiation of HSCs (55, 56). However, advances in single-cell transcriptomics and other multi-omics approaches have refined this understanding, uncovering previously unrecognized HSC subpopulations and revealing the complexity of lineage commitment (57). Hematopoiesis is now viewed as a dynamic continuum, with lineage specification governed by transcriptional states and influenced by transcription factor activity (58-62).

Hematopoiesis is the process of continuously replenishing blood cells from an undifferentiated common precursor, the HSC. HSCs, immunophenotypically defined as CD34⁺, CD38⁻, CD90⁺, CD45RA⁻, possess two defining properties: multipotency, enabling the generation of all differentiated blood cell types, and long-term self-renewal, which ensures the lifelong production of identical progeny through cell division. The regulation of the balance between self-renewal and differentiation is critical for producing mature blood cells while maintaining a stable HSC pool. (63). At the apex of the hematopoietic hierarchy are long-term HSCs (LT-HSCs), a rare population that primarily remains quiescent, typically proliferating only under stress conditions (54). Under physiological conditions, HSCs undergo an asymmetric cell division, resulting in the production of two distinct cell types. One cell is an identical copy of the original HSC, while the other is a multipotent progenitor cell (MPP) (64). These progenitor cells eventually mature into specialized blood cell types, each performing distinct functions essential for maintaining homeostasis and immune defense within the body (**Figure 1**) (54). Further downstream, MPPs give rise to oligopotent progenitors: the lymphoid-primed multipotent progenitors (LMPPs), which preserve stem cell properties (62, 65), and the common myeloid progenitors (CMPs). The myeloid lineage further restricts into granulocyte-monocyte progenitors (GMPs) and megakaryocyte-erythrocyte progenitors (MEPs) (61). The former give rise to terminally differentiated basophils, eosinophils, neutrophils, and macrophages, and the latter terminally differentiate into erythrocytes or megakaryocytes (64). Recent findings suggest that megakaryocytes may arise directly from stem cells (66). The differentiation route that they follow, either step-wise or directly from HSCs, results in functionally distinct megakaryocyte subpopulations (67). LMPPs, in turn, produce common

lymphoid progenitors (CLPs) but retain myeloid differentiation capacity, being also able to differentiate to GMPs (65, 68, 69).

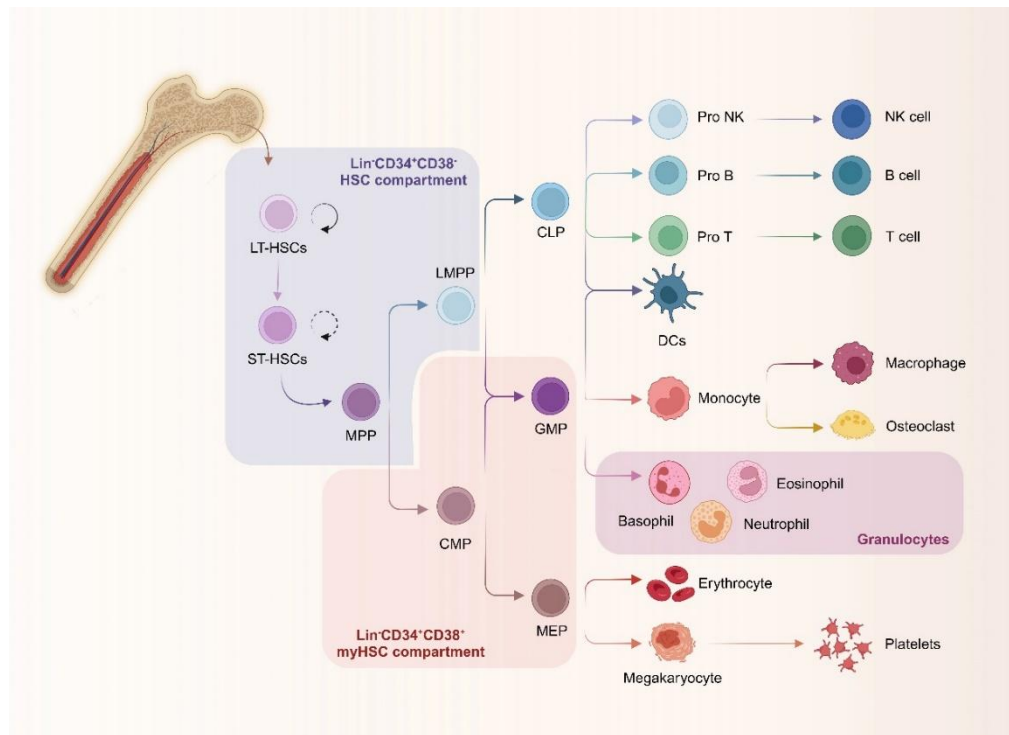


Figure 1. Schematic of adult human hematopoiesis. LT-HSCs give rise to multipotent progenitors (MPPs), which subsequently differentiate into two primary pathways: myeloid-biased common myeloid progenitors (CMPs) and lymphoid-biased lymphoid-primed multipotent progenitors (LMPPs). CMPs further differentiate into megakaryocyte-erythrocyte progenitors (MEPs) and granulocyte/monocyte progenitors (GMPs), while LMPPs generate common lymphoid progenitors (CLPs). MEPs yield megakaryocytes and erythrocytes, while GMPs differentiate into granulocytes, monocytes, and dendritic cells. CLPs predominantly give rise to lymphoid lineages, including natural killer (NK) cells, B cells and T cells. *Figure created using BioRender.*

Although the aforementioned hematopoietic stem and progenitor cell (HSPC) populations are commonly referred to in order to define the differentiation state of cells throughout hematopoiesis, single-cell transcriptomics data have uncovered that hematopoiesis may be far more of a continuous process than originally modeled (70). Moreover, functional analysis of hematopoietic cell states led to the concept of the punctuated continuum hematopoietic model (71). This model proposes the existence of discrete cell states within the continuous transcriptomic landscape, where each state is formed by a heterogeneous pool of cells that are variably primed to give rise to different hematopoietic lineages. Indeed, HSCs demonstrate functional heterogeneity and can differ in their contribution to the lymphoid and myeloid cell lineages. A recent study using DNA barcoding in endogenous adult HSCs in mice to trace the HSC contribution to major hematopoietic cell lineages demonstrated that, although the

majority of HSCs give rise to a single lineage, many HSCs also clonally contribute to multiple lineages, specifically lymphoid and myeloid cells. These results suggested a close developmental relationship between the myeloid and lymphoid lineages (72).

The differentiation potential of HSCs is not static and can be influenced by aging and external stressors (73). In this context, HSCs with a balanced production of lymphoid and myeloid cells are more prevalent during youth (74), whereas aging is associated with increased proportions of HSCs with myeloid-biased output, resulting in myeloid skewing and decreased lymphopoiesis (75-77). Furthermore, it was recently demonstrated that depleting such myeloid-biased HSCs is able to restore characteristic features of a more youthful immune system (78). Changes in differentiation potential can also be triggered by emergency hematopoiesis associated with acute infection, promoting a transcriptional rewiring of HSCs that changes their identity and cellular output from lymphoid- towards myeloid-biased in order to supply elevated numbers of granulocytes (79, 80). Collectively, these data demonstrate that a tight regulation of the differentiation potential of HSCs adapts to specific conditions and is a key mechanism to determine hematopoietic output; and thus, the dominance of aberrant HSCs with altered differentiation is associated with disease-specific abnormal hematopoiesis.

6.1.2 HSC Dysregulation in MDS and CMML

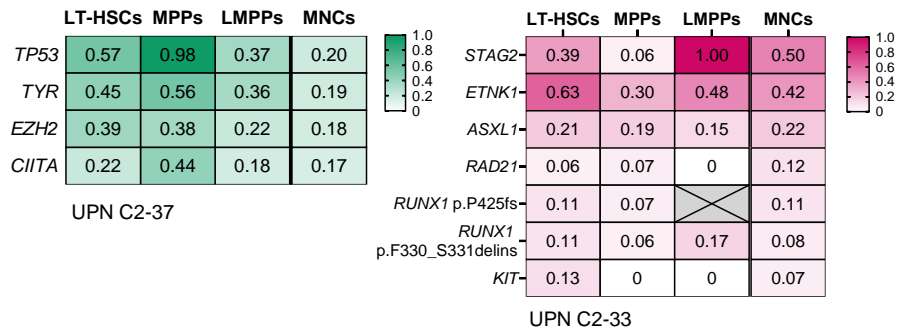
Genetic studies have demonstrated that MDS and CMML arise from HSCs that exhibit aberrant differentiation (6, 81, 82) and persist even during clinical remission to standard therapies (83-85). Elegant clonotypic and transcriptional studies support that immunophenotypically-defined HSPC hierarchies are preserved in MDS and CMML patients, facilitating their isolation and study across genetically diverse patient populations (6, 81, 83, 86).

Malignant HSCs follow distinct myeloid-biased differentiation trajectories, resulting in hierarchies enriched in either CMPs or GMPs (6, 81, 86). These differentiation pathways remain stable throughout HMA therapy, as evidenced in a cohort of over 100 genetically diverse patients, suggesting they represent intrinsic disease mechanisms rather than transient hematopoietic states (83). Genomic and transcriptomic analyses indicate these trajectories originate from either LT-HSCs or LMPPs, each giving rise to distinct CMP or GMP-enriched hierarchies, respectively (83). To maintain consistency, this discussion will use "CMP pattern" to describe LT-HSC-derived hierarchies and "GMP pattern" for those arising from LMPP differentiation.

Mechanistically, distinct MDS and CMML hierarchies are associated with specific genetic and cytogenetic abnormalities. For instance, “CMP pattern” patients are frequently linked to *TP53* mutations and 5q deletions, (6, 86), while the granulomonocytic hierarchy is enriched for mutations in *RUNX1* and *STAG2* (83). These findings align with the emerging concept of mutation-driven HSC fate bias, where specific genetic alterations influence HSC differentiation pathways, guiding their development into distinct HSC hierarchies (87). However, such genotype-hierarchy associations are only observed in a subset of MDS and CMML cases, suggesting that additional factors, such as cooperative genetic interactions or uncharacterized mutations, may also play a role.

Interestingly, driver mutations are almost universally identified in the primitive LT-HSC population, indicating that these cells are consistently either preleukemic or leukemic (6, 83). In contrast, LMPPs in the granulomonocytic trajectory tend to harbor a higher mutational burden, pointing to a potential role for cumulative genetic hits in shaping specific hierarchies (83). These observations highlight the importance of the number and nature of genetic alterations in determining the differentiation trajectories of HSCs and the resultant MDS hierarchies (**Figure 2**). Further genetic and mechanistic studies focusing on HSC biology are essential to unravel the complexities of these differentiation processes and their contribution to MDS pathogenesis.

A. Representative mutational profiles in HSCs and BM MNCs



B. Variant Allele frequencies (VAF) of somatic mutations in patients with hematologic response

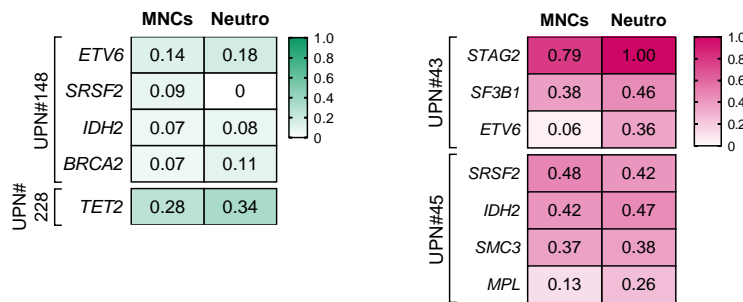


Figure 2. Distribution of Founder Mutations in Hematopoietic Stem and Progenitor Cell (HSPCs) in “CMP Pattern” and “GMP Pattern” MDS/CMML Patients. (A) Variant allele frequencies (VAFs) of somatic mutations in oncogenes and leukemia-associated genes, derived from whole-exome sequencing analyses, are shown across various hematopoietic stem and progenitor cell (HSPC) populations and total BM mononuclear cells (MNCs) in representative “CMP pattern” (left) and “GMP pattern” (right) patients. VAFs are presented without adjustments for copy number variations. Crossed-out boxes indicate instances where specific cell populations were either unavailable or lacked sufficient read coverage at the respective loci, preventing accurate mutation assessment. (B) VAFs of somatic mutations identified in total BM MNCs and neutrophils are displayed for CMP-pattern (left) and GMP-pattern (right) patients during hematologic response to hypomethylating agents (HMAs). Results highlight the stability or evolution of these mutations during treatment. Figure adapted from Ganan-Gomez et al. (83).

The pathogenesis of CMML shares significant similarities with MDS, as both conditions appear to originate from HSCs. Seminal work by Itzykson et al highlights that CMML arises from a CD34⁺CD38⁻CD90⁺ stem cell harboring driver mutations, which confer a competitive advantage over non-clonal HSCs, establishing clonal dominance (88). Among these early mutations, alterations in *TET2* are believed to play an initiating role, promoting clonal expansion and skewing hematopoiesis towards granulomonocytic progenitors (88, 89).

The sequence of genetic events in CMML progression remains under active investigation (13). Founding mutations often involve *TET2*, which may undergo biallelic inactivation through various mechanisms, including mutations on both alleles, copy-neutral loss of heterozygosity (CN-LOH), or microdeletions affecting the 4q24 locus on the unmutated allele (88, 90, 91).

The proposed model suggests a linear and progressive acquisition and accumulation of mutations, where early *SRSF2* mutations often synergize with *TET2* alterations to drive clonal dominance and facilitate the expansion of granulomonocytic progenitors. *In vivo* studies showed that *TET2*-deficient mice develop hematopoiesis with marked granulomonocytic expansion, further supporting this model (92). These findings suggest that co-mutations in *TET2* and *SRSF2* may serve as a genetic hallmark of CMML (52, 88).

Emerging as an early phase in the CMML evolutionary continuum, oligomonocytic CMML (OM-CMML) is characterized by relative monocytosis ($\geq 10\%$ monocytes) with an absolute monocyte count between 0.5 and $1.0 \times 10^9/L$. This condition shares significant overlaps in terms of clinical, morphological, cytogenetic, and molecular features with overt CMML, reflecting their common pathogenic origins (91, 93). Research indicates that approximately 25–30% of OM-CMML cases progress to overt CMML, underscoring its role as a precursor state in disease progression (93). The molecular profile of OM-CMML is characterized by multi-hit *TET2* mutations, often co-occurring with *SRSF2* mutations, further aligning it with the genetic framework of CMML (91). Recognizing OM-CMML as a distinct phase in CMML evolution offers opportunities for earlier diagnosis and targeted interventions, which may alter the disease trajectory and improve patient outcomes (93, 94). Second-order mutations frequently occur at the level of myeloid progenitor cells, such as the MPP and CMP stages. These mutations often involve additional alterations in *TET2* and *SRSF2*, which drive differentiation along the granulocyte-monocyte progenitor (GMP) axis, ultimately resulting in clonal monocytosis (88). Subsequent mutations, including those in *DNMT3A*, *RUNX1*, *SETBP1*, and *SF3B1*, contribute to the development of the myelodysplastic (MD) variant of CMML (95, 96). In parallel, the acquisition of *ASXL1* mutations, activating mutations in the oncogenic RAS pathway, and *JAK2V617F* mutations lead to the myeloproliferative (MP) phenotype of CMML (95-97).

RAS pathway mutations are particularly significant in proliferative CMML, where they enable hypersensitivity GM-CSF, a hallmark of this subtype. This hypersensitivity is accompanied by autonomous growth in granulomonocytic colony cultures, distinguishing proliferative CMML from dysplastic CMML and other MDS subtypes (98). Consistently, RAS pathway mutations, while common in proliferative CMML, are rare in OM-CMML, further delineating the molecular distinctions across the CMML spectrum (93). Additionally, RAS pathway mutations, coupled with somatic copy number alterations, play a critical role in the progression of CMML to AML (97).

Additionally, *ASXL1* mutations, present in about 40% of CMML cases, play a dual role. They act as initiator mutations, driving granulomonocytic differentiation even in the absence of *TET2* mutations, and they can also promote progression to more aggressive forms and AML (96).

6.2 Immune Landscape: Tumor Immunity and Immune Escape

6.2.1 Bone Marrow Microenvironment and Immune Interactions

The immune system, composed of diverse immune cells, plays a central role in recognizing and combating non-self pathogens. In cancer, the dynamic interactions between immune cells, malignant cells, the tumor microenvironment, and therapeutic interventions have become a major area of study for the scientific community (99). Among immune cells, T lymphocytes, with their ability for antigen-specific cytotoxicity, stand out as key members. Their potential in cancer immunotherapy and vaccine development has driven extensive research into their biology and mechanisms of action (100).

T cells are essential for adaptive immunity, coordinating targeted responses to foreign antigens while ensuring tolerance to self-antigens (101). They maintain immune system balance by eliminating pathogens, suppressing the proliferation of malignant cells, and preventing the development of autoimmune conditions (102). The differentiation and functional specialization of T cells is a tightly regulated process critical for effective and supervised immune responses (103, 104).

In the context of cancer, T cells are integral to tumor surveillance, identifying and eliminating malignant cells. However, when T cell differentiation and function are disrupted, immune surveillance mechanisms fail, fostering an immunosuppressive tumor microenvironment that promotes cancer initiation and progression. Dysregulated T cell homeostasis not only facilitates immune evasion but also modulates responses to therapy, significantly influencing clinical outcomes (105). The delicate balance between immunosurveillance and immune escape is essential for preventing malignant transformation. Disruptions in immune regulatory pathways can shift this equilibrium, driving the expansion of malignant clones in numerous cancers (100, 106), including those originating in HSCs (107). Understanding these mechanisms is needed for designing effective strategies to modulate T cell function and improve therapeutic outcomes in cancer patients.

The immune system is essential for preserving hematopoietic equilibrium through its roles in

immune surveillance and tolerance. However, in MDS and CMML, this delicate balance is disrupted, resulting in immune evasion, clonal expansion, and disease progression (108, 109). These myeloid malignancies are characterized by a profoundly dysfunctional immune microenvironment, driven by chronic inflammation and both quantitative and qualitative dysregulation of T cell subpopulations (107, 110). Understanding the role of T cells in MDS and CMML pathogenesis provides a foundation for novel therapeutic approaches targeting immune dysfunction.

6.2.2 T Cell Dysregulation in MDS and CMML

CD4⁺ helper T cells, CD8⁺ cytotoxic T cells, and regulatory T cells (Tregs) each play specialized roles in supporting immune regulation. CD4⁺ T cells interact with other immune cells, such as CD8⁺ T cells, B cells, and antigen-presenting cells, primarily through the secretion of cytokines (111). CD8⁺ T cells are key effectors of cytotoxicity, targeting and eliminating infected or malignant cells. Meanwhile, Tregs are critical for maintaining immune tolerance (112), but in the context of malignancies, they can suppress anti-tumor immunity, thereby facilitating tumor progression (109). In MDS and CMML, both quantitative and qualitative dysregulation of these T cell subsets disrupts the delicate equilibrium between immune activation and suppression.

CD4⁺ T cells

CD4⁺ T cells act as immune orchestrators, supporting CD8⁺ T cells, B cells, and antigen-presenting cells (APCs) through cytokine production, including IFN- γ and TNF- α (111) and proper humoral response. Upon activation of the T-cell receptor (TCR), antigen naïve CD4⁺ T cells differentiate into 6 distinct functional subtypes, namely, Th-1, Th-2, Th-17, Th-22 cells, T follicular helper (Tfh) cells, and Treg cells, each characterized by the secretion of specific cytokines, which functionally activate APCs and CD8⁺ T cells (113).

Traditionally, CD4⁺ T cells have been broadly categorized into two groups, Th-1 and Th-2, based on their cytokine profiles (114). Th-1 cells secrete IFN- γ , TNF- α , and interleukin (IL)-2, which are crucial for cell-mediated immunity and defense against intracellular pathogens (115, 116). In contrast, Th-2 cells secrete IL-4, IL-5, and IL-13, which drive humoral immunity and protect against extracellular pathogens (114). Under normal physiological conditions, the differentiation of Th-1 and Th-2 cells is tightly regulated to maintain a balance between cellular and humoral

immunity. This equilibrium ensures an effective and coordinated immune response while preventing overactivation or suppression.

In MDS and CMML, this balance is disrupted, with a notable reduction in Th-1 cell counts compared to healthy donors (HDs). Reduced Th-1 levels are inversely associated with higher BM blast counts, highlighting their role in regulating malignant cell proliferation and maintaining immune control (117). Additionally, elevated levels of IL-4, predominantly produced by Th-2 cells, serve as an independent predictor of shorter OS in intermediate- to higher-risk MDS patients (118). Interestingly, T cells exposed to monocytes derived from MDS patients exhibit a skewed differentiation towards the Th-2 phenotype (119). This observation supports the notion that Th-2 cells depend on the effective anti-tumor activity of Th-1 cells, rather than directly contributing to tumor evasion through their own polarization (120, 121).

The following sections will delve deeper into the dysregulation of CD4⁺ T cell subsets, highlighting their role in the immune imbalance observed in MDS and CMML.

Th-17/22 cells

Th-17 and Th-22 cells, modulate inflammation and immune activation (122, 123), with overlapping yet distinct contributions to disease progression in MDS and CMML.

Th-17 cells secrete pro-inflammatory cytokines, including IL-17 and IL-23, which are vital for defending against bacterial and fungal infections (124). However, aberrant IL-17 expression has been implicated in autoimmune diseases and cancers, as it fosters a pro-inflammatory cytokine environment that stimulates dysfunctional myeloid cell expansion, promotes angiogenesis, and establishes an immune-suppressive tumor milieu permissive to tumor growth and clonal expansion (125, 126). Lower-risk MDS patients exhibit elevated Th-17 cell counts and IL-17 levels in the PB and BM compared to higher-risk patients, correlating with increased expression of RAR-related orphan receptor genes that drive Th-17 differentiation (127). This pro-inflammatory milieu, marked by elevated cytokines such as IL-6, IL-21, IL-22, and IL-23, leads to increased HSC apoptosis and ineffective hematopoiesis (128, 129).

Th-22 cells secrete IL-22, IL-13, and TNF- α , contributing to both protective immune functions and pathological inflammatory processes (130). IL-22, although protective against tissue inflammation, can also contribute to disease pathogenesis by promoting pro-inflammatory effects (131). In MDS, Th-22 cells are notably elevated in patients with advanced-stage

disease and are closely associated with elevated levels of pro-inflammatory cytokines, including TNF- α and IL-6. This chronic inflammatory signaling likely promotes Th-22 polarization and expansion, further exacerbating immune escape and facilitating clonal evolution (132).

Together, Th-17 and Th-22 cells exemplify the complex interplay between inflammation and immune dysfunction in the pathogenesis of MDS.

T Regulatory cells (Tregs)

Tregs are essential for preserving immune homeostasis by mitigating excessive immune responses against self and non-self antigens. However, Treg cells can also play an active role in inhibiting tumor specific-immunity, thus facilitating immune evasion of cancer cells (133). Tregs exert their immunosuppressive effects through the secretion of cytokines such as IL-10 and TGF- β , thereby inhibiting effective immune activation and antitumor responses (134) by secreting immunosuppressive cytokines (e.g., IL-10 and TGF- β) (135). Increased Treg levels and immunosuppressive activity undermine effective immune activation, resulting in impaired antitumor responses and creating a permissive environment for immune evasion and tumor progression (136).

In MDS and CMML, Treg counts are elevated in the PB and BM of higher-risk patients compared to those with lower disease burden. This increase is thought to result from the expression of tumor-associated antigens on malignant cells during disease progression, which stimulates Treg expansion (137, 138). Interestingly, Treg levels tend to decrease following a positive therapeutic response but rise again with therapy failure, highlighting their dynamic nature in response to treatment (139). These observations suggest that the aberrant expansion and activity of Tregs play a central role in suppressing immune surveillance, thereby promoting the progression of MDS and CMML (137, 140, 141). This underscores the importance of understanding Treg-mediated immune dysfunction in the pathogenesis of these hematologic malignancies.

CD8⁺ cytotoxic T cells

CD8⁺ cytotoxic T cells directly kill tumor cells and function as potent effectors in tumor surveillance and immune defense (142, 143). Upon recognition of pathogens, CD8⁺ T cells activate different mechanisms to kill infected or malignant cells by secreting pro-inflammatory

cytokines such as TNF- α and IFN- γ , releasing cytotoxic mediators (e.g., perforin and granzymes), or activating the Fas/FasL pathway (144). CD8⁺ T cells may also regulate HSC pool dynamics in the BM milieu (145). The functional exhaustion of CD8⁺ T cells, induced by prolonged antigenic stimulation and the immunosuppressive tumor microenvironment, represents a hallmark feature of several cancers (143, 144).

In lower-risk MDS CD8⁺ T cell counts (138, 146), which suppress malignant clones but disrupt normal hematopoiesis, are increased, leading to BM HSPC exhaustion (147). Conversely, in higher-risk MDS, CD8⁺ T cells are reduced in number, exhibit diminished cytotoxic function, and overexpress immune checkpoint proteins like PD-1 and its ligand PD-L1, enabling malignant cells to evade immune detection (148). Using mass cytometry and single-cell RNA sequencing (scRNA-seq), distinct CD8⁺ T cell subsets, such as CD57⁺CXCR3⁺ cells, seemed to be enriched in non-responders to hypomethylating agents (HMAs) and are linked to poor survival outcomes in higher-risk MDS and AML patients (149). These findings support the dynamic interaction between leukemic cells and the immune system, shaping disease progression and therapeutic response.

6.2.3 T Cell Evasion in MDS

Immune evasion is a hallmark of cancer, enabling malignant clones to proliferate and outcompete normal cells (99). This process is particularly pronounced in MDS, where an aging immune system becomes increasingly prone to dysfunction (150). Overexpression of immune checkpoint molecules such as PD-1, PD-L1, and CTLA-4 contributes to T cell exhaustion and creates a tumor microenvironment favorable for immune escape (151).

The interaction between PD-1 and its ligand PD-L1 impairs TCR-mediated T cell activation and cytokine production, undermining immune response. In MDS, PD-1 is upregulated on effector and regulatory T cells, while PD-L1 is overexpressed on CD34⁺ HSPCs, reinforcing the escape of malignant cells from immune surveillance (152-156). Additionally, elevated levels of inflammatory cytokines, including IFN- γ , TNF- α , and S100A9, commonly found in the BM microenvironment of CMML and MDS patients, further enhance PD-1/PD-L1 expression, exacerbating immune evasion (157-159).

CTLA-4, another immune checkpoint receptor, delivers inhibitory signals to T cells, dampening immune responses and facilitating tumor growth (160). Additionally, CTLA-4 expression in MDS and CMML HSPCs correlates with disease progression, showing higher levels in advanced stages and higher-risk subtypes, where it contributes to immune evasion and

transformation to AML (161).

Among the master regulators of immune suppression in cancer are the co-inhibitory receptors TIM-3 and TIGIT, which play significant roles in modulating immune responses. TIM-3 is expressed on a variety of immune cells, including Th-1 cells, CD8⁺ cytotoxic T cells, regulatory T cells (Tregs), and natural killer (NK) cells. It induces apoptosis in Th-1 cells and modulates the production of key cytokines, such as TNF- α and IFN- γ (162, 163). TIM-3 expression is elevated in MDS and CMML BM CD8⁺ T cells and correlates with reduced levels of cytotoxic molecules, such as perforin and granzyme B, alongside increased susceptibility to apoptosis due to CD95 upregulation. This ultimately suppresses CD8⁺ T cell function and enables immune escape (162). Importantly, TIM-3 is overexpressed on MDS/CMML leukemic stem cells, highlighting its potential as a therapeutic target, with dual benefits of depleting malignant cells and restoring immune function (164). TIGIT, another co-inhibitory receptor, is remarkably elevated in higher-risk MDS and contributes to the diminished responsiveness of CD4⁺ T cells, CD8⁺ T cells, and NK cells. Its elevated expression inhibits the production of key effector cytokines, including CD107a, IFN- γ , and TNF- α , thereby facilitating the proliferation of malignant clones (153).

The immune profiles of MDS patients differ significantly based on disease risk (**Figure 3**) (165). Lower-risk MDS is predominantly associated with a pro-inflammatory BM microenvironment, driven in part by activation of the NLRP3 inflammasome. This environment is characterized by an increase in pro-inflammatory T cell populations, such as Th-17 cells, which secrete cytokines including IL-6, IL-21, and IL-23. These cytokines contribute to HSC aberrant differentiation, apoptosis, and impaired hematopoiesis (128, 129). In contrast, higher-risk MDS transitions toward an immunosuppressive state dominated by regulatory T cells (Tregs) (137, 138). These cells suppress immune activation through the secretion of cytokines like IL-10 and TGF- β and by recruiting and inhibiting CD8⁺ T cell activation, thereby promoting immune tolerance and facilitating disease progression (140, 141).

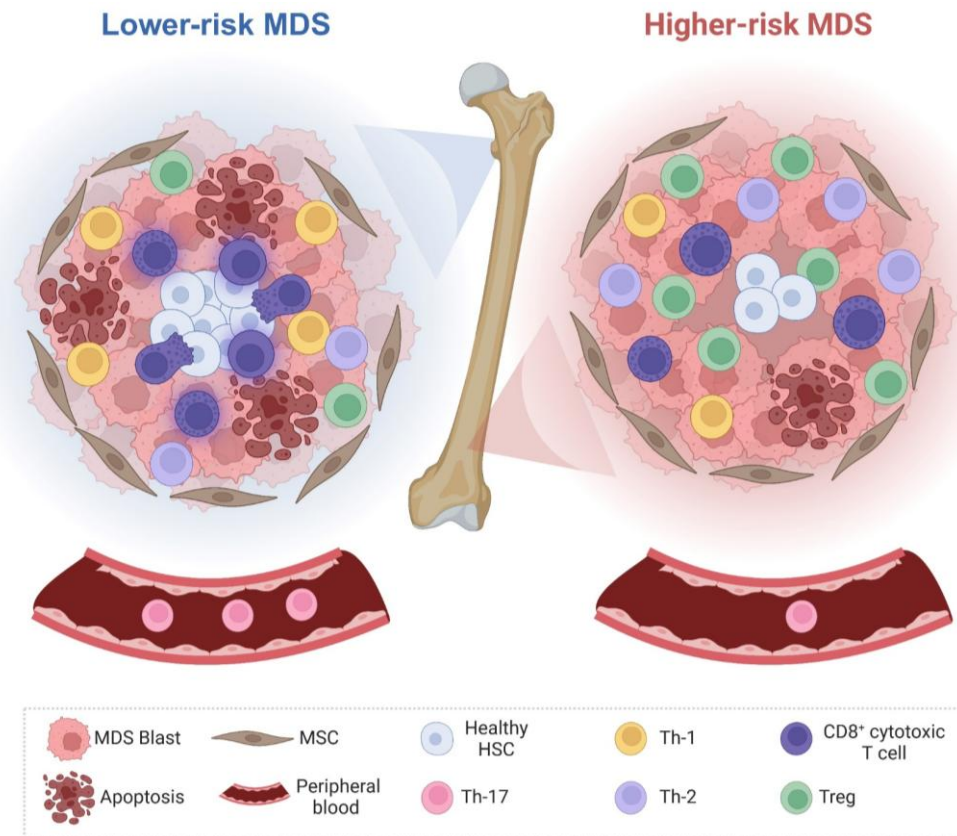


Figure 3. Immune profiles in lower-risk and higher-risk MDS. (Left panel) Lower-risk MDS exhibits intensified immune cell activity, with increased numbers of CD8⁺ T cells displaying enhanced functional activation. (Right panel) In contrast, higher-risk MDS is marked by an immunosuppressive microenvironment that facilitates immune evasion. This stage is characterized by a significant reduction in CD8⁺ T cell numbers and an increase in regulatory T cells (Tregs). MSC: mesenchymal stem cell. Figure adapted from Rodriguez-Sevilla et al. (166).

Immune evasion mechanisms, including altered cytokine profiles and immune checkpoint overexpression, further exacerbate the shift from inflammation in lower-risk MDS to immune suppression in higher-risk cases (167). Elevated levels of cytokines such as IFN- γ and TNF- α found in the BM microenvironment of MDS and CMML patients (157, 158), drive the upregulation of PD-L1 on MDS blasts and PD-1 on HSCs and suppressor cells, reinforcing immune evasion pathways (168). Similarly, molecules like S100A9, a central molecule in MDS pathophysiology (159), induce the expression of programmed death 1 (PD-1) on HSPCs and that of PD-L1 on myeloid-derived suppressor cells (169), while co-inhibitory receptors such as TIM-3 and TIGIT impair antigen presentation and suppress immune responses, further promoting immune escape (169).

Emerging T cell-based therapies offer promising avenues to target dysfunctional T cell populations and enhance antitumor responses. However, despite the therapeutic potential of

these new approaches, the complexity of MDS and CMML-related immune dysregulation has not yet been completely deciphered. Dissecting the interactions between T cell subtypes and malignant cells during disease progression, as well as the dynamic changes in T cell populations in response to therapy, is essential for advancing more effective therapeutic strategies. A detailed exploration of these approaches will be presented in the subsequent section, "Treatment of Myelodysplastic Syndromes and Chronic Myelomonocytic Leukemia".

6.3 The Role of Inflammation in Myeloid Disorders

6.3.1 Chronic Inflammation: A Driver of Hematopoietic Dysregulation

Inflammation is a highly conserved and intricate process that is central to responding to infection, repairing tissue damage, and maintaining homeostasis. However, with aging, the adequate resolution of acute inflammation often diminishes, giving rise to a state of persistent, low-grade inflammation—a phenomenon known as “chronic inflammation” (170). While initially protective, prolonged inflammatory activity can become harmful, contributing to the development of multiple pathologies, including myeloid malignancies (171).

HSCs are a functionally heterogeneous cell population that plays a crucial role in the systemic inflammatory response (172, 173). HSCs respond to external inflammatory signals by adapting their cellular functions, creating a dynamic axis that aligns peripheral stressors with hematopoietic output. (174, 175). In aging individuals, BM HSPCs exhibit a decline in self-renewal potential, coupled with a shift towards myeloid lineage differentiation and compromised immune surveillance, increasing the risk of disease onset (176). This decline is partly driven by a phenomenon termed “inflammaging,” which involves sustained low-grade inflammation and an upregulation of pro-inflammatory cytokines, such as IL-6 and TNF- α , leading to amplified inflammatory signaling at the cellular level (177). Chronic exposure to inflammatory stimuli, whether due to recurrent infections or non-infectious inflammatory triggers, exerts a detrimental effect on HSPC function, particularly impacting self-renewal capacity and inducing a shift from quiescence to active differentiation (178-181). The resultant functional impairment of HSCs is predominantly due to enhanced cellular proliferation rather than an overall suppression of hematopoiesis (182). Over time, this chronic inflammatory state promotes age-related changes within the HSC compartment, leading to the accumulation of DNA damage and somatic mutations (183). Although many of these mutations remain phenotypically silent, some confer proliferative fitness, driving clonal expansion of mutated HSPCs in a process referred to as clonal hematopoiesis of indeterminate potential (CHIP).

Numerous studies have evidenced the central role of inflammatory signaling in driving the initiation and progression of hematologic malignancies, particularly within the evolutionary continuum of myeloid neoplasms (107, 184). Pro-inflammatory cytokines, including IFN- γ , IL-1 β , and TNF- α , have been shown to stimulate clonal expansion of premalignant cells, particularly in cases of clonal hematopoiesis of indeterminate potential (CHIP) driven by *TET2* and *DNMT3A* mutations. Unlike normal HSPCs, these mutant clones display a resistance to depletion by inflammation, providing them with a selective growth advantage (185-188). Thus, chronic inflammatory signaling induces external pressures on HSCs that favor the clonal outgrowth of cells with advantageous mutations, leading to progressive clonal expansion and, potentially, malignancy.

Mutations in *DNMT3A*, *TET2*, and *ASXL1* confer mutant HSPCs with a competitive advantage in inflammatory environments by enabling resistance to inflammation-induced damage, such as apoptosis and exhaustion (189, 190). *TET2* plays a pivotal role in maintaining HSC homeostasis, and its depletion enhances HSC survival and proliferation under inflammatory conditions (191, 192). For example, Tet2-deficient HSPCs exhibit increased expansion in response to inflammatory cytokines like IL-6 and TNF- α and show resistance to demethylation at differentiation-associated transcription factor binding sites. Similarly, *DNMT3A* mutations promote clonal fitness through IFN- γ signaling, as observed in chronic infection models of *Mycobacterium avium* (186) and inflammatory conditions such as ulcerative colitis (193). Mutant *ASXL1* clones further exploit inflammatory signals, with enhanced resistance driven by feedback from mutant progeny cells (194). Together, these findings highlight the role of inflammatory signaling in shaping the clonal dynamics of mutant HSPCs, driving clonal expansion and progression toward overt myeloid neoplasms, such as MDS and CMML.

The nucleotide-binding oligomerization, leucine-rich repeat, and pyrin domains-containing protein 3 (NLRP3) inflammasome, a key biological driver of MDS, triggers pyroptosis, a type of inflammation-mediated cell death (195), causing ineffective hematopoiesis, particularly in the context of *TET2* and *ASXL1* mutations (159). Activation of the NLRP3 inflammasome is induced by both extrinsic factors, such as Toll-like receptor (TLR) signaling, and intrinsic mechanisms, including somatic mutations. This activation leads to the release of pro-inflammatory cytokines IL-1 β and IL-18, which synergize with IL-6, TNF- α , and IL-8 to create a pro-inflammatory microenvironment that sustains the proliferation and survival of aberrant MDS stem cells in preclinical models (175, 186, 196). Collectively, these findings underscore the pivotal role of the NLRP3 inflammasome in fostering a permissive inflammatory niche that supports clonal dominance and disease progression in chronic myeloid neoplasms.

6.3.2 Inflammation and Immune Dysregulation in MDS and CMML

Inflammation and immunity are tightly interconnected, with inflammatory signals driving immune cell activation and responses. The maintenance of a precise equilibrium between pro-inflammatory and anti-inflammatory signals is crucial for preserving immune homeostasis (197). Immune dysregulation, a hallmark of MDS and CMML, significantly affects hematopoiesis and alters both innate and adaptive immunity through the secretion of pro- and anti-inflammatory cytokines (184). T cell-mediated immune imbalance is driven by cell-intrinsic and -extrinsic factors that lead to immune exhaustion, the loss of immune surveillance, and the expansion of mutant clones.

Chronic and unresolved inflammation significantly impairs adaptive immune function. Prolonged exposure to inflammatory stimuli results in a restricted TCR repertoire and diminished potential for memory cell formation (198), and B cells display reduced antibody diversity (199). These inflammation-induced responses result in immune deregulation, which increases the levels of circulating pro-inflammatory cytokines, thus promoting the persistent infiltration of macrophages and neutrophils and hampering tissue homeostasis (200). Thus, chronic inflammation leads to immune dysregulation, which affects immune surveillance and predisposes individuals to cancer, including MDS.

In CHIP, somatic mutations in *DNMT3A*, *TET2*, and *ASXL1* inherently alter immune signaling. The effects of CHIP-related loss-of-function mutations involving epigenetic regulators have been studied extensively to improve the clinical activity of chimeric antigen receptor (CAR) T-cell therapies for hematologic cancers. Indeed, *TET2*-deficient CAR T cells exhibit an abnormal epigenetic landscape and functional changes, characterized by the heightened production of TNF- α , IL-2, and IL-6 upon stimulation and an increased cytotoxic profile (201). Interestingly, *DNMT3A* depletion increases CAR T cells' proliferative capability without inducing the classical exhaustion phenotype acquired upon chronic stimulation, possibly because of increased IL-10 secretion (202). Conversely, *TET2* mutations impair B-cell functions, reducing plasma cell differentiation and antigen-specific antibody production while promoting lymphomagenesis (203). Moreover, *DNMT3A*-deficient B cells, while initially maintaining normal responses to model antigen exposure, eventually progress to an aggressive chronic lymphocytic leukemia (CLL)-like phenotype characterized by high penetrance, underscoring their predisposition to malignant transformation (204, 205).

Regarding the innate immune system, macrophages lacking *TET2* exhibit elevated expression of pro-inflammatory chemokines and cytokines, including IL-1 β , IL-6, IL-8, and IL-

18, compared to their wildtype counterparts (206-208). Furthermore, neutrophils harboring *TET2* mutations display reduced secondary and tertiary granule content, indicative of a less mature phenotype relative to non-mutant cells (209). At the mechanistic level, *TET2* mutations impair the epigenetic regulation of neutrophil maturation, leading to hypermethylated chromatin states and diminished phagocytic function. Collectively, these findings highlight the diverse impact of CHIP mutations across distinct cell types, revealing that their pro-inflammatory effects extend well beyond myeloid cells.

A major challenge in elucidating how pre-leukemic conditions progress into overt hematologic malignancies lies in understanding the mechanisms by which mutant clones outcompete their normal counterparts. Clonal cytopenia of undetermined significance (CCUS)—marked by persistent cytopenias and clonal hematopoiesis but lacking the morphologic or clinical features indicative of MDS (210-212)—presents a crucial opportunity to investigate the immune dysfunction that arises prior to overt disease. In this context, scRNA-seq of BM mononuclear cells (BM MNCs) from CCUS patients with *DNMT3A* or *TET2* mutations has shown that CD8⁺ T effector and NK cells adopt a hyperactivated phenotype. However, this state coincides with significant downregulation of NF- κ B-mediated inflammatory signaling genes, indicating a reduced pro-inflammatory response vital for effective anti-tumor immunity (213). Despite their hyperactivated state, CCUS NK cells secrete significantly less IFN- γ , exhibit impaired cytolytic capabilities, and express increased levels of exhaustion markers (e.g., increased expression of *CD57*, *CD244*, *LAG3*, *TIGIT*, and *PCDC1*). Targeted single-cell DNA sequencing and immunophenotypic analyses revealed that NK cells harbor similar mutational burdens to myelomonocytes, which suggests that MDS driver mutations such as *DNMT3A* or *TET2* affect NK cell functions (213). In MDS and CMML patients, *TET2*-mutated NK cells display diminished immune surveillance of malignant clones, likely due to the reduced expression of killer immunoglobulin-like receptors, perforin, and TNF- α (214). These findings reveal a paradox within the immune microenvironment of pre-leukemic stages, characterized by hyperactivation yet profound functional impairment. Notably, the fact that NK cells harbor mutations at levels comparable to the monocytic and myeloid compartments highlights the significant impact of driver mutations, such as *DNMT3A* and *TET2*, on innate immune dysfunction. This genetic impairment induces irreversible dysfunction in NK cells, profoundly impairing their immune surveillance capacity. Consequently, malignant cells evade immune surveillance, enabling uncontrolled expansion and driving disease progression during these pre-leukemic stages.

Thus, chronic inflammation observed in patients with CHIP or CCUS critically contributes to disease initiation by disrupting immune system regulation. This imbalance is further

pronounced in conditions like MDS and CMML, where T-cell exhaustion undermines antitumor immunity and promotes the rise of immune tolerance.

6.3.3 Inflammation as a Potential Therapeutic Target in MDS and CMML

Inflammation is a key contributor to the development of MDS and CMML, disrupting hematopoiesis and fostering a microenvironment that supports clonal evolution and immune evasion. Targeting inflammatory pathways has emerged as a promising strategy to mitigate immune dysregulation and halt disease progression, particularly in lower-risk patients where inflammation is a dominant factor.

Advances in understanding the molecular mechanisms of inflammation in MDS and CMML have identified several therapeutic targets, currently under investigation in preclinical and clinical settings. Inhibitors of interleukin-1 receptor-associated kinases (IRAK1/4), which mediate Toll-like receptor signaling, have shown promise in reducing inflammatory cytokine production and restoring hematopoietic balance. Targeting the S100A9 signaling pathway, central to inflammation-driven immune suppression and clonal expansion, represents another viable strategy (159). Therapeutic agents targeting the transforming growth factor-beta (TGF- β) pathway, IL-6, TNF- α are also being explored as strategies to reinvigorate immune surveillance and suppress malignant progression (169).

A detailed evaluation of these therapies, including specific drug candidates, mechanisms of action, and ongoing clinical trials, is presented in the "Emerging treatments for MDS and CMML: biological rationales and clinical translation" section of this thesis.

In summary, chronic inflammation perpetuates immune dysregulation and fosters malignant progression in MDS and CMML. By disrupting inflammatory feedback loops, emerging therapies offer the potential to enhance hematopoiesis, reinvigorate immune surveillance, and improve outcomes. Future research should focus on refining these strategies and extend their applicability to higher-risk disease contexts.

6.4 Molecular Pathogenesis of MDS And CMML

The molecular basis of MDS and CMML is primarily driven by the gradual accumulation of genetic alterations in HSCs over time. With aging, HSCs progressively acquire somatic mutations and chromosomal abnormalities, conferring selective advantages to mutant clones

over normal cells (6, 215-217). These genetic changes often originate in small populations of BM cells, a phenomenon termed clonal hematopoiesis of indeterminate potential (CHIP). Over time, additional driver mutations or external pressures, such as chronic inflammation or prior chemotherapy, facilitate the expansion of CHIP clones, leading to overt disease (218). In MDS and CMML, this progression can ultimately result in the transformation to acute myeloid leukemia (AML), often following treatment failure, when malignant clones acquire secondary mutations or undergo clonal evolution (216, 218-220).

Recent advancements in next-generation sequencing (NGS) have significantly expanded our understanding of MDS and CMML, revealing recurrent mutations in key pathways such as DNA methylation, chromatin remodeling, RNA splicing, and signal transduction (221, 222). NGS-targeted panels have become essential for CMML diagnostics, particularly due to the lower prevalence of cytogenetic abnormalities in these patients (observed in 70–80% of cases) and the challenges posed by ambiguous presentations, such as mild dysplasia or monocytosis (28).

6.4.1 Genetic Landscape and Key Mutations in MDS

Cumulative scientific evidence has demonstrated that MDS arises through a multistep process characterized by recurrent genetic mutations or cytogenetic abnormalities, driving the preferential clonal expansion of mutant HSCs over their wildtype counterparts (223). Single-cell technologies and functional studies in murine models have further elucidated the multistep genetic processes driving MDS pathogenesis. These studies reveal that recurrent genetic mutations and cytogenetic aberrations promote clonal dominance of mutant HSCs, facilitating their expansion at the expense of normal hematopoiesis. Understanding the functional impact of these mutations is essential, as they target diverse cellular pathways and contribute to the initiation, progression, and phenotypic variability of MDS (**Figure 4**).

A) Splicing Factors

Splicing factors are genes encoding components of the spliceosome, a complex ribonucleoprotein machinery essential for pre-mRNA processing. The spliceosome ensures the accurate removal of introns and the ligation of exons to produce mature messenger RNA (mRNA) (224). Mutations in spliceosome genes disrupt canonical splicing, resulting in aberrant inclusion of introns or the generation of mis-spliced exons. These events lead to the production of dysfunctional or truncated proteins, which can interfere with normal cellular processes. Such disruptions contribute to the dysplastic phenotypes characteristic of MDS (225).

Mutations in spliceosome components are among the most frequent genetic aberrations in MDS, occurring in up to 60% of cases (226-228). The most commonly affected genes include *SF3B1*, *SRSF2*, *U2AF1*, and *ZRSR2*. These mutations are predominantly heterozygous and are usually mutually exclusive, reflecting distinct pathophysiological roles and selective pressures in HPCs (226, 229). The impact of these mutations extends beyond aberrant splicing, influencing cellular homeostasis, clonal evolution, and disease phenotype. For instance, *SF3B1* mutations are closely associated with the formation of ring sideroblasts, a hallmark feature in a subset of MDS (230). In contrast, mutations in *SRSF2* and *U2AF1* lead to broader defects in hematopoietic differentiation, further contributing to the characteristic dysplasia of the disease (231). These findings underscore the important role of splicing factor mutations in shaping the clinical and molecular phenotype of MDS.

B) Epigenetic Regulators

Epigenetic regulators constitute the second most frequently mutated group of genes in MDS (232). These mutations can be broadly classified into two primary categories: those that disrupt DNA methylation and those that alter histone modification:

- **DNA Methylation Factors:** DNA methylation, particularly at CpG islands within gene promoters and regulatory enhancer regions, is an essential mechanism for controlling gene expression. Alterations in methylation patterns can lead to dysregulated gene activity, commonly resulting in the hypermethylation of tumor suppressor genes and those involved in DNA repair. Such epigenetic changes contribute to the disruption of HSC function in MDS (233). In MDS, hypermethylation frequently affects genes involved in cell proliferation and adhesion, contributing to disease pathogenesis.

Prominent examples of genes frequently affected by DNA methylation include *TET2* and *DNMT3A*, which often acquire frameshift or nonsense mutations (234). These mutations, alongside those in splicing factors, *ASXL1*, and *TP53*, are common in CHIP, indicating their potential role as early or initiating events in disease evolution (235).

- **Histone Modifiers:** Histones, which package DNA into nucleosomes and form chromatin, undergo various post-translational modifications—such as acetylation, methylation, and ubiquitination—that regulate chromatin accessibility and gene expression (236). In MDS, mutations frequently occur in genes encoding histone-modifying enzymes, notably *ASXL1* and *EZH2*, which are often associated with a loss of function (237, 238). These mutations lead to impaired chromatin architecture and

aberrant gene expression patterns, contributing to hematopoietic dysregulation and the development of dysplastic phenotypes.

C) Cohesin Complex Components

The cohesin complex, consisting of proteins such as SMC1A, SMC3, RAD21, STAG1, and STAG2, is essential for maintaining sister chromatid cohesion during mitosis, facilitating post-replicative DNA repair, and regulating transcription (239). Mutations in cohesin complex genes in MDS are typically heterozygous deletions or point mutations, often leading to a loss of function (240). Among these, *STAG2* mutations are the most prevalent, with a reported frequency of 5–10% (241). Disruption of cohesin function contributes to chromosomal instability and transcriptional dysregulation, both of which are critical drivers of clonal evolution and malignant transformation in MDS (242).

D) Transcription Factors

The maintenance of HSC function and the appropriate differentiation of these cells into mature blood cell lineages depend on the tightly regulated activation of lineage-specific transcriptional programs. Transcription factors serve as master regulators of these processes by orchestrating the expression of genes required for proper cellular function, proliferation, and differentiation. In MDS, mutations in critical transcription factors such as *RUNX1*, *GATA2*, and *ETV6* are commonly identified. These genetic alterations play a crucial role in disrupting normal hematopoiesis, driving disease initiation, and contributing to its progression (243-245).

Mutations in these transcription factors disrupt hematopoietic differentiation and increase clonal fitness, driving disease progression. *RUNX1* mutations, often resulting in loss of function or dominant-negative variants, impair lineage commitment and lead to the accumulation of dysplastic cells (245, 246). Alterations in *GATA2* compromise progenitor cell survival and immune function, increasing the risk of transformation to secondary AML (247, 248). Similarly, mutations in *ETV6* contribute to genomic instability, further promoting clonal evolution (244, 249). Collectively, these mutations undermine cellular homeostasis and create a permissive environment for malignant transformation, underscoring their central role in MDS pathogenesis.

E) Signal Transduction Molecules

Signal transduction is the process by which extracellular signals, triggered by the binding of ligands to cell surface receptors, are transmitted through a cascade of intracellular reactions to modulate gene expression, ultimately controlling key cellular processes such as proliferation and apoptosis (250). In MDS, mutations in components of these signaling pathways frequently

result in their constitutive activation, even in the absence of external signals. This aberrant activation disrupts normal regulatory mechanisms, driving uncontrolled cellular proliferation and contributing to disease progression.

Mutations in signal transduction genes, while less frequent in MDS compared to other myeloid neoplasms, occur in approximately 10–15% of cases (251). Commonly mutated genes include members of the RAS signaling pathway (*NRAS*, *KRAS*, *CBL*, *PTPN11*, *NF1*) and *JAK2*. These alterations, often missense mutations or small insertions/deletions, result in persistent activation of downstream signaling cascades, promoting clonal expansion and malignant transformation. Despite their relatively low prevalence, these mutations play a significant role in the pathogenesis of MDS by altering cellular growth dynamics and fostering an environment (i.e., pro-inflammatory) conducive to disease maintenance and progression (252).

F) TP53 Pathway

The TP53 gene, located on the short arm of chromosome 17, encodes the p53 transcription factor, a pivotal regulator of genomic stability. This tumor suppressor plays an essential role in responding to genotoxic stress by orchestrating cellular processes such as cell cycle arrest, DNA repair, and apoptosis, thereby safeguarding genomic integrity (253, 254).

While *TP53* mutations are found in roughly 10% of de novo MDS cases, they are highly prevalent in complex karyotype cases, observed in up to 30-50% of these patients (255, 256). Moreover, *TP53* mutations are detected in roughly 20% of MDS cases with isolated del(5q) and can reach up to 40% in secondary MDS cases (257, 258).

Recent classification systems, including the 5th edition of the World Health Organization (WHO) classification of myeloid neoplasms (3) and the International Consensus Classification (ICC) (259), have recognized multi-hit *TP53*-mutated MDS and AML as distinct clinical entities due to their unique molecular and clinical features. These *TP53* mutations often involve "multi-hit" events, characterized by biallelic inactivation of TP53, typically through a combination of point mutations and chromosomal abnormalities on chromosome 17, and are strongly associated with complex karyotypes (260) and are less commonly associated with mutations in other genes (256). Multi-hit *TP53* mutations are particularly notable for their association with high-risk disease features, a greater likelihood of transformation to AML, and markedly reduced OS, independent of traditional prognostic models such as IPSS-R (256, 261). While the specific type of *TP53* mutation does not seem to influence prognosis, the overall mutational burden and the dominance of *TP53*-mutated clones significantly impact clinical outcomes (261).

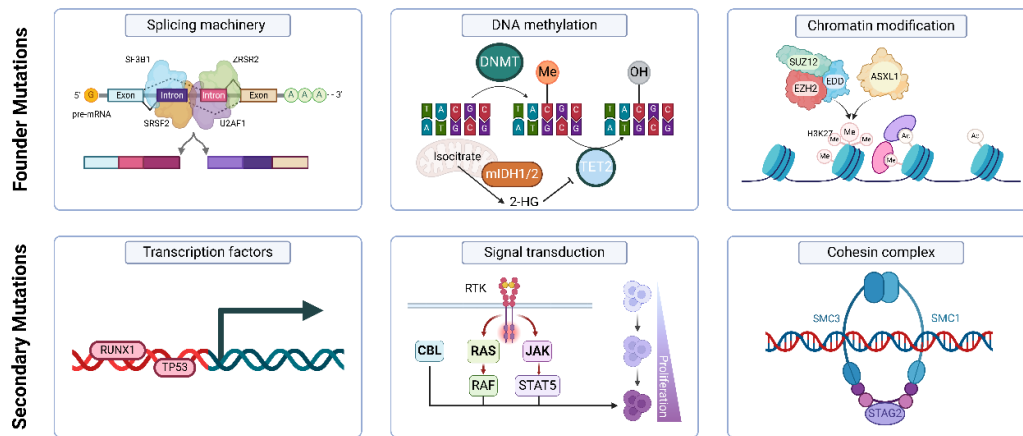


Figure 4. Overview of the somatic mutational landscape in MDS and CMML. The illustration highlights the most frequent somatic mutations involved in disease initiation (founder mutations) and progression to secondary AML (sAML) (secondary mutations). Adapted from Rodriguez-Sevilla et al. (262).

6.4.2 Genetic Landscape and Key Mutations In CMML

CMML is characterized by a high frequency of somatic mutations affecting various biological pathways, with significant overlap with MDS, yet presenting unique molecular features (13). Meggendorfer and colleagues demonstrated that over 90% of CMML cases harbor mutations in at least one of the following nine genes: *TET2*, *SRSF2*, *ASXL1*, *CBL*, *EZH2*, *JAK2*, *KRAS*, *NRAS*, and *RUNX1* (263). In patients with CMML, the somatic mutation burden is estimated at 10–15 variants per kilobase within coding regions of the genome, similar to AML but considerably lower than highly mutagenic cancers such as melanoma and lung cancer (264). These mutations affect a diverse array of cellular processes, including epigenetic regulation, pre-mRNA splicing, signal transduction pathways, transcriptional control, and DNA damage response, as previously detailed.

Epigenetic regulatory genes are among the most frequently mutated in CMML, underscoring their critical role in disease pathogenesis. *TET2* mutations, present in approximately 60% of patients, impair DNA demethylation, leading to dysregulated gene expression. While these mutations do not significantly affect OS (265, 266), their absence in *ASXL1*-mutated CMML patients (*ASXL1**mt*/*TET2**wt*) is linked to worse outcomes and diminished responses to HMAs (267, 268). *ASXL1*, mutated in ~40% of cases, disrupts chromatin regulation by interfering with polycomb-group repressive complexes, promoting transcriptional dysregulation and oncogenesis. In contrast to *TET2*, *ASXL1* mutations are consistently associated with a poor prognosis. *EZH2* mutations, although rare (<5%), frequently co-occur with *ASXL1* mutations, particularly in myeloproliferative (MP) CMML phenotype (269).

Spliceosome mutations, particularly in *SRSF2*, are observed in ~50% of CMML cases (40). While *SRSF2* mutations alone do not appear to have a direct impact on OS (263, 265), they are associated with a distinct disease phenotype, often observed in older patients and characterized by milder anemia and diploid karyotype (40). *SF3B1* mutations, commonly seen in MDS with ring sideroblasts, are present in ~10% of CMML cases and are associated with favorable AML-free survival (95). *U2AF1* and *ZRSR2* mutations are less frequent and lack consistent prognostic significance (226).

Signal transduction pathway mutations, particularly those in the RAS signaling cascade (e.g., *NRAS*, *KRAS*, *CBL*, *PTPN11*), occur in ~30% of CMML patients and are strongly associated with myeloproliferative phenotypes (265). *JAK2V617F* mutations (~10%) are linked to MP-like features, such as elevated hemoglobin and platelet levels, though they do not significantly impact OS or AML transformation rates (270). *CBL* mutations, often accompanied by uniparental disomy on chromosome 11q, are associated with enhanced RAS signaling and proliferative phenotypes (265, 271).

Transcription factor *RUNX1* is frequently mutated in CMML (272). *RUNX1* mutations, observed in 10–15% of cases, are associated with lower platelet counts and higher rates of AML transformation, though they have no clear impact on OS (273, 274). Mutations in other transcription factors are less common. For instance, *GATA2* mutations contribute to hematopoietic dysregulation and disease progression (271).

The sequence of mutational events in CMML is an area of ongoing research. Early driver mutations often occur in *TET2* or *SRSF2* at the HSPC level, promoting clonal hematopoiesis as it was discussed before in “HSC Dysregulation in MDS and CMML”. Secondary mutations, including those in *ASXL1* or *RAS* pathway genes, shape disease phenotypes by accelerating differentiation along the granulocyte-monocyte progenitor (GMP) axis, leading to clonal monocytosis. Subsequent acquisition of mutations in genes such as *RUNX1* and *TP53* drive disease progression and transformation to AML (275).

The integration of NGS and advanced genomic technologies has significantly improved CMML diagnostics while providing a deeper understanding of its molecular basis. These advancements have enhanced prognostic stratification and paved the way for the development of more precise targeted therapies.

6.5 Cytogenetic Landscape of Myelodysplastic Syndromes and Chronic Myelomonocytic Leukemia

Cytogenetic analysis is a core element of the diagnostic evaluation for MDS and CMML, providing critical information for diagnosis, prognosis, and treatment planning (13, 37). A minimum of 20 metaphases is recommended for accurate analysis; however, the detection of a clonal abnormality can yield meaningful clinical insights even with fewer metaphases. When metaphases are insufficient or a normal karyotype is observed, additional genomic techniques such as fluorescence in situ hybridization (FISH), comparative genomic hybridization (CGH) arrays, or single nucleotide polymorphism (SNP) arrays can uncover cryptic abnormalities and enhance the genomic assessment.

Recent advances in technology, particularly optical genome mapping (OGM), have greatly improved the resolution of cytogenetic studies in myeloid neoplasms (276). OGM enables high-resolution imaging of structural variants, balanced translocations, and copy number alterations, often outperforming traditional karyotyping and array-based methods (277). By visualizing long DNA molecules, OGM can uncover cryptic rearrangements and complex abnormalities that are required for better understanding of the disease (278).

OGM has proven particularly valuable for identifying recurrent abnormalities in MDS and CMML, such as complex karyotypes and cryptic deletions (279, 280). For example, OGM can refine the detection of high-risk chromosomal abnormalities, such as those involving chromosome 7, by revealing additional genomic complexities. Its capability to provide comprehensive genomic profiling in a single assay significantly simplifies the diagnostic workflow, reducing the need for multiple sequential tests.

When integrated with conventional cytogenetics and advanced molecular techniques, OGM offers a more complete view of the genomic landscape in MDS and CMML. This integration helps clinicians better understand the genetic drivers of these diseases, enabling more precise patient management and treatment optimization.

6.5.1 Cytogenetic Alterations in Myelodysplastic Syndromes

Cytogenetic abnormalities are a hallmark of MDS, identified in approximately 40–50% of patients with de novo cases and up to 80% of secondary MDS (281-283). Most of these alterations involve the loss of genetic material, either as deletions (partial loss of a chromosome segment) or monosomies (complete loss of a chromosome). In contrast, gains

in genetic material—excluding trisomy 8 (+8)—and structural rearrangements, such as translocations and inversions, are relatively infrequent in MDS (284, 285).

The most common cytogenetic abnormalities in MDS include del(5q) (15%), -7/del(7q) (10%), +8 (8%), and del(20q) (5%) (78,79). Less frequent alterations include -Y, -17/17p-, and -18/18q- (79). Importantly, while these abnormalities are highly characteristic of MDS, they are not pathognomonic and can also be detected in other hematologic disorders, particularly CMML (**Figure 5**).

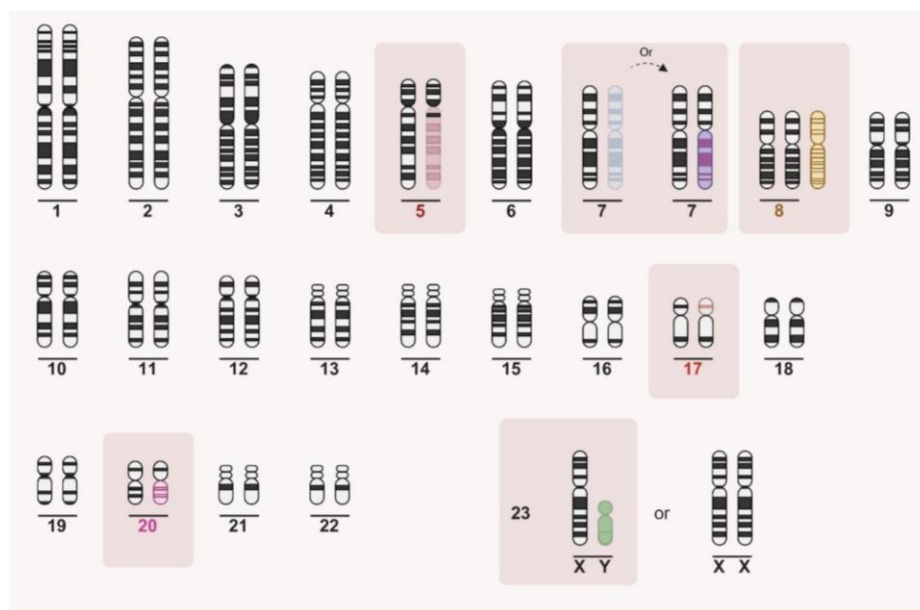


Figure 5. Cytogenetic landscape depicting the most common chromosomal alterations in MDS. Highlighted regions represent recurrent abnormalities, including deletions (del(5q), del(20q), del(7q)), monosomies (-7, -Y), trisomy (+8), and complex karyotypes involving chromosome 17 (-17/17p-). These alterations are critical for diagnosis, prognosis, and treatment planning in MDS. Abbreviations: chr, chromosome. Figure created using BioRender

Cytogenetic abnormalities in MDS can occur as isolated events, in pairs, or as part of a complex karyotype involving three or more aberrancies. Complex karyotypes, which are strongly associated with adverse outcomes, underscore the prognostic significance of both the type and number of cytogenetic alterations (286). These features have been consistently validated as independent prognostic factors, influencing disease trajectory and treatment strategies (285, 287).

A pivotal study by Schanz et al. analyzed 2,902 patients, leading to the development of a cytogenetic scoring system that is now widely used in clinical practice (288). This system categorizes cytogenetic abnormalities into five risk groups based on their prognostic significance and incorporates 20 distinct alterations (**Table 1**). This framework has become

indispensable for risk stratification and therapeutic planning, offering a structured approach to individualized patient care.

Table 1. Prognostic classification of cytogenetic alterations in MDS, as Proposed by Schanz et al. (288).

Risk Group	Cytogenetic Alterations*	Median Survival (Years)
Very Good	-Y, del(11q)	5.4
Good	Normal karyotype, del(5q), del(12p), del(20q), double including del(5q)	4.8
Intermediate	del(7q), +8, +19, i(17q), any other single or double alteration in independent clones	2.7
Poor	-7, inv(3)/t(3q)/del(3q), double including -7/del(7q), complex (3 abnormalities)	1.5
Very Poor	Complex (>3 abnormalities)	0.7

*All abnormalities listed as isolated alterations unless otherwise specified.

This classification remains integral to understanding MDS prognosis, enabling clinicians to tailor therapeutic strategies to individual patient risk profiles.

6.5.2 Cytogenetic Alterations in CMML

Clonal cytogenetic abnormalities are found in approximately 20–30% of CMML cases, a significantly lower frequency compared to their higher prevalence in MDS, reflecting distinct cytogenetic profiles between the two disorders (289-291). These abnormalities are not exclusive to CMML and show significant overlap with those found in other myeloid neoplasms.

The most recurrent abnormalities in CMML include trisomy 8 (+8), monosomy 7 (-7), and partial deletion of the long arm of chromosome 7 (del(7q)). Studies analyzing large cohorts of CMML patients with available cytogenetic data—each involving approximately 400 patients—report that 6–7% of patients have +8, 4–6% exhibit -Y, 3–6% display a complex karyotype, and 1.5–5.5% harbor chromosome 7 abnormalities (289-291). Other classical MDS-associated cytogenetic abnormalities, such as del(5q) or del(20q), are less commonly observed in CMML, occurring in fewer than 1% (289, 290), and ~2% of cases, respectively (289-291).

These findings reveal the cytogenetic complexity of CMML and its shared features with MDS, particularly in terms of recurrent abnormalities. They emphasize the importance of a thorough diagnostic approach that combines clinical, morphological, molecular, and cytogenetic data to achieve accurate diagnosis and better inform patient management.

7. Clinical Manifestations

Some patients with MDS or CMML are asymptomatic and are diagnosed incidentally during routine blood tests that reveal mild cytopenia or monocytosis. However, most patients present with symptoms linked to cytopenias, with anemia being the most common and often the primary reason they seek medical attention. Patients with thrombocytopenia or neutropenia are at increased risk for bleeding and infection, respectively. As the disease advances, patients may develop constitutional symptoms such as fatigue, fever, weight loss, and night sweats, which signal more advanced stages of the disease (13, 37).

Visceromegaly is rare in MDS but is relatively common in CMML, particularly in proliferative forms of the disease characterized by a leukocyte count $\geq 13,000/\text{mm}^3$ (292). In these cases, organ infiltration may lead to additional manifestations, such as splenomegaly, hepatomegaly, cutaneous involvement, gingival hypertrophy, and lymphadenopathy, reflecting the systemic nature of the proliferative variants.

Systemic inflammatory and autoimmune diseases (SIAD) are associated with MDS and CMML in 10–20% of cases and can significantly influence the clinical course of these conditions (293). While the exact impact of SIAD on OS and progression to acute leukemia remains unclear, their presence often complicates management and requires careful therapeutic consideration. Immune thrombocytopenia (ITP) is one of the autoimmune manifestations observed in both MDS and CMML. However, its clinical features and the best approaches for managing it remain poorly understood due to the limited availability of large-scale studies (293, 294).

8. Diagnosis and Classification of Myelodysplastic Syndromes and Chronic Myelomonocytic Leukemia

Despite the progress made with advanced molecular assays, cytological evaluation remains the cornerstone for diagnosing MDS and CMML. BM smears stained with panoptic stain are used to perform a detailed quantitative assessment of dysplasia, while Perls' stain is applied to evaluate iron deposits within the mononuclear phagocyte system and to quantify sideroblasts. PB smears, also stained with panoptic stain, are critical for the qualitative evaluation of dysplastic features and for determining the percentage of circulating blasts.

According to WHO criteria, significant dysplasia is identified in a myeloid lineage (megakaryocytic, erythroid, or granulocytic) when 10% or more of cells in that lineage exhibit dysplastic features (**Table 2**). For accurate assessment, it is recommended to evaluate 30 megakaryocytes, 200 neutrophils, and 200 erythroid precursors. Blast percentages should be determined by performing a differential count on 200 white blood cells in PB and 500 cells in BM (2, 14, 15, 41). Both the WHO classification and various publications from the International Working Group on Morphology of Myelodysplastic Syndromes (IWGM-MDS) describe the following dysplastic features (295-299):

Table 2. Key morphological dysplastic features in MDS and CMML. This table summarizes the main dysplastic findings across the granulocytic, erythroid, and megakaryocytic lineages.

Lineage	Dysplastic Features
Granulopoiesis	unusual cell size (either abnormally large or small), cytoplasmic hypo- or degranulation, Döhle bodies, nuclear hyposegmentation (pseudo Pelger-Huët anomaly), nuclear hypersegmentation, pseudo-Chediak-Higashi granules, Auer rods, ring-shaped nuclei, mirror-image nuclei, and hypercondensed chromatin clumping.
Erythroid	internuclear bridges, nuclear contour irregularities, karyorrhexis, multinuclearity, megaloblastic changes, PAS positivity, cytoplasmic vacuolization, and ring sideroblasts (sideroblasts with five or more hemosiderin granules arranged perinuclearly, covering at least one-third of the nuclear perimeter).
Megakaryopoiesis	hypolobulated or monolobulated megakaryocytes, binucleation, separated nuclei, and micromegakaryocytes.

This classification ensures a systematic evaluation of dysplastic features across hematopoietic lineages (**Figure 6**), providing a robust foundation for accurate diagnosis and characterization of disease.

Although following WHO 2017 criteria a MDS diagnosis could be established in absence of dysplasia based on a list of defining cytogenetic abnormalities, the 2022 update from the International Consensus Classification (ICC) has further evolved the diagnostic criteria for MDS, expanding it to include cases lacking overt dysplasia if certain molecular abnormalities are identified, in addition to some cytogenetic alterations (259). Key markers include biallelic *TP53* mutations (bi*TP53*), complex karyotypes, *SF3B1* mutations with a variant allele frequency (VAF) $\geq 10\%$, isolated deletion of chromosome 5q [del(5q)], and specific alterations on chromosome 7 (such as monosomy 7 or del(7q)).

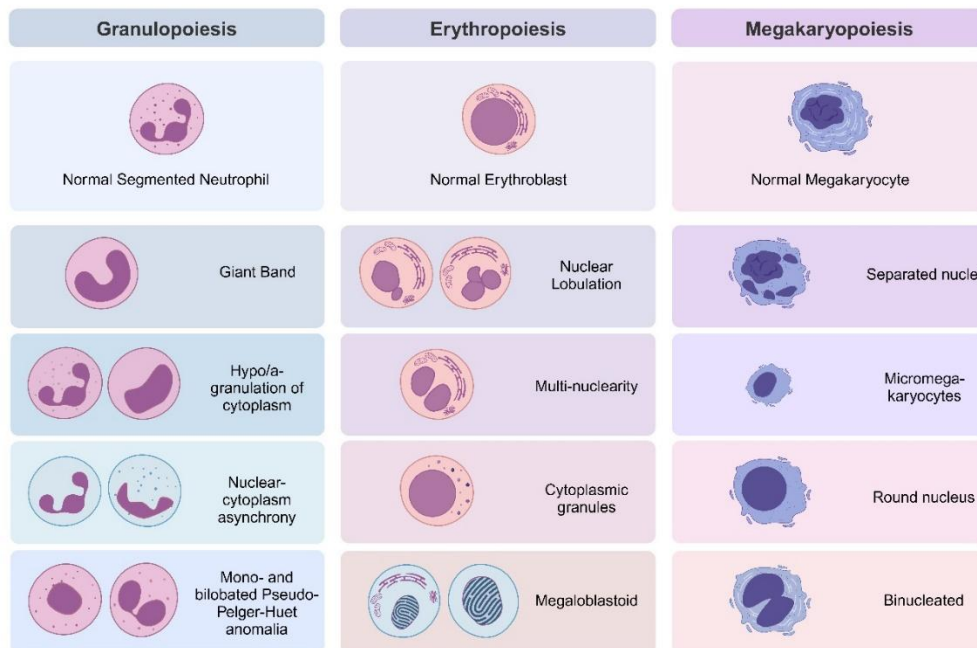


Figure 6. Depiction of myelodysplastic features in hematopoiesis. This illustration highlights the diverse morphological abnormalities observed in MDS and CMML, affecting multiple hematopoietic lineages and demonstrating characteristic dysplastic features across cell types. Figure created using BioRender.

This updated framework builds on a deeper understanding of the molecular landscape of MDS, offering a more comprehensive diagnostic approach for cases that might previously have been categorized as CCUS despite significant clonal abnormalities. By incorporating molecular and cytogenetic findings, the ICC 2022 criteria aim to enhance diagnostic accuracy, enabling the earlier and more precise identification of patients with subtle or early-stage MDS and supporting more effective, targeted clinical management strategies.

8.1 Myeloid Continuum in MDS and CMML Pathogenesis: CHIP, CCUS, CMUS and CCMUS

Hematologic malignancies arise from the clonal expansion of HSCs, driven by mutations that disrupt their finely-tuned regulation of proliferation and differentiation. These clones, depending on their genetic and epigenetic alterations, generate heterogeneous phenotypes. While many mutations remain phenotypically silent, some confer a proliferative advantage, enabling mutant cells to outcompete normal HSPCs. This clonal dominance, when not associated with overt hematologic disease, is referred to as CHIP.

CHIP may evolve into CCUS, in which clonally expanded cells are associated with persistent and unexplained cytopenia (**Figure 7**). Compared with MDS, CCUS has a lower mutation burden, reduced genetic complexity, and no evidence of dysplasia (210-212, 300). However, like MDS patients, CCUS patients have PB cytopenias and often require transfusions (301). A progressive transition between CHIP, CCUS, and MDS is thought likely (300), with CCUS representing an intermediate stage among the clonal hematopoietic disorders (**Figure 7**). *DNMT3A*, *TET2*, and *ASXL1* mutations occur in 70-80% of patients with CHIP or CCUS (302). In MDS, these mutations are linked to a higher clonal burden and an evolving co-mutational landscape that drives disease progression (300).

Clonal monocytosis of undetermined significance (CMUS), a precursor state to CMML, has been increasingly recognized as a distinct clinical entity (259). Analogous to CCUS, CCMUS is characterized by clonal hematopoiesis with mild monocytosis (absolute monocyte count of $0.5\text{--}1.0 \times 10^9/\text{L}$) but lacks the dysplastic or proliferative features typical of overt CMML. For the WHO, CMUS and CCMUS are included within the broad definition of CCUS, reflecting its shared characteristics with other early clonal hematopoietic disorders (2). In contrast, the ICC introduces a distinct category for CMUS, recognizing it as a unique precursor stage (259). Both classifications highlight CMUS as part of the broader spectrum of clonal myeloid neoplasms and stress its potential to progress to CMML, influenced by additional genetic and environmental factors (303).

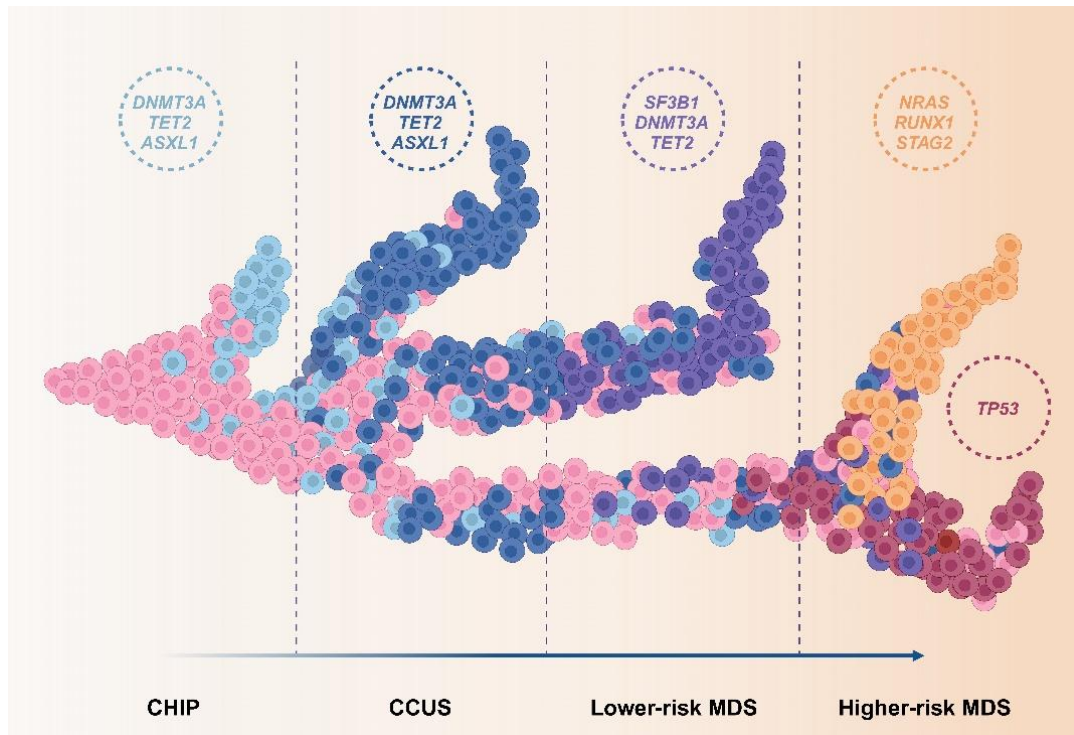


Figure 7. Clonal evolution across the spectrum of myeloid neoplasms. Schematic representation of clonal progression from pre-leukemic stages, CHIP and CCUS, to overt disease, categorized into lower-risk and higher-risk MDS. Colored circles depict the clonal architecture of various mutant clones. Key mutations associated with each stage are indicated within dashed circles. Lower-risk MDS, characterized by an indolent disease course and favorable prognosis, predominantly involves mutations in the *SF3B1* splicing gene. Higher-risk MDS is a more aggressive disease with additional mutations in *TP53*, *RUNX1*, *STAG2*, and *RAS* pathway genes. Adapted from Rodriguez-Sevilla et al. (304).

To better understand how diagnostic and prognostic frameworks in MDS and CMML have evolved, it is important to consider the trajectory of risk stratification tools and classification systems developed over time. These systems have adapted alongside advances in molecular and cytogenetic research, with the goal of improving disease characterization and risk prediction for both MDS and CMML (**Figure 8**). The different diagnostic and prognostic milestones for MDS and CMML will be explained in detail in the following section.



Figure 8. Timeline of diagnostic and prognostic milestones in MDS and CMML. This figure provides a chronological overview of the major diagnostic and prognostic systems developed for MDS and CMML, starting with the introduction of cytogenetic analysis in the 1970s and culminating in the latest advancements in molecular risk stratification models. FAB, French-American-British classification; IPSS, International Prognostic Scoring System; MDAPS, MD Anderson Prognostic Scoring System; WPSS, WHO Prognostic Scoring System; MDS-LR, Low-Risk MDS prognostic model; MDAS, MD Anderson Scoring System for MDS; FPSS, French Prognostic Scoring System; IPSS-R, Revised International Prognostic Scoring System; CPSS, CMML-specific Prognostic Scoring System; GFM Score, Groupe Francophone des Myélodysplasies Score; Mayo Model, Prognostic model developed at the Mayo Clinic for MDS; Mayo Molecular Model, Molecular-based prognostic model from Mayo Clinic for MDS; CPSS-Mol, Molecular-based CMML Prognostic Scoring System; WHO, World Health Organization classification; NGS, Next-Generation Sequencing; ICC, International Consensus Classification; IPSS-M, Molecular International Prognostic Scoring System for MDS; CHRS, Clonal Hematopoiesis Risk Score. Figure created using BioRender.

8.2 Classification of MDS and CMML

8.2.1 The FAB Classification

The French-American-British (FAB) cooperative group introduced the first formal classification system for MDS in 1982 (7). This pioneering classification defined five MDS subtypes based on specific criteria, including the percentage of blasts in PB and BM, the presence of Auer rods (rod-like structures in the cytoplasm of myeloid blasts composed of enzymes such as myeloperoxidase and/or chloroacetate esterase) (305), the monocyte count in PB, and the percentage of ring sideroblast (**Table 3**).

Table 3. FAB classification of MDS

Classification	Peripheral blood	Monocytes >1000/uL	BM Blasts	Ringed sideroblasts (%)
RA	<1%	No	<5%	<15
RARS	<1%	No	<5%	>15
RAEB	<5%	No	5–19%	Variable
RAEB-T	>5%	+/-	20–29%	Variable
CMML	<5%	Yes	<20%	Variable

Abbreviations: RA, Refractory anemia; RARS, Refractory anemia with ringed sideroblasts; RAEB, Refractory anemia with excess blasts; RAEB-T, Refractory anemia with excess blasts in transformation; CMML, Chronic myelomonocytic leukemia.

For almost two decades, the FAB classification has been integral to the diagnosis and classification of MDS. It provided a robust framework for both diagnostic and prognostic evaluation, contributing significantly to the clinical management of these disorders. Notably, within the FAB system, CMML was considered a subtype of MDS, underscoring the close biological and clinical relationship between MDS and CMML in early classification efforts.

The FAB classification also recognized the dual myelodysplastic and myeloproliferative nature of CMML. Importantly, it separated CMML into two forms based on PB white blood cell (WBC) counts: myelodysplastic (MD-CMML) for cases with $WBC < 13 \times 10^9/L$, and myeloproliferative (MP-CMML) for cases with $WBC \geq 13 \times 10^9/L$ (24, 306). Patients with MD-CMML typically present with cytopenias, recurrent infections, and transfusion dependence, whereas MP-CMML often manifests with elevated white blood cell counts, splenomegaly, and systemic symptoms associated with myeloproliferation, such as fatigue, night sweats, bone pain, weight loss, and cachexia (307). This distinction highlighted the clinical heterogeneity of CMML and laid the foundation for its evolving classification in subsequent WHO updates.

8.2.2 The 2001 WHO Classification of Myeloid Neoplasms

The FAB classification for MDS, used for nearly 20 years, was revised in 2001 when the World Health Organization (WHO) introduced a new classification system for hematologic neoplasms, including MDS. Aiming at enhancing diagnostic and prognostic precision over the FAB classification, this update expanded beyond morphology to include cytogenetics, significantly improving the classification and prognostic assessment (308).

The WHO 2001 classification defined eight distinct MDS categories based on the number of cytopenias, blast percentages in PB and BM, the presence of Auer rods, the percentage of ring sideroblasts, and the detection of an isolated 5q deletion (**Table 4**). These criteria were widely accepted by the scientific community, and subsequent validation studies highlighted the prognostic value of these categories.

Based on the WHO 2001 classification, MDS could be stratified into two primary risk groups: low-risk MDS (RA, RARS) and high-risk MDS (RAEB, RCMD, and RCMD-RS). While the 5q-syndrome was generally regarded as low-risk, this distinction was not explicitly addressed within the WHO 2001 framework, leaving some ambiguity regarding its classification (309).

Table 4. The WHO 2001 classification of MDS.

Subtype	PB Blasts	BM Blasts	RS	Cytopenias	Dysplasia
RA	None	<5%	<15%	One or more	Erythroid lineage only
RARS	None	<5%	≥15%	One or more	Erythroid lineage only
RCMD	None	<5%	Variable	One or more	Multilineage
RCMD-RS	None	<5%	≥15%	One or more	Multilineage
RAEB-1	<5%	5–9%	Variable	One or more	Multilineage
RAEB-2*	5–19%	10–19%	Variable	One or more	Multilineage
MDS-del(5q)	<5%	<5%	Variable	One or more	Unilineage
MDS-U	<1%	<5%	Variable	Two or more	Unilineage

*The presence of Auer rods is diagnostic of RAEB-2.

Abbreviations: RA, Refractory anemia; RARS, Refractory anemia with ring sideroblasts; RCMD, Refractory cytopenia with multilineage dysplasia; RCMD-RS, RCMD with ring sideroblasts; RAEB-1, Refractory anemia with excess blasts-1; RAEB-2, Refractory anemia with excess blasts-2; MDS-del(5q), Myelodysplastic syndrome with isolated deletion of chromosome 5q; MDS-U, Myelodysplastic syndrome unclassifiable; PB, Peripheral blood; BM, Bone marrow; RS, Ring sideroblasts.

A significant update in the 2001 WHO classification was the formal introduction of MDS/MPN, acknowledging the coexistence of dysplastic and proliferative features. Within this category, CMML was recognized as the most common subtype, defined by persistent monocytosis (absolute monocyte count $\geq 1 \times 10^9/L$) and dysplasia in one or more myeloid lineages. CMML was further stratified into CMML-1 and CMML-2, based on blast and promonocyte percentages:

- CMML-1: <5% blasts and promonocytes in PB, <10% in BM.
- CMML-2: 5–19% blasts and promonocytes in PB, 10–19% in BM, or the presence of Auer rods.

These adjustments highlighted the heterogeneity and prognostic importance of CMML, forming the basis for future updates.

8.2.3 The 2008 WHO Classification of Myeloid Neoplasms

In 2008, the WHO revised its classification of MDS, refining diagnostic categories to improve clinical and prognostic stratification (25). While maintaining the general categorization into low-risk (RCUD, RARS), intermediate-risk (RCMD, RAEB-1), and high-risk (RAEB-2) subgroups, the update incorporated significant changes to reflect advances in understanding MDS pathogenesis and clinical presentation (**Table 5**).

Patients with persistent cytopenias lacking significant dysplasia but harboring defining cytogenetic abnormalities were classified as unclassifiable MDS, alongside cases with unilineage dysplasia and pancytopenia, or 1% blasts in the PB. The distinction between RCMD and RCMD with ring sideroblasts was removed, supported by evidence that the percentage of ring sideroblasts did not significantly impact survival or leukemic transformation risk (310). The previously defined "5q- syndrome" was expanded into the broader category of MDS with isolated del(5q) to include a wider spectrum of patients harboring this specific cytogenetic abnormality. To address the distinct clinical and pathological characteristics of pediatric cases, the provisional category of *refractory cytopenia of childhood* was introduced, emphasizing the importance of tailored diagnostic criteria for younger patients. Other key updates included redefining refractory anemia as a subtype of RCUD, expanding its classification to encompass refractory anemia, neutropenia, and thrombocytopenia. These conditions are all marked by unilineage dysplasia and restricted to no more than two cytopenias. Cases presenting with pancytopenia were reassigned to the unclassifiable MDS category, reflecting the need for distinct diagnostic criteria. Furthermore, the diagnostic criteria for RAEB-1 were updated, establishing a PB blast count of 2%–<5% as sufficient for diagnosis, independent of BM blast percentages. These changes underscored the commitment to greater diagnostic precision, aligning with the expanding understanding of MDS heterogeneity and its diverse clinical presentations.

Table 5. The WHO 2008 classification of MDS.

Subtype	Cytopenias	PB Blasts	BM Blast s	BM RS	Dysplasia
RCUD	1 or 2	<1	<5	<15	1 lineage
RARS	Anemia	0	<5	≥15	Erythroid only
RCMD	Cytopenia(s)	<1	<5	Indifferent	≥2 lineages
RAEB-1	Cytopenia(s)	<5	5-9	Indifferent	Indifferent
RAEB-2	Cytopenia(s)	5-19	10-19	Indifferent	Indifferent, <i>Auer rods present</i>
MDS with isolated del(5q)	Anemia, Normal or ↑ Platelets	<1	<5	Indifferent	Megakaryocytes (monolobulated nuclei)
MDS-U	Cytopenia(s)	≤1	<5		<10% in ≥1 myeloid lineage Cytogenetic abnormalities

The presence of Auer rods is diagnostic of RAEB-2.

Abbreviations: RCUD, Refractory cytopenia with unilineage dysplasia; RARS, Refractory anemia with ring sideroblasts; RCMD, Refractory cytopenia with multilineage dysplasia; RAEB-1, Refractory anemia with excess blasts-1; RAEB-2, Refractory anemia with excess blasts-2; MDS, Myelodysplastic syndrome; PB, Peripheral blood; BM, Bone marrow; RS, Ring sideroblasts; MDS-U, Myelodysplastic syndrome unclassifiable.

The 2008 WHO classification retained CMML within the MDS/MPN category and preserved its subcategorization into CMML-1 and CMML-2, based on blast and promonocyte percentages in PB and BM. This distinction remained crucial for prognostic evaluation, with CMML-2 associated with higher risks of leukemic transformation and poorer survival outcomes (311).

8.2.4 The 2017 WHO Classification of Myeloid Neoplasms

In 2017, the World Health Organization (WHO) released an updated classification of MDS and CMML, refining diagnostic criteria and stratification while addressing ambiguities in prior frameworks (14). As in earlier iterations, MDS subtypes were categorized into low-risk (e.g., unilineage dysplasia, ring sideroblasts with unilineage dysplasia, isolated del(5q)), intermediate-risk (e.g., multilineage dysplasia, multilineage dysplasia with ring sideroblasts), and high-risk (e.g., excess blasts) groups, based on OS and leukemia progression risk (**Table 6**).

A major change was the removal of blast count requirements specific to non-erythroid cellularity and the reclassification of erythroleukemia. Cases previously considered erythroleukemia were predominantly reclassified as MDS with excess blasts, though the concept of erythroid predominance was retained within this subgroup. Its prognostic significance remains unclear, particularly given associations with adverse-risk cytogenetics and mutations in *RUNX1*, *TP53*, and *ASXL1* (312, 313).

The term “refractory cytopenia” was replaced with “myelodysplastic syndrome” to enhance nomenclature precision, allowing for cases where dysplastic lineage involvement does not match the observed cytopenias. For example, a case with megakaryocytic dysplasia but isolated anemia would now fall under the classification of MDS with unilineage dysplasia. The criteria for unclassifiable MDS were also updated, requiring the presence of 1% blasts in peripheral blood and less than 5% in bone marrow, confirmed in at least two consecutive samples. For MDS with isolated del(5q), the inclusion criteria were expanded to accommodate cases with certain additional cytogenetic abnormalities, provided they did not include monosomy 7 or del(7q), following evidence that these secondary changes do not significantly affect prognosis (314). Cases with $\geq 15\%$ ring sideroblasts, $< 5\%$ blasts, and no del(5q) were reclassified into subgroups based on dysplasia, distinguishing between unilineage and multilineage involvement. Importantly, the presence of *SF3B1* mutations allowed diagnosis of ring sideroblast-associated MDS with as few as 5% sideroblasts.

Table 6. The 2017 WHO classification of MDS.

Subtype	# Dysplastic Lineages	Cytopenias	%RS in BM Erythroid Elements	Blasts (BM/PB)
MDS-SLD	1	1-2	<15% / <5%*	BM <5%, PB <1%
MDS-MLD)	2-3	1-3	<15% / <5%*	BM <5%, PB <1%
MDS-RS				
MDS-RS-SLD	1	1-2	≥15% / ≥5%*	BM <5%, PB <1%
MDS-RS-MLD	2-3	1-3	≥15% / ≥5%*	BM <5%, PB <1%
MDS with Isolated del(5q)	1-3	1-2	Indifferent	BM <5%, PB <1%
MDS-EB:				
-MDS-EB-1	0-3	1-3	Indifferent	BM 5%-9%, or PB 2%-4%
-MDS-EB-2	0-3	1-3	Indifferent	BM 10%-19%, or PB 5%-19%
MDS-U:				
-with 1% Blasts In PB	1-3	1-3	Indifferent	BM <5%, PB = 1%**
-with Single-Lineage Dysplasia And Pancytopenia	1	3	Indifferent	BM <5%, PB <1%
- Based on Cytogenetic Abnormality (no dysplasia)	0	1-3	<15%	BM <5%, PB <1%

* If the *SF3B1* mutation is present

** In two control samples

Abbreviations: MDS-SLD, Myelodysplastic syndrome with single-lineage dysplasia; MDS-MLD, Myelodysplastic syndrome with multilineage dysplasia; MDS-RS, Myelodysplastic syndrome with ring sideroblasts; MDS-RS-SLD, MDS-RS with single-lineage dysplasia; MDS-RS-MLD, MDS-RS with multilineage dysplasia; MDS-EB, Myelodysplastic syndrome with excess blasts; MDS-EB-1, MDS with excess blasts-1; MDS-EB-2, MDS with excess blasts-2; MDS-U, Myelodysplastic syndrome unclassifiable; del(5q), Deletion of the long arm of chromosome 5; PB, Peripheral blood; BM, Bone marrow; RS, Ring sideroblasts.

A notable update for CMML was the reintroduction of the dysplastic (MD-CMML) and proliferative (MP-CMML) subtypes, reflecting their distinct clinical, prognostic, and molecular features (315). CMML was further stratified into three subcategories based on blast percentages:

- CMML-0: <2% blasts in PB and <5% blasts in BM.
- CMML-1: 2–<5% blasts in PB and/or 5–<10% blasts in BM.
- CMML-2: 5–<20% blasts in PB and/or 10–<20% blasts in BM, or the presence of Auer rods regardless of blast count.

This classification aimed to enhance prognostic stratification, with studies suggesting that MP-CMML is associated with shorter OS compared to MD-CMML. However, the distinction between CMML-0 and CMML-1 demonstrated only marginal prognostic differences, indicating areas for further investigation (316)

Diagnostic clarity for CMML was also improved by requiring monocytes to constitute $\geq 10\%$ of PB leukocytes, a threshold that consolidated the distinction between CMML and reactive monocytosis. The inclusion of PCM1-JAK2 rearrangements in the list of eosinophilia-associated abnormalities and the acknowledgment of mutational analysis as a tool for clonality detection marked additional updates. Given the difficulty in excluding reactive monocytosis, common causes such as autoimmune disorders, infections, and malignancies were emphasized in the differential diagnosis. CMML's frequent coexistence with autoimmune conditions further complicates the distinction between clonal monocytosis and reactive processes (317-320).

While clonal markers are detectable in 20–30% of CMML cases using cytogenetic methods, their detection is often challenging. Mutations in *TET2*, *SRSF2*, and *ASXL1* are present in 85–90% of patients (52, 53, 263, 266). However, while frequently observed, these mutations are not specific to the disease, as they are also associated with age-related clonal hematopoiesis (321-323), limiting their diagnostic specificity. Flow cytometry has become a valuable diagnostic tool for CMML by analyzing monocyte subset distributions in peripheral blood (PB) (324). Specifically, patients with CMML exhibit a significant increase in classical monocytes (CD14+/CD16–), accounting for more than 94% of total monocytes. This pattern effectively differentiates CMML from reactive monocytosis and other hematologic conditions with high sensitivity and specificity. Notably, this abnormal monocyte distribution is independent of mutational status, making it a reliable diagnostic marker. Additionally, in patients responding to hypomethylating agents (HMAs), this monocyte profile normalizes, suggesting its potential as a dynamic biomarker for monitoring treatment efficacy (324).

8.2.5 The 2022 WHO Classification of Myeloid Neoplasms

The 2022 WHO classification introduced significant updates to enhance diagnostic accuracy and refine prognostic stratification for MDS and CMML. These revisions integrate molecular and cytogenetic data, aligning the classification system with the latest insights into disease biology and clinical practice (2).

For MDS, the WHO 2022 classification incorporates new molecular features to better stratify disease subtypes. Categories such as MDS-bi*TP53*, characterized by biallelic *TP53* mutations, highlight distinct disease biology and poor prognosis, while MDS-*SF3B1* denotes cases with *SF3B1* mutations associated with favorable outcomes and ring sideroblasts. Additional subtypes include MDS-f, associated with marrow fibrosis, and MDS-h, which

identifies hypoplastic BM, acknowledging distinct pathophysiological features that influence management (**Table 7**). Cases of isolated del(5q) now include those with specific secondary cytogenetic abnormalities, provided they do not involve monosomy 7 or del(7q). Moreover, the presence of ring sideroblasts $\geq 15\%$ or an *SF3B1* mutation allows for the diagnosis of ring sideroblast-associated MDS even with sideroblast levels as low as 5%. These changes reflect the growing importance of integrating genetic and morphological data to enhance classification accuracy and guide personalized treatment strategies.

Table 7. The WHO 2022 classification of MDS.

Subtype	Blasts	Cytogenetics	Mutations
MDS With Defining Genetic Abnormalities			
MDS-5q	<5% BM and <2% PB	5q Deletion Alone, Or With 1 Other Abnormality (Not Monosomy 7 Or 7q Deletion)	
MDS- <i>SF3B1</i>	<5% BM and <2% PB	Absence Of 5q Deletion, Monosomy 7, Or Complex Karyotype	<i>SF3B1</i>
MDS-biTP53	<20% BM and PB	Usually Complex	Two Or More <i>TP53</i> Mutations, Or 1 Mutation With Evidence Of <i>TP53</i> Copy Number Loss Or cnLOH
MDS, Morphologically Defined			
MDS-LB	<5% BM and <2% PB		
MDS-H		$\leq 25\%$ Bone Marrow Cellularity, Age-Adjusted	
MDS-IB			
MDS-IB1	5–9% BM or 2–4% PB		
MDS-IB2	10–19% BM or 5–19% PB or AUER RODS		
MDS-f	5–19% BM; 2–19% PB		

Notes:

a. Detection of $\geq 15\%$ ring sideroblasts may substitute for an *SF3B1* mutation. Acceptable related terminology: MDS with low blasts and ring sideroblasts.

b. Defined as $\leq 25\%$ BM cellularity, age-adjusted.

Abbreviations: MDS-5q, Myelodysplastic syndrome with low blasts and isolated 5q deletion; MDS-*SF3B1*, Myelodysplastic syndrome with low blasts and *SF3B1* mutation; MDS-biTP53, Myelodysplastic syndrome with biallelic *TP53* inactivation; MDS-LB, Myelodysplastic syndrome with low blasts; MDS-H, Myelodysplastic syndrome, hypoplastic; MDS-IB1, Myelodysplastic syndrome with increased blasts 1; MDS-IB2, Myelodysplastic syndrome with increased blasts 2; MDS-f, Myelodysplastic syndrome with fibrosis. BM, Bone marrow; PB, Peripheral blood; cnLOH, Copy neutral loss of heterozygosity.

To elucidate the key advancements introduced in the WHO 2022 classification compared to the 2017 framework, Zhang et al. analyzed clinical outcomes in a cohort of 854 MDS patients

based on both classification systems (325). **Figure 9** provides a detailed visual representation of how patients were reclassified across subtypes, emphasizing the impact of incorporating molecularly defined criteria. Notably, the inclusion of subgroups such as MDS-*SF3B1* and MDS-biTP53 underscores the enhanced precision in diagnostic and prognostic stratification. These molecularly informed updates reflect the growing understanding of disease pathobiology and support more accurate and individualized diagnoses.

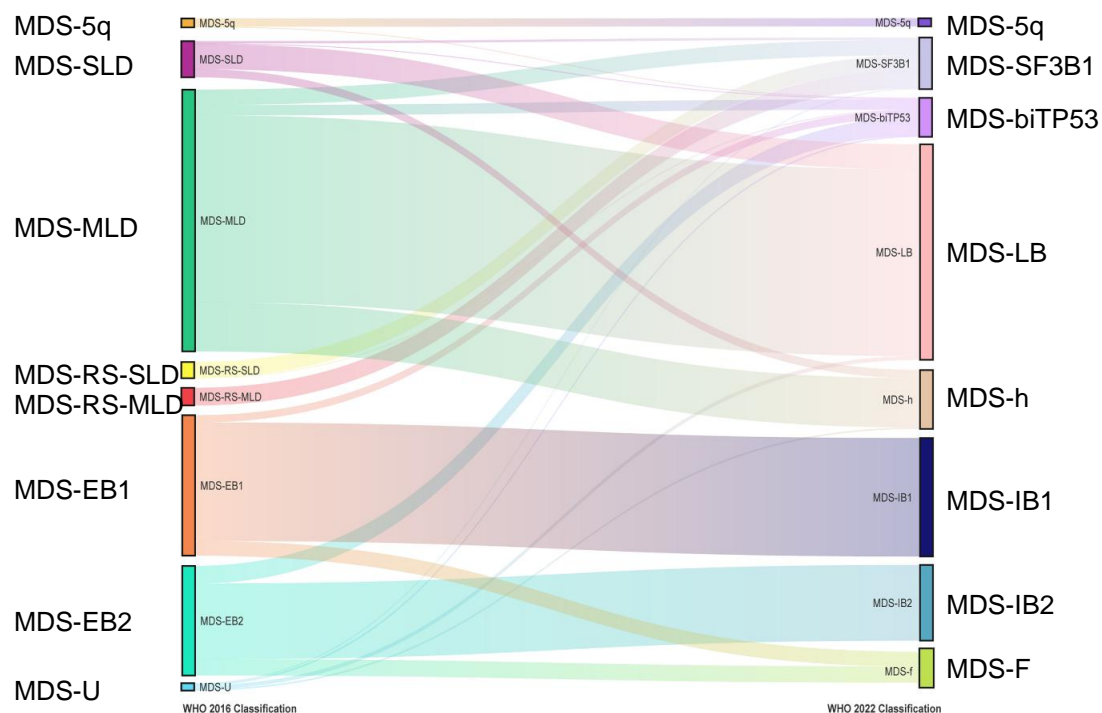


Figure 9. Overview of MDS subtypes according to WHO classifications from 2017 and 2022.

The diagram illustrates the relationship between MDS subtypes as defined by WHO criteria in 2017 and the revised classification in 2022. Key classifications include: MDS-U (MDS unclassifiable), SLD (single lineage dysplasia), MLD (multilineage dysplasia), RS-SLD (ring sideroblasts with SLD), RS-MLD (ring sideroblasts with MLD), EB1/2 (excess blasts types 1 and 2), 5q- (isolated 5q deletion), biTP53 (biallelic TP53 inactivation), LB (low blasts), MDS-*SF3B1* (MDS with low blasts and *SF3B1* mutation), MDS-h (hypoplastic MDS), IB1/2 (increased blasts types 1 and 2), and MDS-f (MDS with fibrosis). This figure is adapted from Zhang et al. (325).

The WHO 2022 classification introduces refined criteria to more clearly differentiate CMML from other overlapping myeloid neoplasms, addressing previous ambiguities and enhancing diagnostic precision (**Table 8**). A major revision includes lowering the threshold for PB monocytosis from $\geq 1.0 \times 10^9/L$ to $\geq 0.5 \times 10^9/L$, broadening the inclusion of cases that meet additional CMML-defining criteria. This adjustment acknowledges the biological and clinical significance of lower monocytosis levels when combined with other diagnostic features. Furthermore, the CMML-0 category has been eliminated, with its cases now incorporated into CMML-1. This consolidation simplifies classification and improves clinical utility, providing a streamlined framework for diagnosis and management.

The revised subcategories CMML-1 and CMML-2 emphasize the importance of molecular and cytogenetic abnormalities in prognosis and treatment planning. The updated classification maintains a distinction between myelodysplastic CMML (MD-CMML), characterized by a white blood cell count (WBC) of $<13 \times 10^9/L$, and myeloproliferative CMML (MP-CMML), defined by $WBC \geq 13 \times 10^9/L$. Additionally, subgroups are further stratified by the percentage of blasts and promonocytes in PB and BM, facilitating more precise risk assessment.

Table 8. The WHO 2022 diagnostic criteria for CMML.

Category	Criteria
Prerequisite Criteria	<ol style="list-style-type: none"> 1. Persistent absolute ($\geq 0.5 \times 10^9/L$) and relative ($\geq 10\%$) PB monocytosis. 2. Blasts constitute $<20\%$ of cells in PB and BM^a. 3. Does not meet diagnostic criteria for chronic myeloid leukemia or other myeloproliferative neoplasms^b. 4. Does not meet diagnostic criteria for myeloid/lymphoid neoplasms with tyrosine kinase fusions^c.
Supporting Criteria	<ol style="list-style-type: none"> 1. Dysplasia involving ≥ 1 myeloid lineage^d. 2. Presence of an acquired clonal cytogenetic or molecular abnormality. 3. Abnormal partitioning of PB monocyte subsets^e.
Requirements for Diagnosis	<ul style="list-style-type: none"> - All prerequisite criteria must be present in every case. - If monocytosis is $\geq 1 \times 10^9/L$: at least one supporting criterion must be met. - If monocytosis is ≥ 0.5 and $< 1 \times 10^9/L$: supporting criteria 1 and 2 must both be met.
Subtyping Criteria	<ul style="list-style-type: none"> - MD-CMML: $WBC < 13 \times 10^9/L$ - MP-CMML: $WBC \geq 13 \times 10^9/L$
Subgrouping criteria (based on percentage of blasts and promonocytes)	<ul style="list-style-type: none"> - CMML-1: $<5\%$ in PB and $<10\%$ in BM - CMML-2: 5–19% in PB and 10–19% in BM

Notes:

- a. Blasts and blast equivalents include myeloblasts, monoblasts, and promonocytes.
 - b. Myeloproliferative neoplasms (MPNs) can present with monocytosis at diagnosis or during disease progression, potentially mimicking CMML. A documented history of MPN excludes CMML. Features of MPN in the BM and/or a high burden of MPN-associated mutations (e.g., JAK2, CALR, or MPL) suggest MPN with monocytosis rather than CMML.
 - c. Criteria for myeloid/lymphoid neoplasms with tyrosine kinase fusions should be specifically ruled out in cases with eosinophilia.
 - d. Morphologic dysplasia should be present in $\geq 10\%$ of cells in a hematopoietic lineage within the BM.
 - e. Based on the detection of increased classical monocytes ($>94\%$) in the absence of known active autoimmune diseases and/or systemic inflammatory syndromes.
- Abbreviations: PB, Peripheral blood; BM, Bone marrow; WBC, White blood cell count; MD, Myelodysplastic; MP, Myeloproliferative.

The diagnostic criteria for CMML are now more comprehensive, requiring persistent absolute monocytosis ($\geq 0.5 \times 10^9/L$ and $\geq 10\%$ of PB leukocytes) and blasts constituting $<20\%$ of cells in PB and BM. Supporting criteria include dysplasia in at least one myeloid lineage, the presence of acquired clonal cytogenetic or molecular abnormalities, and abnormal distribution

of monocyte subsets. **Figure 10** visually demonstrates how cases previously categorized under CMML-0 and CMML-1 in the 2017 WHO classification are redistributed into CMML-1 under the 2022 criteria, reflecting a more refined diagnostic schema.

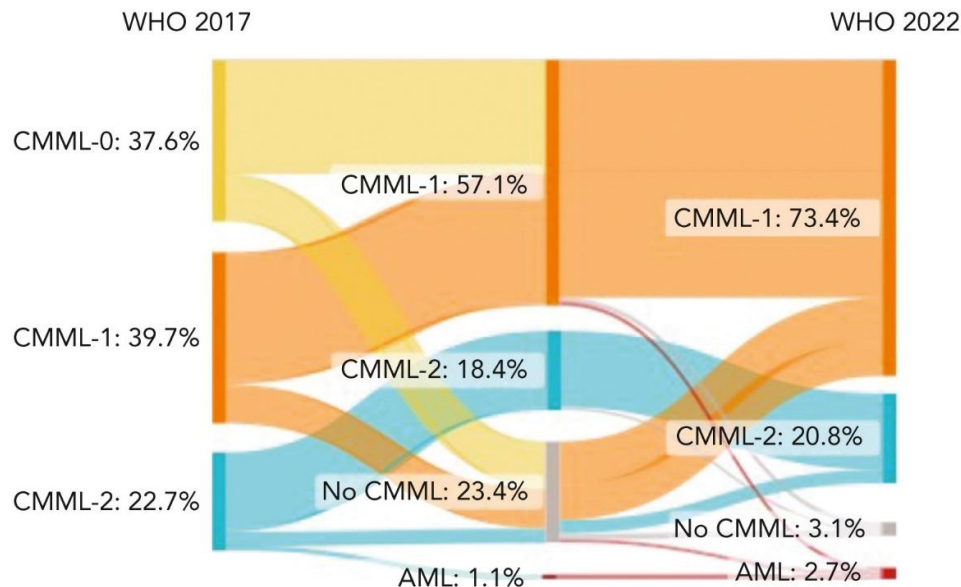


Figure 10. Reclassification of previously diagnosed CMML and monocytosis cases based on the updated WHO 2022 classification. This figure illustrates the diagnostic transitions of 1,279 established CMML cases, re-evaluated from the WHO 2017 classification to the WHO 2022 criteria. "No CMML" indicates cases reclassified with an alternative diagnosis, as they no longer meet the updated CMML criteria. Abbreviations: AML, acute myeloid leukemia. Adapted from Baumgartner F et al. (303).

Collectively, these updates underscore the growing role of molecular and cytogenetic findings in defining CMML subtypes, improving diagnostic accuracy, and guiding more targeted therapeutic strategies. By integrating these advancements, the WHO 2022 classification aligns with contemporary clinical and biological insights, enhancing its applicability in personalized patient management. The following sections will delve further into these prognostic milestones for MDS and CMML.

9 PROGNOSIS

9.1 Prognostic Indices for Myelodysplastic Syndromes

9.1.1 International Prognostic Scoring System (IPSS)

Since its publication in 1997, the International Prognostic Scoring System (IPSS) has been widely adopted as the standard tool for risk stratification in MD (326). This model was developed based on clinical and biological data from 816 patients with de novo MDS classified under the French-American-British (FAB) criteria and managed with supportive care (**Table 9**). IPSS incorporates three independent prognostic variables: BM blast percentage, karyotype, and the number of cytopenias.

Table 9. IPSS variables and scoring criteria

Prognostic Variable	0	0.5	1	1.5	2
BM blasts (%)	<5	5-10	-	11-20	21-30
Karyotype*	Good	Intermediate	Poor	-	-
Number of cytopenias**	0-1	2-3	-	-	-

* Karyotype categories: Good (normal, -Y, del(5q), del(20q) as sole abnormalities); Poor (complex karyotype with ≥ 3 abnormalities or chromosome 7 anomalies); Intermediate (other single or double abnormalities).

**Cytopenias were defined using the following thresholds: hemoglobin <10 g/dL, neutrophils <1,800/ μ L, and platelets <100,000/ μ L.

Based on these scores, patients are stratified into four risk categories with statistically significant differences in OS and risk of progression to AML:

- Low risk (0 points): Median survival of 5.7 years
- Intermediate-1 (0.5–1 point): Median survival of 3.5 years
- Intermediate-2 (1.5–2 points): Median survival of 1.2 years
- High risk (2.5–3.5 points): Median survival of 0.4 years

The IPSS, while widely used for its simplicity, has several limitations. It excludes secondary MDS or proliferative CMML, and uses blast percentage thresholds that do not align with WHO criteria, potentially leading to misclassification of higher-risk cases. The system also fails to account for the severity of cytopenias, disproportionately emphasizes blast percentage over karyotype, and was developed using data in which a significant portion (~30%) of patients lacked cytogenetic information. Furthermore, because it was based on data from tertiary centers, it carries a selection bias and was not designed to address disease progression, limiting its utility in dynamic clinical settings. These shortcomings highlighted the need for more refined models, such as the IPSS-R.

9.1.2 Revised International Prognostic Scoring System (IPSS-R)

Introduced in 2012, the Revised International Prognostic Scoring System (IPSS-R) addressed many of the limitations of the original IPSS by providing a more comprehensive assessment of disease characteristics (327). Developed using data from 7,012 de novo MDS patients, the IPSS-R expanded and refined key prognostic variables, including cytogenetics, BM blast percentages, and cytopenia severity (**Table 10**).

The revision introduced a more detailed stratification of cytogenetic risk, categorizing it into five groups: very good, good, intermediate, poor, and very poor. Blast percentage thresholds were adjusted for greater precision, dividing the original <5% category into $\leq 2\%$ and $>2\text{--}<5\%$. The severity of cytopenias was also incorporated into the scoring system, with defined thresholds for hemoglobin levels, platelet counts, and neutrophil counts. These updates significantly enhanced the system's prognostic accuracy, making it a more robust tool for clinical decision-making.

Table 10. IPSS-R variables and scoring criteria

Prognostic Variable	0	0.5	1	1.5	2	3	4
Cytogenetic risk group*	Very Good	-	Good	-	Intermediate	Poor	Very Poor
BM blasts (%)	≤ 2	-	$>2\text{--}<5$	-	5-10	>10	-
Hemoglobin (g/dL)	≥ 10	-	8- <10	-	<8	-	-
Platelets ($\times 10^9/\text{L}$)	≥ 100	-	50- <100	-	<50	-	-
Neutrophils ($\times 10^9/\text{L}$)	≥ 0.8	<0.8	-	-	-	-	-

* *Cytogenetic Risk Groups*: Very Good (-Y, del(11q) as single alterations); Good (normal, del(5q), del(12p), del(20q) as single or double anomalies with del(5q)); Intermediate (del(7q), +8, +19, i(17q) as single abnormalities); Poor (-7, inv(3)/(3q)/del(3q), double anomalies with -7/del(7q), or complex with three abnormalities); Very Poor (complex with more than three abnormalities).

Based on these refined criteria, the IPSS-R stratifies patients into five distinct risk groups with corresponding median survival estimates:

- Very Low (0-1.5 points): Median survival of 8.8 years
- Low ($>1.5\text{--}3$ points): Median survival of 5.3 years
- Intermediate ($>3\text{--}4.5$ points): Median survival of 3 years
- High ($>4.5\text{--}6$ points): Median survival of 1.6 years
- Very High (>6 points): Median survival of 0.8 years

9.1.3 WHO Classification-Based Prognostic Scoring System (WPSS)

The WHO Classification-Based Prognostic Scoring System (WPSS) provides a dynamic tool for predicting outcomes in MDS by integrating three critical variables: IPSS cytogenetic risk categories, WHO 2001 diagnostic classifications, and transfusion requirements (328). Initially, transfusion dependency was defined by the requirement for at least one transfusion every eight weeks over a duration of four months (**Table 11**). Later revisions substituted this criterion with anemia severity to enhance prognostic precision.

Table 11. WPSS variables and scoring criteria

Prognostic Variable	0	1	2	3
WHO classification	RA, RARS, 5q-	RCMD, RCMD-RS	RAEB-1	RAEB-2
Karyotype*	Good	Intermediate	Poor	-
Transfusion requirement**	No	Yes	-	-

Karyotype:

-Good: Normal, -Y, del(5q), del(20q) as sole abnormalities.

-Poor: Complex (≥3 abnormalities), chromosome 7 alterations.

-Intermediate: Other single or double abnormalities.

Transfusion Requirement: At least one transfusion every 8 weeks over a 4-month period.

The WPSS allows for real-time risk assessment, distinguishing between five risk groups with differing prognostic outcomes, making it a valuable tool for treatment planning and monitoring disease progression.

9.1.4 MD Anderson Global Prognostic Scoring System (MPSS) and Low-Risk Prognostic Scoring System (LR-PSS)

The MD Anderson Global Prognostic Scoring System (MPSS) introduced in 2008, was developed from a cohort of 1,915 patients, extending prognostic evaluation to include secondary MDS, proliferative CMML, MDS/MPN neoplasms, and patients undergoing treatment (329). A key feature of MPSS is its inclusion of host-dependent factors, such as age and ECOG performance status, which acknowledges the influence of patient-specific variables on disease outcomes. However, this broader approach has its limitations, as it may overestimate or underestimate disease-specific risks, particularly in older patients or those with poor functional status, potentially affecting its accuracy in certain clinical scenarios.

9.1.5 GESMD Recommendations for Prognostic Stratification in MDS

In 2020, the Spanish Group of Myelodysplastic Syndromes (GESMD) released guidelines that offer a simplified yet robust framework for risk stratification in MDS (330). These guidelines categorize patients into two main risk groups—high-risk and low-risk—based on a combination of clinical and prognostic factors, providing a practical tool for guiding treatment decisions

- High-risk patients: IPSS intermediate-2 and high; WPSS high and very high; IPSS-R high and very high, or intermediate with at least one of the following features:
 - High or very high-risk cytogenetic abnormalities (IPSS-R)
 - Platelets $<30 \times 10^9/L$
 - Neutrophils $<0.5 \times 10^9/L$
 - BM fibrosis (grades 2–3, European consensus)
 - *TP53* somatic mutation
- Low-risk patients:
 - Patients who do not meet any of the previously mentioned criteria.

9.1.6 Molecular International Prognostic Scoring System (IPSS-M) for Myelodysplastic Syndromes

The clinical and biological complexity of MDS highlights the need for personalized prognostic tools that can improve risk assessment and inform treatment strategies. Traditional systems like the IPSS and IPSS-R have primarily relied on clinical variables and cytogenetic data for patient stratification. However, advancements in high-throughput sequencing have transformed our understanding of MDS, uncovering the critical role of somatic mutations in disease progression and prognosis.

Over the past decade, genomic research has shed light on the stepwise acquisition of genetic alterations in MDS, linking recurrent mutations to disease initiation, clonal hematopoiesis, and progression to AML (221, 235, 255). These mutations often cluster in key biological pathways, including RNA splicing, epigenetic regulation, transcriptional control, and cohesin complex function, driving malignant transformation. While lower-risk MDS typically harbors two or three driver mutations, higher-risk MDS is associated with a greater mutational burden, reflecting its more aggressive clinical behavior (235). Specific mutations, such as those in *TP53*, *NRAS*, *KRAS*, *RUNX1*, *STAG2*, *ASXL1*, and *IDH2*, are more frequently enriched in higher-risk MDS, correlating with poor leukemia-free survival (LFS), OS, and increased likelihood of AML

transformation (221, 331, 332). Paired studies of MDS and secondary AML have revealed that certain mutations, including those in signaling pathways (*FLT3*, *NRAS*, *KRAS*, *PTPN11*), myeloid transcription factors (*RUNX1*, *CEBPA*), and cohesin components (*STAG2*, *RAD21*), often emerge or expand at disease progression (333-335). These insights highlight the dynamic nature of clonal evolution and its impact on prognosis.

In response to these findings, the Molecular International Prognostic Scoring System (IPSS-M) was developed to integrate clinical, cytogenetic, and mutational data into a comprehensive framework for risk assessment. This model incorporates mutations in key adverse effect genes, including *TP53* multi-hit, *FLT3*, and *MLL-PTD*, as robust predictors of poor outcomes. Additional mutations in genes such as *ASXL1*, *BCOR*, *EZH2*, *NRAS*, *RUNX1*, *STAG2*, and *U2AF1* have also been linked to adverse prognosis. By integrating molecular data, IPSS-M offers a more nuanced and precise stratification tool compared to its predecessors, enabling tailored treatment strategies (**Table 12, Figure 11**).

Multi-hit *TP53*-mutated MDS/AML has recently been recognized as a distinct clinical entity, as reflected in the 5th edition of the WHO classification of myeloid neoplasms and the International Consensus Classification (ICC). These cases are associated with high-risk disease features, an increased likelihood of transformation to AML, and poor overall survival.

The introduction of the IPSS-M has reclassified many patients into higher-risk categories, significantly improving prognostic accuracy. However, this enhanced precision has also brought new challenges in tailoring treatment strategies (336). By integrating genetic and clinical factors, the IPSS-M enables earlier identification of patients at risk for disease progression, creating opportunities for timely therapeutic interventions. Furthermore, understanding the sequential genetic alterations driving MDS provides an essential foundation for studying clonal dynamics and tumor burden, paving the way for improved disease management.

Table 12. Adjusted Hazard Ratios and model weights for leukemic transformation or death in MDS patients.

Category	Variable	Adjusted Hazard Ratio (95% CI)	Model Weight
Clinical	Bone marrow blasts (%)	1.07 (1.05–1.09)	0.0704
	min(Platelets, 250) ($\times 10^9/L$)	0.998 (0.997–0.999)	–0.00222
	Hemoglobin (g/dL)	0.84 (0.81–0.88)	–0.171
Cytogenetic	IPSS-R cytogenetic category§	1.33 (1.21–1.47)	0.287
	TP53multihit	3.27 (2.38–4.48)	1.18
	<i>MLLPTD</i>	2.22 (1.49–3.32)	0.798
	<i>FLT3ITD+TKD</i>	2.22 (1.11–4.45)	0.798
	<i>SF3B15q</i>	1.66 (1.03–2.66)	0.504
	<i>NPM1</i>	1.54 (0.78–3.02)	0.430
	<i>RUNX1</i>	1.53 (1.23–1.89)	0.423
	<i>NRAS</i>	1.52 (1.05–2.20)	0.417
	<i>ETV6</i>	1.48 (0.98–2.23)	0.391
	<i>IDH2</i>	1.46 (1.05–2.02)	0.379
Gene Main Effects	<i>CBL</i>	1.34 (0.99–1.82)	0.295
	<i>EZH2</i>	1.31 (0.98–1.75)	0.270
	<i>U2AF1</i>	1.28 (1.01–1.61)	0.247
	<i>SRSF2</i>	1.27 (1.03–1.56)	0.239
	<i>DNMT3A</i>	1.25 (1.02–1.53)	0.221
	<i>ASXL1</i>	1.24 (1.02–1.51)	0.213
	<i>KRAS</i>	1.22 (0.84–1.77)	0.202
	<i>SF3B1α</i>	0.92 (0.74–1.16)	–0.0794

Abbreviations: CI, confidence interval; IPSS-M, International Prognostic Scoring System–Molecular; IPSS-R, International Prognostic Scoring System–Revised; ITD, internal tandem duplication; min, minimum; PTD, partial tandem duplication; TKD, tyrosine kinase domain.

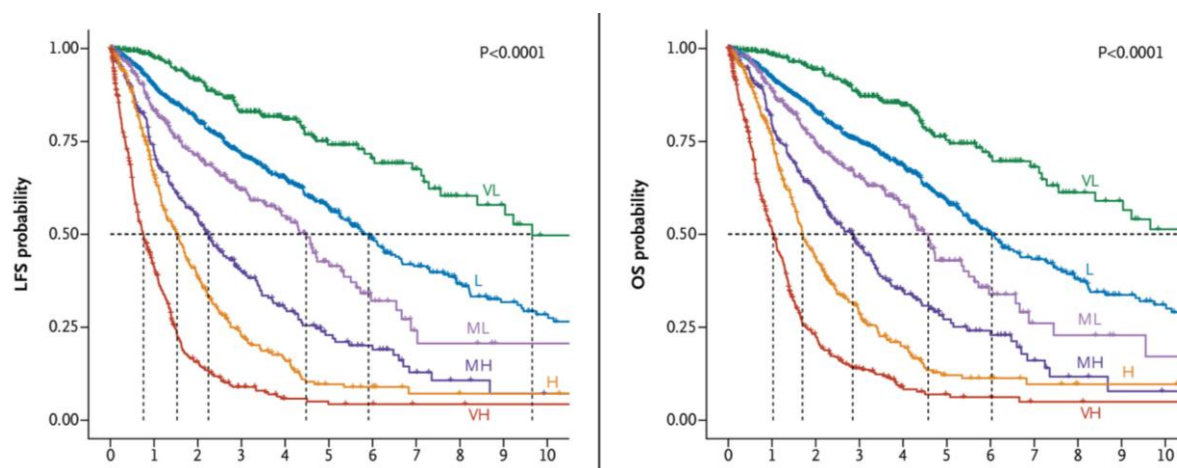


Figure 11. Kaplan–Meier survival analysis for LFS and OS stratified by IPSS-M risk categories. The Kaplan–Meier curves illustrate the estimated probabilities of LFS (left panel) and OS (right panel) across the IPSS-M risk categories: very low (VL), low (L), moderate-low (ML), moderate-high (MH), high (H), and very high (VH). Dashed lines represent the median survival values. The number of patients at risk is displayed below each panel at specified time points. Statistical significance was determined by the investigators using the log-rank test ($P < 0.0001$ for both panels). Adapted from Bernard et al. (33). Abbreviations: OS, overall survival; LFS, leukemia-free survival.

9.2 Prognostic Indices for CMML

9.2.1 MD Anderson Prognostic Scoring System (MDAPS)

The MD Anderson Prognostic Scoring System (MDAPS), developed by Onida et al. in 2002, is based on data from 213 patients diagnosed with CMML (28). This scoring system integrates four prognostic variables that capture key hematological and biological features of the disease:

- Hemoglobin <120 g/L
- Absolute lymphocyte count >2.5 x 10⁹/L
- Presence of circulating myeloid precursors
- BM blasts ≥10%

The inclusion of absolute lymphocyte count and circulating myeloid precursors as prognostic markers was a significant advancement, later validated by subsequent independent studies (337, 338). A follow-up validation study including 250 CMML patients from MD Anderson Cancer Center further reinforced the reliability of the MDAPS (29). The MDAPS stratifies patients into four distinct risk categories with associated median survival rates:

- Low risk: 24 months
- Intermediate-1: 15 months
- Intermediate-2: 8 months
- High risk: 5 months

While MDAPS offers a straightforward framework for risk stratification, its clinical application is limited. Its inability to effectively distinguish high- and low-risk groups for therapeutic decision-making and the relatively poor survival even in the low-risk category highlights this limitation, underscoring the need for more sophisticated models that can better inform risk-adapted treatment strategies and improve patient outcomes.

9.2.2 CMML-specific Prognostic Scoring System (CPSS)

The CMML-specific Prognostic Scoring System (CPSS), published in 2013, is the most widely adopted prognostic tool specifically designed for CMML (31). Developed from a cohort of 558 patients from the Spanish Myelodysplastic Syndromes Registry (RESMD) and externally validated in an independent cohort of 274 patients from the Düsseldorf Registry and the San Matteo Hospital in Pavia, the CPSS introduced a novel approach to CMML risk assessment (**Table 13**).

Notably, CPSS was the first scoring system to incorporate cytogenetics as a prognostic variable in CMML. The cytogenetic risk groups, internationally recognized as the Spanish Cytogenetic Risk Stratification System, were defined by Such et al. in 2011(289)

Table 13. CMML-specific Prognostic Scoring System (CPSS).

SCORE	0	1	2
WHO Category	CMML-1	CMML-2	
FAB Category	CMML-MD	CMML-MP	
Transfusion Dependency (Red Cell Concentrates)	No	Yes	
Cytogenetic Category	Low Risk	Intermediate Risk	High Risk
Cytogenetic Category (GESMD): Low (0 points): Normal, -Y; Intermediate (1 point): Other Abnormalities; High (2 Points): +8, Chromosome 7 Abnormalities, And Complex Karyotype.			
Risk Groups: Low: 0 points, Intermediate-1: 1 points, Intermediate-2: 2-3 points, High: 4-5 points			

Abbreviations: WHO: World Health Organization; CMML: Chronic Myelomonocytic Leukemia; FAB: French-American-British Cooperative Leukemia Group; MD: Myelodysplastic Variant; MP: Myeloproliferative Variant; GESMD: Spanish Group of Myelodysplastic Syndromes. Transfusion dependency for red cell concentrates can be replaced by hemoglobin level (<10 g/dL vs. ≥10 g/dL) (31, 289).

The prognostic grouping facilitates a clear distinction between low-risk (low and intermediate-1) and high-risk (intermediate-2 and high) patients. This differentiation is critical for tailoring risk-adapted therapeutic strategies. Consistent with the GESMD recommendations for high-risk MDS patients, which define high-risk as having an estimated median OS of less than 30 months, the CPSS categories align well with these thresholds, providing a robust framework for clinical decision-making.

An alternative CPSS model was proposed in the same study, replacing transfusion dependency with a hemoglobin threshold of <10 g/dL. While this alternative model demonstrated comparable predictive capacity based on concordance probability estimates, it failed to significantly distinguish four distinct risk groups for leukemic transformation in the validation cohort.

9.2.3 Groupe Français des Myélodysplasies (GFM) Prognostic Score

Developed by the French MDS Group, the GFM score was based on a study of 312 CMML patients and validated in an independent cohort of 165 patients from the Munich Leukemia Laboratory (265). Remarkably, the GFM score integrated molecular data, specifically mutations in the *ASXL1* gene, marking it the first CMML prognostic model to incorporate

genomic insights into risk stratification. The GFM model incorporates five key variables, each of which significantly impacts patient outcomes:

- Age >65 years
- Leukocytes $>15 \times 10^9/L$
- Anemia (Hb <11 g/dL in men; <10 g/dL in women)
- Platelets $<100 \times 10^9/L$
- Presence of *ASXL1* mutation

The GFM score stratifies patients into three risk categories:

- Low risk: Median survival not reached
- Intermediate: 38.5 months
- High risk: 14.4 months

This model has proven valuable in guiding risk-adapted treatment decisions. However, including age as a prognostic factor introduces a notable limitation, as it may overestimate the disease-specific risk in older patients. This overestimation could potentially lead to erroneous therapeutic decisions, disproportionately attributing poor outcomes to CMML in advanced-age individuals, as opposed to other age-related factors or comorbidities.

9.2.4 Mayo Prognostic Model for WHO-defined CMML (Mayo Model)

Published in 2013, the Mayo Model is based on 226 CMML patients from the Mayo Clinic and validated in a cohort from the Moffitt Cancer Center (337). This model specifically focused on clinical variables, as an analysis incorporating cytogenetic and molecular data (mutations in *ASXL1*, *SRSF2*, *SF3B1*, and *U2AF1*) found that only four clinical factors independently predicted prognosis in a multivariable setting. Notably, BM blast percentage, often included in prognostic models, did not emerge as an independent prognostic variable in this model. The four adverse prognostic factors included in the Mayo Model are:

- Hemoglobin <100 g/L
- Monocyte count $>10 \times 10^9/L$
- Platelet count $<100 \times 10^9/L$
- Presence of circulating myeloid precursors (myelocytes)

This model stratifies patients into three risk categories:

- Low risk: 32 months
- Intermediate: 18.5 months
- High risk: 10 months

The Mayo Model's simplicity and reliance on clinical variables make it a practical tool for prognostication and risk stratification in CMML. However, the exclusion of cytogenetic and molecular markers, which are increasingly recognized as critical in understanding disease biology and progression, limits its applicability in modern clinical practice.

9.2.5 Mayo Molecular Model (MMM)

The Mayo Molecular Model (MMM) was introduced as an improvement to the original Mayo Prognostic Model, following a collaborative effort between the Mayo Clinic and the French MDS Group. This collaboration aimed to address discrepancies regarding the prognostic significance of *ASXL1* mutations (339). Using data from 466 patients across both groups, the study confirmed that *ASXL1* mutations, particularly nonsense and frameshift variants, are an independent adverse prognostic factor for OS, although they are not predictive of leukemic transformation.

This integration resulted in a refined risk stratification framework, dividing patients into four distinct groups with significantly different survival outcomes:

- Low risk: Median OS of 97 months
- Intermediate-1 risk: Median OS of 59 months
- Intermediate-2 risk: Median OS of 31 months
- High risk: Median OS of 16 months

This refined stratification confirms the critical role of *ASXL1* mutations in determining patient outcomes and supports tailored therapeutic decisions.

9.2.6 Molecular CMML-specific Prognostic Scoring System (CPSS-Mol)

In 2016, Elena et al. introduced the CPSS-Mol, an updated version of the CPSS, incorporating molecular data to refine risk stratification (340). Developed using a cohort of 214 CMML patients and validated in an independent cohort of 260 patients, this model included four gene

mutations—*ASXL1*, *RUNX1*, *SETBP1*, and *NRAS*—which demonstrated independent adverse prognostic significance (**Table 14**). The addition of these mutations, combined with the Spanish Cytogenetic Risk Stratification System, facilitated the creation of a genetic score to enhance prognostic precision.

The CPSS-Mol comprises the following variables:

- BM blasts $\geq 5\%$
- Leukocytes $\geq 13 \times 10^9/L$
- Transfusion dependency
- Genetic score based on the mutational status of *ASXL1*, *RUNX1*, *SETBP1*, and *NRAS*

Tabla 14. CPSS-Molecular (CPSS-mol)

Score	Cytogenetic Category	<i>ASXL1</i>	<i>NRAS</i>	<i>RUNX1</i>	<i>SETBP1</i>	BM Blasts	WBC	Transfusion Dependency*
0	Low (normal, -Y)	Not Mut	Not Mut	Not Mutated	Not Mut	<5%	<13 x $10^9/L$	No
1	Intermediate (other anomalies)	Mut	Mut	Mut		$\geq 5\%$	$\geq 13 \times 10^9/L$	Yes
2	High (+8, chromosome 7 abnormalities, complex karyotype)				Mut			

*Transfusion dependency can be substituted by hemoglobin level (<10 g/dL vs. ≥ 10 g/dL) (340).

The CPSS-Mol stratifies patients into four distinct prognostic groups with significant differences in OS and risk of leukemic transformation:

- Low risk: Median survival not reached
- Intermediate-1: Median survival of 64 months
- Intermediate-2: Median survival of 37 months
- High risk: Median survival of 18 months

This model offers a comprehensive approach to risk stratification in CMML by integrating genetic and clinical factors, providing a better prognosis assessment.

9.3 Novel Stratification of MDS and CMML and its Clinical Implications

9.3.1 HSPC architecture in MDS and CMML

Advancing personalized treatment approaches for MDS and CMML requires ongoing improvements in patient stratification techniques. Prognostic tools such as the IPSS (326) and its revision (IPSS-R) (327), and the IPSS-M (33) have marked significant progress in risk assessment by incorporating clinical, cytogenetic, and molecular data. However, a critical limitation remains, since these systems do not account for the hierarchical organization of BM HSPCs, a factor increasingly recognized as pivotal in capturing the full complexity of the disease and predicting therapeutic responses.

Ganan-Gomez et al. characterized two distinct subgroups of MDS and CMML patients, differentiated by both immunophenotypic and biological features, driven by the hierarchical organization of BM HSPCs (83). Using a cohort of 123 untreated MDS and CMML BM samples, the study employed unsupervised hierarchical clustering of immunophenotypically defined HSPC populations and principal component analysis to identify two distinct MDS subgroups with unique immunophenotypic profiles.

The first subgroup, designated as the “CMP pattern” (comprising 52% of samples), displayed aberrant differentiation within the myeloid hematopoietic progenitor cell (MyHPC) compartment. This subgroup was marked by an overrepresentation of CMPs and a concomitant reduction in GMPs and MEPs. In contrast, the second subgroup, referred to as the “GMP pattern” (48% of samples), exhibited an enrichment of GMPs alongside a corresponding depletion of CMPs and MEPs.

Moreover, the immunophenotypic composition of the upstream HSC populations in these two MDS subgroups revealed substantial differences. The “CMP pattern” MDS subgroup had an increased proportion of LT-HSCs and MPPs, while the “GMP pattern” MDS subgroup was characterized by an expanded population of LMPPs. The unique HSC architecture observed in the “GMP pattern” MDS subgroup was characterized by a notable expansion of LMPPs, coupled with a reduction in the frequencies of LT-HSCs and MPPs within the total BM MNCs (**Figure 12**). These two distinct MDS differentiation patterns were associated with unique mutational landscapes that likely contribute to the structural differences observed in HSPC hierarchies. Specifically, mutations in *RUNX1*, *BCOR*, *STAG2*, and *DNMT3A* were significantly enriched in “GMP pattern” MDS patients, whereas *TP53* and *U2AF1* mutations were predominantly associated with the “CMP pattern” phenotype (83).

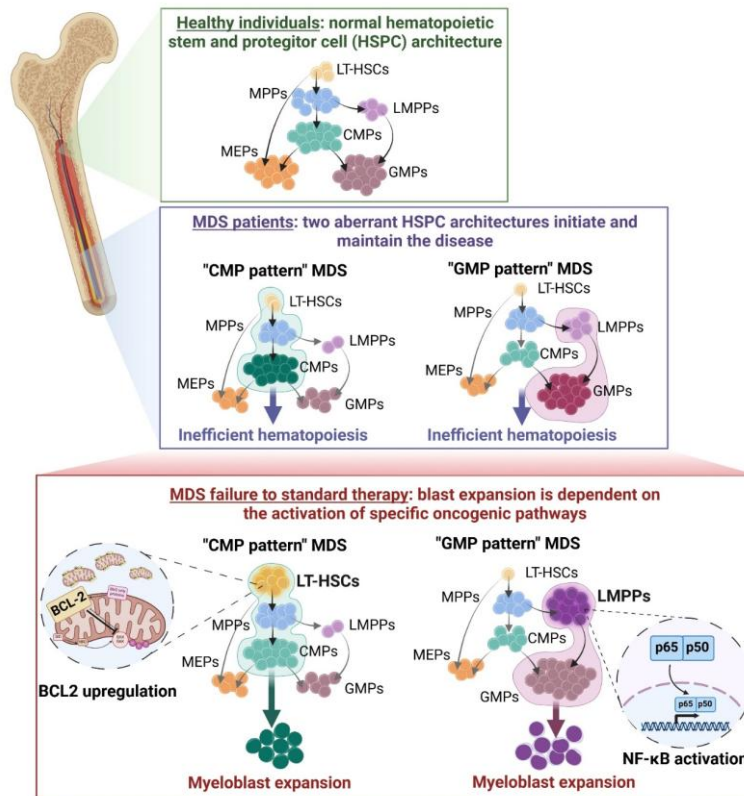


Figure 12. Distinct and Recurrent Cellular Hierarchies drive the maintenance and disease progression of MDS and CMML. Research by Ganan-Gomez et al. illustrates that MDS patients can be classified into two biologically and immunophenotypically distinct subgroups, determined by the organization of HSPC hierarchies. In the “CMP pattern” subgroup, disease progression is driven by LT-HSCs that depend on BCL2 upregulation for survival. In contrast, in the “GMP pattern” subgroup, lymphoid-primed multipotent progenitors (LMPPs) drive progression through upregulated NF-κB signaling pathways. Adapted from Ganan-Gomez et al., *Nature Medicine*, 2022 (83). Figure created using BioRender.

These findings underscore the importance of considering HSPC hierarchies in refining biologically-based stratification systems for MDS and CMML, paving the way for more tailored therapeutic strategies and improved clinical outcomes for patients.

9.3.2 Immunophenotypically Defined HSPC Hierarchies are predictive of MDS and CMML progression

MDS and CMML are highly heterogeneous in their biological and clinical manifestations, necessitating deeper insights into the mechanisms driving disease progression. A critical area of investigation is understanding how blast progression (BP) occurs in distinct HSPC hierarchies, which could inform novel therapeutic approaches to address resistance to current available therapies.

Recent seminal studies have aimed to clarify the biological mechanisms driving BP in the two previously described MDS subgroups, the CMP and GMP patterns, with the goal of identifying novel therapeutic strategies to prevent or address HMA failure. HMA resistance is often independent of the molecular and genetic alterations within the founder clone (341) and BP is primarily driven by the expansion of HSC clones carrying preexisting or newly acquired mutations in genes involved in signal transduction, transcription, and epigenetic regulation (220, 331, 342). This suggests that specific oncogenic pathways, recurrently activated in distinct MDS subgroups, may play a key role in HSC expansion. To test this hypothesis, gene expression profiling was performed in LT-HSC and LMPP populations isolated from MDS patients with “CMP pattern” and “GMP pattern”, respectively, at disease progression (83). These patients had developed higher-risk MDS or AML following resistance to HMA therapy. RNA sequencing revealed that LT-HSCs from “CMP pattern” MDS patients with BP after HMA failure showed substantial upregulation of genes associated with cell proliferation and survival, such as the anti-apoptotic regulator BCL2, in comparison to untreated LT-HSCs. In striking contrast, LMPPs from “GMP pattern” MDS patients with BP exhibited significant upregulation of genes involved in the TNF α -induced NF- κ B signaling pathway, relative to LMPPs from newly diagnosed “GMP pattern” MDS patients.

These observations suggest therapeutic vulnerabilities specific to each subgroup. The “CMP pattern” appears to benefit from targeting BCL2, while the “GMP pattern” may respond more effectively to NF- κ B pathway inhibition. Pharmacological inhibition of these pathways was found to selectively deplete the corresponding MDS stem cell subtypes *in vitro* and reduce tumor burden in patient-derived xenograft models. Moreover, patients with primitive hierarchies demonstrated significantly shorter time to achieve response and more sustained responses to venetoclax-based therapies compared to those with granulomonocytic hierarchies (83). These results provided the rationale for refining patient stratification in venetoclax-based clinical trials, particularly for patients in the “CMP pattern. Additional studies have focused on understanding the mechanisms of venetoclax response and resistance by

analyzing sequential BM samples from MDS patients enrolled in clinical trials. Resistance to venetoclax is frequently associated with upregulation of myeloid cell leukemia 1 (MCL1), a mechanism well-documented in AML, and induced downstream of NF- κ B signaling (343, 344). Preliminary work suggests that MCL1 inhibition, either alone or in combination with venetoclax, could be effective for progressive MDS in patients failing HMA therapy. Preclinical studies in CLL and AML have shown that combining BCL2 and MCL1 inhibitors can have synergistic effects, effectively suppressing leukemic blasts and stem cells (345-347). However, it remains unclear whether these findings are applicable to MDS and CMML.

Further evidence of hierarchy-dependent venetoclax sensitivity was provided by ex vivo drug screening studies, which revealed a negative correlation between AML differentiation levels and venetoclax sensitivity (348). Primitive hierarchies enriched with quiescent leukemic stem cells (LSCs) displayed higher sensitivity, irrespective of prior therapy failure, suggesting that venetoclax sensitivity is more closely associated with disease progression rather than treatment history (349). Similar observations were made in clinical trials of venetoclax-azacitidine; where newly diagnosed AML patients with primitive phenotypes responded better than those with monocytic phenotypes (350, 351), which showed shorter remission durations (351). Primary resistance to venetoclax in monocytic leukemias has been associated with lower BCL2 expression and a greater dependency on MCL1 for survival, reflecting shifts in mitochondrial apoptotic priming (344, 345, 352). In MDS with granulomonocytic hierarchies, relapse after HMA therapy has been linked to *MCL1* upregulation in LMPPs, further underscoring their reliance on NF- κ B signaling and *MCL1* for survival. Similar mechanisms have been observed in CMML with a monocytic bias, suggesting that hierarchy-dependent oncogenic dependencies are a common feature across various stem cell malignancies (83).

Collectively, these studies demonstrated that MDS and AML hierarchies are biomarkers of sensitivity to venetoclax but preserve certain phenotypic plasticity that may be leveraged as a drug resistance mechanism. Therefore, large genomic studies in MDS and AML should take hematopoietic hierarchies into account in order to identify additional associations with genetic drivers that may be valuable to predict drug response to venetoclax.

10. Treatment of Myelodysplastic Syndromes and Chronic Myelomonocytic Leukemia

To date, treatment options for MDS and CMML remain largely palliative, as stem cell transplantation remains as the only curative therapy, and no new curative treatments have emerged in over a decade (353, 354). The clinical heterogeneity of these diseases further complicates treatment decisions, requiring comprehensive prognostic tools to guide therapy based on disease risk.

For lower-risk MDS, characterized by less aggressive disease biology, treatment primarily aims to alleviate cytopenias such as anemia, thrombocytopenia, or neutropenia to improve quality of life. Supportive care remains the cornerstone of therapy and includes red blood cell transfusions, erythropoiesis-stimulating agents (ESAs), thrombopoietin receptor agonists, and iron chelation to manage transfusion-related iron overload (37). Recent advances have expanded treatment options for lower-risk MDS. Luspatercept, an erythroid maturation agent, was approved by the FDA for patients with lower-risk MDS and ring sideroblasts, offering a targeted approach to improve hemoglobin levels and reduce transfusion dependency (355, 356). Similarly, imetelstat, a first-in-class telomerase inhibitor, has demonstrated efficacy in reducing transfusion burden in lower-risk MDS patients with refractory anemia, including those unresponsive to ESAs, marking another significant advancement in therapeutic options (357, 358). These developments reflect a growing focus on addressing the underlying mechanisms of lower-risk MDS while prioritizing symptom management and minimizing treatment-related toxicities rather than altering the disease course directly.

In contrast, higher-risk MDS is marked by a more aggressive clinical trajectory, with a higher likelihood of progression to sAML and significantly diminished survival (327). In these cases, the goal of treatment shifts to modifying the disease course, extending survival, and delaying leukemic transformation. Hypomethylating agents (HMAs) remain the standard of care and provide clinical benefit for some patients, but more than half of treated individuals eventually develop resistance to HMAs. This resistance often leads to disease progression to sAML, with a median survival of only 4–6 months (359, 360). Allogeneic hematopoietic stem cell transplantation (HSCT) remains the sole potentially curative treatment for both MDS and CMML, but it is limited to a small subset of patients due to high transplant-related morbidity and mortality, coupled with the advanced age at diagnosis commonly seen in these diseases (361, 362).

The guidelines developed by the Spanish Group for Myelodysplastic Syndromes (GESMD) underscore the complexities of MDS and CMML and provide a detailed framework for

navigating these challenges (**Figures 13-15**), emphasizing personalized treatment approaches tailored to individual patient profiles (330).

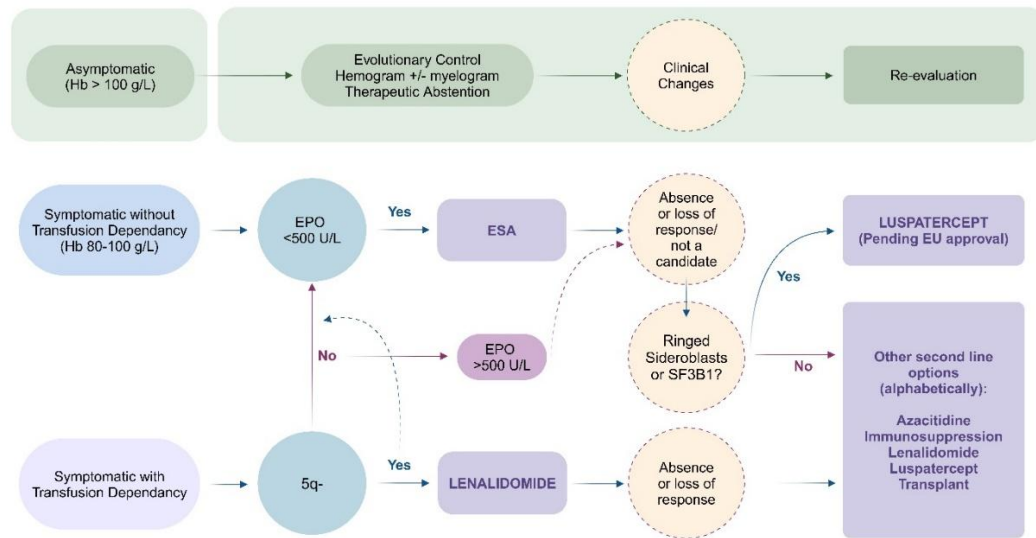


Figure 13. Proposed treatment algorithm for lower-risk MDS patients. BMA, bone marrow aspiration; ESA, erythropoiesis-stimulating agents; IST, immunosuppressive therapy; del(5q), deletion 5q; HCT, hematopoietic cell transplantation. *Figure created using BioRender.*

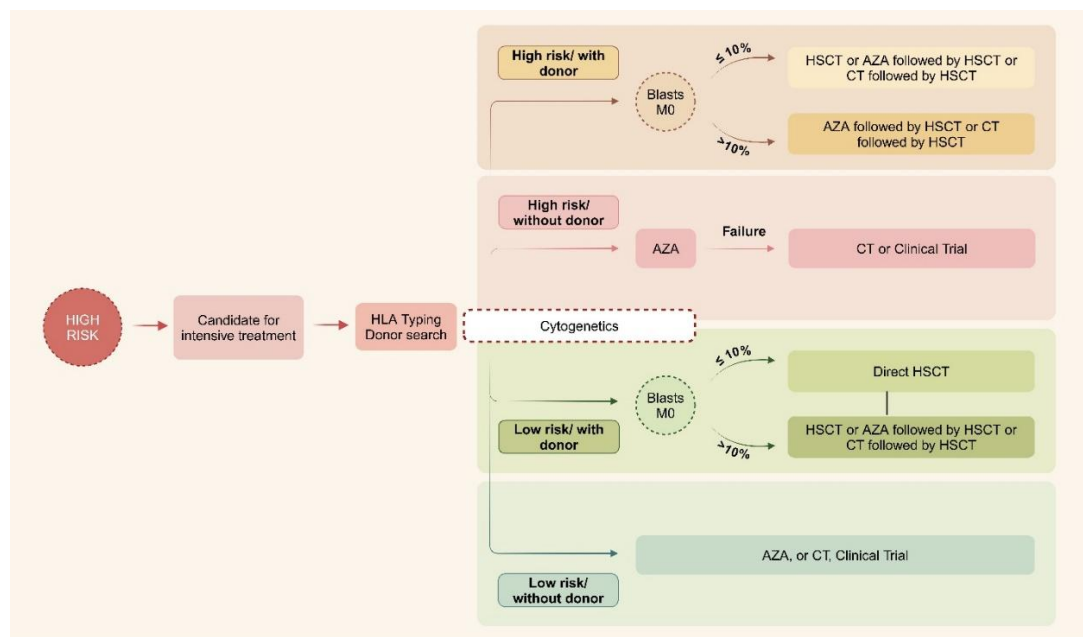


Figure 14. Proposed treatment algorithm for higher-risk MDS patients. High-risk cytogenetic abnormalities: -7 and inv(3)/t(3q)/del(3q) isolated, two abnormalities including -7/del(7q) and complex abnormalities (≥ 3 abnormalities); low-risk: all others. *Figure created using BioRender.*

For CMML, therapeutic options remain limited, with high rates of morbidity, transformation to AML, and poor OS (28, 52). Approximately 50% of CMML patients derive clinical benefit from HMA therapy, but responses are often transient, and HMAs fail to effectively deplete the HSCs

driving disease progression, leaving the tumor burden largely unaddressed. Consequently, outcomes after AML transformation are dismal, with a median survival of just five months (363, 364). These limitations highlight the urgent need for therapies targeting the mechanisms underlying disease persistence and progression. In CMML, guidelines advocate for risk-based therapy, including the use of targeted agents in patients with specific genetic mutations, alongside HSCT for eligible high-risk individuals.

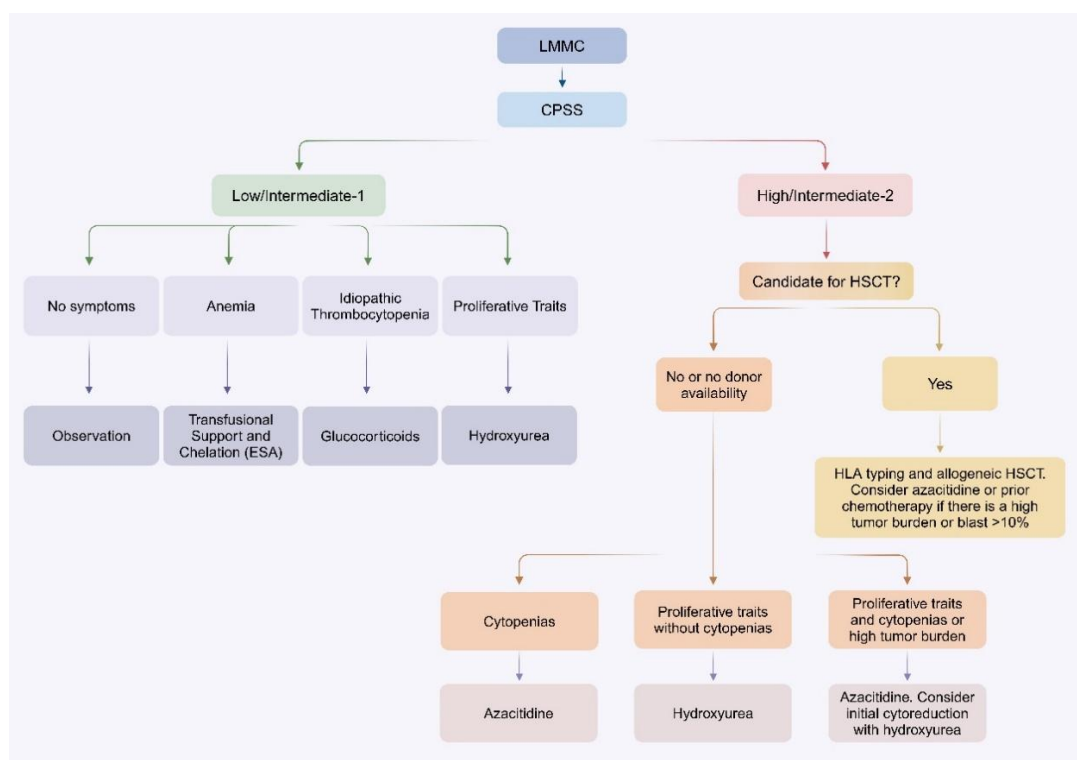


Figure 15. Proposed treatment algorithm for CMML. CMML, Chronic Myelomonocytic Leukemia; CPSS, CMML Prognostic Scoring System; HCT, Hematopoietic Cell Transplant; ESA, Erythropoiesis-Stimulating Agents. Whenever possible, the patient should be included in a clinical trial.

- Consider high risk if: (1) unfavorable prognostic factors are present, such as CPSS-mol: intermediate-2/high, increased BM blast count ($>15\%$ or $>50\%$), severe cytopenias (platelets $<30 \times 10^9/L$, ≥ 2 red blood cell transfusions/month over 6 months, neutrophils $<0.5 \times 10^9/L$) or (2) non-transplant strategies have failed.
- Young patient, good general condition, with no comorbidities.
- Severe leukocytosis (leukocytes $>35 \times 10^9/L$), symptomatic splenomegaly, or other extra-hematologic involvement (e.g., skin infiltration).
- Not indicated: azacitidine in CMML with low/intermediate-1 CPSS and/or proliferative CMML.
- Consider targeted therapies if mutations in *IDH1/2*, *NPM1*, or *FLT3-ITD/TKD* are present.
- It is advisable not to administer concomitantly with azacitidine.

Figure created using BioRender.

Despite incremental improvements in supportive care and the use of HMAs, treatment for MDS and CMML remains largely palliative. In both diseases, HMA therapy typically yields only transient clinical benefits, failing to eradicate the clonal HSCs that drive progression to secondary AML and resulting in dismal outcomes after transformation. Although allogeneic HSCT is the sole potentially curative strategy, it is limited to a small subset of patients due to

advanced age and high transplant-related morbidity. These shortcomings underscore the urgent need for novel, mechanism-based therapies, which will be addressed in the following section.

10.1 Emerging treatments for MDS and CMML: biological rationales and clinical translation

Advances in understanding the molecular and inflammatory mechanisms driving MDS and CMML have paved the way for innovative therapeutic strategies. Both diseases are characterized by abnormal signaling pathways that fuel clonal expansion, immune evasion, and progression to sAML. Key contributors to disease pathology include dysregulated inflammatory networks, and somatic mutations affecting apoptosis, DNA methylation, and chromatin structure.

Emerging treatments are designed to target these underlying mechanisms. Anti-apoptotic protein inhibitors, such as venetoclax, focus on overcoming resistance to cell death and have shown significant promise. Inflammatory pathways, mediated by mutations in genes like *RAS*, are being targeted with agents such as IRAK4 and TLR inhibitors. Meanwhile, therapies targeting inflammatory pathways, driven by mutations in genes like *RAS*, include agents such as IRAK4 and TLR inhibitors. These treatments specifically address the inflammatory microenvironment, which plays a critical role in sustaining disease progression and suppressing immune function (365-367).

Additional novel approaches include epigenetic modulators, signal transduction inhibitors, and immunotherapies, which exploit different vulnerabilities deeply examined in prior sections of this thesis. These targeted therapies offer the potential to improve outcomes by addressing both the intrinsic genetic factors and the extrinsic microenvironmental influences that drive the progression of MDS and CMML.

10.1.1 Therapies targeting anti-apoptotic proteins

Apoptosis, or programmed cell death, is essential for maintaining cellular balance by removing damaged or dysfunctional cells. This process, controlled by intrinsic and extrinsic signaling pathways, is tightly regulated by the BCL2 protein family. The intrinsic apoptosis pathway is triggered by mitochondrial outer membrane permeabilization (MOMP), which

allows the release of cytochrome c into the cytoplasm, activating the apoptosome and downstream caspase signaling (368). The BCL2 protein family is central to regulating this process, with pro-survival proteins (e.g., BCL2, BCL-XL, and MCL1) counteracting pro-apoptotic proteins (e.g., BAX, BAK1, and BH3-only proteins such as BIM, BID, and PUMA) to maintain a delicate balance that preserves mitochondrial integrity (369-371).

Resistance to cell death is a defining feature of cancer progression (99, 372). Overexpression of pro-survival BCL2 family proteins enables cancer cells to evade apoptosis by sequestering pro-apoptotic proteins, thereby preventing MOMP and inhibiting caspase activation. This mechanism has spurred the development of BH3 mimetics—small molecules that mimic BH3-only proteins to antagonize pro-survival BCL2 family members. These agents displace pro-apoptotic proteins, inducing apoptosis in cancer cells with high BCL2 dependency (373).

Venetoclax (ABT-199) is a selective BCL2 inhibitor that disrupts BCL2-mediated survival pathways, promoting BAX and BAK oligomerization to trigger apoptosis (374-376) (**Figure 16**). Since its FDA approval in 2020, venetoclax has markedly improved therapeutic outcomes for AML patients. In older individuals with AML who were not eligible for more aggressive treatment regimens, such as intensive induction chemotherapy, the combination of venetoclax and low-dose cytarabine resulted in high response rates and extended periods of remission (377). Additionally, in previously untreated AML patients who were unable to undergo intensive chemotherapy, those treated with a combination of azacitidine and venetoclax experienced longer overall survival (OS) and higher remission rates compared to those receiving azacitidine alone (378).

The therapeutic potential of venetoclax has also extended to MDS and CMML. A phase Ib trial (NCT02966782) in relapsed/refractory (R/R) MDS patients showed a 39% objective response rate (ORR) when venetoclax was combined with azacitidine (379). Further support came from a phase I/II trial (NCT04160052), where venetoclax combined with azacitidine benefited patients with R/R MDS and CMML (380). Phase II data in high-risk, treatment-naïve MDS patients demonstrated an impressive 80% ORR and a median survival of 26 months. However, resistance to the venetoclax-azacitidine combination remains a challenge, affecting approximately 20% of MDS patients (381, 382). The results of the eagerly anticipated phase III Verona trial (NCT04401748) are expected to provide critical insights into resistance mechanisms and determine whether venetoclax can be incorporated as a newly approved treatment option for high-risk MDS patients, potentially refining therapeutic strategies for this population.

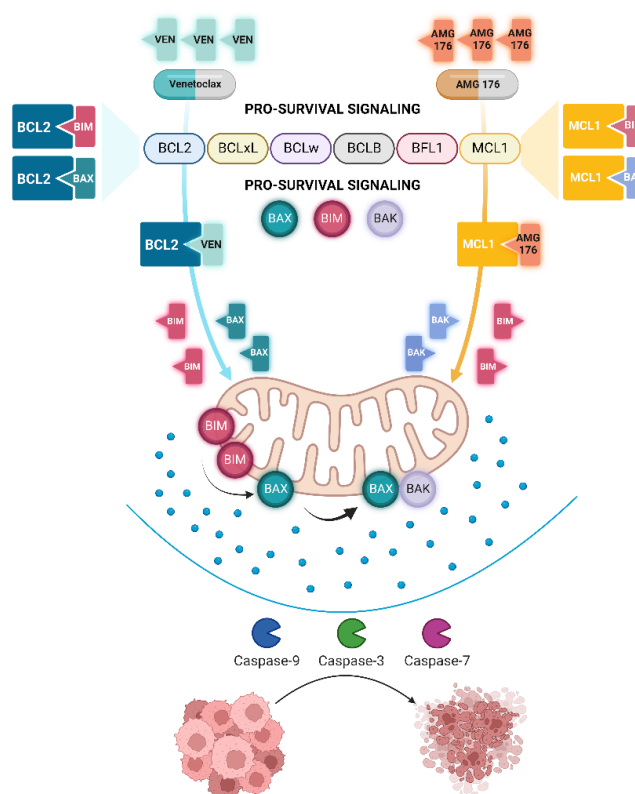


Figure 16. Mechanisms of action of BCL2 and MCL1 inhibition. The anti-apoptotic proteins BCL2 and MCL1 prevent apoptosis by binding to and sequestering the apoptotic effectors BAX/BAK, thereby inhibiting their oligomerization and the initiation of apoptosis. Venetoclax (BCL2) and AMG 176 (MCL1) specifically bind to the BH3 domains of BCL2 and MCL1, respectively. This process disrupts the mitochondrial outer membrane, causing the release of cytochrome c and activating the caspase cascade, ultimately driving cell apoptosis. Adapted from Rodriguez-Sevilla et al. (262).

Preclinical research has provided a deeper understanding of the biological basis for venetoclax resistance and response in MDS and CMML. Molecular profiling of over 400 MDS samples revealed two distinct HSC architectures—long-term HSCs and lymphoid-primed multipotent progenitors (LMPPs)—leading to differentiation along either a CMP or GMP pattern (83). Venetoclax selectively targeted and depleted CMP-pattern HSCs, primarily due to their reliance on BCL2-mediated survival pathways. This depletion was associated with shorter times to achieve complete remission and longer relapse-free survival in clinical studies. In contrast, GMP-pattern HSCs, which are driven by NF- κ B-mediated survival pathways, demonstrated resistance to venetoclax, underscoring the need for alternative therapeutic strategies to address this resistance.

Targeting anti-apoptotic proteins beyond BCL2 offers additional avenues to overcome resistance. GMP-pattern HSCs exhibit upregulation of MCL1, a key effector of NF- κ B signaling and a known driver of venetoclax resistance (345). Preclinical studies indicate that combined

inhibition of BCL2 and MCL1 is effective across MDS subtypes, even in the presence of RAS mutations conferring resistance to venetoclax (383). This rationale has led to a phase I clinical trial of AMG-176, an MCL1 inhibitor, in combination with azacitidine for R/R MDS after HMA failure (NCT05209152). The study's initial phase will establish dosing parameters before extending to venetoclax-naïve and venetoclax-exposed patients, aiming to refine strategies for durable responses in resistant disease

10.1.2 NEDDylation inhibitors

The regulated synthesis, degradation, and clearance of intracellular proteins are essential for maintaining cellular homeostasis. NEDDylation is a multi-step enzymatic process initiated by the NEDD8-activating enzyme (NAE), which conjugates the ubiquitin-like protein NEDD8 (neuronal precursor cell-expressed developmentally downregulated-8) to a conserved lysine residue, thereby promoting protein degradation (384). The best-characterized target of NEDDylation is the cullin-RING E3 ubiquitin ligase (CRL) (385). NEDDylation activates CRLs, enhancing their ability to ubiquitinate substrates that regulate key cellular processes, including cell cycle progression (e.g., p21, p27, cyclin E, c-Myc), DNA damage repair, tumor suppression (e.g., TP53), and stress responses. Elevated levels of NEDD8 and NAE have been observed in cancers such as AML and MDS, where they contribute to tumor growth and enable cells to evade programmed cell death (386, 387)

Pevonedistat (MLN4924), a pioneering NEDDylation inhibitor, targets the adenylation active site of NAE, disrupting CRL activity and triggering several cellular responses, including cell cycle arrest, apoptosis, senescence, and autophagy. Preclinical studies have shown that pevonedistat reduces AML cell colony formation and induces apoptosis *in vitro* (388). Additionally, in AML xenograft models, pevonedistat combined with azacitidine demonstrated synergistic apoptotic effects (389). Clinical evaluations of pevonedistat have yielded promising results. In a phase Ib trial (NCT01814826), pevonedistat combined with azacitidine was well-tolerated in older AML patients ineligible for intensive induction chemotherapy. This combination not only improved response timing and frequency compared to azacitidine alone but also suggested enhanced therapeutic efficacy (390). Subsequently, a phase II trial (NCT03238248) was initiated to assess the combination therapy in patients with MDS refractory to HMA therapy. Preliminary findings from 21 patients with relapsed/refractory (R/R) MDS reported an ORR of 43% (391).

Current clinical trials are investigating the potential of pevonedistat in combination with other agents, including belinostat, fludarabine, and cytarabine, for the treatment of

relapsed/refractory (R/R) MDS (NCT03772925, NCT03813147, and NCT03459859). These studies aim to expand therapeutic options for MDS patients by leveraging NEDDylation inhibition to disrupt tumor cell survival and improve treatment outcomes.

10.1.3 Signal transduction inhibitors

Aberrations in signal transduction pathways are a hallmark of cancer, arising from the activation of oncogenes or the inactivation of tumor suppressor genes (392). These disruptions lead to dysregulated cell cycle progression, uncontrolled proliferation, enhanced survival, and abnormal differentiation of tumor cells. Targeting these pathways offers a promising therapeutic strategy for cancers, including MDS and CMML.

Receptor tyrosine kinases (RTKs) are membrane-bound proteins with intracellular catalytic domains that transmit extracellular signals through intracellular signaling cascades (393). Upon ligand binding, RTKs dimerize, activating their tyrosine kinase domains (TKDs), which then phosphorylate specific residues to initiate downstream signaling pathways (394).

Among these pathways, the RTK-RAS signaling axis is one of the most frequently disrupted in cancer (395, 396). Once activated, RAS proteins stimulate downstream cascades, including the mitogen-activated protein kinase (MAPK) and phosphatidylinositol 3-kinase (PI3K)/protein kinase B (AKT) pathways. These cascades regulate critical processes in tumorigenesis, such as cell survival, metabolism, motility, growth, cell cycle progression, and oncogenic transcription (397). RAS function is inherently dependent on its capacity to bind and hydrolyze GTP. The guanine nucleotide exchange factor (GEF) and GTPase-activating protein (GAP) systems tightly regulate the conversion between the inactive GDP-bound state and the active GTP-bound state of RAS (398). Gain-of-function mutations in RAS isoforms (*HRAS*, *KRAS*, or *NRAS*) are common in many cancers and drive oncogenic transformation by locking RAS in its active, GTP-bound state. This sustains proliferative and survival signaling, providing mutant cells with a growth advantage and making RAS a critical therapeutic target (399). Such alterations provide mutant cells with a significant growth advantage over their normal counterparts and represent a critical target for therapeutic intervention.

While rare in newly diagnosed MDS, RAS-activating mutations are detected in approximately 20% of cases that progress to sAML (334). As a result, therapeutic strategies targeting RAS signaling—either by inhibiting RAS's enzymatic activity or its mediators—are being explored for MDS patients at higher risk of disease progression. One such therapy is rigosertib, a

synthetic benzyl styryl sulfone that selectively disrupts the interaction between RAS and the RAS-binding domain of RAF, a critical effector protein. (400). By blocking downstream MAPK and PI3K/AKT signaling, rigosertib induces cell cycle arrest and apoptosis (401). However, phase III trials (NCT01241500) failed to demonstrate improved survival in MDS patients with excess blasts refractory to HMA therapy (402). Despite these disappointing results, other targeted inhibitors, such as the newly approved KRAS inhibitor MRTX1133 (403), hold promise for patients with *KRAS*-mutant cancer patients.

FMS-like tyrosine kinase 3 (FLT3) is another receptor tyrosine kinase critical for regulating hematopoietic cell survival, proliferation, and differentiation (404). Under normal conditions, FLT3 exists as an inactive monomer but becomes activated upon binding its ligand, FLT3 ligand (FLT3L), triggering receptor dimerization, phosphorylation, and downstream signaling via the PI3K and RAS pathways (405). FLT3 mutations represent common genetic alterations in AML and cause constitutive receptor phosphorylation, leading to the aberrant activation of signaling pathways (406). These mutations include internal tandem duplications (FLT3-ITDs) within the juxtamembrane domain and point mutations in the TKD (FLT3-TKD) (405), with FLT3-ITDs being associated with poor prognosis (407). While FLT3 mutations are infrequent at MDS onset, they are detected in up to 10% of cases progressing to sAML, correlating with accelerated disease transformation and poor outcomes (408).

FLT3 inhibitors are classified into two categories: first-generation multi-kinase inhibitors, such as sorafenib, lestaurtinib, and midostaurin, and next-generation selective inhibitors, including quizartinib, crenolanib, and gilteritinib (409). Current clinical trials (e.g., NCT03661307, NCT04493138, NCT01892371) have yet to provide conclusive evidence regarding the benefit of FLT3 inhibition in this context. Given the significant overlap between MDS progression to sAML and FLT3-mediated pathogenesis, additional studies are urgently needed to clarify the therapeutic potential of FLT3 inhibitors. These investigations should focus on identifying the MDS subpopulations most likely to benefit from FLT3 inhibition and optimizing treatment regimens to address this unmet need. A deeper understanding of the molecular and clinical characteristics of these patients will be critical to advancing targeted therapies for high-risk MDS and CMML.

10.1.4 Isocitrate dehydrogenase inhibitors

Isocitrate dehydrogenase (IDH) is an essential enzyme in the tricarboxylic acid cycle, responsible for catalyzing the reversible conversion of isocitrate into α -ketoglutarate (α -KG).

Heterozygous gain-of-function mutations in *IDH1* and *IDH2* occur in up to 20% of de novo AML patients (410) and 4–12% of newly diagnosed MDS cases (411) carry *IDH1/2* heterozygous gain-of-function mutations affecting the amino acids R132, R172, and R140 (411, 412). These mutations disrupt the normal enzymatic activity of IDH1/2, leading to the production of the oncometabolite 2-hydroxyglutarate (2-HG) in place of α -KG (413, 414). Elevated 2-HG levels inhibit α -KG-dependent dioxygenases, including TET2 and histone demethylases, resulting in aberrant DNA and histone hypermethylation, which impairs hematopoietic differentiation and promotes malignant transformation (415, 416).

IDH1/2 mutations are predominantly found in MDS patients with prior treatment failure, highlighting their role in disease progression (417). The oral agents enasidenib and ivosidenib specifically target *IDH2*- and *IDH1*-mutant cells, respectively, suppressing 2-HG production and promoting differentiation of tumoral cells without causing BM aplasia

Enasidenib (AG-221), a selective IDH2 inhibitor, reduces 2-HG production, promotes cellular differentiation, and avoids BM aplasia. Approved by the FDA in August 2017, enasidenib demonstrated an ORR of 40% in a phase I/II trial involving 239 relapsed/refractory (R/R) *IDH2*-mutated AML patients, including 30 cases progressing from MDS (418). Notably, objective better responses were reported in patients with *IDH2*^{R172} mutations than in those with *IDH2*^{R140} mutations (53.3% vs. 35.4%). More recently, a phase II study (NCT03383575) showed that enasidenib, either alone or combined with azacitidine, is effective in treatment-naïve high-risk MDS patients or those with HMA-refractory disease (419). Similarly, ivosidenib (AG-120), a selective IDH1 inhibitor, received FDA approval in July 2018. In a phase I trial (NCT02074839) involving 179 R/R *IDH1*-mutated AML patients, ivosidenib demonstrated durable remissions with minimal adverse effects, achieving molecular remissions and transfusion independence in some patients (420).

Newer IDH inhibitors are under clinical investigation, including olutasidenib (FT-2102), a potent and selective oral IDH1 inhibitor. Olutasidenib is being evaluated in a phase I/II trial (NCT02719574) either as a monotherapy or in combination with azacitidine or cytarabine for R/R MDS and AML patients (421).

Despite these advances, IDH inhibitors are not curative, likely due to the subclonal nature of *IDH1/2* mutations and their cooperation with other driver mutations, such as *SRSF2*, in promoting leukemogenesis (422). To improve long-term outcomes, future studies must focus on developing combination strategies that target cooperative pathways alongside IDH inhibition.

10.1.5 Inflammation pathway inhibitors

The disruption of innate immune and inflammatory signaling pathways is a defining characteristic of both MDS and CMML (423, 424). To evade immune surveillance, malignant cells deploy various mechanisms, such as reducing their antigenic and/or immunogenic properties and inducing an immunosuppressive microenvironment within the tumor (425). A key contributor to ineffective hematopoiesis in MDS is the aberrant activation of Toll-like receptor (TLR) signaling, which has gained attention as a potential therapeutic target (426-428).

TLRs are pattern-recognition receptors that initiate innate immune responses by detecting extracellular pathogens through pathogen-associated molecular patterns or intracellular damage via damage-associated molecular patterns (429). In humans, 10 TLRs are expressed across a variety of immune cells—such as neutrophils, macrophages, dendritic cells, natural killer cells, and B and T lymphocytes—as well as in non-immune cells like fibroblasts, endothelial cells, and epithelial cells. In HSPCs, TLR activation leads to dimerization of the Toll/interleukin-1 receptor domain, recruiting adaptor proteins such as MyD88 (430), which in turn activates downstream pathways mediated by IRAK family kinases. This results in the production of inflammatory cytokines through interferon regulatory mechanisms (431).

In cancer, TLRs are often overexpressed, with their role in tumor progression varying depending on the cellular context. In MDS, overexpression of TLR2, TLR4, TLR6, and MyD88 in HSPCs contributes to disease pathology. For instance, TLR2 activation induces JMJD3-mediated histone demethylation, which enhances NF- κ B signaling and disrupts erythropoiesis (432). This understanding has led to clinical trials targeting TLR pathways. A phase I/II trial (NCT02363491) investigating tomaralimab (OPN-305), a monoclonal antibody against TLR2, in heavily pretreated transfusion-dependent MDS patients with low- to intermediate-risk disease post-HMA failure, reported an ORR of 50%, indicating that TLR2 inhibition can restore erythropoiesis in specific subsets of patients (433).

Another key mediator of inflammatory signaling is interleukin-1 receptor-associated kinase 4 (IRAK4), which is central to TLR and interleukin-1 receptor-induced activation of the NF- κ B pathway, triggering survival in many cancer types (434). Preclinical studies in MDS and AML have revealed that mutations in U2AF1 and SF3B1 lead to dysregulated splicing of IRAK4, generating a longer isoform (IRAK4-L) that retains exon 4 (435, 436). This isoform amplifies NF- κ B pathway activation compared to the shorter isoform. Genetic inhibition of IRAK4-L expression promotes AML cell differentiation and reduces tumor burden *in vivo*. These findings highlight the potential of targeting IRAK4 to modulate the innate immune system in

hematologic malignancies (437). Furthermore, IRAK signaling has been linked to adaptive resistance in FLT3-mutant AML, underscoring its broader relevance in hematologic malignancies.

These findings paved the way for the development of emavusertib (CA-4948), an oral inhibitor targeting both IRAK4 and FLT3. A phase I/II trial (NCT04278768) demonstrated that emavusertib, either alone or combined with azacitidine or venetoclax, showed efficacy in patients with *SF3B1*, *U2AF1*, or *FLT3* mutations. Among seven MDS patients with spliceosome mutations, 57% achieved marrow complete remission, and one patient attained red blood cell transfusion independence (438).

Other inflammatory pathways, including IL-6, TGF- β , and TNF- α , have also emerged as promising therapeutic targets in MDS and CMML. Despite its role in MDS pathogenesis, targeting IL-6 has shown limited success. For instance, a phase II trial of siltuximab, an anti-IL-6 monoclonal antibody, failed to reduce transfusion burden and was terminated early (439). In contrast, Targeting the TGF- β pathway has shown greater potential in addressing hematopoietic dysfunction. This pathway inhibits hematopoiesis by activating SMAD signaling in HSPCs, and low levels of SMAD7, a natural inhibitor of this process, further worsen the differentiation block. Agents such as galunisertib, a TGF- β receptor kinase inhibitor, have demonstrated the ability to restore hematopoietic differentiation (440), while luspatercept, which was recently approved by the FDA, targets activins within the TGF- β superfamily to promote late-stage erythropoiesis (355). Sotatercept, another activin-targeting agent, has similarly shown potential in restoring hematopoiesis (441). TNF- α , a cytokine involved in bone marrow dysfunction, has also been explored as a therapeutic target. Inhibitors like infliximab and etanercept have shown mixed results. While infliximab yielded a modest ORR of 13.6% in lower-risk MDS patients (NCT00074074), etanercept achieved a higher ORR of 73% in a phase II trial (NCT00118287). However, long-term follow-up revealed no significant impact on the natural course of the disease (442). However, long-term follow-up revealed no significant impact on the natural course of the disease.

These emerging therapies highlight the growing understanding of how inflammatory pathways contribute to MDS and CMML pathogenesis. Future research will be crucial to refine these strategies, optimize their use in combination with existing treatments, and identify the patient populations most likely to benefit.

10.1.6 Immune Checkpoint Inhibitors and T Cell-Based Therapeutic Strategies

Advancements in immunotherapy have opened new avenues for treating MDS and CMML by addressing immune dysregulation that contributes to disease progression and therapeutic resistance. Among these, immune checkpoint inhibitors (ICIs) and T cell-based strategies, such as CAR T cells and bispecific T cell engagers (BiTEs), aim to restore the immune system to effectively target malignant cells.

Over the last decade, the development of immune checkpoint inhibitors targeting CTLA-4 and PD-1 has revolutionized cancer treatment by enhancing T cell-mediated antitumor responses (443). However, their efficacy in the MDS/CMML setting remains limited. For instance, pembrolizumab, a PD-1 inhibitor, showed minimal efficacy as a standalone treatment in intermediate-1/2 and high-risk MDS patients who failed HMA therapy (KEYNOTE-013; NCT01953692) (444). Even in combination with azacitidine, pembrolizumab yielded only a modest ORR of 25% (NCT03094637). Similarly, a basket trial evaluating nivolumab and ipilimumab, targeting PD-1 and CTLA-4, reported limited efficacy in HMA-refractory MDS patients (NCT02530463), suggesting that checkpoint may only benefit specific patient subsets (445). TIM-3, another immune checkpoint, has gained attention due to its expression on both T cells and MDS stem cells, contributing to immune evasion (446). Despite initial promise, TIM-3 inhibitors like sabatolimab have not shown significant improvement over HMA monotherapy in phase III trials (164, 447)

CAR T cell therapy has transformed the treatment of lymphoid malignancies (448-450), but its application in myeloid diseases like MDS and CMML has faced significant challenges. Candidate antigens such as CD123 and CD33 are expressed on both leukemic cells and normal HSCs, increasing the risk of severe off-target toxicities, including prolonged myeloablation (451). Despite these risks, preclinical studies using CAR T cells targeting CD123 or CD33 in xenograft models of MDS and CMML have shown robust efficacy in eliminating leukemic clones, providing a strong rationale for further research (452, 453).

One promising approach is CYAD-01, a CAR T cell product based on the NKG2D receptor, which recognizes stress-induced ligands frequently expressed on malignant cells. A phase I trial demonstrated that CYAD-01 had a tolerable safety profile and preliminary anti-leukemic activity in relapsed or refractory AML and multiple myeloma, with one MDS patient achieving marrow complete remission (454). NKG2D, an activating immunoreceptor, binds to a range of MHC class I-like self-molecules overexpressed in hematological malignancies while being minimally expressed on normal cells,(455), making it an attractive target for CAR T cell therapy

in myeloid cancers (456, 457). However, challenges such as the scalability and feasibility of autologous CAR T cell therapies persist, especially for heavily pretreated MDS patients. Allogeneic CAR T cell therapies, manufactured from healthy donor cells, offer a potential solution by reducing production costs and treatment delays. Nevertheless, issues like graft-versus-host disease and immune rejection must be addressed before these therapies can be widely implemented (458, 459).

A novel class of immunotherapeutic agents, bispecific T cell engagers (BiTEs), is designed to enhance T cell-mediated cytotoxicity by simultaneously binding CD3 on T cells and tumor-specific antigens, thereby promoting targeted immune responses (460). Key targets for BiTEs in myeloid malignancies include CD123 and CD33, both of which are frequently expressed in relapsed/refractory (R/R) MDS and AML. Early-phase trials have demonstrated that BiTEs targeting these antigens can effectively engage T cells and trigger antitumor responses (461). Vibeotamab (NCT05285813) and APVO436 (NCT03647800) are examples of CD3-CD123 BiTEs that have shown preliminary efficacy in R/R MDS and CMML. While these results are encouraging, further studies are needed to identify the most responsive patient subgroups and determine the optimal timing for these interventions (462).

Immune checkpoint inhibitors and T cell-based therapies represent a rapidly growing field of innovation in the treatment of MDS and CMML. Advances in understanding the mechanisms of immune evasion have paved the way for these targeted approaches, offering the potential to overcome the limitations of conventional treatments and improve patient outcomes. However, challenges remain, including the need for precise antigen targeting, optimizing therapeutic combinations, and determining the best timing for interventions to ensure a balance between efficacy and safety

11. Published Reviews Contributing To The Doctoral Framework

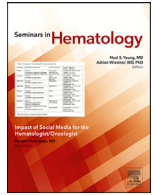
In accordance with the UB 2024 guidelines, this section presents two peer-reviewed literature reviews authored during the development of this doctoral thesis: *"Inflammation in myelodysplastic syndrome pathogenesis"* and *"T-cell dysfunctions in myelodysplastic syndromes"*. While these publications are not listed as primary articles of the thesis, they provide comprehensive theoretical foundations and contextual analysis that complement the research presented herein. Both reviews offer a thorough overview of the current state of immune dysregulation in myelodysplastic syndromes.

First Review

Inflammation in myelodysplastic syndrome pathogenesis

Rodriguez-Sevilla JJ, Colla S

Seminars in Hematology 2024 December; 61(6):385-396.
2024 Impact Factor 5.0
Quartile 1



Inflammation in myelodysplastic syndrome pathogenesis

Juan Jose Rodriguez-Sevilla*, Simona Colla*

Department of Leukemia, The University of Texas MD Anderson Cancer Center, Houston, TX

ARTICLE INFO

Keywords:

Clonal cytopenia of undetermined significance
Clonal hematopoiesis of indeterminate potential
Hematopoietic stem cells
Inflammation
Myelodysplastic syndromes

ABSTRACT

Inflammation is a key driver of the progression of preleukemic myeloid conditions, such as clonal hematopoiesis of indeterminate potential (CHIP) and clonal cytopenia of undetermined significance (CCUS), to myelodysplastic syndromes (MDS). Inflammation is a critical mediator in the complex interplay of the genetic, epigenetic, and microenvironmental factors contributing to clonal evolution. Under inflammatory conditions, somatic mutations in *TET2*, *DNMT3A*, and *ASXL1*, the most frequently mutated genes in CHIP and CCUS, induce a competitive advantage to hematopoietic stem and progenitor cells, which leads to their clonal expansion in the bone marrow. Chronic inflammation also drives metabolic reprogramming and immune system deregulation, further promoting the expansion of malignant clones. This review underscores the urgent need to fully elucidate the role of inflammation in MDS initiation and highlights the potential of the therapeutic targeting of inflammatory pathways as an early intervention in MDS.

© 2024 Elsevier Inc. All rights are reserved, including those for text and data mining, AI training, and similar technologies.

Introduction

Inflammation is an evolutionarily well-conserved and complex mechanism essential for responding to infection and injury and maintaining tissue homeostasis. Chronic inflammation, commonly observed with aging, occurs when acute inflammatory mechanisms fail to eliminate tissue injury, resulting in persistent, low-grade proinflammatory states [1]. Thus, although it is initially protective, inflammation can become maladaptive and detrimental, contributing to the pathogenesis of various diseases, including myeloid neoplasms.

Hematopoietic stem cells (HSCs) are a functionally heterogeneous cell population that plays a crucial role in the systemic inflammatory response [2,3]. HSCs integrate external inflammatory signals into cellular responses, establishing a demand-adapted axis between peripheral stresses and hematopoietic responses [4]. As individuals age, hematopoietic stem and progenitor cells (HSPCs) in the bone marrow (BM) lose their self-renewal capabilities, gain enhanced myeloid differentiation, and develop impaired immune surveillance, thereby increasing disease susceptibility [5]. This progressive loss of fitness is influenced by a phenomenon known as "inflammaging," which is characterized by chronic, low-grade in-

flammation; elevated levels of proinflammatory cytokines, such as interleukin 6 (IL-6) and tumor necrosis factor- α (TNF- α) and proinflammatory cellular activity [6]. Chronic proinflammatory signaling from infections or repetitive sterile inflammation negatively impacts HSPCs' self-renewal, leading to their loss of quiescence and increased differentiation [7–10]. The impairment of HSCs' functions is primarily due to these cells' increased proliferation rather than a systemic inhibitory effect on hematopoiesis [11]. A persistent inflammatory state contributes to the aging-related changes in the HSC compartment and the progressive accumulation of DNA damage and somatic mutations. Although most of these mutations do not have a phenotypic effect, some may endow mutant cells with a proliferative advantage, facilitating their clonal expansion over normal HSPCs. In the absence of overt hematologic disease, this phenomenon is termed clonal hematopoiesis of indeterminate potential (CHIP).

Increasing evidence supports the role of inflammatory signaling in the pathogenesis of hematological diseases, including myelodysplastic syndromes (MDS) [12,13]. Inflammatory molecules, such as interferon- γ (IFN- γ), IL-1 β , and TNF- α , can drive premalignant clonal expansion, particularly in the setting of CHIP induced by HSPC clones carrying mutations in the *tet methylcytosine dioxygenase 2* gene, *TET2*, or the DNA methyltransferase 3 alpha gene, *DNMT3A*. Indeed, unlike their normal counterparts, these clones are intrinsically resistant to inflammation-mediated depletion [14–17]. Therefore, inflammation-induced HSCs' extrinsic alterations induce a selective

* Corresponding authors at: Department of Leukemia, The University of Texas MD Anderson Cancer Center, Houston, TX 77030.

E-mail addresses: jrsevilla@mdanderson.org (J.J. Rodriguez-Sevilla), scolla@mdanderson.org (S. Colla).

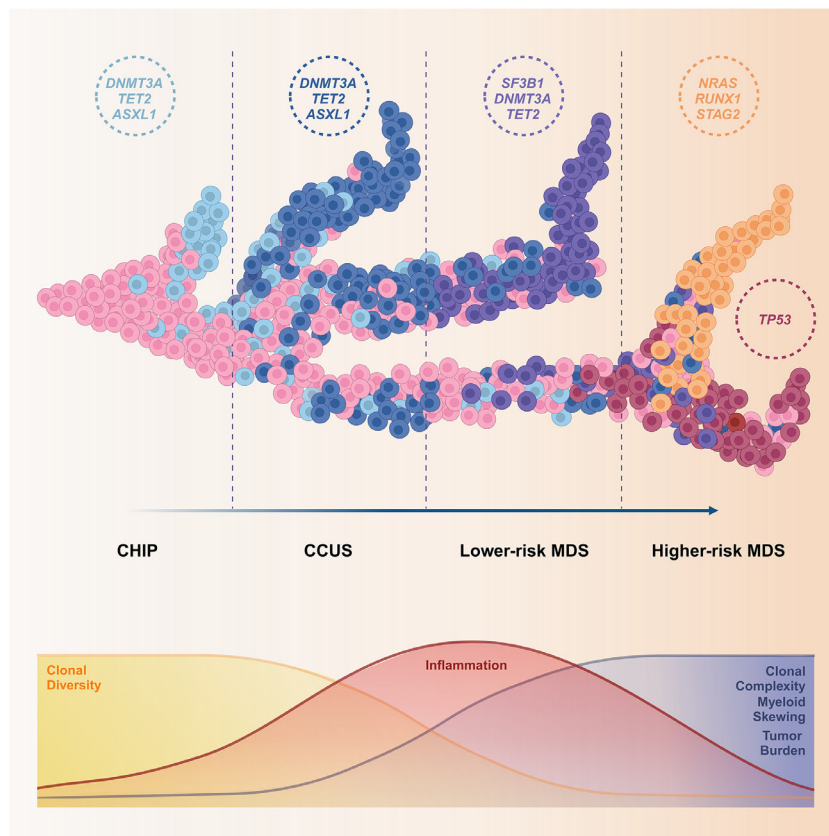


Fig. 1. Clonal evolution across the spectrum of myeloid neoplasms. Schematics of the clonal progression from the pre-leukemic stages of CHIP and CCUS to overt disease, divided into lower-risk and higher-risk MDS. Colored circles represent the clonal architecture of different mutant clones. Key mutations associated with each stage are indicated within dashed circles. The most frequent mutations in CHIP and CCUS are *DNMT3A*, *TET2*, and *ASXL1*. Lower-risk MDS, characterized by an indolent disease course and favorable prognosis, are characterized mainly by mutations in the *SF3B1* splicing gene. Higher-risk MDS is a more aggressive disease carrying additional mutations in *TP53*, *RUNX1*, *STAG2*, and *RAS* pathway genes.

pressure under which mutations in epigenetic modifiers, such as *DNMT3A* and *TET2*, confer a proliferative advantage, which leads to these cells' clonal expansion.

The nucleotide-binding oligomerization, leucine-rich repeat, and pyrin domains-containing protein 3 (NLRP3) inflammasome, a key biological driver of MDS, triggers pyroptosis, a type of inflammation-mediated cell death [18], causing ineffective hematopoiesis, particularly in the setting of mutations in *TET2* and the ASXL transcriptional regulator 1 gene, *ASXL1* [19]. NLRP3 activation and inflammasome formation are driven by cell-extrinsic signals (e.g., Toll-like receptor [TLR] activation) and cell-intrinsic signals (e.g., somatic mutations). The NLRP3 inflammasome also catalyzes the release of the proinflammatory cytokines IL-1 β and IL-18, which, along with IL-6, TNF- α , and IL-8, support the growth of aberrant MDS stem cells in preclinical models [15,20,21].

Myeloid continuum in mds pathogenesis

Hematologic malignancies arise from the expansion of mutated HSC clones with aberrant proliferation or differentiation. Depending on their genetic alterations, these clones induce different heterogeneous phenotypes.

CHIP is a risk factor for hematologic malignancies and for various chronic comorbidities, such as cardiovascular, autoimmune, or autoinflammatory diseases [22–24]. CHIP may evolve into clonal cytopenia of undetermined significance (CCUS), in which clonally expanded cells are associated with persistent and unexplained cytopenia (Fig. 1). Compared with MDS, CCUS has a lower mutation burden, less genetic complexity, and no evidence of dysplasia [25–

28]. However, like MDS patients, CCUS patients have peripheral blood cytopenias and often require transfusions [29]. CCUS is considered a premalignant phase of MDS.

MDS are a group of clonal hematopoietic disorders characterized by ineffective hematopoiesis and a propensity to progress to acute myeloid leukemia (AML). A progressive transition between CHIP, CCUS, and MDS is thought likely [27], with CCUS representing an intermediate stage among the clonal hematopoietic disorders (Fig. 1). *DNMT3A*, *TET2*, and *ASXL1* mutations occur in 70–80% of patients with CHIP or CCUS [30]. In patients with MDS, these genes are associated with an increased tumoral burden and a distinct co-mutational landscape [27].

The transition from CHIP to CCUS and ultimately to MDS involves a complex interplay of genetic, epigenetic, and microenvironmental factors, among which inflammation acts as a critical mediator. This review delves into inflammation's multifaceted role in MDS pathogenesis and emphasizes its impact on HSC function, clonal fitness, immune response, and cellular metabolism during different stages of the disease.

Inflammation and clonal fitness

Inflammation can disrupt the equilibrium among HSC self-renewal, proliferation, and differentiation, a relationship that is pivotal in maintaining blood cell homeostasis. Quiescent HSCs respond to stress, such as that arising from severe infections or systemic inflammation, by increasing their proliferation rate and adapting hematopoiesis output [31,32]. Chronic inflammation may predispose HSCs to the acquisition of somatic mutations by in-

ducing selective pressure, and it can enhance the clonal selection and expansion of aberrant populations by dictating hematopoietic cell fate and differentiation through aberrant proinflammatory signaling [33]. For example, TNF- α signaling promotes HSC survival and induces myeloid differentiation by activating the nuclear factor kappa-light-chain-enhancer of activated B cells (NF- κ B) pathway [34]. Similarly, acute stimulation with IL-1 enhances HSCs' proliferation and promotes their myeloid differentiation, whereas chronic stimulation with IL-1 leads to these cells' regenerative exhaustion [8].

In an inflammatory environment, *DNMT3A*, *TET2*, and *ASXL1* mutations confer a significant competitive advantage to HSCs, possibly because they confer resistance to the deleterious effects of inflammation, such as apoptosis and exhaustion [35–37]. *TET2* plays a pivotal role in the maintenance of HSCs by controlling 5-hydroxymethylcytosine levels at genes that regulate these cells' self-renewal, proliferation, and differentiation [38]. The depletion of *TET2* confers to HSCs a survival advantage and a proliferative phenotype in response to inflammatory challenges [35,39,40]. In studies of competitive clonal hematopoiesis in chimeric mouse models, *tet2*-depleted HSPCs exposed to lipopolysaccharide had higher repopulation rates and elevated serum levels of IL-6, TNF- α , and chemokine ligand 2 (CCL2), indicating an ongoing proinflammatory phenotype [35] (Fig. 2A). Moreover, IL-1 administration significantly expanded *tet2*-depleted HSPCs by enhancing their self-renewal and inhibiting the demethylation of transcription factor binding sites regulating terminal differentiation [41]. The genetic deletion of *Il-1r1* or pharmacologic inhibition of IL-1 β signaling reduced myeloid expansion and clonal evolution [42] and balanced the proinflammatory state [43]. In a colitis model, disrupting the intestinal barrier drove the clonal expansion of *tet2*-depleted HSPCs in an IL-6- and bacterial pathogen-dependent manner [39], whereas antibiotic and anti-TNF- α therapies mitigated these cells' expansion (Fig. 2B). These results show that pathogen-associated inflammatory signaling has a role in triggering the growth of clonal populations [44].

Chronic *Mycobacterium avium* infection conferred a competitive advantage to *dnmt3a*-depleted HSPCs transplanted into mice [15]. The depletion of the IFN- γ receptor gene *Ifngr* rescued this advantage (Fig. 2C). Without chronic infection, IFN- γ promoted the competitive advantage of *dnmt3a*-depleted HSPCs, suggesting that IFN- γ signaling is sufficient to improve these cells' fitness. These results are supported by the observation that *DNMT3A* clonal burden is correlated with IFN- γ serum levels in patients with ulcerative colitis [45] (Fig. 2B).

In a zebrafish model of clonal HSPC expansion, frameshift mutations in *asxl1* led to an increased transcriptional inflammatory gene signature in mature myeloid cells but an anti-inflammatory gene signature in myeloid progenitor cells (Fig. 2D). In this setting, the CRISPR-adapted deletion of the anti-inflammatory nuclear receptor subfamily 4A1 gene, *nr4a1*, inhibited HSCs' clonal expansion, which suggests that the clonal fitness of the *asxl1*-mutant clones was driven by their enhanced resistance to the inflammatory signals activated by their mutant mature progeny [46].

CCUS HSPCs exhibit an enhanced myeloid-biased differentiation trajectory characterized by an increased frequency of committed myeloid progenitors and early myeloid or lymphoid progenitors [47]. However, compared with elderly healthy donors, CCUS patients have significantly fewer BM CD34⁺CD38⁻ HSCs and CD34⁺CD38⁺ HSPCs, which demonstrates that myeloid priming is the result of aberrant differentiation towards the myeloid lineage rather than a numerical expansion of downstream myeloid progenitor cells. Further transcriptomic analysis showed that HSCs from CCUS patients had significantly upregulated expression genes involved in the TNF α -mediated NF- κ B pathway, including the downstream target IL-1 β , compared with those from elderly healthy

donors. Given that chronic IL-1 β exposure drives HSC differentiation towards myelopoiesis at the expense of erythropoiesis and lymphopoiesis, these results may explain why CCUS HSCs are myeloid-primed [47]. These data demonstrate that CCUS HSCs with MDS driver mutations evade aging-induced phenotypic degeneration and exhibit aberrant myeloid skewing, possibly because of enhanced inflammatory signaling-induced expansion.

Integrative molecular profiling of more than 400 MDS patient samples revealed that MDS HSCs in one of 2 differentiation states, long-term HSCs or lymphoid-primed multipotent progenitors, give rise to distinct patterns of progenitor differentiation (a "common myeloid progenitor pattern" or a "granulocytic-monocytic progenitor pattern," respectively) [48]. Extensive preclinical and clinical analyses suggest that MDS is maintained by one of 2 conserved, hierarchically distinct cellular architectures in which cell type-specific survival pathways drive therapy resistance and disease progression. RNA sequencing analysis demonstrated that long-term HSCs from patients with "common myeloid progenitor pattern" MDS progressing to a blast phase after hypomethylating agent therapy failure exhibited significant upregulation of proliferation- and survival-promoting genes, including the BCL2 apoptosis regulator gene, *BCL2*. In contrast, lymphoid-primed multipotent progenitors from patients with "granulocytic-monocytic progenitor pattern" MDS showed the significant upregulation of genes involved in the TNF- α -induced NF- κ B signaling pathway, which was associated with an increase in phospho-NF- κ B/p65⁺ blasts and showed a decreased expression of genes involved in the regulation of cell proliferation and mitochondrial respiration. This proinflammatory signature suggests that lymphoid-primed multipotent progenitors lose their differentiation capability and acquire a protective, stem cell-like quiescent state during disease progression.

In summary, these data suggest that inflammation selects the expansion of HSPCs with CHIP-associated driver mutations by creating a supportive niche for leukemic stem cells. Each mutation engages different cytokine-specific pathways and alters gene expression to sustain the inflammatory response. Although the cell-autonomous proliferation of mutant HSPCs contributes to these cells' expansion, the proinflammatory environment is a major determinant of these cells' clonal dominance, which suggests that mutant HSPCs not only gain a proliferative advantage in an inflammatory microenvironment but also perpetuate a self-reinforcing inflammatory cytokine milieu.

Inflammation and the immune system

Inflammation and immunity are intrinsically linked. Inflammatory signals drive immune cell activation and response, and the balance between proinflammatory and anti-inflammatory signals is crucial for maintaining immune homeostasis [49]. Immune dysregulation, a hallmark of MDS, significantly affects hematopoiesis and alters both innate and adaptive immunity through the secretion of pro and anti-inflammatory cytokines [13]. T cell-mediated immune imbalance is driven by cell-intrinsic and -extrinsic factors that lead to immune exhaustion, the loss of immune surveillance, and the expansion of mutant clones.

Adaptive immune function declines under unresolved and chronic inflammation. Under inflammatory stimuli, T cells develop a restricted T-cell receptor repertoire and decreased memory cell potential [50], and B cells display reduced antibody diversity [51]. These inflammation-induced responses result in immune deregulation, which increases the levels of circulating proinflammatory cytokines, thus promoting the persistent infiltration of macrophages and neutrophils and hampering tissue homeostasis [52]. Thus, chronic inflammation leads to immune dysregulation, which affects immune surveillance and predisposes individuals to cancer, including MDS.

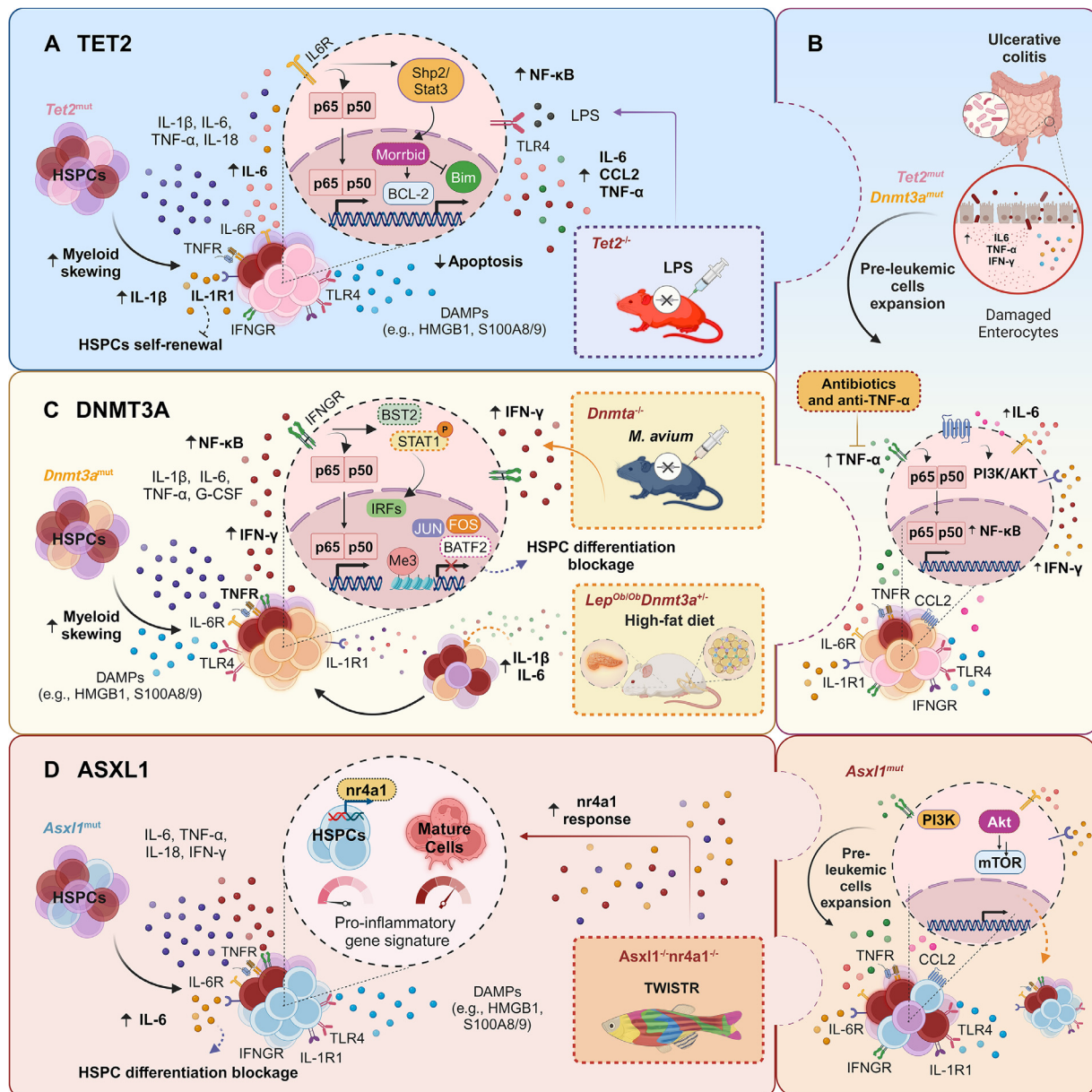


Fig. 2. Current working models of hematopoietic clonal fitness driven by *TET2*, *DNMT3A*, and *ASXL1* mutations under chronic inflammation. (A) *Tet2*-mutant HSPCs undergo enhanced myeloid differentiation and clonal expansion through proinflammatory signals (e.g., IL-6, IL-1 β , and TNF- α), which promote the hyperactivation of the NF- κ B and Shp2/Stat3 pathways and induce a selective advantage of *TET2* mutant clones. In *tet2* knockout mouse models, exposure to LPS induces a proinflammatory phenotype characterized by the secretion of IL-6, TNF- α , and CCL2, which reinforces clonal fitness. (B) Colitis murine models show that intestinal barrier disruption induces clonal expansion of *tet2*- and *dnt3a*-depleted HSPCs, which is mediated by IL-6 and IFN- γ , respectively. (C) *Dnmt3a*-depleted HSPCs are influenced by the inflammatory microenvironment through IFN- γ secretion, as demonstrated by studies using *Mycobacterium avium* exposure. In *Lep^{Ob/Ob}* mice, heterozygous *dnt3a* deletion leads to bone marrow adipocyte accumulation and increased secretion of IL-6, IL-1 β , and TNF- α , sustaining the inflammatory milieu and promoting malignant expansion. (D) *Asxl1*-mutant HSPCs exhibit increased resistance to inflammatory signals via nr4a1, a critical factor in promoting clonal expansion. Biallelic loss of *nr4a1* disrupts the ability of *asxl1*-mutant clones to establish clonal dominance. Hyperactive AKT/mTOR signaling induced by *ASXL1* mutations results in aberrant proliferation and HSC dysfunction associated with DNA damage accumulation.

Akt = protein kinase B; BATF2 = basic leucine zipper ATF-like transcription factor 2; Bcl-2 = B-cell lymphoma 2; BST2 = bone marrow stromal antigen 2; CCL2 = C-C motif chemokine ligand 2; DAMPs = damage-associated molecular patterns; FOS = FBJ murine osteosarcoma viral oncogene homolog; G-CSF = granulocyte colony-stimulating factor; HMGB1 = high mobility group box 1; HSPCs = hematopoietic stem and progenitor cells; IFN- γ = interferon gamma; IFNGR = interferon gamma receptor; IL-1R1 = interleukin 1 receptor type 1; IL6R = interleukin 6 receptor; IRF1 = interferon regulatory factor 1; JUN = AP-1 transcription factor subunit; LPS = lipopolysaccharide; Me3 = trimethylation; *M. Avium* = *Mycobacterium avium*; Morb1 = myeloid RNA regulator of bim-induced death; mTOR = mammalian target of rapamycin; NF- κ B = nuclear factor kappa B; nr4a1 = nuclear receptor subfamily 4 group A member 1; PI3K = phosphoinositide 3-kinase; S100A8/9 = calprotectin; STAT1 = signal transducer and activator of transcription 1; TLR4 = toll-like receptor 4; TNF- α = tumor necrosis factor alpha; TNFR = tumor necrosis factor receptor; TWISTR = tissue editing with inducible stem cell tagging via recombination.

In CHIP, somatic mutations in *DNMT3A*, *TET2*, and *ASXL1* can intrinsically lead to altered immune signaling (Fig. 3). The effects of CHIP-related loss-of-function mutations involving epigenetic regulators have been studied extensively to improve the efficacy of chimeric antigen receptor (CAR) T-cell therapies for hematologic

cancers after the unexpected finding that CAR T cells originated from a single clone in which lentiviral vector-mediated insertion of the CAR transgene disrupting the *TET2* gene induced complete remission in a patient with chronic lymphocytic leukemia. Indeed, *TET2*-deficient CAR T cells exhibit an abnormal epigenetic land-

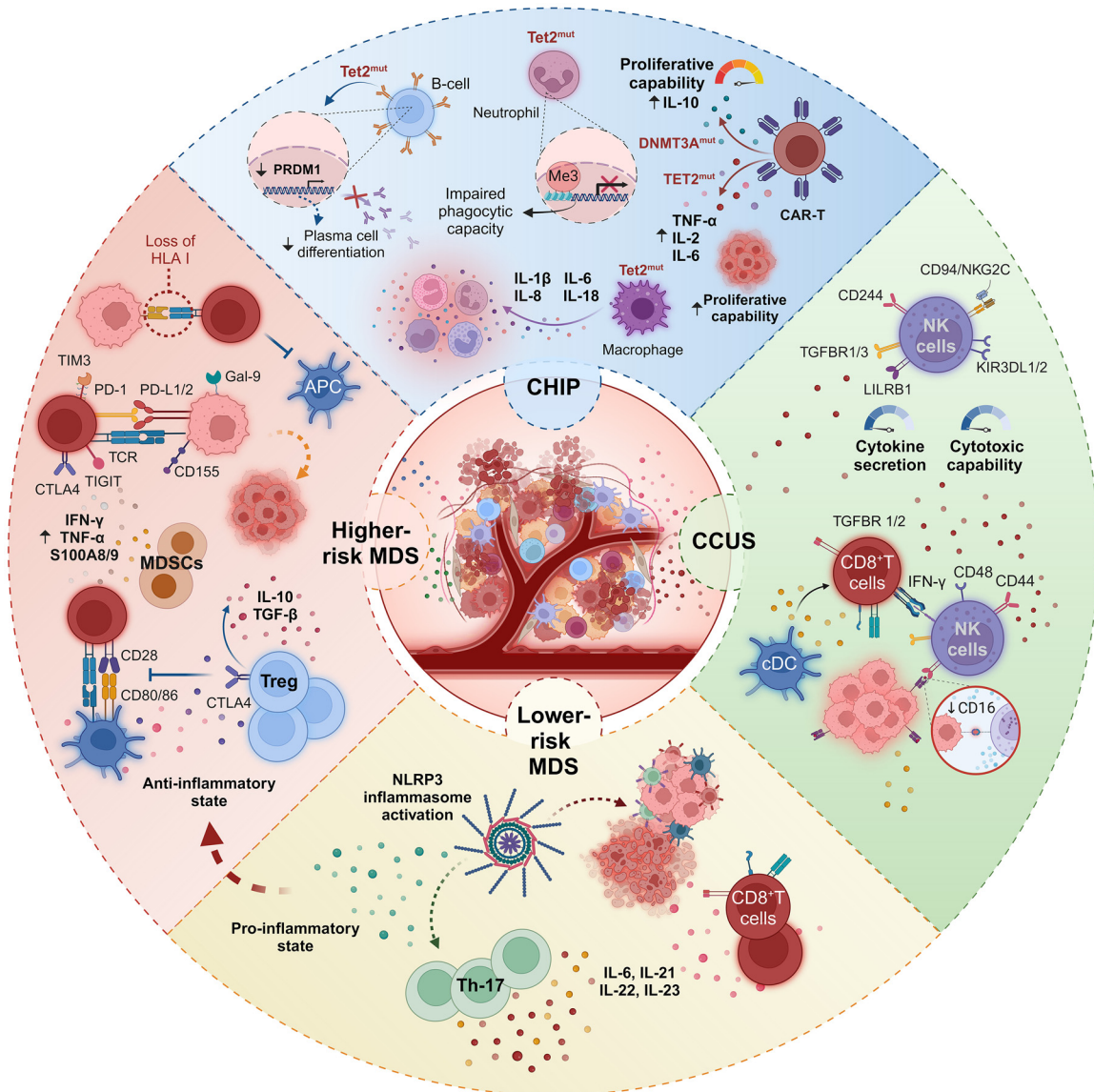


Fig. 3. Inflammation-induced immune imbalance contributes to immune evasion and malignant clone evolution. Top, CHIP-mutated genes *TET2* and *DNMT3A* significantly impact innate and adaptive immune responses. *TET2*-deficient CAR-T cells exhibit increased production of proinflammatory cytokines $\text{TNF-}\alpha$, IL-2, and IL-6, along with enhanced cytotoxic profiles. *DNMT3A* depletion results in increased CAR-T cell proliferation. *Tet2* mutations in macrophages lead to elevated levels of IL-1 β , IL-6, IL-8, and IL-18, while *Tet2*-mutant neutrophils show impaired phagocytic capacity. B cells with *Tet2* mutations undergo impaired plasma cell differentiation because of reduced PRDM1 expression. Right, in CCUS, the immune system is hyperactivated, and NK cells have reduced cytokine secretion and tumor-killing capacities. Bottom, lower-risk MDS are characterized by a proinflammatory state driven by the activation of the NLRP3 inflammasome and the expansion of Th-17 cells. Cytokines secreted by Th-17 cells (e.g., IL-6, IL-21, IL-22, and IL-23) create an inflammatory environment that leads to HSC exhaustion and ineffective hematopoiesis. Left, immunosuppression is a hallmark of higher-risk MDS. Regulatory T (Treg) cells significantly expand and promote an immunosuppressive environment by secreting the anti-inflammatory cytokines IL-10 and TGF- β . Myeloid-derived suppressor cells further contribute to this anti-inflammatory milieu. Upregulating immune checkpoint molecules (e.g., PD-1 and CTLA-4) enables malignant cells to escape immune surveillance. APC = antigen-presenting cells; CTLA-4 = cytotoxic T lymphocyte-associated protein 4; cDC = conventional dendritic cells; MDSCs = myeloid-derived suppressor cells; Gal-9 = galectin-9; HLA I = human leukocyte antigen I; KIR3DL1 = killer-cell immunoglobulin-like receptor; LILRB1 = leukocyte immunoglobulin-like receptor B1; Me3 = trimethylation; NKG2C = natural killer group 2 member C; NLRP3 = NOD-like receptor protein 3; PD-1 = programmed cell death protein 1; PD-L1/2 = programmed death-ligand 1/2; PRDM1 = B lymphocyte-induced maturation protein 1; TCR = T cell receptor; TGFBR1/2/3 = transforming growth factor beta receptor 1/2/3; TIGIT = T cell immunoreceptor with Ig and Itim domain; TIM3 = T cell immunoglobulin and mucin-domain containing-3.

scape and functional changes, characterized by the heightened production of $\text{TNF-}\alpha$, IL-2, and IL-6 upon stimulation and an increased cytotoxic profile [53]. Interestingly, *DNMT3A* depletion increases CAR T cells' proliferative capability without inducing the typical exhaustion phenotype acquired upon chronic stimulation, possibly because of increased IL-10 secretion [54]. In contrast, the depletion of CHIP-related mutations involving epigenetic regulators impairs the function of B cells. Indeed, *TET2* deletion reduces the expression of the plasma cell-defining transcription factor PR/SET domain 1 (*PRDM1*), affects plasma cell differentiation, decreases

the production of antigen-specific antibodies upon secondary immunization, and promotes B-cell lymphomagenesis [55]. *DNMT3A*-deficient B cells normally respond to model antigen exposure but develop an aggressive, chronic lymphocytic leukemia-like disease with high penetrance [56,57].

In the innate immune system landscape, *TET2*-depleted macrophages express higher levels of proinflammatory chemokines and cytokines (IL-1 β , IL-6, IL-8, and IL-18) than wild-type macrophages [58–60]. Moreover, *TET2*-mutated neutrophils have a lower content of secondary and tertiary granules, which suggests

that they achieve a less mature stage than their wild-type counterparts [61]. Mechanistically, *TET2* mutations disrupt the epigenetic regulation of neutrophil development, resulting in a more hypermethylated chromatin profile and an impaired phagocytic capacity. Together, these observations underscore the plasticity of CHIP mutations on different cell types and reveal that these mutations' proinflammatory effects extend far beyond myeloid cells.

Our limited understanding of how mutant cells expand over their normal counterpart has hindered the development of strategies to prevent or delay the evolution of CCUS to MDS. Single-cell RNA sequencing (scRNA-seq) of BM mononuclear cells from CCUS patients with *DNMT3A* or *TET2* mutations revealed that CD8⁺ T effector and NK cells exhibit a hyperactivated state associated with a downregulation of NF- κ B-mediated inflammatory signaling genes, which suggests a decreased proinflammatory response that is crucial for effective antitumor activity. Despite their hyperactivated state, CCUS NK cells secrete significantly less IFN- γ , exhibit impaired cytolytic capabilities, and expressed increased levels of exhaustion markers (e.g., increased expression of *CD57*, *CD244*, *LAG3*, *TIGIT 1*, and *PCDC1*). Targeted single-cell DNA sequencing and immunophenotypic analyses revealed that NK cells harbor similar mutational burdens to myelomonocytes, which suggests that MDS driver mutations such as *DNMT3A* or *TET2* affect NK cell functions [62]. *TET2*-mutated NK cells from MDS patients showed suppressed immune surveillance of malignant clones because of a reduced expression of killer immunoglobulin-like receptors, perforin, and TNF- α [63]. These findings demonstrate that in CCUS, the immune microenvironment is activated but hyporesponsive. Specifically, CCUS NK cells harbor genetic mutations and are irreversibly dysfunctional, thus enabling malignant cell expansion, disease progression, and MDS onset.

The immune profiles of lower-risk and higher-risk MDS differ substantially [64]. Lower-risk MDS is characterized by a persistent inflammatory environment in the BM, mainly mediated by activated NLRP3 inflammasome and an expansion of proinflammatory T cells, such as T helper 17 cells. T helper 17 cells stimulate the secretion of several inflammatory-associated cytokines (e.g., IL-6, IL-21, IL-22, IL-23), which leads to a proinflammatory milieu, increases HSCs' apoptosis and results in ineffective hematopoiesis [65,66]. In contrast, higher-risk MDS exhibits an immunosuppressive state dominated by the expansion of regulatory T cells, which suppresses the immune activation induced by malignant cells by secreting IL-10 and transforming growth factor beta (TGF- β) [67] and recruiting activated CD8⁺ T cells [68,69]. Regulatory T cells regulate antitumor immunity and disease progression in MDS [68,70,71] (Fig. 3).

The immune surveillance escape is also associated with a shift in the cytokine milieu from the proinflammatory state observed in lower-risk MDS to the anti-inflammatory state of higher-risk MDS [72]. Among the immune evasion mechanisms, the overexpression of immune checkpoints plays a critical role [73–75]. Indeed, inflammatory cytokines, such as IFN- γ and TNF- α , are present at high levels in the BM microenvironment of MDS patients [76,77] and upregulate programmed death-ligand 1 (PD-L1) expression on MDS blasts [78], enabling their escape from immune surveillance. Similarly, S100A9, a central molecule in MDS pathophysiology [19], induces the expression of programmed death 1 (PD-1) on HSPCs and that of PD-L1 on myeloid-derived suppressor cells [79]. Other co-inhibitory receptors, such as T-cell immunoglobulin and mucin domain-containing protein 3 (TIM3) and T-cell immunoreceptor with Ig and immunoreceptor tyrosine-based inhibitory motif domains (TIGIT) [80], induce immune evasion [73] through human leukocyte antigen loss, which inhibits neoantigen presentation by dendritic cells [81,82].

Overall, chronic inflammation in patients with CHIP or CCUS critically contributes to disease initiation by disrupting immune

system regulation. This imbalance is further exacerbated in MDS, in which T-cell exhaustion accelerates the collapse of antitumor immunity and fosters the development of immune tolerance.

Inflammation and metabolism

Inflammatory conditions can significantly affect metabolism, which regulates HSC function [83]. Inflammation-induced HSC dysfunction primarily manifests as a failure to maintain appropriate metabolic and mitochondrial regulation [83,84]. HSC states such as quiescence, proliferation, and differentiation have distinct metabolic demands and mitochondrial functions [85] and exhibit unique gene expression profiles and epigenetic landscapes [86,87]. Typically, quiescent HSCs derive their energy through glycolysis to avoid generating reactive oxygen species (ROS) from oxidative phosphorylation, which can induce DNA damage [88]. In cancer, including myeloid neoplasms, chronic inflammation-driven metabolic reprogramming can sustain malignant cell growth and survival [89].

Mutant HSPCs exhibit metabolic alterations that enhance survival and self-renewal and affect myeloid differentiation through extrinsic mechanisms involving the HSC niche [90]. HSCs' transition from quiescence to proliferation leads to metabolic changes associated with substantial epigenetic remodeling. DNA demethylation, regulated by the alpha-ketoglutarate (α -KG)-dependent enzyme *TET2* and its cofactor, ascorbate [91–93], occurs during HSC metabolic activation [94] and differentiation [95]. Under DNA damage or replication stress conditions engaged by an inflammatory microenvironment, which increases ROS production and affects mitochondria function [96,97], HSCs undergo epigenetic changes and have decreased autophagic activity. Because the depletion of *TET2* and *DNMT3A* activates cyclic guanosine monophosphate–adenosine monophosphate synthase signaling and the type I interferon pathway [98], loss-of-function mutations affecting these epigenetic factors further increase inflammation and the expansion of mutant clones (Fig. 4).

Obesity, diabetes, and metabolic syndromes are characterized by chronic inflammation and elevated proinflammatory immune cells in adipose tissues [99]. An obesity-induced proinflammatory state can compromise the HSC niche and disrupt the environmental signaling that regulates HSC maintenance and self-renewal [100]. Moreover, obesity promotes the progression of pre-leukemic CHIP clones [101,102]. Indeed, in mice with early obesity induced by the homozygous obese spontaneous mutation (Ob/Ob mice), heterozygous deletion of *dnmt3a* led to a significant increase of IL-6 and TNF- α secretion by mutant myeloid-derived HSCs, which underscores the impact of obesity in enhancing inflammatory states and driving the expansion of pre-leukemic clones. In *dnmt3a*-mutant mice, obesity and a high-fat diet exacerbated inflammation and metabolic dysfunction, thus promoting the expansion of mutant cells [102]. In this setting, HSCs' *dnmt3a* haploinsufficiency led to a higher proinflammatory environment, which resulted in weight gain and insulin resistance (Fig. 4). These data highlight the synergistic effect of *dnmt3a* loss and a high-fat diet in driving clonal expansion and metabolic alterations through a proinflammatory milieu.

The intimate connection between inflammation-driven metabolic changes and epigenetic regulation is tightly linked to clonal growth and increased HSC proliferation [103,104]. Dysfunctional metabolism increases the risk of proinflammatory CHIP, further exacerbating inflammation-induced metabolic conditions such as insulin resistance and atherosclerosis [105].

Compared with those from elderly healthy donors, HSCs from CCUS patients have significantly upregulated genes involved in translation, respiratory electron transport, and mitochondrial translation initiation, which underscores these cells' state of metabolic

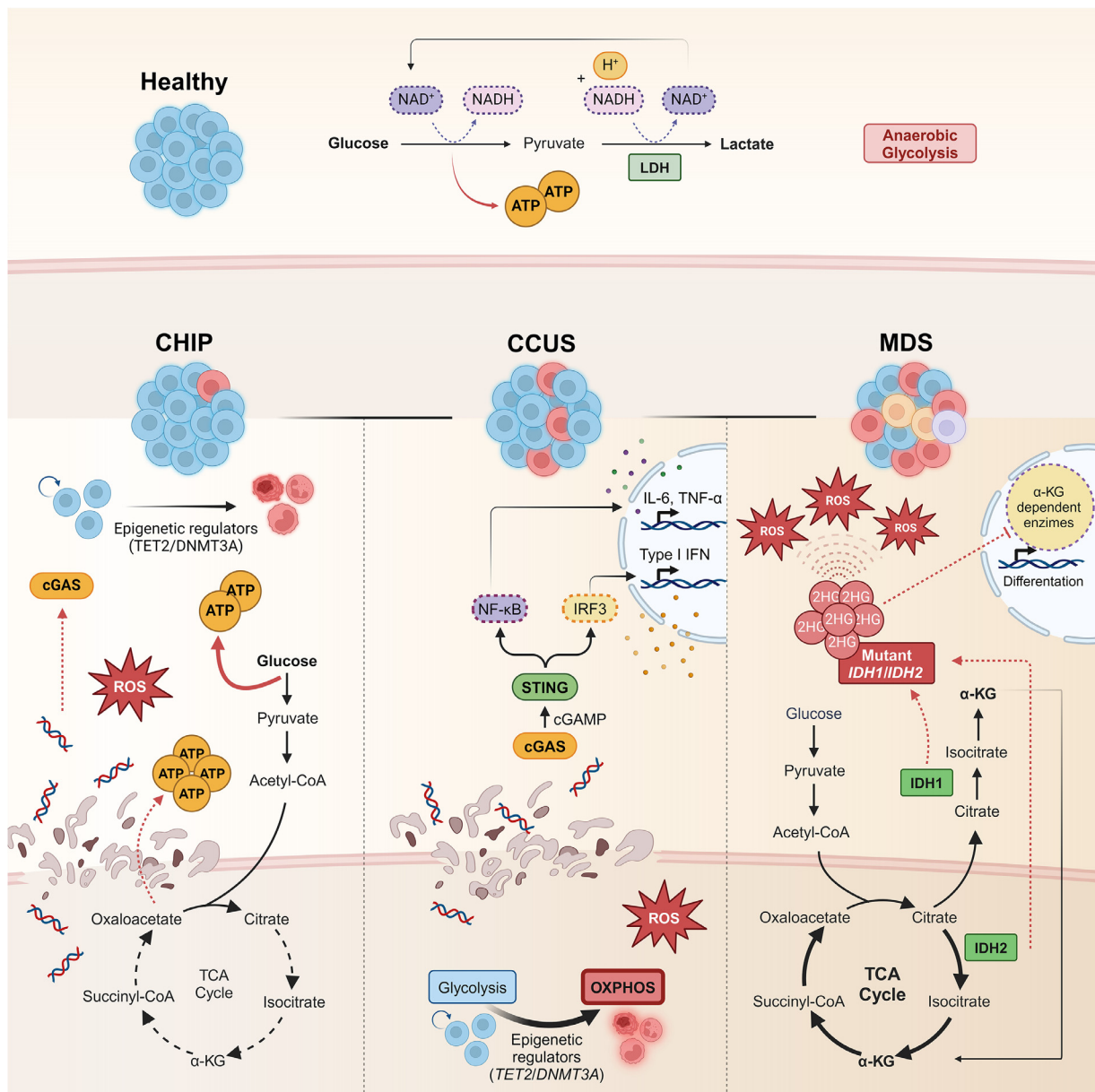


Fig. 4. Inflammation-driven metabolic rewiring in CHIP, CCUS, and MDS. Top, healthy HSCs primarily rely on anaerobic glycolysis to meet their energy demands. This metabolic state effectively limits the production of ROS, while preserving mitochondrial membrane integrity, crucial for maintaining quiescence and long-term stem cell potential. Bottom, the epigenetic regulators DNMT3A and TET2 shift the HSC metabolic landscape towards an aerobic state, which enhances glycolysis and oxidative phosphorylation to sustain clonal expansion and survival, leading to increased ROS production. In CCUS, excessive mitochondrial distress and fragmentation further increase ROS production, which leads to the release of mitochondrial DNA into the cytoplasm. Cytosolic DNA activates the DNA sensor cGAS-STING pathway, which triggers a cascade mediated by NF- κ B activation and interferon regulatory factor 3 (IRF3) transcription, modulating the expression of IL-6, TNF- α , and genes involved in the type I interferon pathway. Under these conditions, HSCs switch their metabolism from anaerobic glycolysis to mitochondrial oxidative metabolism to meet the high-energy demands required for sustaining activated myeloid differentiation. MDS HSCs have increased glycolysis and fatty acid oxidation. Mutations in the metabolic enzymes IDH1 and IDH2 contribute to metabolic dysfunction by promoting the accumulation of the oncometabolite 2-hydroxyglutarate (2-HG), which inhibits α -KG-dependent enzymes, including TET2. In the presence of IDH1/2 mutations, high levels of 2-HG induce hypermethylation of histones and DNA, thus changing HSCs' epigenetic profile and significantly impairing hematopoietic differentiation.

ATP = adenosine triphosphate; cGAS = cyclic GMP-AMP synthase; H^+ = proton; IDH1/2 = isocitrate dehydrogenase 1/2; LDH = lactate dehydrogenase; NAD^+ = nicotinamide adenine dinucleotide; NADH = reduced nicotinamide adenine dinucleotide; NF- κ B = nuclear factor kappa B; OXPHOS = oxidative phosphorylation; ROS = reactive oxygen species; STING = stimulator of interferon genes; TCA = tricarboxylic acid cycle; TNF- α = tumor necrosis factor alpha; α -KG = alpha-ketoglutarate.

activation [62]. Targeted ion chromatography-mass spectrometry analysis revealed that CCUS CD34⁺ HSPCs have significantly up-regulated intermediates in the tricarboxylic acid cycle pathway but downregulated intermediates in glycolysis. These results suggest that HSCs, which rely on anaerobic glycolysis to maintain their quiescent state [106] under homeostatic conditions, switch to mitochondrial oxidative metabolism in CCUS to meet the high-energy demands necessary to sustain activated myeloid differentiation [107,108] (Fig. 4). Moreover, compared with BM mononuclear

cells from CHIP patients, those from CCUS patients have significantly higher rates of mitochondrial fragmentation [109]. Dysfunctional mitochondria may accumulate owing to restricted autophagy or mitophagy, further promoting the release of mitochondrial ROS and other contents into the cytoplasm, which leads to inflammatory signaling activation and myeloid expansion [110].

MDS HSCs exhibit elevated levels of aerobic glycolysis and fatty acid oxidation [111]. This metabolic shift is partly regulated by metabolic enzymes such as isocitrate dehydrogenase 1 and 2

(IDH1/2) and epigenetic factors like TET2. IDH, a key enzyme in the tricarboxylic acid cycle, reversibly converts isocitrate to α -ketoglutarate (α -KG). Mutations in IDH1/2, which are observed in 4–12% of MDS patients [112], decrease the proteins' ability to convert isocitrate to α -KG but enhance their ability to catalyze the reduction of α -KG to 2-hydroxyglutarate (2-HG) [113,114]. 2-HG, a competitive inhibitor of α -KG-dependent dioxygenases (e.g., TET enzyme family members), induces the hypermethylation of histones and DNA [115] and impairs hematopoietic differentiation by altering epigenetic patterns and cell fate [116] (Fig. 4).

Interestingly, the histone variant macroH2A1.1 (mH2A1.1) links epigenetics with inflammation and metabolism [117]. The overexpression of mH2A1.1 in MDS mesenchymal cells leads to the activation of TLR4- and NF- κ B-mediated pathways, which induces a proinflammatory microenvironment and impairs the hematopoietic niche through increased ROS production and the nuclear localization of lactate dehydrogenase. The relationship among metabolism, epigenetic regulators, and somatic mutations is bidirectional, with epigenetic modifications driving metabolic changes and contributing to disease progression.

MDS cells display 2 metabolomic profiles based on BM blast counts [118–120]. Patients with lower blast counts (<5%) accumulate glycolytic metabolites, whereas those with higher blast counts (>5%) show enhanced electron transport chain and increased oxidative phosphorylation activity. However, mitochondrial oxidative phosphorylation efficiency is impaired in MDS, resulting in reduced adenosine triphosphate synthesis, increased ROS production, and elevated lactate dehydrogenase activity, which suggests that MDS cells compensate for aberrant metabolism by shifting to anaerobic glycolysis for energy production.

Lower-risk MDS are characterized by increased apoptosis and ineffective erythropoiesis, in which mitochondrial dysfunction plays a crucial role. Mitochondrial DNA mutations and altered nuclear-encoded mitochondrial proteins contribute to dyserythropoiesis, iron accumulation, and elevated ROS production, which causes cell damage and promotes MDS maintenance [121,122]. This metabolic disruption leads to significant energy deficiency and is closely associated with iron overload, given that iron chelation therapy partially restores energy metabolism in peripheral blood mononuclear cells [123]. In HSCs from *cb1^{ΔE8/9}/runx1^{S291fs}* mice and MDS patients with *RUNX1* or *ASXL1* mutations, excessive mitochondrial fragmentation triggers inflammatory signaling activation and ineffective hematopoiesis in a manner dependent on dynamin-related protein 1 [109], a master regulator of mitochondrial fission, which suggests that mitochondrial fragmentation is a key trigger of MDS pathogenesis [124].

In conclusion, the interplay between dysregulated metabolism and proinflammatory alterations establishes a complex immune-metabolic network within the BM, significantly contributing to the pathogenesis of the early and late stages of MDS.

Targeting inflammation

Deregulated inflammatory signaling, a hallmark of MDS, is therapeutically targetable. The inflammatory cytokine profiles of CHIP and CCUS are similar to those of MDS [125], which demonstrates that inflammation promotes disease initiation. Therefore, targeting inflammation has become a promising strategy for treating patients with MDS in its early stages, and numerous clinical trials of agents targeting several inflammatory pathways are underway [126] (Table 1). However, as the clonal complexity of MDS increases, intrinsic factors, such as the effects of cooperative mutations, and extrinsic factors, such as increased immune suppression that contributes to the expansion of mutant cells, may limit the efficacy of anti-inflammatory therapies.

One potential therapeutic target in MDS is IL-1 β . The fully human monoclonal antibody canakinumab, which targets the IL-1 β signaling pathway by blocking the interaction of IL-1 β with IL-1R1, improved hemoglobin levels in patients with CHIP-associated mutations, particularly those with DNMT3A and TET2 mutations [127]. In a heavily pretreated cohort of patients with lower-risk MDS, canakinumab was well-tolerated and demonstrated target engagement but limited efficacy (NCT04239157) [128]. Sequential scRNA-seq of HSPCs and BM mononuclear cells obtained during therapy revealed that canakinumab significantly decreased TNF- α -mediated inflammatory signaling in IL-1R1-expressing hematopoietic populations and rescued ineffective erythropoiesis in MDS with lower genetic complexity.

Several other trials of agents targeting IL-1 β are enrolling patients with CCUS and lower-risk MDS (NCT05641831, NCT04798339, NCT04239157). IL-1R-associated kinases (IRAKs) are key mediators of TLR and IL-1R1 signaling [129], and these kinases' interaction with upstream TLR pathway regulators (e.g., myeloid differentiation primary response protein 88) is critical in MDS pathogenesis [130]. Emavusertib (CA-4948), an oral IRAK4 inhibitor, elicited an overall response rate of 57% in patients with spliceosome-mutated MDS after hypomethylating agent failure [131].

Although IL-6 has a critical role in MDS pathogenesis, treatments targeting IL-6 have shown limited success in MDS patients. A double-blind, phase II clinical trial of siltuximab, a chimeric anti-IL-6 monoclonal antibody, did not reduce red blood cell transfusion burden [132] and was terminated early. HT-6184, an allosteric inhibitor of the NLRP3/never in mitosis gene A (NIMA)-related kinase 7 (NEK7) inflammasome, suppresses myeloid skewing, downregulates the proinflammatory cytokines IL-1 β and IL-6, and restores erythroid differentiation in MDS BM mononuclear cells [133]. An ongoing phase II trial (CTRI/2023/11/059758) is assessing the safety and clinical efficacy of HT-6184 in patients with lower-risk MDS.

Another emerging therapeutic target in MDS is the TGF- β pathway. TGF- β pathway activation inhibits MDS HSPCs' differentiation into committed progenitors [134]. Reduced levels of small mother against decapentaplegic 7 (SMAD7), a negative regulator of TGF- β signaling, increase TGF- β activity and suppress hematopoiesis [135]. Galunisertib, a TGF- β kinase receptor type I inhibitor, hinders SMAD2/3 activation, alleviates MDS HSCs' differentiation blockage *in vitro* and *in vivo*, and has shown an acceptable safety profile in phase I studies [136,137]. Luspatercept [138] and sotatercept [139] target other regulators of the TGF- β signaling pathway (e.g., activin ligands) and restore later hematopoiesis stages [140,141]. Interestingly, while luspatercept primarily targets late-stage erythropoiesis and promotes terminal erythroid differentiation by inhibiting the TGF- β signaling pathway, HT-6184 inhibits the priming and activation of the NLRP3 inflammasome, a key mediator of chronic inflammation in MDS. However, no direct evidence suggests that HT-6184 targets a specific stage of erythropoiesis in MDS.

In addition to direct anti-inflammatory strategies, other approaches can mitigate the effects of mutations in HSCs. For example, vitamin C enhances the hypomethylating activity of the functional TET2 protein encoded by the wild-type allele [142]. In a randomized, placebo-controlled phase II clinical trial (NCT03682029), patients with lower-risk MDS who received oral vitamin C supplementation had significantly improved overall survival. In addition, because inflammation significantly impacts the interplay between metabolism and malignant clonal expansion, biguanides (e.g., metformin), which inhibit respiratory complex I and decrease adenosine triphosphate synthesis and have been shown to reduce oxidative phosphorylation in myeloid malignancies [143], are being evaluated as a therapeutic strategy for CCUS (NCT04741945).

Table 1

List of clinical trials of agents targeting inflammatory-related pathways.

Therapy	Target	Clinical trial phase	Target MDS population	Number of patients enrolled	Type of response	NCT number/reference
Toll like receptor signaling pathway inhibitors						
Tomaralimab	TLR2	1/2 C	Lower and intermediate-risk MDS (R/R)	51	HI 50% TI > 8w 17% mOS 8.2m	NCT02363491 [144]
CX-01	TLR2	1 C	Intermediate and higher-risk MDS (R/R)	9		NCT02995655 [145]
Bortezomib	TLR2	2 C	Lower and intermediate-risk MDS	15	ORR 20% SD 53% PD 27% ORR 57%	NCT01891968 [146]
Emavusertib	IRAK4	1/2B R	Higher-risk MDS (R/R)	7		NCT04278768 [147]
R289	IRAK1/IRAK4	1 R	Low-risk MDS (R/R)	NA	NA	NCT05308264
Fostamatinib	SYK	1	Lower and higher-risk MDS	5	NA	NCT05030675 [148]
Inflammatory cytokine signaling pathway inhibitors						
Canakinumab	IL-1 β	2 R	Cohort 1: R/R Lower-risk MDS (TD) Cohort 2: Lower-risk MDS (TD) Cohort 3: Lower-risk MDS Cohort 4: CCUS Higher-risk CCUS*	25	HI 17.3%	NCT04239157 [128]
Canakinumab	IL-1 β	2 R		NA	NA	NCT05641831
Canakinumab	IL-1 β	2 T	Lower and intermediate-risk MDS (TD)	NA	NA	NCT05237713
Canakinumab	IL-1 β	1B/2 R	Lower-risk MDS (TD)	9	SD 100%	NCT04798339 [149]
Infliximab	TNF- α	2 C	Lower and intermediate-risk MDS	43	ORR: 13.6%	NCT00074074 [150]
Etanercept	TNF- α	1/2 C	Lower, intermediate and higher-risk MDS	29	ORR 73% (at 3m)	NCT00118287
Siltuximab	IL-6	2 T	Lower and intermediate-risk MDS (TD)	50	Early termination due to lack of efficacy	NCT01513317
ARRY614	p38-MAPK	1 C	Lower and intermediate-risk MDS	45	HI 32% TI > 20w 12%	NCT00916227 [151]
BMS-986253	IL-8	1/2 T	Lower and higher-risk MDS	NA	NA	NCT05148234
Inflammasome inhibitors						
HT-6184	NEK7/NLRP3	2 R	Lower-risk MDS	NA	NA	2023/11/059758 [†]
DFV890	NLRP3	1 R	Lower and intermediate-risk MDS	NA	NA	NCT05552469
TGF- β pathway inhibitors						
Vactosertib	TGF- β	1/2 C	Lower and intermediate-risk MDS (R/R)	NA	NA	NCT03074006
Sotatercept	TGF- β	2 C	Lower and intermediate-risk MDS (TD)	74	HI-E 58%	NCT01736683 [139]
Galunisertib	TGF- β	2/3 C	Lower and intermediate-risk MDS	41	HI-E 24.4%	NCT02008318 [152]
Luspatercept	TGF- β	2 C	Lower and intermediate-risk MDS (TD)	58	HI-E 63%	NCT01749514 NCT02268383 [153]
Luspatercept	TGF- β	3 C	Lower and intermediate-risk MDS with ring sideroblasts (TD)	153	TI > 8w 38% TI > 12w 28% HI-E 53%	NCT02631070 [154]
Luspatercept	TGF- β	3 ANR	Lower-risk MDS (TD)	178	TI > 12w + HI-E 58.5% HI-E > 8w 74.1% TI > 12w 66.7%	NCT03682536 [138]
Targeted therapy						
Ivosidenib	IDH1	2 R	IDH1-mutant CCUS	NA	NA	NCT05030441
Enasidenib	IDH2	1 ANR	IDH2-mutant CCUS	NA	NA	NCT05102370
Metabolic pathway inhibitors						
Atorvastatin or Rosuvastatin	OXPHOS	2 R	CCUS and lower-risk MDS	16	NA	NCT05483010
Curcumin	Systemic inflammation	2 R	CCUS and lower-risk MDS	NA	NA	NCT06063486
Vitamin C	TET2 rescue	2 ANR	CCUS and lower-risk MDS	109	5y-OS 70%	NCT03682029 [155]
Vitamin C	TET2 rescue	2 R	TET2-mutant CCUS	10	ORR 0%	NCT03418038 [156]

ANR = active not recruiting; C = completed; CCUS = clonal cytopenia of undetermined significance; mDoR = median duration of response; HI = hematologic improvement; HI-E = erythroid HI; m = months; MDS = myelodysplastic syndromes, mOS = median overall survival; NA = not available; ORR = overall response rate; OXPHOS = oxidative phosphorylation; PD = progressive disease; R = recruiting; R/R = relapse/refractory; SD = stable disease; T = terminated; TD = transfusion dependence; TI = transfusion independence; w = weeks; y = years.

* Any of the following: isolated somatic spliceosome mutation (*SRSF2*, *SF3B1*, *U2AF1*, or *ZRSR2*) at any variant allelic frequency (VAF); isolated *TP53* mutations with a VAF > 5%; at least 1 mutation in *TET2*, *DMNT3A*, or *ASXL1* at any VAF together with at least 1 other known myeloid pathogenic somatic mutation or known pathogenic germline mutation that predisposes to myeloid malignancies as determined by next-generation sequencing and bone marrow biopsy; a *TET2*, *DMNT3A*, or *ASXL1* mutation with a VAF > 10% together with another *TET2*, *DMNT3A*, or *ASXL1* with a VAF > 10%; the presence of 2 or more known myeloid pathogenic somatic or germline mutations (other than *TET2*, *ASXL1*, *DMNT3A*, *TP53*, or spliceosome mutations) with a VAF > 10%.

[†] Secondary Identification: HT-6184-MDS-001 Version No. 3.0. A study of HT-6184 in subjects with MDS and symptomatic anemia.

Conclusions

Most patients with MDS have limited treatment options and dismal outcomes. At the onset of the disease, almost all HSPCs harbor pathogenic genetic alterations [48], suggesting that no other therapies, except for allogeneic HSC transplantation, can cure MDS. Therapeutic strategies targeting the biological mechanisms underlying the preleukemic stage of MDS may improve the dismal outcomes MDS patients experience.

Inflammation is emerging as a key regulator of myeloid malignancy development and progression [12]. Several preclinical studies showed that mitigating inflammation could delay or prevent the progression of CHIP to MDS. However, most of these studies were performed using murine models. Although similar inflammatory processes are likely involved in leukemogenesis in patients with CHIP- or CCUS-related mutations, further studies in humans are needed to fully elucidate the role of inflammation in MDS initiation.

Declaration of competing interest

The authors declare that they have no known competing financial interests or personal relationships that could have appeared to influence the work reported in this paper.

CRediT authorship contribution statement

Juan Jose Rodriguez-Sevilla: Writing – original draft. **Simona Colla:** Writing – review & editing.

Acknowledgments

This work was supported by philanthropic contributions to The University of Texas MD Anderson Cancer Center's MDS/AML Moonshot and by the Edward P. Evans Foundation. J.J.R.-S. is the recipient of MD Anderson's Odyssey fellowship. Figures were created using Biorender.com.

References

- [1] Furman D, Campisi J, Verdin E, et al. Chronic inflammation in the etiology of disease across the life span. *Nat Med* 2019;25(12):1822–32.
- [2] Pietras EM. Inflammation: a key regulator of hematopoietic stem cell fate in health and disease. *Blood* 2017;130(15):1693–8.
- [3] Mitroulis I, Kalafati L, Bornhäuser M, Hajishengallis G, Chavakis T. Regulation of the bone marrow niche by inflammation. *Front Immunol* 2020;11:1540.
- [4] Takizawa H, Boettcher S, Manz MG. Demand-adapted regulation of early hematopoiesis in infection and inflammation. *Blood* 2012;119(13):2991–3002.
- [5] Mejia-Ramirez E, MC Florian. Understanding intrinsic hematopoietic stem cell aging. *Haematologica* 2020;105(1):22–37.
- [6] Fulop T, Larbi A, Dupuis G, et al. Immunosenescence and inflamm-aging as two sides of the same coin: friends or foes? *Front Immunol* 2017;8:1960.
- [7] Matatall KA, Jeong M, Chen S, et al. Chronic Infection depletes hematopoietic stem cells through stress-induced terminal differentiation. *Cell Rep* 2016;17(10):2584–95.
- [8] Pietras EM, Mirantes-Barbeito C, Fong S, et al. Chronic interleukin-1 exposure drives haematopoietic stem cells towards precocious myeloid differentiation at the expense of self-renewal. *Nat Cell Biol* 2016;18(6):607–18.
- [9] Essers MA, Offner S, Blanco-Bose WE, et al. IFN α activates dormant haematopoietic stem cells in vivo. *Nature* 2009;458(7240):904–8.
- [10] Pietras EM, Lakshminarasimhan R, Techner JM, et al. Re-entry into quiescence protects hematopoietic stem cells from the killing effect of chronic exposure to type I interferons. *J Exp Med* 2014;211(2):245–62.
- [11] Bogeska R, Mikecin AM, Kaschutnig P, et al. Inflammatory exposure drives long-lived impairment of hematopoietic stem cell self-renewal activity and accelerated aging. *Cell Stem Cell* 2022;29(8):1273–84.e8.
- [12] Balandran JC, Lasry A, Aifantis I. The role of inflammation in the initiation and progression of myeloid neoplasms. *Blood Cancer Discov* 2023;4(4):254–266.
- [13] Ganan-Gomez I, Wei Y, Starczynowski DT, et al. Deregulation of innate immune and inflammatory signaling in myelodysplastic syndromes. *Leukemia* 2015;29(7):1458–69.
- [14] Florez MA, Tran BT, Wathan TK, DeGregori J, Pietras EM, King KY. Clonal hematopoiesis: mutation-specific adaptation to environmental change. *Cell Stem Cell* 2022;29(6):882–904.
- [15] Hormaechea-Agulla D, Matatall KA, Le DT, et al. Chronic infection drives Dnmt3a-loss-of-function clonal hematopoiesis via IFN γ signaling. *Cell Stem Cell* 2021;28(8):1428–42.e6.
- [16] SanMiguel JM, Young K, Trowbridge JJ. Hand in hand: intrinsic and extrinsic drivers of aging and clonal hematopoiesis. *Exp Hematol* 2020;91:1–9.
- [17] Jakobsen NA, Turkalj S, Zeng AGX, et al. Selective advantage of mutant stem cells in human clonal hematopoiesis is associated with attenuated response to inflammation and aging. *Cell Stem Cell* 2024;31:1127–44 E17August 01, 2024.
- [18] Bergsbaken T, Fink SL, Cookson BT. Pyroptosis: host cell death and inflammation. *Nat Rev Microbiol* 2009;7(2):99–109.
- [19] Basiorika AA, McGraw KL, Eksioglu EA, et al. The NLRP3 inflammasome functions as a driver of the myelodysplastic syndrome phenotype. *Blood* 2016;128(25):2960–75.
- [20] Caiado F, Pietras EM, Manz MG. Inflammation as a regulator of hematopoietic stem cell function in disease, aging, and clonal selection. *J Exp Med* 2021;218(7):e20201541.
- [21] Schinke C, Giricz O, Li W, et al. IL8-CXCR2 pathway inhibition as a therapeutic strategy against MDS and AML stem cells. *Blood* 2015;125(20):3144–52.
- [22] Jaiswal S, Ebert BL. Clonal hematopoiesis in human aging and disease. *Science* 2019;366(6465):eaan4673.
- [23] David C, Duployez N, Eloy P, et al. Clonal haematopoiesis of indeterminate potential and cardiovascular events in systemic lupus erythematosus (HEMATOPLUS study). *Rheumatology (Oxford)* 2022;61(11):4355–63.
- [24] Arends CM, Weiss M, Christen F, et al. Clonal hematopoiesis in patients with anti-neutrophil cytoplasmic antibody-associated vasculitis. *Haematologica* 2020;105(6):e264–e2e7.
- [25] Cargo CA, Rowbotham N, Evans PA, et al. Targeted sequencing identifies patients with preclinical MDS at high risk of disease progression. *Blood* 2015;126(21):2362–5.
- [26] Malcovati L, Galli A, Travaglino E, et al. Clinical significance of somatic mutation in unexplained blood cytopenia. *Blood* 2017;129(25):3371–8.
- [27] Bejar RCHIP. ICUS, CCUS and other four-letter words. *Leukemia* 2017;31(9):1869–71.
- [28] Bewersdorf JP, Ardasheva A, Podoltsev NA, et al. From clonal hematopoiesis to myeloid leukemia and what happens in between: Will improved understanding lead to new therapeutic and preventive opportunities? *Blood Rev* 2019;37:100587.
- [29] DeZern AE, Malcovati L, Ebert BL. CHIP, CCUS, and other acronyms: definition, implications, and impact on practice. *Am Soc Clin Oncol Educ Book* 2019;39:400–10.
- [30] Weeks LD, Niroula A, Neuberg D, et al. Prediction of risk for myeloid malignancy in clonal hematopoiesis. *NEJM Evidence* 2023;2(5):EVID0a2200310.
- [31] Laurenti E, Gottgens B. From haematopoietic stem cells to complex differentiation landscapes. *Nature* 2018;553(7689):418–26.
- [32] Hajishengallis G, Li X, Chavakis T. Immunometabolic control of hematopoiesis. *Mol Aspects Med* 2021;77:100923.
- [33] Avagyan S, Zon LI. Clonal hematopoiesis and inflammation—the perpetual cycle. *Trends Cell Biol* 2023;33(8):695–707.
- [34] Yamashita M, Passequé E. TNF- α coordinates hematopoietic stem cell survival and myeloid regeneration. *Cell Stem Cell* 2019;25(3):357–72.e7.
- [35] Cai Z, Kotzin JJ, Ramdas B, et al. Inhibition of inflammatory signaling in tet2 mutant preleukemic cells mitigates stress-induced abnormalities and clonal hematopoiesis. *Cell Stem Cell* 2018;23(6):833–49.e5.
- [36] Kovtonyuk LV, Fritsch K, Feng X, Manz MG, Takizawa H. Inflamm-aging of hematopoiesis, hematopoietic stem cells, and the bone marrow microenvironment. *Front Immunol* 2016;7:502.
- [37] Jakobsen NA, Turkalj S, Zeng AGX, et al. Selective advantage of mutant stem cells in human clonal hematopoiesis is associated with attenuated response to inflammation and aging. *Cell Stem Cell*. 1127–1144.
- [38] Moran-Crusio K, Reavie L, Shih A, et al. Tet2 loss leads to increased hematopoietic stem cell self-renewal and myeloid transformation. *Cancer cell* 2011;20(1):11–24.
- [39] Meisel M, Hinterleitner R, Pacis A, et al. Microbial signals drive pre-leukaemic myeloproliferation in a Tet2-deficient host. *Nature* 2018;557(7706):580–4.
- [40] Caiado F, Kovtonyuk LV, Gonullu NG, Fullin J, Boettcher S, Manz MG. Aging drives Tet2+/- clonal hematopoiesis via IL-1 signaling. *Blood* 2023;141(8):886–903.
- [41] McClatchy J, Strogantsev R, Wolfe E, et al. Clonal hematopoiesis related TET2 loss-of-function impedes IL1 β -mediated epigenetic reprogramming in hematopoietic stem and progenitor cells. *Nat Commun* 2023;14(1):8102.
- [42] McClatchy J, Strogantsev R, Wolfe E, et al. Clonal hematopoiesis related TET2 loss-of-function impedes IL1 β -mediated epigenetic reprogramming in hematopoietic stem and progenitor cells. *Nat Commun* 2023;14(1):8102.
- [43] Burns SS, Kumar R, Pasupuleti SK, So K, Zhang C, Kapur R. IL-1r1 drives leukemogenesis induced by Tet2 loss. *Leukemia* 2022;36(10):2531–4.

- [44] Zeng H, He H, Guo L, et al. Antibiotic treatment ameliorates Ten-eleven translocation 2 (TET2) loss-of-function associated hematological malignancies. *Cancer Lett* 2019;467:1–8.
- [45] Zhang CRC, Nix D, Gregory M, et al. Inflammatory cytokines promote clonal hematopoiesis with specific mutations in ulcerative colitis patients. *Exp Hematol* 2019;80:36–41.e3.
- [46] Avagyan S, Henninger JE, Mannherz WP, et al. Resistance to inflammation underlies enhanced fitness in clonal hematopoiesis. *Science* 2021;374(6568):768–72.
- [47] Ganan-Gomez I, Chien KS, Ma F, et al. The transcriptional and epigenetic reprogramming of aged hematopoietic stem cells drives myeloid rewiring in clonal hematopoiesis-associated cytopenias. *Blood* 2021;138:3273.
- [48] Ganan-Gomez I, Yang H, Ma F, et al. Stem cell architecture drives myelodysplastic syndrome progression and predicts response to venetoclax-based therapy. *Nat Med* 2022.
- [49] Cicchese JM, Evans S, Hult C, et al. Dynamic balance of pro- and anti-inflammatory signals controls disease and limits pathology. *Immunol Rev* 2018;285(1):147–67.
- [50] Joshi NS, Cui W, Chande A, et al. Inflammation directs memory precursor and short-lived effector CD8⁺T Cell fates via the graded expression of T-bet transcription factor. *Immunity* 2007;27(2):281–95.
- [51] Cain D, Kondo M, Chen H, Kelsoe G. Effects of acute and chronic inflammation on b-cell development and differentiation. *J Investigat Dermatol* 2009;129(2):266–77.
- [52] Chen L, Deng H, Cui H, et al. Inflammatory responses and inflammation-associated diseases in organs. *Oncotarget* 2018;9(6):7204–18.
- [53] Fraietta JA, Nobles CL, Sammons MA, et al. Disruption of TET2 promotes the therapeutic efficacy of CD19-targeted T cells. *Nature* 2018;558(7709):307–12.
- [54] Prinzing B, Zebley CC, Petersen CT, et al. Deleting DNMT3A in CAR T cells prevents exhaustion and enhances antitumor activity. *Science translational medicine* 2021;13(620):eab0272.
- [55] Dominguez PM, Ghamlouch H, Rosikiewicz W, et al. TET2 deficiency causes germinal center hyperplasia, impairs plasma cell differentiation, and promotes b-cell lymphomagenesis. *Cancer Discov* 2018;8(12):1632–53.
- [56] Mahajan VS, Mattuo H, Sun N, et al. B1a and B2 cells are characterized by distinct CpG modification states at DNMT3A-maintained enhancers. *Nat Commun* 2021;12(1):2208.
- [57] Biran A, Yin S, Kretzmer H, et al. Activation of notch and myc signaling via b-cell-restricted depletion of dnmt3a generates a consistent murine model of chronic lymphocytic leukemia. *Cancer Res* 2021;81(24):6117–30.
- [58] Jaiswal S, Natarajan P, Silver AJ, et al. Clonal hematopoiesis and risk of atherosclerotic cardiovascular disease. *New Eng J Med* 2017;377(2):111–21.
- [59] Fuster JJ, MacLauchlan S, Zuriaga MA, et al. Clonal hematopoiesis associated with TET2 deficiency accelerates atherosclerosis development in mice. *Science* 2017;355(6327):842–7.
- [60] Zhang Q, Zhao K, Shen Q, et al. Tet2 is required to resolve inflammation by recruiting Hdac2 to specifically repress IL-6. *Nature* 2015;525(7569):389–93.
- [61] Huerga Encabo H, Aramburu IV, Garcia-Albornoz M, et al. Loss of TET2 in human hematopoietic stem cells alters the development and function of neutrophils. *Cell Stem Cell* 2023;30(6):781–99.e9.
- [62] Ganan-Gomez I, Kumar B, Rodriguez Sevilla JJ, et al. Mutant natural killer cell dysfunction enables the immune escape of premalignant MDS cell clones. *Blood* 2023;142(Supplement 1):514.
- [63] Boy M, Bisio V, Zhao LP, et al. Myelodysplastic Syndrome associated TET2 mutations affect NK cell function and genome methylation. *Nat Commun* 2023;14(1):588.
- [64] Peng X, Zhu X, Di T, et al. The yin-yang of immunity: immune dysregulation in myelodysplastic syndrome with different risk stratification. *Front Immunol* 2022;13:994053.
- [65] Zhang Z, Li X, Guo J, et al. Interleukin-17 enhances the production of interferon- γ and tumour necrosis factor- α by bone marrow T lymphocytes from patients with lower risk myelodysplastic syndromes. *Eur J Haematol* 2013;90(5):375–84.
- [66] Kordasti SY, Afzali B, Lim Z, et al. IL-17-producing CD4(+) T cells, pro-inflammatory cytokines and apoptosis are increased in low risk myelodysplastic syndrome. *Br J Haematol* 2009;145(1):64–72.
- [67] Aggarwal S, van de Loosdrecht AA, Alhan C, Ossenkoppele GJ, Westers TM, Bontkes HJ. Role of immune responses in the pathogenesis of low-risk MDS and high-risk MDS: implications for immunotherapy. *Br J Haematol* 2011;153(5):568–81.
- [68] Kordasti SY, Ingram W, Hayden J, et al. CD4+CD25high Foxp3+ regulatory T cells in myelodysplastic syndrome (MDS). *Blood* 2007;110(3):847–50.
- [69] Giovazzino A, Leone S, Rubino V, et al. Reduced regulatory T cells (Treg) in bone marrow preferentially associate with the expansion of cytotoxic T lymphocytes in low risk MDS patients. *Br J Haematol* 2019;185(2):357–60.
- [70] Lambert C, Wu Y, Aanei C. Bone Marrow Immunity and Myelodysplasia. *Front Oncol* 2016;6:172.
- [71] Hamdi W, Ogawara H, Handa H, Tsukamoto N, Nojima Y, Murakami H. Clinical significance of regulatory T cells in patients with myelodysplastic syndrome. *Eur J Haematol* 2009;82(3):201–7.
- [72] Garcia-Manero G, Chien KS, Montalban-Bravo G. Myelodysplastic syndromes: 2021 update on diagnosis, risk stratification and management. *Am J Hematol* 2020;95(11):1399–420.
- [73] Tsvetkov N, Gusak A, Morozova E, et al. Immune checkpoints bone marrow expression as the predictor of clinical outcome in myelodysplastic syndrome. *Leukemia Res Rep* 2020;14:100215.
- [74] Meng F, Li L, Lu F, et al. Overexpression of TIGIT in NK and t cells contributes to tumor immune escape in myelodysplastic syndromes. *Front Oncol* 2020;10:1595.
- [75] Tsvetkov NY, Morozova EV, Epifanovskaya OS, et al. Profile of checkpoint molecules expression on bone marrow cell populations in patients with high-risk myelodysplastic syndrome. *Blood* 2020;136:43–4.
- [76] Kitagawa M, Saito I, Kuwata T, et al. Overexpression of tumor necrosis factor (TNF)-alpha and interferon (IFN)-gamma by bone marrow cells from patients with myelodysplastic syndromes. *Leukemia* 1997;11(12):2049–54.
- [77] Stifter G, Heiss S, Gastl G, Tzankov A, Stauder R. Over-expression of tumor necrosis factor-alpha in bone marrow biopsies from patients with myelodysplastic syndromes: relationship to anemia and prognosis. *Eur J Haematol* 2005;75(6):485–91.
- [78] Kondo A, Yamashita T, Tamura H, et al. Interferon-gamma and tumor necrosis factor-alpha induce an immunoinhibitory molecule, B7-H1, via nuclear factor-kappaB activation in blasts in myelodysplastic syndromes. *Blood* 2010;116(7):1124–31.
- [79] Cheng P, Eksioğlu EA, Chen X, et al. S100A9-induced overexpression of PD-1/PD-L1 contributes to ineffective hematopoiesis in myelodysplastic syndromes. *Leukemia* 2019;33(8):2034–46.
- [80] Wolf Y, Anderson AC, Kuchroo VK. TIM3 comes of age as an inhibitory receptor. *Nat Rev Immunol* 2020;20(3):173–85.
- [81] Montes P, Bernal M, Campo LN, et al. Tumor genetic alterations and features of the immune microenvironment drive myelodysplastic syndrome escape and progression. *Cancer Immunol Immunother* 2019;68(12):2015–2027.
- [82] Montes P, Kerick M, Bernal M, et al. Genomic loss of HLA alleles may affect the clinical outcome in low-risk myelodysplastic syndrome patients. *Oncotarget* 2018;9(97):36929–44.
- [83] Chandel NS, Jasper H, Ho TT, Passequé E. Metabolic regulation of stem cell function in tissue homeostasis and organismal ageing. *Nat Cell Biol* 2016;18(8):823–32.
- [84] Shyh-Chang N, Daley GQ, Cantley LC. Stem cell metabolism in tissue development and aging. *Development* 2013;140(12):2535–47.
- [85] Papa L, Djedaini M, Hoffman R. Mitochondrial role in stemness and differentiation of hematopoietic stem cells. *Stem Cells Int* 2019;2019:4067162.
- [86] Cedar H, Bergman Y. Epigenetics of haematopoietic cell development. *Nat Rev Immunol* 2011;11(7):478–88.
- [87] MacArthur BD, Ma'ayan A, Lemischka IR. Systems biology of stem cell fate and cellular reprogramming. *Nat Rev Mol Cell Biol* 2009;10(10):672–81.
- [88] Suda T, Takubo K, Semenza GL. Metabolic regulation of hematopoietic stem cells in the hypoxic niche. *Cell Stem Cell* 2011;9(4):298–310.
- [89] Xu X, Peng Q, Jiang X, et al. Metabolic reprogramming and epigenetic modifications in cancer: from the impacts and mechanisms to the treatment potential. *Experiment Mol Med* 2023;55(7):1357–70.
- [90] Verovskaya EV, Dellorusso PV, Passequé E. Losing sense of self and surroundings: hematopoietic stem cell aging and leukemic transformation. *Trends Mol Med* 2019;25(6):494–515.
- [91] Ko M, Bandukwala HS, An J, et al. Ten-Eleven-Translocation 2 (TET2) negatively regulates homeostasis and differentiation of hematopoietic stem cells in mice. *Proc Natl Acad Sci U S A* 2011;108(35):14566–71.
- [92] Cimmino L, Dolgalev I, Wang Y, et al. Restoration of TET2 function blocks aberrant self-renewal and leukemia progression. *Cell* 2017;170(6):1079–95.e20.
- [93] Agathocleous M, Meacham CE, Burgess RJ, et al. Ascorbate regulates haematopoietic stem cell function and leukaemogenesis. *Nature* 2017;549(7673):476–81.
- [94] Ho TT, Warr MR, Adelman ER, et al. Autophagy maintains the metabolism and function of young and old stem cells. *Nature* 2017;543(7644):205–10.
- [95] Cabezas-Wallscheid N, Klimm D, Hansson J, et al. Identification of regulatory networks in HSCs and their immediate progeny via integrated proteome, transcriptome, and DNA methylome analysis. *Cell Stem Cell* 2014;15(4):507–22.
- [96] Li X, Li C, Zhang W, Wang Y, Qian P, Huang H. Inflammation and aging: signaling pathways and intervention therapies. *Signal Transduct Target Ther* 2023;8(1):239.
- [97] Ho YH, Méndez-Ferrer S. Microenvironmental contributions to hematopoietic stem cell aging. *Haematologica* 2020;105(1):38–46.
- [98] Cobo I, Tanaka TN, Chandra Mangalhar K, et al. DNA methyltransferase 3 alpha and TET methylcytosine dioxygenase 2 restrain mitochondrial DNA-mediated interferon signaling in macrophages. *Immunity* 2022;55(8):1386–401.e10.
- [99] Reilly SM, Saltiel AR. Adapting to obesity with adipose tissue inflammation. *Nat Rev Endocrinol* 2017;13(11):633–43.
- [100] Bowers E, Singer K. Obesity-induced inflammation: the impact of the hematopoietic stem cell niche. *JCI Insight* 2021;6(3):e145295.
- [101] Pasupuleti SK, Ramdas B, Burns SS, et al. Obesity-induced inflammation exacerbates clonal hematopoiesis. *J Clin Invest* 2023;133(11):e163968.
- [102] Reyes JM, Tovy A, Zhang L, et al. Hematologic DNMT3A reduction and high-fat diet synergize to promote weight gain and tissue inflammation. *iScience* 2024;27(3):109122.
- [103] Wu D, Hu D, Chen H, et al. Glucose-regulated phosphorylation of TET2 by AMPK reveals a pathway linking diabetes to cancer. *Nature* 2018;559(7715):637–41.
- [104] Lee MK, Dragoljevic D, Veiga CB, Wang N, Yvan-Charvet L, Murphy AJ. Interplay between clonal hematopoiesis of indeterminate potential and metabolism. *Trends Endocrinol Metab* 2020;31(7):525–35.

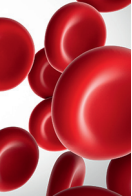
- [105] Furer N, Kaushansky N, Shlush LI. The vicious and virtuous circles of clonal hematopoiesis. *Nat Med* 2021;27(6):949–50.
- [106] Chandel NS, Jasper H, Ho TT, Passegue E. Metabolic regulation of stem cell function in tissue homeostasis and organismal ageing. *Nat Cell Biol* 2016;18(8):823–32.
- [107] Testa U, Labbaye C, Castelli G, Pelosi E. Oxidative stress and hypoxia in normal and leukemic stem cells. *Exp Hematol* 2016;44(7):540–60.
- [108] Kang YA, Paik H, Zhang SY, et al. Secretory MPP3 reinforce myeloid differentiation trajectory and amplify myeloid cell production. *J Exp Med* 2023;220(8):e20230088.
- [109] Aoyagi Y, Hayashi Y, Harada Y, et al. Mitochondrial fragmentation triggers ineffective hematopoiesis in myelodysplastic syndromes. *Cancer Discov* 2022;12(1):250–69.
- [110] Yeaton A, Cayanen G, Loghavi S, et al. The impact of inflammation-induced tumor plasticity during myeloid transformation. *Cancer Discov* 2022;12(10):2392–413.
- [111] Balaian E, Wobus M, Bornhäuser M, Chavakis T, Sockel K. Myelodysplastic syndromes and metabolism. *Int J Mol Sci* 2021;22(20):11250.
- [112] DiNardo CD, Jabbour E, Ravandi F, et al. IDH1 and IDH2 mutations in myelodysplastic syndromes and role in disease progression. *Leukemia* 2016;30(4):980–4.
- [113] Dang L, White DW, Gross S, et al. Cancer-associated IDH1 mutations produce 2-hydroxyglutarate. *Nature* 2009;462(7274):739–44.
- [114] Ward PS, Patel J, Wise DR, et al. The common feature of leukemia-associated IDH1 and IDH2 mutations is a neomorphic enzyme activity converting alpha-ketoglutarate to 2-hydroxyglutarate. *Cancer cell* 2010;17(3):225–34.
- [115] Xu W, Yang H, Liu Y, et al. Oncometabolite 2-hydroxyglutarate is a competitive inhibitor of α -ketoglutarate-dependent dioxygenases. *Cancer cell* 2011;19(1):17–30.
- [116] Figueroa ME, Abdel-Wahab O, Lu C, et al. Leukemic IDH1 and IDH2 mutations result in a hypermethylation phenotype, disrupt TET2 function, and impair hematopoietic differentiation. *Cancer cell* 2010;18(6):553–67.
- [117] Giallongo C, Culmacare I, Giallongo S, et al. MacroH2A1.1 as a crossroad between epigenetics, inflammation and metabolism of mesenchymal stromal cells in myelodysplastic syndromes. *Cell Death Disease* 2023;14(10):686.
- [118] Poulaki A, Katsila T, Stergiou IE, et al. Bioenergetic profiling of the differentiating human mds myeloid lineage with low and high bone marrow blast counts. *Cancers* 2020;12(12):3520.
- [119] Stevens BM, Engel KL, Gillen AE, et al. Unique metabolic vulnerabilities of myelodysplastic syndrome stem cells. *Blood* 2021;138:1511.
- [120] Stevens BM, Khan N, D'Alessandro A, et al. Characterization and targeting of malignant stem cells in patients with advanced myelodysplastic syndromes. *Nat Commun* 2018;9(1):3694.
- [121] Wulfert M, Küpper AC, Tappich C, et al. Analysis of mitochondrial DNA in 104 patients with myelodysplastic syndromes. *Exp Hematol* 2008;36(5):577–86.
- [122] Visconte V, Avishai N, Mahfouz R, et al. Distinct iron architecture in SF3B1-mutant myelodysplastic syndrome patients is linked to an SLC25A37 splice variant with a retained intron. *Leukemia* 2015;29(1):188–95.
- [123] Cilloni D, Ravera S, Calabrese C, et al. Iron overload alters the energy metabolism in patients with myelodysplastic syndromes: results from the multicenter FISM BIOFER study. *Scient Rep* 2020;10(1):9156.
- [124] Smirnova E, Griparic L, Shurland DL, van der Blik AM. Dynamin-related protein Drp1 is required for mitochondrial division in mammalian cells. *Mol Biol Cell* 2001;12(8):2245–56.
- [125] Nielsen AB, Hansen JW, Ørskov AD, et al. Inflammatory cytokine profiles do not differ between patients with idiopathic cytopenias of undetermined significance and myelodysplastic syndromes. *Hemasphere* 2022;6(5):e0713.
- [126] Rodríguez-Sevilla JJ, Adema V, García-Manero G, Colla S. Emerging treatments for myelodysplastic syndromes: biological rationales and clinical translation. *Cell Rep Med* 2023;4(2):100940.
- [127] Woo J, Lu D, Lewandowski A, et al. Effects of IL-1 β inhibition on anemia and clonal hematopoiesis in the randomized CANTOS trial. *Blood Adv* 2023;7(24):7471–84.
- [128] Rodríguez Sevilla JJ, Adema V, Chien KS, et al. A Phase 2 study of canakinumab in patients with lower-risk myelodysplastic syndromes or chronic myelomonocytic leukemia. *Blood* 2023;142:1866.
- [129] Rhyasen GW, Starczynowski DT. IRAK signalling in cancer. *Br J Cancer* 2015;112(2):232–7.
- [130] Choudhary GS, Pellagatti A, Agianian B, et al. Activation of targetable inflammatory immune signaling is seen in myelodysplastic syndromes with SF3B1 mutations. *eLife* 2022;11:e78136.
- [131] García-Manero G, Winer ES, DeAngelo DJ, et al. Phase 1/2a study of the IRAK4 inhibitor CA-4948 as monotherapy or in combination with azacitidine or venetoclax in patients with relapsed/refractory (R/R) acute myeloid leukemia or myelodysplastic syndrome. *J Clin Oncol* 2022;40(16 suppl):7016.
- [132] García-Manero G, Gartenberg G, Steensma DP, et al. A phase 2, randomized, double-blind, multicenter study comparing siltuximab plus best supportive care (BSC) with placebo plus BSC in anemic patients with International Prognostic Scoring System low- or intermediate-1-risk myelodysplastic syndrome. *Am J Hematol* 2014;89(9):E156–62.
- [133] Rabinovich E, Fromowitz A, Ajibade O, et al. The Dual inflammatory/myddosome inhibitor HT-6184 restores erythropoiesis in MDS/AML. *Blood* 2023;142:1417.
- [134] Verma A, Deb DK, Sassano A, et al. Activation of the p38 mitogen-activated protein kinase mediates the suppressive effects of type I interferons and transforming growth factor- β on normal hematopoiesis. *J Biol Chem* 2002;277(10):7726–35.
- [135] Zhou L, McMahon C, Bhagat T, et al. Reduced SMAD7 leads to overactivation of TGF- β signaling in MDS that can be reversed by a specific inhibitor of TGF- β receptor I Kinase. *Cancer Res* 2011;71(3):955–63.
- [136] Rodon J, Carducci MA, Sepulveda-Sánchez JM, et al. First-in-human dose study of the novel transforming growth factor- β receptor I kinase inhibitor LY2157299 monohydrate in patients with advanced cancer and glioma. *Clin Cancer Res* 2015;21(3):553–60.
- [137] Herbertz S, Sawyer JS, Stauber AJ, et al. Clinical development of galunisertib (LY2157299 monohydrate), a small molecule inhibitor of transforming growth factor-beta signaling pathway. *Drug Des Devel Ther*. 2015;9:4479–99.
- [138] Platzbecker U, Della Porta MG, Santini V, et al. Efficacy and safety of luspatercept versus epoetin alfa in erythropoiesis-stimulating agent-naïve, transfusion-dependent, lower-risk myelodysplastic syndromes (COMMANDS): interim analysis of a phase 3, open-label, randomised controlled trial. *Lancet* 2023;402(10399):373–85.
- [139] Komrokji R, García-Manero G, Ades L, et al. Sotatercept with long-term extension for the treatment of anaemia in patients with lower-risk myelodysplastic syndromes: a phase 2, dose-ranging trial. *Lancet Haematol* 2018;5(2):e63–72.
- [140] Suragani RN, Cadena SM, Cawley SM, et al. Transforming growth factor- β superfamily ligand trap ACE-536 corrects anemia by promoting late-stage erythropoiesis. *Nat Med* 2014;20(4):408–14.
- [141] Carrancio S, Markovics J, Wong P, et al. An activin receptor IIA ligand trap promotes erythropoiesis resulting in a rapid induction of red blood cells and haemoglobin. *Bri J Haematol* 2014;165(6):870–82.
- [142] Cimmino L, Dolgalev I, Wang Y, et al. Restoration of TET2 function blocks aberrant self-renewal and leukemia progression. *Cell* 2017;170(6):1079–95.e20.
- [143] You R, Wang B, Chen P, et al. Metformin sensitizes AML cells to chemotherapy through blocking mitochondrial transfer from stromal cells to AML cells. *Cancer Letters* 2022;532:21582.
- [144] García-Manero G, Jabbour EJ, Konopleva MY, et al. A Clinical Study of Tomaralimab (OPN-305), a Toll-like Receptor 2 (TLR-2) Antibody, in Heavily Pre-Treated Transfusion Dependent Patients with Lower Risk Myelodysplastic Syndromes (MDS) That Have Received and Failed on Prior Hypomethylating Agent (HMA) Therapy. *Blood* 2018;132(Supplement 1):798.
- [145] Huselton E, Cashen AF, DiPersio JF, et al. Updated study results of CX-01, an inhibitor of CXCL12/CXCR4, and azacitidine for the treatment of hypomethylating agent refractory AML and MDS. *Blood* 2019;134(Supplement 1):3915.
- [146] Daher M, Hidalgo Lopez JE, Randhawa JK, et al. An exploratory clinical trial of bortezomib in patients with lower risk myelodysplastic syndromes. *Am J Hematol* 2017;92(7):674–82.
- [147] García-Manero G, Winer ES, DeAngelo DJ, et al. S129: TAKEAIM LEUKEMIA-a phase 1/2a study of the IRAK4 inhibitor emavusertib (CA-4948) as monotherapy or in combination with azacitidine or venetoclax in relapsed/refractory AML or MDS. *HemaSphere* 2022;6:30–1.
- [148] Montalbán-Bravo G, Borthakur G, Chien KS, et al. A phase I open label study of fostamatinib, a SYK Inhibitor, in patients with lower-risk myelodysplastic syndromes and chronic myelomonocytic leukemia. *Blood* 2022;140(Supplement 1):9816–17.
- [149] Sallman DA, Hunter AM, Xie Z, et al. Phase 1b/2 Study evaluating the safety and efficacy of canakinumab with darbepoetin alfa in patients with lower-risk myelodysplastic syndromes (MDS) who have failed erythropoietin stimulating agents (ESA). *Blood* 2023;142:4620.
- [150] Baron F, Suci S, Amadori S, et al. Value of infliximab (Remicade®) in patients with low-risk myelodysplastic syndrome: final results of a randomized phase II trial (EORTC trial 06023) of the EORTC Leukemia Group. *Haematologica* 2012;97(4):529–33.
- [151] García-Manero G, Khoury HJ, Jabbour E, et al. A Phase I Study of Oral AR-RY-614, a p38 MAPK/Tie2 Dual Inhibitor, in Patients with Low or Intermediate-1 Risk Myelodysplastic Syndromes. *Clin Cancer Res* 2015;21(5):985–94.
- [152] Santini V, Valcárcel D, Platzbecker U, et al. Phase II study of the ALK5 inhibitor galunisertib in very low-, low-, and intermediate-risk myelodysplastic syndromes. *Clin Cancer Res* 2019;25(23):6976–85.
- [153] Platzbecker U, Germing U, Götze KS, et al. Luspatercept for the treatment of anaemia in patients with lower-risk myelodysplastic syndromes (PACE-MDS): a multicentre, open-label phase 2 dose-finding study with long-term extension study. *Lancet Oncol* 2017;18(10):1338–47.
- [154] Fenaux P, Platzbecker U, Mufti GJ, et al. Luspatercept in patients with lower-risk myelodysplastic syndromes. *N Engl J Med* 2020;382(2):140–51.
- [155] Mikkelsen SU VA, Nielsen A, Hansen J, et al. Vitamin C supplementation in patients with clonal cytopenia of undetermined significance or low-risk myeloid malignancies: results from EVI-2, a randomized, placebo-controlled phase 2 study. *EHA* 2024.
- [156] Xie Z, McCullough K, Lasho TL, et al. Phase II study assessing safety and preliminary efficacy of high dose intravenous ascorbic acid in patients with TET2 mutant clonal cytopenias. *Blood* 2023;142:4611.

Second Review

T-cell dysfunctions in myelodysplastic syndromes

Rodriguez-Sevilla JJ, Colla S

Blood 2024 April;143(14):1329-1343.
2024 Impact Factor 21.0
Quartile 1



T-cell dysfunctions in myelodysplastic syndromes

Juan Jose Rodriguez-Sevilla and Simona Colla

Department of Leukemia, The University of Texas MD Anderson Cancer Center, Houston, TX

Escape from immune surveillance is a hallmark of cancer. Immune deregulation caused by intrinsic and extrinsic cellular factors, such as altered T-cell functions, leads to immune exhaustion, loss of immune surveillance, and clonal proliferation of tumoral cells. The T-cell immune system contributes to the pathogenesis, maintenance, and progression of myelodysplastic syndrome (MDS).

Here, we comprehensively reviewed our current biological knowledge of the T-cell compartment in MDS and recent advances in the development of immunotherapeutic strategies, such as immune checkpoint inhibitors and T-cell- and antibody-based adoptive therapies that hold promise to improve the outcome of patients with MDS.

Introduction

T cells play a key role in adaptive immunity by orchestrating immune responses against foreign antigens while preserving self-tolerance. T cells maintain immune homeostasis by overcoming pathogens, arresting the clonal expansion of cancer cells, and preventing the development of autoimmune (AI) diseases. T-cell differentiation and functional specialization are tightly regulated processes, which are essential for effective immune responses.

T cells play a key role in tumor surveillance by identifying and eliminating tumoral cells. T cells' aberrant differentiation and function can disrupt immune surveillance mechanisms and foster an immunosuppressive tumor microenvironment, which promotes cancer initiation and progression. Moreover, deregulated T-cell homeostasis can affect clinical outcomes in patients with cancer by modulating therapy responses.¹ Regulated immunity prevents or delays the appearance of malignant clones through innate antitumor activity or specific recognition of neoantigens. Given that tumor immunity arises from a balance between immunosurveillance and immune escape, errors in the immune regulatory pathways can lead to malignant clone expansion in many cancers,^{2,3} including those affecting hematopoietic stem cells (HSCs).⁴

Mounting experimental evidence demonstrates that immune deregulation in the hematopoietic niche and chronic inflammation due to aberrant secretion of cytokines by immune cells have prominent roles in the pathogenesis and progression of myelodysplastic syndromes (MDS). Progression of MDS to acute myeloid leukemia (AML) is associated with an increased inflammatory signature, which significantly affects the composition of the immune microenvironment and impairs immune cells' function.^{4,5}

T lymphocytes are key effectors of cell-mediated immune responses against tumor cells, and these cells' alterations

contribute to immune dysfunction in MDS and expansion of malignant clones.^{6,7} Here, we comprehensively overview: (1) how T-cell subtypes' composition and functional alterations contribute to MDS initiation, maintenance, and progression; (2) whether T cells are biomarkers of response to treatment; and (3) the recent strides toward the development of novel T-cell-based therapeutic approaches to treat MDS.

T-cell subtypes and immune deregulation in MDS

CD4⁺ helper T (Th), CD8⁺ cytotoxic T, and regulatory T (Treg) cells play distinct functional roles in regulating the immune response. Immune-mediated cell death of pathogens and cancer cells is mainly mediated by CD8⁺ and CD4⁺ T cells, whereas Treg cells regulate immune tolerance and modulate immune responses (Figure 1).⁷ The absolute number of peripheral blood (PB) CD4⁺ T cells is reduced in patients with MDS compared with that of healthy donors (HDs), which results in a lower PB CD4⁺/CD8⁺ T-cell ratio.⁸ Indeed, the age-adjusted CD4/CD8 ratio is decreased in patients with MDS with both lower- and higher-risk MDS when compared with HDs, due to a decreased numbers of CD4⁺ T cells in these patients rather than an expansion of CD8⁺ T cells.⁹ Given that CD4/CD8 ratio is a conventional measure of immune function and response,¹⁰ these studies suggest that the immune system is severely impaired in MDS.

CD4⁺ T cells

CD4⁺ T cells are highly functionally heterogeneous and have a central role in tumor immunity by enhancing the effect of CD8⁺ cytotoxic T cells, mediating humoral responses, and secreting effector cytokines, such as interferon gamma (IFN- γ) and tumor necrosis factor- α (TNF- α).¹¹

CD4 is a glycoprotein located on the surface of CD4⁺ T cells, dendritic cells (DCs), monocytes, and macrophages.¹² CD4 serves as a coreceptor for the T-cell receptor (TCR), which

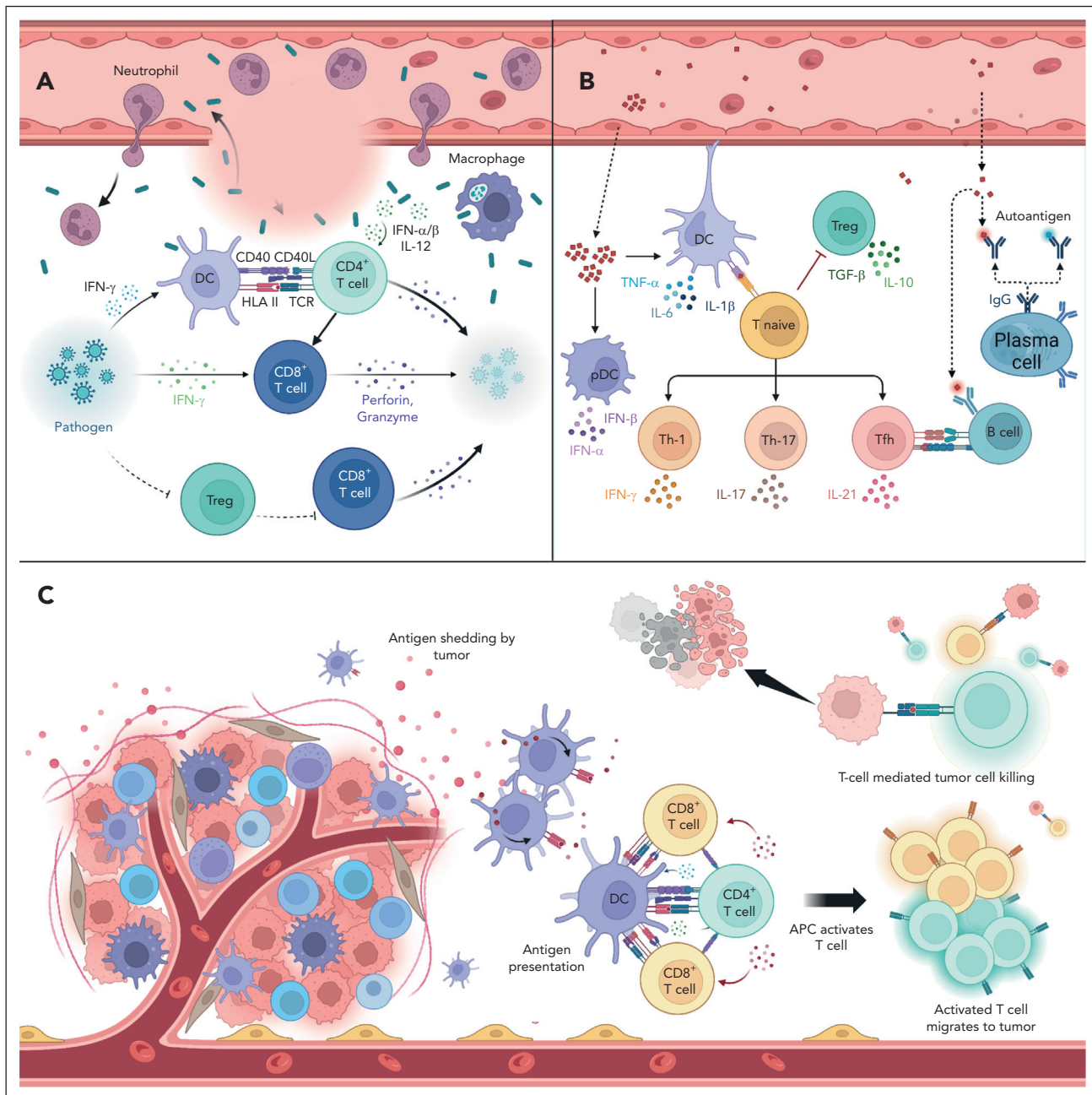


Figure 1. Role of T cells in infection, autoimmunity, and cancer. (A) During infection, CD8⁺ T cells directly recognize and eliminate pathogenic peptides presented on the surfaces of infected cells. (B) T cells do not react against self-antigens owing to central and peripheral immunogenic tolerance. Failure of the checkpoints described in panels A and B can cause uncontrolled expansion of self-reactive T cells, which leads to the development of AI diseases. (C) In steady-state, T cells survey, patrol, identify, and destroy abnormal cells, including cancer cells. pDC, plasmacytoid DC.

engages with antigenic peptides presented by the HLA class II molecules, and facilitates communication with antigen-presenting cells (APCs), such as DCs (Figure 1).¹³

CD4⁺ T cells activate cytotoxic T cells, B lymphocytes, innate immune cells (eg, DCs, basophils, and neutrophils), and nonimmune cells.¹³ Upon activation of the TCR, antigen naïve CD4⁺ T cells differentiate into 6 distinct functional subtypes, namely, Th-1, Th-2, Th-17, Th-22 cells, T follicular helper (Tfh) cells, and Treg cells, each characterized by the secretion of specific cytokines, which are essential to functionally activate APCs and CD8⁺ T cells (Figure 1).¹⁴

Differentiated CD4⁺ T cells are classically divided in 2 groups, Th-1 and Th-2 cells, based on the cytokines they release.¹⁵ Th-1 cells secrete IFN- γ , TNF- α , and interleukin-2 (IL-2), which promote cell-mediated immunity and control infections induced by intracellular pathogens.^{16,17} Th-2 cells secrete IL-4, IL-5, IL-10, and IL-13, which mediate humoral immune responses and resistance to external pathogens.¹⁵ Under physiological conditions, the differentiation of Th-1/Th-2 cells is balanced, which leads to a tight regulation of the cellular and humoral immune response.

However, the Th-1/Th-2 ratio is altered in MDS because the number of Th-1 cells is lower than that in HDs. Significantly

decreased Th-1 cell counts are inversely correlated with higher blast counts in the BM of patients with MDS.¹⁸ Moreover, a high level of IL-4, a cytokine that is mainly produced by Th-2 cells, is an independent factor that predicts shorter overall survival in patients with intermediate- to higher-risk MDS.¹⁹ Interestingly, T cells cultured in the presence of MDS-derived monocytes are significantly skewed toward Th-2 differentiation,²⁰ which supports the hypothesis that Th-2 cells rely on Th-1 cells' effective anticancer immunity instead of driving tumor evasion by their own polarization.^{21,22}

Th-17 cells

Th-17 cells are a subset of CD4⁺ T cells that mainly secrete the proinflammatory cytokines IL-17 and IL-23 and protect the body from bacterial and fungal infections (Figure 1).²³ IL-17 facilitates and induces an inflammatory cytokine environment, and abnormal expression of IL-17 has been reported in patients with AI diseases and cancers.²⁴ IL-17-induced inflammatory mediators, such as granulocyte-colony stimulating factor, IL-6, and C-X-C motif Chemokine Ligand 1 (CXCL1) stimulate the expansion and recruitment of dysfunctional myeloid cells and establish a proangiogenic and immune suppressive tumor environment that enhances tumor growth and clonal expansion. Notably, IL-17 enhances the development and progression of a wide array of malignancies.²⁵

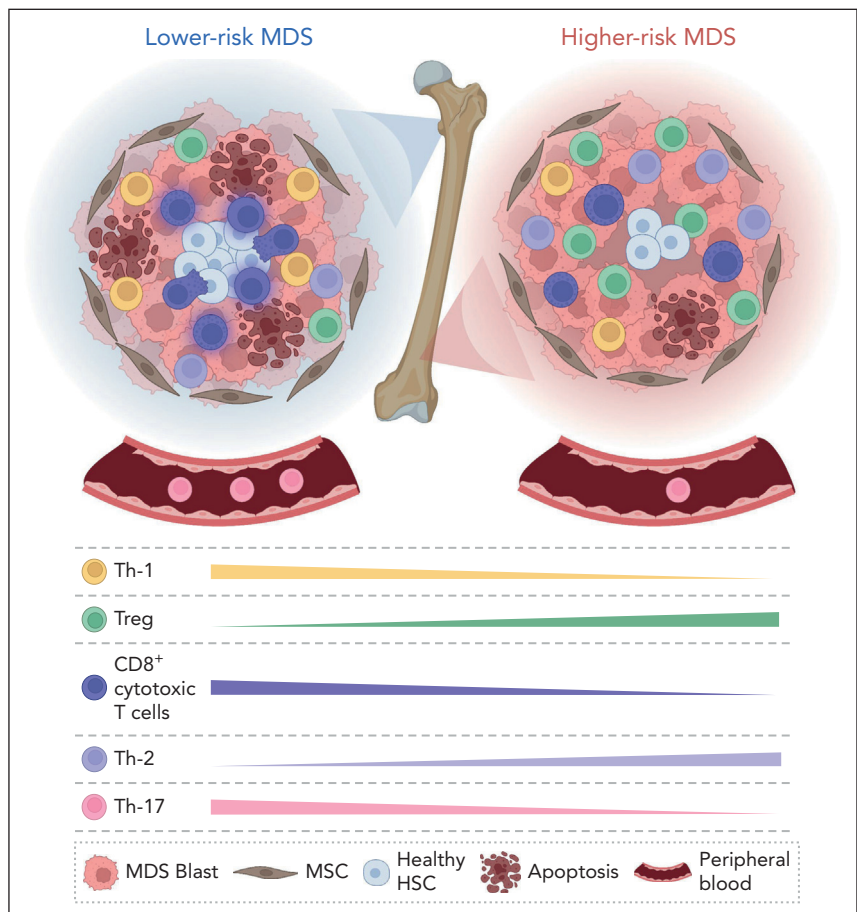
Patients with lower-risk MDS have significantly higher Th-17 cell counts and IL-17 levels in the PB and BM than those with higher-risk MDS (Figure 2). Additionally, PB cells from patients with lower-risk MDS have significantly increased expression of the RAR-related orphan receptor gene family, which encode key transcription factors inducing Th-17 lineage commitment.²⁶ In patients with lower-risk MDS, Th-17 cells stimulate secretion of several inflammatory-associated cytokines (eg, IL-6, IL-21, IL-22, and IL-23), which results in a proinflammatory milieu and leads to increased HSC apoptosis and ineffective BM hematopoiesis (Figure 2).^{27,28}

Th-22 cells

Th-22 cells are a subset of Th cells that mainly secrete IL-22, IL-13, and TNF- α .²⁹ Naïve CD4⁺ T cells differentiate into Th-22 cells after IL-6 and TNF- α stimulation.³⁰ IL-22, a member of the IL-10 family, protects tissues from inflammation but can also elicit proinflammatory effects, contributing to disease pathogenesis.³¹ Indeed, IL-22 has a pathogenic role in several AI diseases.³²

In MDS, the number of Th-22 cells is increased in the PB of late-stage patients compared with that of early-stage patients and correlates with TNF- α and IL-6 levels.³³ This observation suggests that exacerbation of inflammatory cytokine signaling during MDS progression may polarize and expand Th-22 cells,

Figure 2. Immune deregulation in lower-risk MDS and higher-risk MDS. (Left panel) Lower-risk MDS are characterized by the hyperfunction of immune cells. CD8⁺ T cells are increased in number and functionally activated. (Right panel) Higher-risk MDS are characterized by an immunosuppressive environment that causes immune escape. CD8⁺ T cells are significantly decreased, whereas the number of Treg cells is increased. MSC, mesenchymal stem cell.



thereby further contributing to immune escape and clonal evolution (Figure 2).

Tfh cells

Tfh cells represent a subpopulation of CD4⁺Th cells, characterized by the surface expression of CXCR5, inducible costimulatory molecule (ICOS), programmed cell death protein 1 (PD-1), and transcription factor B-cell lymphoma 6.³⁴ Tfh cells mainly secrete IL-21, which induces the proliferation and differentiation of B cells into antibody-producing cells (Figure 1).³⁵ The binding of CXCL13 to its receptor CXCR5 regulates lymphocyte infiltration within the tumor microenvironment, thus affecting responsiveness to immune- and cytotoxic-targeted therapies.³⁶

In MDS, patients with lower-risk disease have significantly decreased PB Tfh cell counts compared with HDs.³⁷ These findings were supported by preclinical studies in the *NUP98-HOXD13* mouse MDS model that showed reduced PB and BM numbers and aberrant function of Tfh cells. Further in vitro experiments using this system demonstrated that Tfh cells' reduction and dysfunction hindered antibody production by B cells, which suggests that Tfh cells have a role in regulating humoral immunity.^{38,39} Moreover, patients with MDS with AI diseases have a higher number of PB Tfh cells than that of those without AI diseases,⁴⁰ but whether these cells can mediate immune deregulation in this setting remains to be defined.

Treg cells

Treg cells have an established role in suppressing abnormal/excessive immune responses to self- and nonself-antigens to maintain immune homeostasis. However, Treg cells can also play an active role in inhibiting tumor-specific immunity, thus facilitating immune evasion of cancer cells.⁴¹ Treg cells are divided into different subsets, such as naïve cells, central memory cells, effector memory (emTreg) cells, and effector Treg cells based on these cells' differentiation state and immunosuppressive potential.⁴² Treg cells modulate immune reactions and affect immune surveillance⁴³ by secreting immunosuppressive cytokines (eg, IL-10 and TGF- β ; Figure 1).⁴⁴ Thus, elevated Treg counts and function result in defective immune activation and compromised antitumor immunity.⁴⁵

In MDS, the number of Treg cells in the PB and BM of patients with higher-risk MDS is increased compared with that in lower-risk patients,^{46,47} possibly because the expression of tumor-associated antigens on MDS cells during disease evolution. Treg cells decrease after response to therapy but increase again at therapy failure.⁴⁸ These findings suggest that aberrant expansion of Treg cells drives immune surveillance suppression in MDS, thereby contributing to disease progression (Figure 2).^{46,49,50}

CD8⁺ cytotoxic T cells

CD8⁺ cytotoxic T cells directly kill tumor cells and are the most powerful effectors of surveillance and immune defense against cancer cells.^{51,52} The CD8 glycoprotein is located on the membrane of CD8⁺ T cells, which recognize specific antigens bound to the HLA class I molecules on the surface of APCs. Upon recognition of pathogens, CD8⁺ T cells activate different mechanisms to kill infected or malignant cells by secreting

proinflammatory cytokines such as TNF- α and IFN- γ , releasing cytotoxic mediators (eg, perforin and granzymes), or activating the Fas/FasL pathway (Figure 1).⁵³ CD8⁺ T cells also regulate HSC pool dynamics in the BM milieu.⁵⁴ Exhaustion and functional impairment of CD8⁺ T cells in response to the tumor microenvironment or chronic antigenic stimulation⁵² is a hallmark of many cancers.⁵³

In MDS, patients with lower-risk disease have higher CD8⁺ T-cell counts.^{47,55} However, while suppressing the malignant clone, CD8⁺ T cells also affect normal hematopoiesis, resulting in the apoptosis observed in the BM of these patients (Figure 2).⁵⁶ In higher-risk MDS, CD8⁺ T cells are decreased, have lower cytotoxicity capability and overexpress the PD-1/PD ligand 1 (PD-L1), which enhances the ability of tumor cells to evade the host immune surveillance⁵⁷ by reducing TCR-induced redirected toxicity.⁵⁸

$\gamma\delta$ T cells

Although $\gamma\delta$ T cells are a minor subset of T cells (1%-10% of circulating PB T cells⁵⁹), they constitute an important component of innate immunity and play a key role in the rapid response to pathogens and tumoral cells.^{60,61} $\gamma\delta$ T cells display distinct TCR γ and δ ($\gamma\delta$ TCR) chains that are heterogeneous in structure and function.⁶² Specifically, $\gamma\delta$ T-cell subsets characterized by the expression of V δ 1 and V δ 2 chains exhibit distinct tissue tropisms. The V δ 1⁺ subset is preferentially enriched in mucosal tissues, whereas the V δ 2⁺ subset is frequently encountered in the PB and lymphoid organs.⁶³ These findings suggest that $\gamma\delta$ T cells are functionally specialized to execute specific immune surveillance functions in different tissue environments.

$\gamma\delta$ T cells are reduced in patients with lower-risk MDS, mainly in patients with associated AI diseases.⁶⁴ Additionally, in vitro studies showed that, independently of any MDS risk stratification, $\gamma\delta$ T cells do not expand in response to bromohalohydrin pyrophosphate (a potent stimulator of human $\gamma\delta$ T cells) and do not proliferate after IL-2 stimulation,⁶⁴ which suggests these cells' irreversible functional impairment.

A summary of the quantitative and qualitative changes in T-cell subsets among different MDS genetic subgroups is included in supplemental Tables 1 and 2 (available on the *Blood* website), respectively.

Inflammation and the immune system in MDS

Inflammation, a pivotal driver of MDS pathogenesis, significantly induces progressive dysfunction in the hematopoietic niche^{4,65,66} and affects the immune response.⁶⁷⁻⁶⁹ The MDS proinflammatory milieu attracts regulatory and suppressive immune cells, thereby inhibiting immune surveillance of malignant clones through the elevated production of inflammatory cytokines such as TNF- α , IFN- γ , IL-6, IL-1 β , and IL-8.¹⁴ Several clinical studies are currently investigating the potential to inhibit dysregulated inflammatory signaling in MDS by targeting key hub mediators such as IRAK1 and IRAK4, as well as ligands and receptors, including S100A9, CD33, IL-1 β , IL1RAP, and TGF- β .

A better understanding of the molecular and cellular mechanisms through which the inflammatory environment contributes to immune system dysfunction could allow the development of new therapeutic strategies, particularly in patients with lower-risk MDS.

TCR repertoire in patients with MDS

The TCR plays a fundamental role as a transmembrane glycoprotein in the immunological synapse. The TCR is a

heterodimeric protein that is formed by the combination of either α and β ($\alpha\beta$ TCR) or γ and δ ($\gamma\delta$ TCR) chains. Expression of either $\alpha\beta$ or $\gamma\delta$ TCRs on T cells are crucial for antigen recognition and immune responses.⁷⁰

The populations of cells with unique TCR sequences are known as the TCR repertoire (Figure 3). Development of the TCR repertoire is a dynamic process that occurs over a lifetime. However, the diversity of the TCR repertoire dramatically decreases during the seventh and eighth decades of life, which

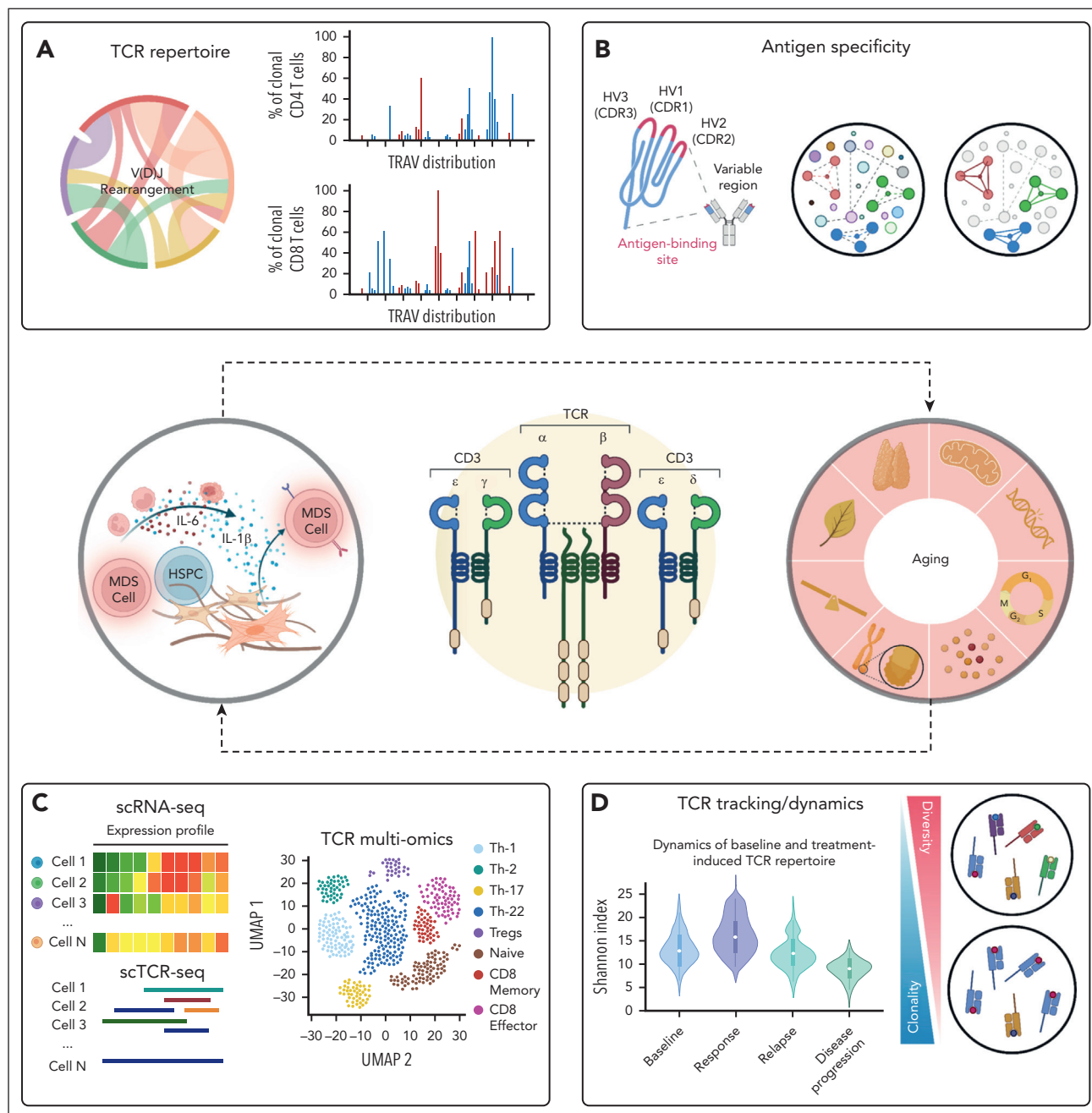


Figure 3. Integrative approach dissecting TCR complexity. TCR repertoire is regulated during thymocyte development and drives the generation of $\alpha\beta$ and $\gamma\delta$ T lymphocytes. Chronic inflammatory states or physiological aging can hinder TCR development and function. (A) TCR clonotype frequency distribution. (B) Prediction of TCR binding specificity and putative antigens. (C) Gene expression profile of clonotypes within a TCR cluster. (D) Comparison of clonotype tracking and repertoire diversity across different groups of patients with varying treatment responses. HV, hypervariable region; HSPC, hematopoietic stem and progenitor cell; TRAV, T-cell receptor alpha variable region.

affects the recognition of a wide range of antigenic targets and immune functions (Figure 3).⁷¹

Analysis of the TCR repertoire provides a holistic representation of the extensive versatility and breadth of the immune T-cell compartment. Clonal T cells can be identified by analyzing the third complementarity determining region (CDR3) of the TCR, a hypervariable domain that directly binds to antigenic cell-surface peptides, named HLA proteins. In normal T-cell homeostasis, a restricted number of T cells are activated and undergo intermittent clonal expansion that is triggered by foreign antigens. However, viral infections, AI diseases and clonal T-cell malignancies induce an excessive clonal T-cell expansion.⁷²⁻⁷⁴

In MDS, the diversity of the TCR repertoire correlates with response to various therapeutic approaches (Figure 3). As an example, sequential analyses of the $\alpha\beta$ TCR repertoire identified a significant group of T cells that shared identical CDR3 lengths and involvement of variable TCR β chains which declined in patients with clinical responses to immunosuppression therapies.⁷⁵⁻⁷⁸ Moreover, although significant skewness in CDR3 length is detected in patients with MDS compared with that in HDs,⁷⁹ treatment with hypomethylating agents (HMAs) increased the TCR diversity.⁸⁰ In addition, patients with MDS whose disease responds to HMA treatment show TCR clonotype expansion, whereas patients with MDS whose disease is refractory to HMA therapy exhibited TCR clonotype contraction.⁸¹ These data suggest that the TCR clonotype diversity contributes to response to HMA therapy. Our unpublished data also show that patients whose disease respond to venetoclax-based therapy have a higher count of T-cell clonotypes and T-cell diversity, whereas reduction of these cells' clonotypes predicts disease progression. Together, these results highlight the potential role of adoptive immunotherapy strategies to enhance therapy efficacy in improving the survival of patients with MDS.

However, to date, it is not yet known whether the increase in TCR diversity or the emergence of new TCR clonotypes in patients whose disease responds to therapy is directly related to the therapeutic effect of the treatment (ie, increased release of neoantigens) or is induced by the reduction in tumor burden, which leads to the restoration of hematopoiesis. Further randomized clinical trials evaluating the differential impact of each therapy on the immune microenvironment may provide insights into T-cell adaptive immunity and establish a causal relationship between TCR dynamics and the pathogenesis and progression of MDS.

T-cell evasion in MDS

Immune evasion is a hallmark of cancer that enables malignant cell clones to expand and overpopulate healthy tissues.⁸² Immune evasion is especially relevant in patients with MDS whose aged immune system is vulnerable.⁸³ The overexpression of immune checkpoint proteins, such as PD-1/PD-L1 and cytotoxic T lymphocyte-associated protein 4 (CTLA-4) on T cells, leads to T-cell exhaustion and transition toward an immune-evading tumor microenvironment (Figure 4).⁸⁴

The interaction of PD-1 with its ligand PD-L1 (Figure 5) suppresses TCR-mediated T-cell proliferation and the release of cytokines that regulate immune activation, thus compromising

immune response. In MDS, PD-1/PD-L1 expression is significantly altered. MDS CD34⁺ hematopoietic stem and progenitor cells overexpress PD-L1, effector T cells and Treg cells upregulate PD-1.^{57,85-88} Secreted inflammatory cytokines, such as IFN- γ , TNF- α , and S100A9, which are present at high levels in the BM microenvironment of patients with MDS,⁸⁹⁻⁹¹ induce PD-1 and/or PD-L1 upregulation on MDS cells, thus facilitating MDS cells' escape from immune surveillance.

CTLA-4 is a costimulatory receptor that delivers a potent inhibitory signal to T cells, leading to restriction of immune responses.⁹² Thus, CTLA-4 expression on tumor cells induces an immunosuppressive state and allows tumor growth (Figure 4). In MDS, CTLA-4 levels correlate with disease stage and the risk of progression to AML (being overexpressed in higher-risk MDS compared with lower-risk MDS).⁹³

Other co-inhibitory receptors, such as the T-cell immunoglobulin and mucin domain 3 (TIM-3), and the T-cell immunoglobulin and immunoreceptor tyrosine-based inhibitory motif (ITIM) domain (TIGIT) are also associated with immune evasion (Figure 4). TIM-3 is a checkpoint receptor that was initially identified on terminally differentiated Th-1 and CD8⁺ T cells. TIM-3 is also expressed on other immune cells, such as Treg and natural killer (NK) cells. TIM-3 inhibits Th-1 cells' responses by inducing Th-1 cell-mediated apoptosis and regulates the expression of cytokines, such as TNF- α and IFN- γ .^{94,95}

Immune evasion, mainly mediated by the overexpression of immune checkpoints, plays a crucial role in the development and progression of MDS. Th-1, CD8⁺ and Treg cells have high TIM-3 expression, which further increases over the course of the disease.⁹⁴⁻⁹⁶ The overexpression of TIM-3 in MDS CD8⁺ T cells is correlated with reduced levels of perforin and granzyme B, and upregulation of the death receptor CD95, which affects these cells' cytotoxicity and killing capabilities and leads to their susceptibility to cell death, respectively, thus facilitating immune escape.⁹⁴ Importantly, TIM-3 is also overexpressed in MDS/AML leukemic stem cells and blasts, which suggests that monoclonal antibodies targeting TIM-3 may have a dual anti-cancer effect by directly depleting the leukemic clone while potentiating the immune response.⁹⁷

TIGIT levels are increased in patients with higher-risk MDS⁸⁵ and lead to CD4⁺ T, CD8⁺ T, and NK cells' hyporesponsiveness upon stimulation and these cells' decreased secretion capability of effector cytokines (eg, CD107a, IFN- γ and TNF- α), which results in malignant clonal expansion and tumor escape.⁸⁵

T-cell-based therapeutic approaches in MDS

Current treatment options for patients with MDS are mainly based on supportive care or HMA-based therapies. Except for allogeneic stem cell transplantation, which is limited to eligible patients, no new curative treatments have been developed for MDS in the last 10 years.⁹⁸

Several exploratory clinical trials targeting signaling pathways, cell death regulators or immune cell dysfunction are currently under development.⁹⁹ Harnessing the power of immune cells, especially T cells, to increase antitumor responses has emerged

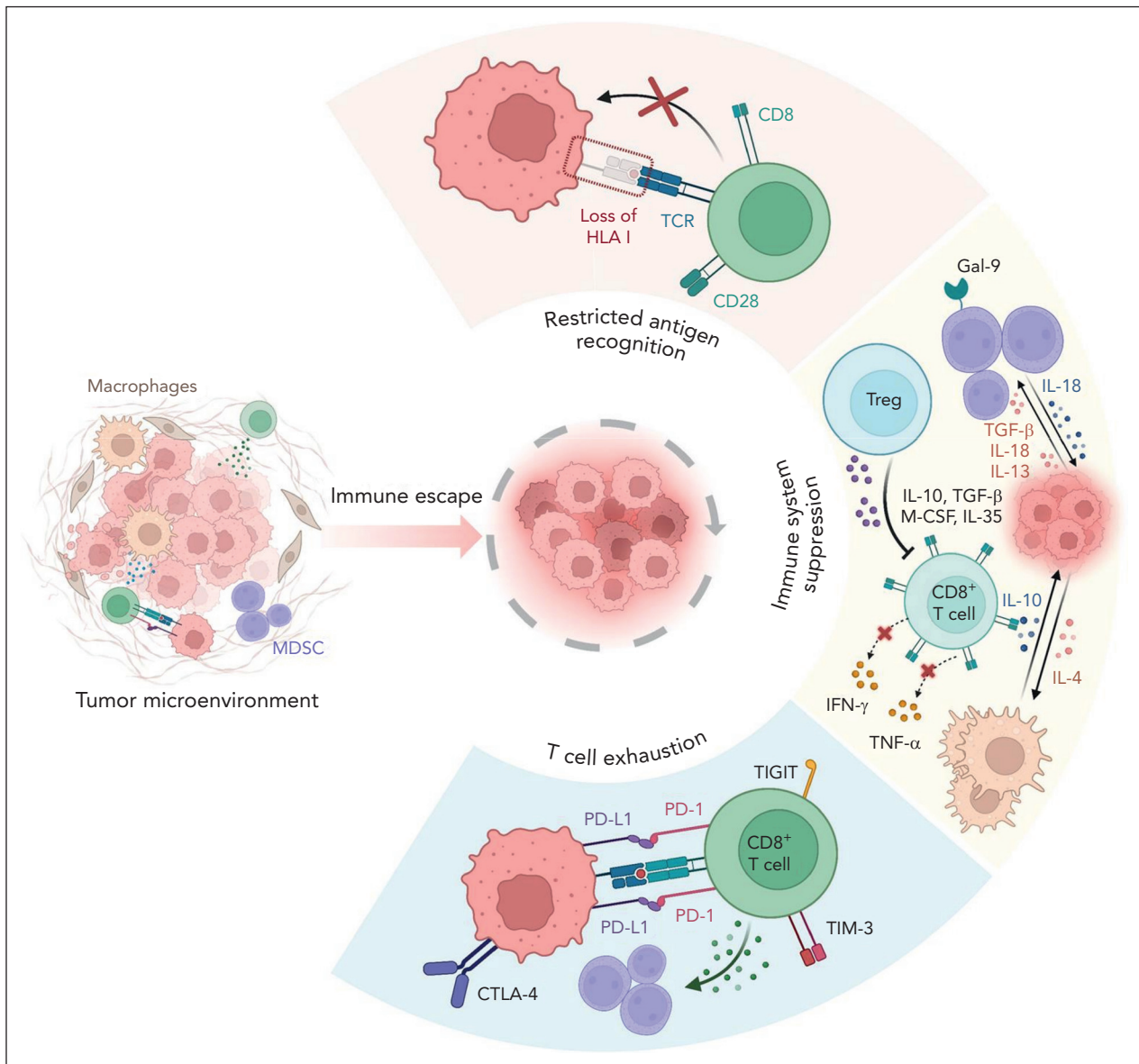


Figure 4. Mechanisms of tumor evasion in MDS. MDS cells escape immune responses and bypass immune-mediated attacks by restricting their antigen recognition, dysregulating several immune checkpoints, and inducing T-cell exhaustion. Gal-9, galectin-9; MDSC, myeloid-derived suppressor cell.

as a promising approach in the management of hematologic malignancies.³ Immune checkpoint inhibitors, chimeric antigen receptor (CAR) T-cell therapies, and novel approaches based on expanded/activated $\gamma\delta$ T cells and bispecific T-cell engagers (BiTEs) are promising therapeutic options to treat patients with MDS (Figure 5; Table 1).

Checkpoint inhibitors are monoclonal antibodies that reactivate the immune system against malignant cells by blocking the interactions of immune function inhibitory receptors with their ligands (Figure 5). To date, treatments targeting PD-1, PD-L1 or CTLA-4-mediated interactions showed modest response rates in MDS.^{100,101} Indeed, pembrolizumab (MK3475), a humanized IgG4 monoclonal antibody that blocks the interaction of PD-1 with PD-L1, showed no clinical activity as single agent in patients with intermediate-1/2 and higher-risk MDS whose disease previously failed HMA therapy (KEYNOTE-013 study;

NCT01953692)¹⁰⁰ and pembrolizumab in combination with azacytidine only modestly improved these patients' overall response rate (25%) (NCT03094637; Table 1).¹⁰¹ These studies suggest that checkpoint inhibitors targeting the PD-1-mediated signaling pathway cannot overcome the poor outcomes of patients with MDS whose disease failed HMA therapy. However, a phase 2 basket clinical trial of PD-1 and CTLA-4 inhibitors (nivolumab and ipilimumab, respectively) alone or in combination with azacytidine (NCT02530463) showed clinical activity and a tolerable safety profile in patients with frontline and HMA therapy-refractory MDS, respectively (Table 1).¹⁰³

A phase 1b clinical trial (NCT03066648) of the immune checkpoint inhibitor sabatolimab (a humanized monoclonal antibody that targets TIM-3) in combination with HMA therapy showed antileukemic activity and emerging response durability in patients with higher-risk MDS (Table 1).¹⁰⁴ However, another

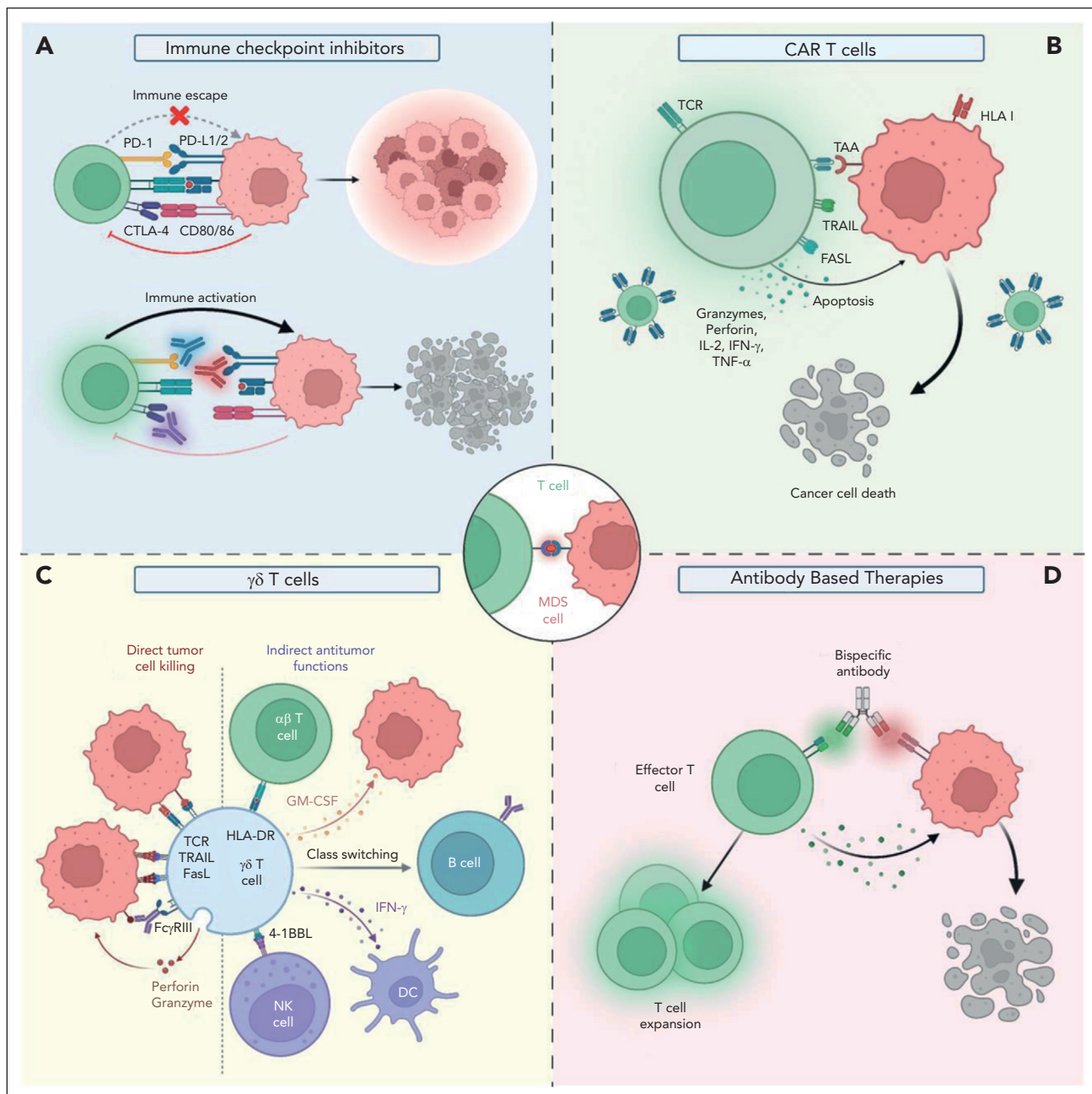


Figure 5. Emerging T-cell-based therapies in MDS. T-cell-based treatment strategies, such as immune checkpoint inhibitors, CAR T-cell therapies, expanded/activated $\gamma\delta$ T cells, and BiTEs hold promise to achieve robust antileukemic activities in MDS while avoiding T-cell cytotoxicity against healthy tissues. (A) Immune checkpoint inhibitors. (B) CAR T cells. (C) $\gamma\delta$ T cells. (D) Antibody-based therapies. Fc γ RIII, low-affinity IgG receptor type 3; GM-CSF, granulocyte-macrophage colony-stimulating factor; TAA, tumor-associated antigen; TRAIL, TNF-related apoptosis inducing ligand.

clinical trial of sabatolimab in combination with HMA therapy (NCT03946670; STIMULUS-MDS1) did not show any significant improvement in complete remission (CR) or progression-free-survival when compared with HMA therapy alone.¹⁰⁵

The STIMULUS-MDS2 study, a phase 3, randomized trial evaluating the clinical effects of sabatolimab alone or in combination with azacytidine in higher-risk MDS (NCT04266301) is currently ongoing and aims to provide definitive evidence of the potential long-term benefits of sabatolimab in combination with HMA therapy in patients with higher-risk MDS⁹⁷.

CAR T-cell therapies have revolutionized the treatment in lymphoid malignancies (Figure 5).¹¹⁴⁻¹¹⁶ However, the identification of CAR T-cell-specific antigenic targets in MDS remains challenging.¹¹⁷ Current CAR T-cell therapies in MDS target the myeloid CD123 and CD33 antigens which are concomitantly expressed on normal HSCs, thereby resulting in off-target toxicities with profound myeloablation.¹¹⁷ Recent preclinical studies based on the administration of MDS-derived CAR T cells against CD123 or CD33 in primary MDS/AML-derived xenograft models showed significant efficacy in depleting leukemic clones.^{118,119}

Table 1. Select targeted T-cell therapies currently in MDS clinical trials

Therapy	Target	Phase	Enrolled patients	Response rate OS rate and mOS	AEs grade ≥3	NCT number/ reference
Immune checkpoint inhibitors	PD-1	1b	N = 28 lower- and higher-risk MDS (HMA failure)	Overall ORR: 0% SD: 44% mOS: 6 mo 2-y OS (overall): 17% 2-y OS (intermediate-1): 46% 2-y OS (intermediate-2 and higher-risk): 0%	Gastro-enteritis: 4% Pain: 4% TLS: 4%	NCT01953692 ¹⁰⁰
		2	N = 37 20 HMA failure n = 17 frontline	HMA-refractory ORR: 25% CR: 5% mCR: 10% HI: 10% mOS: 5.8 mo Frontline cohort ORR: 76% CR: 18% mCR: 29% HI: 6% mOS: not reached (mFU: 12.8 mo)	Neutropenia: 32% Pneumonia: 24% FN: 18% Anemia: 12%	NCT03094637 ¹⁰¹
Nivolumab and/or ipilimumab ± azacytidine	PD-1 (Nivo) CTLA-4 (ipi)	2	N = 76 n = 35 HMA-failure n = 41 frontline	ORR: 13% (Nivo; HMA-failure) ORR: 35% (ipi; HMA-failure) ORR: 75% (Nivo + Aza; frontline) ORR: 71% (ipi + aza; frontline) CR/CRp: 15% (Nivo; HMA-failure) CR/CRp: 0% (ipi; HMA-failure) CR/CRp: 50% (Nivo + Aza; frontline) CR/CRp: 38% (ipi + Aza; frontline) mOS: 8 mo (ipi or Nivo; HMA-failure) mOS: not reached (ipi + Aza; frontline) mOS: 12 mo (Nivo + Aza; frontline)	NS	NCT02530463 ¹⁰²
		Basket exploratory phase 2	N = 26 n = 11 HMA-failure n = 15 frontline	Ipi + Nivo (HMA-refractory cohort) ORR: 36% CR: 9%; CRi: 9% HI: 18% mPFS: 7.1 mo mOS: 11.4 mo Ipi + Nivo + Aza (frontline cohort) ORR: 67% CR: 5% HI: 5% mPFS: 10 mo mOS: 12 mo	Infection: 55% FN: 46% Rash: 24% Elevated AST/ALT: 24%	NCT02530463 ¹⁰³
Sabatolimab + HMAs	TIM-3	1b	53 MDS	ORR: 57% mDOR: 16.1 mo	Neutropenia: 47% Thrombocytopenia: 43% FN: 36% Anemia: 28%	NCT03066648 ¹⁰⁴

AEs, adverse effects; Aza, azacytidine; CMML, chronic myelomonocytic leukemia; CRh, complete response with complete cytogenetic remission; CRi, complete response with incomplete count recovery; CRp, complete remission with incomplete platelet recovery; CRS, cytokine release syndrome; DOR, duration of response; FN, febrile neutropenia; HI, hematological improvement; HR, higher-risk; iipi, ipilimumab; IR, infusion-related reaction; mCR, marrow complete response; mFU, median follow-up; mOS, median overall survival; PR, partial response; mPFS, median progression-free survival; NA, not available; Nivo, nivolumab; ORR, overall response rate; OS, overall survival; PD, progressive disease; RFS, relapse-free survival; SD, stable disease; TLS, tumor lysis.

Table 1 (continued)

Therapy	Target	Phase	Enrolled patients	Response rate OS rate and mOS	AEs grade ≥3	NCT number/ reference
Sabatolimab + HMAs	TIM-3	2	N = 65 higher-risk MDS	Overall ORR: 68% CR: 22% mOS: 22.8 mo mPFS: 11.1 mo	Neutropenia: 56% Thrombocytopenia: 37% FN: 35% Anemia: 23% Leukopenia: 23%	NCT03946670 ¹⁰⁵
Adoptive T-cell therapies	CYAD-01	1	22 total 1 R/R MDS N = 24 n = 3 R/R MDS n = 1 CMML n = 20 R/R AML	Patient achieved mCR	CRS: 31% Lymphopenia: 19% Transient CRS grade 3	NCT03018405 ¹⁰⁶ NCT03927261 ¹⁰⁷
	PRGN-3006 Ultra CAR T cells	1/1b		ORR MDS/CMML: 0% ORR (AML): 30% (1 CRi, 1 CRh, 1 PR)		
Bispecific antibodies	Flotetuzumab	1/2	N = 5 R/R MDS N = 46 n = 39 R/R AML n = 7 R/R MDS	1 evaluable patient: PD patients with MDS NE: 1 SD: 3 mCR: 3 mCR + HI: 44% HI: 11% CRi: 56%	No results reported CRS: 8.7% Anemia: 4.3% IRR: 4.3% Infusion reaction: 4%	NCT02152956 ^{108,109} NCT03647800 ¹¹⁰
	APVO436	1b	23 total 9 R/R MDS 12 AML 2 CMML			NCT05285813 ¹¹¹
	Vibecotamab	2	N = 68 R/R HR-MDS R/R AML	No results reported	No results reported	NCT03915379 ¹¹²
	JNJ-67571244	1		No reported results	No results reported	NCT03516591 ¹¹³
	AMV564	1				

AEs, adverse effects; Aza, azacitidine; CMML, chronic myelomonocytic leukemia; CRh, complete response with complete cytogenetic remission; CRi, complete response with incomplete count recovery; CRp, complete remission with incomplete platelet recovery; CRS, cytokine release syndrome; DOR, duration of response; FN, febrile neutropenia; HI, hematological improvement; HR, higher-risk; ipi, ipilimumab; IRR, infusion-related reaction; mCR, marrow complete response; mFU, median follow-up; mOS, median overall survival; PR, partial response; mPFS, median progression-free survival; NA, not available; NE, not evaluable; Nivo, nivolumab; ORR, overall response rate; OS, overall survival; PD, progressive disease; RFS, relapse-free survival; SD, stable disease; TLS, tumor lysis.

A phase 1 clinical trial (NCT03018405) in patients with AML, multiple myeloma, and MDS after HMA failure assessed the efficacy of the autologous CAR T product CYAD-01 based on the natural killer group 2D (NKG2D) receptor.¹⁰⁶ NKG2D is an activating immunoreceptor, which plays a pivotal role in anti-tumor immunity by binding to numerous and highly diversified MHC class I-like self-molecules.¹²⁰ The expression of NKG2D ligands is largely absent on healthy cells but elevated in hematological malignancies.^{121,122} The study, which mainly enrolled patients with relapsed or refractory (R/R) AML and multiple myeloma (only 1 MDS patient was included and achieved a marrow CR; Table 1) showed that the treatment with CYAD-01 was well tolerated and had an antileukemic activity.¹⁰⁶

The quality of T cells from patients with MDS who previously received many other therapies hinders the efficacy of autologous CAR T in MDS. Thus, the feasibility of treatments based on the administration of “off-the-shelf” products or allogeneic CAR T cells generated from HDs is currently under investigation. Allogeneic products do not require patient-specific manufacturing, which lowers the costs and reduces the time to infusion,¹²³ the latter being particularly problematic in patients with higher-risk features who may experience disease progression before autologous CAR T-cell treatments are available. However, side effects induced by graft-versus-host disease and risk of host immune rejection still remain challenges to overcome before successfully implementing allogeneic CAR T cells into clinical practice.¹²⁴

$\gamma\delta$ T cells represent an appealing treatment for MDS in light of these cells’ favorable safety profile, potent and wide-ranging antitumor capabilities, and their potential for allogeneic administration (Figure 5).¹²⁵ Currently, several ongoing clinical trials based on expanded/activated $\gamma\delta$ T cells after allogeneic stem cell transplantation (NCT03533816, NCT03849651) aim to maximize the antitumor response and minimize graft-versus-host disease in patients with AML and patients with MDS. However, a better understanding of the mechanisms underlying the antitumor activities of $\gamma\delta$ T cells and their interactions with the tumor microenvironment remains a crucial point to be addressed before developing effective $\gamma\delta$ T-cell-based therapies in MDS.

Bispecific antibodies (BiTEs) are recombinant antibodies designed to recognize and bind 2 different antigens or 2 different epitopes on the same antigen (Figure 5). BiTEs target CD3 and tumor-specific antigens simultaneously, thereby promoting T-cell-induced cytotoxicity.¹²⁶

An increasing number of BiTEs against tumor-specific antigens are under evaluation in R/R MDS and AML, including those targeting the CD123 (NCT02152956, NCT03647800, NCT05285813) and CD33 (NCT03915379, NCT03516591) antigens (Table 1).¹²⁷ As an example, an open-label phase 2 trial of the dual CD3-CD123 inhibitor vibecotamab (NCT05285813) is actively accruing patients with R/R MDS and AML harboring at least 20% of aberrant myeloblasts with CD123 expression. However, another ongoing multicenter phase 1b clinical trial of the dual CD3-CD123 inhibitor APVO436 (NCT03647800) is showing modest efficacy in R/R MDS and AML patients (Table 1).¹¹⁰ These

findings, although preliminary, highlight the need to better understand which cohort of patients with MDS might benefit from this immune approach and when, during disease stages, these bispecific antibodies might be effective to improve patient survival.

Immunosuppressive therapy (IST) in MDS

In a subset of patients with lower-risk MDS, PB cytopenias are caused by hyperactive T cells that suppress hematopoiesis through the direct attack on BM cells or the release of a variety of inflammatory cytokines, such as IFN- γ , TNF- α , and IL-17, as also observed in aplastic anemia.¹²⁸ This cohort of patients may benefit of IST. The most used IST involves the administration of cyclosporine (CsA) or antithymocyte globulin (ATG), either as monotherapy or in combination. CsA is a calcineurin inhibitor, which effectively suppresses CD4⁺ T cells, enhances cytotoxic lymphocyte function, and inhibits the release of TNF- α .¹²⁹ ATG is a mixture of purified polyclonal IgG derived from rabbits or horses immunized with human thymocytes that induces immune modulation mainly through T cells’ complement-dependent lysis and apoptosis.¹³⁰ Based on National Comprehensive Cancer Network guidelines, IST is indicated as a treatment option for symptomatic anemia in lower-risk, non-del(5q) MDS, particularly in patients younger than 60 years old, with $\leq 5\%$ blasts in the BM, hypocellular BM, paroxysmal nocturnal hemoglobinuria, or STAT3 mutant cytotoxic T-cell clones.¹³¹

CsA and ATG combination therapy have shown response rates of up to 51% in patients with lower-risk MDS.¹³² A recent systematic review and meta-analysis of patients with MDS treated with IST that includes 9 prospective cohort studies and 13 clinical trials showed an overall response rate of 42.5%, including a CR rate of 12.5% and red blood cell transfusion independence rate of 33.4%.¹³³ Future randomized clinical trials are critically warranted to definitively determine the impact of IST on response and survival in patients with MDS.¹³³

Conclusions

Impaired immune functions in the MDS microenvironment enable tumoral cell immune escape, which contributes to disease initiation and maintenance. Further T-cell alterations during MDS progression induce autoimmunity, aberrant release of cytokines, and attenuation or loss of immune surveillance, which results in the proliferation of the malignant clone.

Dysregulation of immune checkpoints (ie, PD-1/PD-L1, CTLA-4, TIM-3, and TIGIT) on T cells is a key mechanism of immune evasion. Thus, emerging T-cell-based therapies, including immune checkpoint inhibitors, CAR T-cell therapy, expanded/activated $\gamma\delta$ T-cell injections, and BiTEs offer promising avenues to target dysfunctional T-cell populations and enhance anti-tumor responses in MDS (Figure 5).

A better understanding of how different T-cell subtypes and MDS cells interact during disease evolution and how T-cell subpopulations dynamically change after therapy remains a future challenge for the development of more effective

therapeutic combinations for improving the outcome of patients with MDS.

Acknowledgments

The authors thank Helen T. Chifotides and Kelly A. Soltysiak for editing the manuscript. Figures were created using [Biorender.com](#).

This work was supported by philanthropic contributions to The University of Texas MD Anderson Cancer Center’s myelodysplastic syndrome/acute myeloid leukemia Moon Shot, by the Umberto Veronesi Foundation, and by the Edward P. Evans Foundation. J.J.R.-S. is the recipient of the MDACC Odyssey fellowship.

Authorship

Contribution: J.J.R.-S. and S.C. wrote the manuscript; and J.J.R.-S. created the figures.

Conflict-of-interest disclosure: The authors declare no competing financial interests.

ORCID profile: S.C., [0000-0001-6583-8910](#).

Correspondence: Juan Jose Rodriguez-Sevilla, Department of Leukemia, The University of Texas MD Anderson Cancer Center, 1515 Holcombe Blvd, Houston, TX 77030; email: jrsevilla@mdanderson.org; and Simona Colla, Department of Leukemia, The University of Texas MD Anderson Cancer Center, 1515 Holcombe Blvd, Houston, TX 77030; email: scolla@mdanderson.org.

Footnotes

Submitted 3 November 2023; accepted 12 January 2024; prepublished online on *Blood First Edition* 18 January 2024. <https://doi.org/10.1182/blood.2023023166>.

The online version of this article contains a data supplement.

REFERENCES

1. Xia A, Zhang Y, Xu J, Yin T, Lu XJ. T cell dysfunction in cancer immunity and immunotherapy. *Front Immunol*. 2019;10:1719.

2. Disis ML. Immune regulation of cancer. *J Clin Oncol*. 2010;28(29):4531-4538.

3. Waldman AD, Fritz JM, Lenardo MJ. A guide to cancer immunotherapy: from T cell basic science to clinical practice. *Nat Rev Immunol*. 2020;20(11):651-668.

4. Balandrán JC, Lasry A, Aifantis I. The role of inflammation in the initiation and progression of myeloid neoplasms. *Blood Cancer Discov*. 2023;4(4):254-266.

5. Chokr N, Patel R, Wattamwar K, Chokr S. The rising era of immune checkpoint inhibitors in myelodysplastic syndromes. *Adv Hematol*. 2018;2018:2458679.

6. Lynch OF, Calvi LM. Immune dysfunction, cytokine disruption, and stromal changes in myelodysplastic syndrome: a review. *Cells*. 2022;11(3):580.

7. Simoni Y, Chapuis N. Diagnosis of myelodysplastic syndromes: from immunological observations to clinical applications. *Diagnostics (Basel)*. 2022;12(7):1659.

8. Symeonidis A, Kourakli A, Katevas P, et al. Immune function parameters at diagnosis in patients with myelodysplastic syndromes: correlation with the FAB classification and prognosis. *Eur J Haematol*. 1991;47(4):277-281.

9. Zou JX, Rollison DE, Boulware D, et al. Altered naive and memory CD4+ T-cell homeostasis and immunosenescence characterize younger patients with myelodysplastic syndrome. *Leukemia*. 2009;23(7):1288-1296.

10. Xu L-P, Luo X-H, Chang Y-J, et al. High CD4/CD8 ratio in allografts predicts adverse outcomes in unmanipulated HLA-mismatched/haploidentical hematopoietic stem cell transplantation for chronic myeloid leukemia. *Ann Hematol*. 2009;88(10):1015-1024.

11. Tay RE, Richardson EK, Toh HC. Revisiting the role of CD4+ T cells in cancer immunotherapy—new insights into old paradigms. *Cancer Gene Ther*. 2021;28(1-2):5-17.

12. Jardine L, Barge D, Ames-Draycott A, et al. Rapid detection of dendritic cell and monocyte disorders using CD4 as a lineage marker of the human peripheral blood antigen-presenting cell compartment. *Front Immunol*. 2013;4:495.

13. Zhu J, Paul WE. CD4 T cells: fates, functions, and faults. *Blood*. 2008;112(5):1557-1569.

14. Chatzileontiadou DSM, Sloane H, Nguyen AT, Gras S, Grant EJ. The many faces of CD4(+) T cells: immunological and structural characteristics. *Int J Mol Sci*. 2020;22(1):73.

15. Mosmann TR, Cherwinski H, Bond MW, Giedlin MA, Coffman RL. Two types of murine helper T cell clone. I. Definition according to profiles of lymphokine activities and secreted proteins. *J Immunol*. 1986;136(7):2348-2357.

16. Tan Y, Tan Y, Li J, et al. Combined IFN-γ and IL-2 release assay for detect active pulmonary tuberculosis: a prospective multicentre diagnostic study in China. *J Transl Med*. 2021;19(1):289.

17. Li X, Kömer H, Liu X. Susceptibility to intracellular infections: contributions of TNF to immune defense. *Front Microbiol*. 2020;11:1643.

18. Wang X, Wu DP, He G, Miao M, Sun A. Research of subset and function of Th cells in bone marrow of myelodysplastic syndrome patients. *Blood*. 2005;106(11):4913.

19. Liu Z, Xu X, Zheng L, et al. The value of serum IL-4 to predict the survival of MDS patients. *Eur J Med Res*. 2023;28(1):7.

20. van Leeuwen-Kerkhoff N, Westers TM, Poddighe PJ, de Groot TD, Kordasti S, van de Loosdrecht AA. Thrombomodulin-expressing monocytes are associated with low-risk features in myelodysplastic syndromes and dampen excessive immune activation. *Haematologica*. 2020;105(4):961-971.

21. Hamilton DH, Bretscher PA. Different immune correlates associated with tumor progression and regression: implications for prevention and treatment of cancer. *Cancer Immunol Immunother*. 2008;57(8):1125-1136.

22. Hamilton D, Ismail N, Kroeger D, Rudulier C, Bretscher P. Macrophage immunology and immunotherapy of cancer. *Immunotherapy*. 2009;1(3):367-383.

23. Romagnani S, Maggi E, Liotta F, Cosmi L, Annunziato F. Properties and origin of human Th17 cells. *Mol Immunol*. 2009;47(1):3-7.

24. Nistala K, Wedderburn LR. Th17 and regulatory T cells: rebalancing pro- and anti-inflammatory forces in autoimmune arthritis. *Rheumatology (Oxford)*. 2009;48(6):602-606.

25. Zhao J, Chen X, Herjan T, Li X. The role of interleukin-17 in tumor development and progression. *J Exp Med*. 2020;217(1):e20190297.

26. Castro G, Liu X, Ngo K, et al. RORγt and RORα signature genes in human Th17 cells. *PLoS One*. 2017;12(8):e0181868.

27. Zhang Z, Li X, Guo J, et al. Interleukin-17 enhances the production of interferon-γ and tumour necrosis factor-α by bone marrow T lymphocytes from patients with lower risk myelodysplastic syndromes. *Eur J Haematol*. 2013;90(5):375-384.

28. Kordasti SY, Afzali B, Lim Z, et al. IL-17-producing CD4(+) T cells, pro-inflammatory cytokines and apoptosis are increased in low risk myelodysplastic syndrome. *Br J Haematol*. 2009;145(1):64-72.

29. Hossein-Khannazer N, Zian Z, Bakkach J, et al. Features and roles of T helper 22 cells in immunological diseases and malignancies. *Scand J Immunol*. 2021;93(5):e13030.

30. Jiang S, Dong C. A complex issue on CD4(+) T-cell subsets. *Immunol Rev*. 2013;252(1):5-11.

31. Saxton RA, Henneberg LT, Calafiore M, et al. The tissue protective functions of interleukin-22 can be decoupled from pro-inflammatory actions through

- structure-based design. *Immunity*. 2021; 54(4):660-672.e9.
32. Yamamoto-Furusho JK, Miranda-Pérez E, Fonseca-Camarillo G, Sánchez-Muñoz F, Dominguez-Lopez A, Barreto-Zuñiga R. Colonic epithelial upregulation of interleukin 22 (IL-22) in patients with ulcerative colitis. *Inflamm Bowel Dis*. 2010; 16(11):1823.
 33. Shao LL, Zhang L, Hou Y, et al. Th22 cells as well as Th17 cells expand differentially in patients with early-stage and late-stage myelodysplastic syndrome. *PLoS One*. 2012; 7(12):e51339.
 34. Jogdand GM, Mohanty S, Devadas S. Regulators of Tfh cell differentiation. *Front Immunol*. 2016;7:520.
 35. Qi H. T follicular helper cells in space-time. *Nat Rev Immunol*. 2016;16(10):612-625.
 36. Kazanietz MG, Durando M, Cooke M. CXCL13 and its receptor CXCR5 in cancer: inflammation, immune response, and beyond. *Front Endocrinol (Lausanne)*. 2019; 10:471.
 37. Lampropoulou P, Verigou E, Symeonidis A, Gogos C, Solomou EE. Characterization of T follicular helper cells in patients with low risk myelodysplastic syndromes. *Blood*. 2013; 122(21):4729.
 38. Lin YW, Slape C, Zhang Z, Aplan PD. NUP98-HOXD13 transgenic mice develop a highly penetrant, severe myelodysplastic syndrome that progresses to acute leukemia. *Blood*. 2005;106(1):287-295.
 39. Jiang H, Cui N, Yang L, et al. Altered follicular helper T cell impaired antibody production in a murine model of myelodysplastic syndromes. *Oncotarget*. 2017;8(58):98270-98279.
 40. Xiao N, He X, Niu H, et al. Increased circulating CD4(+)CXCR5(+) cells and IgG4 levels in patients with myelodysplastic syndrome with autoimmune diseases. *J Immunol Res*. 2021;2021:4302515.
 41. Zou W. Regulatory T cells, tumour immunity and immunotherapy. *Nat Rev Immunol*. 2006;6(4):295-307.
 42. Shevryev D, Tereshchenko V. Treg heterogeneity, function, and homeostasis. *Front Immunol*. 2019;10:3100.
 43. Wang C, Yang Y, Gao S, et al. Immune dysregulation in myelodysplastic syndrome: clinical features, pathogenesis and therapeutic strategies. *Crit Rev Oncol Hematol*. 2018;122:123-132.
 44. Aggarwal S, van de Loosdrecht AA, Alhan C, Ossenkoppele GJ, Westers TM, Bontkes HJ. Role of immune responses in the pathogenesis of low-risk MDS and high-risk MDS: implications for immunotherapy. *Br J Haematol*. 2011;153(5):568-581.
 45. Nishikawa H, Koyama S. Mechanisms of regulatory T cell infiltration in tumors: implications for innovative immune precision therapies. *J Immunother Cancer*. 2021;9(7):e002591.
 46. Kordasti SY, Ingram W, Hayden J, et al. CD4+CD25high Foxp3+ regulatory T cells in myelodysplastic syndrome (MDS). *Blood*. 2007;110(3):847-850.
 47. Giovazzino A, Leone S, Rubino V, et al. Reduced regulatory T cells (Treg) in bone marrow preferentially associate with the expansion of cytotoxic T lymphocytes in low risk MDS patients. *Br J Haematol*. 2019; 185(2):357-360.
 48. Kotsianidis I, Bouchliou I, Nakou E, et al. Kinetics, function and bone marrow trafficking of CD4+CD25+FOXP3+ regulatory T cells in myelodysplastic syndromes (MDS). *Leukemia*. 2009;23(3): 510-518.
 49. Lambert C, Wu Y, Aanei C. Bone marrow immunity and myelodysplasia. *Front Oncol*. 2016;6:172.
 50. Hamdi W, Ogawara H, Handa H, Tsukamoto N, Nojima Y, Murakami H. Clinical significance of regulatory T cells in patients with myelodysplastic syndrome. *Eur J Haematol*. 2009;82(3):201-207.
 51. Raskov H, Orhan A, Christensen JP, Gögenur I. Cytotoxic CD8+ T cells in cancer and cancer immunotherapy. *Br J Cancer*. 2021;124(2):359-367.
 52. Szabo PA, Levitin HM, Miron M, et al. Single-cell transcriptomics of human T cells reveals tissue and activation signatures in health and disease. *Nat Commun*. 2019; 10(1):4706.
 53. Philip M, Schietinger A. CD8+ T cell differentiation and dysfunction in cancer. *Nat Rev Immunol*. 2022;22(4):209-223.
 54. Geerman S, Brasser G, Bhushal S, et al. Memory CD8(+) T cells support the maintenance of hematopoietic stem cells in the bone marrow. *Haematologica*. 2018; 103(6):e230-e233.
 55. Lopes MR, Traina F, Campos PdM, et al. IL10 inversely correlates with the percentage of CD8+ cells in MDS patients. *Leuk Res*. 2013;37(5):541-546.
 56. Zheng Z, Qianqiao Z, Qi H, Feng X, Chunkang C, Xiao L. In vitro deprivation of CD8+ CD57+ T cells promotes the malignant growth of bone marrow colony cells in patients with lower-risk myelodysplastic syndrome. *Exp Hematol*. 2010;38(8):677-684.
 57. Yang H, Bueso-Ramos C, DiNardo C, et al. Expression of PD-L1, PD-L2, PD-1 and CTLA4 in myelodysplastic syndromes is enhanced by treatment with hypomethylating agents. *Leukemia*. 2014; 28(6):1280-1288.
 58. Sand K, Theorell J, Bruserud Ø, Bryceson YT, Kittang AO. Reduced potency of cytotoxic T lymphocytes from patients with high-risk myelodysplastic syndromes. *Cancer Immunol Immunother*. 2016;65(9): 1135-1147.
 59. Colonna-Romano G, Aquino A, Bulati M, et al. Impairment of gamma/delta T lymphocytes in elderly: implications for immunosenescence. *Exp Gerontol*. 2004; 39(10):1439-1446.
 60. Hayday AC. Gammadelta T cells and the lymphoid stress-surveillance response. *Immunity*. 2009;31(2):184-196.
 61. Kunzmann V, Wilhelm M. Anti-lymphoma effect of gammadelta T cells. *Leuk Lymphoma*. 2005;46(5):671-680.
 62. Zhao Y, Niu C, Cui J. Gamma-delta (γδ) T cells: friend or foe in cancer development? *J Transl Med*. 2018;16(1):3.
 63. Mensurado S, Blanco-Domínguez R, Silva-Santos B. The emerging roles of γδ T cells in cancer immunotherapy. *Nat Rev Clin Oncol*. 2023;20(3):178-191.
 64. Kiladjian JJ, Visentin G, Viey E, et al. Activation of cytotoxic T-cell receptor γδ T lymphocytes in response to specific stimulation in myelodysplastic syndromes. *Haematologica*. 2008;93(3):381-389.
 65. Barreyro L, Chlon TM, Starczynowski DT. Chronic immune response dysregulation in MDS pathogenesis. *Blood*. 2018;132(15): 1553-1560.
 66. Sallman DA, List A. The central role of inflammatory signaling in the pathogenesis of myelodysplastic syndromes. *Blood*. 2019; 133(10):1039-1048.
 67. Ganán-Gómez I, Wei Y, Starczynowski DT, et al. Dereglulation of innate immune and inflammatory signaling in myelodysplastic syndromes. *Leukemia*. 2015;29(7): 1458-1469.
 68. Mayle A, Yang L, Rodriguez B, et al. Dnmt3a loss predisposes murine hematopoietic stem cells to malignant transformation. *Blood*. 2015;125(4):629-638.
 69. Li Z, Cai X, Cai C-L, et al. Deletion of Tet2 in mice leads to dysregulated hematopoietic stem cells and subsequent development of myeloid malignancies. *Blood*. 2011;118(17): 4509-4518.
 70. Pellicci DG, Uldrich AP, Le Nours J, et al. The molecular bases of δ/αβ T cell-mediated antigen recognition. *J Exp Med*. 2014; 211(13):2599-2615.
 71. Naylor K, Li G, Vallejo AN, et al. The influence of age on T cell generation and TCR diversity. *J Immunol*. 2005;174(11): 7446-7452.
 72. Young NS, Maciejewski JP, Sloand E, et al. The relationship of aplastic anemia and PNH. *Int J Hematol*. 2002;76(Suppl 2): 168-172.
 73. Wechsler J, Bagot M, Nikolova M, et al. Killer cell immunoglobulin-like receptor expression delineates in situ Sézary syndrome lymphocytes. *J Pathol*. 2003; 199(1):77-83.
 74. Kuhn R, Sandu I, Agrafiotis A, et al. Clonally expanded virus-specific CD8 T cells acquire diverse transcriptional phenotypes during acute, chronic, and latent infections. *Front Immunol*. 2022;13: 782441.

75. Kochenderfer JN, Kobayashi S, Wiedner ED, Su C, Molldrem JJ. Loss of T-lymphocyte clonal dominance in patients with myelodysplastic syndrome responsive to immunosuppression. *Blood*. 2002;100(10):3639-3645.
76. Epperson DE, Nakamura R, Sauntharajah Y, Melenhorst J, Barrett AJ. Oligoclonal T cell expansion in myelodysplastic syndrome: evidence for an autoimmune process. *Leuk Res*. 2001;25(12):1075-1083.
77. Sloand EM, Mainwaring L, Fuhrer M, et al. Preferential suppression of trisomy 8 compared with normal hematopoietic cell growth by autologous lymphocytes in patients with trisomy 8 myelodysplastic syndrome. *Blood*. 2005;106(3):841-851.
78. Wlodarski MW, Gondek LP, Nearman ZP, et al. Molecular strategies for detection and quantitation of clonal cytotoxic T-cell responses in aplastic anemia and myelodysplastic syndrome. *Blood*. 2006;108(8):2632-2641.
79. Fozza C, Contini S, Galleu A, et al. Patients with myelodysplastic syndromes display several T-cell expansions, which are mostly polyclonal in the CD4(+) subset and oligoclonal in the CD8(+) subset. *Exp Hematol*. 2009;37(8):947-955.
80. Fozza C, Corda G, Barraqueddu F, et al. Azacitidine improves the T-cell repertoire in patients with myelodysplastic syndromes and acute myeloid leukemia with multilineage dysplasia. *Leuk Res*. 2015;39(9):957-963.
81. Abbas HA, Reville PK, Jiang X, et al. Response to hypomethylating agents in myelodysplastic syndrome is associated with emergence of novel TCR clonotypes. *Front Immunol*. 2021;12:659625.
82. Hanahan D. Hallmarks of cancer: new dimensions. *Cancer Discov*. 2022;12(1):31-46.
83. Fane M, Weeraratna AT. How the ageing microenvironment influences tumour progression. *Nat Rev Cancer*. 2020;20(2):89-106.
84. Seidel JA, Otsuka A, Kabashima K. Anti-PD-1 and anti-CTLA-4 therapies in cancer: mechanisms of action, efficacy, and limitations. *Front Oncol*. 2018;8:86.
85. Meng F, Li L, Lu F, et al. Overexpression of TIGIT in NK and T cells contributes to tumor immune escape in myelodysplastic syndromes. *Front Oncol*. 2020;10:1595.
86. Haroun F, Solola SA, Nassereldine S, Tabbara I. PD-1 signaling and inhibition in AML and MDS. *Ann Hematol*. 2017;96(9):1441-1448.
87. Coats T, Smith Ae, Mourikis TP, Irish JM, Kordasti S, Mufti GJ. Mass cytometry reveals PD1 upregulation is an early step in MDS disease progression. *Blood*. 2016;128(22):4296.
88. Tsvetkov NY, Morozova EV, Epifanovskaya OS, et al. Profile of checkpoint molecules expression on bone marrow cell populations in patients with high-risk myelodysplastic syndrome. *Blood*. 2020;136(suppl 1):43-44.
89. Kitagawa M, Saito I, Kuwata T, et al. Overexpression of tumor necrosis factor (TNF)-alpha and interferon (IFN)-gamma by bone marrow cells from patients with myelodysplastic syndromes. *Leukemia*. 1997;11(12):2049-2054.
90. Stifter G, Heiss S, Gastl G, Tzankov A, Stauder R. Over-expression of tumor necrosis factor-alpha in bone marrow biopsies from patients with myelodysplastic syndromes: relationship to anemia and prognosis. *Eur J Haematol*. 2005;75(6):485-491.
91. Basiorka AA, McGraw KL, Eksioglu EA, et al. The NLRP3 inflammasome functions as a driver of the myelodysplastic syndrome phenotype. *Blood*. 2016;128(25):2960-2975.
92. Thompson CB, Allison JP. The emerging role of CTLA-4 as an immune attenuator. *Immunity*. 1997;7(4):445-450.
93. Aref S, El Agdar M, El Sebaie A, Abouzeid T, Sabry M, Ibrahim L. Prognostic value of CD200 expression and soluble CTLA-4 concentrations in intermediate and high-risk myelodysplastic syndrome patients. *Asian Pac J Cancer Prev*. 2020;21(8):2225-2230.
94. Tao J, Li L, Wang Y, Fu R, Wang H, Shao Z. Increased TIM3+CD8+T cells in myelodysplastic syndrome patients displayed less perforin and granzyme B secretion and higher CD95 expression. *Leuk Res*. 2016;51:49-55.
95. Fu R, Li L, Hu J, et al. Elevated TIM3 expression of T helper cells affects immune system in patients with myelodysplastic syndrome. *J Invest Med*. 2019;67(8):1125-1130.
96. Tsvetkov N, Gusak A, Morozova E, et al. Immune checkpoints bone marrow expression as the predictor of clinical outcome in myelodysplastic syndrome. *Leuk Res Rep*. 2020;14:100215.
97. Zeidan AM, Giagounidis A, Sekeres MA, et al. STIMULUS-MDS2 design and rationale: a phase III trial with the anti-TIM-3 sabatolimab (MBG453) + azacitidine in higher risk MDS and CMML-2. *Future Oncol*. 2023;19(9):631-642.
98. Garcia-Manero G, Chien KS, Montalban-Bravo G. Myelodysplastic syndromes: 2021 update on diagnosis, risk stratification and management. *Am J Hematol*. 2020;95(11):1399-1420.
99. Rodriguez-Sevilla JJ, Adema V, Garcia-Manero G, Colla S. Emerging treatments for myelodysplastic syndromes: biological rationales and clinical translation. *Cell Rep Med*. 2023;4(2):100940.
100. Garcia-Manero G, Ribrag V, Zhang Y, Farooqui M, Marinello P, Smith BD. Pembrolizumab for myelodysplastic syndromes after failure of hypomethylating agents in the phase 1b KEYNOTE-013 study. *Leuk Lymphoma*. 2022;63(7):1660-1668.
101. Chien KS, Kim K, Nogueras-Gonzalez GM, et al. Phase II study of azacitidine with pembrolizumab in patients with intermediate-1 or higher-risk myelodysplastic syndrome. *Br J Haematol*. 2021;195(3):378-387.
102. Garcia-Manero G, Sasaki K, Montalban-Bravo G, et al. A phase II study of nivolumab or ipilimumab with or without azacitidine for patients with myelodysplastic syndrome (MDS). *Blood*. 2018;132(suppl 1):465-465.
103. Morita K, Kantarjian HM, Montalban-Bravo G, et al. A phase II study of double immune checkpoint inhibitor blockade with nivolumab and ipilimumab with or without azacitidine in patients with myelodysplastic syndrome (MDS). *Blood*. 2020;136(suppl 1):7-9.
104. Brunner AM, Esteve J, Porkka K, et al. Efficacy and safety of sabatolimab (MBG453) in combination with hypomethylating agents (HMAs) in patients (Pts) with very high/high-risk myelodysplastic syndrome (vHR/HR-MDS) and acute myeloid leukemia (AML): final analysis from a phase Ib study. *Blood*. 2021;138(suppl 1):244.
105. Zeidan AM, Ando K, Rauzy O, et al. Sabatolimab plus hypomethylating agents in previously untreated patients with higher-risk myelodysplastic syndromes (STIMULUS-MDS1): a randomised, double-blind, placebo-controlled, phase 2 trial. *Lancet Haematol*. 2024;11(1):e38-e50.
106. Sallman DA, Kerre T, Havelange V, et al. CYAD-01, an autologous NKG2D-based CAR T-cell therapy, in relapsed or refractory acute myeloid leukaemia and myelodysplastic syndromes or multiple myeloma (THINK): haematological cohorts of the dose escalation segment of a phase 1 trial. *Lancet Haematol*. 2023;10(3):e191-e202.
107. Sallman DA, Elmariah H, Sweet K, et al. Phase 1/1b safety study of Prgn-3006 Ultracar-T in patients with relapsed or refractory CD33-positive acute myeloid leukemia and higher risk myelodysplastic syndromes. *Blood*. 2022;140(suppl 1):10313-10315.
108. Vey N, Davidson-Moncada J, Uy GL, et al. Interim results from a phase 1 first-in-human study of flotetuzumab, a CD123 x CD3 bispecific DART molecule, in AML/MDS. *Ann Oncol*. 2017;28(suppl 5):v355.
109. Vey N, Davidson-Moncada J, Uy GL, et al. Interim results from a Phase 1 First-in-Human Study of Flotetuzumab, a CD123 x CD3 Bispecific DART® Molecule, in AML/MDS. *ESMO*. 2017.
110. Uckun FM, Watts J, Mims AS, et al. A clinical phase 1B study of the CD3xCD123 bispecific antibody APVO436 in patients with relapsed/refractory acute myeloid leukemia or myelodysplastic syndrome. *Cancers (Basel)*. 2021;13(21):5287.
111. Nguyen D, Ravandi F, Wang SA, et al. A phase II study of vibecotamab, a CD3-CD123

- bispecific T-cell engaging antibody, for MDS or CMML after hypomethylating failure and in MRD-positive AML. *Blood*. 2023;142(suppl 1):322.
112. Nair-Gupta P, Diem M, Reeves D, et al. A novel C2 domain binding CD33xCD3 bispecific antibody with potent T-cell redirection activity against acute myeloid leukemia. *Blood Adv*. 2020;4(5):906-919.
 113. Garcia-Manero G, Jacoby M, Sallman DA, Han T, Guenot J, Feldman E. A phase I study of AMV564 in patients with intermediate or high-risk myelodysplastic syndromes. *J Clin Oncol*. 2019;37(suppl 15):TPS7071.
 114. Neelapu SS, Locke FL, Bartlett NL, et al. Axicabtagene ciloleucel CAR T-cell therapy in refractory large B-cell lymphoma. *N Engl J Med*. 2017;377(26):2531-2544.
 115. Schuster SJ, Bishop MR, Tam CS, et al. Tisagenlecleucel in adult relapsed or refractory diffuse large B-cell lymphoma. *N Engl J Med*. 2019;380(1):45-56.
 116. Abramson JS, Palomba ML, Gordon LI, et al. Lisocabtagene maraleucel for patients with relapsed or refractory large B-cell lymphomas (TRANSCEND NHL 001): a multicentre seamless design study. *Lancet*. 2020;396(10254):839-852.
 117. Chua CC, Cheok KPL. Taking a step forward in CAR T-cell therapy for acute myeloid leukaemia and myelodysplastic syndrome. *Lancet Haematol*. 2023;10(3):e161-e162.
 118. Stevens BM, Zhang W, Pollyea DA, et al. CD123 CAR T cells for the treatment of myelodysplastic syndrome. *Exp Hematol*. 2019;74:52-63.e3.
 119. Kenderian SS, Ruella M, Shestova O, et al. CD33-specific chimeric antigen receptor T cells exhibit potent preclinical activity against human acute myeloid leukemia. *Leukemia*. 2015;29(8):1637-1647.
 120. Liu H, Wang S, Xin J, Wang J, Yao C, Zhang Z. Role of NKG2D and its ligands in cancer immunotherapy. *Am J Cancer Res*. 2019;9(10):2064-2078.
 121. Diermayr S, Himmelreich H, Durovic B, et al. NKG2D ligand expression in AML increases in response to HDAC inhibitor valproic acid and contributes to allorecognition by NK-cell lines with single KIR-HLA class I specificities. *Blood*. 2008;111(3):1428-1436.
 122. Driouk L, Gicobi J, Kamihara Y, et al. Chimeric antigen receptor T cells targeting NKG2D-ligands show robust efficacy against acute myeloid leukemia and T-cell acute lymphoblastic leukemia. *Blood*. 2019;134(suppl 1):1930-1931.
 123. Heine R, Thielen FW, Koopmanschap M, et al. Health economic aspects of chimeric antigen receptor T-cell therapies for hematological cancers: present and future. *Hemasphere*. 2021;5(2):e524.
 124. Depil S, Duchateau P, Grupp SA, Mufti G, Poirot L. 'Off-the-shelf' allogeneic CAR T cells: development and challenges. *Nat Rev Drug Discov*. 2020;19(3):185-199.
 125. Bucchieri S, Guggino G, Caccamo N, Li Donni P, Dieli F. Efficacy and safety of $\gamma\delta$ T cell-based tumor immunotherapy: a meta-analysis. *J Biol Regul Homeost Agents*. 2014;28(1):81-90.
 126. Haber L, Olson K, Kelly MP, et al. Generation of T-cell-redirecting bispecific antibodies with differentiated profiles of cytokine release and biodistribution by CD3 affinity tuning. *Sci Rep*. 2021;11(1):14397.
 127. Allen C, Zeidan AM, Bewersdorf JP. BiTEs, DARTs, BiKEs and TriKEs are antibody based therapies changing the future treatment of AML? *Life (Basel)*. 2021;11(6):465.
 128. Teramura M, Kimura A, Iwase S, et al. Treatment of severe aplastic anemia with antithymocyte globulin and cyclosporin A with or without G-CSF in adults: a multicenter randomized study in Japan. *Blood*. 2007;110(6):1756-1761.
 129. Tsuda K, Yamanaka K, Kitagawa H, et al. Calcineurin inhibitors suppress cytokine production from memory T cells and differentiation of naïve T cells into cytokine-producing mature T cells. *PLoS One*. 2012;7(2):e31465.
 130. Mohty M. Mechanisms of action of antithymocyte globulin: T-cell depletion and beyond. *Leukemia*. 2007;21(7):1387-1394.
 131. *NCCN Guidelines Version Myelodysplastic Syndromes (1.2023)*. National Comprehensive Cancer Network; 2023.
 132. Haider M, Al Ali N, Padron E, et al. Immunosuppressive therapy: exploring an underutilized treatment option for myelodysplastic syndrome. *Clin Lymphoma Myeloma Leuk*. 2016;(16 suppl):S44-S48.
 133. Stahl M, Bewersdorf JP, Giri S, Wang R, Zeidan AM. Use of immunosuppressive therapy for management of myelodysplastic syndromes: a systematic review and meta-analysis. *Haematologica*. 2020;105(1):102-111.

© 2024 American Society of Hematology. Published by Elsevier Inc. All rights are reserved, including those for text and data mining, AI training, and similar technologies.

Supplementary Table 1. Quantitative changes in T cell subsets among different MDS subgroups

Cell populations	Healthy Donors	Lower-Risk MDS	Higher-risk MDS	MDS-SLD	MDS-MLD	MDS-EB	MDS-RS/MDS-SF3B1	MDS-5q	References	
% of PB T cells (range) (CD3 ⁺)	(n=18) 66 (43–82)	(n=22) 62 (10–85)	(n=9) 66 (53–92)						Sand et al., Oncoimmunology. 2013 ¹	
% of BM T cells (range) (CD3 ⁺)				(n=70) 71 ± 12	(n=64) 69.9 ± 10	(n=2) 52 ± 28	(n=56) 71.9 ± 13	(n=8) 78.6 ± 5	Fattizzo et al., Front. Oncol. 2022 ²	
PB CD4 ⁺ T cells										
% of CD4 ⁺ (CD3 ⁺ CD4 ⁺ CD8 ⁺) (range)	(n=18) 68 (36–85)	(n=22) 69 (45–89)	(n=9) 57 (40–87)						Sand et al., Oncoimmunology. 2013 ¹	
% of CD4 ⁺ naïve (CD45RA ⁺ CD62L ⁺) (range)	(n=18) 32 (3–51)	(n=22) 26 (9–62)	(n=9) 33 (7–51)							
% of CD4 ⁺ central memory (CD45RA ⁺ CD62L ⁺) (range)	(n=18) 34 (20–55)	(n=22) 28 (19–65)	(n=9) 29 (14–48)							
% of CD4 ⁺ effector memory (CD45RA ⁺ CD62L ⁺) (range)	(n=18) 31 (15–76)	(n=22) 32 (12–54)	(n=9) 36 (17–64)							
% of CD4 ⁺ terminal effector (CD45RA ⁺ CD62L ⁺) (range)	(n=18) 2 (0.4–7)	(n=22) 5 (0.5–17)	(n=9) 2 (0.3–32)							
% of BM Th-1 (IFN-γ producing CD4 ⁺ T cells)	(n=15) 0.48 ± 0.10	(n=18) 0.36 ± 0.11							Wang et al., Blood 2005 ³	
% of BM Th-2 (IL-4 producing CD4 ⁺ T cells)	(n=15) 0.24 ± 0.19	(n=18) 0.76 ± 0.35								
BM Th-1/Th-2 ratio	(n=15) 2.31 ± 0.76	(n=18) 0.51 ± 0.13								
% of CD4 ⁺ (95% CI)	(n=18) 40.2 (36.4–44.0)						(n=31) 41.1 (35.1–47.0)	(MDS-EB-1, n=9) 35.7 (26.3–45.1) (MDS-EB-2, n=7) 46.2 (34.3–58.2)	(n=9) 45.5 (38.8–52.1)	Hamdi et al., Int. J. Lab. Hematol. 2009 ⁴
CD4 ⁺ cells (×10 ⁹ /L) (range)	(n=18) 0.73 (0.64–0.83)						(n=15) 0.46 (0.31–0.61)	(n=7) 0.79 (0.30–1.18)	(n=4) 0.68 (0.36–1.01)	
% of Th-1 (95% CI)	(n=18) 17.5						(n=31) 18.6	(MDS-EB-1, n=9) 23.9 (16.3–31.5)	(n=9) 19.8 (13.0–26.6)	

	(12.9–22.0)		(15.5–21.7)	(MDS-EB-2, n=7) 20.7 (11.1–30.2)				
% of Th-2 (95% CI)	(n=18) 1.8 (1.2–2.3)		(n=31) 2.2 (1.6–2.8)	(MDS-EB-1, n=9) 2.8 (1.8–3.8) (MDS-EB-2, n=7) 2.4 (0.1–4.6)	(n=9) 2.6 (1.5–3.7)			
Th-1/Th-2 ratio (range)	(n=18) 14.5 (9.3–19.7)		(n=15) 11.2 (4.8–17.7)	(n=7) 5.7 (3.4–8.0)	(n=4) 11.2 (5.9–16.6)			
Th-1 cells ($\times 10^9/L$) (range)	(n=18) 0.17 (0.12–0.21)		(n=15) 0.09 (0.06–0.12)	(n=7) 0.10 (0.02–0.17)	(n=4) 0.18 (0.05–0.31)			
CD4/CD8 ratio (95% CI)	(n=17) 1.23 (0.97–1.50)		(n=31) 2.30 (1.47–3.14)	(MDS-EB-1, n=9) 2.25 (1.20–3.31) (MDS-EB-2, n=7) 2.34 (0.83–3.84)	(n=9) 2.19 (1.75–2.63)			
% of CD4 ⁺ T helper						(n=11) 48%		Hamdi et al., Int. J. Lab. Hematol. 2009
Th-17 cells (CD3⁺CD4⁺IL-17⁺IFN-γ)								
% of BM Th-17 % of PB Th-17						(n=11) ~1.6% ~2.2%		Balaian et al., Ann. Hematol. 2016 ⁵
PB T follicular helper cells								
% of CD4 ⁺ CXCR5 ⁺		MDS with autoimmune disease (n=21: MDS-SLD n=3; MDS-MLD n=6; MDS-EB n=12) 19.02 \pm 3.23						
% of PD1 ⁺ CD4 ⁺ CXCR5 ⁺		MDS with no autoimmune disease (n=21: MDS-SLD n=4; MDS-MLD n=5; MDS-RS n=1, MDS-EB n=11) 13.46 \pm 3.32						
		MDS with autoimmune disease (MDS-SLD n=3; MDS-MLD n=6; MDS-EB n=12) 4.09 \pm 2.29%						
		MDS with no autoimmune disease (MDS-SLD n=4; MDS-MLD n=5; MDS-RS n=1, MDS-EB n=11) 7.85 \pm 5.28%						
% of CD4 ⁺ ICOS ⁺ (estimated for CD4 ⁺ T cells)	(n=10) 8.69 \pm 4.08	(n=20) 5.34 \pm 1.44						Xiao et al., J Immunol. Res. 2021 ⁷
T Regulatory cells								
								Lampropoulou et al., Blood 2013 ⁸

Supplementary Table 2. Qualitative changes in T cell subsets among different MDS subgroups

Cell populations	Healthy Donors	Higher-risk MDS	TP53 status		References
			Wild-type TP53	Mutant TP53	
PB CD3 ⁺ T cells					
% of PD-1 ⁺ (range)			(n=30) 5.465 (1.37-43)	(n=30) 4.485 (0.64-21.1)	Sallman et al., Blood 2020 ⁹
% of TIM-3 ⁺ (range)			(n=30) 1.74 (0.17-15.8)	(n=30) 1.9 (0.35-9.72)	
% of LAG-3 ⁺ (range)			(n=30) 0.51 (0.037-13.3)	(n=30) 0.315 (0.025-2.54)	
% of OX-40 ⁺ (range)			(n=30) 7.195 (1.11-28.5)	(n=30) 3.2 (0.95-30.8)	
% of CTLA-4 ⁺ (range)			(n=30) 0.235 (0.043-5.22)	(n=30) 0.13 (0.027-1.74)	
% of 4-1BB ⁺ (range)			(n=30) 12.2 (1.28-39.1)	(n=30) 13.1 (0.26-63.3)	
% of ICOS ⁺ (range)			(n=30) 7.15 (0.29-34.4)	(n=30) 12.7 (0.77-42.3)	
% of TIGIT ⁺ (standard deviation)	(n=20) 18.32 ± 23.38	(n=26) 35.42 ± 15.55	Meng et al. <i>Front. Oncol.</i> 2020 ¹⁰		
% of CD226 ⁺ (standard deviation)	(n=20) 70.96 ± 10.25	(n=26) 53.85 ± 13.70			
% of PD-1 ⁺ (standard deviation)	(n=20) 12.73 ± 8.841	(n=26) 31.11 ± 15.62			
BM exhaustion markers			(n=17) ↑ PD-1 ⁺ ↑ TIM-3 ⁺ ↑ CTLA4 ⁺ ↑ LAG3 ⁺		Jiang et al., <i>Blood</i> 2023 ¹¹
PB Th cells (CD3 ⁺ CD4 ⁺)					
% of PD-1 ⁺ (range)			(n=30) 4.33 (0.78-42.1)	(n=30) 3.725 (0.49-15.9)	Sallman et al., Blood 2020 ⁹
% of TIM-3 ⁺ (range)			(n=30) 2.12 (0.18-22.1)	(n=30) 2.15 (0.45-10.5)	
% of LAG-3 ⁺ (range)			(n=30) 0.695 (0.036-18.4)	(n=30) 0.39 (0.029-2.91)	
% of OX-40 ⁺ (range)			(n=30) 7.675 (1.04-35.2)	(n=30) 3.75 (1.23-35.1)	
% of CTLA-4 ⁺ (range)			(n=30) 0.225 (0.025-5.62)	(n=30) 0.13 (0.026-1.71)	
% of 4-1BB ⁺ (range)			(n=30) 7.675 (0.73-31)	(n=30) 5.475 (0.2-67.2)	
% of ICOS ⁺ (range)			(n=30)	(n=30)	

				11.3 (0.84-45.7)		18.05 (1.5-57) (n=17) ↑ TIM-3* ↑ LAG-3* ~CTLA4* ~PD-1*		Jiang et al., <i>Blood</i> 2023 ¹¹
BM exhaustion markers								
% of TIGIT* (standard deviation)		(n=20) 15.05 ± 15.43	(n=26) 18.18 ± 9.187					Meng et al. <i>Front Oncol.</i> 2020 ¹⁰
% of CD226* (standard deviation)		(n=20) 67.03 ± 14.19	(n=26) 59.47 ± 19.65					
% of PD-1* (standard deviation)		(n=20) 11.64 ± 13.15	(n=26) 17.53 ± 7.731					
T Regulatory cells (CD3*CD4*CD25*CD127 ^{low/-})								
% of PD-1* (range)				(n=30) 5.195 (0.89-72.5)		(n=30) 3.58 (0.4-17.6)		Sallman et al., <i>Blood</i> 2020 ⁹
% of TIM-3* (range)				(n=30) 4.72 (0.28-70.9)		(n=30) 2.85 (1.9-11.6)		
% of LAG-3* (range)				(n=30) 2.425 (0.069-62.3)		(n=30) 1.865 (0.049-16.7)		
% of OX-40* (range)				(n=30) 10.4 (1.54-46.2)		(n=30) 5.82 (2.17-39.6)		
% of CTLA-4* (range)				(n=30) 1.3 (0.14-18.2)		(n=30) 0.75 (0.16-9.35)		
% of 4-1BB* (range)				(n=30) 10.85 (1.95-70.9)		(n=30) 6.01 (1.29-29.4)		
% of ICOS* (range)				(n=30) 14.45 (1.41-68.4)		(n=30) 16.85 (2.17-48.4)		
CD8* cytotoxic T cells (CD3*CD8*)								
% of PD-1* (range)				(n=30) 26.9 (10.1-59.6)		(n=30) 24.15 (2.14-49)		Sallman et al., <i>Blood</i> 2020 ⁹
% of TIM-3* (range)				(n=30) 1.59 (0.091-16.8)		(n=30) 1.55 (0.12-9.34)		
% of LAG-3* (range)				(n=30) 0.485 (0.061-9.39)		(n=30) 0.245 (0-7.01)		
% of OX-40* (range)				(n=30) 6.435 (1.27-30.2)		(n=30) 2.34 (0.54-14)		
% of CTLA-4* (range)				(n=30) 0.105 (1-6.43)		(n=30) 0.0445 (0-0.7)		
% of 4-1BB* (range)				(n=30) 19.65 (2.2-85.8)		(n=30) 37.85 (0.62-77.5)		
% of ICOS* (range)				(n=30) 1.43 (0.18-30.9)		(n=30) 4.93 (0.046-28)		
% of TIGIT* (standard deviation)		(n=20) 13.97 ± 14.76	(n=26) 49.41 ± 19.58					Meng et al. <i>Front. Oncol.</i> 2020 ¹⁰
% of CD226* (standard deviation)		(n=20)	(n=26)					

% of PD-1 ⁺ (standard deviation)	73.37 ± 11.79 (n=20)	60.46 ± 12.81 (n=26)	
	13.19 ± 13.03	47.88 ± 20.22	
BM exhaustion markers			<div> <div>(n=17)</div> <div> <div>↑ TIM-3⁺</div> <div>↑ LAG-3⁺</div> <div>↑ CTLA4⁺</div> <div>↑ PD-1⁺</div> <div>↑ TIGIT⁺</div> </div> </div>
			Jiang et al., <i>Blood</i> 2023 ¹¹

Abbreviations: BM: bone marrow; CTLA-4: cytotoxic T lymphocyte-associated protein 4; EM: effector memory; LAG-3: lymphocyte activation gene 3; ICOS: inducible T cell Costimulator; PB: peripheral blood; BM, bone marrow; MDS: myelodysplastic syndromes; PD-1: programmed cell death protein 1; TIGIT: T cell immunoglobulin and ITIM domain; TIM-3: T cell immunoglobulin and mucin domain

REFERENCES

1. Sand KE, Rye KP, Mannsåker B, Bruserud O, Kittang AO. Expression patterns of chemokine receptors on circulating T cells from myelodysplastic syndrome patients. *Oncoimmunology*. 2013;2(2):e23138.
2. Fattizzo B, Levati GV, Giannotta JA, et al. Low-Risk Myelodysplastic Syndrome Revisited: Morphological, Autoimmune, and Molecular Features as Predictors of Outcome in a Single Center Experience. *Front Oncol*. 2022;12:795955.
3. Wang X, Wu DP, He G, Miao M, Sun A. Research of Subset and Function of Th Cells in Bone Marrow of Myelodysplastic Syndrome Patients. *Blood*. 2005;106(11):4913-4913.
4. Hamdi W, Ogawara H, Handa H, Tsukamoto N, Nojima Y, Murakami H. Clinical significance of regulatory T cells in patients with myelodysplastic syndrome. *European Journal of Haematology*. 2009;82(3):201-207.
5. Balaian E, Schuster C, Schönefeldt C, et al. Selective expansion of regulatory T cells during lenalidomide treatment of myelodysplastic syndrome with isolated deletion 5q. *Annals of Hematology*. 2016;95(11):1805-1810.
6. Coats T, Smith Ae, Mourikis TP, Irish JM, Kordasti S, Mufti GJ. Mass Cytometry Reveals PD1 Upregulation Is an Early Step in MDS Disease Progression. *Blood*. 2016;128(22):4296.
7. Xiao N, He X, Niu H, et al. Increased Circulating CD4(+)CXCR5(+) Cells and IgG4 Levels in Patients with Myelodysplastic Syndrome with Autoimmune Diseases. *J Immunol Res*. 2021;2021:4302515.

8. Lampropoulou P, Verigou E, Symeonidis A, Gogos C, Solomou EE. Characterization Of T Follicular Helper Cells In Patients With Low Risk Myelodysplastic Syndromes. *Blood*. 2013;122(21):4729-4729.
9. Sallman DA, McLemore AF, Aldrich AL, et al. TP53 mutations in myelodysplastic syndromes and secondary AML confer an immunosuppressive phenotype. *Blood*. 2020;136(24):2812-2823.
10. Meng F, Li L, Lu F, et al. Overexpression of TIGIT in NK and T Cells Contributes to Tumor Immune Escape in Myelodysplastic Syndromes. *Front Oncol*. 2020;10:1595.
11. Jiang L, Huang X, Zhou X, et al. High Expressions of Checkpoint Receptors in T Cells Subsets of Myelodysplastic Syndromes Patients with TP53 Mutations. *Blood*. 2023;142:4614.

HYPOTHESIS & OBJECTIVES

Hypothesis 1:

Venetoclax resistance in myelodysplastic syndromes (MDS) and chronic myelomonocytic leukemia (CMML) is driven by distinct molecular, cellular, and immune-mediated mechanisms, including hematopoietic stem cell (HSC) differentiation hierarchies, co-mutational patterns, and inflammatory signaling. Together, these factors shape therapeutic responses and resistance, presenting opportunities to identify novel biomarkers and therapeutic targets.

Objectives:

1. **Molecular and Cellular Mechanisms of Venetoclax Resistance:** Investigate molecular and cellular biomarkers predictive of venetoclax response and resistance in MDS and CMML by:
 - Exploring differentiation hierarchies within the HSC compartment.
 - Assessing the impact of co-mutational patterns on therapy resistance.
 - Examining the roles of NF- κ B and MCL1-mediated survival pathways in venetoclax resistance using single-cell multi-omics, flow cytometry, and *in vitro/in vivo* models.
2. **Clinical and Translational Implications:** Develop predictive biomarkers and therapeutic strategies to improve patient stratification and treatment efficacy.
 - Identifying biomarkers predictive of response to venetoclax-based treatments.
 - Proposing a rationale for a combination therapy targeting resistant HSC populations and inflammatory pathways to overcome resistance.

Hypothesis 2:

Inflammatory signaling and immune dysregulation are central to disease progression and therapeutic resistance in MDS and CMML. Aberrant inflammatory pathways influence HSC survival, differentiation, and immune interactions, promoting clonal evolution and disease persistence. Targeting these mechanisms, with a focus on key mediators such as MCL1 and IL-1 β , offers potential for novel therapeutic strategies.

Objectives:

1. **Role of Inflammation in Disease Progression:** Examine the contribution of inflammatory signaling to clonal expansion, immune evasion, and therapeutic resistance in MDS and CMML by:
 - Profiling pro-inflammatory cytokines and their downstream effects on hematopoietic progenitors and immune cells.
 - Investigating the role of chronic inflammation in shaping the bone marrow microenvironment and fostering a permissive state for mutant HSC survival.
2. **Functional and Molecular Analysis of HSCs:** Characterize inflammation-driven mechanisms that affect HSC survival, differentiation, and clonal evolution by:
 - Examining the transcriptional and epigenetic responses of HSCs to inflammatory cytokines, with an emphasis on IL-1 β signaling pathways.
 - Investigating how molecular adaptations in HSCs, including shifts toward myeloid-biased progenitor states, contribute to therapeutic resistance.
3. **Therapeutic Implications of IL-1 β Inhibition:** Evaluate the translational potential of

targeting IL-1 β signaling to modulate inflammation and improve therapeutic outcomes:

- Assessing the effects of IL-1 β inhibitor, Canakinumab, on inflammatory cytokine levels and hematopoietic function in a clinical trial setting.
 - Examining the relationship between IL-1 β activity and somatic mutations, such as *TET2* and *DNMT3A*, which amplify inflammatory responses and clonal dominance.
4. **Immune System Dynamics and T Cell Functionality:** Investigate the role of immune cell dysfunction, particularly T cells, in MDS and CMML pathogenesis by:
- Profiling immune effector cells, including CD8⁺ T cells and NK cells, to identify functional impairments and exhaustion markers.
 - Analyzing ligand-receptor interactions between immune cells and hematopoietic progenitors within the inflammatory microenvironment.
 - Evaluating how IL-1 β inhibition affects T cell activity and restores immune functionality.
5. **Survival Mechanisms and MCL1 Dependency:** Assess the contribution of MCL1 to inflammation-driven survival mechanisms in resistant and high-risk disease subsets:
- Investigating the interplay between inflammatory signaling pathways and MCL1-mediated survival of mutant HSCs and downstream progenitors.
 - Evaluating the potential of targeting MCL1 as a therapeutic strategy, particularly in the context of venetoclax resistance and RAS-mutant CMML.

Hypothesis 3:

CMML is a highly heterogeneous disease, with distinct co-mutational patterns that influence its clinical presentation, progression, and treatment responses. Understanding the cooperative effects of these mutations and their impact on hematopoietic differentiation and clonal evolution will refine stratification models and inform therapeutic approaches.

Objectives:

1. **Characterization of Co-Mutational Patterns:** Identify and classify recurrent co-mutational patterns in CMML to define genomic subtypes by:
 - Leveraging next-generation sequencing (NGS) to profile somatic mutations across a large CMML cohort.
 - Applying computational clustering methods to reveal mutational co-occurrence and subgroup-defining patterns.
2. **Clonal Dynamics and Evolution:** Explore the role of co-mutational patterns in clonal architecture and evolution by:
 - Assessing clonal dominance and subclonal dynamics at diagnosis and progression using variant allele frequency (VAF) distributions.
 - Studying the temporal changes in clonal populations, including the emergence or expansion of high-risk mutations during disease progression.
 -
3. **Phenotypic, Clinical, and Prognostic Associations:** Determine how co-mutational patterns shape disease phenotype and clinical outcomes by:
 - Examining the relationship between specific co-mutational patterns and disease phenotypes, including hematologic parameters, bone marrow

- morphology, and patterns of clonal evolution
- Correlating mutational clusters with overall survival, leukemia-free survival, and therapeutic resistance
- 4. **Refinement of CMML Stratification Models:** Integrate molecular data with clinical stratification to improve CMML classification by:
 - Improving existing prognostic models with genomic subtypes to provide better risk stratification.
 - Developing tools to guide patient selection for targeted therapies and combination approaches.

Together, these objectives aim to deepen our understanding of the complex molecular, cellular, and immune mechanisms that drive disease progression and resistance in MDS and CMML. By investigating the roles of hematopoietic stem cell hierarchies, inflammatory signaling, and immune dysregulation, this thesis seeks to uncover how these interconnected processes contribute to clonal evolution, therapeutic resistance, and disease persistence. In addressing these challenges, this research aims to identify novel biomarkers and therapeutic targets, ultimately paving the way for more effective treatment strategies for patients who currently face limited options.

METHODS & RESULTS

The methods and results are detailed in the four published articles that comprise this thesis:

First publication: Rodriguez-Sevilla JJ, Ganan-Gomez I, Ma F, Chien K, Del Rey M, Loghavi S, Montalban-Bravo G, Adema V, Wildeman B, Kanagal-Shamanna R, Bazinet A, Chifotides HT, Thongon N, Calvo X, Hernández-Rivas JM, Díez-Campelo M, Garcia-Manero G, Colla S. Hematopoietic stem cells with granulo-monocytic differentiation state overcome venetoclax sensitivity in patients with myelodysplastic syndromes. **Nat Commun.** 2024 Mar 18;15(1):2428. doi: 10.1038/s41467-024-46424-3. PMID: 38499526; PMCID: PMC10948794. *Impact factor: 16.6*

Second publication: Montalban-Bravo G*, Thongon N*, Rodriguez-Sevilla JJ*, Ma F, Ganan-Gomez I, Yang H, Kim YJ, Adema V, Wildeman B, Tanaka T, Darbaniyan F, Al-Atrash G, Dwyer K, Loghavi S, Kanagal-Shamanna R, Song X, Zhang J, Takahashi K, Kantarjian H, Garcia-Manero G, Colla S. Targeting MCL1-driven anti-apoptotic pathways overcomes blast progression after hypomethylating agent failure in chronic myelomonocytic leukemia. **Cell Rep Med.** 2024 Jun 18;5(6):101585. doi: 10.1016/j.xcrm.2024.101585. Epub 2024 May 22. PMID: 38781960; PMCID: PMC11228590. *Impact factor: 16.98*

Third publication: Rodriguez-Sevilla JJ, Adema V, Chien K, Loghavi S, Ma F, Yang H, Montalban-Bravo G, Huang X, Joseph J, Bodden K, Garcia-Manero G, Calvo X, Colla S. Biological and Clinical Effects of Canakinumab in Patients with Lower-Risk Myelodysplastic Syndromes: Results from a Phase 2 Trial. **Nat Commun.** 2024 (accepted). *Impact factor: 16.6*

Fourth publication: Montalban-Bravo G, Rodriguez-Sevilla JJ, Swanson DM, Kanagal-Shamanna R, Hammond D, Chien K, Sasaki K, Jabbour E, DiNardo C, Takahashi K, Short N, Issa GC, Pemmaraju N, Kadia T, Ravandi F, Daver N, Borthakur G, Loghavi S, Pierce S, Bueso-Ramos C, Kantarjian H, Garcia-Manero G. Influence of co-mutational patterns in disease phenotype and clinical outcomes of chronic myelomonocytic leukemia. **Leukemia.** 2024 May;38(5):1178-1181. doi: 10.1038/s41375-024-02190-1. Epub 2024 Feb 28. PMID: 38418609. *Impact factor: 12.8*

First publication

Hematopoietic stem cells with granulo-monocytic differentiation state overcome venetoclax sensitivity in patients with myelodysplastic syndrome

Rodriguez-Sevilla JJ, Ganan-Gomez I, Ma F, Chien K, Del Rey M, Loghavi S, Montalban-Bravo G, Adema V, Wildeman B, Kanagal-Shamanna R, Bazinet A, Chifotides HT, Thongon N, Calvo X, Hernández-Rivas JM, Díez-Campelo M, Garcia-Manero G, Colla S


Nature Communications 2024 Mar 18;15(1):2428.
2024 Impact Factor 14.7
Quartile 1

Hematopoietic stem cells with granulo-monocytic differentiation state overcome venetoclax sensitivity in patients with myelodysplastic syndromes

Received: 25 August 2023

Accepted: 9 February 2024

Published online: 18 March 2024

 Check for updates

Juan Jose Rodriguez-Sevilla^{1,6}, Irene Ganan-Gomez^{1,6}, Feiyang Ma², Kelly Chien¹, Monica Del Rey³, Sanam Loghavi⁴, Guillermo Montalban-Bravo¹, Vera Adema¹, Bethany Wildeman¹, Rashmi Kanagal-Shamanna⁴, Alexandre Bazinet¹, Helen T. Chifotides¹, Natthakan Thongon¹, Xavier Calvo⁵, Jesús María Hernández-Rivas³, Maria Díez-Campelo³, Guillermo Garcia-Manero¹ & Simona Colla¹✉

The molecular mechanisms of venetoclax-based therapy failure in patients with acute myeloid leukemia were recently clarified, but the mechanisms by which patients with myelodysplastic syndromes (MDS) acquire secondary resistance to venetoclax after an initial response remain to be elucidated. Here, we show an expansion of MDS hematopoietic stem cells (HSCs) with a granulo-monocytic-biased transcriptional differentiation state in MDS patients who initially responded to venetoclax but eventually relapsed. While MDS HSCs in an undifferentiated cellular state are sensitive to venetoclax treatment, differentiation towards a granulo-monocytic-biased transcriptional state, through the acquisition or expansion of clones with *STAG2* or *RUNX1* mutations, affects HSCs' survival dependence from BCL2-mediated anti-apoptotic pathways to TNF α -induced pro-survival NF- κ B signaling and drives resistance to venetoclax-mediated cytotoxicity. Our findings reveal how hematopoietic stem and progenitor cell (HSPC) can eventually overcome therapy-induced depletion and underscore the importance of using close molecular monitoring to prevent HSPC hierarchical change in MDS patients enrolled in clinical trials of venetoclax.

The hematopoietic stem cell (HSC) hierarchy of myelodysplastic syndromes (MDS) predicts the biological mechanisms of progression after the failure of frontline hypomethylating agents (HMAs) and can guide the design or choice of second-line therapeutic approaches¹. We

previous showed that, compared with those with a “granulocytic-monocytic progenitor (GMP) pattern” of differentiation, MDS patients with an immunophenotypic “common myeloid progenitor (CMP) pattern” of differentiation who received venetoclax-based therapy had

¹Department of Leukemia, The University of Texas MD Anderson Cancer Center, Houston, TX, USA. ²Department of Molecular, Cell and Developmental Biology, University of California Los Angeles, Los Angeles, CA, USA. ³Hematology Department, University Hospital of Salamanca, IBSAL Cancer Center, Salamanca, Spain. ⁴Department of Hematopathology, The University of Texas MD Anderson Cancer Center, Houston, TX, USA. ⁵Laboratori de Citologia Hematològica, Servei de Patologia, Grup de Recerca Translacional en Neoplàsies Hematològiques (GRETNHE), Hospital del Mar Research Institute (IMIM), Barcelona, Spain. ⁶These authors contributed equally: Juan Jose Rodriguez-Sevilla, Irene Ganan-Gomez. ✉e-mail: scolla@mdanderson.org

a shorter cumulative time to complete remission and a longer recurrence-free survival duration, primarily because venetoclax can efficiently target only “CMP pattern” HSCs, whose survival depends on BCL2.

However, MDS patients eventually failed venetoclax-based therapy after a short period of time².

Here, to dissect the cellular and molecular mechanisms of venetoclax-based therapy failure, we performed multi-omic analyses of sequential samples from MDS patients whose disease initially responded to venetoclax-based therapy but then relapsed.

Results

Although further confirmed in a larger cohort of samples ($n = 28$; 12 “CMP pattern” MDS and 16 “GMP pattern” MDS) (Supplementary Fig. 1a, b and Supplementary Data 1), our survival analysis of MDS patients who were enrolled in clinical trials of venetoclax-based therapy and had longer follow-up (median time, 20.1 months) showed that those with “CMP pattern” MDS eventually lose response and/or progress to acute myeloid leukemia (AML) after an initial remission ($n = 6$ of 6 “CMP pattern” MDS patients with an initial response who did not discontinue the study) (Supplementary Data 1). These results suggest that alternative approaches are needed for these patients, who would otherwise have no other therapeutic options.

To dissect the cellular and molecular mechanisms of secondary venetoclax-based therapy failure, we performed multi-omics analyses of sequential samples from 6 “CMP pattern” MDS patients (Supplementary Data 2) whose initial disease response to venetoclax-based therapy was associated with HSC depletion (Supplementary Fig. 1c).

These analyses showed that the “CMP pattern” immunophenotypic architecture (Supplementary Fig. 2a) and the hematopoietic stem and progenitor cell (HSPC) transcriptomic signature (Supplementary Fig. 2b, c) persisted at disease recurrence in the 3 patients with *TP53* mutations (UPN#3, UPN#4, and UPN#6), which is consistent with previous findings that *TP53* mutations confer an intrinsic resistance to BCL2 inhibition³.

However, the HSPC hierarchy switched to “GMP pattern” MDS in the other 3 patients (UPN#1, UPN#2, and UPN#11) before venetoclax failure (Fig. 1a, b and Supplementary Fig. 3a–d). In all 3 patients, this immunophenotypic hierarchical change was associated with the acquisition or selection of clones with *STAG2* or *RUNX1* mutations, which we previously found to be enriched in “GMP pattern” MDS¹ (Fig. 1c and Supplementary Fig. 3e, f). Single-cell RNA-sequencing (scRNA-seq) analyses of mononuclear cells (MNCs) from sequential bone marrow (BM) samples from 2 of the 3 patients (Fig. 1d and Supplementary Fig. 3g) confirmed that HSCs were significantly depleted during disease remission but expanded at therapy failure (Supplementary Fig. 3h). Differential expression analyses of sequential BM samples collected during different disease stages showed that the acquisition of *STAG2*- or *RUNX1*-mutant clones not only rewired MDS HSPCs' differentiation state towards a myeloid-biased transcriptional signature (Supplementary Fig. 4a) but also changed HSCs' survival dependence from BCL2-mediated anti-apoptotic pathways to TNF α -induced pro-survival NF- κ B signaling, thus enabling HSCs to evade the cytotoxic effects of venetoclax (Fig. 1e and Supplementary Fig. 4b–d).

Importantly, 3 of the 4 patients with “CMP pattern” MDS whose disease was refractory to venetoclax-based therapy (UPN#8, UPN#9, and UPN#12) carried subclones with *STAG2* and/or *RUNX1* mutations at the time of clinical trial enrollment (Supplementary Data 2). During venetoclax therapy, these clones underwent clonal evolution (Supplementary Fig. 5a), which switched the HSPC hierarchy from “CMP pattern” to “GMP pattern” MDS (Supplementary Fig. 5b). These data confirm that *STAG2* and/or *RUNX1* mutations drive venetoclax resistance by reprogramming the HSPC architecture.

Interestingly, trisomy 8 was significantly associated with *STAG2* mutations ($P = 0.03$) and conferred a shorter duration of response to

venetoclax-based therapy regardless of prior treatment in patients with “CMP pattern” MDS but not those with “GMP pattern” MDS ($n = 53$ patients treated with venetoclax-based therapies for whom immunophenotypic data were available) (Supplementary Fig. 6a, Supplementary Data 3). These results suggest that trisomy 8 is also a predictive biomarker of venetoclax resistance in patients with “CMP pattern” MDS.

Discussion

The current standard of care for MDS patients is HMA therapy, which results in clinical improvements in over 50% of patients. However, the disease eventually becomes resistant to these agents. Patients with HMA-resistant MDS develop progressive cytopenias or secondary AML and have a median survival duration of only 4–6 months⁴.

Venetoclax-based therapy in patients whose disease previously failed HMA therapy holds promise for improving these patients' dismal survival. However, whereas the molecular and biological mechanisms of resistance to venetoclax have recently been recently elucidated in AML^{5–7}, we still do not know why MDS patients whose disease failed HMA therapy acquire secondary resistance to venetoclax after an initial response⁸.

Our study revealed the molecular mechanisms of venetoclax-based therapy failure in MDS. HSPCs exposed to venetoclax undergo survival pressure, which results in the acquisition or expansion of clones carrying specific genetic alterations that change these cells' dependence on BCL2-mediated pathways to NF- κ B-mediated anti-apoptotic pathways for survival (Fig. 1f).

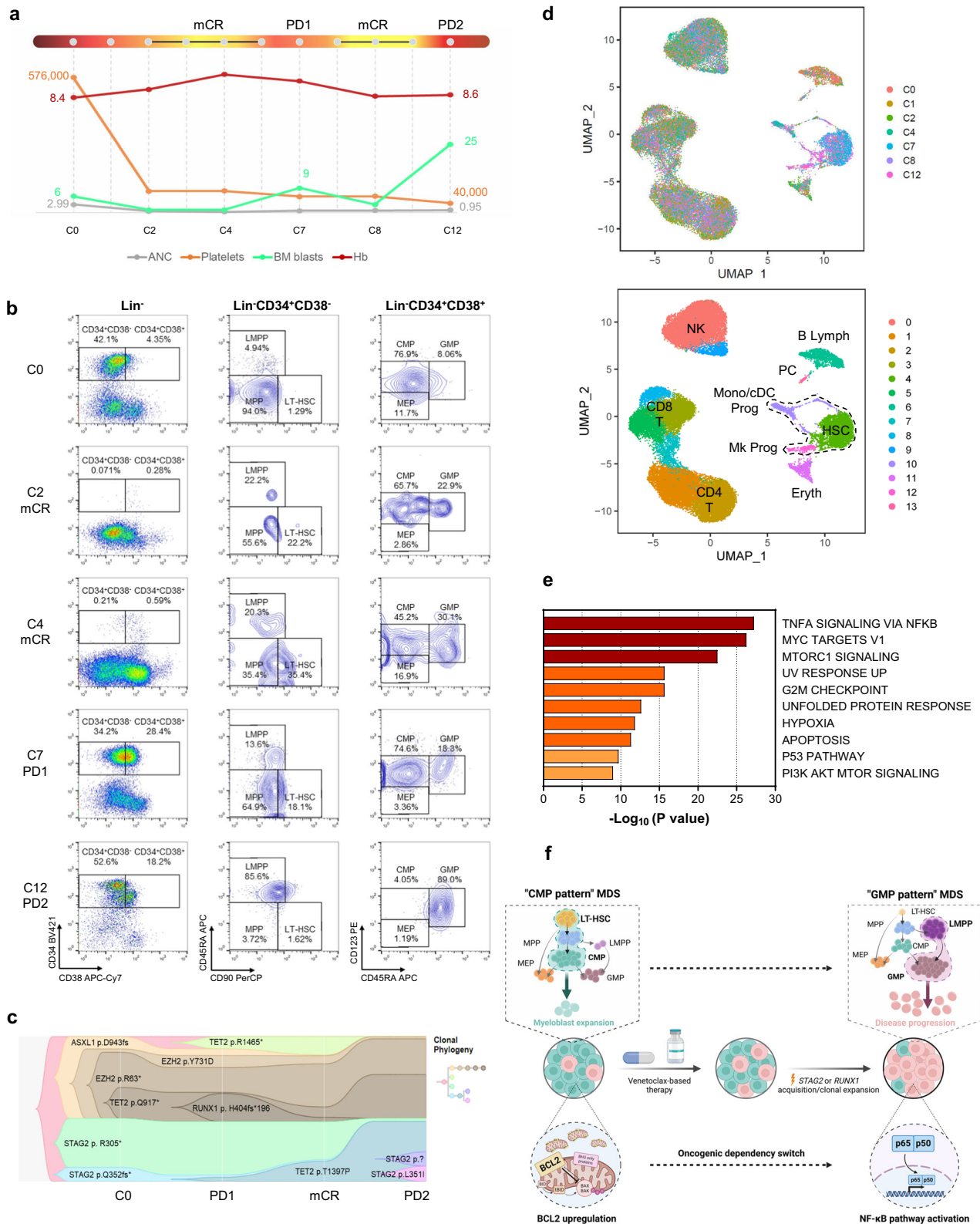
These results suggest that MDS patients receiving venetoclax-based therapy should be monitored closely for the acquisition or expansion of clones with *STAG2* or *RUNX1* mutations and enrolled in clinical trials of agents targeting NF- κ B signaling effectors, such as MCL1, before their disease undergoes HSC transcriptional reprogramming and becomes resistant to venetoclax.

Methods

The research complies with the ethical regulations (MD Anderson Cancer Center IRB-approved human sample protocol PA15-0926).

Human primary samples and clinical data analysis

We analyzed MDS patients who received venetoclax-based therapy at MD Anderson Cancer Center. Patients were enrolled in 1 of 3 phase I/II clinical trials (NCT04160052², NCT04550442⁹, or NCT04655755¹⁰). Patient characteristics, laboratory values, and BM data, including cytogenetics and next-generation sequencing (NGS) data, were assessed before venetoclax-based therapy, and thereafter as clinically warranted. Genomic DNA was extracted from whole BM aspirates and subjected to 81-gene target polymerase chain reaction-based sequencing using an NGS platform as described previously¹¹. Testing was performed in a Clinical Laboratory Improvement Amendments-certified laboratory. Risk stratification was performed using the Revised International Prognostic Scoring System (IPSS-R), and MDS was classified as lower-risk (IPSS-R score ≤ 3.5) or higher-risk (IPSS-R score > 4) MDS^{12,13}. Disease response was categorized according to the International Working Group 2006 criteria for MDS, and patients with responsive disease included those with complete response (CR), marrow CR (mCR), hematologic improvement (HI), or a combination of mCR and HI¹⁴. Response duration was defined as the time from first documented response to first documented disease progression or death, whichever occurred first. To evaluate the mechanisms of secondary venetoclax-based therapy failure, we analyzed 28 MDS patients enrolled in the 3 clinical trials in whom HMA therapy had failed. To evaluate the impact of trisomy 8 on the survival of MDS patients treated with venetoclax-based therapy, we analyzed the clinical data of 53 patients who were enrolled in the 3 clinical trials regardless of prior therapies and for whom immunophenotypic data were available.



Samples were obtained in accordance with the Declaration of Helsinki from MD Anderson's Department of Leukemia under protocol PA15-0926 with the approval of the corresponding Institutional Review Boards. Written informed consent to report any information (including age, sex, and clinical parameters) was obtained from all donors, and all diagnoses were confirmed by dedicated hematopathologists. The clinical characteristics of the patients included in this study are shown in Supplementary Data 1–4. MNCs were isolated from each

sample using the standard gradient separation approach with Ficoll-Paque PLUS (GE Healthcare Lifesciences, Pittsburgh, PA).

Flow cytometry and fluorescence-activated cell sorting (FACS)

Quantitative flow cytometric analyses and FACS of human live MNCs were performed using a previously described gating strategy and antigen panel¹⁵ and antibodies against CD2 (RPA-2.10; 1:20), CD3 (SK7; 1:10), CD14 (MφP9; 1:20), CD19 (SJ25C1; 1:10), CD20 (2H7; 1:10), CD34

Fig. 1 | Mutation-induced MDS HSCs' transcriptional reprogramming overcomes venetoclax-based therapy vulnerability. **a** Schematic of UPN#1's clinical course. After HMA therapy failure (cycle 0 [C0]), UPN#1 received 5-azacitidine (75 mg/m² for 5 days) and venetoclax (400 mg/m² for 14 days) every month. The patient had mCR at cycle 2 (C2); however, after the venetoclax dose was reduced to 100 mg/m², the patient had an initial disease progression (PD1) at cycle 7 (C7). The patient had mCR after the venetoclax dose was increased to 200 mg/m² at cycle 8 (C8) but had progression to AML (PD2) at cycle 12 (C12). Hb, hemoglobin; ANC, absolute neutrophil count. Units: blasts, %; Hb, g/dL; ANC, ×10⁹/L; platelets, ×10⁹/L. **b** Flow cytometry plots of lineage (Lin) CD34⁺CD38⁺ HSCs and Lin⁺CD34⁺CD38⁺ myeloid hematopoietic progenitor cells in the BM of UPN#1 at sequential timepoints before and during venetoclax-based therapy. LT-HSC long-term hematopoietic stem cells, MPP multipotent progenitors, LMPP lymphoid-primed multipotent progenitors, CMP common myeloid progenitors, GMP granulocytic-monocytic progenitors, MEP megakaryocyte erythroid progenitors. **c** Fish plot of the clonal evolution pattern inferred from NGS data for UPN#1. Phylogenetic trees

show the estimated order of mutation acquisition and the proportion of subclones with different combinations of mutations at each timepoint. In UPN#1, clonal evolution was associated with the immunophenotypic HSPC hierarchical change and the acquisition of 2 *STAG2* mutations. **d** UMAP plots of scRNA-seq data from BM MNCs isolated from UPN#1 (*n* = 39,206). Each dot represents 1 cell. Different colors indicate sample origin (top) and cluster identity (bottom). HSC hematopoietic stem cell, Mk megakaryocytic, Mono monocytic, cDC classic dendritic, Prog progenitors, Eryth erythroblasts, NK natural killer cells, Lymph lymphocytes, PC plasma cells. Dotted lines indicate the HSPC compartment. **e** Pathway enrichment analysis of the genes that were significantly upregulated in HSCs from UPN#1 (cluster 4 in **d**) at the time of PD2 compared with those in HSCs at the time of PD1 (*P* adj ≤ 0.05). The top 10 Hallmark gene sets are shown. **f** Proposed working model of venetoclax-based therapy failure. After an initial response to venetoclax-based therapy, the acquisition or expansion of clones with *STAG2* or *RUNX1* mutations reprograms the HSPC hierarchy and switches HSCs' dependence from BCL2- to NF-κB-mediated survival programs, which leads to secondary venetoclax-based therapy failure.

(581; 1:20), CD56 (B159; 1:40), CD123 (9F5; 1:20), and CD235a (HIR2; 1:40; all from BD Biosciences, Franklin Lakes, NJ); CD4 (S3.5; 1:20), CD11b (ICRF44; 1:20), CD33 (P67.6; 1:20), and CD90 (SE10; 1:10; all from Thermo Fisher Scientific, Waltham, MA); CD7 (6B7; 1:20) and CD38 (HIT2; 1:20; both from BioLegend, San Diego, CA); CD10 (SJ5-IB4; 1:20; Leinco Technologies, St. Louis, MO); and CD45RA (HI100; 1:10; Tonbo Biosciences, San Diego, CA).

FACS-purified samples were acquired with a BD Influx Cell Sorter (BD Biosciences), and the cell populations were analyzed using FlowJo software (version 10.7.1, Ashland, OR). All experiments included single-stained controls and were performed at MD Anderson's South Campus Flow Cytometry and Cellular Imaging Facility.

scRNA-seq

scRNA-seq was performed as we described previously¹. Briefly, FACS-purified live BM MNCs were prepared and sequenced at MD Anderson's Advanced Technology Genomics Core. Sample concentration and cell suspension viability were evaluated using a Countess II FL Automated Cell Counter (Thermo Fisher Scientific) and manual counting. Samples were normalized for input onto the Chromium Single Cell A Chip Kit (10x Genomics, Pleasanton, CA), in which single cells were lysed and barcoded for reverse-transcription. The pooled single-stranded, barcoded cDNA was amplified and fragmented for library preparation. Pooled libraries were sequenced on a Nova-Seq6000 SP 100-cycle flow cell (Illumina, San Diego, CA).

The sequencing analysis was carried out using 10X Genomics' Cell Ranger software (version 3.0.2). Fastq files were generated using the Cell Ranger MkFastq pipeline (version 3.0.2). Raw reads were mapped to the human reference genome (refdata-cellranger-GRCh38-3.0.0) using the Cell Ranger Count pipeline. Multiple samples were aggregated using the Cell Ranger Aggr pipeline. The digital expression matrix was analyzed with the R package Seurat (version 3.0.2)¹⁶ to identify different cell types and signature genes for each. Cells with fewer than 500 unique molecular identifiers or greater than 50% mitochondrial expression were removed from further analysis. The Seurat function NormalizeData was used to normalize the raw counts. Variable genes were identified using the FindVariableFeatures function. The ScaleData function was used to scale and center expression values in the dataset, and the number of unique molecular identifiers was regressed against each gene. Uniform manifold approximation and projection (UMAP) was used to reduce the dimensions of the data, and the first 2 dimensions were used in the plots. The FindClusters function was used to cluster the cells. Marker genes for each cluster were identified using the FindAllMarkers function. Cell types were annotated based on the marker genes and their match to canonical markers^{17,18}. Pathway analyses of differentially expressed genes were

conducted using Metascape¹⁹. The GMP enrichment score was calculated based on a previously validated GMP expression signature²⁰.

Statistics and reproducibility

Statistical analyses were performed using R (version 4.0.320), Jamovi (version 2.0.021), and GraphPad (version 9.0.0, San Diego, CA). The 2-tailed Student t-test or Mann-Whitney test, as appropriate, and chi-square test were used to compare continuous and categorical variables, respectively. The multiple test analyses included in Supplementary Data 3 were corrected using the Bonferroni adjustment. No statistical method was used to predetermine sample size. No data were excluded from the analyses. Patient samples were selected based on of diagnosis regardless of sex and gender because MDS affect both females and males. The sex of the patients included in this study is indicated in Supplementary Data 1 and 3. Mutations with variant allele frequency values below 2% were excluded from the plot to model clonal evolution. A comprehensive summary of the mutations for UPN#1, UPN#2, UPN#11, UPN #8, UPN#9, and UPN#12 at every timepoint is provided in Supplementary Data 4. Fish plot visualization was performed using the timescape package (version 3.14) in R (version 4.2.2). The graphical abstract was made using BioRender.

Reporting summary

Further information on research design is available in the Nature Portfolio Reporting Summary linked to this article.

Data availability

Data sets generated in this study using scRNA-seq have been deposited at GEO under accession code [GSE241417](https://www.ncbi.nlm.nih.gov/geo/query/acc.cgi?acc=GSE241417). Source data are provided as a Source data file. Source data are provided with this paper.

References

1. Ganan-Gomez, I. et al. Stem cell architecture drives myelodysplastic syndrome progression and predicts response to venetoclax-based therapy. *Nat. Med.* **28**, 557–567 (2022).
2. Bazinet, A. et al. Azacitidine plus venetoclax in patients with high-risk myelodysplastic syndromes or chronic myelomonocytic leukaemia: phase 1 results of a single-centre, dose-escalation, dose-expansion, phase 1-2 study. *Lancet Haematol.* **9**, e756–e765 (2022).
3. Nechiporuk, T. et al. The TP53 apoptotic network is a primary mediator of resistance to BCL2 inhibition in AML cells. *Cancer Discov.* **9**, 910–925 (2019).
4. Jabbour, E. et al. Outcome of patients with myelodysplastic syndrome after failure of decitabine therapy. *Cancer* **116**, 3830–3834 (2010).

5. Pei, S. et al. Monocytic subclones confer resistance to venetoclax-based therapy in patients with acute myeloid leukemia. *Cancer Discov.* **10**, 536–551 (2020).
6. Jones, C. L. et al. Nicotinamide metabolism mediates resistance to venetoclax in relapsed acute myeloid leukemia stem cells. *Cell Stem Cell* **27**, 748–764.e744 (2020).
7. Stevens, B. M. et al. Fatty acid metabolism underlies venetoclax resistance in acute myeloid leukemia stem cells. *Nat. Cancer* **1**, 1176–1187 (2020).
8. Rodriguez-Sevilla, J. J., Adema, V., Garcia-Manero, G. & Colla, S. Emerging treatments for myelodysplastic syndromes: Biological rationales and clinical translation. *Cell Rep. Med.* **4**, 100940 (2023).
9. Desikan, S. P. et al. Results of a phase 1 trial of azacitidine with venetoclax in relapsed/refractory higher-risk myelodysplastic syndrome (MDS). *J. Clin. Oncol.* **40**, e19068–e19068 (2022).
10. Bataller, A. et al. Phase 1/2 study of oral decitabine/cedazuridine in combination with venetoclax in treatment-naïve higher-risk myelodysplastic syndromes or chronic myelomonocytic leukemia. *HemaSphere* **7**, <https://doi.org/10.1097/01.HS9.0000967600.18588.ff> (2023).
11. Kanagal-Shamanna, R. et al. Principles of analytical validation of next-generation sequencing based mutational analysis for hematologic neoplasms in a CLIA-certified laboratory. *Expert Rev. Mol. Diagn.* **16**, 461–472 (2016).
12. Greenberg, P. L. et al. Revised international prognostic scoring system for myelodysplastic syndromes. *Blood* **120**, 2454–2465 (2012).
13. Pfeilstöcker, M. et al. Time-dependent changes in mortality and transformation risk in MDS. *Blood* **128**, 902–910 (2016).
14. Cheson, B. D. et al. Revised recommendations of the International Working Group for Diagnosis, Standardization of Response Criteria, Treatment Outcomes, and Reporting Standards for Therapeutic Trials in Acute Myeloid Leukemia. *J. Clin. Oncol.* **21**, 4642–4649 (2003).
15. Ganan-Gomez, I., Clise-Dwyer, K. & Colla, S. Isolation, culture, and immunophenotypic analysis of bone marrow HSPCs from patients with myelodysplastic syndromes. *STAR Protoc.* **3**, 101764 (2022).
16. Stuart, T. et al. Comprehensive integration of single-cell data. *Cell* **177**, 1888–1902.e1821 (2019).
17. Velten, L. et al. Human haematopoietic stem cell lineage commitment is a continuous process. *Nat. Cell Biol.* **19**, 271–281 (2017).
18. Buenrostro, J. D. et al. Integrated single-cell analysis maps the continuous regulatory landscape of human hematopoietic differentiation. *Cell* **173**, 1535–1548.e1516 (2018).
19. Zhou, Y. et al. Metascape provides a biologist-oriented resource for the analysis of systems-level datasets. *Nat. Commun.* **10**, 1523 (2019).
20. Karamitros, D. et al. Single-cell analysis reveals the continuum of human lympho-myeloid progenitor cells. *Nat. Immunol.* **19**, 85–97 (2018).

Acknowledgements

This work was supported by philanthropic contributions to MD Anderson's AML and MDS Moon Shot Program and Support Grant CA016672,

the Umberto Veronesi Foundation, and the Edward P. Evans Foundation to Dr. Simona Colla. Dr Maria Díez-Campelo was supported by the UMBRELLA Project (PI20/00970). J.J.R.-S. is a recipient of MD Anderson's Odyssey Fellowship. This work used MD Anderson's South Campus Flow Cytometry and Cellular Imaging Facility and its Advanced Technology Genomics Core, both of which are supported in part by the NIH through MD Anderson's Cancer Center Support Grant (P30 CA16672).

Author contributions

S.C. designed the research; J.J.R.-S. guided the research; J.J.R.-S., I.G.-G., M.D.R., V.A., B.W., and N.T. performed experiments; J.J.R.-S., K.C., G.M.-B., and A.B. analyzed the clinical data; R.K.-S. and S.L. analyzed the genomic data; F.M. analyzed the scRNA-seq data; J.J.R.-S. and I.G.-G. analyzed the flow cytometry data; H.T.C. edited the manuscript. X.C., M.-D.C., J.M.H.-R., and G.G.-M. made critical intellectual contributions throughout the project; S.C. wrote the manuscript.

Competing interests

G.G.-M. reports clinical funding from AbbVie and Amgen. All other authors report no competing interests relative to this work.

Additional information

Supplementary information The online version contains supplementary material available at <https://doi.org/10.1038/s41467-024-46424-3>.

Correspondence and requests for materials should be addressed to Simona Colla.

Peer review information *Nature Communications* thanks the anonymous reviewer(s) for their contribution to the peer review of this work. A peer review file is available.

Reprints and permissions information is available at <http://www.nature.com/reprints>

Publisher's note Springer Nature remains neutral with regard to jurisdictional claims in published maps and institutional affiliations.

Open Access This article is licensed under a Creative Commons Attribution 4.0 International License, which permits use, sharing, adaptation, distribution and reproduction in any medium or format, as long as you give appropriate credit to the original author(s) and the source, provide a link to the Creative Commons licence, and indicate if changes were made. The images or other third party material in this article are included in the article's Creative Commons licence, unless indicated otherwise in a credit line to the material. If material is not included in the article's Creative Commons licence and your intended use is not permitted by statutory regulation or exceeds the permitted use, you will need to obtain permission directly from the copyright holder. To view a copy of this licence, visit <http://creativecommons.org/licenses/by/4.0/>.

© The Author(s) 2024

Description of Additional Supplementary Files

File Name: Supplementary Data 1

Description: Characteristics of MDS patients treated with venetoclax-based therapy at the time of progression after HMA therapy (n=28).

File Name: Supplementary Data 2

Description: Characteristics of patients with "CMP pattern" MDS (n=10) who failed venetoclaxbased therapy.

File Name: Supplementary Data 3

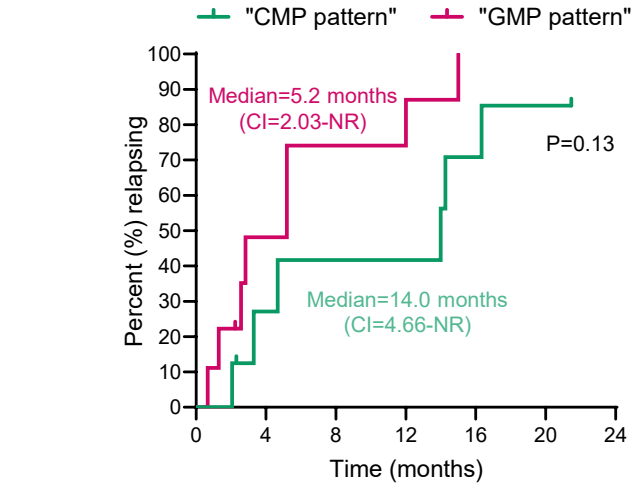
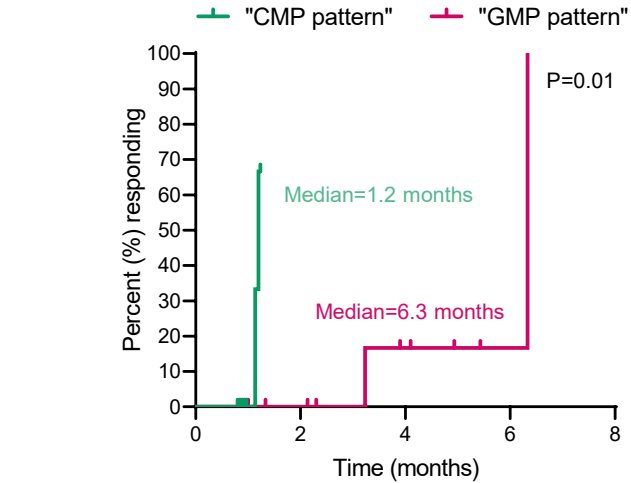
Description: Characteristics of MDS patients at the time of enrollment in clinical trials of venetoclax-based therapy regardless of prior therapies (n=53)

File Name: Supplementary Data 4

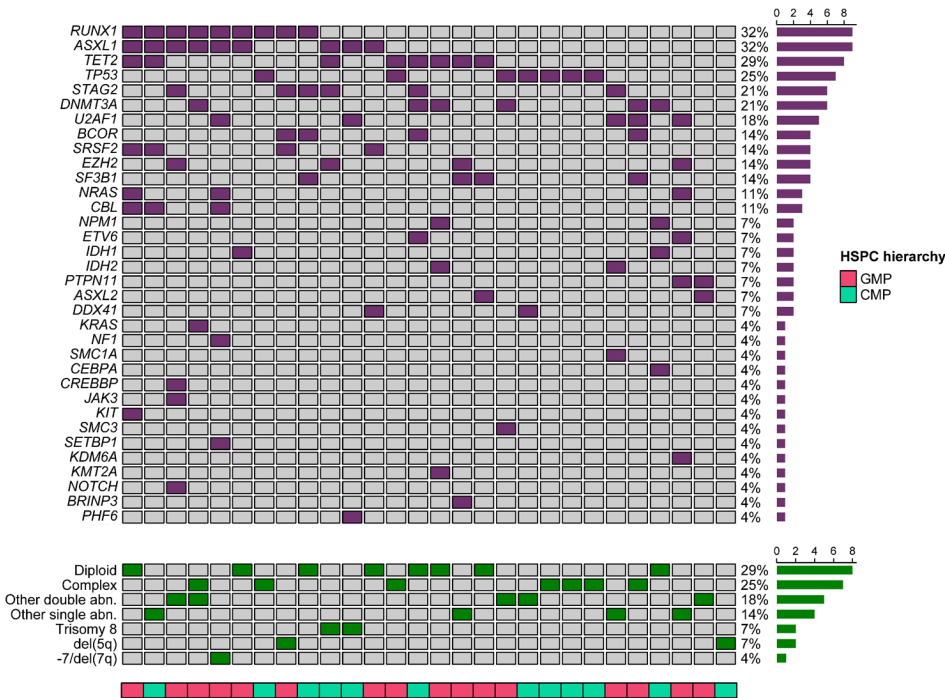
Description: Summary of mutations in patients with secondary (UPN#1, UPN#2, UPN#11) and primary (UPN#8, UPN#9, UPN#12) failure to venetoclax-based therapy

Supplementary Figure 1

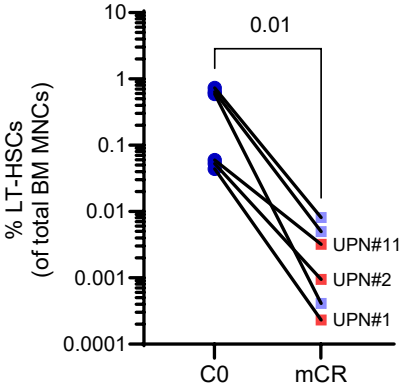
a



"GMP pattern"	9	4	2	2	0	0	0
"CMP pattern"	8	5	4	4	2	1	0

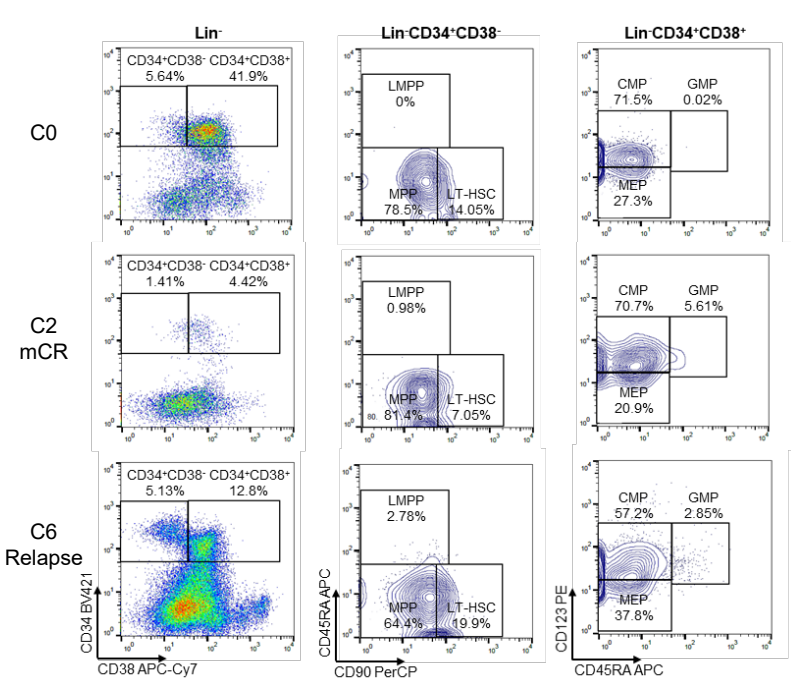
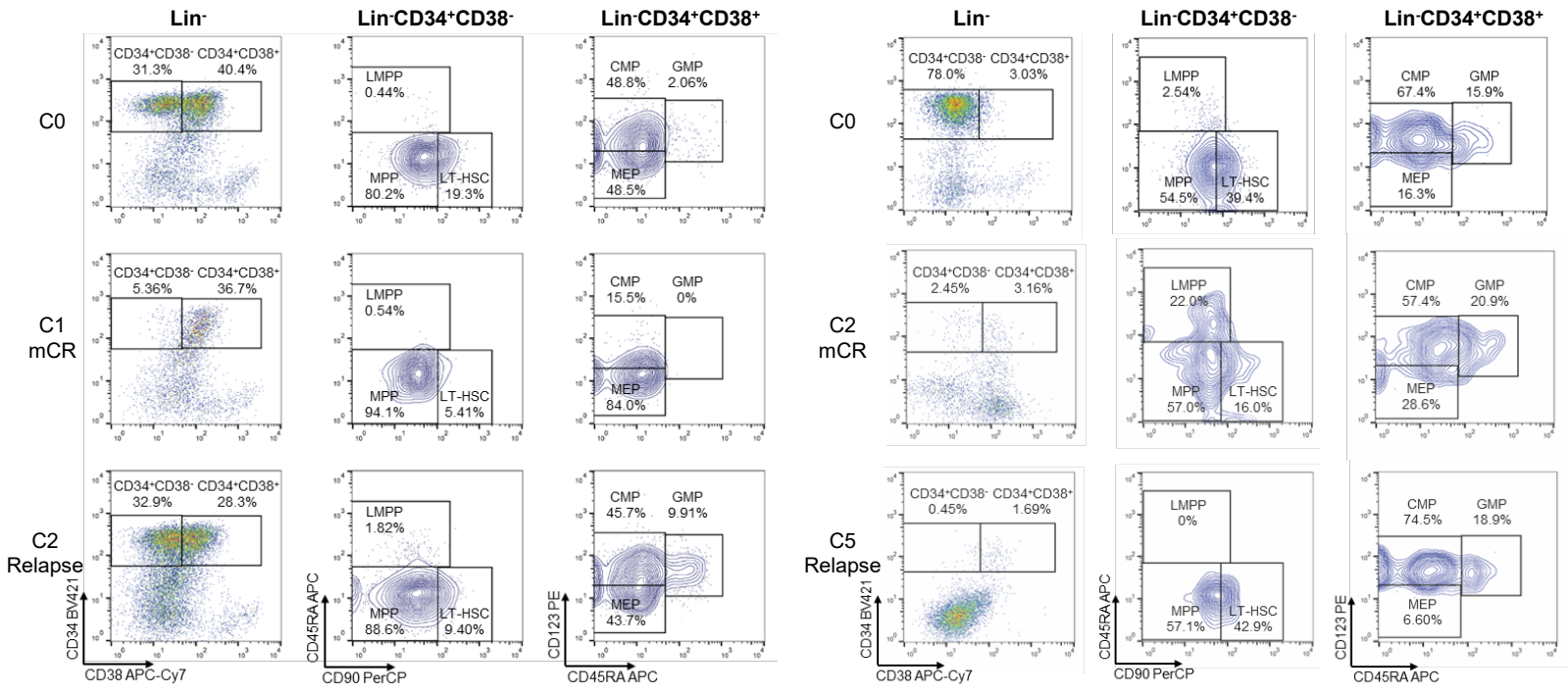


c

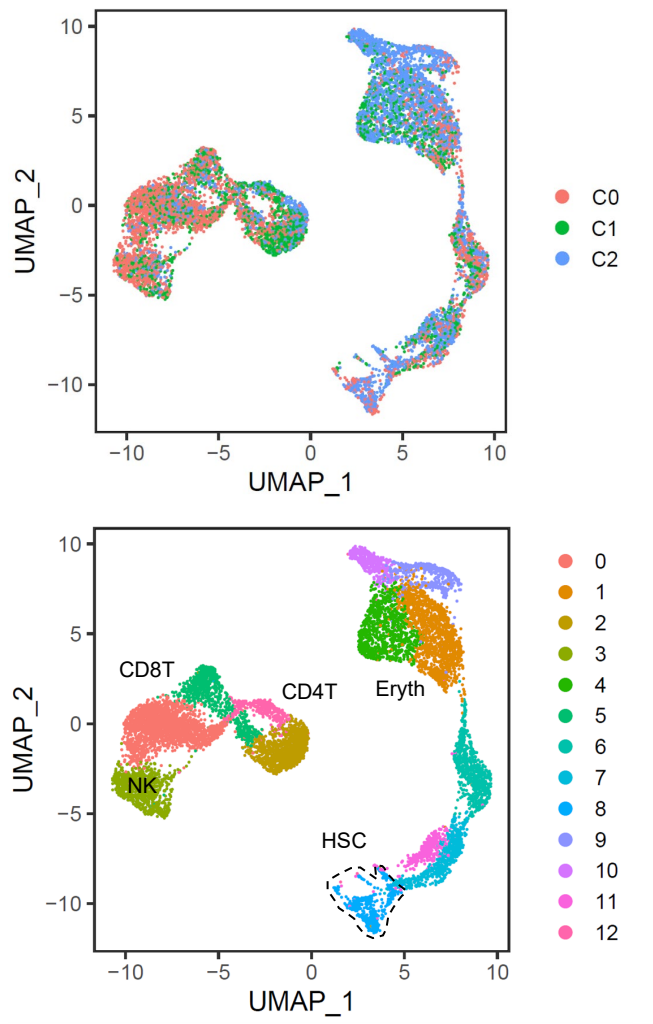


Supplementary Figure 2

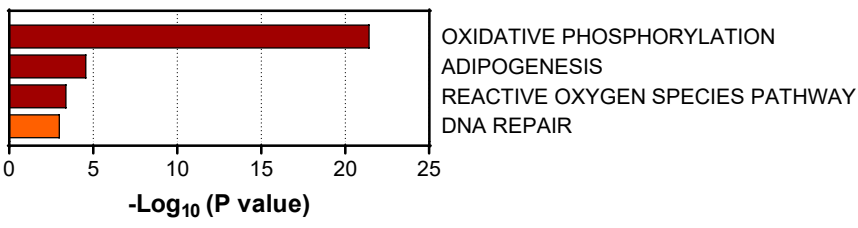
a



b

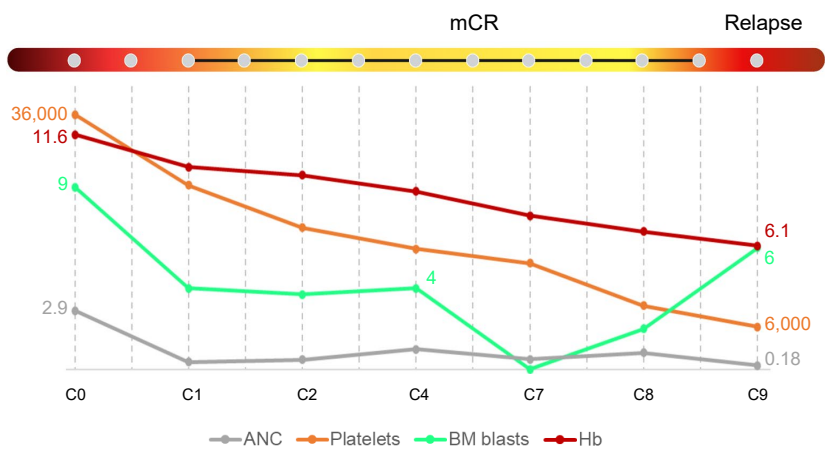


c

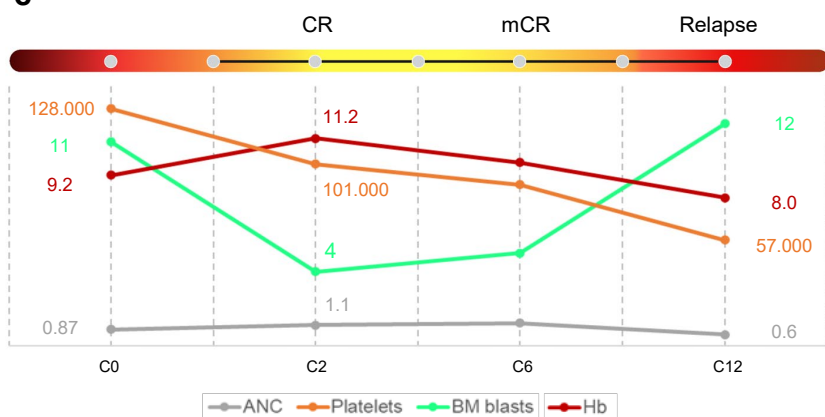


Supplementary Figure 3

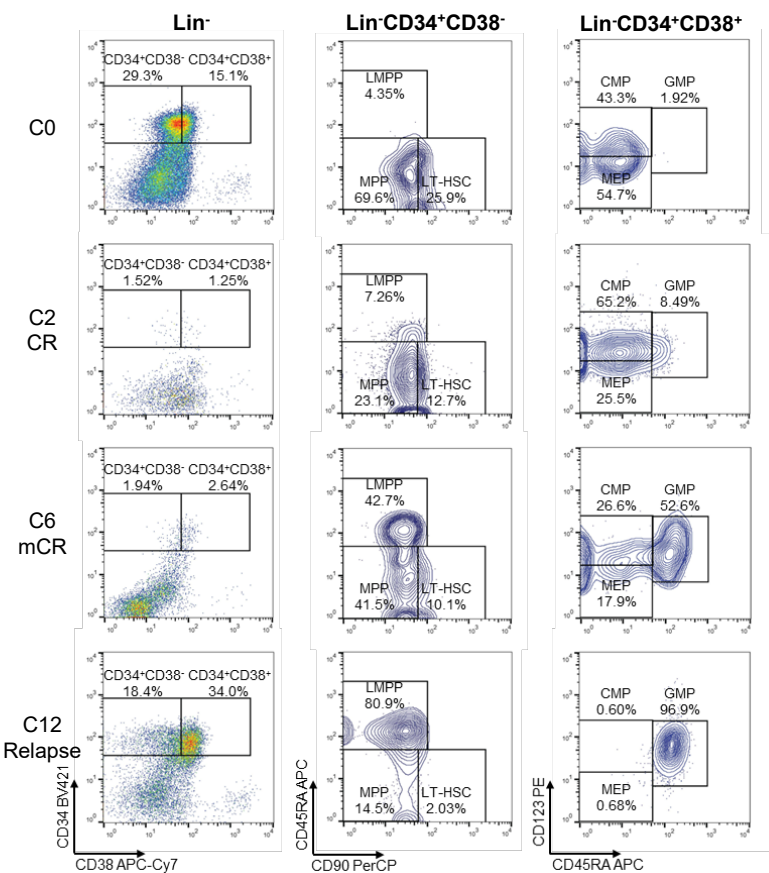
a



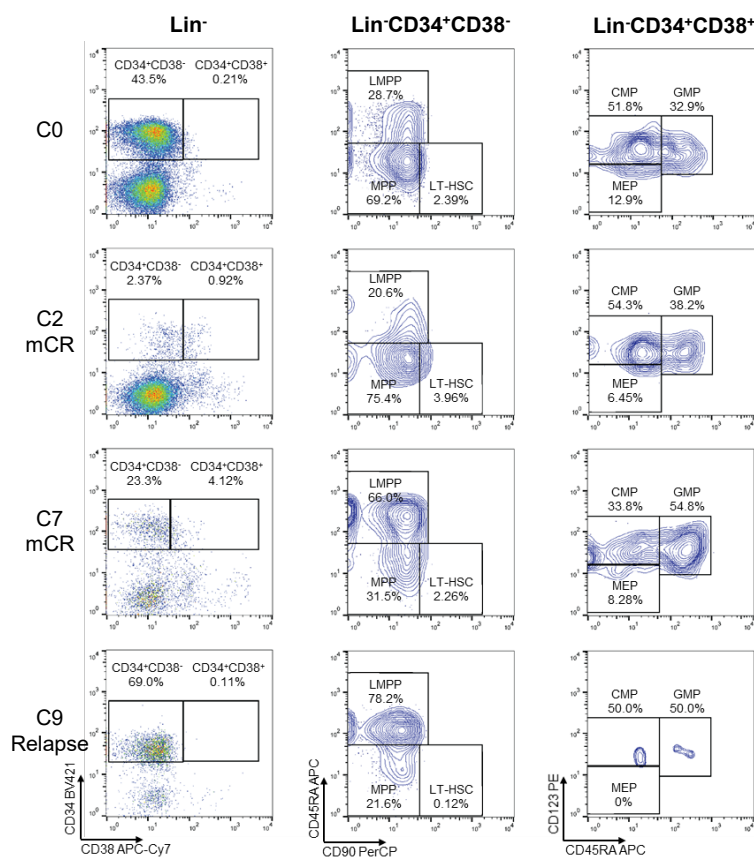
c



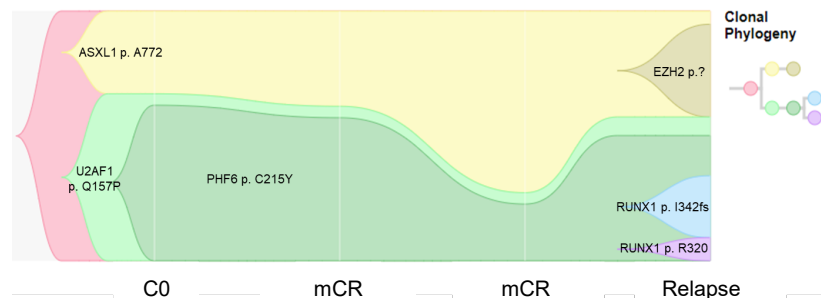
d



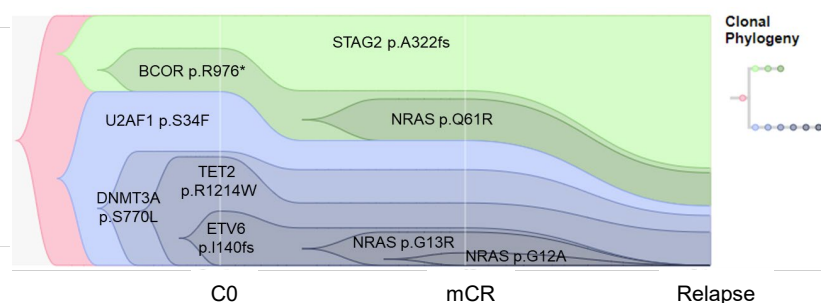
b



e

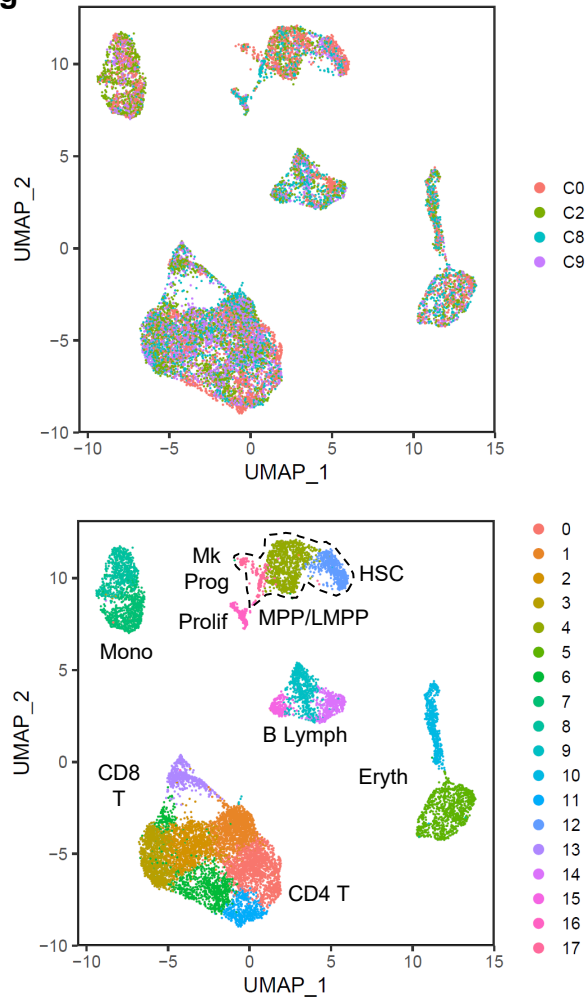


f

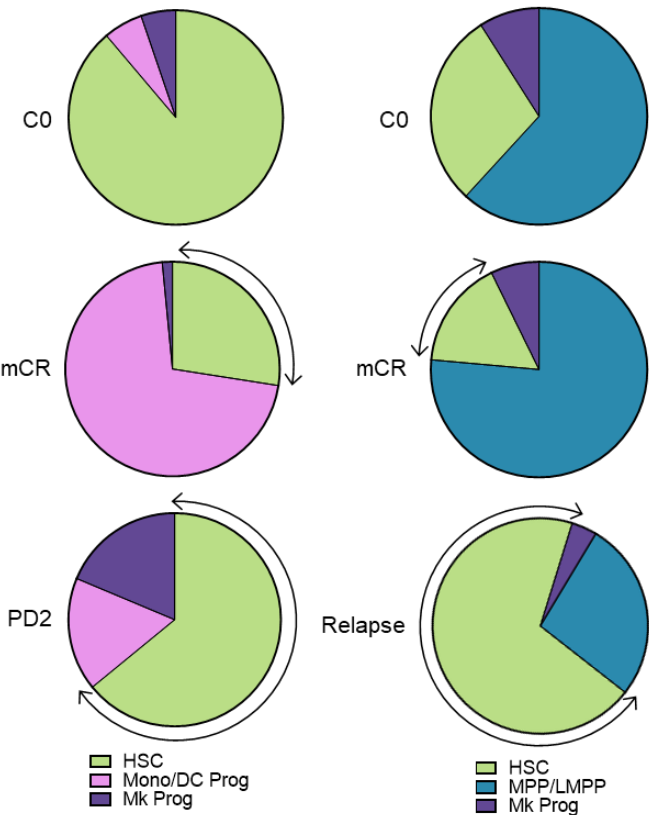


Supplementary Figure 3 (continue)

g

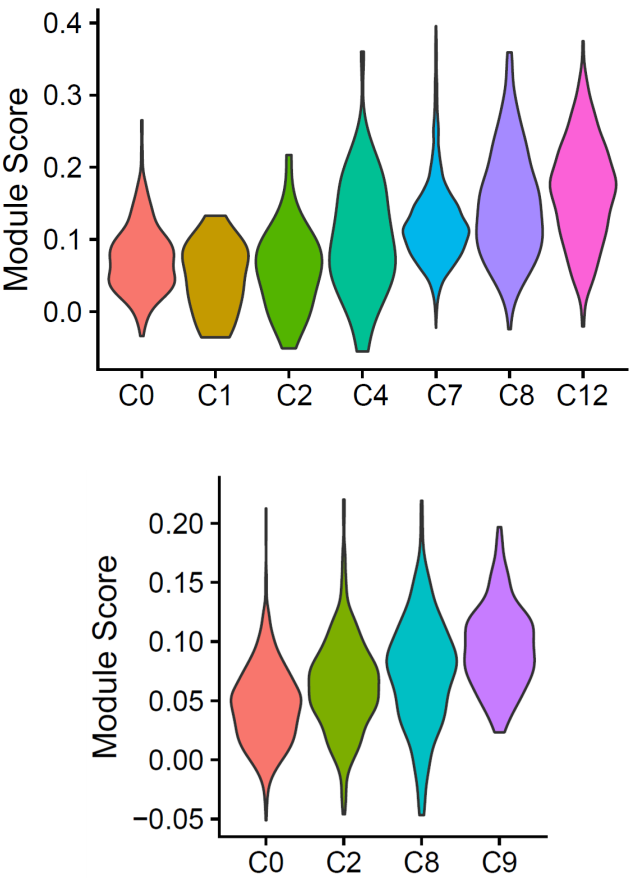


h

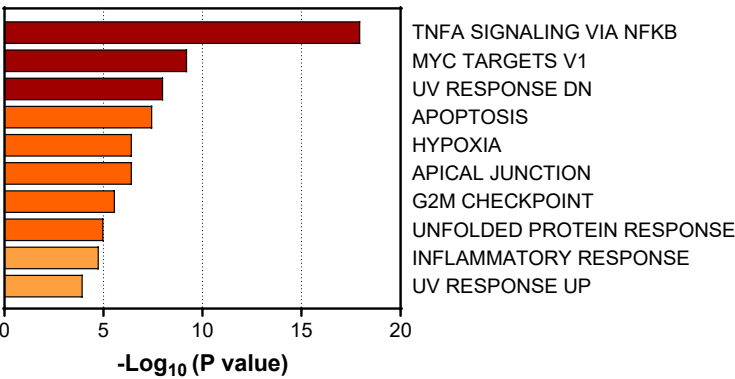


Supplementary Figure 4

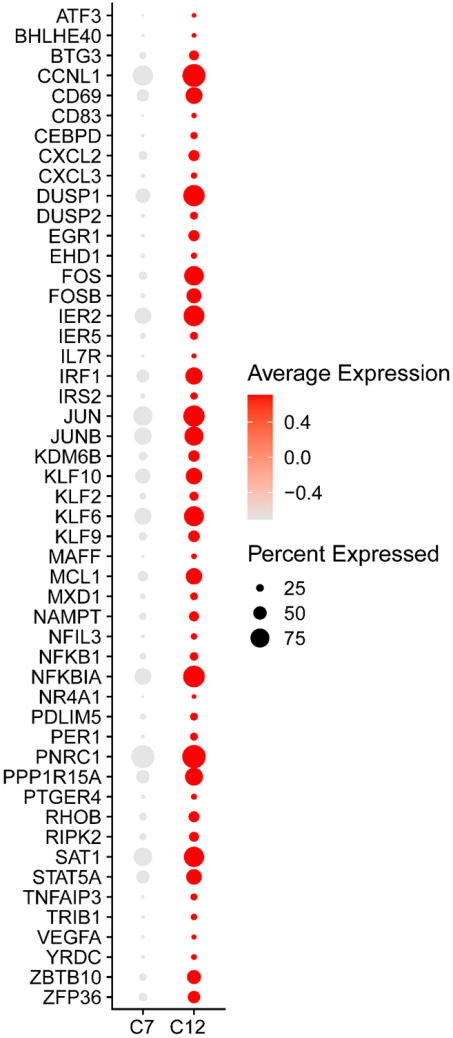
a



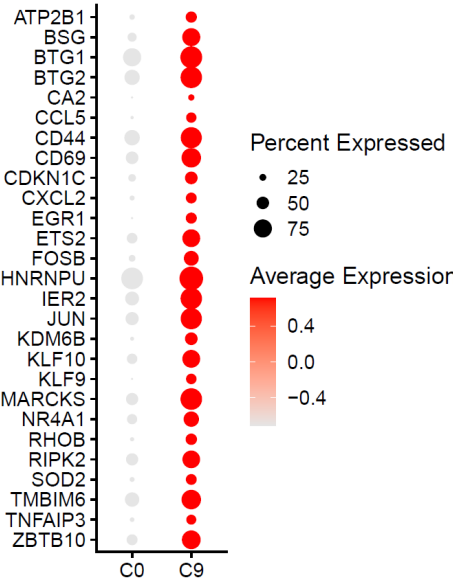
c



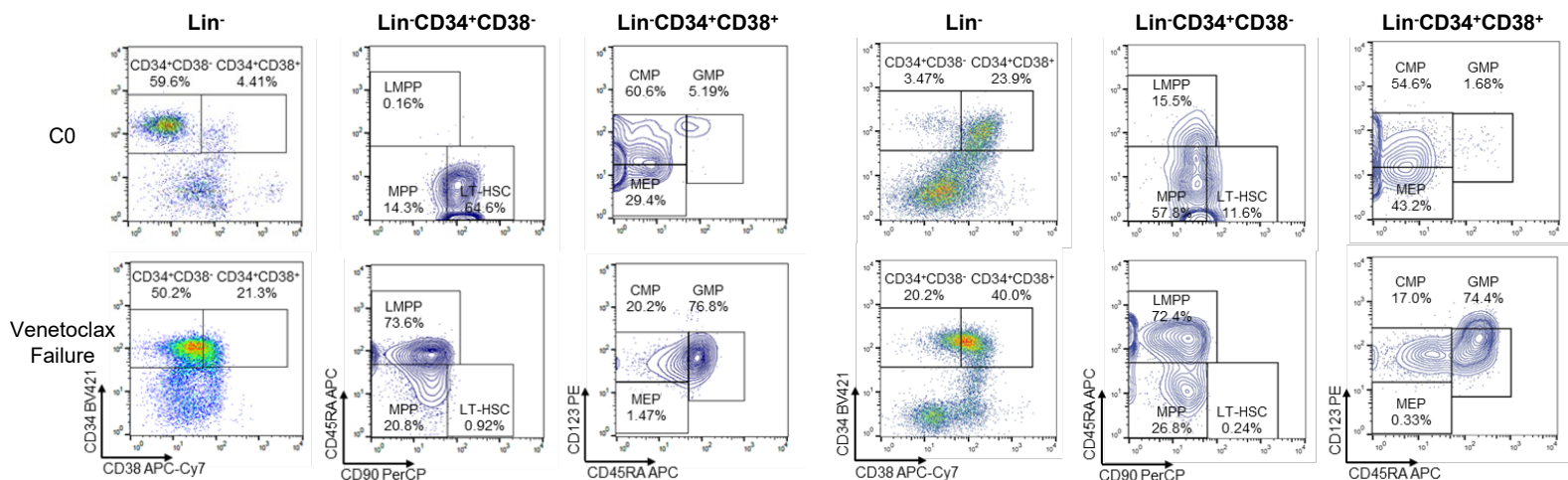
b



d

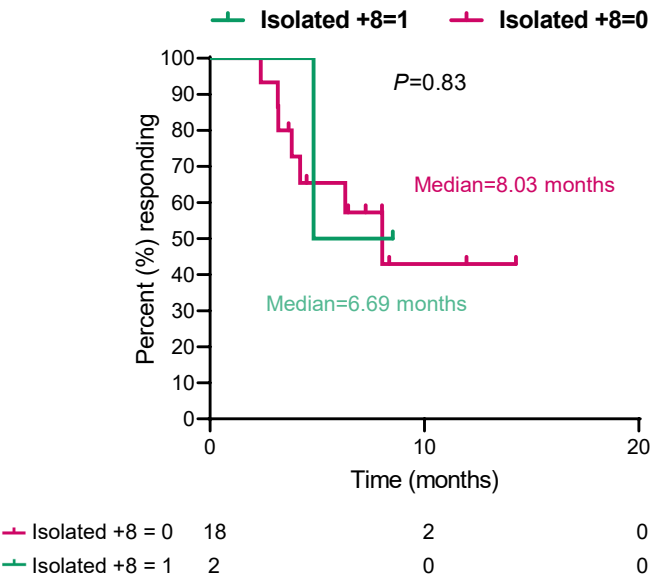
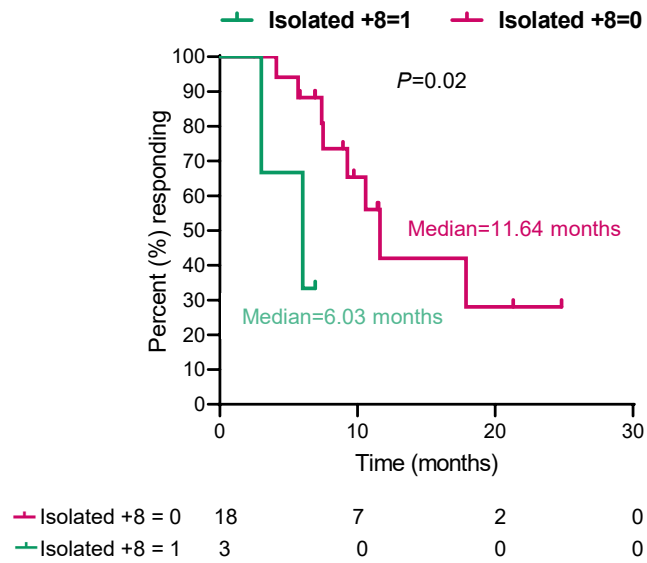


a



Supplementary Figure 6

a



Second publication

**Targeting MCL1-driven anti-apoptotic pathways
overcomes blast progression after
hypomethylating agent failure in chronic
myelomonocytic leukemia.**

Montalban-Bravo G*, Thongon N*, Rodriguez-Sevilla JJ*, Ma F,
Ganan-Gomez I, Yang H, Kim YJ, Adema V, Wildeman B, Tanaka
T, Darbaniyan F, Al-Atrash G, Dwyer K, Loghavi S, Kanagal-
Shamanna R, Song X, Zhang J, Takahashi K, Kantarjian H, Garcia-
Manero G, Colla S.

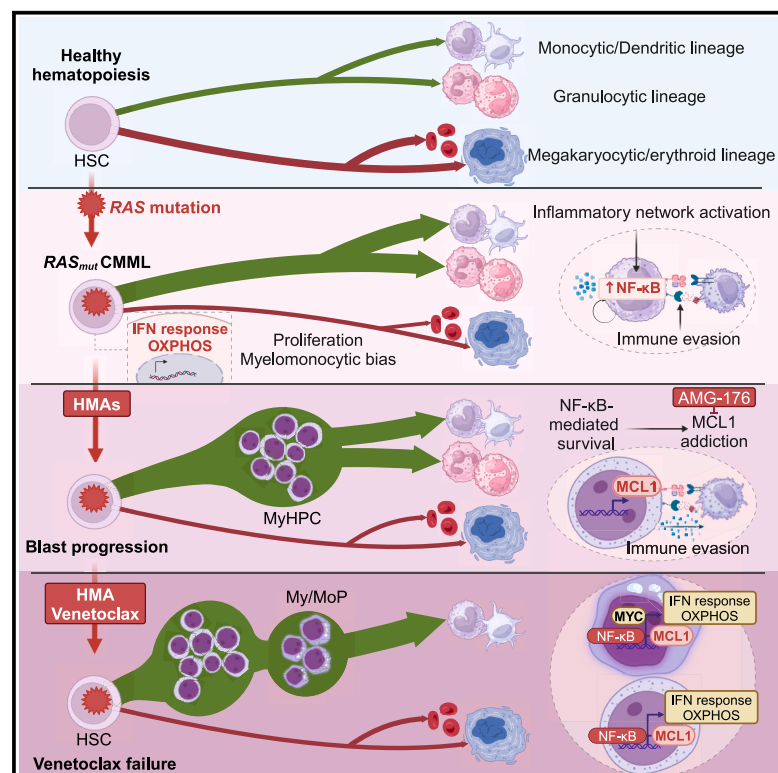
Cell Rep Med. 2024 Jun 18;5(6):101585.

Impact factor: 11.7

Quartile 1

Targeting MCL1-driven anti-apoptotic pathways overcomes blast progression after hypomethylating agent failure in chronic myelomonocytic leukemia

Graphical abstract



Authors

Guillermo Montalban-Bravo,
 Natthakan Thongon,
 Juan Jose Rodriguez-Sevilla, ...,
 Hagop Kantarjian,
 Guillermo Garcia-Manero, Simona Colla

Correspondence

scolla@mdanderson.org

In brief

In brief, Montalban-Bravo et al. show that *RAS* pathway mutations induce multi-step reprogramming of distinct cellular populations in CMML. Expansion of myeloid progenitors at blast progression following hypomethylating agent therapy is driven by NF- κ B pathway activation and MCL1 dependency. These data support the potential of NF- κ B-targeted therapies in CMML.

Highlights

- *RAS* mutations induce inflammatory network activation and immune evasion in CMML
- Expansion of NF- κ B-dependent HSPCs drives blast progression (BP) after HMA therapy
- *RAS* mutant CMML HSPCs rely on MCL1 for survival during BP
- NF- κ B pathway activation in *RAS* mutant HSPCs drives venetoclax resistance



Article

Targeting MCL1-driven anti-apoptotic pathways overcomes blast progression after hypomethylating agent failure in chronic myelomonocytic leukemia

Guillermo Montalban-Bravo,^{1,7} Natthakan Thongon,^{1,7} Juan Jose Rodriguez-Sevilla,^{1,7} Feiyang Ma,² Irene Ganan-Gomez,¹ Hui Yang,¹ Yi June Kim,¹ Vera Adema,¹ Bethany Wildeman,¹ Tomoyuki Tanaka,¹ Faezeh Darbaniyan,³ Gheath Al-Atrash,⁴ Karen Dwyer,⁴ Sanam Loghavi,⁶ Rashmi Kanagal-Shamanna,⁶ Xingzhi Song,⁵ Jianhua Zhang,⁵ Koichi Takahashi,¹ Hagop Kantarjian,¹ Guillermo Garcia-Manero,¹ and Simona Colla^{1,8,*}

¹Department of Leukemia, The University of Texas MD Anderson Cancer Center, Houston, TX, USA

²Department of Molecular, Cell and Developmental Biology, University of California Los Angeles, Los Angeles, CA, USA

³Department of Biostatistics, The University of Texas MD Anderson Cancer Center, Houston, TX, USA

⁴Department of Stem Cell Transplantation and Hematopoietic Biology and Malignancy, The University of Texas MD Anderson Cancer Center, Houston, TX, USA

⁵Department of Genomic Medicine, The University of Texas MD Anderson Cancer Center, Houston, TX, USA

⁶Department of Hematopathology, The University of Texas MD Anderson Cancer Center, Houston, TX, USA

⁷These authors contributed equally

⁸Lead contact

*Correspondence: scolla@mdanderson.org

<https://doi.org/10.1016/j.xcrm.2024.101585>

SUMMARY

RAS pathway mutations, which are present in 30% of patients with chronic myelomonocytic leukemia (CMML) at diagnosis, confer a high risk of resistance to and progression after hypomethylating agent (HMA) therapy, the current standard of care for the disease. Here, using single-cell, multi-omics technologies, we seek to dissect the biological mechanisms underlying the initiation and progression of RAS pathway-mutated CMML. We identify that RAS pathway mutations induce transcriptional reprogramming of hematopoietic stem and progenitor cells (HSPCs) and downstream monocytic populations in response to cell-intrinsic and -extrinsic inflammatory signaling that also impair the functions of immune cells. HSPCs expand at disease progression after therapy with HMA or the BCL2 inhibitor venetoclax and rely on the NF-κB pathway effector MCL1 to maintain survival. Our study has implications for the development of therapies to improve the survival of patients with RAS pathway-mutated CMML.

INTRODUCTION

Chronic myelomonocytic leukemia (CMML), a clonal disorder of mutant hematopoietic stem cells (HSCs),¹ is characterized by myelodysplastic and myeloproliferative bone marrow (BM) features,^{2,3} and a high risk of progression to acute myeloid leukemia (AML).^{4–6} Hypomethylating agent (HMA) therapy, the current standard of care for most patients with CMML,⁷ can overcome CMML cells' aberrant proliferation and achieve improved outcomes in some patients. However, most patients only have transient responses to HMA therapy, owing to these agents' inability to effectively deplete HSCs and decrease tumor burden. CMML patients whose disease undergoes transformation to AML upon HMA therapy failure have dismal clinical outcomes.^{8,9}

Despite advances in the genetic characterization of CMML, the development of alternative frontline treatments or more effective second-line therapies to improve the outcomes of CMML patients with high-risk biological features has been delayed because of an incomplete understanding of the ways in which different hematopoietic populations that persist

throughout HMA therapy contribute to disease maintenance and progression.

Mutations in *RAS* pathway signaling genes (*BRAF*, *CBL*, *KRAS*, *NF1*, *NRAS*, and *PTPN11*) confer adverse biological features that increase the risk of disease progression and poor overall survival, particularly when they are concurrently present with loss-of-function mutations in the ASXL transcriptional regulator 1 gene, *ASXL1*.¹⁰

Herein, we used single-cell technology-based approaches to elucidate the biological and molecular landscape of *RAS* pathway-mutated CMML to guide the selection of future therapeutic interventions and achieve durable responses in CMML patients in whom blast progression (BP) occurs after failure to HMA therapy.

RESULTS

Mutations in *RAS* pathway signaling genes predict a high risk of CMML BP after HMA therapy failure

We first evaluated whether specific mutations predict a high risk of CMML BP in a cohort of 108 CMML patients who received



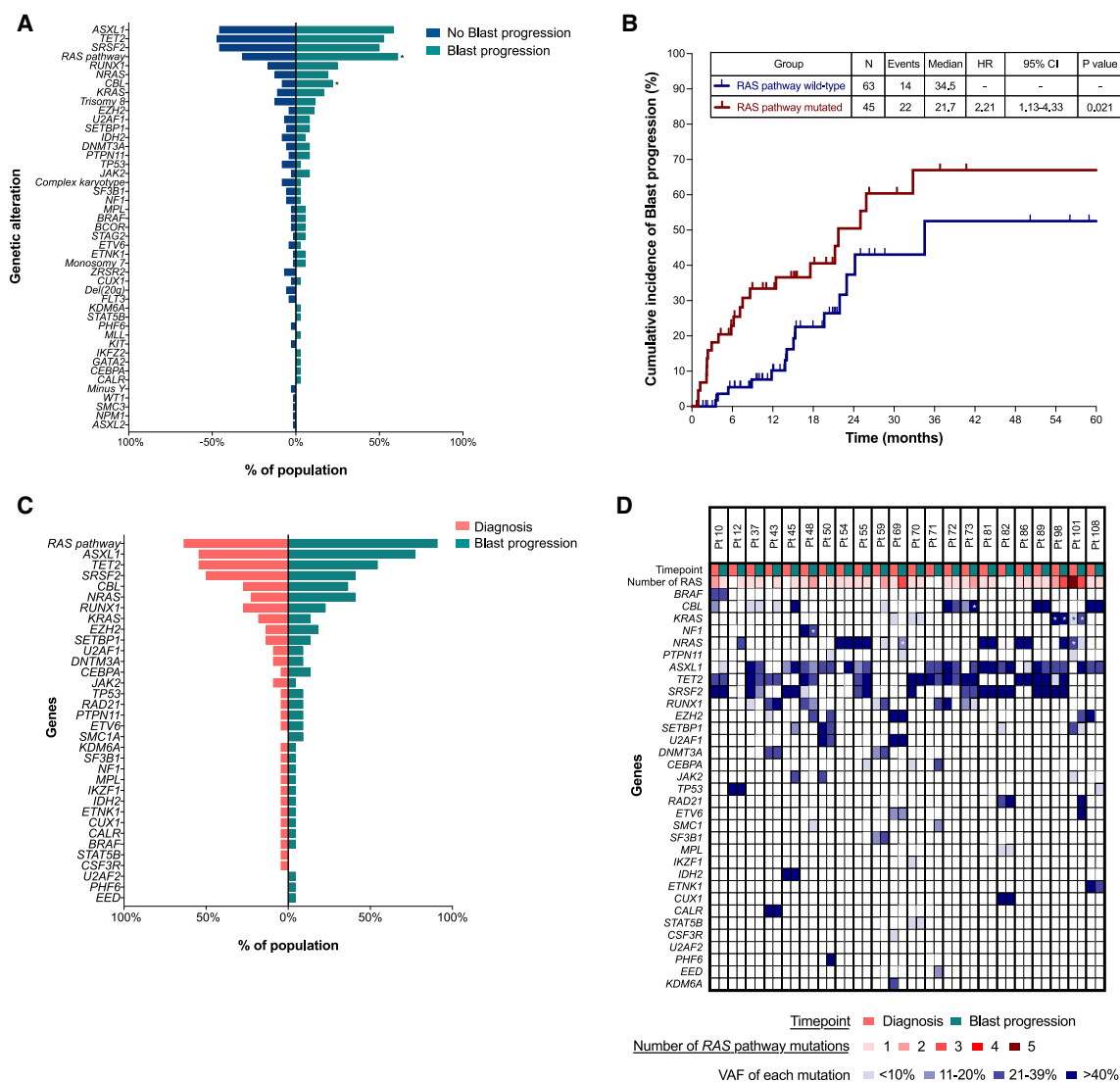


Figure 1. Mutations in RAS pathway signaling genes predict a high risk of CMML BP after HMA therapy failure

(A) Bar chart showing the frequencies of detectable mutations and cytogenetic abnormalities among 108 CMML patients who received HMA therapy and whose disease progressed (green) or did not progress (blue). Asterisks indicate significantly different frequency changes ($p < 0.05$).

(B) Kaplan-Meier survival curves showing the cumulative incidence of BP after HMA therapy in previously untreated CMML patients with or without RAS pathway mutations. N, number; HR, hazard ratio; CI, confidence interval.

(C) Bar chart showing the overall frequencies of detectable mutations among 22 CMML patients whose disease progressed and in whom targeted sequencing was performed at the time of BP. Mutations at diagnosis and BP are indicated by pink and green, respectively. Paired samples were analyzed.

(D) Detected mutations and their variant allele frequencies (VAFs) in matched samples obtained at diagnosis and at the time of BP in the 22 CMML patients shown in (C). Columns represent the mutations and VAFs from sequential samples of individual CMML patients at diagnosis and BP. Patient identifiers are shown at the top of each column. Asterisks indicate the presence of multiple mutations in a particular gene. The numbers of RAS mutations are shown in blue gradient. The VAFs of each mutation are shown in blue gradient.

HMA therapy (Table S1). After a median follow-up of 19 months (95% confidence interval [CI], 15.8–23.9 months), 57 patients experienced HMA therapy failure; 36 patients had BP at the time of therapy failure. Mutations in RAS pathway genes were significantly associated with BP (odds ratio = 3.35; 95% CI, 1.46–7.70; $p = 0.004$) (Figure 1A) and shorter time to BP (hazard ratio = 2.21; 95% CI, 1.13–4.33; $p = 0.021$) (Figure 1B). Similarly, logistic regression analysis showed that RAS pathway mutations

were associated with a higher risk of BP ($p = 0.01158$) (Table S2). To assess whether BP was associated with mutations that were not detected at diagnosis or with the clonal expansion of pre-existing mutations, we sequenced BM cells isolated from samples collected at the time of BP after HMA failure from 22 of the 36 patients and compared the cells' genomic landscape with that of BM cells isolated at diagnosis (Figure 1C). Among 22 patients with BP, 14 (64%) had RAS pathway mutations at diagnosis,

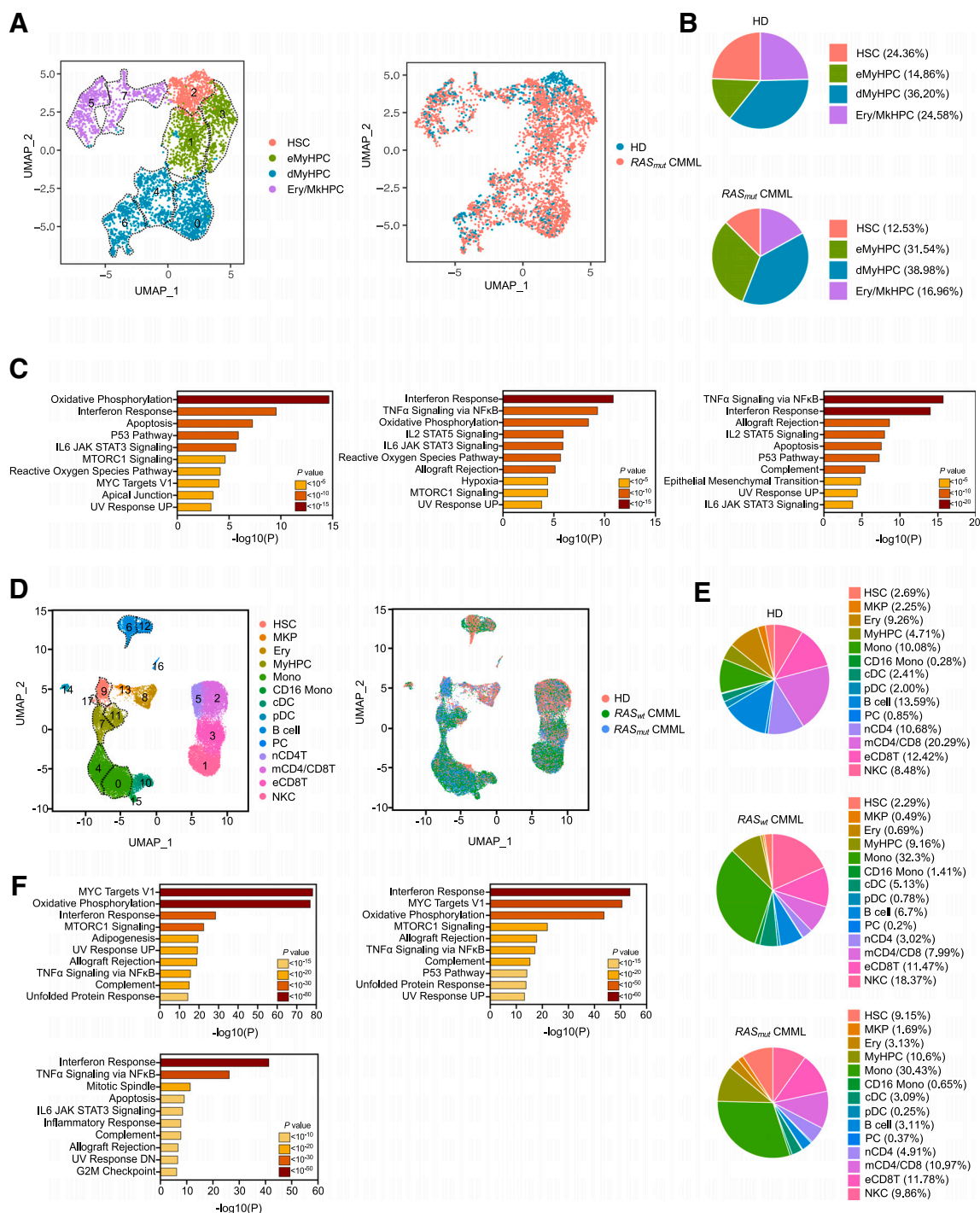


Figure 2. RAS pathway-mutated CMML cells activate cell-intrinsic and -extrinsic inflammatory networks

(A) UMAP of scRNA-seq data for pooled single Lin[−]CD34⁺ cells isolated from BM samples of two HDs ($n = 895$) and five RAS pathway mutant CMML patients ($n = 3,161$). Each dot represents one cell. Different colors represent the cluster cell-type identity (left) or sample origin (right). HSC, hematopoietic stem cells; eMyHPC, early myeloid progenitor cells; dMyHPC, differentiated myeloid progenitors; Ery/MkHPC, erythroid/megakaryocyte hematopoietic progenitor cells. Dashed lines indicate single clusters in each cell-type population.

(B) Distribution of HD (top) and RAS pathway mutant CMML (bottom) Lin[−]CD34⁺ cell types among the clusters shown in (A).

(C) Pathway enrichment analysis of the genes that were significantly upregulated in HSCs (left), eMyHPCs (middle), and dMyHPCs (right) from the five RAS pathway mutant CMML samples shown in (A) compared with those from HD samples (adjusted $p \leq 0.05$). The top 10 hallmark gene sets are shown.

(legend continued on next page)

and 20 (91%) had *RAS* pathway mutations at BP. Nine patients (41%) acquired newly detectable *RAS* pathway mutations at BP (4 patients had no detectable *RAS* pathway mutations at diagnosis, and 5 patients acquired other *RAS* pathway mutations). Of the 14 patients with *RAS* pathway-mutated CMML at diagnosis, 10 had BP without *RAS* pathway mutation-induced clonal evolution (Figure 1D).

These results were validated using single-cell DNA sequencing coupled with cell-surface immunophenotyping analysis of mononuclear cells (MNCs) isolated from sequential BM samples obtained at the time of diagnosis or BP from two representative *RAS* pathway-mutated CMML patients whose disease never responded to therapy (Figures S1A and S1B) or underwent clonal evolution after an initial response (Figures S2A and S2B). Taken together, these data demonstrate that patients with *RAS* pathway-mutated CMML have a high risk of BP at the time of HMA therapy failure. This observation has important clinical implications in light of our recent study showing that *RAS* pathway mutations also drive resistance to and/or BP following venetoclax-based second-line therapy.¹¹ These data underscore the urgent need to dissect the biological mechanisms of *RAS* pathway mutation-induced therapy resistance, as such an understanding could lead to the development of future therapeutic approaches to prevent or overcome disease progression.

***RAS* pathway mutations activate cell-intrinsic and -extrinsic inflammatory networks**

To dissect the molecular mechanisms underlying the progression of *RAS* pathway-mutated CMML, we first evaluated the molecular determinants of disease initiation. We performed single-cell RNA sequencing (scRNA-seq) analysis of lineage-negative (Lin[−]) CD34⁺ hematopoietic stem and progenitor cells (HSPCs) isolated from five untreated *RAS* pathway mutant CMML patients and two age-matched healthy donors (HDs) (Table S3). This analysis identified eight cellular clusters driven by the differentiation profile of the cells (Figure 2A), which we defined based on the differential expression of validated lineage-specific transcriptional factors (TFs) and cellular markers^{12,13} (Figure S3A; Table S4). Compared with HSPCs from HDs, Lin[−]CD34⁺ HSPCs from *RAS* pathway mutant CMML patients had a predominant myeloid differentiation route with higher frequencies of early myeloid hematopoietic progenitor cells (eMyHPCs) (clusters 1 and 3, characterized by the high expression of *CD34*, *BTF3*, and *CEBPA* but low expression of *CD38*) and more differentiated MyHPCs (dMyHPCs) (clusters 0, 4, and 6, marked by the expression of *CEBPD* and/or *CEBPA*, as well as that of *MPO*) at the expense of more primitive HSCs (cluster 2,

marked by the high expression of *MLLT3*, *MEG3*, and *CLEC9A*), and erythroid/megakaryocyte (Ery/Mk) HPCs (clusters 5 and 7, marked by the expression of *KLF1*, *GATA1*, and *GATA2*) (Figure 2B). Differential expression analysis revealed that genes upregulated in *RAS* pathway mutant CMML HSCs compared with HD HSCs were mainly involved in oxidative phosphorylation, interferon (IFN) response, and apoptosis (Figures 2C and S3B). Similar results were observed in eMyHPCs and dMyHPCs (Figure 2C).

To evaluate the contribution of downstream myelo/monocytic (My/Mo) populations to disease maintenance, we performed scRNA-seq analysis of BM MNCs isolated from three HDs, and five untreated *RAS* pathway mutant CMML samples. To dissect the specific role of *RAS* pathway mutations in disease initiation, we also included BM MNCs from three untreated *RAS* pathway wild-type CMML samples. This analysis identified 18 cellular clusters inclusive of all major BM cell types that we defined based on the expression of lineage-specific TFs and cellular markers and using the single-cell transcriptome to protein prediction with deep neural network pipeline^{14,15} (Figures 2D and S3C; Table S5). Consistent with the predominant myeloid differentiation bias of CMML HSPCs, differential analysis of BM cell lineage composition revealed that the monocyte population (clusters 0 and 4) increased in BM CMML samples compared with that in BM HD samples, regardless of the presence of *RAS* pathway mutations (Figure 2E).

However, although CMML monocytes from *RAS* pathway wild-type CMML underwent transcriptional reprogramming compared with those from HDs, *RAS* pathway mutant monocytes had significantly enhanced upregulation of IFN and NF- κ B signaling-mediated inflammatory responses compared with *RAS* pathway wild-type monocytes (Figures 2F and S4A).

Inflammatory networks modulate the immune microenvironment and contribute to immune escape.¹⁶ To assess whether CMML monocytes directly suppress the immune response and whether *RAS* pathway mutations modulate such interactions, we dissected the intercellular crosstalk and communication networks between CMML cells and all other BM cells. We inferred cell-to-cell communications from the combined expression of multi-subunit ligand-receptor complexes using CellPhoneDB, a repository of ligands and receptors and their interactions.¹⁷ After generating a homeostatic interactome of BM MNCs from HDs, we analyzed the cellular communication networks that were upregulated in *RAS* pathway wild-type and mutant CMML BM samples (Figure S4B; Table S6). Compared with HD MNCs, *RAS* pathway mutant CMML MNCs had significantly more ligand-receptor interactions

(D) UMAP of scRNA-seq data for pooled single MNCs isolated from BM samples of three HDs ($n = 12,836$), three *RAS* pathway wild-type (*RAS_{wt}*) ($n = 16,038$), and five *RAS* pathway mutant (*RAS_{mut}*) ($n = 12,234$) CMML patients. Each dot represents one cell. Different colors represent the cluster cell-type identity (left) or sample origin (right). HSC, hematopoietic stem cells; MKP, megakaryocyte precursors; Ery, erythroid precursors; MyHPC, myeloid hematopoietic progenitor cells; Mono, monocytes; CD16 Mono, non-classical CD16⁺ monocytes; cDC, classical dendritic cells; pDC, plasmacytoid dendritic cells; B cell, B lymphocytes; PC, plasma cells; nCD4T, naive CD4⁺ T cells; mCD4/CD8, memory CD4⁺ and CD8⁺ T cells; eCD8T, effector CD8⁺ T cells; NK, natural killer cells. Dashed lines indicate single clusters in each cell-type population.

(E) Distribution of HD (top), and *RAS* pathway wild-type (*RAS_{wt}*) (middle) or mutant (*RAS_{mut}*) CMML (bottom) BM MNC populations among the clusters shown in (D).

(F) Pathway enrichment analysis of the genes that were significantly upregulated in *RAS* pathway wild-type (top left) or mutant (top right) CMML monocyte clusters compared with those in HD and *RAS* pathway mutant monocyte clusters compared with those in *RAS* pathway wild-type monocyte clusters (bottom left) (adjusted $p \leq 0.05$). The top 10 hallmark gene sets are shown.

involving monocytes, classical dendritic cells (cDCs), plasmacytoid DCs (pDCs), MyHPCs, effector CD8⁺ T (eCD8T) cells, and natural killer (NK) cells (Figure S4B). Monocytes, cDCs, and immune populations from patients with *RAS* pathway mutant CMML gained significantly more ligand-to-receptor interactions compared with those without *RAS* pathway mutations (Figure S4B). Specifically, expression levels of chemokine genes (*CCL3* and *CCL3L1*) and cytokine genes (*IL1B*, *TNFSF10*, *MIF*, and *HGF*) involved in inflammatory signaling and NF- κ B-mediated cell survival were significantly increased in CMML monocytes, cDCs, pDCs, and MyHPCs, and enriched in patients with *RAS* pathway mutations (Figure S4C). Monocytes and cDCs from patients with *RAS* pathway mutations expressed higher levels of the receptors of these ligands (*CCR1*, *CCR5*, *CD74*, and *TNFRSF10B*), which suggests that an aberrant feedback loop among different cell types preferentially contributes to CMML maintenance in *RAS* pathway mutant CMML. Together, these data are consistent with previous findings showing that, in other cancers, NF- κ B signaling activation is essential for *RAS* pathway mutation-induced tumorigenesis.^{18–21}

CMML monocytes, pDCs, and cDCs also gained cell-to-cell interactions with NK and eCD8T cells. Interactions involving the HLA-E-KLRG1/2, CDH1-KLRG1, LGALS9-HAVCR2, and TGFB1-TGFB1/3 ligand-receptor pairs (known to inhibit the immune cell functions^{22–29}) were the most common (Figure S4C; Table S6). To evaluate whether CMML BM monocytes and immune cells spatially co-localized, we performed multiplex immunofluorescence analysis of BM biopsy sections obtained from CMML patients ($n = 4$) at the time of diagnosis. This analysis revealed that BM monocytes (CD14⁺CD68⁺ cells) resided within a median of 19.73 μ m (95% CI, 12.75–32.25 μ m) from CD8⁺ T cells and 22.62 μ m (95% CI, 15.73–32.17 μ m) from NK cells (CD3⁺CD56⁺ cells; Figures S5A and S5B), which suggests that these cell populations interact with each other. Accordingly, both CMML NK cells (cluster 1) and eCD8T cells (cluster 3) had increased expression levels of immune checkpoint genes associated with these cells' exhaustion (e.g., *KLRG1*, *KLRG1*, *TIGIT*, *LAG3*, *CD244*, *B3GAT1*, and *CD160*) compared with those from HDs (Figure S5C).^{30–32} To further characterize the functional state of CD8⁺ T and NK cells in CMML, we evaluated the expression of activation markers on these cells after antigen exposure. After co-culture with K562 AML cells, the frequencies of IFN- γ ⁺ CD8⁺ T cells and activated CD16⁺ NK cells were significantly lower in *RAS* pathway mutant CMML but not in *RAS* pathway wild-type CMML, compared with those in HDs (Figure S5D). In addition, IFN- γ ⁺ CD8⁺ T cells and NK cells from patients with *RAS* pathway mutant CMML, but not those from *RAS* pathway wild-type CMML, had significantly lower IFN- γ and perforin expression levels, respectively (Figure S5D).

Taken together, these data suggest that CMML HSPCs and downstream My/Mo cells undergo significant transcriptional re-wiring and that *RAS* pathway mutations enhance the activation of cell-intrinsic and -extrinsic inflammatory networks in CMML monocyte populations to maintain cell proliferation and suppress the immune microenvironment, thus enabling immune escape and clonal expansion.

***RAS* pathway-mutated HSCs upregulate NF- κ B transcriptional programs and drive CMML BP after HMA therapy failure**

To evaluate the cellular and molecular dynamics of CMML progression, we performed scRNA-seq analysis of Lin[−]CD34⁺ HSPCs isolated from BM samples sequentially obtained from five *RAS* pathway mutant CMML patients at diagnosis and BP (Figures 3A and S6A; Table S7). HSPCs isolated from BM samples obtained at BP maintained aberrant differentiation toward the My/Mo lineage (Figure 3B) and had upregulated genes belonging to the NF- κ B signaling pathway (Figure 3C). Importantly, *MCL1*, an anti-apoptotic member of the BCL2 family and a downstream effector of the NF- κ B pathway, was significantly upregulated in HSCs (cluster 6) and eMyHPCs (clusters 0 and 1) at BP compared with those at diagnosis (Figures S6B and S6C; Table S8).

To evaluate whether HSPCs' transcriptional changes at BP resulted from epigenetic reprogramming in the more primitive HSCs, we performed single-cell assays for transposase-accessible chromatin with high-throughput sequencing (scATAC-seq) to profile the chromatin accessibility landscape in Lin[−]CD34⁺ HSPCs isolated from BM samples sequentially obtained from three *RAS* pathway mutant CMML patients at diagnosis or BP. Our analysis identified five clusters with distinct TF binding motif enrichment in the open chromatin regions (Figures 3D and S6D; Table S9). MyHPCs (clusters 1 and 2) were characterized by open chromatin regions in the binding motifs of the myeloid TFs *SPI1B* and *CEBPA* and TFs belonging to the *FOS* and *JUN* families. HSCs (clusters 0 and 4) had the highest activities of TFs involved in stemness maintenance, such as *HLF* and TFs belonging to the nuclear retinoid receptor and *EGR* families. Ery/MkHPCs (cluster 3) were characterized by open chromatin regions in binding motifs for GATA TFs.

Consistent with our transcriptomic data, HSCs at BP had increased open chromatin peaks at the promoters of genes involved in NF- κ B pathway activation and inflammatory response pathways (Figure 3E), including *MCL1* (Figure S6E; Table S10). HSCs also showed increased open chromatin peaks of genes involved in NF- κ B pathway activation and inflammatory response pathways at the genes' distal elements, which define cell identity and differentiation trajectories more precisely than promoter regions do³³ (Figures 3F and S6F).

Taken together, these data suggest that *RAS* pathway-mutated CMML HSCs exacerbate the activation of inflammatory and NF- κ B pathway transcriptional programs and promote transcriptional upregulation of NF- κ B signaling-mediated anti-apoptotic pathways to maintain survival at BP after HMA failure.

***RAS* pathway-mutated CMML cells rely on *MCL1* overexpression to maintain their survival at BP**

To elucidate whether MyHPCs' transcriptional and epigenetic reprogramming drives BP, we performed scRNA-seq analysis of MNCs isolated from sequential *RAS* pathway-mutated CMML BM samples obtained from six CMML patients at diagnosis and BP (Figures 4A and S7A; Table S11). MNCs at BP had a significantly higher frequency of CD34⁺ MyHPCs (22.5% vs. 2.8%, respectively; clusters 7, 8, and 14) compared with those at diagnosis (Figures 4B and S7B). These results were confirmed

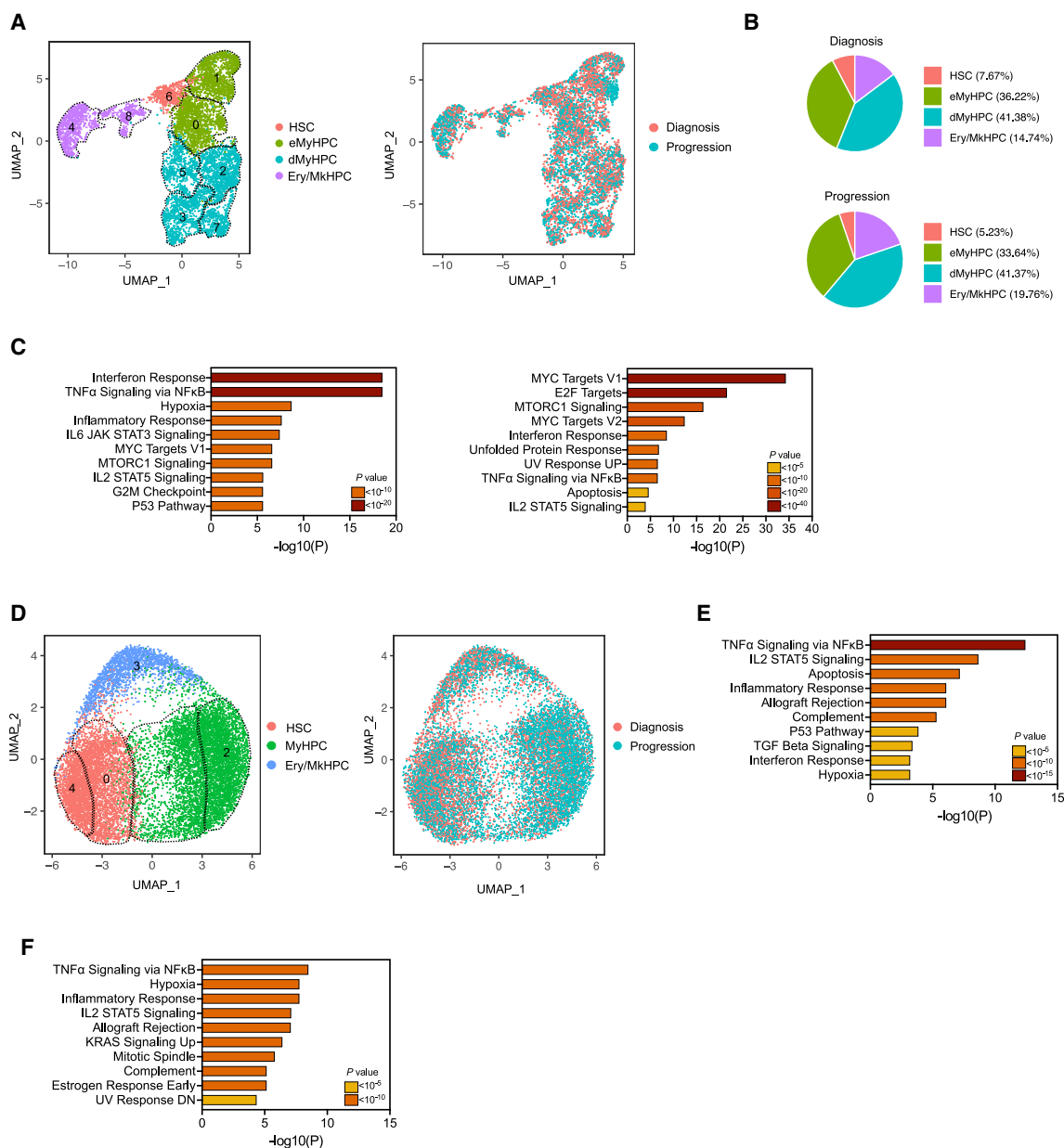


Figure 3. *RAS* pathway-mutated HSCs undergo epigenetic reprogramming and drive CMML BP after HMA therapy failure

(A) UMAP of scRNA-seq data for pooled single Lin⁺CD34⁺ cells isolated from BM samples of five *RAS* pathway mutant CMML patients at diagnosis ($n = 1,840$) and at BP after HMA therapy failure ($n = 1,711$). Each dot represents one cell. Different colors represent the cluster cell-type identity (left) or sample origin (right). HSC, hematopoietic stem cells; eMyHPC, early myeloid hematopoietic progenitor cells; dMyHPC, differentiated myeloid hematopoietic progenitor cells; Ery/MkHPC, erythroid/megakaryocyte hematopoietic progenitor cells. Dashed lines indicate single clusters in each cell-type population.

(B) Distribution of Lin⁺CD34⁺ cell types at diagnosis (top) and BP (bottom) among the clusters shown in (A).

(C) Pathway enrichment analysis of the genes that were significantly upregulated in HSCs (left) and dMyHPCs (right) at the time of BP after HMA therapy failure compared with those at diagnosis (adjusted $p \leq 0.05$). The top 10 hallmark gene sets are shown.

(D) UMAP of scATAC-seq data for pooled Lin⁺CD34⁺ cells isolated from BM samples obtained from three *RAS* pathway mutant CMML patients at diagnosis ($n = 5,066$) and at BP after HMA therapy failure ($n = 8,603$). Each dot represents one cell. Different colors represent the cluster identity (left) or sample of origin (right). HSC, hematopoietic stem cells; MyHPC, myeloid progenitor cells; Ery/MkHPC, erythroid/megakaryocyte hematopoietic progenitor cells.

(E) Pathway enrichment analysis of genes whose promoters were enriched in open chromatin regions in HSCs (clusters 0 and 4, shown in D) at the time of BP as compared with those at diagnosis ($p \leq 10^{-4}$). The top 10 hallmark gene sets are shown.

(F) Pathway enrichment analysis of genes whose distal elements were enriched in open chromatin regions in HSCs (clusters 0 and 4, shown in D) at the time of BP as compared with those at diagnosis (adjusted $p \leq 0.05$). The top 10 hallmark gene sets are shown.

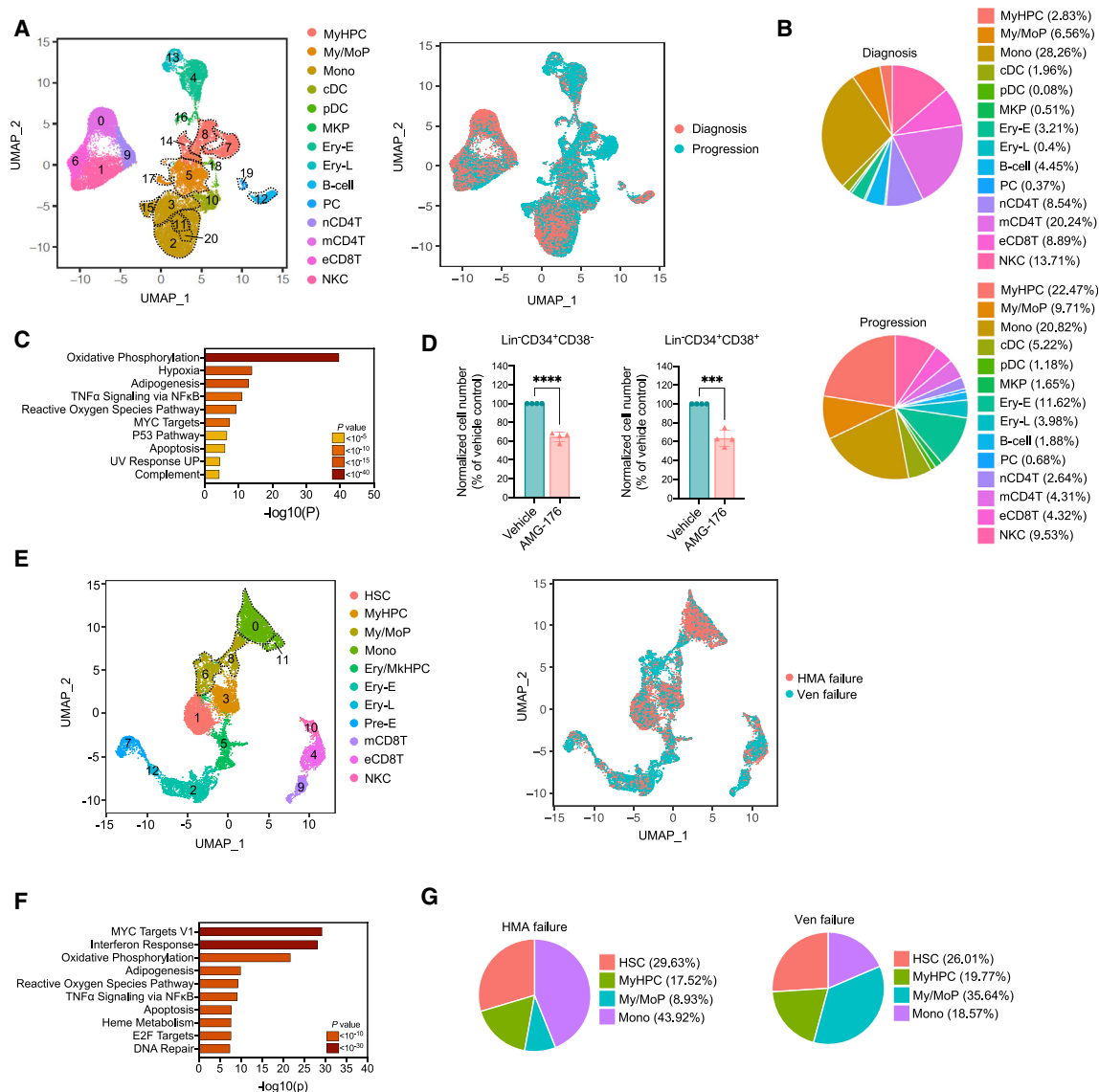


Figure 4. *RAS* pathway-mutated CMML cells rely on *MCL1* overexpression to maintain their survival at BP

(A) UMAP of scRNA-seq data for pooled single MNCs isolated from BM samples of six *RAS* pathway mutant CMML patients at diagnosis ($n = 16,372$) and at BP after HMA therapy failure ($n = 19,541$). Each dot represents one cell. Different colors represent the cluster cell-type identity (left) or sample of origin (right). MyHPC, myeloid hematopoietic progenitor cells; My/MoP, myelo/monocytic progenitors; Mono, monocytes; cDC, classical dendritic cells; pDC, plasmacytoid dendritic cells; MKP, megakaryocyte precursors; Ery-E, early erythroid precursors; Ery-L, late erythroid precursors; B cell, B lymphocytes; PC, plasma cells; nCD4T, naive CD4⁺ T cells; mCD4T, memory CD4⁺ T cells; eCD8T, effector CD8⁺ T cells; NKC, natural killer cells. Dashed lines indicate single clusters in each cell-type population.

(B) Distribution of MNC populations at diagnosis (top) and progression (bottom) among the clusters shown in (A).

(C) Pathway enrichment analysis of the genes that were significantly upregulated in the monocytic populations (clusters 2, 3, 11, 15, and 20) shown in (A) at the time of BP after HMA therapy failure compared with those at diagnosis (adjusted $p \leq 0.05$). The top 10 hallmark gene sets are shown.

(D) Numbers of live Lin⁺CD34⁺CD38⁻ HSCs and Lin⁺CD34⁺CD38⁺ MyHPCs from CMML patients with BP after treatment with vehicle or AMG-176 ($n = 4$, 20 nM) for 48 h. Lines represent means \pm SD. Statistical significance was calculated using a two-tailed Student's *t* test (*** $p < 0.001$, **** $p < 0.0001$).

(E) UMAP of scRNA-seq data for pooled single MNCs isolated from BM samples obtained from a representative CMML patient at the time of BP after HMA therapy failure ($n = 6,209$) and subsequent failure to venetoclax-based therapy ($n = 6,795$). Each dot represents one cell. Different colors represent the cluster cell-type identity (left) or the sample of origin (right). HSC, hematopoietic stem cells; MyHPC, myeloid hematopoietic progenitor cells; My/MoP, myelo/monocytic progenitors; Mono, monocytes; Ery/MkHPC, erythroid/megakaryocytic hematopoietic progenitor cells; Ery-E, early erythroid precursors; Ery-L, late erythroid precursors; Pre-E, pre-erythrocytes; mCD8T, memory CD8⁺ T cells; eCD8T, effector CD8⁺ T cells; NKC, natural killer cells.

(F) Pathway enrichment analysis of the genes that were significantly upregulated in MyHPCs at the time of venetoclax failure compared with those at the time of BP after HMA therapy failure (adjusted $p \leq 0.05$). The top 10 hallmark gene sets are shown.

(G) Distribution of myeloid cell types among the myeloid compartments at BP after HMA therapy failure (left) and venetoclax-based therapy failure (right).

by flow cytometry analysis of Lin[−]CD34⁺ cells in 70% of the patients (Figure S7C), which suggests that BP after HMA therapy is mostly driven by the expansion of the HSPC compartment. Consistent with our results in the Lin[−]CD34⁺ compartment, differential expression analysis confirmed that MyHPCs at BP had upregulated genes involved in TNF- α -mediated NF- κ B activation (Figure S7D), including *MCL1* (Figures S7E and S7F; Table S12). The upregulation of these genes was maintained in downstream My/Mo progenitors (My/MoPs; clusters 5 and 17) and was significantly increased in the monocytic populations (clusters 2, 3, 11, 15, and 20) (Figures 4C and S7G; Table S12). Consistent with these transcriptomic results, CD34⁺ BM cells from patients with *RAS* pathway mutant CMML at BP ($n = 2$) had higher *MCL1* protein expression than did cells from patients at diagnosis ($n = 3$; Figure S7H).

MNCs at BP exacerbated the cellular communication networks between cDCs, MyHPCs, My/MoPs, pDCs, monocytes, and eCD8T cells, compared with MNCs at baseline. Exacerbation of the cellular communication networks mainly occurred through immune-suppressive interactions between the LGALS9-HAVCR2 ligand-receptor pair, as well as increased CCL3/CCR1 and HGF/CD44 interactions between monocytes, MyMoPs and MyHPCs (Figures S8A and S8B; Table S13).

To determine whether *MCL1* upregulation was a hallmark of BP in *RAS* pathway mutant CMML or a general mechanism of treatment resistance and progression in CMML, we performed scRNA-seq analysis of BM MNCs isolated from *RAS* pathway wild-type CMML samples at diagnosis ($n = 3$) and BP after HMA failure ($n = 3$) (Figures S9A and S9B; Table S14). *RAS* pathway wild-type BM MNCs at progression had a higher frequency of MyHPCs compared with those at diagnosis (8.1% vs. 3.9%, respectively; cluster 7; Figure S9C). MyHPCs at BP upregulated genes involved in TNF- α -mediated NF- κ B activation but not *MCL1* (Figures S9D and S9E; Table S15). Similar data were also observed in downstream My/MoPs and monocytes (Figure S9D; Table S15). Consistent with these findings, CD34⁺ BM cells from patients with *RAS* pathway wild-type CMML at diagnosis ($n = 3$) and BP ($n = 3$) had similar *MCL1* protein expression levels (Figure S7H).

Together, these data suggest that only *RAS* pathway-mutated CMML MyHPCs and monocytes rely on *MCL1*-driven anti-apoptotic pathways to maintain survival and expand after therapy failure. To test this hypothesis, we treated Lin[−]CD34⁺ HSPCs isolated from the BM of patients with *RAS* pathway-mutated CMML with the *MCL1* inhibitor AMG-176³⁴ (at a dose that did not deplete Lin[−]CD34⁺CD38[−] or Lin[−]CD34⁺CD38⁺ HSPCs isolated from the BM of HDs in co-culture system with mesenchymal stromal cells; Figure S10A). AMG-176 significantly decreased the numbers of Lin[−]CD34⁺CD38[−] and Lin[−]CD34⁺CD38⁺ HSPCs isolated from BM samples obtained from patients with *RAS* pathway-mutated CMML at BP (Figure 4D). AMG-176 did not significantly affect the survival of HSPCs isolated from BM samples obtained from patients at diagnosis (Figure S10B), which confirms that CMML HSPCs maintain an intact apoptotic program at disease initiation. Consistent with our scRNA-seq analysis showing that *MCL1* was not upregulated in *RAS* pathway wild-type HSPCs, the treatment with AMG-176 did not deplete

RAS pathway wild-type HSPCs at the time of BP after HMA failure (Figure S10C).

Importantly, *BCL2* was not overexpressed in either *RAS* pathway mutant CMML HSPCs or downstream My/Mo populations at BP after HMA therapy failure (Figure S10D). *BCL2* expression was significantly downregulated at progression in MyHPCs and My/MoPs from CMML patients without detectable *RAS* pathway mutations at the time of BP (Figure S10E). These findings are consistent with our previous clinical observation that CMML patients in whom HMA therapy has failed do not benefit from second-line therapy with venetoclax.¹¹ Indeed, scRNA-seq analysis of MNCs isolated from sequential BM samples obtained from one representative *RAS* pathway mutant CMML patient whose disease progressed after HMA therapy failure and did not respond to venetoclax therapy (Figures 4E and S10F; Table S16) revealed that MyHPCs further exacerbate the expression of genes involved in TNF- α -mediated NF- κ B pathway activation (Figure 4F), including *MCL1* (Figure S10G). Venetoclax failure was associated with a significant expansion of downstream My/MoPs in the myeloid compartment (Figure 4G) and these cells' high expression of *MCL1* (Figure S10G).

Taken together, our findings suggest that venetoclax therapy cannot overcome HMA failure-induced transcriptional reprogramming in My/MoPs and provide a rationale for targeting effectors of the NF- κ B signaling pathway, such as *MCL1*, in patients with *RAS* pathway mutant CMML to improve the dismal outcome of CMML patients whose disease is resistant to available therapies.

DISCUSSION

Whereas the dissection of the molecular landscape of CMML initiation and progression has significantly advanced our understanding of the pathogenesis of CMML,^{1,35–38} the development of more effective therapeutic approaches to improve patient survival has been delayed by our limited understanding of the ways in which genetic alterations affect distinct transcriptional states of My/Mo differentiation.

Mutations in *RAS* pathway genes, which are present in 30% of CMML patients,³⁸ are enriched during disease progression in up to 90% of the cases and predict a higher risk of and a shorter time to relapse after HMA and venetoclax therapy.³⁹ Currently, there are no other therapies that improve the survival duration of patients with *RAS* pathway-mutated CMML.

Using single-cell multi-omics technologies, we sought to dissect the biological mechanisms behind *RAS* pathway mutation-induced CMML evolution with the overall goal of identifying cellular vulnerabilities that could be therapeutically targeted to halt disease progression. We found that, at disease initiation, *RAS* pathway mutant CMML HSPCs significantly upregulated genes involved in the cell-intrinsic IFN signaling pathway such as *IRF1*, *IRF7*, *IRF9*, *IFI44*, *IFI44L*, *IFIH1*, *IFIT3*, or *STAT2* that drive these cells' differentiation toward the My/Mo lineage while maintaining an intact apoptotic program. Consistent with this observation and prior studies showing that *KRAS* or *NRAS* mutations directly activate intrinsic IFN-stimulated genes,⁴⁰ IFN signaling activation in HSPCs was not associated with IFN receptor (*IFNAR1*, *IFNAR2*, *IFNGR1*, or *IFNG2*) or ligand (*IFNG* or

IFNA) overexpression. In addition, this inflammatory reprogramming was exacerbated in downstream *RAS* pathway mutant monocyte populations, which expressed high levels of cytokines and cell surface receptors involved in NF- κ B pathway activation and immune evasion. These results suggest that disease initiation and maintenance, as a result of *RAS* pathway mutations, rely on the activation of both cell-intrinsic and -extrinsic inflammatory networks in distinct cell populations and provide a rationale for using inhibitors of NF- κ B-associated inflammatory signaling cascades as a frontline treatment for patients with *RAS* pathway-mutated CMML. These findings, which are consistent with previous studies showing the role of inflammatory cell populations in myeloid malignancies,^{41,42} have significant implications since several inflammation-targeting therapies that are currently in clinical development have shown great potential to treat patients with myeloid malignancies.^{43–45}

Consistent with the long-standing observation that inhibition of apoptosis contributes to therapy resistance and cancer progression, we found that *RAS* pathway mutant CMML HSPCs isolated from BM samples at the time of BP depended on MCL1, an anti-apoptotic downstream effector of the NF- κ B pathway, to maintain their survival and undergo clonal expansion. Consistent with this observation, we had demonstrated previously that TNF- α -mediated NF- κ B pathway activation represents a cell-intrinsic adaptive mechanism to overcome cell death in response to therapeutic pressure.⁴⁶ In addition, our findings align with prior data demonstrating that *RAS* mutations can directly induce NF- κ B hyperactivation.^{21,47} Notably, targeting MCL1 activity with the small molecule AMG-176 only significantly depleted HSPCs from *RAS* mutant CMML but not those from *RAS* wild-type CMML, a finding that supports the selective use of MCL1 inhibitors to treat patients with *RAS* pathway mutant CMML in whom BP occurs at the time of HMA therapy failure. These results are consistent with previous findings showing that CMML monocytes rely on MCL1, but not BCL2, for survival,⁴⁸ and that *NRAS*-mutant monocytic subclones that emerge at AML relapse depend on MCL1, not BCL2, for energy production.⁴⁹ Consistent with this observation, our scRNA-seq analysis of BM MNCs from one representative patient with venetoclax-resistant disease confirmed that BCL2 inhibition cannot overcome the activation of NF- κ B pathway-mediated inflammatory and survival mechanisms in HSPCs and downstream My/Mo populations.

In conclusion, this study highlights the importance of dissecting how specific genetic drivers affect the cell-of-origin in cancer to gain mechanistic insights into therapy failure and, thereby, develop selective therapeutic approaches to halt disease progression. Given that the *RAS* pathway mutation-induced reprogramming of CMML cells is a multi-step process that affects multiple biological signaling pathways (e.g., inflammation, apoptosis, and immune escape) in distinct BM cell types, our findings also suggest that only combination therapies that simultaneously target these pathways could effectively overcome disease progression and prolong the survival of patients whose disease is resistant to current therapeutic approaches.

Limitations of the study

In this study, we used 3' RNA-seq by 10X Genomics, which evaluates RNA transcript expression levels for individual genes at the

single-cell level but does not capture the entire RNA sequence, hence not allowing inference of the complete cDNA sequence and somatic mutation detection. Therefore, we were not able to correlate transcriptome to *RAS* pathway mutation status with single-cell resolution in all sequenced cases. Although we attempted to mitigate this intrinsic limitation to our sequencing technique by selecting samples with high *RAS* pathway mutant variant allele frequencies (VAFs), future studies will require the use of alternative single-cell sequencing technologies able to simultaneously capture genotype and transcriptome at the single-cell level to invariably characterize the specific features of *RAS* pathway mutant vs. wild-type cells. In an attempt to mitigate the impact of such a limitation in our identification of MCL1 upregulation as a preferential *RAS* mutant cell survival mechanism, we confirmed MCL1 upregulation at the protein level by evaluating *RAS* pathway mutant samples with high VAFs. In addition, although we were able to confirm the selective sensitivity of *RAS* pathway mutant Lin[−]CD34⁺ cells to MCL1 inhibition at the time of progression after HMA therapy failure, there are inherent limitations to the extent to which these studies can capture the *in vivo* effects of MCL1 inhibition and how this could affect distinct cell types and functionalities. Finally, although we validated our transcriptomic findings related to cell-cell communication networks between key BM populations with multiplex immunofluorescence and immunophenotypic immune cell characterization, future studies will require deeper investigation and validation of these interactions.

STAR★METHODS

Detailed methods are provided in the online version of this paper and include the following:

- KEY RESOURCES TABLE
- RESOURCE AVAILABILITY
 - Lead contact
 - Materials availability
 - Data and code availability
- EXPERIMENTAL MODEL AND STUDY PARTICIPANT DETAILS
 - Primary human samples
- METHOD DETAILS
 - Clinical data analysis
 - Flow cytometry analysis and fluorescence-activated cell sorting (FACS)
 - Multiplex imaging assay
 - Western blot
 - T cell and NK cell cytokine secretion assays
 - scRNA-seq analysis and bioinformatic pipeline
 - scATAC-seq analysis and bioinformatic pipeline
 - scDNA and protein-seq analysis
 - Primary cell culture assays
- QUANTIFICATION AND STATISTICAL ANALYSIS

SUPPLEMENTAL INFORMATION

Supplemental information can be found online at <https://doi.org/10.1016/j.xcrm.2024.101585>.

ACKNOWLEDGMENTS

This work was supported by philanthropic contributions to MD Anderson's AML/MDS Moon Shot, the Edward P. Evans Foundation, and the National

Institutes of Health through a Leukemia SPORE grant awarded to the MD Anderson Cancer Center (P50 CA100632). J.J.R.-S. is a recipient of the Odyssey Fellowship awarded by the MD Anderson Cancer Center. This work used MD Anderson's South Campus Flow Cytometry & Cellular Imaging Facility and the Advanced Technology Genomics Core at the MD Anderson Cancer Center; the facilities are supported in part by the National Institutes of Health (National Cancer Institute) through MD Anderson's Cancer Center Support Grant (P30 CA16672). The authors thank Joseph Munch for assistance with manuscript editing. The authors give thanks for the technical support of the following Translational Molecular Pathology-Immunoprofiling Laboratory members: Daniela E. Duenas, Mario L. Marques-Piubelli, Mei Jiang, Beatriz Sanchez-Espidion, Salome McAllen, and Jianling Zhou. The graphical abstract was created with [Biorender.com](https://biorender.com).

AUTHOR CONTRIBUTIONS

G.M.-B. and S.C. designed the research. N.T., J.J.R.-S., I.G.-G., H.Y., V.A., and B.W. performed the experiments. F.M. analyzed scRNA and scATAC-seq data. S.L., R.K.-S., X.S., and J.Z. analyzed targeted DNA sequencing data. Y.J.K., T.T., and K.T. performed scDNA and protein-seq experiments. K.D. analyzed the flow cytometry data. G.M.-B. and J.J.R.-S. identified the clinical samples included in the study. G.M.-B. and F.D. analyzed the clinical data. G.A.-A. provided the HD samples. H.K. and G.G.-M. made critical intellectual contributions throughout the study. G.M.-B. and S.C. wrote the manuscript.

DECLARATION OF INTERESTS

G.M.-B. declares research support from Rigel Pharmaceuticals, IFM Therapeutics, and Takeda Oncology. K.T. declares support from Symbio Pharmaceuticals, Novartis, Celgene/BMS, and GSK, and honoraria from Mission Bio and Illumina. H.K. declares research support from and an advisory role at Actinium and research support from AbbVie, Agio, Amgen, Ariad, Astex, Bristol Myers Squibb, Cyclacel, Daiichi-Sankyo, Immunogen, Jazz Pharma, Novartis, and Pfizer. G.G.-M. declares research support from and an advisory role at Bristol Myers Squibb, Astex, and Helsinn, and research support from Amphenova, Novartis, AbbVie, H3 Biomedicine, Onconova, and Merck. S.C. declares research support from Amgen.

DECLARATION OF GENERATIVE AI AND AI-ASSISTED TECHNOLOGIES IN THE WRITING PROCESS

During the preparation of this work, S.C. used Grammarly to correct grammar mistakes. After using this tool, S.C. reviewed and edited the content as needed. S.C. takes full responsibility for the content of the publication.

Received: December 4, 2022

Revised: November 27, 2023

Accepted: April 30, 2024

Published: May 22, 2024

REFERENCES

- Itzykson, R., Kosmider, O., Renneville, A., Morabito, M., Preudhomme, C., Berthon, C., Adès, L., Fenaux, P., Platzbecker, U., Gagey, O., et al. (2013). Clonal architecture of chronic myelomonocytic leukemias. *Blood* 121, 2186–2198. <https://doi.org/10.1182/blood-2012-06-440347>.
- Arber, D.A., Orazi, A., Hasserjian, R., Thiele, J., Borowitz, M.J., Le Beau, M.M., Bloomfield, C.D., Cazzola, M., and Vardiman, J.W. (2016). The 2016 revision to the World Health Organization classification of myeloid neoplasms and acute leukemia. *Blood* 127, 2391–2405. <https://doi.org/10.1182/blood-2016-03-643544>.
- Vardiman, J.W., Thiele, J., Arber, D.A., Brunning, R.D., Borowitz, M.J., Porwit, A., Harris, N.L., Le Beau, M.M., Hellström-Lindberg, E., Tefferi, A., and Bloomfield, C.D. (2009). The 2008 revision of the World Health Organization (WHO) classification of myeloid neoplasms and acute leukemia: rationale and important changes. *Blood* 114, 937–951. <https://doi.org/10.1182/blood-2009-03-209262>.
- Patnaik, M.M., Padron, E., LaBorde, R.R., Lasho, T.L., Finke, C.M., Hanson, C.A., Hodnefield, J.M., Knudson, R.A., Ketterling, R.P., Al-kali, A., et al. (2013). Mayo prognostic model for whom-defined chronic myelomonocytic leukemia: ASXL1 and spliceosome component mutations and outcomes. *Leukemia* 27, 1504–1510. <https://doi.org/10.1038/leu.2013.88>.
- Onida, F., Kantarjian, H.M., Smith, T.L., Ball, G., Keating, M.J., Estey, E.H., Glassman, A.B., Albitar, M., Kwari, M.I., and Beran, M. (2002). Prognostic factors and scoring systems in chronic myelomonocytic leukemia: a retrospective analysis of 213 patients. *Blood* 99, 840–849.
- Patnaik, M.M., Itzykson, R., Lasho, T.L., Kosmider, O., Finke, C.M., Hanson, C.A., Knudson, R.A., Ketterling, R.P., Tefferi, A., and Solary, E. (2014). ASXL1 and SETBP1 mutations and their prognostic contribution in chronic myelomonocytic leukemia: a two-center study of 466 patients. *Leukemia* 28, 2206–2212. <https://doi.org/10.1038/leu.2014.125>.
- Pleyer, L., Leisch, M., Kourakli, A., Padron, E., Maciejewski, J.P., Xicoy Cirici, B., Kaivers, J., Ungerstedt, J., Heibl, S., Patiou, P., et al. (2021). Outcomes of patients with chronic myelomonocytic leukaemia treated with non-curative therapies: a retrospective cohort study. *Lancet. Haematol.* 8, e135–e148. [https://doi.org/10.1016/S2352-3026\(20\)30374-4](https://doi.org/10.1016/S2352-3026(20)30374-4).
- Alfonso, A., Montalban-Bravo, G., Takahashi, K., Jabbour, E.J., Kadia, T., Ravandi, F., Cortes, J., Estrov, Z., Borthakur, G., Pemmaraju, N., et al. (2017). Natural history of chronic myelomonocytic leukemia treated with hypomethylating agents. *Am. J. Hematol.* 92, 599–606. <https://doi.org/10.1002/ajh.24735>.
- Montalban-Bravo, G., Kanagal-Shamanna, R., Li, Z., Hammond, D., Chien, K., Rodriguez-Sevilla, J.J., Sasaki, K., Jabbour, E., DiNardo, C., Takahashi, K., et al. (2023). Phenotypic subtypes of leukaemic transformation in chronic myelomonocytic leukaemia. *Br. J. Haematol.* 203, 581–592. <https://doi.org/10.1111/bjh.19060>.
- Itzykson, R., Kosmider, O., Renneville, A., Gelsi-Boyer, V., Meggendorfer, M., Morabito, M., Berthon, C., Adès, L., Fenaux, P., Beyne-Rauzy, O., et al. (2013). Prognostic score including gene mutations in chronic myelomonocytic leukemia. *J. Clin. Oncol.* 31, 2428–2436. <https://doi.org/10.1200/JCO.2012.47.3314>.
- Montalban-Bravo, G., Hammond, D., DiNardo, C.D., Konopleva, M., Borthakur, G., Short, N.J., Ramos-Perez, J., Guerra, V., Kanagal-Shamanna, R., Naqvi, K., et al. (2021). Activity of venetoclax-based therapy in chronic myelomonocytic leukemia. *Leukemia* 35, 1494–1499. <https://doi.org/10.1038/s41375-021-01240-2>.
- Paul, F., Arkin, Y., Giladi, A., Jaitin, D.A., Kenigsberg, E., Keren-Shaul, H., Winter, D., Lara-Astiaso, D., Gur, M., Weiner, A., et al. (2015). Transcriptional Heterogeneity and Lineage Commitment in Myeloid Progenitors. *Cell* 163, 1663–1677. <https://doi.org/10.1016/j.cell.2015.11.013>.
- Giladi, A., Paul, F., Herzog, Y., Lubling, Y., Weiner, A., Yofe, I., Jaitin, D., Cabezas-Wallscheid, N., Dress, R., Ginhoux, F., et al. (2018). Single-cell characterization of haematopoietic progenitors and their trajectories in homeostasis and perturbed haematopoiesis. *Nat. Cell Biol.* 20, 836–846. <https://doi.org/10.1038/s41556-018-0121-4>.
- Lian, Q., Xin, H., Ma, J., Konnikova, L., Chen, W., Gu, J., and Chen, K. (2020). Artificial-cell-type aware cell-type classification in CITE-seq. *Bioinformatics* 36, i542–i550. <https://doi.org/10.1093/bioinformatics/btaa467>.
- Zhou, Z., Ye, C., Wang, J., and Zhang, N.R. (2020). Surface protein imputation from single cell transcriptomes by deep neural networks. *Nat. Commun.* 11, 651. <https://doi.org/10.1038/s41467-020-14391-0>.
- Hamarsheh, S., Groß, O., Brummer, T., and Zeiser, R. (2020). Immune modulatory effects of oncogenic KRAS in cancer. *Nat. Commun.* 11, 5439. <https://doi.org/10.1038/s41467-020-19288-6>.
- Efremova, M., Vento-Tormo, M., Teichmann, S.A., and Vento-Tormo, R. (2020). CellPhoneDB: inferring cell-cell communication from combined expression of multi-subunit ligand-receptor complexes. *Nat. Protoc.* 15, 1484–1506. <https://doi.org/10.1038/s41596-020-0292-x>.

18. Chenette, E.J. (2009). Cancer: A Ras and NF-kappaB pas de deux. *Nat. Rev. Drug Discov.* 8, 932. <https://doi.org/10.1038/nrd3060>.
19. Datta, J., Bianchi, A., De Castro Silva, I., Deshpande, N.U., Cao, L.L., Mehra, S., Singh, S., Rafie, C., Sun, X., Chen, X., et al. (2022). Distinct mechanisms of innate and adaptive immune regulation underlie poor oncologic outcomes associated with KRAS-TP53 co-alteration in pancreatic cancer. *Oncogene* 41, 3640–3654. <https://doi.org/10.1038/s41388-022-02368-w>.
20. Daniluk, J., Liu, Y., Deng, D., Chu, J., Huang, H., Gaiser, S., Cruz-Monserrate, Z., Wang, H., Ji, B., and Logsdon, C.D. (2012). An NF-kappaB pathway-mediated positive feedback loop amplifies Ras activity to pathological levels in mice. *J. Clin. Invest.* 122, 1519–1528. <https://doi.org/10.1172/JCI59743>.
21. Hamarsheh, S., Osswald, L., Saller, B.S., Unger, S., De Feo, D., Vinnakota, J.M., Konantz, M., Uhl, F.M., Becker, H., Lübbert, M., et al. (2020). Oncogenic Kras(G12D) causes myeloproliferation via NLRP3 inflammasome activation. *Nat. Commun.* 11, 1659. <https://doi.org/10.1038/s41467-020-15497-1>.
22. Morandi, F., Airolidi, I., and Pistoia, V. (2014). IL-27 driven upregulation of surface HLA-E expression on monocytes inhibits IFN-gamma release by autologous NK cells. *J. Immunol. Res.* 2014, 938561. <https://doi.org/10.1155/2014/938561>.
23. Pereira, B.I., Devine, O.P., Vukmanovic-Stejic, M., Chambers, E.S., Subramanian, P., Patel, N., Virasami, A., Sebire, N.J., Kinsler, V., Valdovinos, A., et al. (2019). Senescent cells evade immune clearance via HLA-E-mediated NK and CD8(+) T cell inhibition. *Nat. Commun.* 10, 2387. <https://doi.org/10.1038/s41467-019-10335-5>.
24. Ramsuran, V., Naranbhai, V., Horowitz, A., Qi, Y., Martin, M.P., Yuki, Y., Gao, X., Walker-Sperling, V., Del Prete, G.Q., Schneider, D.K., et al. (2018). Elevated HLA-A expression impairs HIV control through inhibition of NKG2A-expressing cells. *Science* 359, 86–90. <https://doi.org/10.1126/science.aam8825>.
25. Banh, C., Fugère, C., and Brossay, L. (2009). Immunoregulatory functions of KLRG1 cadherin interactions are dependent on forward and reverse signaling. *Blood* 114, 5299–5306. <https://doi.org/10.1182/blood-2009-06-228353>.
26. Lou, C., Wu, K., Shi, J., Dai, Z., and Xu, Q. (2022). N-cadherin protects oral cancer cells from NK cell killing in the circulation by inducing NK cell functional exhaustion via the KLRG1 receptor. *J. Immunother. Cancer* 10, e005061. <https://doi.org/10.1136/jitc-2022-005061>.
27. Yang, R., Sun, L., Li, C.F., Wang, Y.H., Yao, J., Li, H., Yan, M., Chang, W.C., Hsu, J.M., Cha, J.H., et al. (2021). Galectin-9 interacts with PD-1 and TIM-3 to regulate T cell death and is a target for cancer immunotherapy. *Nat. Commun.* 12, 832. <https://doi.org/10.1038/s41467-021-21099-2>.
28. Slattery, K., Woods, E., Zaiatz-Bittencourt, V., Marks, S., Chew, S., Conroy, M., Goggins, C., MacEochagain, C., Kennedy, J., Lucas, S., et al. (2021). TGFbeta drives NK cell metabolic dysfunction in human metastatic breast cancer. *J. Immunother. Cancer* 9, e002044. <https://doi.org/10.1136/jitc-2020-002044>.
29. Chakravarthy, A., Khan, L., Bensler, N.P., Bose, P., and De Carvalho, D.D. (2018). TGF-beta-associated extracellular matrix genes link cancer-associated fibroblasts to immune evasion and immunotherapy failure. *Nat. Commun.* 9, 4692. <https://doi.org/10.1038/s41467-018-06654-8>.
30. Yu, L., Liu, X., Wang, X., Yan, F., Wang, P., Jiang, Y., Du, J., and Yang, Z. (2021). TIGIT(+) TIM-3(+) NK cells are correlated with NK cell exhaustion and disease progression in patients with hepatitis B virus-related hepatocellular carcinoma. *Oncolimmunology* 10, 1942673. <https://doi.org/10.1080/2162402X.2021.1942673>.
31. Juno, J.A., Stalker, A.T., Waruk, J.L., Oyugi, J., Kimani, M., Plummer, F.A., Kimani, J., and Fowke, K.R. (2015). Elevated expression of LAG-3, but not PD-1, is associated with impaired iNKT cytokine production during chronic HIV-1 infection and treatment. *Retrovirology* 12, 17. <https://doi.org/10.1186/s12977-015-0142-z>.
32. Chan, I.S., Knutsdottir, H., Ramakrishnan, G., Padmanaban, V., Warriar, M., Ramirez, J.C., Dunworth, M., Zhang, H., Jaffee, E.M., Bader, J.S., and Ewald, A.J. (2020). Cancer cells educate natural killer cells to a metastasis-promoting cell state. *J. Cell Biol.* 219. <https://doi.org/10.1083/jcb.202001134>.
33. Corces, M.R., Buenrostro, J.D., Wu, B., Greenside, P.G., Chan, S.M., Koenig, J.L., Snyder, M.P., Pritchard, J.K., Kundaje, A., Greenleaf, W.J., et al. (2016). Lineage-specific and single-cell chromatin accessibility charts human hematopoiesis and leukemia evolution. *Nat. Genet.* 48, 1193–1203. <https://doi.org/10.1038/ng.3646>.
34. Caenepeel, S., Brown, S.P., Belmontes, B., Moody, G., Keegan, K.S., Chui, D., Whittington, D.A., Huang, X., Poppe, L., Cheng, A.C., et al. (2018). AMG 176, a Selective MCL1 Inhibitor, Is Effective in Hematologic Cancer Models Alone and in Combination with Established Therapies. *Cancer Discov.* 8, 1582–1597. <https://doi.org/10.1158/2159-8290.CD-18-0387>.
35. Awada, H., Nagata, Y., Goyal, A., Asad, M.F., Patel, B., Hirsch, C.M., Kuzmanovic, T., Guan, Y., Przychodzen, B.P., Aly, M., et al. (2019). Invariant phenotype and molecular association of biallelic TET2 mutant myeloid neoplasia. *Blood Adv.* 3, 339–349. <https://doi.org/10.1182/bloodadvances.2018024216>.
36. Carr, R.M., Vorobyev, D., Lasho, T., Marks, D.L., Tolosa, E.J., Vedder, A., Almada, L.L., Yurchenko, A., Padiou, I., Alver, B., et al. (2021). RAS mutations drive proliferative chronic myelomonocytic leukemia via a KMT2A-PLK1 axis. *Nat. Commun.* 12, 2901. <https://doi.org/10.1038/s41467-021-23186-w>.
37. Zhang, Y., He, L., Selimoglu-Buet, D., Jegu, C., Morabito, M., Willekens, C., Diop, M.K., Gonin, P., Lapiere, V., Droin, N., et al. (2017). Engraftment of chronic myelomonocytic leukemia cells in immunocompromised mice supports disease dependency on cytokines. *Blood Adv.* 1, 972–979. <https://doi.org/10.1182/bloodadvances.2017004903>.
38. Patel, B.J., Przychodzen, B., Thota, S., Radivoyevitch, T., Visconte, V., Kuzmanovic, T., Clemente, M., Hirsch, C., Morawski, A., Souaid, R., et al. (2017). Genomic determinants of chronic myelomonocytic leukemia. *Leukemia* 31, 2815–2823. <https://doi.org/10.1038/leu.2017.164>.
39. Montalban-Bravo, G., Hammond, D., DiNardo, C.D., Konopleva, M., Borthakur, G., Short, N.J., Ramos-Perez, J., Guerra, V., Kanagal-Shamanna, R., Naqvi, K., et al. (2021). Activity of venetoclax-based therapy in chronic myelomonocytic leukemia. *Leukemia* 35, 1494–1499. <https://doi.org/10.1038/s41375-021-01240-2>.
40. Reggiardo, R.E., Maroli, S.V., Halasz, H., Ozen, M., Hrabeta-Robinson, E., Behera, A., Peddu, V., Carrillo, D., LaMontagne, E., Whitehead, L., et al. (2022). Mutant KRAS regulates transposable element RNA and innate immunity via KRAB zinc-finger genes. *Cell Rep.* 40, 111104. <https://doi.org/10.1016/j.celrep.2022.111104>.
41. Ferrall-Fairbanks, M.C., Dhawan, A., Johnson, B., Newman, H., Volpe, V., Letson, C., Ball, M., Hunter, A.M., Balasis, M.E., Kruer, T., et al. (2022). Progenitor Hierarchy of Chronic Myelomonocytic Leukemia Identifies Inflammatory Monocytic-Biased Trajectory Linked to Worse Outcomes. *Blood Cancer Discov.* 3, 536–553. <https://doi.org/10.1158/2643-3230.BCD-21-0217>.
42. Chen, X., Eksioğlu, E.A., Zhou, J., Zhang, L., Djou, J., Fortenberry, N., Epling-Burnette, P., Van Bijnen, S., Dolstra, H., Cannon, J., et al. (2013). Induction of myelodysplasia by myeloid-derived suppressor cells. *J. Clin. Invest.* 123, 4595–4611. <https://doi.org/10.1172/JCI67580>.
43. Garcia-Manero, G., Winer, E.S., DeAngelo, D.J., Tarantolo, S.R., Sallman, D.A., Dugan, J., Groepper, S., Giagounidis, A., Gotze, K.S., Metzler, K., et al. (2022). Phase 1/2a study of the IRAK4 inhibitor CA-4948 as monotherapy or in combination with azacitidine or venetoclax in patients with relapsed/refractory (R/R) acute myeloid leukemia or myelodysplastic syndrome. *J. Clin. Oncol.* 40, 7016. https://doi.org/10.1200/JCO.2022.40.16_suppl.7016.
44. Hunter, A.M., Newman, H., Dezern, A.E., Steensma, D.P., Niyongere, S., Roboz, G.J., Mo, Q., Chan, O., Gerds, A., Sallman, D.A., et al. (2021).

- Integrated Human and Murine Clinical Study Establishes Clinical Efficacy of Ruxolitinib in Chronic Myelomonocytic Leukemia. *Clin. Cancer Res.* 27, 6095–6105. <https://doi.org/10.1158/1078-0432.CCR-21-0935>.
45. Walker, A.R., Byrd, J.C., Blachly, J.S., Bhatnagar, B., Mims, A.S., Orwick, S., Lin, T.L., Crosswell, H.E., Zhang, D., Minden, M.D., et al. (2020). Entospletinib in Combination with Induction Chemotherapy in Previously Untreated Acute Myeloid Leukemia: Response and Predictive Significance of HOXA9 and MEIS1 Expression. *Clin. Cancer Res.* 26, 5852–5859. <https://doi.org/10.1158/1078-0432.CCR-20-1064>.
46. Ganan-Gomez, I., Yang, H., Ma, F., Montalban-Bravo, G., Thongon, N., Marchica, V., Richard-Carpentier, G., Chien, K., Manyam, G., Wang, F., et al. (2022). Stem cell architecture drives myelodysplastic syndrome progression and predicts response to venetoclax-based therapy. *Nat. Med.* 28, 557–567. <https://doi.org/10.1038/s41591-022-01696-4>.
47. Tago, K., Funakoshi-Tago, M., Ohta, S., Kawata, H., Saitoh, H., Horie, H., Aoki-Ohmura, C., Yamauchi, J., Tanaka, A., Matsugi, J., and Yanagisawa, K. (2019). Oncogenic Ras mutant causes the hyperactivation of NF-kappaB via acceleration of its transcriptional activation. *Mol. Oncol.* 13, 2493–2510. <https://doi.org/10.1002/1878-0261.12580>.
48. Sevin, M., Debeurme, F., Laplane, L., Badel, S., Morabito, M., Newman, H.L., Torres-Martin, M., Yang, Q., Badaoui, B., Wagner-Ballon, O., et al. (2021). Cytokine-like protein 1-induced survival of monocytes suggests a combined strategy targeting MCL1 and MAPK in CMMML. *Blood* 137, 3390–3402. <https://doi.org/10.1182/blood.2020008729>.
49. Pei, S., Pollyea, D.A., Gustafson, A., Stevens, B.M., Minhajuddin, M., Fu, R., Riemondy, K.A., Gillen, A.E., Sheridan, R.M., Kim, J., et al. (2020). Monocytic Subclones Confer Resistance to Venetoclax-Based Therapy in Patients with Acute Myeloid Leukemia. *Cancer Discov.* 10, 536–551. <https://doi.org/10.1158/2159-8290.CD-19-0710>.
50. Hao, Y., Hao, S., Andersen-Nissen, E., Mauck, W.M., 3rd, Zheng, S., Butler, A., Lee, M.J., Wilk, A.J., Darby, C., Zager, M., et al. (2021). Integrated analysis of multimodal single-cell data. *Cell* 184, 3573–3587.e29. <https://doi.org/10.1016/j.cell.2021.04.048>.
51. Vento-Tormo, R., Efremova, M., Botting, R.A., Turco, M.Y., Vento-Tormo, M., Meyer, K.B., Park, J.-E., Stephenson, E., Polanski, K., Goncalves, A., et al. (2018). Single-cell reconstruction of the early maternal–fetal interface in humans. *Nature* 563, 347–353. <https://doi.org/10.1038/s41586-018-0698-6>.
52. Kanagal-Shamanna, R., Singh, R.R., Routbort, M.J., Patel, K.P., Medeiros, L.J., and Luthra, R. (2016). Principles of analytical validation of next-generation sequencing based mutational analysis for hematologic neoplasms in a CLIA-certified laboratory. *Expert Rev. Mol. Diagn.* 16, 461–472. <https://doi.org/10.1586/14737159.2016.1142374>.
53. DeLong, E.R., DeLong, D.M., and Clarke-Pearson, D.L. (1988). Comparing the areas under two or more correlated receiver operating characteristic curves: a nonparametric approach. *Biometrics* 44, 837–845.
54. Cheson, B.D., Bennett, J.M., Kopecky, K.J., Büchner, T., Willman, C.L., Estey, E.H., Schiffer, C.A., Doehner, H., Tallman, M.S., Lister, T.A., et al. (2003). Revised recommendations of the International Working Group for Diagnosis, Standardization of Response Criteria, Treatment Outcomes, and Reporting Standards for Therapeutic Trials in Acute Myeloid Leukemia. *J. Clin. Oncol.* 21, 4642–4649. <https://doi.org/10.1200/JCO.2003.04.036>.
55. Cheson, B.D., Greenberg, P.L., Bennett, J.M., Lowenberg, B., Wijermans, P.W., Nimer, S.D., Pinto, A., Beran, M., de Witte, T.M., Stone, R.M., et al. (2006). Clinical application and proposal for modification of the International Working Group (IWG) response criteria in myelodysplasia. *Blood* 108, 419–425. <https://doi.org/10.1182/blood-2005-10-4149>.
56. Woll, P.S., Kjällquist, U., Chowdhury, O., Doolittle, H., Wedge, D.C., Thongjuea, S., Erlandsson, R., Ngara, M., Anderson, K., Deng, Q., et al. (2014). Myelodysplastic syndromes are propagated by rare and distinct human cancer stem cells in vivo. *Cancer Cell* 25, 794–808. <https://doi.org/10.1016/j.ccr.2014.03.036>.
57. Will, B., Zhou, L., Vogler, T.O., Ben-Neriah, S., Schinke, C., Tamari, R., Yu, Y., Bhagat, T.D., Bhattacharyya, S., Barreiro, L., et al. (2012). Stem and progenitor cells in myelodysplastic syndromes show aberrant stage-specific expansion and harbor genetic and epigenetic alterations. *Blood* 120, 2076–2086. <https://doi.org/10.1182/blood-2011-12-399683>.
58. Adema, V., Ma, F., Kanagal-Shamanna, R., Thongon, N., Montalban-Bravo, G., Yang, H., Peslak, S.A., Wang, F., Acha, P., Sole, F., et al. (2022). Targeting the EIF2AK1 signaling pathway rescues red blood cell production in SF3B1-mutant myelodysplastic syndromes with ringed sideroblasts. *Blood Cancer Discov.* 3, 554–567. <https://doi.org/10.1158/2643-3230.BCD-21-0220>.
59. Zhou, Y., Zhou, B., Pache, L., Chang, M., Khodabakhshi, A.H., Tanaseichuk, O., Benner, C., and Chanda, S.K. (2019). Metascape provides a biologist-oriented resource for the analysis of systems-level datasets. *Nat. Commun.* 10, 1523. <https://doi.org/10.1038/s41467-019-09234-6>.
60. Thongon, N., Ma, F., Santoni, A., Marchesini, M., Fiorini, E., Rose, A., Adema, V., Ganan-Gomez, I., Groarke, E.M., Gutierrez-Rodriguez, F., et al. (2021). Hematopoiesis under telomere attrition at the single-cell resolution. *Nat. Commun.* 12, 6850. <https://doi.org/10.1038/s41467-021-27206-7>.
61. Buenrostro, J.D., Corces, M.R., Lareau, C.A., Wu, B., Schep, A.N., Aryee, M.J., Majeti, R., Chang, H.Y., and Greenleaf, W.J. (2018). Integrated Single-Cell Analysis Maps the Continuous Regulatory Landscape of Human Hematopoietic Differentiation. *Cell* 173, 1535–1548.e16. <https://doi.org/10.1016/j.cell.2018.03.074>.
62. Morita, K., Wang, F., Jahn, K., Hu, T., Tanaka, T., Sasaki, Y., Kuipers, J., Loghavi, S., Wang, S.A., Yan, Y., et al. (2020). Clonal evolution of acute myeloid leukemia revealed by high-throughput single-cell genomics. *Nat. Commun.* 11, 5327. <https://doi.org/10.1038/s41467-020-19119-8>.

STAR★METHODS

KEY RESOURCES TABLE

REAGENT or RESOURCE	SOURCE	IDENTIFIER
Antibodies		
Anti-human CD2	BD Biosciences	Cat#: 555326; RRID: AB_395733
Anti-human CD3	BD Biosciences	Cat#: 349201; RRID: AB_400405
Anti-human CD4	ThermoFisher	Cat#: MHCD0401; RRID:AB_10392546
Anti-human CD7	BioLegend	Cat#: 343104; RRID: AB_1659216
Anti-human CD11b	ThermoFisher	Cat#: 11-0118-42; RRID: AB_1582242
anti-human CD14	BD Biosciences	Cat#: 347493; RRID: AB_400311
Anti-human CD19	BD Biosciences	Cat#: 340409; RRID: AB_400024
Anti-human CD20	BD Biosciences	Cat#: 555622; RRID: AB_395988
Anti-human CD33	ThermoFisher	Cat#: 11-0337-42; RRID: AB_1603221
Anti-human CD56	BD Biosciences	Cat#: 562794; RRID: AB_2737799
Anti-human CD235	BD Biosciences	Cat#: 559943; RRID: AB_397386
Anti-human CD34	BD Biosciences	Cat#: 562577; RRID: AB_2687922
Anti-human CD38	BioLegend	Cat#: 303534; RRID: AB_2561605
Anti-human CD3	BioLegend	Cat#: 317339; RRID: AB_2563407
Anti-human CD4	BioLegend	Cat#: 300502; RRID: AB_314070
Anti-human CD8	BioLegend	Cat#: 344710; RRID: AB_2044010
Anti-human CD56	BioLegend	Cat#: 362544; RRID: AB_2565922
Anti-human CD16	BioLegend	Cat#: 302028; RRID: AB_893262
Anti-Human IFN- γ	BD Biosciences	Cat#: 554702; RRID: AB_398580
Anti-human Perforin	BioLegend	Cat#: 308130; RRID: AB_2687190
Zombie UV	BioLegend	Cat#: 423107
Protein Transport Inhibitor Cocktail	eBioscience	Cat#: 00-4980-93
Fc Receptor Binding Inhibitor Polyclonal Antibody	ThermoFisher	Cat#: 14-9161-73
CD3e	Cell Signaling Technology	Cat#: 85061BF; RRID: AB_2721019
CD4	Abcam	Cat#: ab133616; RRID: AB_2750883
CD8	Thermo Scientific	Catalog#: MA5-13473; RRID: AB_11000353
CD14	Abcam	Cat#: ab183322; RRID: AB_2909463
CD68, Clone PG-M1	Dako	Cat#: M0876; RRID: AB_2074844
CD56	Dako	Cat#: M7304; RRID: AB_2750583
DAPI	Akoya Biosciences	Cat#: FP1490; RRID: N/A
MCL1	Cell Signaling Technology	Cat#: 4572; RRID:AB_2281980
Vinculin	Sigma-Aldrich	Cat#: V9131; RRID:AB_477629
Biological samples		
Bone marrow aspirates from healthy donors	AllCells (Alameda, CA) and MD Anderson's Department of Stem Cell Transplantation	N/A
Bone marrow aspirates from CMML patients	MD Anderson Bank	N/A
Human bone marrow-derived mesenchymal stem cells	Cells provided by Dr. M. Andreeff	N/A
Chemicals, peptides, and recombinant proteins		
AMG-176	Med Chem Express	Cat#: HY-101565

(Continued on next page)

Continued

REAGENT or RESOURCE	SOURCE	IDENTIFIER
Critical commercial assays		
Cytofix/Cytoperm kit	BD Biosciences	Cat#: 554714
Deposited data		
scRNA-seq data	This paper	GEO: GSE218390
scATAC-seq data	This paper	GEO: GSE218390
scDNA-seq data	This paper	GEO: GSE218390
Experimental models: Cell lines		
K562 cells	ATCC	ATCC CCL243
Software and algorithms		
SPSS 23.0	SPSS, Inc	https://www.ibm.com/products/spss-statistics
R v4.1.2	R Core Team	https://www.r-project.org
Seurat v4 R package	Hao et al. ⁵⁰	https://github.com/satijalab/seurat
CellphoneDB	Vento-Tormo et al. ⁵¹	https://www.cellphonedb.org/
GraphPad Prism version 10.0	GraphPad software	https://www.graphpad.com/
Spotfire	TIBCO	N/A
FlowJo	BD Biosciences	https://www.flowjo.com/
GSEA	Metascape	https://metascape.org/
Spotfire	TIBCO	https://www.spotfire.com/
Other		
Ficoll-Paque PLUS	ThermoFisher	Cat#:45-001-752
CD34 Microbead Kit	Miltenyi Biotec	Cat#:130-046-702
NK Cell Isolation Kit	Miltenyi Biotec	Cat#: 130-092-657
Opal 9 Kit	Akoya Biosciences	Cat#: NEL797001KT
Qubit	Thermo Fisher Scientific	N/A

RESOURCE AVAILABILITY

Lead contact

Further information and requests for resources and reagents should be directed to and will be fulfilled by the lead contact, Simona Colla (scolla@mdanderson.org).

Materials availability

This study did not generate new unique reagents.

Data and code availability

- scRNA-seq, scATAC-seq, and scDNA-seq data are accessible at GEO under accession number GSE218390. No custom computer codes were generated in this study.
- The [lead contact](#) can provide any additional information required to reanalyze the data reported in this work paper upon request.

EXPERIMENTAL MODEL AND STUDY PARTICIPANT DETAILS

Primary human samples

BM aspirates were obtained from patients with CMML who were seen in the Department of Leukemia at the University of Texas MD Anderson Cancer Center. Samples were obtained with the approval of the Institutional Review Board and in accordance with the Declaration of Helsinki. CMML diagnoses were assigned according to the World Health Organization criteria.³

RAS pathway mutations were identified by targeted amplicon-based next-generation sequencing (NSG).⁵² Genomic DNA was extracted from whole BM aspirate samples and was subject to targeted PCR-based sequencing using an NGS platform evaluating a total of 81 genes, as previously described.⁵² This analysis was performed within the MDACC CLIA-certified Molecular Diagnostics Laboratory after informed consent (additional details in [supplemental information](#)). For NGS-based analysis, the limit of detection for

variant calling was 2%. Previously described somatic mutations registered at the Catalog of Somatic Mutations in Cancer (COSMIC; <http://cancer.sanger.ac.uk/cosmic>) were considered potential driver mutations.

All available samples carrying *RAS* pathway mutations were included in the study. Baseline BM aspirates were collected from patients before any treatment. Sequential BM samples were collected after HMA or venetoclax therapy failure. The clinical characteristics of the patients with *RAS* pathway mutated CMML are shown in Tables S1 and S3. BM samples from HDs were obtained from AllCells (Alameda, CA) and the Department of Stem Cell Transplantation at MD Anderson Cancer Center. Written informed consent was obtained from all donors.

MNCs were collected from each BM sample immediately after BM aspiration using the standard gradient separation approach with Ficoll-Paque PLUS (catalog number #45-001-752, Thermo Fisher Scientific). MNCs were cryopreserved and stored in liquid nitrogen until they were used. For cell sorting applications, MNCs were enriched in CD34⁺ cells using magnetic-activated cell sorting (MACS) with the CD34 Microbead Kit (catalog number #130-046-702, Miltenyi Biotec, Germany) and further purified by fluorescence-activated cell sorting (FACS) as described below.

METHOD DETAILS

Clinical data analysis

A clinical dataset of 108 CMML patients treated with HMA therapy at the Department of Leukemia at the University of Texas MD Anderson Cancer Center was evaluated to identify predictors of therapy outcomes. HMA therapy failure was defined as a lack of response (based on IWG 2006 criteria) after at least 4 cycles of therapy or as relapse or progression after any number of cycles of therapy. Blast progression (BP) was defined as 1) the presence of >5% blasts in the BM at the time of primary HMA failure in patients with <5% blasts at baseline or an increase of at least 50% blasts in patients with 5–9% blasts at baseline; 2) BM blasts >20% or myeloid sarcoma regardless of primary or secondary failure; 3) BM blasts >5% at the time of secondary HMA failure (relapse or progression). Associations between gene mutations and BP were assessed using data from 108 patients whose samples were sequenced using the 81-gene panel; these analyses were performed at MD Anderson Cancer Center. Clinical datasets were analyzed using the SPSS 23.0 (SPSS, Inc., Chicago, IL, USA) and R (version 3.5.1) statistical software programs. Logistical regression analysis was performed using clinical, cytogenetic, and molecular characteristics in correlation with responses to HMA therapy. The dataset was randomly divided into a training set (30 patients with BP) and a testing set (5 patients with BP). A combination rule derived from selected features was trained using logistic regression in the training set and a fixed model in the testing set. Receiver operating characteristic (ROC) curves were generated using the “pROC” package in R (version 3.6.0). The 95% CIs for the areas under the ROC curves were estimated using the DeLong method.⁵³ The chi-square or Fisher exact test was used to analyze differences between categorical variables. Survival curves were generated using the Kaplan-Meier method and compared using log rank tests. Responses to HMA- or venetoclax-based therapies were evaluated based on the International Working group 2003⁵⁴ and 2006⁵⁵ criteria for patients with secondary AML or CMML, respectively.

Flow cytometry analysis and fluorescence-activated cell sorting (FACS)

Quantitative flow cytometry and FACS analyses of Lin[−]CD34⁺ cells were performed using previously described staining protocols^{56,57} and antibodies against CD2, FITC, RPA-2.10, BD Biosciences, 555326; CD3, FITC, SK7, BD Biosciences, 349201; CD4, FITC, S3.5, Thermo Fisher, MHCD0401; CD7, FITC, 6B7, BioLegend, 343104; CD11b, FITC, ICRF44, Thermo Fisher, 11-0118-42; CD14, FITC, MφP9, BD Biosciences, 347493; CD19, FITC, SJ25C1, BD Biosciences, 340409; CD20, FITC, 2H7, BD Biosciences, 555622; CD33, FITC, P67.6, Thermo Fisher, 11-0337-42; CD56, FITC, B159, BD Biosciences, 562794; CD235a, FITC, HIR2, BD Biosciences, 559943; CD34, BV421, 581, BD Biosciences, 562577; CD38, APC, HIT2, BioLegend, 303534, as we described previously.⁵⁸

Samples used for flow cytometry and FACS were acquired with a BD LSR Fortessa and a BD Influx Cell Sorter (BD Biosciences), respectively. The cell populations were analyzed using FlowJo software (<https://www.flowjo.com>). All experiments included single-stained controls and were performed at the South Campus Flow Cytometry & Cellular Imaging Facility at MD Anderson Cancer Center.

Multiplex imaging assay

BM core biopsies were used for multiplex immunofluorescence assessment. We optimized and validated a multiplex immunofluorescence panel using antibodies against CD3e, CD4, CD8, CD14, CD56, and CD68. Each antibody was assessed by multiplex immunofluorescence using the Opal 9 kit (catalog #NEL797001KT; Akoya Biosciences, Marlborough, MA), according to the following clones and dilutions: CD3e (clone D7A6E(AM), Cell Signaling Technology, 1:100), CD4 (clone EPR6855, Abcam, 1:200), CD8 (clone C8/144B, Thermo Scientific, 1:25), CD14 (clone SP192, Abcam, 1:100), CD56 (clone 123C3, Dako, 1:25), and CD68 (clone PG-M1, Dako, 1:50). The slides were imaged using the Vectra Polaris spectral imaging system (Akoya Biosciences, Marlborough, MA) using the fluorescence protocol at 10 nm λ from 420 nm to 720 nm. Both germinal center and interfollicular areas from lymph nodes with reactive lymphoid hyperplasia were used as positive controls. Each marker was analyzed at the single-cell level, and a supervised algorithm for phenotyping was built for each marker. Cell density for each marker and combinations of phenotypes were consolidated using Spotfire software (TIBCO Spotfire). The nearest neighbor analysis was performed using R version 4.2.1.

Western blot

BM CD34⁺ cells were enriched from BM MNCs using magnetic sorting with the CD34 Microbead Kit (Miltenyi Biotec). Cells were re-suspended in Mammalian Cell & Tissue Extraction Kit buffer (BioVision Incorporated) and incubated on ice for 10 min. Lysates were then collected after centrifugation at 12,000 rpm at 4°C for 20 min. The amount of protein was quantified using the Qubit Protein Assay Kit and a Qubit Fluorometer (Thermo Fisher Scientific). SDS-PAGE and Western blotting were performed following standard protocols. Blotted membranes were incubated with primary monoclonal antibodies against human MCL1 (#4572S; 1:750 dilution; Cell Signaling Technology) and vinculin (hVIN-1; 1:2,000 dilution; Sigma-Aldrich). Membranes were developed using the SuperSignal West Pico PLUS Chemiluminescent Substrate (Thermo Fisher Scientific) in a KwikQuant Imager (Kindle Biosciences). Vinculin was used as a loading control, and lysates from the myeloma cell line JJN3 were used as positive controls.

T cell and NK cell cytokine secretion assays

NK cells were isolated from BM MNCs obtained from HDs, and RAS pathway mutant or wild-type CMML patients by negative magnetic selection using the NK Cell Isolation Kit (Miltenyi Biotec). NK cells or BM MNCs were mixed with the human erythroleukemia cell line K562 at a target-to-effector ratio of 1:1. Cells were incubated for 4 h at 37°C in 5% CO₂ in the presence of a protein transport inhibitor cocktail (eBioscience 00-4980-93) for 4 h. After incubation, cells were harvested, washed with PBS, and stained with the viability dye Zombie UV. Cells were washed with PBS and resuspended in the presence of an Fc receptor-binding inhibitor antibody (ThermoFisher) for 20 min. NK cells and BM MNCs were stained with antibodies against CD3 (AF700, BioLegend). NK cells were further stained with antibodies against CD56 (PE-Dazle 594) and CD16 (PerCP-Cy5.5), whereas BM MNCs were stained with antibodies against CD4 (PE-Dazzle 594) and CD8 (PerCP-Cy5.5). Cells were then washed, fixed, and permeabilized using the Cytofix/Cytoperm kit (BD Biosciences) and intracellularly stained with antibodies against IFN- γ (APC, BD Biosciences) and perforin (BV711, BioLegend). Samples were acquired with a BD Fortessa (BD Biosciences), and cell populations were analyzed using FlowJo software (version 10.7.1, Ashland, OR).

scRNA-seq analysis and bioinformatic pipeline

ScRNA-seq analysis was performed as we described previously.⁵⁸ Live Lin[−]CD34⁺ cells and live MNCs were isolated by FACS. Sample preparation and sequencing were performed at the Advanced Technology Genomics Core at MD Anderson Cancer Center. Sample concentration and cell suspension viability were evaluated using a Countess II FL Automated Cell Counter (Thermo Fisher Scientific). Samples were normalized for input onto the Chromium Single Cell A Chip Kit (10X Genomics), and single cells were lysed and barcoded for reverse transcription. Equal amounts of each uniquely indexed sample library were pooled together. Pooled libraries were sequenced using a NovaSeq6000 SP 100-cycle flow cell (Illumina). After sequencing, raw reads were aligned to the human genome (hg38), and the digital expression matrix was generated using cellranger count. Individual samples were merged to generate the digital expression matrix using cellranger aggr. The Seurat package in R was used to analyze the digital expression matrix. Cells with less than 100 genes and less than 500 unique molecular identifiers detected were not analyzed further. The Seurat function NormalizeData was used to normalize the raw counts. Variable genes were identified using the FindVariableGenes function. The Seurat ScaleData function was used to scale and center expression values in the dataset for dimensional reduction. Default parameters were used for the Seurat functions. When needed, samples were integrated using the Seurat functions FindIntegrationAnchors and IntegrateData. Principal component analysis and Uniform Manifold Approximation and Projection (UMAP) were used to reduce the dimensions of the data, and the first 2 dimensions were used in plots. To cluster the cells and determine the marker genes for each cluster, we used the FindClusters and FindAllMarkers functions, respectively. Differential expression analysis of the samples was performed using the FindMarkers function and the Wilcoxon rank-sum test. The Benjamini-Hochberg procedure was applied to adjust the false discovery rate. Functional enrichment analysis was performed using the Metascape software (<https://metascape.org/gp/index.html#/main/step1>).⁵⁹ The human hallmark gene set was used. Analyses were performed using gene annotation available in 2020–2023.

CellphoneDB (v2.0.0)¹⁷ was used to analyze the ligand–receptor interactions. Briefly, each cell type was separated by disease classification, and a separate run was performed for each disease classification. The connectome web was plotted using the igraph package in R.

scATAC-seq analysis and bioinformatic pipeline

ScATAC-seq analysis was performed as we described previously.⁵⁸ The scATAC-seq Low Cell Input Nuclei Isolation protocol (10X Genomics) was used to isolate nuclei from FACS-purified cells. Extracted nuclei were used for the consecutive steps of the scATAC-seq library preparation protocol following 10X Genomics guidelines. Equal molar concentrations of uniquely indexed samples were pooled together. Pooled libraries were sequenced using a NextSeq500 150-cycle flow cell (Illumina). Reads were aligned to human (hg38) genomes, and peaks were called using the cellranger-atac count pipeline. Individual samples were merged using the cellranger-atac pipeline to generate the peak-barcode matrix and TF-barcode matrix. To identify specific TF activity for each cell cluster, we used the R package Seurat to analyze the TF-barcode matrix. The raw counts were normalized by the sequencing depth for each cell and scaled for each TF using the NormalizeData and ScaleData functions. Principal component analysis and UMAP were applied to reduce the dimensions of the data, and the first 2 dimensions were plotted. The FindClusters function was used to cluster the cells. The FindAllMarkers function was used to determine the TF markers for each cluster. Differential analysis of TF activity in the samples

was performed using the FindMarkers function and the Wilcoxon rank-sum test. Cluster identity was determined based on the activity of master regulators of lineage commitment, as we⁶⁰ and others^{33,61} described previously. Cluster-specific peaks were determined using the FindAllMarkers function, and differentially accessible peaks between the samples were determined using the FindMarkers function. Each peak was associated with a specific gene based on its distance to that gene's transcription start site (TSS). Peaks overlapping with a promoter region (–1,000 bp, +100 bp) of any TSS were annotated as peaks in promoters, whereas peaks not in promoter regions but within 200 kb of the closest TSS were annotated as peaks in the distal elements. Peaks not mapped in either the promoters or distal elements were annotated as peaks in intergenic regions.

scDNA and protein-seq analysis

Simultaneous analyses of DNA mutations and the cell-surface immunophenotype (scDNA and protein-seq) were performed as we described previously⁶² and according to the Mission Bio protocol using the custom-designed 37-gene myeloid panel kit and 48 oligo-conjugated antibodies against all major BM cell types (Biolegend). Briefly, cryopreserved BM MNCs were thawed, quantified, and then stained with the pool of the oligo-conjugated antibodies. Stained cells were washed and loaded onto the Tapestry machine for single-cell encapsulation, lysis, and barcoding. DNA libraries were extracted from the droplets followed by the purification using Ampure XP beads (Beckman Coulter). Then, the supernatant was incubated with biotinylated oligonucleotides (Integrated DNA Technologies) to capture the antibody tags, followed by purification using streptavidin beads (Thermo Fisher Scientific). Purified DNA and antibody-tagged libraries were indexed and then sequenced on the Illumina NovaSeq 6000 or NextSeq 500 systems with 150 bp paired-end multiplexed runs.

The resulting files containing DNA and protein data were visualized using the Mission Bio Mosaic library version 1.8. Only manually curated and whitelisted variants were used. Variants were filtered using the below setting: min_dp = 5, min_gq = 0, min_vaf = 21, max_vaf = 100, min_prct_cells = 0, min_mut_prct_cells = 0, and min_std = 0. Protein reads were normalized by centered log ratio, and subsequently underwent dimensionality reduction and clustering using Mosaic 'run_pca' (components = 15), 'run_umap' (attribute = 'pca', n_neighbors = 20, metric = 'cosine', min_dist = 0), and 'cluster' (attribute = 'umap', method = 'graph-community', k = 150). Default parameters were used unless otherwise specified, and randomness was controlled in all steps. Heatmaps were separately visualized in R using the ComplexHeatmap package (<https://bioconductor.org/packages/release/bioc/html/ComplexHeatmap.html>).

Primary cell culture assays

FACS-purified Lin[–]CD34⁺ HSPCs were resuspended in cytokine-free sterile RPMI medium supplemented with 10% FBS, 1% penicillin-streptomycin, and 0.1% amphotericin B and plated in 48-well plates previously seeded with low-passage ($p \leq 4$) healthy BM-derived human mesenchymal cells. Co-cultures were incubated at 37°C in a 5% CO₂ atmosphere. After treatment with vehicle or AMG-176 (20 nM) for 48 h, cells were harvested and stained for quantitative flow cytometric analysis using the antibody panel described above and with AccuCheck Counting Beads (Thermo Fisher Scientific) added to each tube.

QUANTIFICATION AND STATISTICAL ANALYSIS

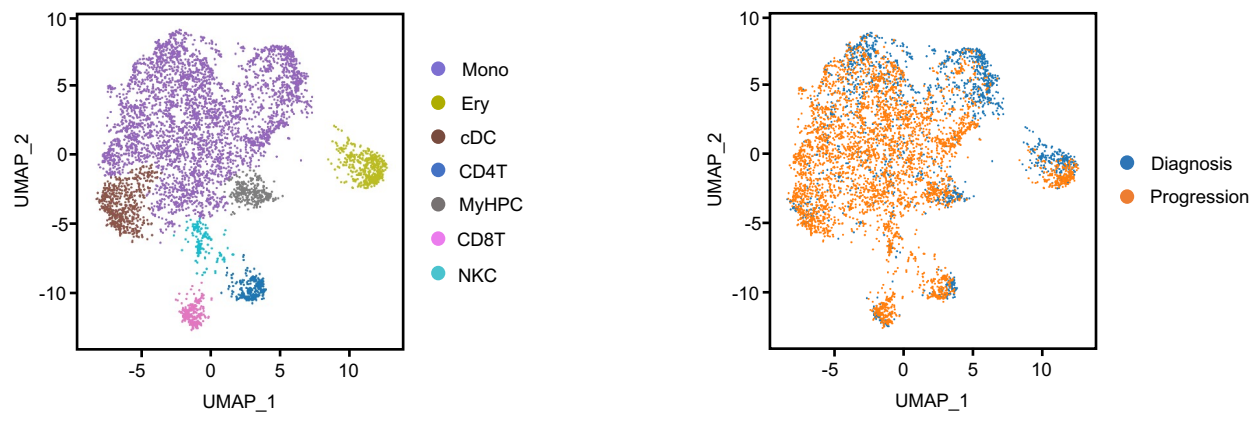
Statistical analysis of flow cytometry data was performed using Prism 8 software (<https://www.graphpad.com>). The figure legends include the statistical test(s) used in each experiment. Statistical significance was represented as * $p < 0.05$, ** $p < 0.01$, *** $p < 0.001$, and **** $p < 0.0001$. In all analyses involving human samples, investigators were blinded to sample annotations and patient outcomes. For replicated experiments, the number of replicates is indicated in the figure legends. No statistical method was used to predetermine the sample size. No data were excluded from the analyses. The experiments were not randomized. Statistical analysis for blast progression and survival in the clinical cohort was performed as specified in the “clinical data analysis” section ([method details](#)).

Supplemental information

**Targeting MCL1-driven anti-apoptotic pathways
overcomes blast progression after hypomethylating
agent failure in chronic myelomonocytic leukemia**

Guillermo Montalban-Bravo, Natthakan Thongon, Juan Jose Rodriguez-Sevilla, Feiyang Ma, Irene Ganan-Gomez, Hui Yang, Yi June Kim, Vera Adema, Bethany Wildeman, Tomoyuki Tanaka, Faezeh Darbaniyan, Gheath Al-Atrash, Karen Dwyer, Sanam Loghavi, Rashmi Kanagal-Shamanna, Xingzhi Song, Jianhua Zhang, Koichi Takahashi, Hagop Kantarjian, Guillermo Garcia-Manero, and Simona Colla

A



B

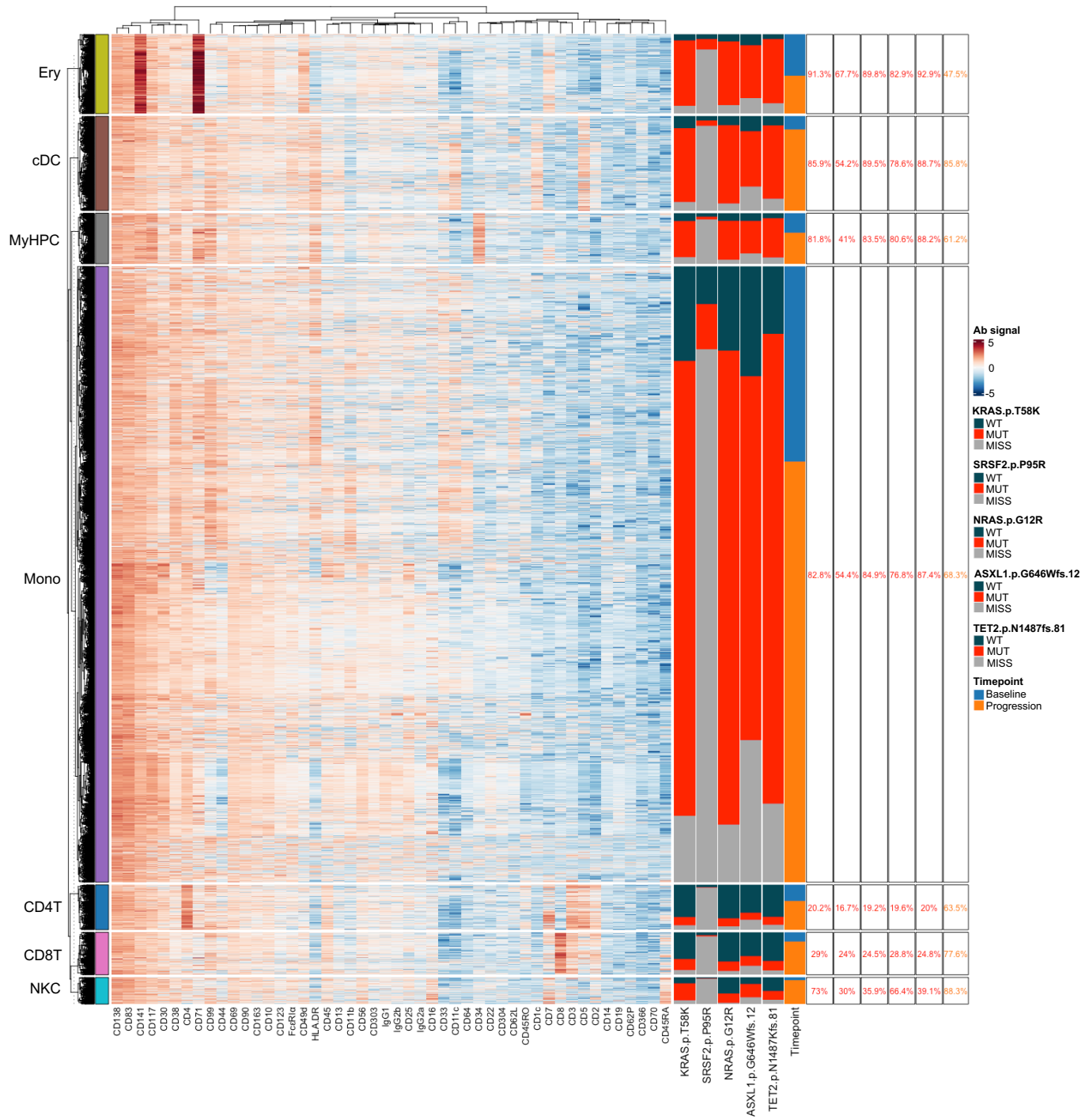
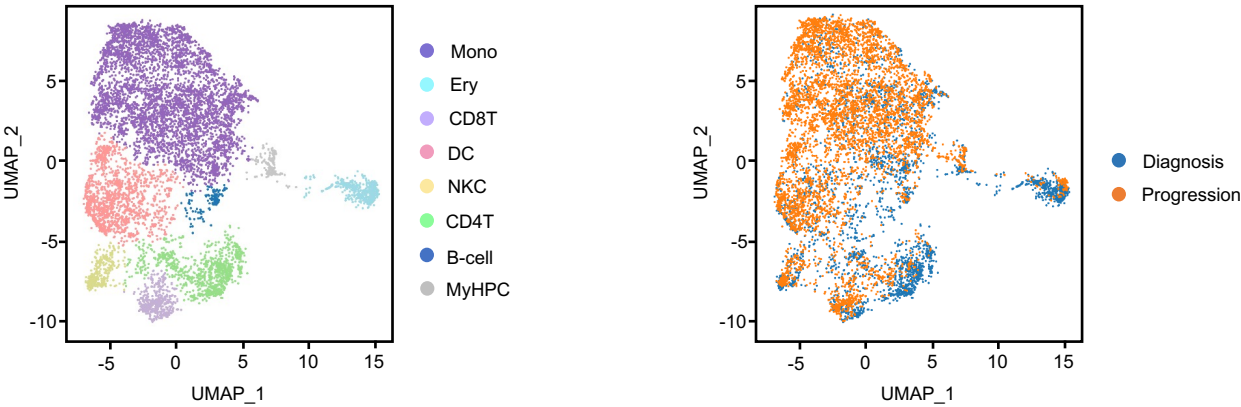


Figure S1. Mutations in *RAS* pathway signaling genes predict a high risk of CMML BP after HMA therapy failure. Related to Figure 1. (A) UMAP of scDNA and protein-seq data for pooled MNCs isolated from BM samples obtained from a CMML patient with pre-existing *KRAS*^{T58K} and *NRAS*^{G12R} mutations at diagnosis (n=1,826) and at BP after HMA therapy failure (n=4,001) included in the CMML patient cohort in Figure 1 and evaluated patient samples in Figure 4. BP was not associated with the clonal evolution of these mutations as they both had approximately 50% VAF at the onset of the disease. Each dot represents one cell. Cells are clustered based on immunophenotypic markers. Different colors represent cluster identity (left) or origin (right). Mono, monocytes; Ery, erythroid precursors; cDC, classical dendritic cells; CD4T, CD4⁺ T cells; MyHPC, myeloid hematopoietic progenitor cells; CD8T, CD8⁺ T cells; NKC, natural killer cells. **(B)** Heatmap displaying DNA and protein reads from each sequenced cell type shown in Fig. S1A. Colors for protein data correspond to antibody-oligonucleotide intensity signals. High protein expression is depicted in red, and low protein expression is depicted in blue. DNA colors correspond to the genotypes for each individual mutation per cell read (wild-type = dark grey, mutant = red, missing = light grey) based on cluster. Percentages correspond to the frequencies of mutant reads within each cluster for a given mutation.

A



B

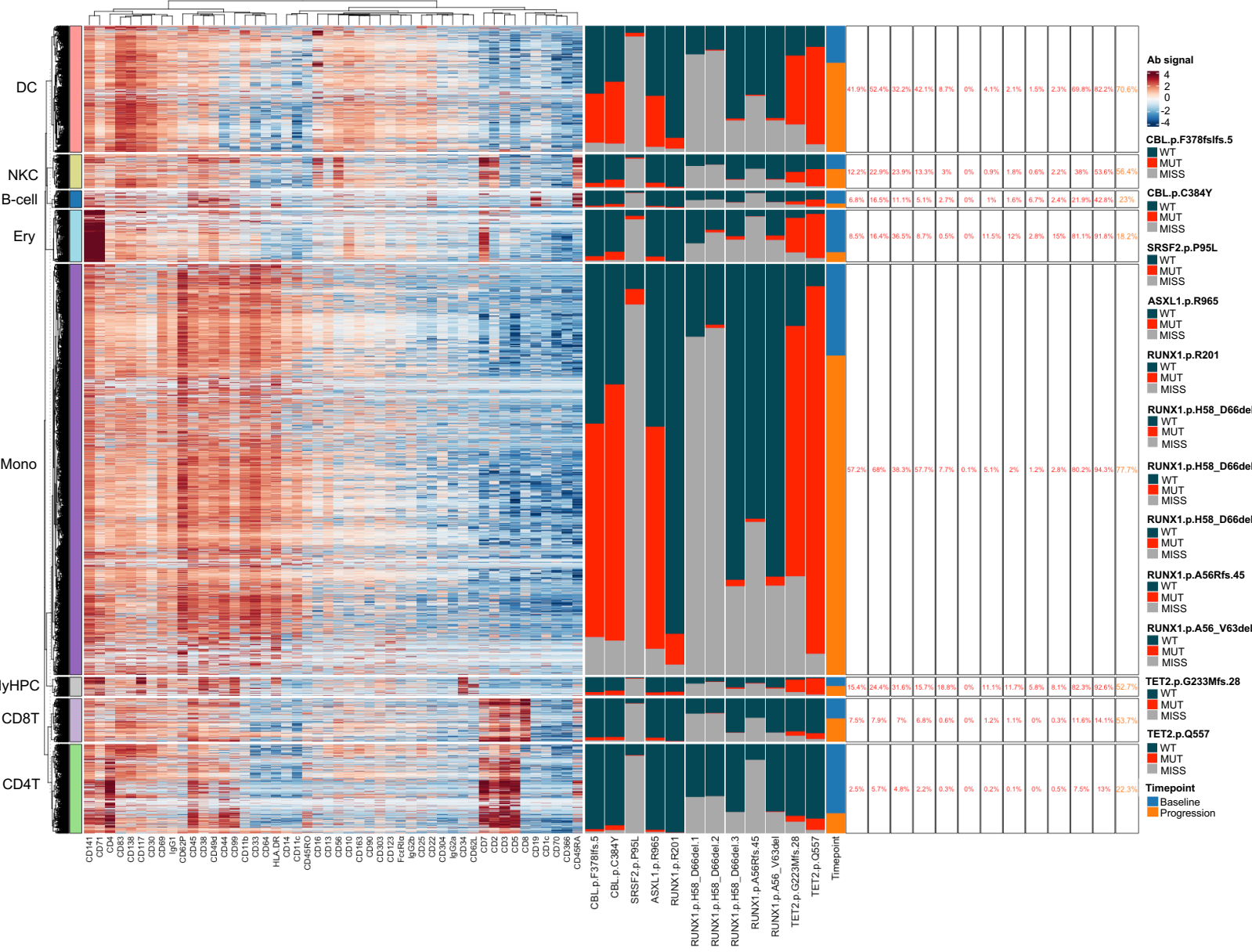


Figure S2. *RAS* pathway mutant clones expand at BP after HMA therapy failure in CMML. Related to Figure 1. (A) UMAP of scDNA and protein-seq data for pooled MNCs isolated from BM samples obtained from a CMML patient at diagnosis (n=3,213) and at BP after HMA therapy failure (n=5,342) included in the CMML patient cohort in Figure 1 and evaluated patient samples in Figure 4. BP was associated with the clonal evolution of a pre-existing *CBL*^{F378Ifs} mutation and the acquisition of a previously undetected *CBL*^{C384Y} mutation. Each dot represents one cell. Cells are clustered based on immunophenotypic markers. Different colors represent cluster identity (left) or origin (right). Mono, monocytes; Ery, erythroid precursors; CD8T, CD8⁺ T cells; DC, classical dendritic cells; NKC, natural killer cells; CD4T, CD4⁺ T cells; B cell, B lymphocytes, MyHPC; myeloid hematopoietic progenitor cells. **(B)** Heatmap displaying DNA and protein reads from each sequenced cell type as shown in Fig. S2A. Colors for protein data correspond to antibody-oligonucleotide intensity signals. Red indicates high protein expression, and blue indicates low protein expression. Colors for DNA data correspond to the genotype for each individual mutation per cell read (wild-type = dark grey, mutant = red, missing = light grey) based on cluster. Percentages correspond to the frequencies of mutant reads within each cluster for a given mutation.

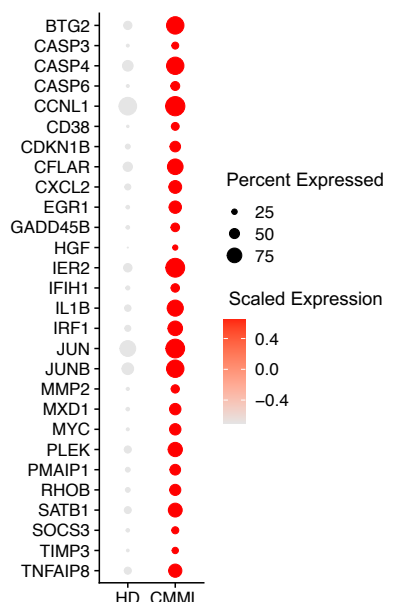
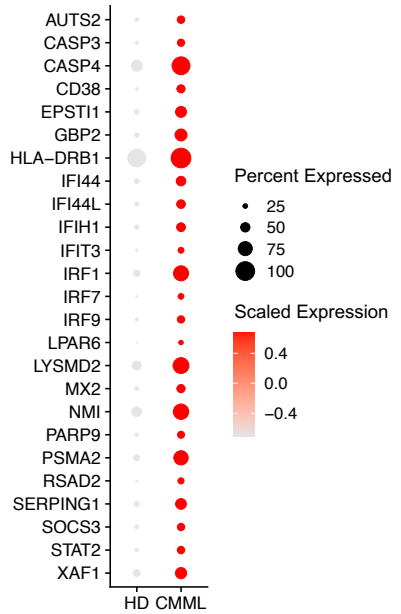
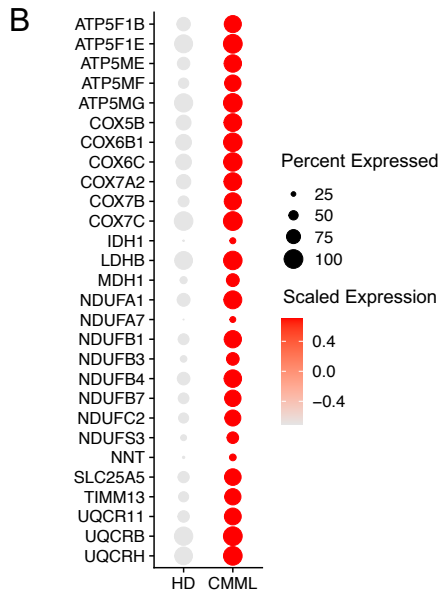
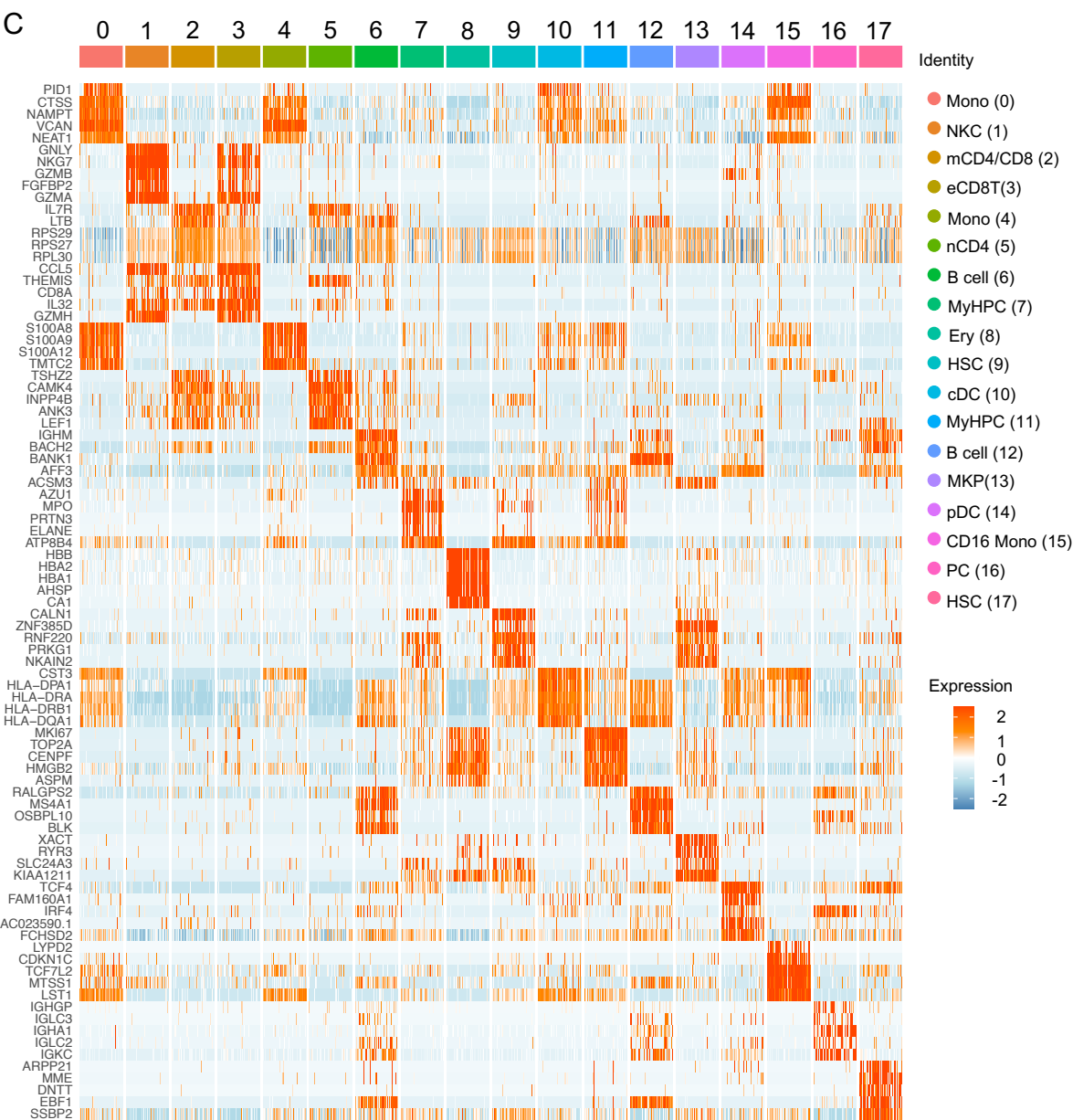
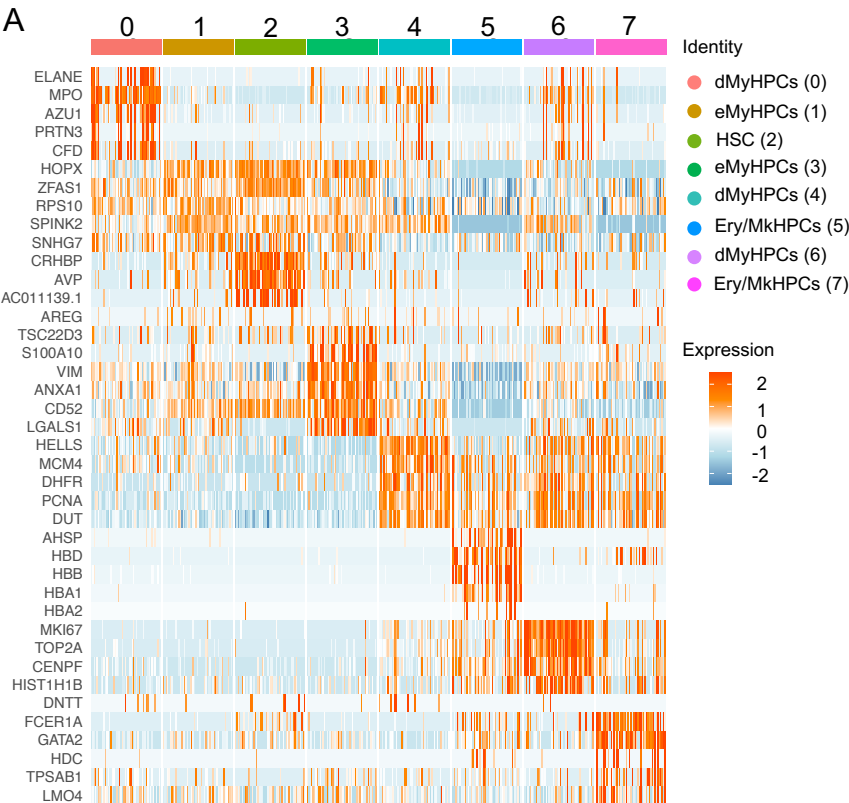


Figure S3. *RAS* pathway mutated CMML cells activate cell-intrinsic and -extrinsic inflammatory networks. Related to Figure 2. (A) Heatmap of the expression levels of the top 5 genes enriched in each of the 8 clusters shown in Fig. 2A. (B) Dot plots of the genes belonging to oxidative phosphorylation (top), IFN response (middle), and apoptosis (bottom) pathways that were significantly overexpressed in the CMML HSCs shown in Fig. 2A compared with those in HD HSCs. The scaled expression represents z scores across conditions. (C) Heatmap of the expression levels of the top 5 genes enriched in each of the 18 clusters shown in Fig. 2D.

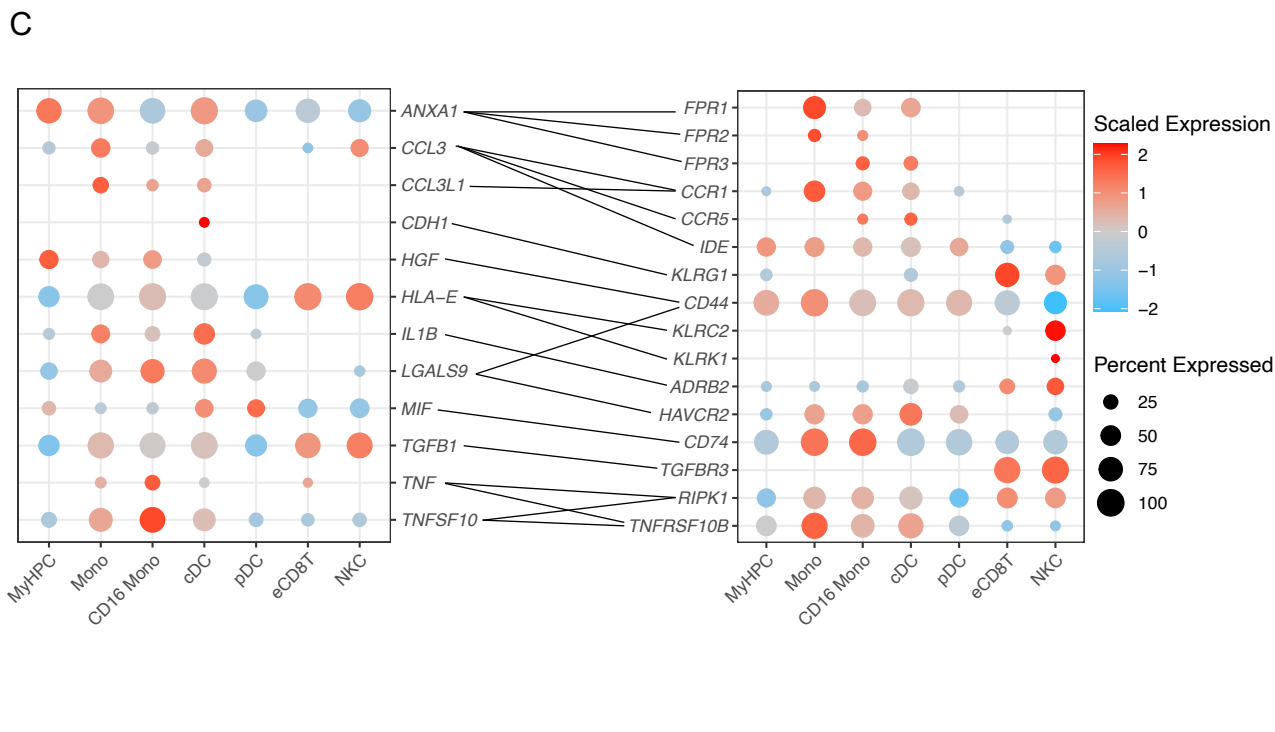
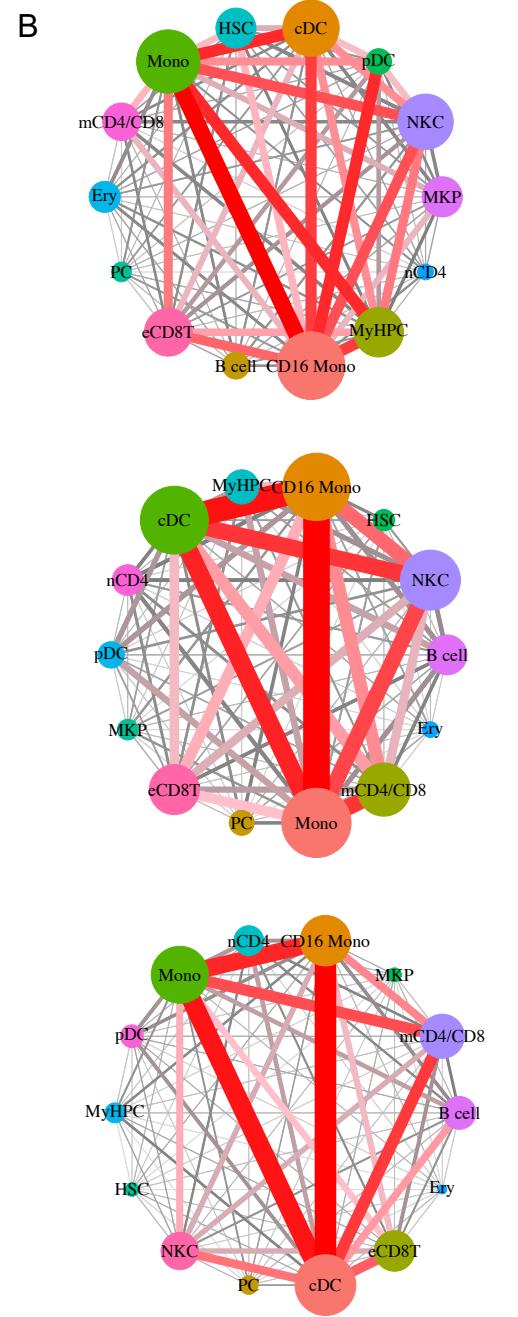
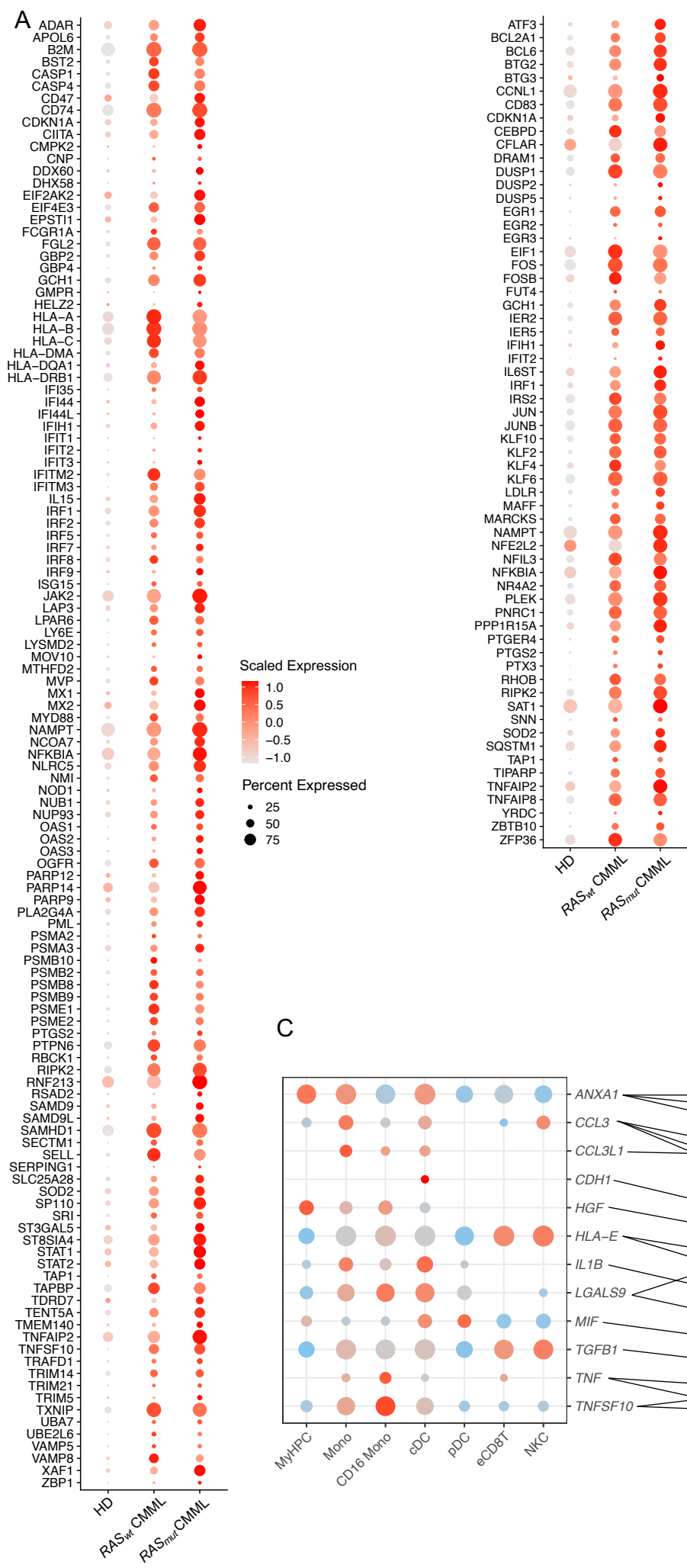


Figure S4. *RAS* pathway mutated CMML cells activate inflammatory networks and establish inhibitory immune interactions.
Related to Figure 2. (A) Dot plots of the genes belonging to IFN response (left) and NF- κ B signaling (right) pathways that were significantly overexpressed in *RAS* pathway mutant and/or wild-type CMML monocytes shown in Fig. 2D compared with those in HD monocytes. The scaled expression represents z scores across conditions. **(B)** Connectome web analysis of interactions between BM MNC populations that were significantly increased in *RAS* pathway wild-type (top) or mutant (middle) CMML compared to those of HDs, or in *RAS* pathway mutant CMML compared to *RAS* pathway wild-type CMML (bottom). The vertex (i.e., colored cell node) size is proportional to the number of interactions to and from each cell type, and the thickness of each connecting line is proportional to the number of interactions between 2 nodes. **(C)** Dot plots showing the most significant ligand- (left) to-receptor (right) interactions gained in MNCs from *RAS* pathway mutant CMML patients compared with those from *RAS* pathway wild-type CMML. Lines represent connections between ligands and their corresponding receptors. Color saturation indicates the level of gene expression. Dot size indicates the percentage of each cell type expressing the gene. The scaled expression represents z scores across conditions.

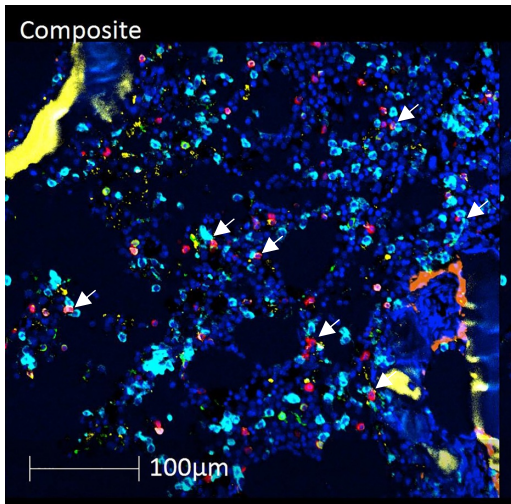
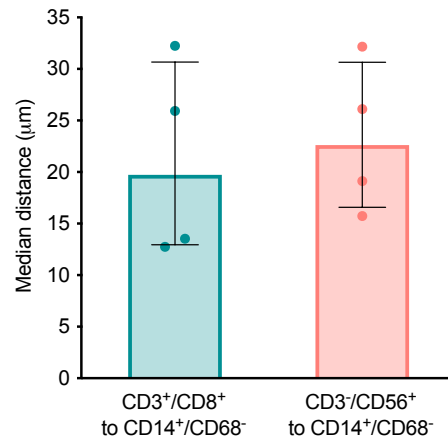
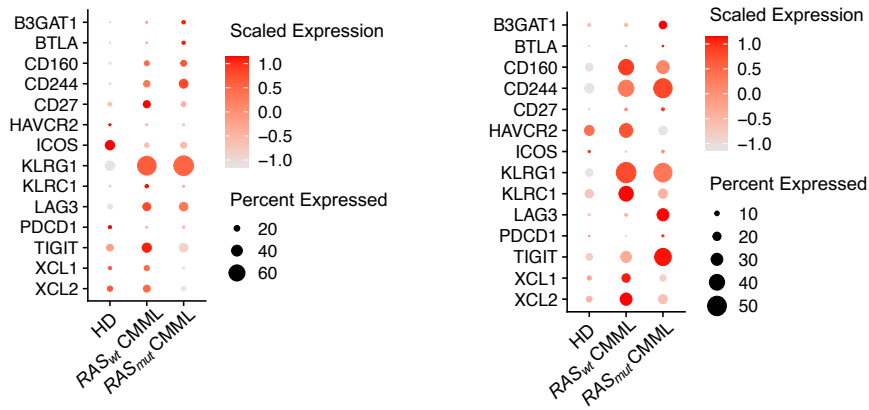
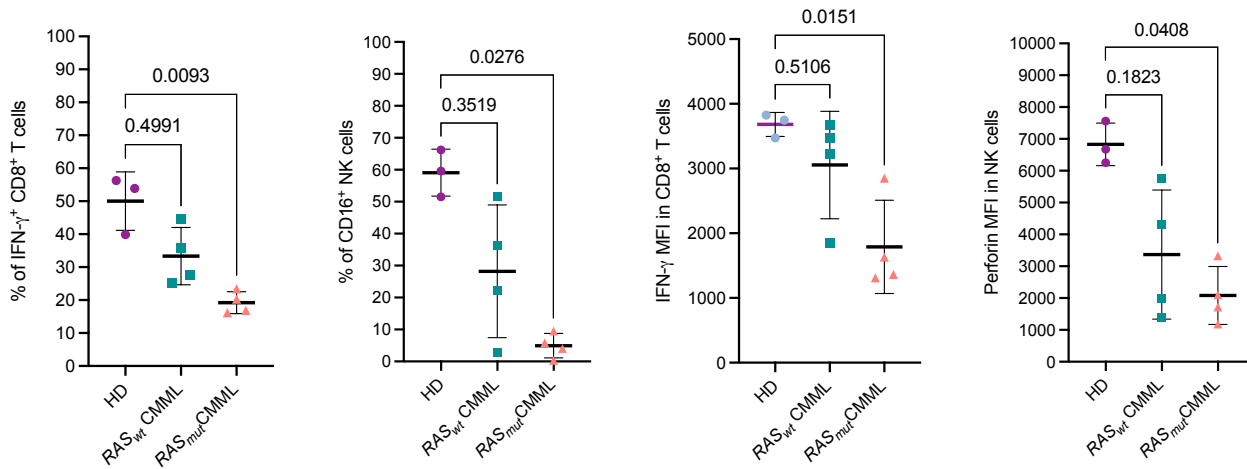
A**B****C****D**

Figure S5. Immune cells are in a dysfunctional state in CMML and spatially co-localize with monocytic populations. Related to Figure 2. (A) Representative multiplex immunofluorescence image of a selected BM section area (20× magnification). Cells were stained with antibodies against CD3 (red), CD4 (green), CD8 (magenta), CD14 (cyan), CD56 (orange), and CD68 (yellow). White arrows indicate the interactions between CD14⁺ monocytes and CD3⁺ T cells. (B) The median distance between CD14⁺/CD68⁻ monocytes and CD3⁺/CD8⁺ T cells (left) or CD3⁻/CD56⁺ NK cells (right) in BM sections obtained from CMML patients (n=4) at the time of diagnosis. (C) Dot plot of exhaustion markers in effector CD8⁺ T (left) and NK (right) cells from HDs, and *RAS* pathway wild-type (*RAS_{wt}*) or mutant (*RAS_{mut}*) CMML. The scaled expression represents z scores across conditions. (D) Frequencies of IFN- γ ⁺ CD8⁺ T cells (far left), CD16⁺ NK cells (middle left), and mean fluorescent intensity (MFI) of IFN- γ ⁺ in CD8⁺ T cells (middle right) or perforin in NK cells (far right) from the BM of HDs (n=3) and *RAS* pathway wild-type (*RAS_{wt}*) or mutant (*RAS_{mut}*) CMML (n=4). Lines represent means. Statistical significance was calculated using the Kruskal-Wallis test.

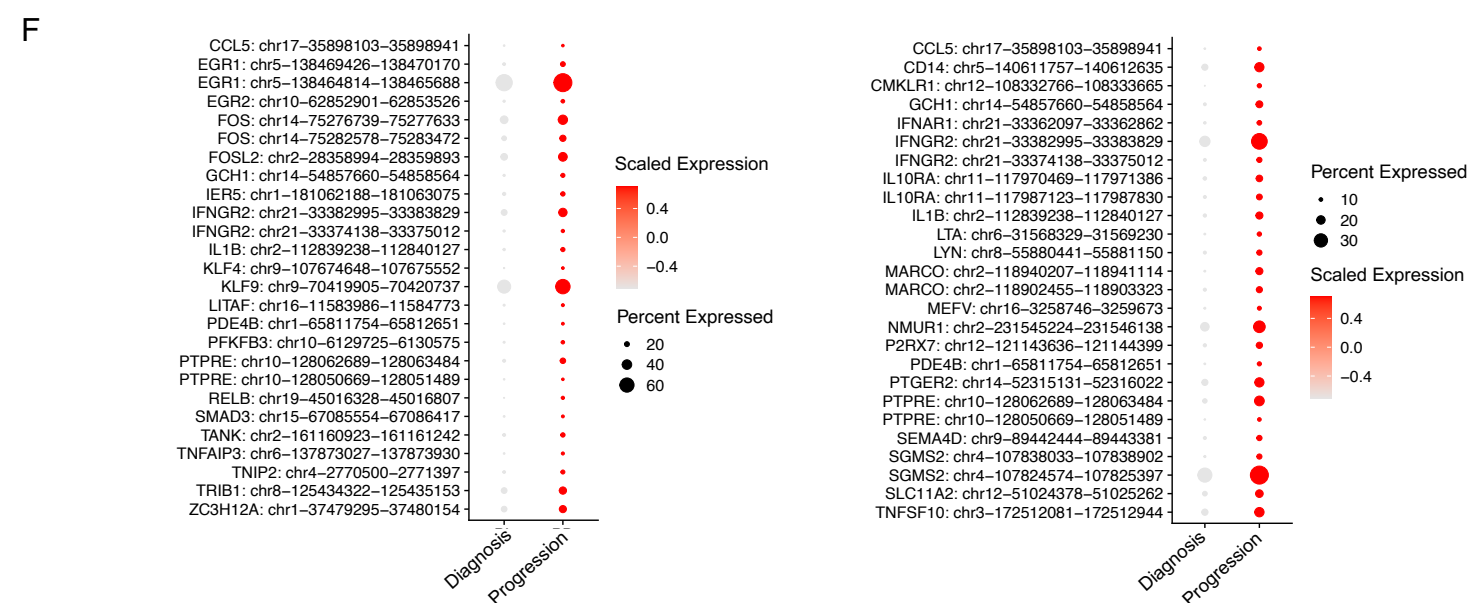
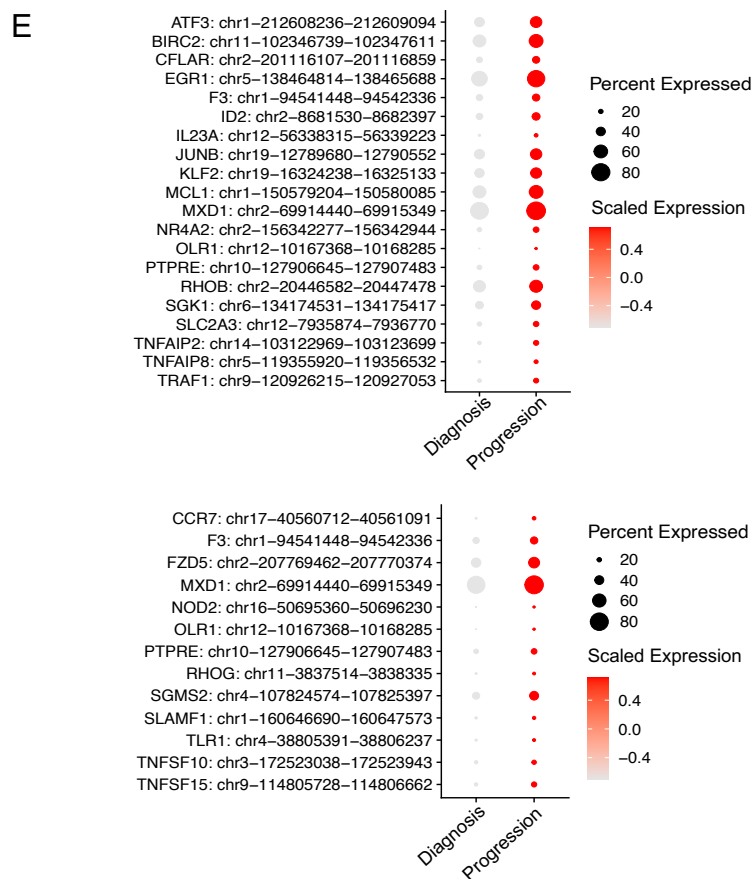
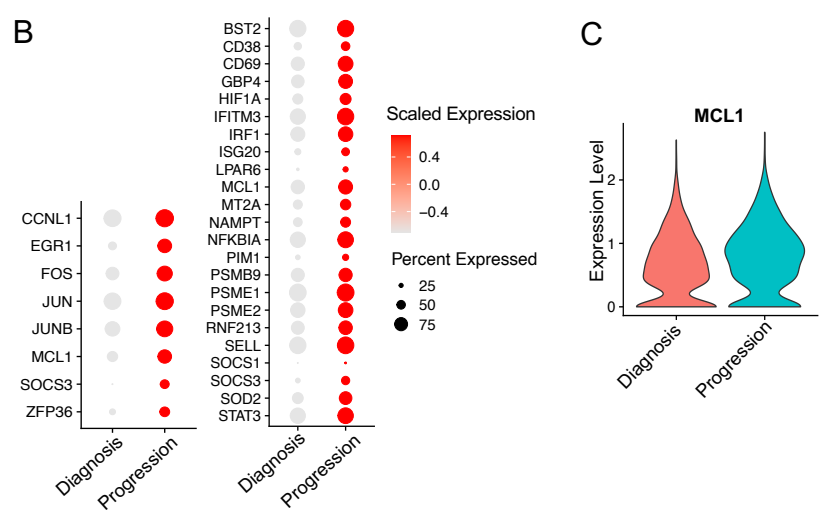
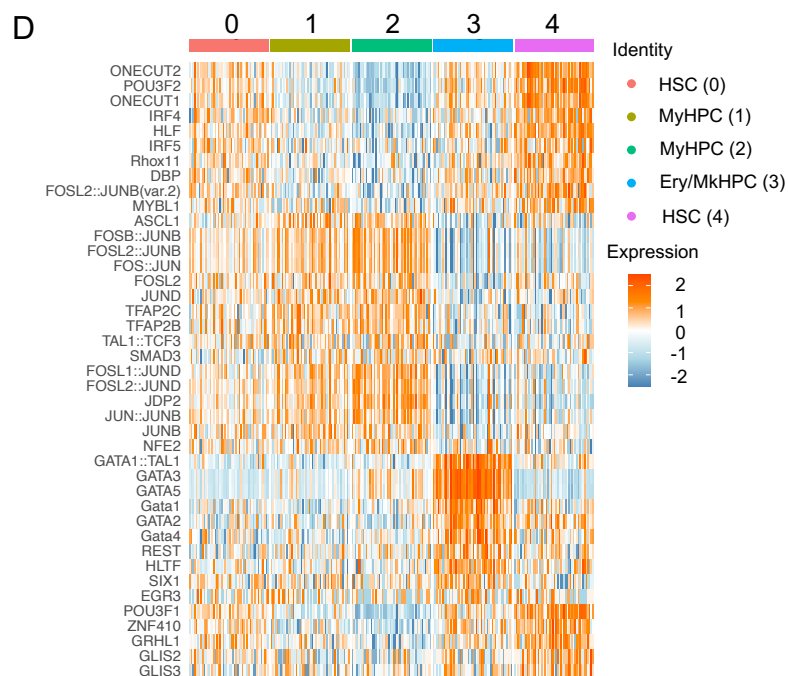


Figure S6. *RAS* pathway–mutated HSCs undergo epigenetic reprogramming and drive CMML BP after HMA therapy failure.
Related to Figure 3. (A) Heatmap of the expression levels of the top 5 genes enriched in each of the 9 clusters shown in Fig. 3A. (B) Dot plots of genes belonging to the NF- κ B signaling pathway that were significantly upregulated in *RAS* mutant CMML HSCs (left) and eMyHPCs (right) at BP compared with those at diagnosis (adjusted $P \leq 0.05$). The scaled expression represents z scores across conditions. (C) Violin plots of *MCL1* expression levels of *RAS* pathway mutant CMML HSCs at diagnosis and BP (adjusted $P = 2.55 \times 10^{-4}$). (D) Heatmap of the activity of the top 10 TFs enriched in each of the 5 clusters shown in Fig. 3D. (E) Dot plots of genes involved in the NF- κ B signaling (top) or inflammatory response (bottom) pathways whose promoters had increased open chromatin peaks in CMML HSCs at BP compared with those at diagnosis ($P \leq 10^{-4}$). The scaled expression represents z scores across conditions. (F) Dot plots of genes involved in the NF- κ B signaling (left) or inflammatory response (right) pathways whose distal regulatory elements had increased open chromatin peaks in CMML HSCs at BP compared with those at diagnosis (adjusted $P \leq 0.05$). The scaled expression represents z scores across conditions.

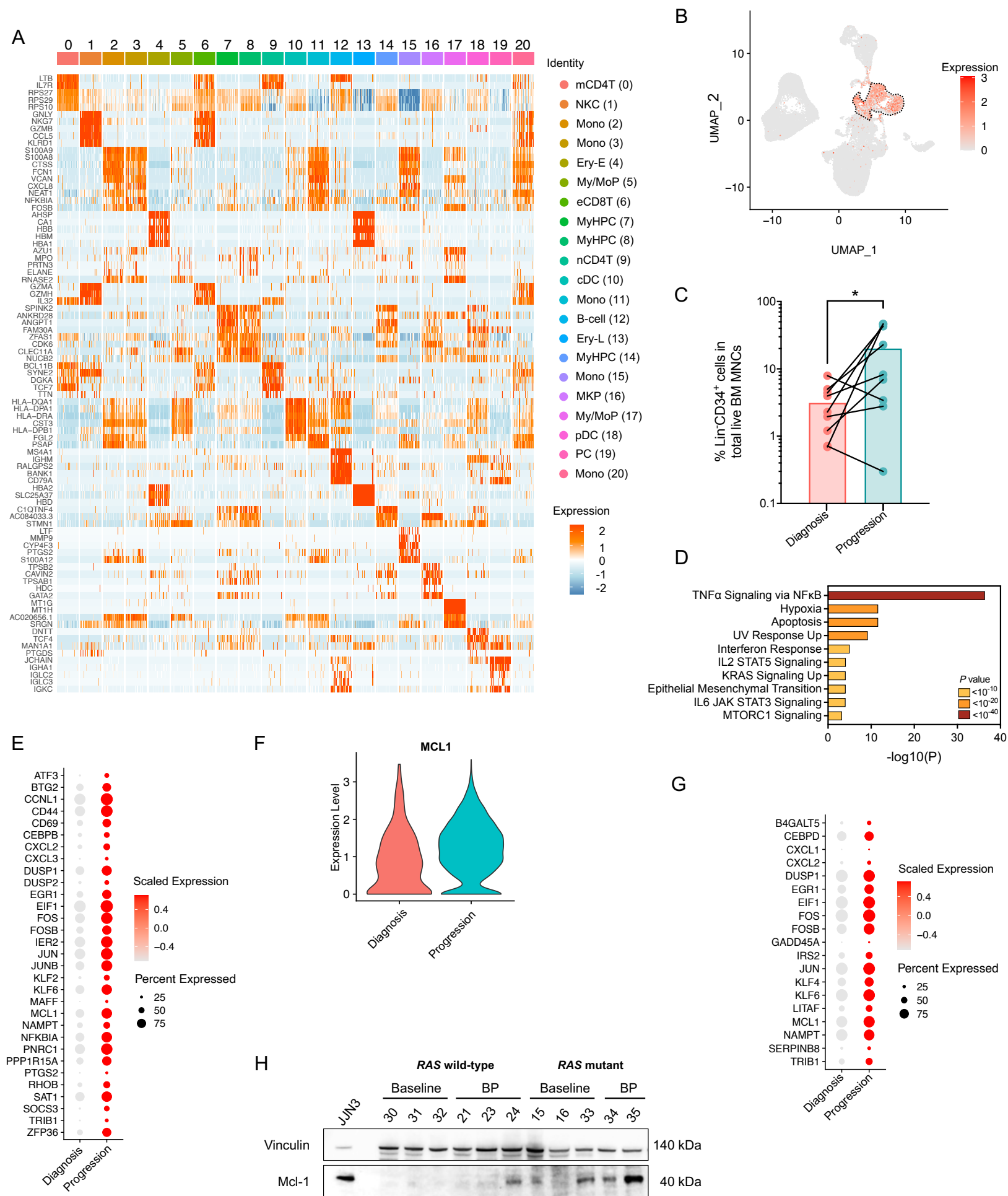
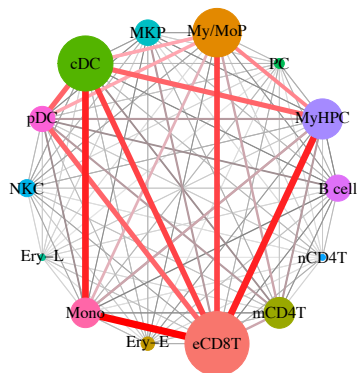


Figure S7. *RAS* pathway mutated CMML cells upregulate NF- κ B survival pathways, including *MCL1*, at BP. Related to Figure 4. (A) Heatmap of the expression levels of the top 5 genes enriched in each of the 21 clusters shown in Fig. 4A. **(B)** UMAP of the distribution of CD34 expression levels across the clusters, as shown in Fig. 4A. Red shading indicates normalized gene expression. Dashed lines indicate MyHPCs. **(C)** Frequency of Lin⁻CD34⁺ cells in MNCs from *RAS* mutant CMML BM samples sequentially collected at diagnosis and BP after HMA therapy failure (n=9). Statistical significance was calculated using a paired two-tailed Student's t-test (* $P < 0.05$). **(D)** Pathway enrichment analysis of the genes that were significantly upregulated in *RAS* mutant MyHPCs at the time of BP compared with those at diagnosis (adjusted $P \leq 0.05$). The top 10 hallmark gene sets are shown. **(E)** Dot plots of genes belonging to the NF- κ B signaling pathway that were significantly upregulated in CMML MyHPCs at BP compared with those at diagnosis (adjusted $P \leq 0.05$). The scaled expression represents z scores across conditions. **(F)** Violin plots of *MCL1* expression levels of *RAS* pathway mutant CMML MyHPCs at diagnosis and BP (adjusted $P = 1.12 \times 10^{-15}$). **(G)** Dot plots of genes belonging to the NF- κ B signaling pathway that were significantly upregulated in *RAS* pathway mutant CMML monocytes at BP compared with those at diagnosis (adjusted $P \leq 0.05$). The scaled expression represents z scores across conditions. **(H)** Western blot analysis of MCL1 expression levels in CD34⁺ BM cells isolated from CMML patients at baseline (*RAS* pathway wild-type, n=3; *RAS* pathway mutant, n=3) or at BP (*RAS* pathway wild-type, n=3; *RAS* pathway mutant, n=2). Vinculin was used as a loading control. JJN3 cells are shown as positive controls. The numbers above each case correspond to the patient's UPN (as detailed in Supplementary Table S3).

A



B

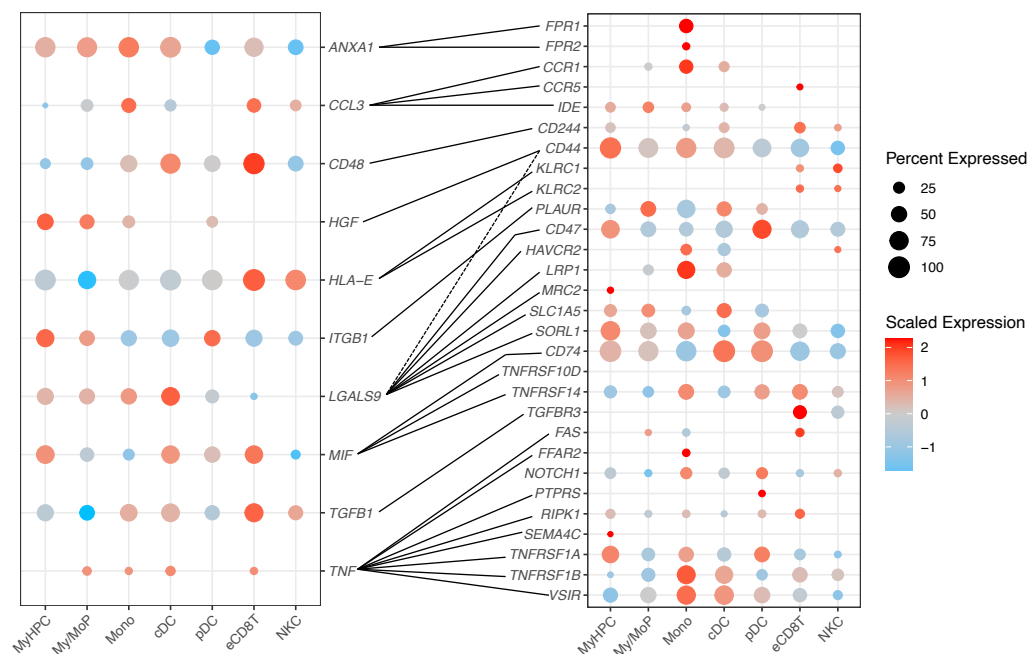
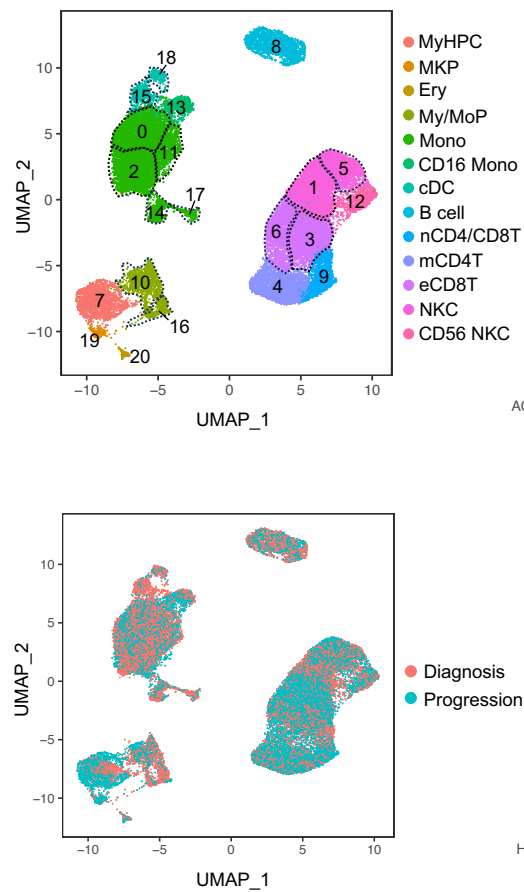
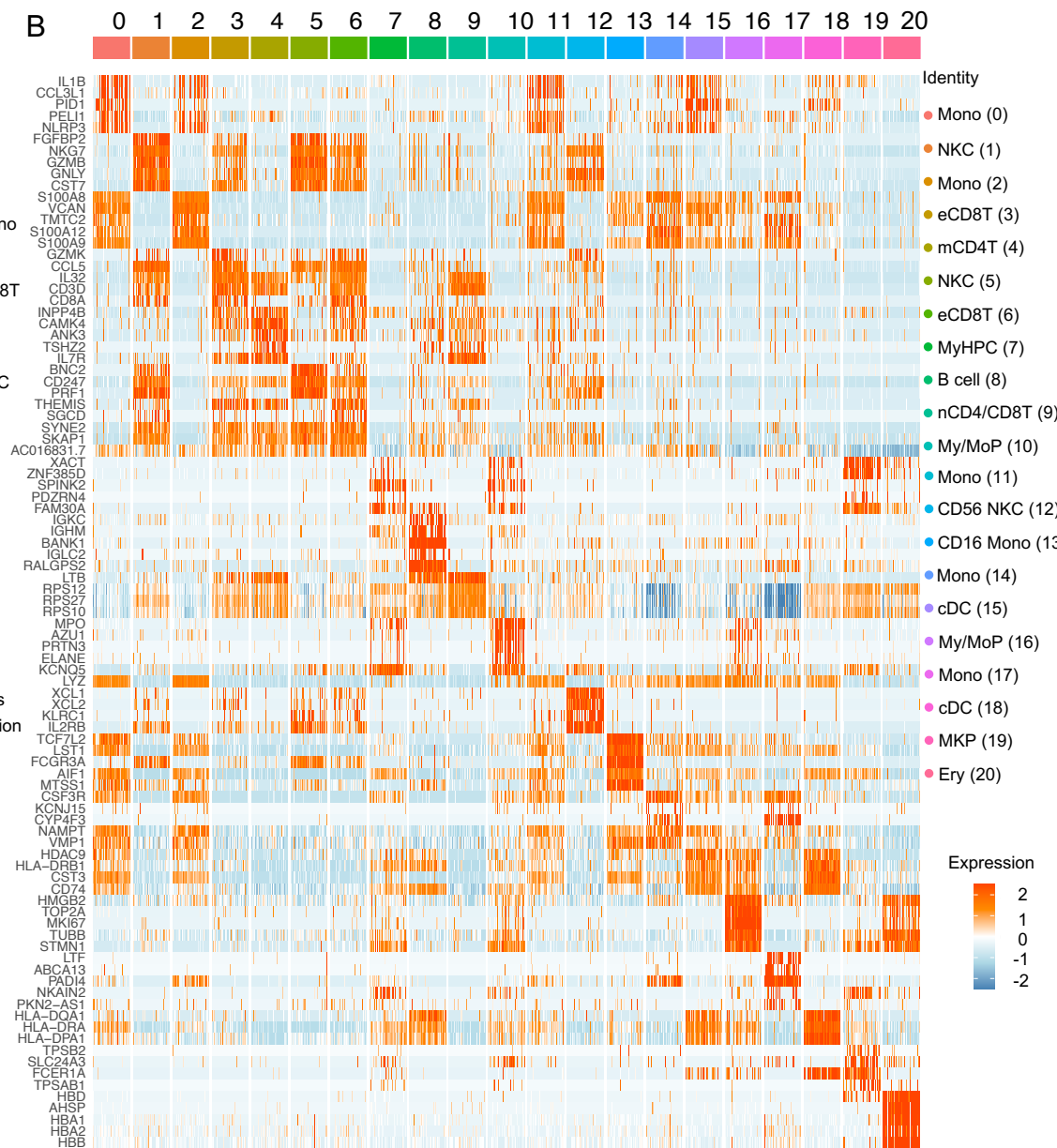


Figure S8. *RAS* pathway mutated CMML MNCs at BP exacerbate the cellular communication networks observed at the time of diagnosis . Related to Figure 4. (A) Connectome web analysis of interactions that were significantly increased in BM MNCs from *RAS* pathway mutant CMML patients at BP compared to those at the time of diagnosis. The vertex (i.e., colored cell node) size is proportional to the number of interactions to and from each cell type, and the thickness of each connecting line is proportional to the number of interactions between 2 nodes. **(B)** Dot plots showing the most significant ligand- (left) to-receptor (right) interactions that were gained in MNCs from *RAS* pathway mutant CMML at diagnosis compared with those at BP (adjusted $P \leq 0.05$). Lines represent connections between ligands and their corresponding receptors. Color saturation indicates the level of gene expression. Dot size indicates the percentage of each cell type expressing the gene. The scaled expression represents z scores across conditions.

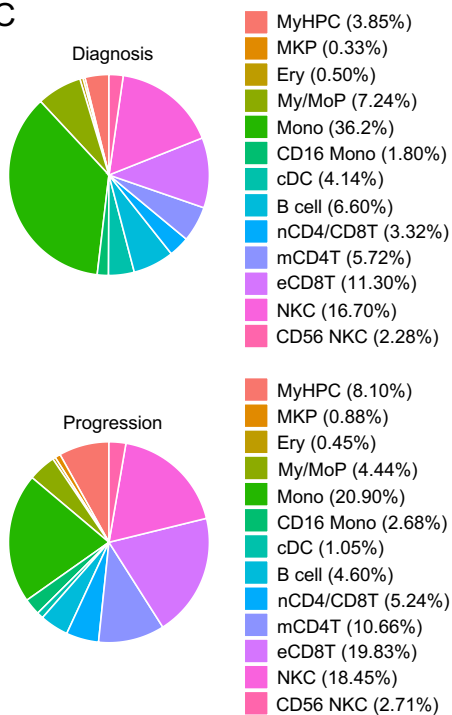
A



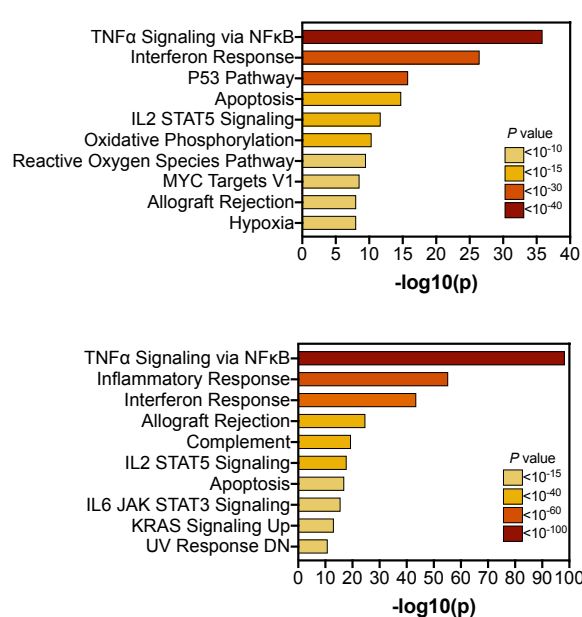
B



C



D



E

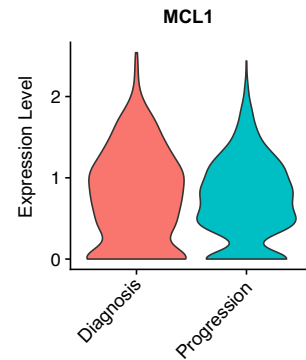


Figure S9. *RAS* pathway wildtype CMML cells do not upregulate *MCL1*-driven antiapoptotic responses at BP. Related to Figure 4.

(A) UMAP of scRNA-seq data for pooled single MNCs isolated from 3 BM samples isolated from *RAS* pathway wild-type CMML patients at diagnosis (n=16,070) and BP after HMA therapy failure (n=17,747). Each dot represents one cell. Different colors represent the cluster cell type identity (top) or sample origin (bottom). MyHPC, myeloid hematopoietic progenitor cells; MKP, megakaryocytic progenitor cells; Ery, erythroid precursors; My/MoP, myelo/monocytic progenitors; Mono, monocytes; CD16 Mono, CD16⁺ non-classical monocytes; cDC, classical dendritic cells; B cell, B lymphocytes; nCD4/CD8T, naïve CD4⁺ and CD8⁺ T cells; mCD4T, memory CD4⁺ T cells; eCD8T, effector CD8⁺ T cells; NKC, natural killer cells; CD56 NKC, CD56⁺ natural killer cells. Dashed lines indicate single clusters in each cell type population. **(B)** Heatmap of the expression levels of the top 5 genes enriched in each of the 21 clusters shown in Supplementary Fig. S9A. **(C)** Distribution of MNC populations at diagnosis (top) and BP (bottom) among the clusters shown in Fig. S9A. **(D)** Pathway enrichment analysis of the genes that were significantly upregulated in MyHPCs (top) and monocytes (bottom) from *RAS* pathway wild-type CMML at the time of BP compared with those at diagnosis (adjusted $P \leq 0.05$). The top 10 hallmark gene sets are shown. **(E)** Violin plots of *MCL1* expression levels in *RAS* pathway wild-type CMML MyHPCs at diagnosis and BP (adjusted $P =$ no significant differences).

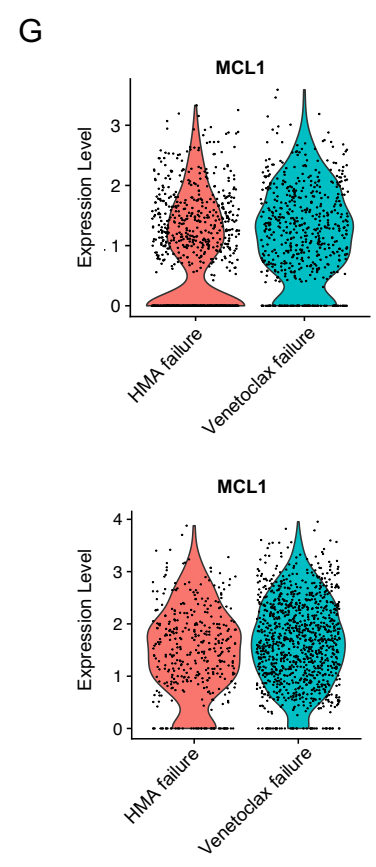
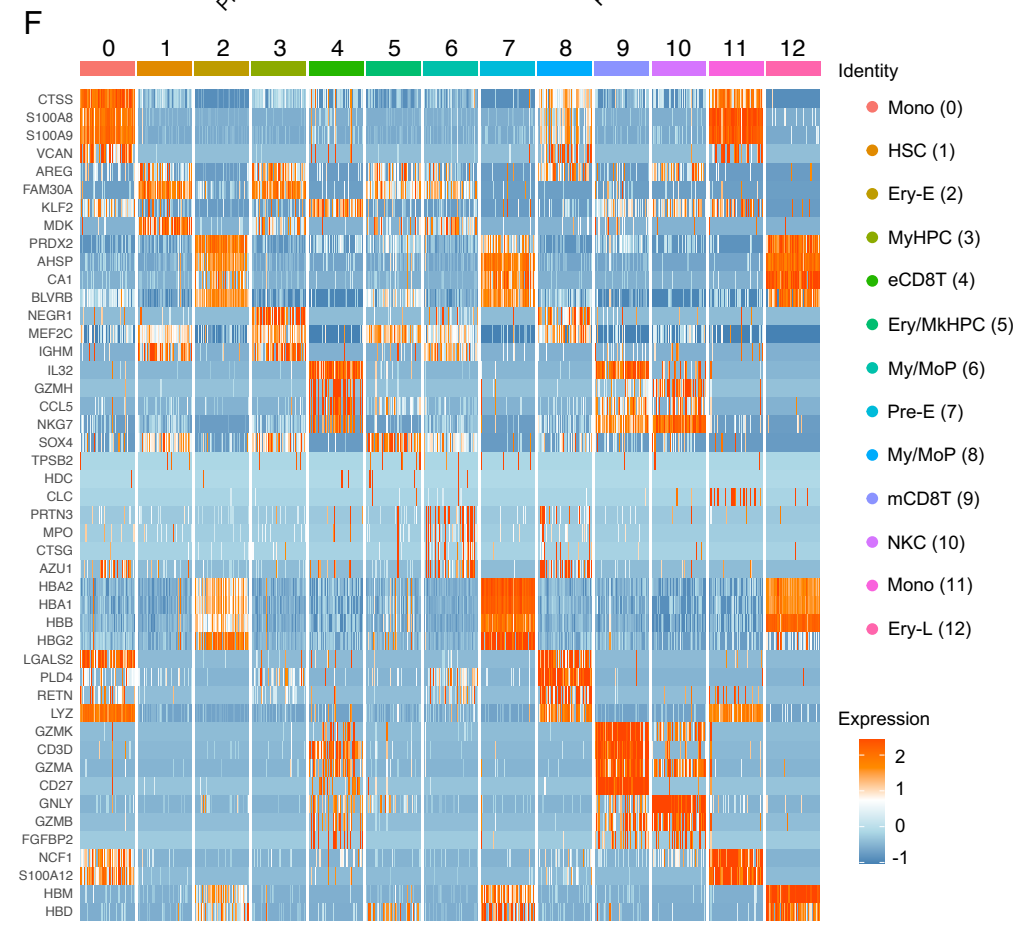
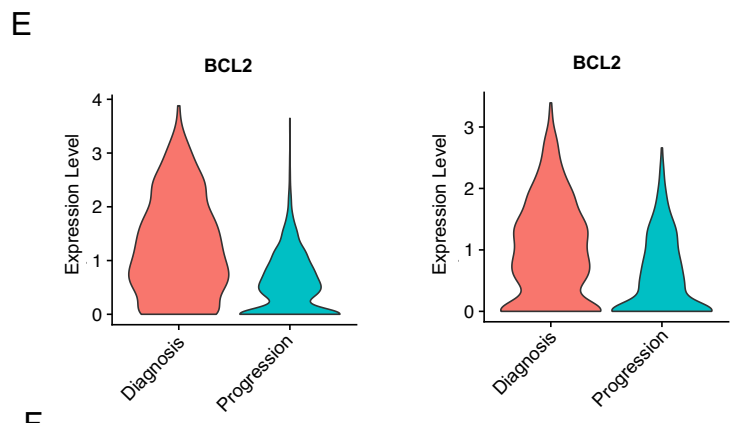
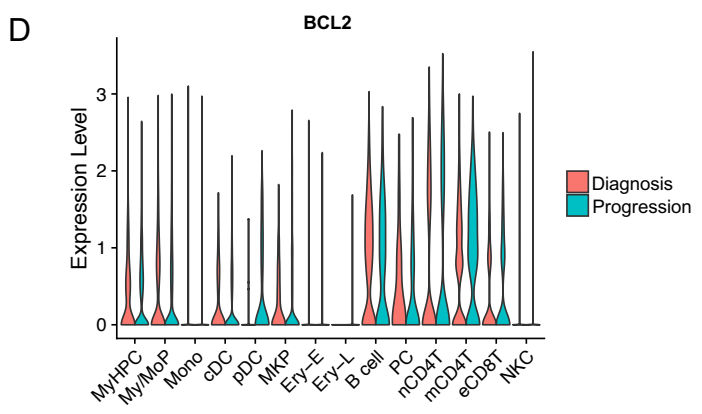
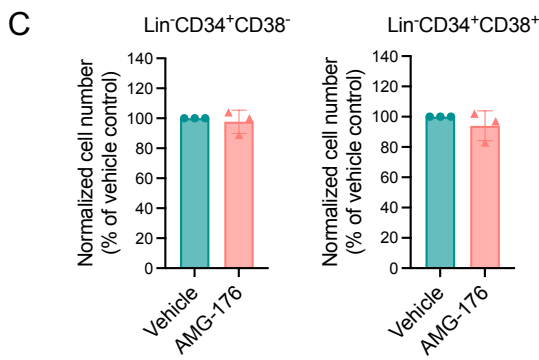
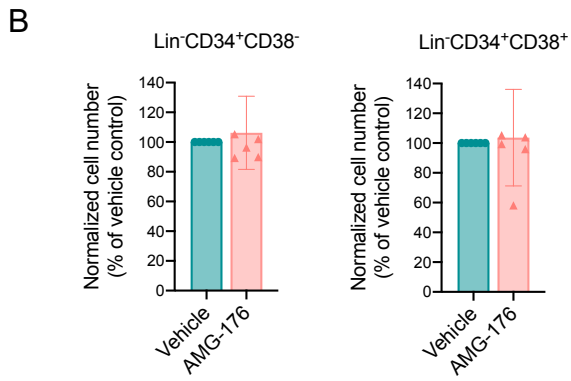
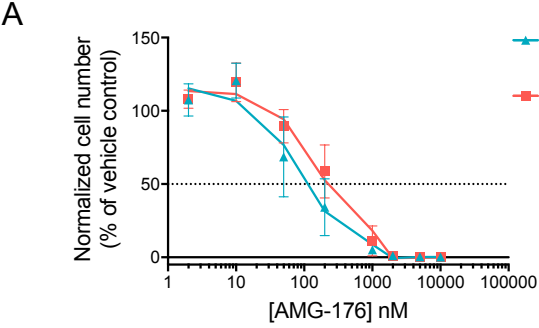


Figure S10. *RAS* pathway mutated CMML cells, but not *RAS* pathway wildtype CMML cells, rely on *MCL1* overexpression to maintain their survival at BP. Related to Figure 4. (A) Number of live cultured Lin⁻CD34⁺CD38⁻ and Lin⁻CD34⁺CD38⁺ cells from HD BM samples (n=2) after 48 hours of treatment with AMG-176. Lines represent means \pm SEMs. (B) Number of live Lin⁻CD34⁺CD38⁻ HSCs and Lin⁻CD34⁺CD38⁺ MyHPCs from *RAS* pathway mutant CMML patients at diagnosis and after treatment with vehicle or AMG-176 (n=6, 20nM) for 48 hours. Lines represent means \pm SDs. A paired two-tailed Student t-test revealed no significant differences. (C) Number of live Lin⁻CD34⁺CD38⁻ HSCs and Lin⁻CD34⁺CD38⁺ MyHPCs from *RAS* pathway wild-type CMML patients at BP after HMA failure and after treatment with vehicle or AMG-176 (n=4, 20nM) for 48 hours. Lines represent means \pm SDs. A paired two-tailed Student t-test revealed no significant differences. (D) Violin plots of *BCL2* expression levels across each *RAS* pathway mutant CMML MNC population at diagnosis compared with those at BP (no significant difference was detected). (D) Violin plots of *BCL2* expression levels in MyHPCs (left) and My/MoPs (right) from *RAS* pathway wild-type CMML at diagnosis compared with those at BP (adjusted $P = 5.45 \times 10^{-54}$ and 1.13×10^{-24} , respectively). (F) Heatmap of the expression levels of the top 5 genes enriched in each of the 13 clusters shown in Fig. 4E. (G) Violin plots of *MCL1* expression levels in *RAS* pathway mutant MyHPCs (top) and My/MoPs (bottom) at the time of BP after HMA therapy failure compared with those at venetoclax failure (adjusted $P = 1.12 \times 10^{-15}$ and no significant difference, respectively).

Third publication

The IL-1 β inhibitor canakinumab in previously treated lower-risk myelodysplastic syndromes: a phase 2 clinical trial.

Rodriguez-Sevilla JJ, Adema V, Chien K, Loghavi S, Ma F, Yang H, Montalban-Bravo G, Huang X, Calvo X, Joseph J, Bodden K, Garcia-Manero G, Colla S.

Nature Communications. 2024
2024 Impact Factor 14.7
Quartile 1

The IL-1 β inhibitor canakinumab in previously treated lower-risk myelodysplastic syndromes: a phase 2 clinical trial

Received: 15 July 2024

Accepted: 6 November 2024

Published online: 13 November 2024

 Check for updates

A list of authors and their affiliations appears at the end of the paper

In myelodysplastic syndromes (MDS), the IL-1 β pathway is upregulated, and previous studies using mouse models of founder MDS mutations demonstrated that it enhances hematopoietic stem and progenitor cells' (HSPCs') aberrant differentiation towards the myeloid lineage at the expense of erythropoiesis. To evaluate whether targeting the IL-1 β signaling pathway can rescue ineffective erythropoiesis in patients with MDS, we designed a phase 2 non-randomized single-arm clinical trial (NCT04239157) to assess the safety profile and efficacy of the IL-1 β inhibitor canakinumab in previously treated lower-risk MDS patients. We enrolled 25 patients with a median age of 74 years; 60% were male, 16% had lower-risk MDS, 84% had intermediate-1 risk MDS according to the International Prognostic Scoring System score, and 80% failed hypomethylating agent therapy. The study met the primary endpoint of defining the clinical activity of canakinumab, and the secondary objective of determining the safety profile, including the rate of transfusion independence, the duration of response, progression-free survival, leukemia-free survival, and overall survival. The overall response rate was 17.4%, with all responses including hematological improvement. Sequential post-hoc prospective single-cell RNA sequencing analyses of HSPCs and bone marrow mononuclear cells at different time points during therapy showed that canakinumab's on-target effects in hematopoietic populations expressing the IL-1 β receptor decreased the TNF-mediated inflammatory signaling pathway but rescued ineffective erythropoiesis only in the context of lower genetic complexity. This study demonstrates that better stratification strategies could target lower-risk MDS patients more effectively.

Increasing evidence supports the role of inflammatory signaling in the pathogenesis of myeloid malignancies, including myelodysplastic syndromes (MDS)^{1,2}. Several inflammatory factors, such as IFN- γ , IL-1 β , and TNF- α , are critical drivers of premalignant clonal expansion, particularly in the setting of clonal hematopoiesis of indeterminate

potential (CHIP) induced by *TET2*- and *DNMT3A*-mutant HSPC clones, which, unlike their healthy counterparts, are intrinsically resistant to inflammation-mediated depletion^{3,4}.

Interleukin-1 β (IL-1 β) is a proinflammatory cytokine crucial to host-defense responses to infection and injury and activating the

✉ e-mail: scolla@mdanderson.org

innate immune system⁵. Secreted IL-1 β binds to its receptor (IL-1R1) and triggers a signaling cascade that controls the gene expression of multiple transcription factors, growth factors, and other cytokines involved in hematological functions⁶. Activating this signaling cascade cooperatively induces the expression of canonical IL-1 target genes, such as *IL-6*, *IL-8*, or *IL-1 β* ⁷, which enhances myeloid skewing⁸ and results in ineffective erythropoiesis. A deregulated IL-1 β -mediated signaling pathway occurs during aging⁹ and in many human diseases, including hematopoietic malignancies and cardiovascular disorders¹⁰. Moreover, recent studies using mouse models of CHIP induced by *Tet2* deletion demonstrated that IL-1 β significantly expanded the mutant clone by enhancing *Tet2*-depleted HSPCs' self-renewal capability and inhibiting the demethylation of transcription factor binding sites related to terminal differentiation compared with their wild-type counterparts. More importantly, the genetic deletion of *IL-1r1* in *Tet2*-knockout HSPCs or the pharmacologic inhibition of IL-1 β signaling by the IL-1R1 antagonist anakinra reduced myeloid expansion and clonal evolution¹¹. These results align with previous results showing that the loss of *IL-1r1* in *Tet2*-knockout HSPCs rescues several abnormalities associated with *Tet2* deficiency, including the expansion of the HSC compartment, the pro-inflammatory state, and the myeloid-lymphoid imbalance¹². Together, these data underscore the urgent need to clarify whether targeting the IL-1 β pathway is a potential intervention strategy to overcome aberrant myeloid differentiation and clonal expansion in human early-stage myeloid neoplasms, such as clonal cytopenias of undetermined significance (CCUS) or lower-risk MDS.

Canakinumab (Novartis, Basel, Switzerland), a fully human monoclonal antibody, targets the IL-1 β signaling pathway by blocking the interaction of IL-1 β with IL-1R1, thus inhibiting IL-1 β downstream target activation and preventing inflammatory mediator production. In the CANTOS (Canakinumab Anti-Inflammatory Thrombosis Outcome Study) trial, canakinumab treatment improved hemoglobin levels and peripheral blood anemia in patients with CHIP-associated mutations, particularly those with *DNMT3A* and *TET2* mutations¹³.

Here, we present the results of a clinical trial evaluating the safety profile and clinical and biological effects of the IL-1 β inhibitor canakinumab in patients with lower-risk MDS. Our work demonstrates that canakinumab rescues ineffective erythropoiesis and overcomes transfusion dependency in the context of MDS with lower genetic complexity.

Results

Patient cohort

Between August 2020 and June 2023, 27 patients were enrolled in a phase 2 clinical trial of canakinumab. Two patients were ineligible, and 25 received treatment (Fig. 1). After performing a short exploratory dose-finding run-in phase, we found no dose-limiting toxicity, and the recommended phase 2 canakinumab dose was established as 300 mg. The baseline patient characteristics are described in Table 1 and Supplementary Table 1. The cohort's median age was 74 years (range 58–88). Of the 25 patients, 15 (60%) were men, and 22 (88%) were White, one (4%) was Asian, and one (4%) was African American; the race of one patient (4%) was unknown. Five patients (20%) did not receive hypomethylating agent (HMA) therapy, and 20 patients (80%) had failed HMA therapy. Patients who experienced HMA failure received a median number of 6 prior cycles of HMAs (range 4–36); 55% of them had primary HMA therapy failure. Twenty-four patients (96%) had transfusion dependency, defined as the need for transfusion 8 weeks before canakinumab initiation because of a hemoglobin level of less than 8 g/dL. Among patients with transfusion dependency, the median baseline transfusion burden was 3 units of packed red blood cells (PRBCs) per 8 weeks (range 0–16). Fourteen patients (56%) had a normal karyotype, and one patient (4%) had a complex karyotype by conventional cytogenetic analysis. The most common mutations identified by targeted NGS involved *SF3B1* (40%), *TET2* (32%), and

DNMT3A (28%). A detailed representation of the clinical characteristics, including the cytogenetic and mutational profiles, of each patient is shown in Supplementary Fig. 1, and detailed information on their molecular profiles is shown in Supplementary Table 2. The BM counts and morphological changes observed during treatment are included in Supplementary Table 3. Five patients (20%) had low (L), six (24%) had moderate low (ML), seven (28%) had moderate high (MH), five (20%) had high (H), and two (8%) had very high (VH) molecular IPSS (IPSS-M) risk.

Safety profile of canakinumab

Canakinumab demonstrated an overall safe profile in all 25 patients. No patient discontinued therapy, but some non-fatal treatment-emergent adverse events occurred. The most common overall treatment-emergent adverse event was neutropenia. The median duration of grade 3 or higher neutropenia was 14 days (range 5–36), and the median absolute neutrophil count nadir was 0.540 (range 0.150–0.990). One death from sepsis (owing to a lung infection due to methicillin-resistant *Staphylococcus epidermidis*) occurred on day seven after canakinumab initiation and was deemed unrelated to treatment. No patient experienced dose reductions or was removed from the study due to canakinumab-related adverse events. The adverse events that occurred during therapy are summarized in Supplementary Table 4. Patients' hematological parameters at multiple time points during canakinumab treatment are summarized in Supplementary Fig. 2A.

Efficacy of canakinumab treatment

Of the 25 patients, 23 were evaluable for response (Fig. 2A and Supplementary Table 1). The overall response rate was 17.4% (95% CI 4.9–38.8). Among the 4 responders, 3 failed HMA therapy before study entry. Erythroid and platelet hematological improvement (HI-E and HI-P) were observed in three patients (13%) and one patient (4%), respectively. The HI rate (including HI-E and HI-P) was 17.4% (95% credible interval [7.1% and 37.4%, respectively], based on a Bayesian prior distribution of Beta [1.0, 1.0]). Hematological improvement was exploratorily reassessed according to the IWG 2018 guidelines, and the HI-E was 13.8% (95% credible interval [4.0%, 28.2%]) (Supplementary Table 5). The four patients' response durations were 12.9, 12.1, 5.1, and 3.1 months, respectively. Transfusion independence (TI) was achieved in three patients whose median duration of response was 8.53 months (95% CI 0.41–16.1). Two patients (UPN-01 and UPN-02), including one patient who was highly transfusion-dependent and who received more than six units of PRBC before canakinumab therapy initiation, had a stable response for over 12 months (Supplementary Table 5). Thirteen patients (56.5%) had stable disease, but in six patients (26.1%), the disease progressed during therapy, and of these six patients, one patient developed acute myeloid leukemia at disease progression (Fig. 2A).

After a median follow-up of 24.9 months (95% CI 19.4, not estimable [NE]), the median OS for the entire cohort was 17.3 months (95% CI 14.3, NE), the median PFS was 17.3 months (95% CI 7.73, NE) (Supplementary Fig. 2B, C), and the median LFS was 16.3 months (95% CI: 14.3, NE). When patients were stratified by HMA therapy status, the median OS was 29.4 months (95% CI 16.34, NE) in the HMA-naïve cohort ($n = 5$) and 17.3 months (95% CI 9.67, NE) in the HMA failure cohort ($n = 20$; $P = 0.64$) (Fig. 2B).

Patients were further classified according to the IPSS-M into higher-risk (HR [VH, MH, and H]) and lower-risk (LR [ML and L]) cohorts. All patients with progressive disease (PD) were HR by IPSS-M (42.8% vs. 0%, $P = 0.01$), while all responders (HI) were LR by IPSS-M (36.3% vs. 0%, $P = 0.01$). When we performed a separate univariate analysis to evaluate any associations between the IPSS-M classification and OS or PFS (Fig. 2C), the median OS for the HR IPSS-M and LR IPSS-M groups were 14.3 months and 29.4 months, respectively ($P = 0.03$).

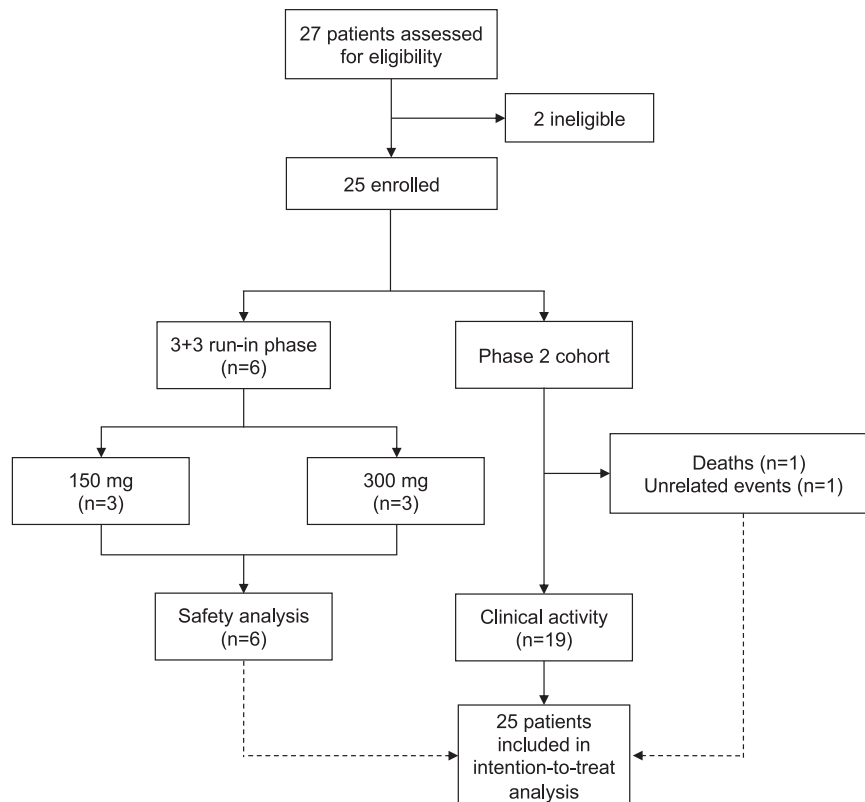


Fig. 1 | Schematic of the clinical trial. The diagram summarizes the flowchart of the clinical trial.

Moreover, the HR IPSS-M and LR IPSS-M groups had 1-year PFS rates of 42.9% and 80.0%, respectively ($P = 0.0087$) (Fig. 2C). The significant association between IPSS-M risk category and OS ($P = 0.04$) and PFS ($P = 0.01$) was further confirmed using the Cox proportional hazards model, accounting for age and prior HMA treatment status (Supplementary Table 6).

Canakinumab induces HSPCs' differentiation in patients with MDS

To evaluate the biological effects of canakinumab on hematopoiesis, we performed sequential post-hoc scRNA-seq analysis of Lin⁺CD34⁺ HSPCs obtained before and during treatment from a representative patient with a *DNMT3A* mutation (UPN-02), who had stable Ht-E after two cycles of canakinumab (Fig. 3A, B and Supplementary Data 1). This analysis revealed that canakinumab increased HSCs' differentiation towards the erythroid and myeloid lineage (Fig. 3C). Differential expression analysis revealed that genes involved in the NF- κ B signaling pathway, including *IL-1 β* , *CXCL2*, *CXCL3*, and *MIF*, were significantly downregulated in HSCs obtained at canakinumab response compared with those in HSCs obtained before treatment (Fig. 3D, Supplementary Fig 3A, B, and Supplementary Data 2). Given that HSCs expressed *IL-1 β* and *IL-1R1* (Supplementary Fig 3C), these data confirmed canakinumab's on-target engagement. ScRNA-seq analysis of MNCs obtained before and after canakinumab administration (Fig. 3E; Supplementary Data 3) revealed that the expression of major regulators of the NF- κ B and inflammatory signaling pathways in MDS, including *TLR2*, *KDM6B*, *REL*, and *NLRP3*, were significantly downregulated in the monocyte population (Fig. 3F, Supplementary Data 4 and Supplementary Fig 3D), which also expressed *IL-1 β* and *IL-1R1* (Supplementary Fig 3E). Consistent with this observation, the levels of several pro-inflammatory cytokines, including IL-1 β , IL-18, IL-6, and IFN- γ , were reduced in BM plasma collected at the time of canakinumab response compared with those in BM plasma collected before treatment (Supplementary Fig 4). This broad spectrum

of pro-inflammatory cytokine inhibition was associated with a recovery of BM erythroblasts (12% vs. 32%; Supplementary Table 3) and significant changes in the immune microenvironment, including a decrease in the CD8⁺GZMK⁺ memory T-cell population (Fig. 3G and Supplementary Fig 5A–C), which is associated with several inflammatory conditions and further enhances the release of pro-inflammatory cytokines^{14–16}. Consistent with this observation, when we inferred cell-to-cell communication from the combined expression of multi-subunit ligand–receptor complexes using CellPhoneDB¹⁷, we observed that before canakinumab treatment, CD8⁺GZMK⁺ T cells were predicted to interact with the monocyte population significantly, and these interactions were significantly inhibited by canakinumab (Supplementary Fig 5D). Specifically, the expression levels of ligands and receptors known to drive monocyte migration (e.g., *a4b1:PLAUR*, *CCL3/CCL3L1/CCL5:CCR1*)^{18–20} and differentiation into highly pro-inflammatory macrophages (e.g., IFN- γ :IFNR, *LTB:LTBR*)^{21,22} were significantly decreased after treatment (Supplementary Fig 5E, Supplementary Data 5).

Further analyses showed that canakinumab treatment did not rescue aberrant erythroid differentiation in lower-risk MDS patients with *SF3B1* mutations (40% of the patients in our cohort), as demonstrated by scRNA-seq analyses of Lin⁺CD34⁺ HSPCs (Fig. 4A, B; Supplementary Data 6) and MNCs (Fig. 4C, D; Supplementary Data 7) isolated from 2 representative patients with *SF3B1* mutations whose best response was stable disease (UPN-07 and UPN-14). Given that *IL-1 β* was expressed in both HSCs and monocytes (Supplementary Fig 6A) and that canakinumab significantly decreased NF- κ B-mediated inflammatory signaling in these populations (Fig. 4E, F; Supplementary Data 8, 9), these data suggest that the IL-1 β -mediated inflammatory pathway does not drive the ineffective erythropoiesis induced by *SF3B1* mutations. Similar data were obtained for 2 other patients with splicing factor mutations whose disease progressed after canakinumab therapy (UPN-12 and UPN-20) (Supplementary Fig 6B–E; Supplementary Data 10–12).

Table 1 | Characteristics of the 25 patients enrolled in the canakinumab trial

Characteristic	
Age, y, median (range)	74 (58–88)
Male, n (%)	15 (60)
Hemoglobin, g/dL, median (range)	8.2 (6.6–9.5)
WBC × 10 ⁹ /L, median (range)	3.2 (2.2–5.9)
ANC × 10 ⁹ /L, median (range)	1.7 (0.38–3.96)
Platelets × 10 ⁹ /L, median (range)	129 (16–430.0)
Bone marrow blast %, median (range)	2 (1–4)
WHO 2022 diagnosis, n (%)	
MDS-LB	12 (48)
MDS-SF3B1	11 (44)
MDS-5q	1 (4)
MDS-f	1 (4)
IPSS, n (%)	
Low	4 (16)
Intermediate-1	21 (84)
IPSS-R, n (%)	
Low	12 (48)
Intermediate	12 (48)
High	1 (4)
IPSS-M, n (%)	
Low	5 (20)
Moderate low	6 (24)
Moderate high	7 (28)
High	5 (20)
Very high	2 (8)
Number of mutations per patient, median (range)	3 (1–10)
Number of pre-treatment PRBC units ^a , median (range)	3 (0–16)
Transfusion dependency, n (%)	24 (96)
Prior HMA treatment, n (%)	20 (80)
Number of prior lines of therapy, median (range)	2 (1–5)

Data are median (range), n (%), or n/N (%). WBC white blood cells, ANC absolute neutrophil counts, WHO World Health Organization, MDS-LB MDS with low blasts, MDS-5q MDS with low blasts and isolated 5q deletion, MDS-SF3B1 MDS with low blasts and SF3B1 mutation, MDS-f MDS with fibrosis, Complex ≥ 3 alterations, Mutations ≥ 5% percentage, HMA hypomethylating agent, PRBC packed red blood cell, IPSS International Prognostic Scoring System, IPSS-R Revised International Prognostic Scoring System, IPSS-M Molecular International Prognostic Scoring System.
^aBaseline transfusion status was defined during the 8-week period prior to canakinumab initiation.

Discussion

Extensive preclinical studies using mouse models of early-stage MDS demonstrated that genetically and pharmacologically targeting the IL-1β inflammatory signaling pathway rescues aberrant myeloid differentiation, overcomes ineffective erythropoiesis, and arrests clonal expansion^{11,12}. To validate these results in the human setting, we conducted a clinical trial of the IL-1β inhibitor canakinumab in patients with lower-risk MDS.

Canakinumab was safe and well-tolerated, with no dose reductions or treatment discontinuation during the study. Cytopenia (occurring in 64% of patients) was the most common grade 3 or higher treatment-emergent adverse event, which may reflect a combination of heightened myelosuppression induced by the treatment or simply the natural history of patients with lower-risk MDS. In contrast to

previous clinical trials in the setting of chronic inflammatory diseases, no grade 3 or 4 infection events were observed^{23,24}.

It is worth noting that we initially used the IPSS and IPSS-R criteria^{25,26} and defined our patients’ risk as lower-risk MDS because of these patients’ baseline single cytopenias, low number of blasts, lower frequencies of *TP53* mutations (*n* = 2,8%), and complex karyotype (*n* = 1,4%). However, 80% of patients previously received other therapies, including HMA therapy (median number of cycles = 6). The overall median number of prior lines of therapies was 2 (interquartile range 1–3). In addition, 80% of the patients were transfusion-dependent. When patients were re-classified according to the IPSS-M score system²⁷, we found that 56% of patients had features of higher-risk disease and were in the MH, H, and VH subgroups. Notably, the IPSS-M score stratification in lower-risk and higher-risk diseases remained significantly associated with OS and PFS.

Canakinumab elicited an overall response rate of 17% (13% HI-E and 4% HI-P), with a median response duration of 8.5 months among responders. We acknowledge the advantages of the IWG 2018 criteria, particularly in refining transfusion burden assessment and hematologic improvement in lower-risk MDS. Although our trial was designed before 2018 using IWG 2006 response criteria, we retrospectively collected transfusion burden data for 16 weeks before canakinumab initiation when possible. The re-analysis with IWG 2018 criteria confirmed that three of four patients who achieved HI maintained responses beyond 16 weeks. However, due to the shortcomings of retrospective data collection, we adhered to the response criteria outlined in our original protocol.

All patients whose disease responded to canakinumab belonged to the lower-risk group by IPSS-M (HI: 36.4%; 4/11), whereas all patients whose disease progressed during treatment were in the higher-risk group (43%, 6/14). Interestingly, the only two patients with HI-E for over 12 months and red blood cell TI (UPN-01 and UPN-02) harbored founder *TET2* or *DNMT3A* mutations, respectively.

Patients with *SF3B1* mutations (40% of the patients in our cohort) did not respond to canakinumab. These results are consistent with the different pathogenic mechanisms of ineffective erythropoiesis caused by *SF3B1* mutations, which induce the aberrant splicing of heme transporters in the mitochondria of erythroblastic cells²⁸. Lower HLA-DR expression levels in *SF3B1* mutant monocytes²⁹ may also affect canakinumab’s efficacy in reducing the interactions with CD8⁺GZMK⁺ T cells, which is predicted to drive monocytes’ migration and differentiation into highly pro-inflammatory macrophages. In addition, previous studies showed that *SF3B1*-mutant MDS have lower inflammatory signatures (including lower levels of IL-1β) compared to lower-risk MDS without *SF3B1* mutations, particularly those with isolated 5q deletion, which are predicted to respond to anti-inflammatory therapy³⁰. Consistent with these findings, canakinumab treatment was associated with prolonged response and transfusion independence in the one patient with MDS-5q (UPN-01) included in our study.

Resistance to canakinumab treatment was also associated with high genetic complexity, which suggests that beyond inflammation, other intrinsic factors (e.g., cooperative mutation effects) and extrinsic factors (e.g., the exacerbation of immune suppression) contribute to patients’ cytopenias and mutant cells’ clonal expansion.

Consistent with preclinical studies in mice¹¹, our study shows that pharmacologically targeting the IL-1β pathway represents a promising therapeutic strategy for improving hematologic parameters and reducing inflammatory cytokine levels in patients with early-stage disease (Supplementary Fig 7).

Given the accumulating evidence of innate immune activation in the pathobiology of MDS and its inflammatory BM microenvironment, particularly in the early stage of the disease, combinations of canakinumab with other anti-inflammasome inhibitors, such as those targeting the NLRP1- or NLRP3-mediated pathways, which neutralize the

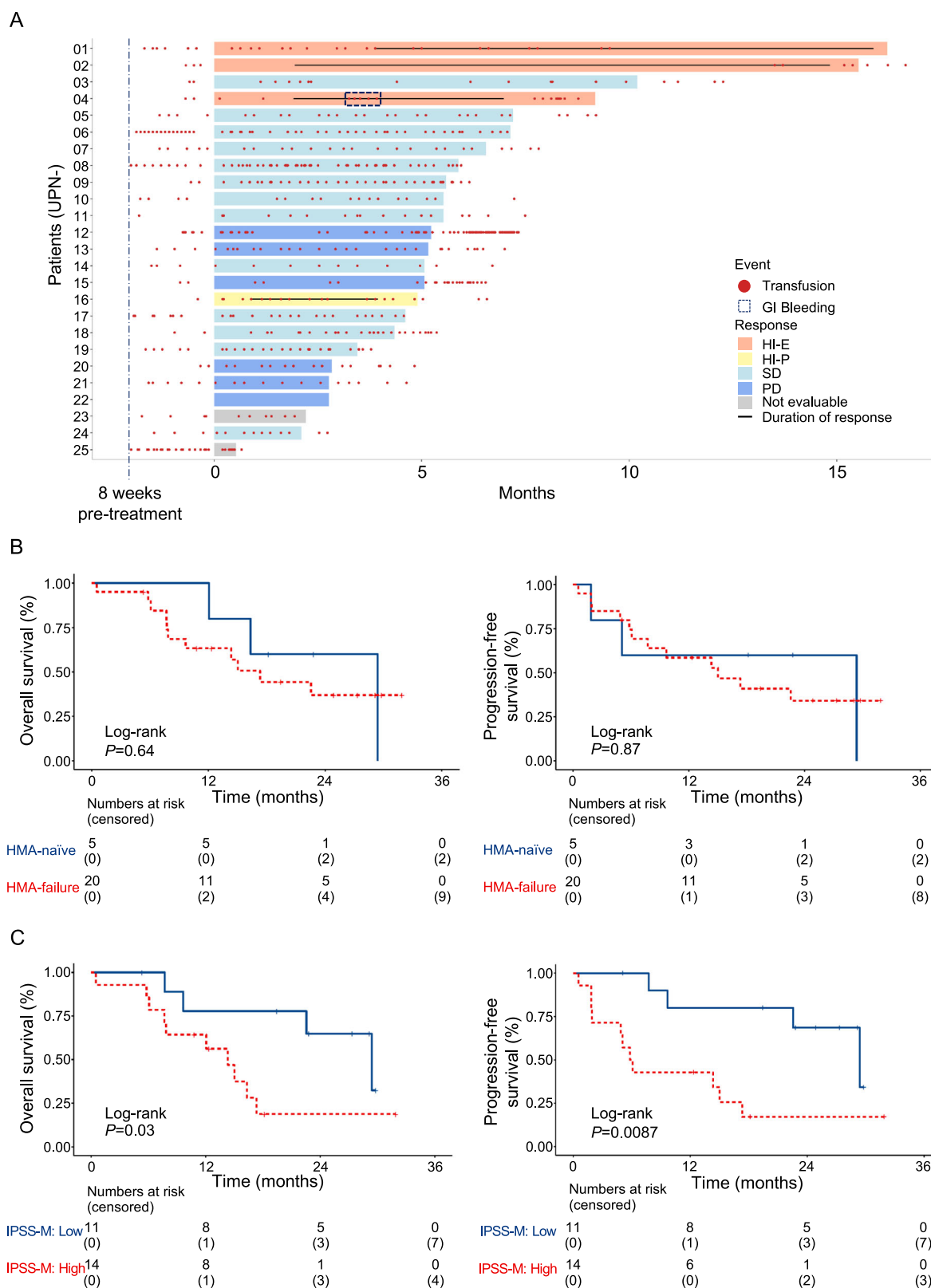
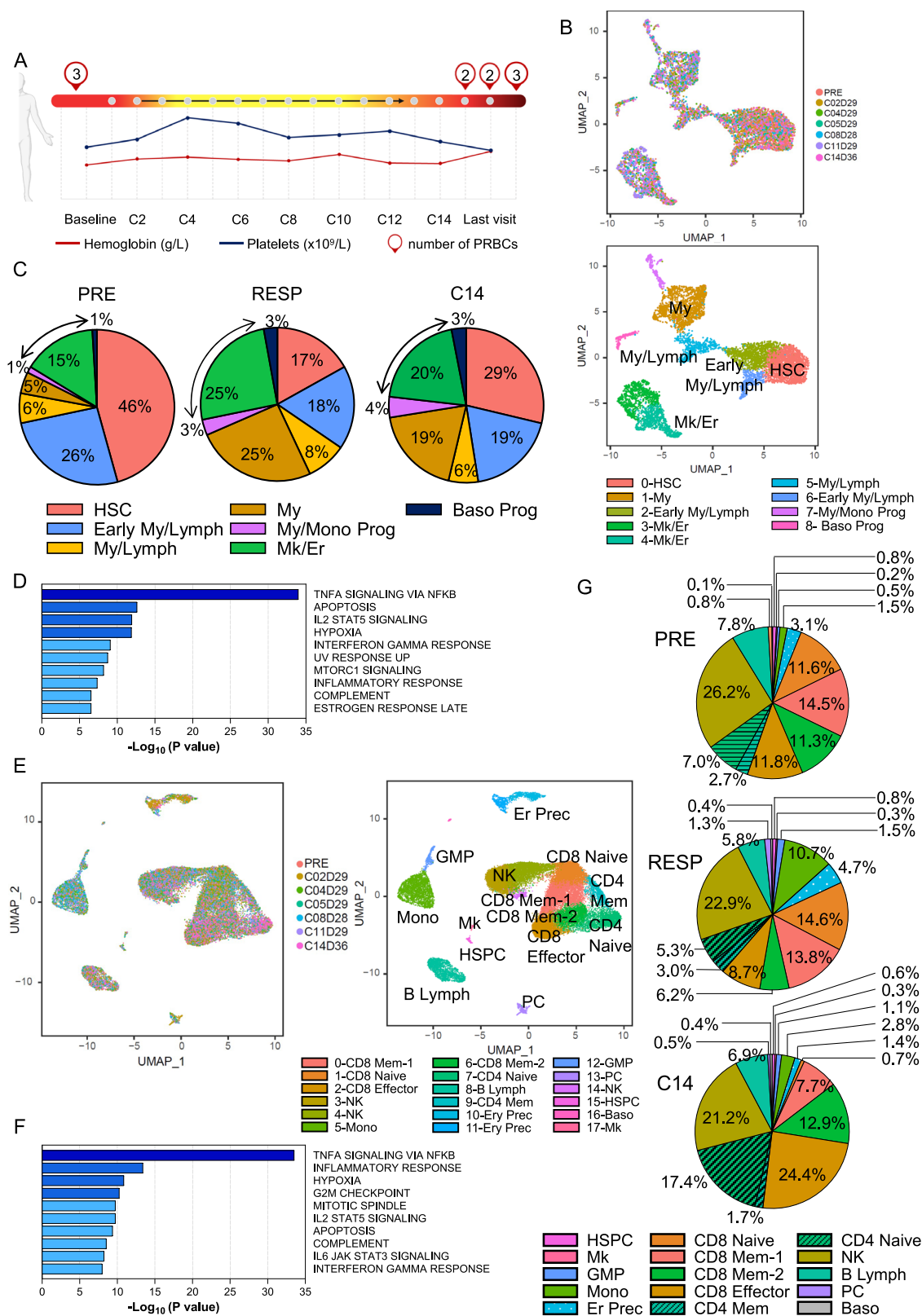


Fig. 2 | Efficacy of canakinumab in lower-risk MDS patients. **A** Swimmer's plot showing transfusions, treatment durations, and responses of MDS patients enrolled in the canakinumab trial ($n = 25$). Red dots represent independent evaluations of transfusion needs in each patient; the dotted square represents the GI bleeding time in patient UPN-04. GI, gastrointestinal; black lines represent the duration of response. HI-E, hematological improvement-erythroid; HI-P, hematological

improvement-platelets; SD, stable disease; PD, progressive disease.

B Kaplan-Meier survival estimate curves for overall survival (left) and progression-free survival (right) stratified by HMA therapy status. **C** Kaplan-Meier survival estimate curves for overall survival (left) and progression-free survival (right) stratified by IPSS-M risk. Source data are provided as a Source Data file.



pyroptotic cell death³¹ and erythropoietin elaboration³² induced by high levels of the alarmin S100A9 observed in the BM of lower-risk MDS patients, may be beneficial in overcoming ineffective erythropoiesis in these patients.

This work has limitations inherent to an early dose-finding study, including the need for a control group and a small sample size. Acknowledging that our patient cohort may not recapitulate the

broader lower-risk MDS population is also essential. The enrollment of patients who were previously heavily treated and/or with high-risk genetic features may not be optimal for evaluating response to IL-1 β inhibition. Indeed, although canakinumab demonstrated an efficient on-target effect at the administered dose, our findings suggest its efficacy is limited to patients with lower genetic complexity. Therefore, future studies should consider the stratification of the patients based

Fig. 3 | Targeting the IL-1 β pathway overcomes ineffective erythropoiesis in lower-risk-MDS. A Schematic of hemoglobin and platelet levels in patient UPN-02 and the number of packed red blood cell (PRBC) units received before and after therapy. The black arrow indicates the response duration. C, cycle. Created in BioRender. Rodríguez-Sevilla, J.J., (2024) <https://www.biorender.com/t63n194>. **B** UMAP plot of scRNA-seq data from Lin^{CD34}⁺ cells from the BM of patient UPN-02 before (PRE; $n = 1381$) and after 2, 4, 5, 8, 11, and 14 cycles of canakinumab treatment ($n = 5721$). Different colors represent the sample (left) and cluster (right) identities. My, myeloid; Lymph, lymphoid; HSC, hematopoietic stem cell; Mk, megakaryocytic; Er, erythroid. **C** Cluster distribution of Lin^{CD34}⁺ cells from the BM before canakinumab treatment (PRE) and at the time of response (cycles 2, 4, 5, 8, and 11) or relapse (cycle 14), represented as the percentage of cells in each cluster. Black arrows indicate the Mk/Er clusters. RESP, response. For the Mk/Er clusters, comparing samples C2, C4, C5, C8, C11, and C14 to the PRE sample: $P = 0.92$, 0.00077 , 4.57×10^{-6} , 0.097 , 1.06×10^{-45} , and 0.0015 , respectively; two-sided Chi-square test. **D** Pathway enrichment analysis of genes significantly ($P \leq 0.05$) downregulated in HSCs after 2 cycles of canakinumab treatment compared with

those before treatment. The top 10 Hallmark gene sets are shown. **E** UMAP plot of scRNA-seq data from BM MNCs isolated from patient UPN-02 before canakinumab treatment (PRE; $n = 2980$) and after 2, 4, 5, 8, 11, and 14 cycles of treatment ($n = 27,913$). Different colors represent the sample (left) and cluster (right) identities. **F** Pathway enrichment analysis of genes significantly ($P \leq 0.05$) downregulated in monocytes after 2 cycles of canakinumab treatment compared with those before treatment. The top 10 Hallmark gene sets are shown. **G** Cluster distribution of BM MNCs before canakinumab treatment (PRE), at the time of response (cycles 2, 4, 5, 8, and 11) or relapse (cycle 14), represented as the percentage of cells in each cluster. For the memory-2 T cell cluster, comparing samples C2, C4, C5, C8, C11, and C14 to the PRE sample: $P = 7.49 \times 10^{-27}$, 1.50×10^{-7} , 0.021 , 1.22×10^{-30} , 7.67×10^{-30} , and 0.036 , respectively; two-sided Chi-square test. HSPC, hematopoietic stem and progenitor cell; Mk, megakaryocytic; GMP, granulomonocytic progenitor; Mono, monocytic; Er, erythroid; Prec, precursor; NK, natural killer; Lymph, lymphoid; PC, plasma cell; Baso, basophil; mem, memory; RESP, response. Source data are provided as a Source Data file.

on genetic and molecular profiles to identify specific features that predict a favorable response to IL-1 β inhibition.

In conclusion, further clinical trials of canakinumab in patients with CCUS or lower-risk MDS defined based on the IPSS-M classification will clarify whether the modulation of IL-1 β -induced inflammation can improve these patients' peripheral blood cytopenias and reduce their risk of developing cardiovascular disorders, thus modifying the course of the disease.

Methods

The research complies with all relevant ethical regulations: MD Anderson Cancer Center IRB-approved human sample protocol PA15-0926. This study was conducted at the University of Texas MD Anderson Cancer Center (Houston, TX, USA) and was approved by MD Anderson's Institutional Review Board. It was performed in accordance with the ethical principles of the World Medical Association Declaration of Helsinki. All patients provided informed written consent. This study is registered at ClinicalTrials.gov (NCT04239157, <https://clinicaltrials.gov/study/NCT04239157>). No deviations from the protocol occurred.

Study design and participants

Between August 2020 and June 2023, patients with relapsed/refractory lower-risk MDS, defined as low or intermediate-1 risk by the International Prognostic Scoring System (IPSS)²⁵ or a score of ≤ 3.5 by the Revised IPSS (IPSS-R)²⁶, with a hemoglobin level < 10 g/dL and symptomatic anemia or transfusion dependency (defined as the need for transfusion eight weeks before treatment for hemoglobin levels less than 8 g/dL) were eligible for the study. Although the IPSS/IPSS-R was developed for untreated patients, its use in the risk stratification of patients with relapsed/refractory MDS was warranted, as no other prognostication tools are available.

Additional eligibility criteria included (1) age ≥ 18 years; (2) Eastern Cooperative Oncology Group (ECOG) performance status score ≤ 2 ; (3) completion of previous antineoplastic agents, including cytotoxic, biological, immunological, and investigational agents, at least 2 weeks before the start of the trial; and (4) adequate organ function (total bilirubin $\leq 3.0 \times$ upper limit of normal [ULN], alanine aminotransferase and aspartate aminotransferase $\leq 3.0 \times$ ULN, serum creatinine clearance > 30 mL/min by the Cockcroft-Gault formula).

Sex-based analyses were not performed in the clinical trial. Males and females had comparable distributions in the clinical trial cohort. The sex of all patients is included in Supplementary Table 1. Gender is not relevant to this study. Due to the limited number of subjects enrolled in the clinical trial, disaggregated analysis by sex should be interpreted with caution.

Hydroxyurea was allowed for patients with rapidly proliferative disease at any time before or during the study if considered in the patient's best interest. However, none of the patients in the trial received hydroxyurea before or during canakinumab administration. Patients with previously untreated MDS, uncontrolled infection, or pregnancy/lactation were excluded.

Procedure

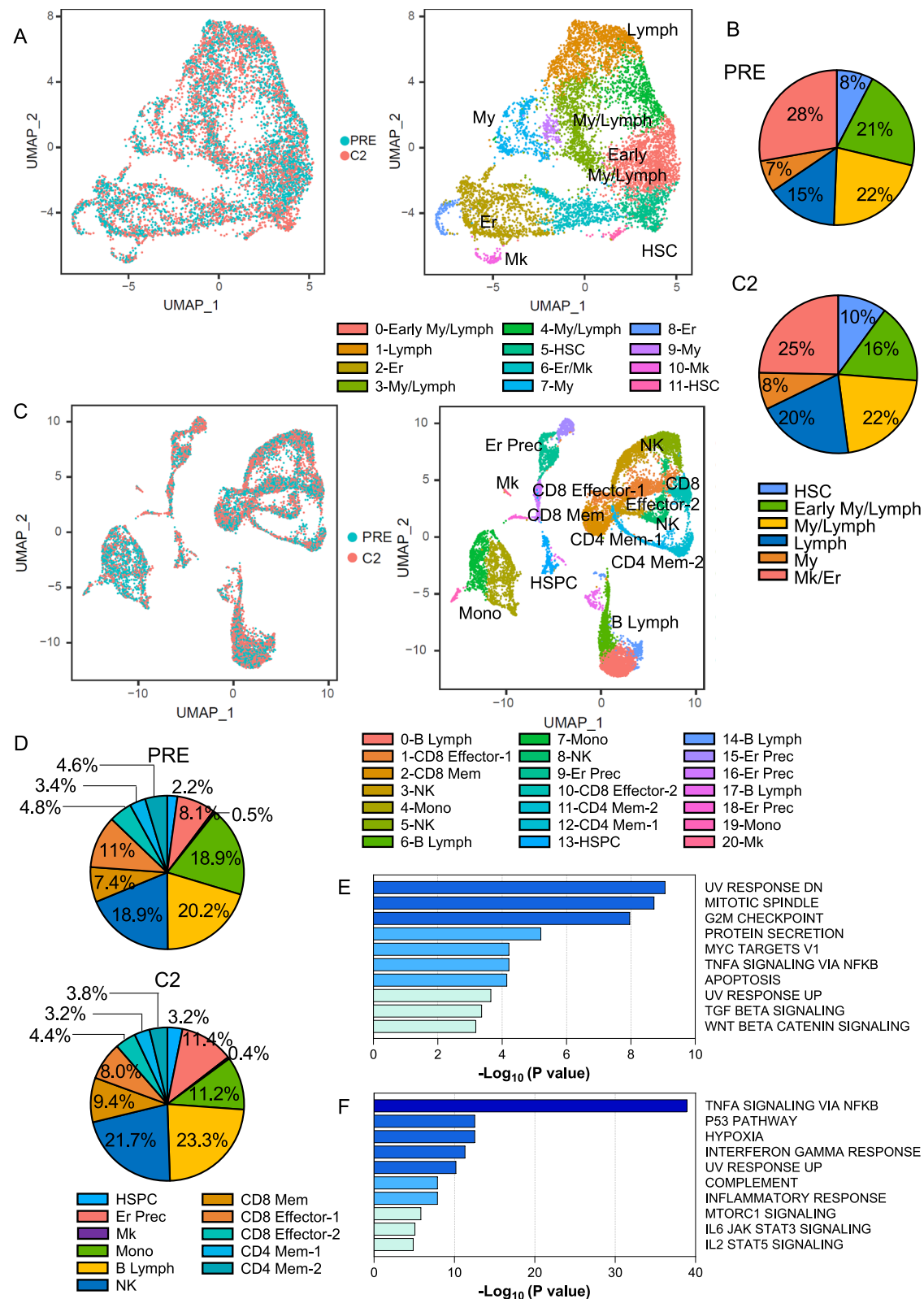
This was an open-label, single-arm, phase 2 clinical trial. Patients were enrolled from September 2020 through November 2022. Since canakinumab was not previously studied in MDS, we first performed a short exploratory dose-finding run-in phase using a standard 3 + 3 design with subcutaneous canakinumab given at 150 mg (first dose level) and then 300 mg (second dose level). After this first phase, all newly recruited patients received 300 mg of subcutaneous canakinumab. Canakinumab was supplied by Novartis (Basel, Switzerland) and administered subcutaneously on day 1 of a 4-week cycle. The study's primary endpoint was the clinical activity of canakinumab, which was determined by the rate of hematologic improvement (HI). Secondary objectives were the safety profile, including the rate of transfusion independence (TI), the duration of response (DoR), progression-free survival (PFS), leukemia-free survival (LFS), and overall survival (OS).

Study assessments

Bone marrow (BM) aspirations and/or biopsies, flow cytometry, conventional cytogenetics, and mutation analyses using an 81-gene next-generation sequencing (NGS) panel³³ were performed before therapy. Additional BM aspirations and/or biopsies were performed at cycle 2, day 28 (± 3 days), and then every three cycles after that or more frequently as clinically warranted. Unless no response was achieved after six or more cycles, canakinumab was continued until disease progression, unacceptable toxicity, the development of concurrent severe illness, patient refusal, or non-compliance. Safety was evaluated in all patients who received at least one canakinumab dose by adverse event (AE) assessment, clinical laboratory test results, physical examinations, and vital signs. AEs were graded according to the National Cancer Institute Common Terminology Criteria for Adverse Events (NCI-CTCAE) version 5.0.

Single-cell RNA sequencing (scRNA-seq)

FACS-purified live lineage (Lin)^{CD34}⁺ or BM mononuclear cells (MNCs) were processed and sequenced at MD Anderson's Advanced Technology Genomics Core, as previously described³⁴. Sample concentration and cell suspension viability were evaluated using a Countess II FL Automated Cell Counter (ThermoFisher Scientific, Waltham, MA) and manual counting. Samples were normalized for input onto the



Chromium Single Cell A Chip Kit (10x Genomics, Pleasanton, CA), in which single cells were lysed and barcoded for reverse transcription. The pooled, single-stranded, barcoded cDNA was amplified and fragmented for library preparation. Pooled libraries were sequenced on a NovaSeq6000 SP 100-cycle flow cell (Illumina, San Diego, CA).

Sequencing analysis was performed using 10x Genomics' Cell Ranger software (v4.0.0 for samples UPN-07 and UPN-14 or v6.1.0 for all other samples). Fastq files were generated using the Cell Ranger

MkFastq pipeline. Raw reads were mapped to the human reference genome (refdata-cellranger-GRCh38-3.0.0) using the Cell Ranger Count pipeline. Intron reads were not counted. The digital expression matrix was analyzed with the R package Seurat (version 4.0.3-5.1.0)³⁵ to identify each cell type and signature gene. Cells with fewer than 500 unique molecular identifiers or greater than 50% mitochondrial expression were excluded from further analysis. The Seurat function NormalizedData was used to normalize the raw counts. Variable genes

Fig. 4 | Canakinumab treatment fails to rescue anemia in patients with MDS with SF3B1 mutations. A UMAP plot of scRNA-seq data from Lin⁺CD34⁺ cells from the BM of patients UPN-07 and UPN-14 before canakinumab treatment (PRE; $n = 3814$) and after 2 cycles (C2) of canakinumab treatment ($n = 4043$). Each dot represents a single cell. Different colors represent the sample (left) and cluster (right) identities. Lymph, lymphoid; My, myeloid; Er, erythroid; HSC, hematopoietic stem cell; Mk, megakaryocytic. **B** Cluster distribution of Lin⁺CD34⁺ cells isolated from the BM before canakinumab treatment (PRE) and during cycle 2 (C2) of canakinumab treatment, represented as the percentage of cells in each cluster shown in Fig. 4A. **C** UMAP plot of scRNA-seq data from BM MNCs isolated from patients UPN-07 and UPN-14 before canakinumab treatment (PRE; $n = 6580$) and after 2 cycles (C2) of canakinumab treatment ($n = 7356$). Different colors represent the sample (top) and cluster (bottom) identities. Er, erythroid; Prec, precursor; NK, natural killer; Mk, megakaryocytic; Mem, memory; HSPC, hematopoietic stem and

progenitor cell; Mono, monocytic; Lymph, lymphoid. **D** Cluster distribution of BM MNCs before canakinumab treatment (PRE) and at the end of cycle 2 (C2) of canakinumab treatment, represented as the percentage of cells in each cluster shown in Fig. 4C. HSPC, hematopoietic stem and progenitor cell; Mk, megakaryocytic; Mono, monocytic; Er, erythroid; Prec, precursor; NK, natural killer; Lymph, lymphoid. **E** Pathway enrichment analysis of genes significantly ($P \leq 0.05$) downregulated in HSCs from patients UPN-07 and UPN-14 at the end of cycle 2 of canakinumab treatment compared with those in HSCs before canakinumab treatment. The top 10 Hallmark gene sets are shown. **F** Pathway enrichment analysis of genes significantly ($P \leq 0.05$) downregulated in monocytes from patients UPN-07 and UPN-14 at the end of cycle 2 of canakinumab treatment compared with those in monocytes before canakinumab treatment. The top 10 Hallmark gene sets are shown. Source data are provided as a Source Data file.

were identified using the FindVariableFeatures function. The ScaleData function was used to scale and center expression values in the dataset, and the number of unique molecular identifiers was regressed against each gene. Uniform manifold approximation and projection (UMAP) was used to reduce the data dimensions, and the first two dimensions were used in the plots. The FindClusters function was used to cluster the cells. Marker genes for each cluster were identified using the FindAllMarkers function. Cell types were annotated based on the marker genes and their match to canonical markers^{36–39}. Pathway analyses of differentially expressed genes were conducted using Metascape, based on the two-sided hypergeometric test. The Benjamini-Hochberg procedure is used for multiple comparison corrections⁴⁰.

CellPhoneDB (v2.0.0)¹⁷ was used to analyze ligand–receptor interactions. The connectome web was plotted using the igraph package in R.

Quantification of cytokines, chemokines, and growth factors in BM plasma

EGF, eotaxin, G-CSF, GM-CSF, IFN- α 2, IFN- γ , IL-1 α , IL-1 β , IL-1RA, IL-2, IL-3, IL-4, IL-5, IL-6, IL-7, IL-8, IL-10, IL-12 (p40), IL-12 (p70), IL-13, IL-15, IL-17A, IL-17E/IL-25, IL-17F, IL-18, IL-22, IP-10, MCP-1, M-CSF, MIG, MIP-1 α , MIP-1 β , PDGF-AA, PDGF-AB/BB, TNF- α , TNF- β , VEGFA, and RANTES were simultaneously quantified from the plasma collected from the BM of patients enrolled in the clinical trials using the MILLIPLEX Human Cytokine/Chemokine/Growth Factor Panel A (HCYTA-60K-PX38, Millipore, Burlington, MA) according to the manufacturer's guidelines. Samples were assayed neat, and 50 μ L of a 1:1 mixture of the sample and assay buffer was added to each assay plate well. For the detection of RANTES, the samples were initially diluted with the assay buffer to 1:100. Briefly, 25 μ L of the 38-analyte bead mixture was added to each plate well, and the plate was incubated overnight at 4 °C. The following day, the plate was incubated at room temperature for 30 min with shaking at 500 rpm. After three washes, 25 μ L of detection antibody was added to each well, and the plate was incubated for 1 h at room temperature with shaking at 500 rpm. Then, 25 μ L of streptavidin–phycoerythrin solution was added to each well, and the plate was incubated for 30 min at room temperature with shaking at 500 rpm. After three wash steps, 150 μ L of xMAP Sheath Fluid Plus (4050021, Thermo Fisher, Waltham, MA) was added to each well. The acquisition was performed using the Luminex 200 system and xPONENT version 4.2 software. Analysis was performed using the Bio-Plex Manager version 6.1 software.

Statistical analysis

Responses were assessed using the modified International Working Group 2006 criteria for MDS⁴¹. The overall response rate (ORR) included complete response (CR), marrow CR (mCR), hematological improvement (HI), and a combination of mCR and HI. The patients' demographic and clinical characteristics and safety data were summarized using descriptive statistics such as means and standard

deviations or medians and ranges. Toxicity type, severity, and attribution were summarized for each patient using frequency tables. For the efficacy analysis, we estimated the HI rate for canakinumab and the 95% confidential intervals (CIs) using the normal approximation method. Transfusion independence (TI) was defined as no transfusion requirements during an 8-week period or longer. The distribution of time-to-event endpoints (OS, PFS, LFS, and DoR) was estimated using the Kaplan–Meier method and compared using the log-rank test. The analysis was further strengthened using the Cox proportional hazards model. OS was defined as the time from the start of therapy to death or last follow-up, with patients alive at the time of the last follow-up censored without event. PFS was defined as the time from diagnosis to disease progression or death from MDS. LFS was defined as the time from the start of therapy to transformation to AML or death from any cause, whichever occurred first. DoR was defined as the time from the first response to the time of first objective documentation of disease progression or death from any cause, whichever occurred first. The median follow-up was determined using the reverse Kaplan–Meier method. Statistical analyses were performed using the R platform (version 4.2.2). Figures were generated using GraphPad Prism (version 10.0.0). Oncoplot visualization was performed using the software package ComplexHeatmap (version 2.14.0). Swimmers plot visualization was performed using the software packages swimplot (version 1.2.0) and ggplot2 (version 3.4.3). Fig. 3A and the graphical abstract were made using Biorender.com.

The sample size of this study after the run-in phase ensures that a posterior credible interval for the HI rate has a width of 0.27 at most under the assumption of a HI rate of 20%. The data cutoff date for this analysis was June 11, 2023. Data were reviewed and analyzed by the contract research organization and the authors; all authors had access to the primary clinical trial data.

Experimental data analysis

Quantitative data were analyzed with GraphPad Prism 10 software (GraphPad, La Jolla, CA). Figure legends indicate the statistical tests used in each experiment. Statistically significant differences in the figures are indicated as * $P < 0.05$, ** $P < 0.01$, *** $P < 0.001$, and **** $P < 0.0001$.

Reporting summary

Further information on research design is available in the Nature Portfolio Reporting Summary linked to this article.

Data availability

To respect participant confidentiality, the study clinical data are not publicly available. Requests for deidentified data should be directed to the corresponding author. The corresponding author will make the data available immediately upon request for scientific non-profit purposes and further elaboration. The granted access to the data will not have any time limitation. The study protocol is also available upon

request to the corresponding author. The datasets generated using scRNA-seq have been deposited under the accession code [GSE237148](https://www.ncbi.nlm.nih.gov/bioproject/1000000000). The remaining data are available within the Article, Supplementary Information, or Supplementary Data file. Source data are provided as a Source Data file. Source data are provided with this paper.

Code availability

The R scripts and Seurat objects are available on the GitHub page: https://github.com/mafeiyang/Canakinumab_LR-MDS.

References

- Balandrán, J. C., Lasry, A. & Aifantis, I. The role of inflammation in the initiation and progression of myeloid neoplasms. *Blood Cancer Discov.* **4**, 254–266 (2023).
- Ganan-Gomez, I. et al. Deregulation of innate immune and inflammatory signaling in myelodysplastic syndromes. *Leukemia* **29**, 1458–1469 (2015).
- Florez, M. A. et al. Clonal hematopoiesis: mutation-specific adaptation to environmental change. *Cell Stem Cell* **29**, 882–904 (2022).
- Hormaechea-Agulla, D. et al. Chronic infection drives Dnmt3a-loss-of-function clonal hematopoiesis via IFN γ signaling. *Cell Stem Cell* **28**, 1428–1442.e1426 (2021).
- Mayer-Barber, K. D. & Yan, B. Clash of the Cytokine Titans: counter-regulation of interleukin-1 and type I interferon-mediated inflammatory responses. *Cell Mol. Immunol.* **14**, 22–35 (2017).
- Martín-Sánchez, F. et al. Inflammasome-dependent IL-1 β release depends upon membrane permeabilisation. *Cell Death Differ.* **23**, 1219–1231 (2016).
- Weber, A., Wasiliew, P. & Kracht, M. Interleukin-1 (IL-1) pathway. *Sci. Signal.* **3**, cm1 (2010).
- Pietras, E. M. et al. Chronic interleukin-1 exposure drives haematopoietic stem cells towards precocious myeloid differentiation at the expense of self-renewal. *Nat. Cell Biol.* **18**, 607–618 (2016).
- Mitchell, C. A. et al. Stromal niche inflammation mediated by IL-1 signalling is a targetable driver of haematopoietic ageing. *Nat. Cell Biol.* **25**, 30–41 (2023).
- Svensson, E. C. et al. TET2-Driven clonal hematopoiesis and response to Canakinumab: an exploratory analysis of the CANTOS Randomized Clinical Trial. *JAMA Cardiol.* **7**, 521–528 (2022).
- McClatchy, J. et al. Clonal hematopoiesis related TET2 loss-of-function impedes IL1 β -mediated epigenetic reprogramming in hematopoietic stem and progenitor cells. *Nat. Commun.* **14**, 8102 (2023).
- Burns, S. S. et al. IL-1r1 drives leukemogenesis induced by Tet2 loss. *Leukemia* **36**, 2531–2534 (2022).
- Woo, J. et al. Effects of IL-1 β inhibition on anemia and clonal hematopoiesis in the randomized CANTOS trial. *Blood Adv.* **7**, 7471–7484 (2023).
- Mogilenko, D. A. et al. Comprehensive profiling of an aging immune system reveals clonal GZMK(+) CD8(+) T cells as conserved hallmark of inflammaging. *Immunity* **54**, 99–115.e112 (2021).
- Jonsson, A. H. et al. Granzyme K(+) CD8 T cells form a core population in inflamed human tissue. *Sci. Transl. Med.* **14**, eabo0686 (2022).
- Lasry, A. et al. An inflammatory state remodels the immune microenvironment and improves risk stratification in acute myeloid leukemia. *Nat. Cancer* **4**, 27–42 (2023).
- Efremova, M., Vento-Tormo, M., Teichmann, S. A. & Vento-Tormo, R. CellPhoneDB: inferring cell-cell communication from combined expression of multi-subunit ligand-receptor complexes. *Nat. Protoc.* **15**, 1484–1506 (2020).
- Hindy, G. et al. Increased soluble urokinase plasminogen activator levels modulate monocyte function to promote atherosclerosis. *J. Clin. Investig.* **132**. <https://doi.org/10.1172/jci158788> (2022).
- Rawat, K. et al. CCL5-producing migratory dendritic cells guide CCR5+ monocytes into the draining lymph nodes. *J. Exp. Med.* **220**. <https://doi.org/10.1084/jem.2022129> (2023).
- Ozga, A. J., Chow, M. T. & Luster, A. D. Chemokines and the immune response to cancer. *Immunity* **54**, 859–874 (2021).
- Luque-Martin, R. et al. IFN- γ drives human monocyte differentiation into highly proinflammatory macrophages that resemble a phenotype relevant to Psoriasis. *J. Immunol.* **207**, 555–568 (2021).
- Wimmer, N. et al. Lymphotoxin β receptor activation on macrophages induces cross-tolerance to TLR4 and TLR9 ligands. *J. Immunol.* **188**, 3426–3433 (2012).
- Ridker, P. M. et al. Antiinflammatory therapy with Canakinumab for Atherosclerotic Disease. *N. Engl. J. Med.* **377**, 1119–1131 (2017).
- Ridker, P. M. et al. Effect of interleukin-1 β inhibition with canakinumab on incident lung cancer in patients with atherosclerosis: exploratory results from a randomised, double-blind, placebo-controlled trial. *Lancet* **390**, 1833–1842 (2017).
- Greenberg, P. et al. International scoring system for evaluating prognosis in myelodysplastic syndromes. *Blood* **89**, 2079–2088 (1997).
- Greenberg, P. L. et al. Revised international prognostic scoring system for myelodysplastic syndromes. *Blood* **120**, 2454–2465 (2012).
- Bernard, E. et al. Molecular international prognostic scoring system for myelodysplastic syndromes. *NEJM Evid.* **1**, EV1-Doa2200008 (2022).
- Clough, C. A. et al. Coordinated missplicing of TMEM14C and ABCB7 causes ring sideroblast formation in SF3B1-mutant myelodysplastic syndrome. *Blood* **139**, 2038–2049 (2022).
- Winter, S. et al. Mutations in the splicing factor SF3B1 are linked to frequent emergence of HLA-DR(low/neg) monocytes in lower-risk myelodysplastic neoplasms. *Leukemia* **38**, 1427–1431 (2024).
- Schneider, M. et al. Activation of distinct inflammatory pathways in subgroups of LR-MDS. *Leukemia* **37**, 1709–1718 (2023).
- Basiorka, A. A. et al. The NLRP3 inflammasome functions as a driver of the myelodysplastic syndrome phenotype. *Blood* **128**, 2960–2975 (2016).
- Cluzeau, T. et al. Pro-inflammatory proteins S100A9 and tumor necrosis factor- α suppress erythropoietin elaboration in myelodysplastic syndromes. *Haematologica* **102**, 2015–2020 (2017).
- Kanagal-Shamanna, R. et al. Principles of analytical validation of next-generation sequencing based mutational analysis for hematologic neoplasms in a CLIA-certified laboratory. *Expert Rev. Mol. Diagn.* **16**, 461–472 (2016).
- Rodriguez-Sevilla, J. J. et al. Hematopoietic stem cells with granulomonocytic differentiation state overcome venetoclax sensitivity in patients with myelodysplastic syndromes. *Nat. Commun.* **15**, 2428 (2024).
- Stuart, T. et al. Comprehensive integration of single-cell data. *Cell* **177**, 1888–1902.e1821 (2019).
- Laurenti, E. et al. The transcriptional architecture of early human hematopoiesis identifies multilevel control of lymphoid commitment. *Nat. Immunol.* **14**, 756–763 (2013).
- Laurenti, E. et al. CDK6 levels regulate quiescence exit in human hematopoietic stem cells. *cell stem cell* **16**, 302–313 (2015).
- Velten, L. et al. Human haematopoietic stem cell lineage commitment is a continuous process. *Nat. Cell Biol.* **19**, 271–281 (2017).
- Belluschi, S. et al. Myelo-lymphoid lineage restriction occurs in the human haematopoietic stem cell compartment before lymphoid-primed multipotent progenitors. *Nat. Commun.* **9**, 4100 (2018).
- Zhou, Y. et al. Metascape provides a biologist-oriented resource for the analysis of systems-level datasets. *Nat. Commun.* **10**, 1523 (2019).
- Cheson, B. D. et al. Clinical application and proposal for modification of the International Working Group (IWG) response criteria in myelodysplasia. *Blood* **108**, 419–425 (2006).

Acknowledgements

This study was funded by Novartis (Basel, Switzerland). This work was supported by philanthropic contributions to MD Anderson's AML and

MDS Moon Shot Program and the Edward P. Evans Foundation. J.J.R.-S. is a recipient of MD Anderson's Odyssey Fellowship. This work used MD Anderson's South Campus Flow Cytometry and Cell Sorting Core Laboratory, ORION Core, and Sequencing and Microarray Facility, all of which are supported in part by the National Institutes of Health/National Cancer Institute through MD Anderson's Cancer Center Support Grant (P30 CA16672). The authors thank Joseph Munch for assistance with manuscript editing. We thank the patients who participated in this trial, their families, and the clinical and research staff at MD Anderson Cancer Center. The sponsor had no role in the study design, data collection interpretation, or manuscript writing.

Author contributions

J.J.R.-S., V.A., K.S.C., G.M.-B., H.Y., J.J., X.C., and K.B. collected and curated the clinical data. S.L. provided pathological interpretation of the clinical samples and correlative molecular data. G.G.-M. designed the clinical study. F.M. analyzed the scRNA-seq data. X.H. performed the biostatistical analyses. V.A. and S.C. designed and interpreted all biological studies. J.J.R.-S. and S.C. wrote the manuscript.

Competing interests

G.G.-M. declares research funding from Astex Pharmaceuticals, Novartis, Abbvie, BMS, Genentech, Aprea Therapeutics, Curis, Gilead Sciences; consulting fees from Astex Pharmaceuticals, Acceleron Pharma, and BMS; and payments or honoraria from Astex Pharmaceuticals, Acceleron Pharma, Abbvie, Novartis, Gilead Sciences, Curis, Genentech, and BMS. All other authors declare no competing interests.

Additional information

Supplementary information The online version contains supplementary material available at <https://doi.org/10.1038/s41467-024-54290-2>.

Correspondence and requests for materials should be addressed to Simona Colla.

Peer review information *Nature Communications* thanks Shahram Kordasti, Elena Torre, Hong Wang, and the other, anonymous, reviewer(s) for their contribution to the peer review of this work. A peer review file is available.

Reprints and permissions information is available at <http://www.nature.com/reprints>

Publisher's note Springer Nature remains neutral with regard to jurisdictional claims in published maps and institutional affiliations.

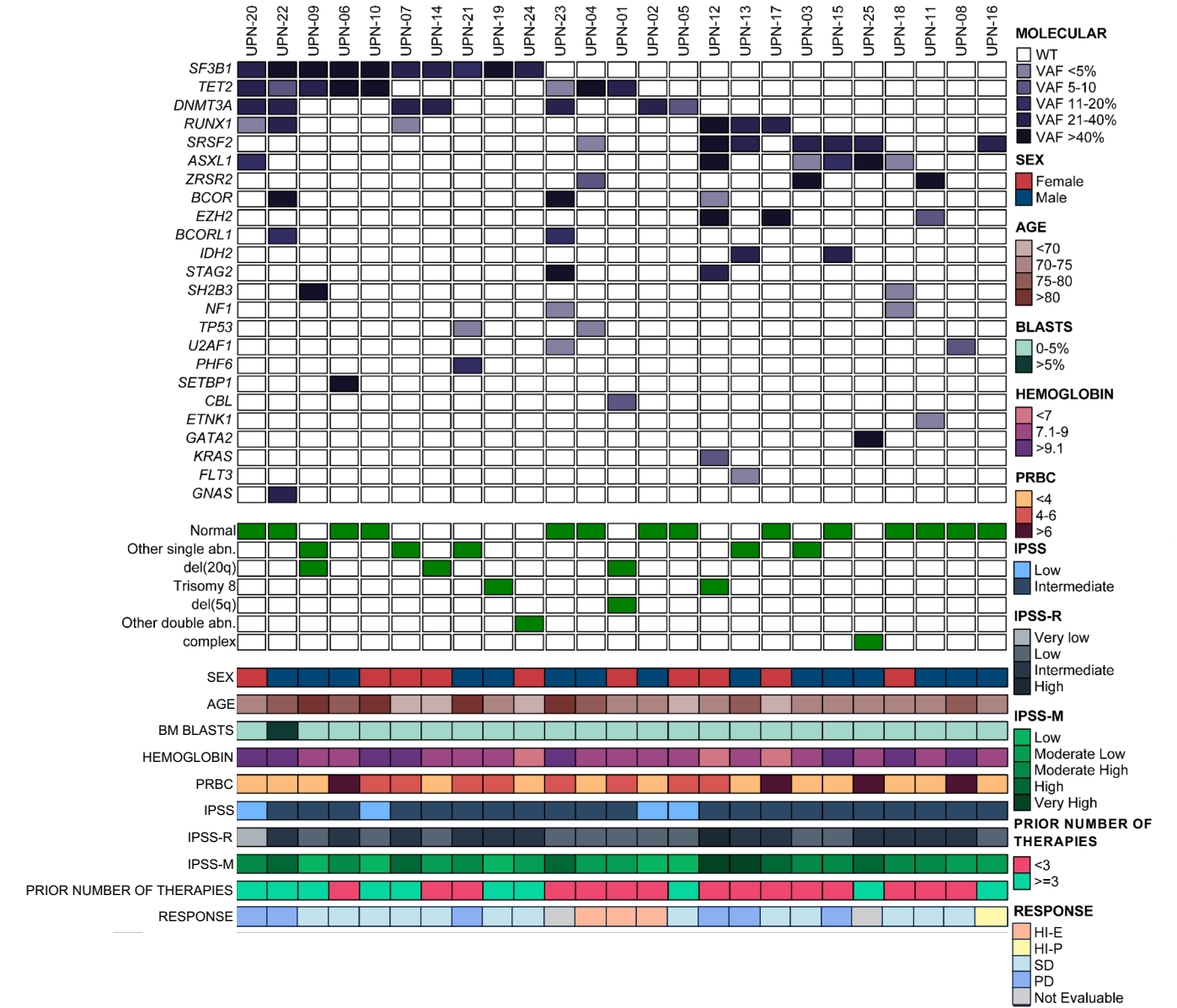
Open Access This article is licensed under a Creative Commons Attribution-NonCommercial-NoDerivatives 4.0 International License, which permits any non-commercial use, sharing, distribution and reproduction in any medium or format, as long as you give appropriate credit to the original author(s) and the source, provide a link to the Creative Commons licence, and indicate if you modified the licensed material. You do not have permission under this licence to share adapted material derived from this article or parts of it. The images or other third party material in this article are included in the article's Creative Commons licence, unless indicated otherwise in a credit line to the material. If material is not included in the article's Creative Commons licence and your intended use is not permitted by statutory regulation or exceeds the permitted use, you will need to obtain permission directly from the copyright holder. To view a copy of this licence, visit <http://creativecommons.org/licenses/by-nc-nd/4.0/>.

© The Author(s) 2024

Juan Jose Rodriguez-Sevilla^{1,6}, Vera Adema^{1,6}, Kelly S. Chien^{1,6}, Sanam Loghavi², Feiyang Ma³, Hui Yang¹, Guillermo Montalban-Bravo¹, Xuelin Huang⁴, Xavier Calvo⁵, Joby Joseph¹, Kristy Bodden¹, Guillermo Garcia-Manero¹ & Simona Colla¹✉

¹Department of Leukemia, The University of Texas MD Anderson Cancer Center, Houston, TX, USA. ²Department of Hematopathology, The University of Texas MD Anderson Cancer Center, Houston, TX, USA. ³Department of Molecular, Cell and Developmental Biology, University of California Los Angeles, Los Angeles, CA, USA. ⁴Department of Biostatistics, The University of Texas MD Anderson Cancer Center, Houston, TX, USA. ⁵Laboratori de Citologia Hematològica, Servei de Patologia, Grup de Recerca Translacional Neoplàsies Hematològiques (GRETNHE), Hospital del Mar Research Institute (IMIM), Barcelona, Spain. ⁶These authors contributed equally: Juan Jose Rodriguez-Sevilla, Vera Adema, Kelly S. Chien. ✉ e-mail: scolla@mdanderson.org

Supplementary Figure 1

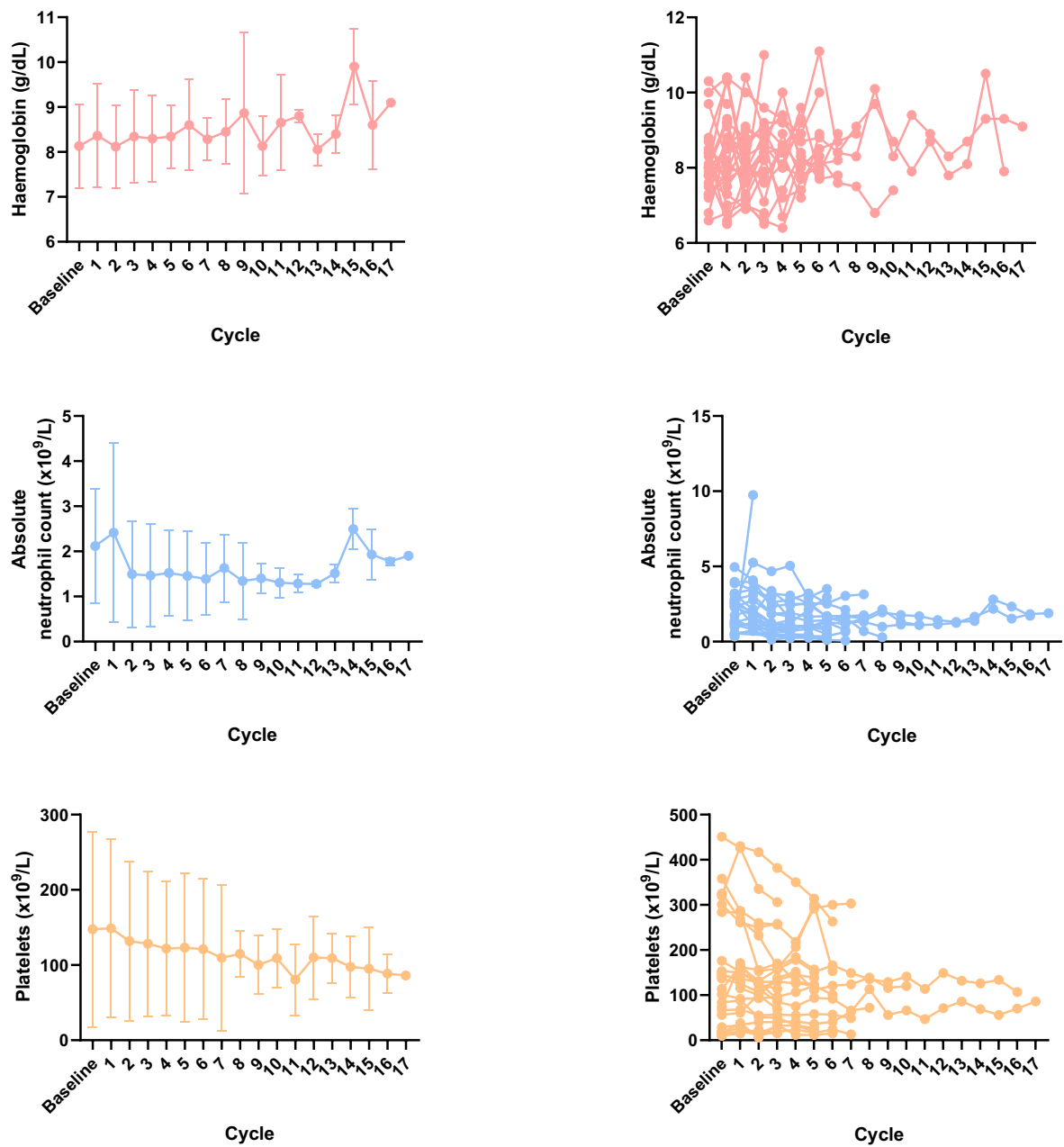


Supplementary Figure 1. Mutations and cytogenetic abnormalities of enrolled patients.

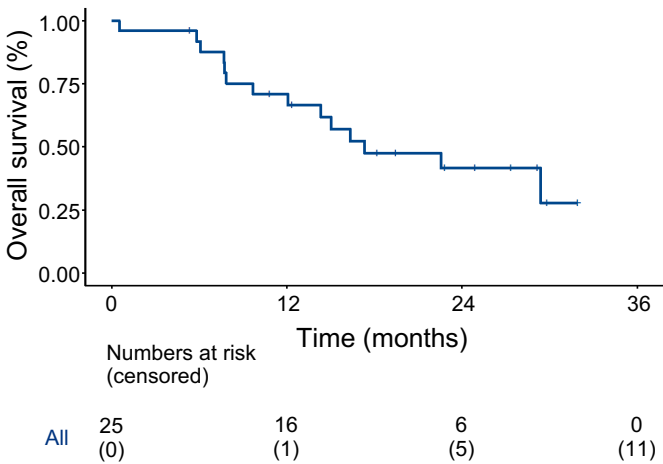
Oncoplot of the molecular landscapes, cytogenetic alterations, clinical characteristics, and canakinumab responses of the patients included in the clinical trial (n=25). Abn, abnormality; BM, bone marrow; HI-E, erythroid hematologic improvement; HI-P, platelet hematologic improvement; IPSS, International Prognostic Scoring System; IPSS-M, Molecular International Prognostic Scoring System; IPSS-R, Revised International Prognostic Scoring System; PD, progression disease; PRBC, packed red blood cell; SD, stable disease.

Supplementary Figure 2

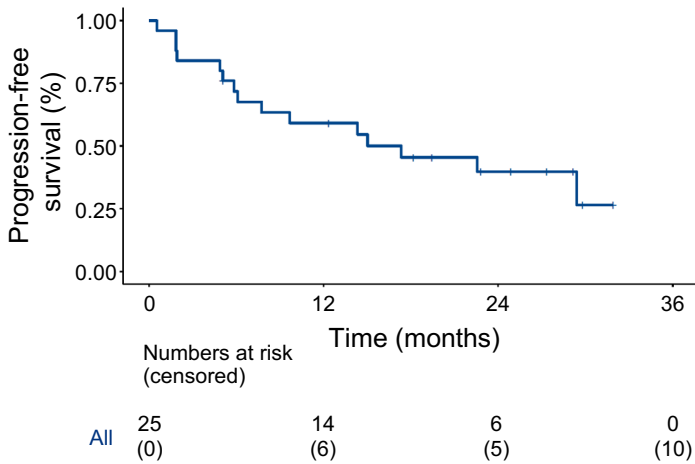
A



B



C



Supplementary Figure 2. Efficacy of canakinumab in lower-risk MDS patients.

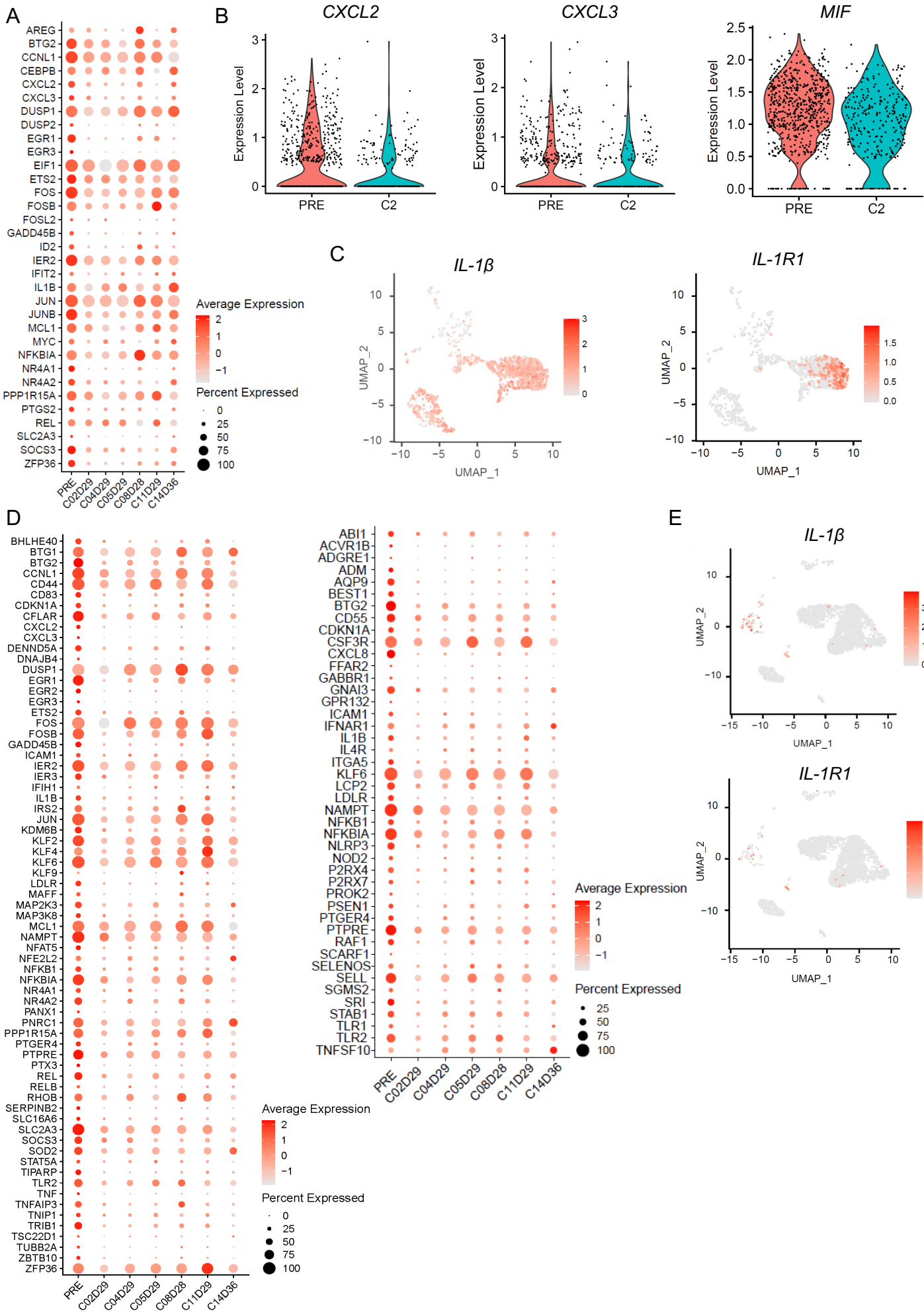
(A) Evolution of hematological parameters during canakinumab treatment. Shown are the median hemoglobin level (top), absolute neutrophil count (middle), and platelet count (bottom) for the entire population (left) and for each patient (right; n=25).

(B) Kaplan-Meier survival estimate curves for overall survival for the whole cohort (n=25).

(C) Kaplan-Meier survival estimate curves for progression-free survival for the whole cohort (n=25).

Source data are provided as a Source Data file.

Supplementary Figure 3



Supplementary Figure 3. Targeting the IL-1 β pathway overcomes ineffective erythropoiesis in lower-risk-MDS.

(A) Dot plot of the significantly expressed genes involved in TNF- α signaling through NF- κ B ($P \leq 0.05$) in HSCs obtained before and after canakinumab treatment, as shown in Figure 3B.

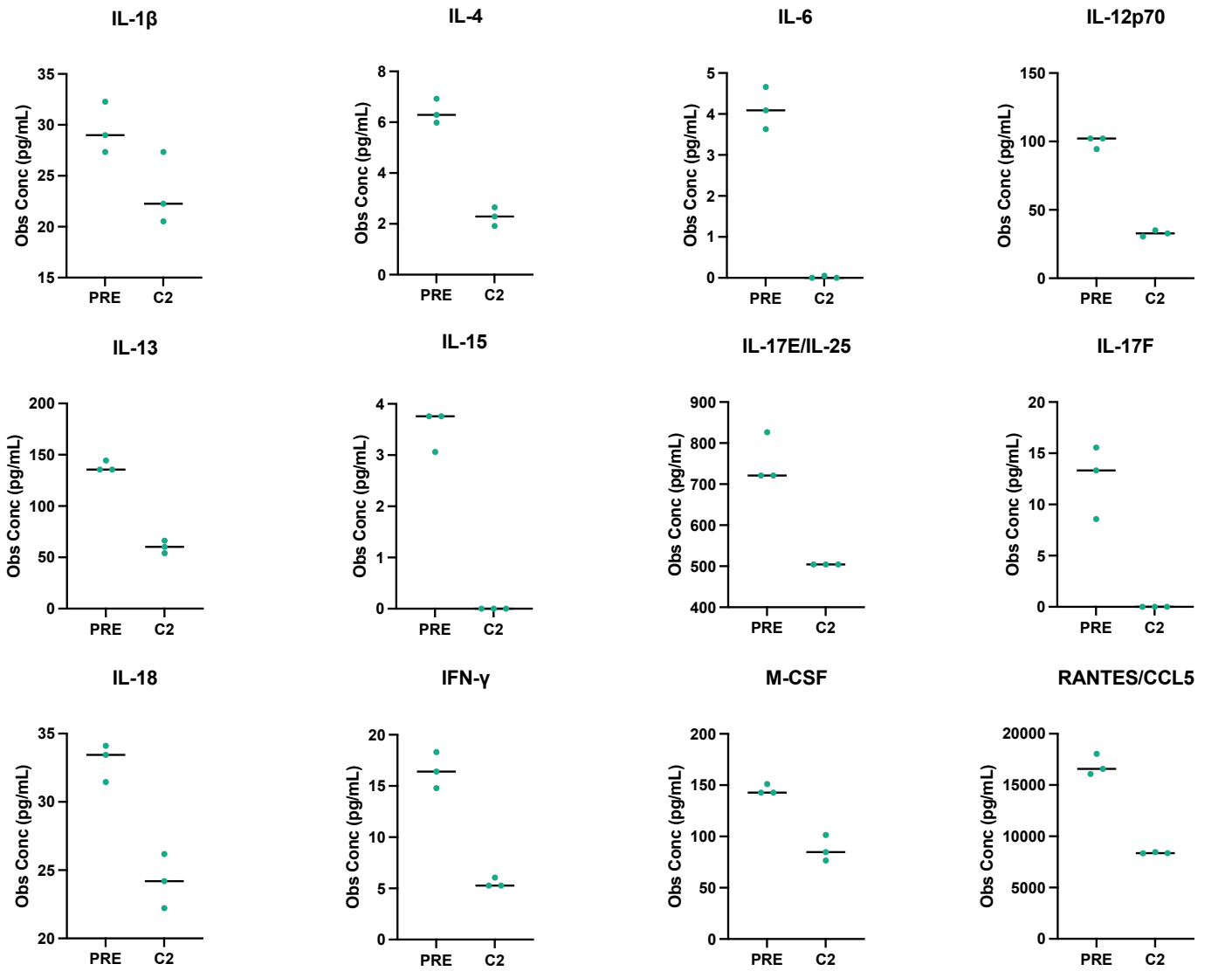
(B) *CXCL2*, *CXCL3*, and *MIF* expression in HSCs from patient UPN-02 before canakinumab treatment (PRE) and at the end of cycle 2 (C2) of canakinumab treatment. Each dot represents the expression level in a single cell ($P = 3.18 \times 10^{-10}$, 0.02, and 4.3×10^{-8} , respectively).

(C) Expression levels of *IL-1 β* (left) and *IL-1R1* (right) in Lin-CD34⁺ cells from patient UPN-02.

(D) Dot plot of the expression levels of genes involved in TNF- α signaling through NF- κ B (left) and inflammatory signaling (right) pathways that were significantly ($P \leq 0.05$) differentially expressed between monocytes (Figure 3E) obtained before and after cycle 2 (C2) of canakinumab treatment.

(E) Expression levels of *IL-1 β* (top) and *IL-1R1* (bottom) in BM MNCs from patient UPN-02 before canakinumab treatment.

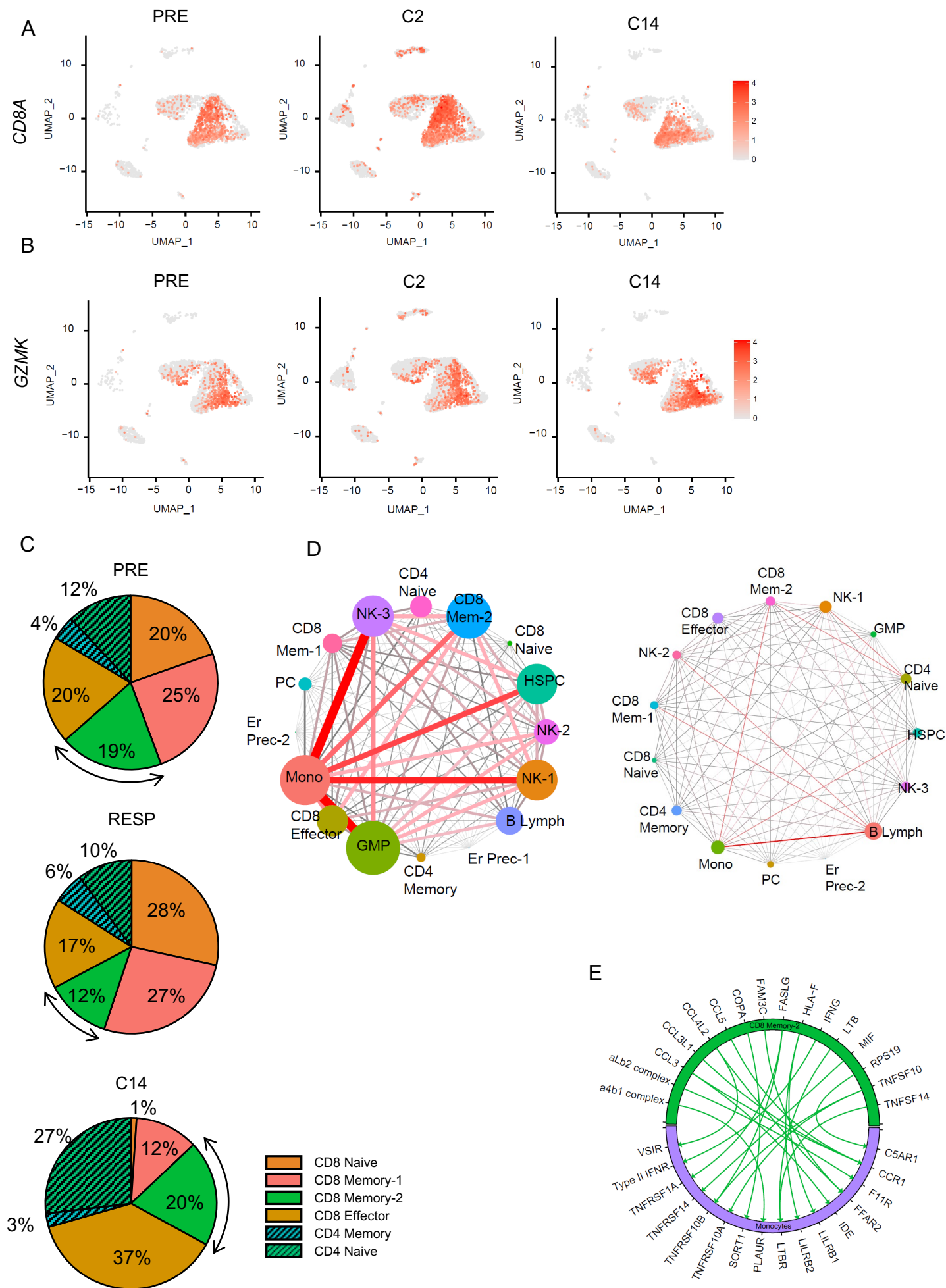
Supplementary Figure 4



Supplementary Figure 4. Decrease of BM pro-inflammatory cytokines during response to canakinumab treatment.

BM plasma concentrations (pg/mL) of the cytokines that were decreased after cycle 2 (C2) of canakinumab treatment in patient UPN-02. Technical replicate raw values are plotted. Lines represent the median. Source data are provided as a Source Data file.

Supplementary Figure 5



Supplementary Figure 5. Modulating the IL-1 β pathway changes the BM immune microenvironment.

(A) Expression levels of *CD8A* in MNCs isolated from the BM of patient UPN-02 before canakinumab treatment (PRE; left) and at the end of cycle 2 (C2; middle) and cycle 14 (C14; right) of canakinumab treatment.

(B) Expression levels of *GZMK* in MNCs isolated from patient UPN-02 before canakinumab treatment (PRE; left) and at the end of cycle 2 (C2; middle) and cycle 14 (C14; right) of canakinumab treatment.

(C) Cluster distribution of T-cell subtypes in the BM T-cell populations before canakinumab treatment (PRE; top) and at the time of response when the patient was transfusion-independent (cycles 2, 4, 5, 8, and 11) (middle) and cycle 14 (C14; bottom) of canakinumab treatment, represented as the percentage of cells in each cluster. Black arrows indicate T cells that represent the CD8⁺GZMK⁺ T-cell population. Clusters were grouped based on the cell lineage annotation. RESP, response.

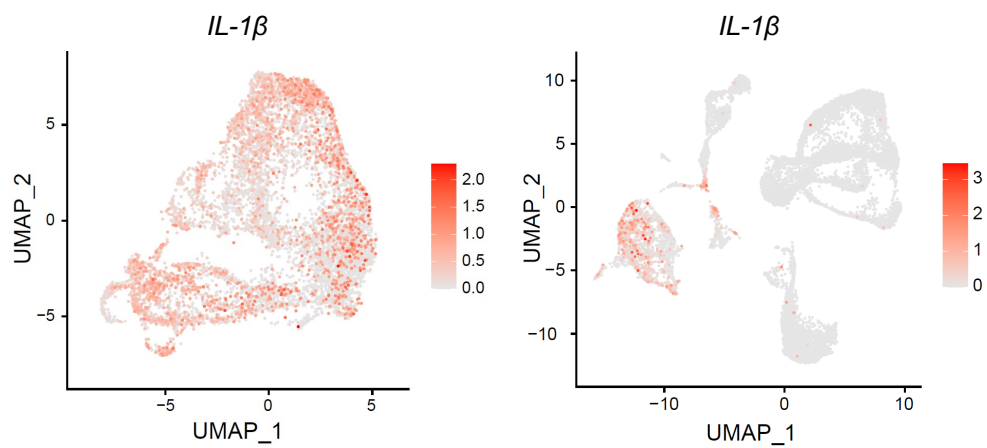
(D) Connectome web analysis of interacting cell types among MNCs isolated from the BM of patient UPN-02 before canakinumab treatment (left) and after 2 cycles of canakinumab treatment (right). The vertex size (i.e., colored cell node) is proportional to the number of interactions to and from each cell type, and the thickness of each connecting line is proportional to the number of interactions between 2 nodes. NK, natural killer; Mem, memory; PC, plasma cell; HSPC, hematopoietic stem and progenitor cell; Er, erythroid; Prec, precursor; Mono, monocytic; Lymph, lymphoid; GMP, granulo-monocytic progenitor.

(E) Circle plot showing the most significant ligand-to-receptor interactions between CD8⁺GZMK⁺ T cells and monocytes that were gained from before canakinumab treatment to the end of cycle 2 (C2) of canakinumab treatment.

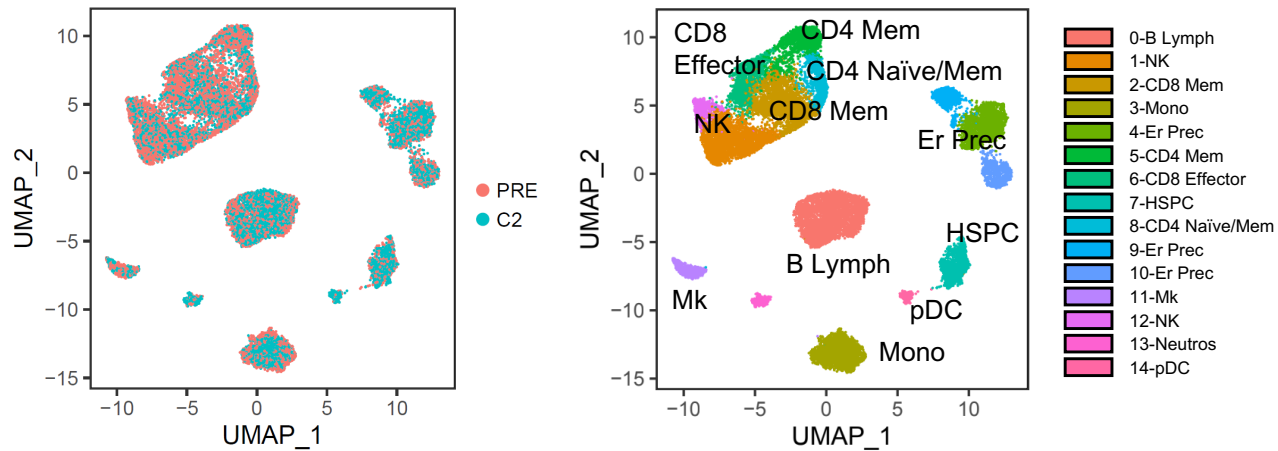
Source data are provided as a Source Data file.

Supplementary Figure 6

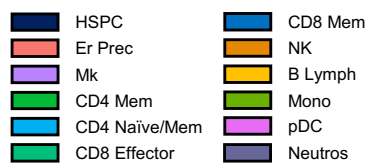
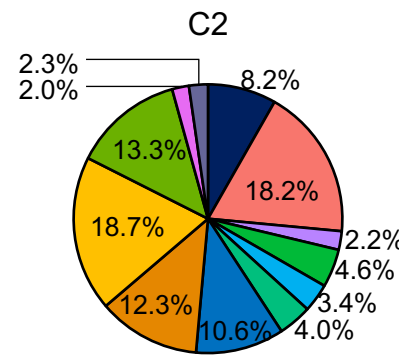
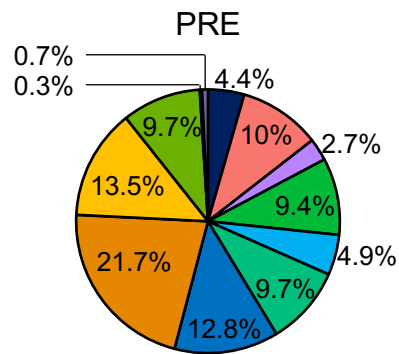
A



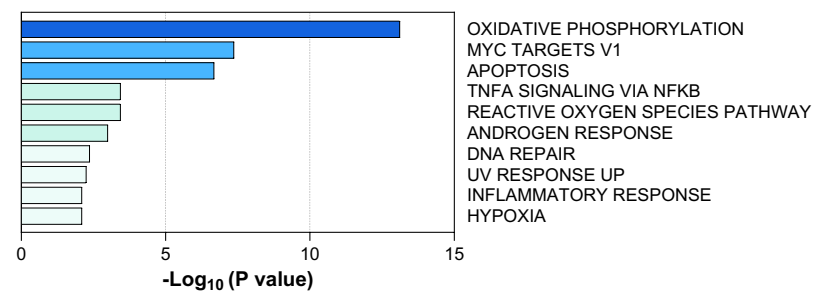
B



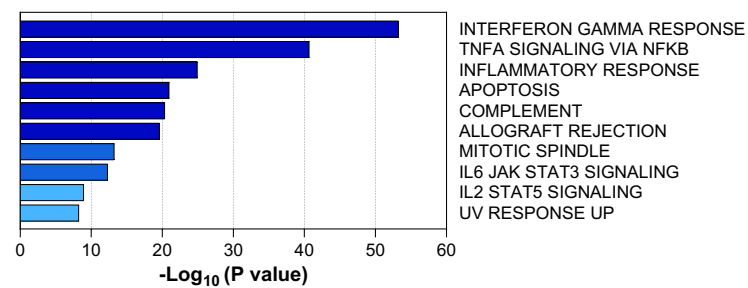
C



D



E



Supplementary Figure 6. Canakinumab treatment fails to rescue anemia in patients with MDS with *SF3B1* mutations.

(A) *IL-1 β* expression levels in Lin-CD34⁺ cells (left) and BM MNCs (right) from patients UPN-07 and UPN-14.

(B) UMAP plot of scRNA-seq data from BM MNCs isolated from UPN-12 and UPN-20 patients before canakinumab treatment (PRE; n = 9,798) and after 2 cycles (C2) of canakinumab treatment (n = 11,249). Each dot represents one cell. Different colors represent the sample (left) and cluster (right) identities. Er, erythroid; Prec, precursor; NK, natural killer; Mk, megakaryocytic; Mem, memory; Neutros, neutrophils; HSPC, hematopoietic stem and progenitor cell; Mono, monocytic; Lymph, lymphoid; pDC, plasmacytoid dendritic cells.

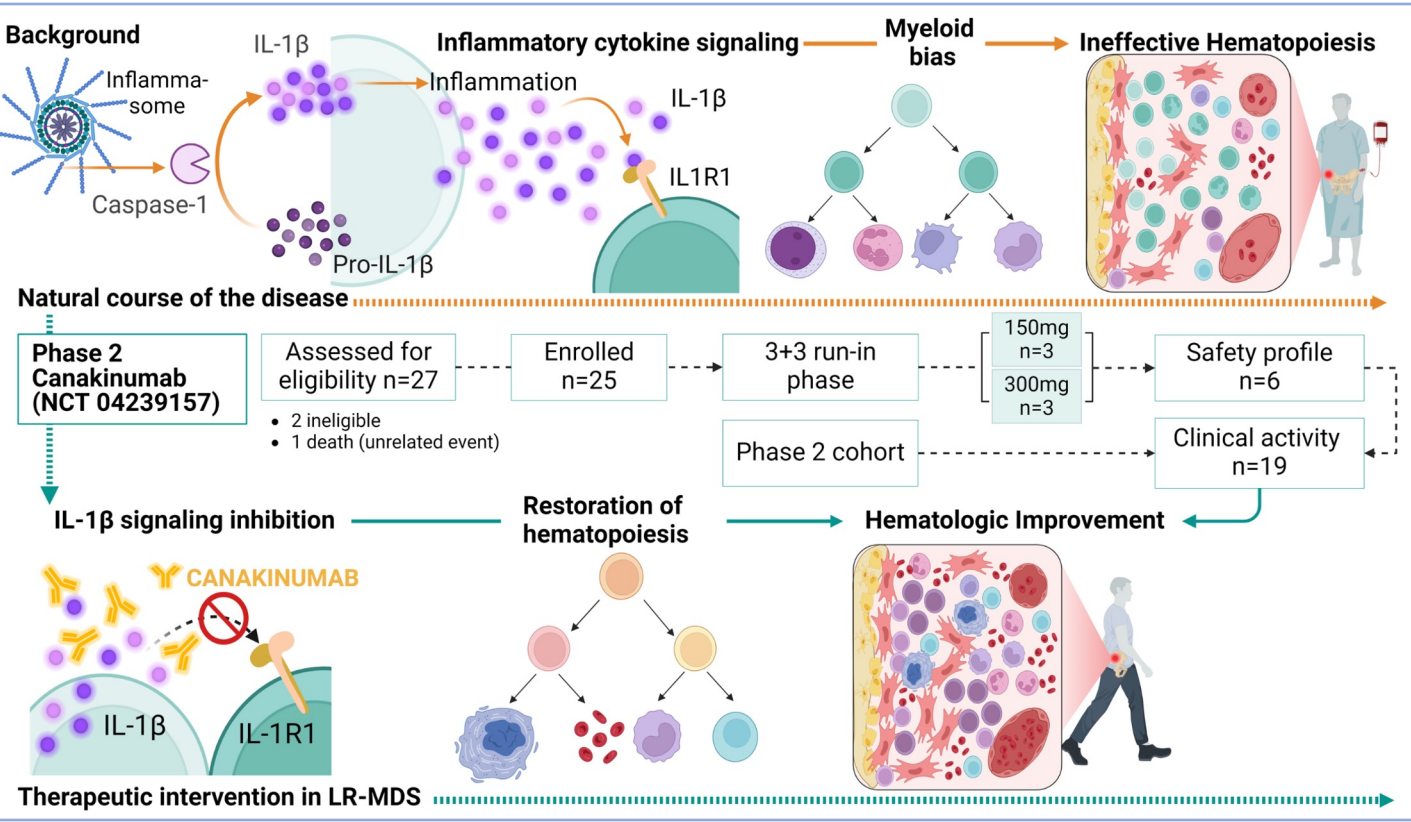
(C) Cluster distribution of BM MNCs before canakinumab treatment (PRE) and at the end of cycle 2 (C2) of canakinumab treatment, represented as the percentage of cells in each cluster shown in Supplementary Figure 6B. Clusters were grouped based on the cell lineage annotation. HSPC, hematopoietic stem and progenitor cell; Mk, megakaryocytic; GMP, granulo-monocytic progenitor; Mono, monocytic; Er, erythroid; Prec, precursor; NK, natural killer; Lymph, lymphoid; pDC, plasmacytoid dendritic cells; Neutros, neutrophils.

(D) Pathway enrichment analysis of genes significantly ($FDR < 0.05$) downregulated in HSPCs from patients UPN-12 and UPN-20 at the end of cycle 2 of canakinumab treatment compared with those in HSPCs before canakinumab treatment. The top 10 Hallmark gene sets are shown.

(E) Pathway enrichment analysis of genes significantly ($FDR < 0.05$) downregulated in monocytes from patients UPN-12 and UPN-20 at the end of cycle 2 of canakinumab treatment compared with those in monocytes before canakinumab treatment. The top 10 Hallmark gene sets are shown.

Source data are provided as a Source Data file.

Supplementary Figure 7



Supplementary Figure 7. Proposed working model.

Inflammatory signaling mediated by the overexpression of IL-1 β drives aberrant differentiation in early-stage MDS. Canakinumab, targeting the IL-1 β -mediated pathway, rescued ineffective erythropoiesis in lower-risk MDS patients with lower genetic complexity.

Created in BioRender. "Rodriguez-Sevilla JJ*, Adema V*, Chien K*, ..., Colla S."
<https://BioRender.com/t63n194>".

Supplementary Table 1. Baseline characteristics of the patients (n=25) enrolled in the canakinumab trial.

Patient ID	Diagnosis	WHO 2022	BM blasts (%)	Hb (g/dL)	ANC (x10 ⁹ /L)	Platelets (x10 ⁹ /L)	Karyotype	Somatic mutations* (VAF%)	Response to Canakinumab	Previous treatments	HMA resistance	scRNA-seq***
UPN-01	MDS with isolated del(5q)	MDS-5q	2	8.5	1.08	52	46,XX,del(5q)(q11.2q33),del(20)(q11.2q13.3)[12]	<i>TET2</i> c.3954+1G>T (26), <i>CBL</i> T402_S403del (10)	HI-E & HI-P	Oral Cedazuridine/decitabine, Lenalidomide low dose	Secondary	
UPN-02	MDS-MLD	MDS-LB	2	7.5	2.75	154	46,XY[18]	<i>DNMT3A</i> P743S (33)	HI-E	ESA, dexamethasone	-	
UPN-03	MDS-MLD	MDS-LB	2	7.3	1.48	126	46,XY,del(12)(p13p11.2)[13]/46,XY[7]	<i>ZRSR2</i> S40* (80), <i>SRSF2</i> P95L (29), <i>ASXL1</i> E635fs*14 (5)	SD	ESA	-	
UPN-04	MDS-MLD	MDS-LB	2	7.3	1.12	101	46,XY[20]	<i>TET2</i> T730fs*21, Y1245fs*22, R1261H (66, 14, 6), <i>ZRSR2</i> C172fs*66 K16fs*4 (10, 10), <i>SRSF2</i> P96A (3), <i>TP53</i> R273L (1)	HI-E	Decitabine	Secondary	
UPN-05	MDS-MLD (MF-2)	MDS-f	1	6.8	2.81	358	46,XX[9]	<i>DNMT3A</i> Y660C (8)	SD	ESA, Decitabine, Luspatercept	Primary	
UPN-06	MDS-RS-MLD	MDS- <i>SF3B1</i>	4	8.2	2.76	21	46,XY[20]	<i>SF3B1</i> K700E (51), <i>TET2</i> D1640fs*55 (46), <i>SETBP1</i> G870S (45)	SD	Decitabine, Luspatercept	Primary	
UPN-07	MDS-RS-MLD	MDS- <i>SF3B1</i>	1	8.1	3.75	60	46,XX,t(1;3)(p36.1;q21)[18]/46,XX[2]	<i>SF3B1</i> K700E (37), <i>DNMT3A</i> P624fs*26 (33), <i>RUNX1</i> T234fs*3 (3)	SD	Oral Cedazuridine/decitabine, alloSCT, Decitabine, post alloSCT	Secondary	
UPN-08	MDS-MLD	MDS-LB	1	8.1	0.56	16	46,XY[20]	<i>U2AF1</i> S34F (9)	SD	Decitabine	Primary	

UPN-09	MDS-RS-SLD	MDS-SF3BI	2	8.5	3.96	430	46,XY,del(20)(q11.2q13.3)[19]/46,idem,del(9)(p12)[1]	<i>SH2B3</i> c.1023_1024insA (63), <i>SF3BI</i> K700E (47), <i>TET2</i> K982fs*25 (11)	SD	ESA, Decitabine, Luspatercept	Secondary	
UPN-10	MDS-RS-MLD	MDS-SF3BI	3	9.2	1.42	283	46,XX[20]	<i>SF3BI</i> H662Y (47) <i>TET2</i> E782*, T1093fs*12, G1316S, N1387T, Q1654fs*6 (43, 12, 5, 3, 1)	SD	Decitabine, ESA, Luspatercept	Secondary	
UPN-11	MDS-MLD	MDS-LB	3	8.5	0.55	140	46,XY[20]	<i>ZRSR2</i> H325fs*15 (66), <i>EZH2</i> c.118-2del (7), <i>ETNK1</i> G156D (2)	SD	Azacitidine	Secondary	
UPN-12	MDS-MLD	MDS-LB	4	8.4	3.15	19	47,XX,+8[2]/46,XX[18]	<i>RUNX1</i> Y140fs*4, A142fs*2 (44, 42), <i>ASXL1</i> I814fs*4 (43), <i>EZH2</i> H279R (42), <i>SRSF2</i> P95R (41), <i>STAG2</i> K917fs*2 (37), <i>KRAS</i> A18D (8), <i>BCOR</i> L371fs (2)	PD	Azacitidine, Daptomycin	Primary	
UPN-13	MDS-SLD	MDS-LB	2	8.4	1.74	325	46,XY,i(14)(q10)[10]/46,XY[1]	<i>IDH2</i> R140Q (38), <i>SRSF2</i> P95H (36), <i>RUNX1</i> S388* (33), <i>FLT3</i> D835H (5)	PD	Azacitidine, Enasidenib	Secondary	
UPN-14	MDS-RS-MLD	MDS-SF3BI	5	7.8	2.06	113	46,XX,del(20)(q11.2q13.3)[13]/46,XX[7]	<i>DNMT3A</i> P904L (39), <i>SF3BI</i> K700E (38)	SD	ESA, Luspatercept	-	
UPN-15	MDS-RS-MLD	MDS-LB	3	9.5	1.38	157	46,XY[16]	<i>SRSF2</i> P95_R102del (25), <i>IDH2</i> R140Q (24), <i>ASXL1</i> G646fs*11 (17)	PD	ESA	-	
UPN-16	MDS-RS-MLD	MDS-LB	2	8.5	2.57	86	46,XY[20]	<i>SRSF2</i> P95R (35%)**	HI-P	ESA + Lenalidomide, Azacitidine, Luspatercept	Primary	

UPN-17	TR-MDS-MLD	MDS-LB	3	6.6	2.64	84	46,XX[20]	<i>EZH2</i> c.1852-1G>A (83), <i>RUNX1</i> c.57_58del (34)	SD	Decitabine	Primary	
UPN-18	MDS-MLD	MDS-LB	3	8.4	0.49	20	46,XX[13]	<i>ASXL1</i> E727* (5), <i>NFI</i> c.2251G>C (4), <i>SH2B3</i> S256fs*12 (2)	SD	Oral Decitabine	Secondary	
UPN-19	MDS-RS-MLD	MDS- <i>SF3B1</i>	1	7.3	1.98	426	47,XY,+8[20]	<i>SF3B1</i> K700E (41)	SD	ESA, oral Decitabine, Azacitidine, Promacta, Luspatercept	Primary	
UPN-20	MDS-RS-MLD	MDS- <i>SF3B1</i>	2	8.8	1.28	143	46,XX[20]	<i>TET2</i> L1621fs*38 (39), <i>DNMT3A</i> P904L (38), <i>SF3B1</i> K700E (35), <i>ASXL1</i> G646fs*11 (18), <i>RUNX1</i> T358fs*242 (1)	PD	ESA, Azacitidine, Luspatercept	Primary	
UPN-21	MDS-RS-MLD	MDS- <i>SF3B1</i>	1	7.1	1.52	129	46,XY,del(13)(q12q14)[2]/46,XY[4]	<i>SF3B1</i> K666T (19), <i>PHF6</i> Q7* (13), <i>TP53</i> H179L (3)	PD	ESA, Luspatercept	-	
UPN-22	MDS-RS-MLD	MDS- <i>SF3B1</i>	4	9.1	1.45	174	46,XY[20]	<i>SF3B1</i> K700E (46), <i>BCOR</i> L1612fs*6 (44), <i>DNMT3A</i> R882H (39), <i>GNAS</i> R201H (25), <i>RUNX1</i> P384fs*217 (23), <i>TET2</i> c.3501-2A>G(9), <i>BCORLI</i> Q1001fs*5, Q1156fs*5, Y502*, Y1520* (17, 6, 6, 5)	PD	Azacitidine, Procrit, Luspatercept	Primary	
UPN-23 ⁺	MDS-MLD	MDS-LB	1	8.5	0.38	31	46,XY[20]	<i>BCOR</i> c.4326+1g>A (86), <i>STAG2</i> S202* (84), <i>U2AF1</i> S34F (44), <i>DNMT3A</i> R882C (30), <i>BCORLI</i>	Not evaluable	Azacitidine	Primary	

UPN-24	MDS-RS-SLD	MDS-SF3BI	1	7.8	3.88	130	46,XX,+1,der(17)(q10;p10)[20]	L1605fs*43 (16), NF1 R2258* (4), TET2 S1290fs*11 (2)	SD	ESA, Luspatercept, Azacitidine	Secondary	
UPN-25 [†]	MDS/MPN-RS-T	MDS-SF3BI	2	7.7	1.9	130	47,XY,del(12)(p11.2),+19[17]/48,ide m,+21[2]/46,XY[1]	ASXL1 G1198fs*20 (45), GATA2 R396W (43), SRSF2 P95L (34)	Not evaluable	Oral Decitabine, Lenalidomide, Luspatercept, CA4948	Primary	

EB: excess of blasts; ESA: erythropoietin stimulating agent; F: female; HI-E: erythroid hematological improvement; HI-P: platelet hematological improvement; IPSS: International Prognostic Scoring System; IPSS-R: Revised-IPSS; M: male; MDS: myelodysplastic syndromes; MF: myelofibrosis; MLD: multilineage dysplasia; MPN: myeloproliferative neoplasms; PD: progressive disease; RS: ringed sideroblasts; SD: stable disease; TR: treatment-related.

*81 gene panel of the most mutated genes in myeloid neoplasia.

**SRSF2 mutation identified as unique somatic mutation 37.1 months before treatment with canakinumab and after 14 days 7.5, and 13.7 months of treatment with canakinumab (VAFs: 40%, 31%, and 44%)

*** scRNA-seq includes Lin⁺CD34⁺ and BM MNCs.

[†] Response assessment in patients UPN-23 and UPN-25 was not available owing to the patient's inability to complete a minimum of two cycles and obtain a bone marrow aspiration due to extended recovery time from a trochanteric fracture in one patient and early death in the other, respectively.

^{††} Dose finding run-in phase

UPN-05 was reclassified as MDS/MPN, not otherwise specified, at 4.6 months after canakinumab initiation. Bone marrow analysis at the time of clinical trial enrollment revealed dyserythropoiesis, with peripheral blood showing anemia and mild leukocytosis (10.5 x10⁹/L), leading to the initial diagnosis of MDS-f. However, the patient developed significant thrombocytosis (824 x10⁹/L) and leukocytosis (13.7 x10⁹/L), leading to repeat bone marrow analysis and consequent reclassification to MDS/MPN, not otherwise specified.

Supplementary Table 2. Summary of baseline mutations before canakinumab treatment.

Patient ID	Gene	NM	cDNA	AA change	VAF (%)
UPN-01	<i>TET2</i>	NM_001127208.2	c.3954+1G>T	p.?	26
UPN-01	<i>CBL</i>	NM_005188.4	c.1204_1209del	p.T402_S403del	10
UPN-02	<i>DNMT3A</i>	NM_022552.4	c.2227C>T	p.P743S	33
UPN-03	<i>ZRSR2</i>	NM_005089.3	c.119C>G	p.S40*	80
UPN-03	<i>SRSF2</i>	NM_003016.4	c.284C>T	p.P95L	29
UPN-03	<i>ASXL1</i>	NM_015338.6	c.1900_1922del	p.E635fs*14	5
UPN-04	<i>TET2</i>	NM_001127208.2	c.2188del	p.T730fs*21	66
UPN-04	<i>TET2</i>	NM_001127208.2	c.3732_3733del	p.Y1245fs*22	14
UPN-04	<i>ZRSR2</i>	NM_005089.3	c.515del	p.C172fs*66	10
UPN-04	<i>ZRSR2</i>	NM_005089.3	c.46_47insGGCCGCCCTGA	p.K16fs*4	10
UPN-04	<i>TET2</i>	NM_001127208.2	c.3782G>A	p.R1261H	6
UPN-04	<i>SRSF2</i>	NM_003016.4	c.286C>G	p.P96A	3
UPN-04	<i>TP53</i>	NM_000546.5	c.818G>T	p.R273L	1
UPN-05	<i>DNMT3A</i>	NM_022552.4	c.1979A>G	p.Y660C	8
UPN-06	<i>SF3B1</i>	NM_012433.3	c.2098A>G	p.K700E	51
UPN-06	<i>TET2</i>	NM_00112720	c.4919del	p.D1640fs*55	46
UPN-06	<i>SETBP1</i>	NM_015559.3	c.2608G>A	p.G870S	45
UPN-07	<i>SF3B1</i>	NM_012433.3	c.2098A>G	p.K700E	37
UPN-07	<i>DNMT3A</i>	NM_022552.4	c.1871_1874del	p.P624fs*26	33
UPN-07	<i>RUNX1</i>	NM_001754.4	c.701del	p.T234fs*3	3
UPN-08	<i>U2AF1</i>	NM_006758.2	c.101C>T	p.S34F	9
UPN-09	<i>SH2B3</i>	NM_005475.3	c.1023_1024insA	p.?	63
UPN-09	<i>SF3B1</i>	NM_012433.3	c.2098A>G	p.K700E	47
UPN-09	<i>TET2</i>	NM_00112720	c.2943del	p.K982fs*25	11
UPN-10	<i>SF3B1</i>	NM_012433.3	c.1984C>T	p.H662Y	47
UPN-10	<i>TET2</i>	NM_001127208.2	c.2344G>T	p.E782*	43
UPN-10	<i>TET2</i>	NM_001127208.2	c.3278_3281del	p.T1093fs*12	12
UPN-10	<i>TET2</i>	NM_001127208.2	c.4081G>A	p.G1361S	5
UPN-10	<i>TET2</i>	NM_001127208.2	c.4160A>C	p.N1387T	3
UPN-10	<i>TET2</i>	NM_001127208.2	c.4959_4960del	p.Q1654fs*6	1
UPN-11	<i>ZRSR2</i>	NM_005089.3	c.969_972dupAAAG	p.H325fs*15	66
UPN-11	<i>EZH2</i>	NM_004456.5	c.118-2del	p.?	7
UPN-11	<i>ETNK1</i>	NM_018638.5	c.467G>A	p.G156D	2
UPN-12	<i>RUNX1</i>	NM_001754.4	c.419_422del	p.Y140fs*4	44
UPN-12	<i>ASXL1</i>	NM_015338.6	c.2439del	p.I814fs*4	43
UPN-12	<i>RUNX1</i>	NM_001754.4	c.423_424insA	p.A142fs*2	42
UPN-12	<i>EZH2</i>	NM_004456.5	c.836A>G	p.H279R	42
UPN-12	<i>SRSF2</i>	NM_003016.4	c.284C>G	p.P95R	41
UPN-12	<i>STAG2</i>	NM_006603.5	c.2747_2748insCTTA	p.K917fs*2	37
UPN-12	<i>KRAS</i>	NM_004985.5	c.53C>A	p.A18D	8
UPN-12	<i>BCOR</i>	NM_017745.6	c.1112delinsGTTCTC	p.L371fs	2
UPN-13	<i>IDH2</i>	NM_002168.3	c.419G>A	p.R140Q	38
UPN-13	<i>SRSF2</i>	NM_003016.4	c.284C>A	p.P95H	36
UPN-13	<i>RUNX1</i>	NM_001754.4	c.1163C>A	p.S388*	33
UPN-13	<i>FLT3</i>	NM_004119.3	c.2503G>C	p.D835H	5

UPN-14	<i>DNMT3A</i>	NM_022552.4	c.2711C>T	p.P904L	39
UPN-14	<i>SF3B1</i>	NM_012433.3	c.2098A>G	p.K700E	38
UPN-15	<i>SRSF2</i>	NM_003016.4	c.284_307del	p.P95_R102del	25
UPN-15	<i>IDH2</i>	NM_002168.3	c.419G>A	p.R140Q	24
UPN-15	<i>ASXL1</i>	NM_015338.6	c.1934dupG	p.G646fs*11	17
UPN-16	<i>SRSF2</i>	NM_003016.4	c.284C>G	p.P95R	35
UPN-17	<i>EZH2</i>	NM_004456.5	c.1852-1G>A	p.?	83
UPN-17	<i>RUNX1</i>	NM_001754.4	c.57_58del	p.?	34
UPN-18	<i>ASXL1</i>	NM_015338.6	c.2179G>T	p.E727*	5
UPN-18	<i>NF1</i>	NM_001042492.3	c.2251G>C	p.?	4
UPN-18	<i>SH2B3</i>	NM_005475.3	c.765dupC	p.S256fs*12	2
UPN-19	<i>SF3B1</i>	NM_012433.3	c.2098A>G	p.K700E	41
UPN-20	<i>TET2</i>	NM_001127208.2	c.4862_4866del	p.L1621fs*38	39
UPN-20	<i>DNMT3A</i>	NM_022552.4	c.2711C>T	p.P904L	38
UPN-20	<i>SF3B1</i>	NM_012433.3	c.2098A>G	p.K700E	35
UPN-20	<i>ASXL1</i>	NM_015338.6	c.1934dupG	p.G646fs*11	18
UPN-20	<i>RUNX1</i>	NM_001754.4	c.1070dupC	p.T358fs*242	1
UPN-21	<i>SF3B1</i>	NM_012433.3	c.1997A>C	p.K666T	19
UPN-21	<i>PHF6</i>	NM_032458.3	c.19C>T	p.Q7*	13
UPN-21	<i>TP53</i>	NM_000546.5	c.536A>T	p.H179L	3
UPN-22	<i>SF3B1</i>	NM_012433.3	c.2098A>G	p.K700E	46
UPN-22	<i>BCOR</i>	NM_017745.6	c.4834dupC	p.L1612fs*6	44
UPN-22	<i>DNMT3A</i>	NM_022552.4	c.2645G>A	p.R882H	39
UPN-22	<i>GNAS</i>	NM_000516.6	c.602G>A	p.R201H	25
UPN-22	<i>RUNX1</i>	NM_001754.4	c.1145_1148dupCGCC	p.P384fs*217	23
UPN-22	<i>BCORL1</i>	NM_021946.4	c.3001dupC	p.Q1001fs*5	17
UPN-22	<i>TET2</i>	NM_00112720	c.3501-2A>G	p.?	9
UPN-22	<i>BCORL1</i>	NM_021946.4	c.3466dupC	p.Q1156fs*60	6
UPN-22	<i>BCORL1</i>	NM_021946.4	c.1505_1506insGGACCCA	p.Y502*	6
UPN-22	<i>BCORL1</i>	NM_021946.4	c.4560C>G	p.Y1520*	5
UPN-23	<i>BCOR</i>	NM_017745.6	c.4326+1G>A	p.?	86
UPN-23	<i>STAG2</i>	NM_006603.5	c.605C>A	p.S202*	84
UPN-23	<i>U2AF1</i>	NM_006758.2	c.101C>T	p.S34F	44
UPN-23	<i>DNMT3A</i>	NM_022552.4	c.2644C>T	p.R882C	30
UPN-23	<i>BCORL1</i>	NM_021946.4	c.4813dupC	p.L1605fs*43	16
UPN-23	<i>NF1</i>	NM_00104249	c.6772C>T	p.R2258*	4
UPN-23	<i>TET2</i>	NM_001127208.2	c.3868_3869insGGGT	p.S1290fs*11	2
UPN-24	<i>SF3B1</i>	NM_012433.3	c.2098A>G	p.K700E	39
UPN-25	<i>ASXL1</i>	NM_015338.6	c.3591_3592dupTG	p.G1198fs*20	45
UPN-25	<i>GATA2</i>	NM_032638.5	c.1186C>T	p.R396W	43
UPN-25	<i>SRSF2</i>	NM_003016.4	c.284C>T	p.P95L	34

Supplementary Table 3. Bone marrow count or morphological changes observed during canakinumab treatment.

Patient ID	Time point	Cellularity	Blasts (%)	Erythroblasts (%)	Monocytes (%)	ME ratio	Dysplasia
UPN-01	baseline	40	2	47	1	0.7	GEM
UPN-01	response	40	1	40	2	1	GM
UPN-02	baseline	85	2	12	4	6.6	GM
UPN-02	response	60	1	32	2	2	GEM
UPN-02	LOR	NA	NA	NA	NA	NA	NA
UPN-03	baseline	85	2	18	2	4	GEM
UPN-03	C2	NA	1	14	8	5.4	GE (unable to assess M)
UPN-03	C5	65	3	24	6	3	GEM
UPN-04	baseline	70	2	39	1	1	GEM
UPN-04	C2	60	3	9	8	9.5	GEM
UPN-04	C5	45	2	6	1	12	GEM
UPN-05	baseline	95	Unable to assess	Unable to assess	Unable to assess	Unable to assess	M (unable to assess E and G)
UPN-05	C2	Unable to assess	Unable to assess	Unable to assess	Unable to assess	Unable to assess	Unable to assess
UPN-05	C5	Unable to assess	Unable to assess	Unable to assess	Unable to assess	Unable to assess	Unable to assess
UPN-06	baseline	80	4	58	1	0.5	GEM
UPN-06	C2	85	3	67	2	0.4	EM
UPN-06	C5	90	2	59	1	0.4	GEM
UPN-07	baseline	45	1	3	14	21.5	GM
UPN-07	C2	60	1	5	7	15.7	GM
UPN-07	C5	10	0	7	2	9.6	G (unable to assess E and M)
UPN-08	baseline	10	1	16	5	1.2	Minimal GE
UPN-08	C2	5	0	8	8	6.8	GE (unable to assess M)
UPN-08	C5	30	1	28	3	1.9	Minimal GE (unable to assess M)
UPN-09	baseline	85	2	56	2	0.7	EM
UPN-09	C2	75	1	40	2	1.3	EM
UPN-09	C5	95	1	45	2	1.1	EM
UPN-10	baseline	80	3	64	3	0.5	GEM
UPN-10	C2	65	1	34	2	1.6	GEM
UPN-11	baseline	40	3	32	2	1.5	GEM
UPN-11	C2	30	4	43	2	1.2	GEM
UPN-11	C5	45	4	42	2	1.3	GEM
UPN-12	baseline	100	4	43	2	1.1	GEM
UPN-12	C2	90	7	59	2	0.6	GEM
UPN-12	40	95	7	46	0	1	GEM
UPN-12	C5	95	6	54	2	0.7	GEM
UPN-13	baseline	90	2	40	4	1.4	GEM
UPN-13	C2	65	5	43	1	1.2	GEM
UPN-13	C5	60	9	37	3	1.5	EM
UPN-14	baseline	60	1	36	3	1.4	GEM
UPN-14	C2	70	1	38	3	1.1	GEM
UPN-14	C5	60	1	31	2	1.5	EM

UPN-15	baseline	60	3	40	3	1.2	GEM
UPN-15	C2	65	2	40	3	1.2	GEM
UPN-15	C5	95	37	27	11	2.6	N/A
UPN-16	baseline	40	2	31	1	1.9	GEM
UPN-16	response	40	1	43	2	1	EM
UPN-16	LOR	30	2	43	4	1	GEM
UPN-17	baseline	45	3	8	5	10.4	NA
UPN-17	C2	65	1	1	2	64.5	M
UPN-17	C5	70	1	1	8	90	NA
UPN-18	baseline	35	2	31	2	1.5	G
UPN-18	C2	75	3	15	3	3.6	GEM
UPN-18	C5	NA	NA	NA	NA	NA	NA
UPN-19	baseline	80	1	52	3	0.7	GEM
UPN-19	C2	60	1	42	2	1.1	GEM
UPN-19	C4	70	1	52	1	0.7	EM (unable to assess G)
UPN-20	baseline	35	3	29	5	1.7	EM
UPN-20	C2	50	8	36	2	1.4	EM
UPN-20	C5	NA	NA	NA	NA	NA	NA
UPN-21	baseline	<5	3	23	8	2.2	GEM
UPN-21	C2	40	6	42	3	1	GEM
UPN-21	C5	NA	NA	NA	NA	NA	NA
UPN-22	baseline	70	6	65	1	0.4	EM
UPN-22	C2	50	15	49	1	0.9	E
UPN-22	C5	NA	NA	NA	NA	NA	NA
UPN-23	baseline	Unable to assess	1	9	3	4.9	GE (unable to assess M)
UPN-23	C2	NA	NA	NA	NA	NA	NA
UPN-23	C5	NA	NA	NA	NA	NA	NA
UPN-24	baseline	70	1	33	0	1.6	EM
UPN-24	C2	60	4	49	1	0.8	EM
UPN-25	baseline	Unable to assess	2	3	32	23.2	G (unable to assess E and M)
UPN-25	C2	NA	NA	NA	NA	NA	NA
UPN-25	C5	NA	NA	NA	NA	NA	NA

LOR, loss of response; C2, cycle 2; C4, cycle 4; C5, cycle 5. NA, not available; GEM, granulocytic, erythroid and megakaryocytic dysplasia; G, granulocytic dysplasia; GM, granulocytic and megakaryocytic dysplasia; EM, erythroid and megakaryocytic dysplasia

Supplementary Table 4. Treatment-emergent adverse events by grade in the entire cohort (n=25).

	Grade 1-2	Grade-3	Grade-4	Grade-5
Total number of events	218 (80)	44 (16)	9 (3)	1 (0.4)
Neutropenia	9 (36)	10 (40)	5 (20)	0
Fatigue	20 (80)	3 (12)	0	0
Gastrointestinal	20 (80)	0	0	0
Skin lesions	18 (72)	2 (8)	0	0
Elevated liver function tests	16 (64)	2 (8)	0	0
Surgical/Medical Procedures	16 (64)	0	0	0
Myalgias/Arthralgias	14 (56)	1 (4)	0	0
Electrolyte/Glucose Abnormalities	14 (56)	0	0	0
Respiratory	13 (52)	1 (4)	0	0
Anemia	3 (12)	10 (40)	1 (4)	0
Infection	9 (36)	4 (16)	0	1 (4)
Thrombocytopenia	7 (28)	4 (16)	3 (12)	0
Acute kidney injury	11 (44)	1 (4)	0	0
Psychiatric and Neurologic	9 (36)	0	0	0
Cardiac	7 (28)	1 (4)	0	0
Anorexia/Malnutrition	7 (28)	1 (4)	0	0
Fever/Chills or Infusion Reaction	6 (24)	1 (4)	0	0
Bleeding/Bruising	5 (20)	2 (8)	0	0
Headache	6 (24)	0	0	0
Urinary Symptoms	4 (16)	1 (4)	0	0

Supplementary Table 5. Transfusion burden before canakinumab treatment and response assessment.

Patient ID	PRBCs			Platelet Transfusion		Hb* (g/dL)		Platelets* (x10 ⁹ /L)		Transfusion Burden**			Response		Duration of response (months)
	8 weeks	16 weeks		8 weeks	16 weeks	8 weeks	16 weeks	8 weeks	16 weeks	modified IWG 2006**	IWG 2006	IWG 2018	IWG 2006	IWG 2018	
UPN-01	6	10		2	2	8.5	8.4	52	82.8	TD	TD	HTB	HI-E	HI-E	11.99
UPN-02	3	8		0	0	7.5	7.5	154	150.2	TD	TID	HTB	HI-E	HI-E	12.88
UPN-03	2	NC		0	NC	7.3	7.7	126	120.4	TD	TID	NE	SD	NE	-
UPN-04	2	3		0	0	7.3	7.7	101	101.6	TD	TID	LTB	HI-E	HI-E	5.06
UPN-05	4	8		0	0	6.8	7.9	358	349.0	TD	TD	HTB	SD	SD	-
UPN-06	15	19		2	6	8.2	7.8	21	18.5	TD	TD	HTB	SD	SD	-
UPN-07	5	12		0	0	8.1	7.6	60	66.6	TD	TD	HTB	SD	SD	-
UPN-08	9	12		1	1	8.1	7.1	16	10.2	TD	TD	HTB	SD	SD	-
UPN-09	2	NC		0	NC	8.5	7.8	430	374.3	TD	TID	NE	SD	NE	-
UPN-10	4	8		0	0	9.2	8.2	283	243.7	TD	TD	HTB	SD	SD	-
UPN-11	1	4		0	0	8.5	8.1	140	161.9	TD	TID	LTB	SD	SD	-
UPN-12	6	NC		6	NC	8.4	7.9	19	15.4	TD	TD	NE	PD	NE	-
UPN-13	3	7		0	0	8.4	7.7	325	297.1	TD	TID	LTB	PD	PD	-
UPN-14	3	8		0	0	7.8	8.4	113	105.2	TD	TID	HTB	SD	SD	-
UPN-15	2	6		0	0	9.5	8.5	157	158.3	TD	TID	LTB	PD	PD	-
UPN-16	1	4		0	0	8.5	7.3	86	56.5	TD	TID	LTB	HI-P	SD	3.06
UPN-17	7	10		0	0	6.6	7.5	84	94.2	TD	TD	HTB	SD	SD	-
UPN-18	2	6		2	5	8.4	8.8	20	35.4	TD	TID	LTB	SD	SD	-
UPN-19	5	7		0	0	7.3	7.3	426	402.3	TD	TD	LTB	SD	SD	-
UPN-20	2	4		0	0	8.8	8.8	143	137.3	TD	TID	LTB	PD	PD	-
UPN-21	5	7		0	0	7.1	8.0	129	131.1	TD	TD	LTB	PD	PD	-
UPN-22	0	0		0	0	9.1	9.0	174	142.9	TI	TID	NTD	PD	PD	-
UPN-23	4	8		2	3	8.5	8.4	31	20.8	TD	TD	HTB	NE [†]	NE [†]	-
UPN-24	3	5		0	0	7.8	8.0	130	180.0	TD	TID	LTB	SD	SD	-
UPN-25	16	37		0	0	7.7	7.8	130	117.6	TD	TD	HTB	NE [†]	NE [†]	-

PRBC, packed red blood cell; NC, not collected; NE, not evaluable; NTD, non-transfused; LTb, low transfusion burden; HTB, high transfusion burden; TD, transfusion-dependent; TID, transfusion independent; HI-E, erythroid hematological improvement; HI-P, platelet hematological improvement; SD, stable disease; PD progressive disease.

Hb and PLT measurements to determine the baseline Hb values were performed at least every 2 weeks during the 8-week (and 16-week) screening period, when possible.

**Transfusion dependency is the need for a prior transfusion in the past 8 weeks for a hemoglobin level < 8g/dL.

+ Response assessment in patients UPN-23 and UPN-25 was unavailable owing to the patients' inability to complete a minimum of two cycles and obtain a bone marrow aspiration.

Supplementary Table 6. Multivariate analysis for overall survival and progression-free survival.

Analysis of overall survival (two-sided Wald tests for Cox proportional hazards models. Adjustments for multiple comparisons were not performed).

	Hazard Ratio	P-value
Age>75 vs. <75	1.23	0.71
IPSS-M High vs. Low	3.66	0.04
HMA-failure vs. HMA-naïve	1.38	0.63

Analysis of Progression-Free Survival

	Hazard Ratio	P-value
Age>75 vs. <75	1.82	0.29
IPSS-M High vs. Low	4.6	0.01
HMA-failure vs. HMA-naïve	0.81	0.75

HMA, hypomethylating agent; IPSS-M, Molecular International Prognostic Scoring System.

*Patients were classified according to the IPSS-M into higher-risk (very high, moderately high, and high) and lower-risk (very low, moderately low, and low) cohorts.

Fourth publication

Influence of co-mutational patterns in disease phenotype and clinical outcomes of chronic myelomonocytic leukemia

Montalban-Bravo G, Rodriguez-Sevilla JJ, Swanson DM, Kanagal-Shamanna R, Hammond D, Chien K, Sasaki K, Jabbour E, DiNardo C, Takahashi K, Short N, Issa GC, Pemmaraju N, Kadia T, Ravandi F, Daver N, Borthakur G, Loghavi S, Pierce S, Bueso-Ramos C, Kantarjian H, Garcia-Manero G.

Leukemia. 2024 May;38(5):1178-1181. Impact factor: 12.8
Quartile 1

LETTER



MYELODYSPLASTIC NEOPLASM

Influence of co-mutational patterns in disease phenotype and clinical outcomes of chronic myelomonocytic leukemia

Guillermo Montalban-Bravo¹✉, Juan Jose Rodriguez-Sevilla¹, David Michael Swanson², Rashmi Kanagal-Shamanna³, Danielle Hammond¹, Kelly Chien¹, Koji Sasaki¹, Elias Jabbour¹, Courtney DiNardo¹, Koichi Takahashi¹, Nicholas Short¹, Ghayas C. Issa¹, Naveen Pemmaraju¹, Tapan Kadia¹, Farhad Ravandi¹, Naval Daver¹, Gautam Borthakur¹, Sanam Loghavi³, Sherry Pierce¹, Carlos Bueso-Ramos³, Hagop Kantarjian¹ and Guillermo Garcia-Manero¹

© The Author(s), under exclusive licence to Springer Nature Limited 2024

Leukemia (2024) 38:1178–1181; <https://doi.org/10.1038/s41375-024-02190-1>

TO THE EDITOR:

Chronic myelomonocytic leukemia (CMML) is a clonal disorder of mutant hematopoietic stem/progenitor cells (HSPCs) [1] characterized by high risk of progression to acute myeloid leukemia (AML) [2]. Integration of molecular data with clinical and cytogenetic features has allowed developing multiple prognostic risk models applicable in clinical practice [3, 4]. Despite these advances, our ability to accurately predict disease transformation and our understanding on how distinct genomic events cooperate to determine the disease behavior remains limited. Although previous studies have reported the potential cooperative effects of specific mutations [5, 6], determining if certain recurrent cooperative genomic patterns predict for disease phenotype and clinical outcomes could help define diseases subsets to optimize patient management and direct translational efforts aimed at developing rationally designed novel combinations.

In order to evaluate further if distinct genomic profiles, characterized by recurrent co-occurrence of somatic mutations, define clinicopathologic subgroups of CMML with distinct outcomes, we evaluated a cohort of patients with CMML, defined using the WHO 2016 classification [7], and used computational methods to identify unique clusters defined by recurrent co-mutational patterns and define their clinical features and outcomes. Akaike information criterion (AIC) method was applied to evaluate mixture model components defining clusters solely based on mutational profile. Mutation data was obtained using an amplicon-based next-generation sequencing platform, as detailed in Supplementary Methods, and was available in all 296 patients included in this discovery cohort. Expectation-maximization (EM) algorithm was used for mixture model fitting to multivariate binary data. Unsupervised cluster membership was chosen as a function of the component with the highest weight for any individual, and we examined means of cluster centers. Generalized linear models were used to study the association of overall response (ORR), complete remission (CR), and risk factors. Overall survival (OS) was calculated as the time from diagnosis to

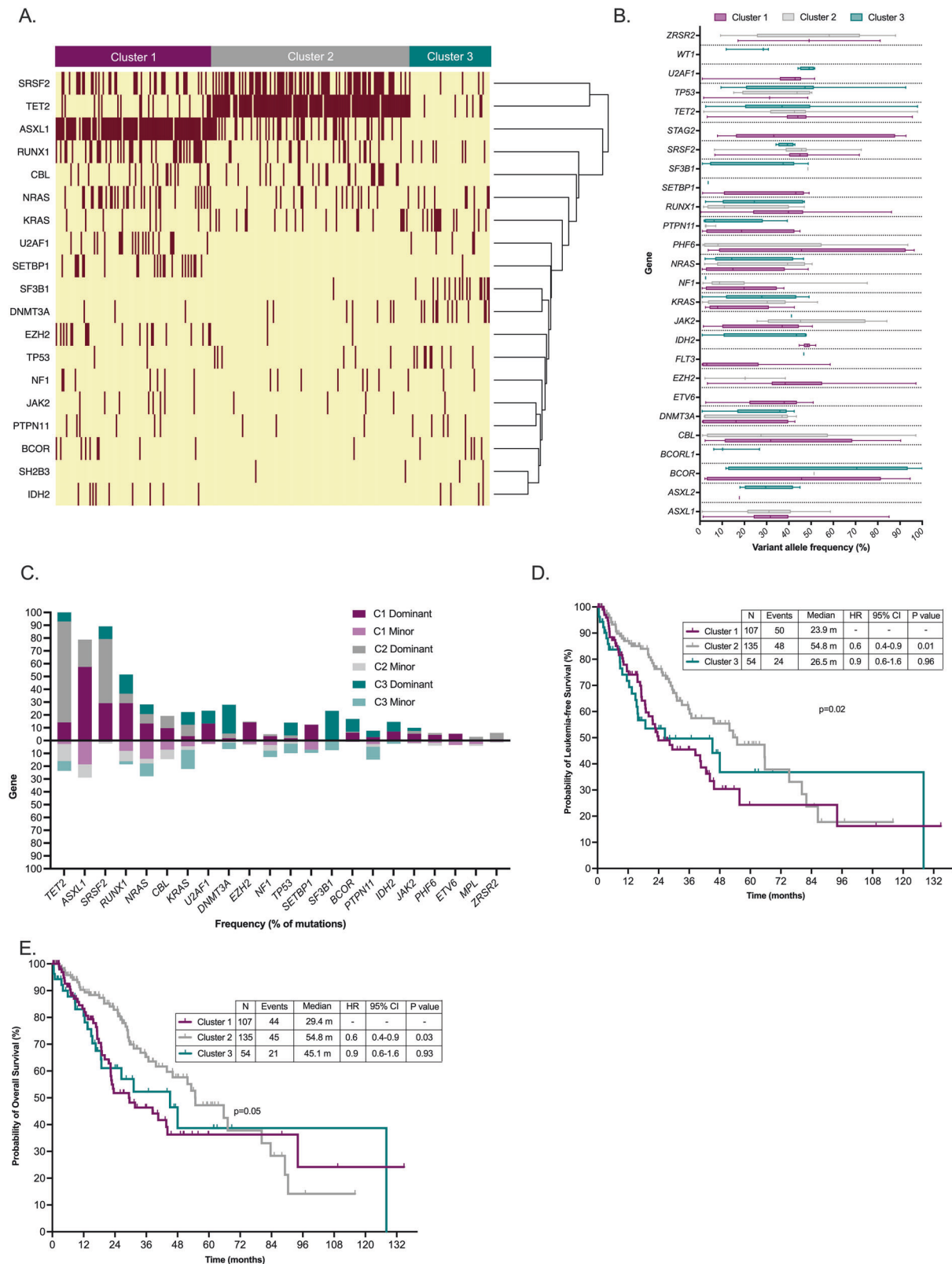
death or last follow-up date. Leukemia-free survival (LFS) was calculated from the time of diagnosis until transformation to AML, death or last follow-up date. Patients who were alive at their last follow-up were censored on that date. The Kaplan–Meier product limit method was used to estimate the median OS, EFS, and for each clinical/demographic factor. Univariate and multivariate Cox proportional hazards regression analyses were used to identify any association with each of the variables and survival outcomes. Statistical analyses were performed using R version 4.0.3, Jamovi version 2.0.0, SPSS Statistics version 28 (IBM), and GraphPad version 9.0.0 (San Diego, CA).

A total of 296 patients were included in the analysis. Patient characteristics of the entire cohort are shown in Supplementary Table S1. Frequency of identified somatic mutations among the entire population is shown in Supplementary Fig. S1. Based on the frequency and co-occurrence of identified somatic mutations, we aimed to identify patient clusters with shared genomic profiles and overall co-mutation patterns. We examined AIC over 2 to 5 mixture model components and arrived at 3 by optimization of AIC and clinical understanding of co-mutational patterns. We fit mixture models to the multivariate binary mutation data using the EM algorithm and 5 randomly chosen starting values without consideration of patient outcomes. Unsupervised cluster membership was chosen as a function of the component with the highest weight for any individual, and we examined differences between cluster means. Mutation frequencies among each of the defined clusters are shown in Fig. 1A. Cluster 1 (C1, $n = 107$), was characterized by high frequency of *ASXL1* mutations (86%), with lower *TET2* mutation frequency (20%), and enrichment of *RUNX1* (35%), *NRAS* (28%) and *U2AF1* (18%) mutations. *SETBP1* and *EZH2* mutations were nearly exclusively observed in C1 (16% and 20% of C1 pts, respectively). All pts with *ETV6* and *STAG2* mutations belonged to this cluster. Cluster 2 (C2, $n = 135$) was defined by universal presence of *TET2* mutations (93%) with frequent *SRSF2* co-mutation (56%) and lower frequency of *ASXL1* (34%), *RUNX1* (15%) or *NRAS* (12%) mutations, compared to C1. Despite their

¹Department of Leukemia, The University of Texas MD Anderson Cancer Center, Houston, TX, USA. ²Department of Biostatistics, The University of Texas MD Anderson Cancer Center, Houston, TX, USA. ³Department of Hematopathology, The University of Texas MD Anderson Cancer Center, Houston, TX, USA. ✉email: G.Montalban1@mdanderson.org

Received: 2 January 2024 Revised: 13 February 2024 Accepted: 15 February 2024

Published online: 28 February 2024



overall low frequency, *BRAF* mutations were restricted to C2, while *CBL* mutations were observed at similar frequencies in C1 (16%) and C2 (18%). This suggests that co-mutation profiles and genomic context differs among genes involved in *RAS* pathway signaling. Cluster 3 (C3, $n = 54$) included a minor and more

genomically heterogeneous group enriched for *SF3B1* (25%), *KRAS* (24%), *DNMT3A* (22%) and *TP53* (15%) mutations, with absence of *ASXL1* mutations, and low frequency of *TET2* (12%) mutations. All *BCORL1* and *WT1* mutations and most *ASXL2* and *CEBPA* mutations were in C3. Given the heterogeneity within this cluster, we then

Fig. 1 **Mutational composition and clinical outcomes of genomic clusters in CMML.** **A** Oncoplot showing hierarchical clustering based on co-mutation profiles of 296 patients with CMML. Cells in red wine color correspond to presence of mutation, those in yellow to lack of mutation. Cases are clustered by mixture model component defined clusters based on frequency and patterns of appearance of mutations on individual patients. **B** Variant allele frequencies (VAFs) of identified mutations in each individual clusters. Median and ranges are shown for each individual mutation. Statistical comparisons were performed using the Mann–Whitney test ($*P < 0.05$). **C** Frequency of likely clonal hierarchy (dominant or minor clone) of identified mutations within each CMML genetic cluster. Clonal relationships were tested using Pearson goodness-of-fit tests with clonal heterogeneity being defined in cases with goodness-of-fit $p < 0.05$ suggesting significant variability of VAF distributions reflecting presence of several clones. **D** Kaplan–Meier survival estimate curve for leukemia-free survival according to clusters. Patients were attributed a cluster by unsupervised cluster membership defined as a function of component with highest weight for a cluster for each individual patient. **E** Kaplan–Meier survival estimate curve for overall survival according to clusters. Patients were attributed a cluster by unsupervised cluster membership defined as a function of component with highest weight for a cluster for each individual patient.

sought to evaluate the presence of unique genomic subclusters. To do so, we evaluated co-mutational profiles among patients assigned to cluster 3 based on attributed cluster weights. Although no statistically significant subclusters had been identified by our initial AIC and EM algorithm, this analysis revealed six distinct subclusters (Supplementary Fig. S2) defined by presence of *SF3B1* with or without *DNMT3A* co-mutation (C3a, $n = 15$), *KRAS* mutations (C3b, $n = 12$), *DNMT3A* mutations in the absence of *SF3B1* or *TP53* mutations (C3c, $n = 4$), *TP53* mutations (C3c, $n = 8$), other not-otherwise specifiable recurrent co-mutational profiles (C3d, $n = 8$) and a subset with no detectable somatic mutations among evaluated genes (C3f, $n = 7$).

Next, to determine if the clonal dominance and architecture among recurrent or specific somatic mutations define each of the clusters, we evaluated the allele frequency distribution and likely mutation dominance among the unique clusters (Fig. 1B, C, Supplementary Figs. S3–S4). This analysis revealed that *RUNX1* mutations not only were more frequent among C1 but appeared at higher median VAF compared to other clusters (C1: 40%, C2: 11%, C3: 25%, $p = 0.003$). Consistent with the higher median VAF of *RUNX1* mutations in C1, *RUNX1* mutations were more likely to appear within dominant clones in C1 compared to C2 (C1: 32/43 [74%]; C2: 10/26 [39%]; $p = 0.003$). Mutations in *U2AF1* had mildly higher median VAF in C3 compared to cluster 1 (49% vs 43%, $p = 0.017$). Analysis of clonal dominance revealed that among C1, majority of patients had *ASXL1* mutations within dominant clones (dominant $n = 71/94$ [76%] and minor $n = 23/94$ [25%], respectively). This was also the case among C2 (dominant: $n = 30/45$ [67%] vs minor: $n = 15/45$ [33%], respectively). Despite higher frequency of *TET2* mutations in C2, majority of mutations involving *TET2* appeared within dominant clones irrespective of cluster (85% vs 89% in C1 and C2, respectively, $p = 0.754$). However, *TET2* multihit loss (defined as ≥ 2 *TET2* mutations and/or *TET2* VAF $\geq 55\%$, implying a biallelic alteration due to loss of heterozygosity or 4q24 deletion, as previously reported [8, 9]) was significantly enriched among C2 when compared to C1 (C1: 9/18 [50%]; C2: 33/93 [73.8%]; $p = 0.038$). Mutations in *SRSF2* and *U2AF1* where almost invariably present within dominant clones while *NRAS*, *CBL* or *KRAS* mutations could be found in similar frequencies as part of dominant or minor clones among all clusters.

To determine if these unique genomic clusters are associated to specific phenotypic features, we evaluated the clinicopathologic and cytogenetic features of each cluster (Supplementary Table S1). Cluster 1 was enriched in MP-CMML (C1: 64%; C2: 48%; C3: 52%, $p < 0.001$) and had higher frequency of del(7q)/-7 (C1: 11%; C2 0%, C3: 6%, $p < 0.001$) and trisomy 8 (C1: 15%, C2: 7%, C3: 6%, $p = 0.05$). Complex karyotype (C1: 1%, C2: 1%, C3: 22%, $p < 0.001$) was nearly exclusive of C3, while C2 was more likely to be associated with a normal karyotype (C1: 59%; C1: 73%; C3: 41%, $p < 0.001$) and higher median hemoglobin (C1: 9.8 g/dL; C2: 12.1 g/dL, C3: 9.7 g/dL, $p < 0.001$).

A total of 55 (19%) patients experienced progression to AML including 21 (20%), 26 (19%) and 8 (15%) in C1, C2, and C3, respectively. To evaluate if unique dynamic genomic evolution defines each of the clusters, we aimed to study the clonal changes

associated with AML progression among each cluster. Matched NGS at the time of transformation to AML was available in 36 (C1: $n = 13$; C2 $n = 19$; C3: $n = 4$) of the 55 (65%) patients who had progression to AML (Supplementary Fig. S5). Expansion of pre-existing clones (defined as increase of VAF to a higher group as defined in Supplementary Fig. S5) was observed in 8 (62%), 4 (21%) and 2 (50%) patients in C1, C2 and C3 at transformation, respectively (Supplementary Fig. S6). Only one patient in C1 and two patients in C2 had no changes in clonal architecture at transformation. Among these 3 patients, sequential cytogenetic evaluation revealed no changes at transformation compared to diagnosis. Overall, acquisition or expansion of *NRAS* ($n = 12$, 33%), *CBL* ($n = 7$, 19%), *RUNX1* ($n = 6$, 17%), *NPM1* ($n = 5$, 14%), *ASXL1* ($n = 5$, 14%) and *PHF6* ($n = 5$, 14%) were the most common events and were present in $>10\%$ of patients. Acquisition of new *NRAS*, *RUNX1* and *ASXL1* mutations, more commonly present in C1 at diagnosis, was observed in 32%, 19% and 19% of patients in C2 at transformation.

With a median follow up of 31.1 months (95% CI 25.3–36.9 months), a total of 216 patients received therapy including 195 (66%) receiving hypomethylating-agent (HMA)-based therapies. No significant differences in ORR or CR rates following IWG 2006 criteria were observed based on mutation clusters (Supplementary Table S1). By univariate analysis, patients in C1 and C3 had significantly worse LFS (C1: 23.9 months [95% CI 7.7–40.1], C2: 54.8 months [95% CI 34.8–74.9 months], C3: 26.5 months [95% CI 0.0–63.8 months], $p = 0.02$, Fig. 1D) and OS (C1: 29.4 months [95% CI 14.2–44.5 months], C2: 54.8 months [95% CI 40.7–68.9 months], C3: 45.1 months [95% CI 22.9–67.4 months], $p = 0.05$, Fig. 1E) than those in C2. Survival differences among patients in C3 based on genomic subclusters are detailed in Supplementary Fig. S7. Overall, no significant differences in OS or LFS were observed among subclusters. To evaluate if mutation clusters predicted for survival outcomes we fitted Cox proportional hazards models, regressing OS and LFS on normalized cluster weights with adjustment for age and sex (Supplementary Tables S2–S3). We performed 2 degree of freedom likelihood ratio tests on cluster weight in all models regardless of covariate adjustment, finding their contribution to explaining variation in the survival outcomes ($p < 0.015$ in all cases). Use of Cox proportional hazards models confirmed that, when corrected by age and sex, cluster annotation by attributed cluster weights predicted for LFS and OS.

In conclusion, our data confirms prior reports suggesting that certain mutations co-occur in CMML [5, 6] and identifies three major genomic-defined disease clusters: C1 defined by dominant *ASXL1* and *RUNX1* mutations, frequent *SETPB1* and *EZH2* mutations and lack of *TET2* enrichment; C2 defined by multihit *TET2* and *SRSF2* co-dominance and a more heterogeneous C3 encompassing six unique subclusters defined by *SF3B1*, *KRAS*, *DNMT3A*, *TP53* mutations as well as non-recurrent co-mutations or those with no detectable mutations. Although further validation and refinement of these disease clusters is needed in larger cohorts of patients, while accounting for specific previously reported mutational combinations (such as those involving *ASXL1* and *TET2*), our data

might help improve disease classification by considering genomic composition.

DATA AVAILABILITY

The datasets generated during and/or analyzed during the current study are not publicly available due to patient privacy concerns but are available from the corresponding author on reasonable request.

REFERENCES

1. Itzykson R, Kosmider O, Renneville A, Morabito M, Preudhomme C, Berthon C, et al. Clonal architecture of chronic myelomonocytic leukemias. *Blood*. 2013;121:2186–98.
2. Patnaik MM, Padron E, LaBorde RR, Lasho TL, Finke CM, Hanson CA, et al. Mayo prognostic model for WHO-defined chronic myelomonocytic leukemia: ASXL1 and spliceosome component mutations and outcomes. *Leukemia*. 2013;27:1504–10.
3. Padron E, Garcia-Manero G, Patnaik MM, Itzykson R, Lasho T, Nazha A, et al. An international data set for CMML validates prognostic scoring systems and demonstrates a need for novel prognostication strategies. *Blood Cancer J*. 2015;5:e333.
4. Elena C, Galli A, Such E, Meggendorfer M, Germing U, Rizzo E, et al. Integrating clinical features and genetic lesions in the risk assessment of patients with chronic myelomonocytic leukemia. *Blood*. 2016;128:1408–17.
5. Coltro G, Mangaonkar AA, Lasho TL, Finke CM, Pophali P, Carr R, et al. Clinical, molecular, and prognostic correlates of number, type, and functional localization of TET2 mutations in chronic myelomonocytic leukemia (CMML)-a study of 1084 patients. *Leukemia*. 2020;34:1407–21.
6. Itzykson R, Kosmider O, Renneville A, Gelsi-Boyer V, Meggendorfer M, Morabito M, et al. Prognostic score including gene mutations in chronic myelomonocytic leukemia. *J Clin Oncol*. 2013;31:2428–36.
7. Arber DA, Orazi A, Hasserjian R, Thiele J, Borowitz MJ, Le Beau MM, et al. The 2016 revision to the World Health Organization classification of myeloid neoplasms and acute leukemia. *Blood*. 2016;127:2391–405.
8. Garcia-Gisbert N, Arenillas L, Roman-Bravo D, Rodríguez-Sevilla JJ, Fernandez-Rodríguez C, Garcia-Avila S, et al. Multi-hit TET2 mutations as a differential molecular signature of oligomonocytic and overt chronic myelomonocytic leukemia. *Leukemia*. 2022;36:2922–6.
9. Awada H, Nagata Y, Goyal A, Asad MF, Patel B, Hirsch CM, et al. Invariant phenotype and molecular association of biallelic TET2 mutant myeloid neoplasia. *Blood Adv*. 2019;3:339–49.

ACKNOWLEDGEMENTS

This work was supported in part by the University of Texas MD Anderson Cancer Center Support Grant CA016672 (all authors) and the University of Texas MD Anderson MDS/AML Moon Shot (GM-B, RK-S, CBB, CC, KT, KAS, CB-R, HK, and GG-M). JJR-S is a recipient of MD Anderson's Odyssey Fellowship.

AUTHOR CONTRIBUTIONS

G. Montalban-Bravo, J.J. Rodríguez-Sevilla and G. García-Manero designed the study, analyzed the data and participated in writing the manuscript. K. Sasaki, F. Ravandi, N. Dayer, K. Takahashi, D. Hammond, K. Chien, N. J. Short, C. DiNardo, E. Jabbour, G. Borthakur, N. Pemmaraju, T. Kadia, G. C. Issa, H. Kantarjian and G. García-Manero contributed patients and participated in analyzing the data and writing the manuscript. S. Pierce collected and analyzed data. S. Loghavi and R. Kanagal-Shamanna performed histopathological analysis and sequencing analysis. D. M Swanson developed mixture and time-to-event models. R. Kanagal-Shamanna, S. Loghavi and C. Bueso-Ramos reviewed bone marrow morphologic and genetic findings, analyzed the data and contributed in writing the manuscript.

COMPETING INTERESTS

KS declares honoraria from Otsuka Pharma, and consultancy fee from Pfizer Japan. MK declares consulting and honoraria from AbbVie, Genentech, F. Hoffman La-Roche, Stemline Therapeutics, Amgen, Forty-Seven, and Kisoji; research funding and/or clinical trial support from AbbVie, Genentech, F. Hoffman La-Roche, Eli Lilly, Cellectis, Calithera, Ablynx, Stemline Therapeutics, Agios, Ascentage, and Astra Zeneca; and stock options/royalties from Reata Pharmaceutical. HK declares research support from AbbVie, Agios, Amgen, Ariad, Astex, BMS, Cyclacel, Daiichi-Sankyo, Immunogen, Jazz Pharma, Novartis, and Pfizer, honoraria from AbbVie, Actinium, Agios, Amgen, Immunogen, Orsinex, Pfizer, and Takeda, and an advisory role with Actinium. GG-M declares support from and an advisory role with Celgene Corporation, Astex, and Amphivena, and grant/research support 15 from Helsinn, Novartis, AbbVie, Onconova, H3 Biomedicine, and Merck. The rest of authors declare no competing financial interests.

ADDITIONAL INFORMATION

Supplementary information The online version contains supplementary material available at <https://doi.org/10.1038/s41375-024-02190-1>.

Correspondence and requests for materials should be addressed to Guillermo Montalban-Bravo.

Reprints and permission information is available at <http://www.nature.com/reprints>

Publisher's note Springer Nature remains neutral with regard to jurisdictional claims in published maps and institutional affiliations.

Springer Nature or its licensor (e.g. a society or other partner) holds exclusive rights to this article under a publishing agreement with the author(s) or other rightsholder(s); author self-archiving of the accepted manuscript version of this article is solely governed by the terms of such publishing agreement and applicable law.

Supplementary Information for
Influence of Co-mutational Patterns in Disease Phenotype and Clinical Outcomes of Chronic
Myelomonocytic Leukemia

Table of Contents

Content	Page
Supplementary Methods	
PCR-based NGS 81-gene panel	2
Computational and study methodology	4
Supplementary Tables	
Table S1. Clinicopathologic features and response outcomes of CMML genomic clusters	5
Table S2. Cox proportional hazard model for overall survival	7
Table S3. Cox proportional hazard model for leukemia-free survival	8
Supplementary Figures	
Figure S1. Frequency of identified somatic mutations in the total cohort	9
Figure S2. Genomic subclusters among patients classified as cluster 3	10
Figure S3. Variant allele frequency distributions of most common somatic mutations	11
Figure S4. Mutation dominance distribution by CMML cluster	12
Figure S5. Heatmap of clonal architecture at diagnosis and AML for each CMML cluster	13
Figure S6. Frequency of emerging or expanding somatic mutations at transformation by CMML cluster	14
Figure S7. Survival outcomes based on cluster 3 genomic subclusters	15

PCR-based next generation sequencing (NGS) 81-Gene panel

<i>Gene</i>	Exons (codons) tested
<i>ANKRD26</i>	1 (1-6)
<i>ASXL1</i>	11-12 (362-1442), 12 (1450-1542)
<i>ASXL2</i>	11-12 (381-1436)
<i>BCOR</i>	2-4 (1-511), 4-12 (515-1547), 13-15 (1550-1644), 15 (1663-1722)
<i>BCORL1</i>	1-6 (1-1261), 6 (1292-1323), 6-12 (1326-1700), 12 (1706-1712)
<i>BRAF</i>	11 (439-478), 15 (581-620)
<i>BRINP3</i>	2-8 (1-767)
<i>CALR</i>	9 (352-418)
<i>CBL</i>	7-9 (336-477)
<i>CBLB</i>	7-10 (282-469)
<i>CBLC</i>	7-9 (336-454), 10 (465-475)
<i>CEBPA</i>	1 (1-90), 1 (249-358), 1 (128-175), 1 (178-201)
<i>CREBBP</i>	1-8 (1-608), 9-30 (615-1724), 31 (2238-2443), 31 (2049-2235), 31 (1725-1943), 31 (1950-2042)
<i>CRLF2</i>	6 (217-256)
<i>CSF3R</i>	14 (575-622), 17 (681-800), 17 (822-864)
<i>CUX1</i>	2-6 (11-172), 6-9 (174-241), 10-14 (248-408)
<i>DDX41</i>	1-11 (1-410), 12 (416-418), 12-17 (420-623)
<i>DNMT3A</i>	8-22 (286-862), 23 (866-913)
<i>EED</i>	1-2 (1-69), 2-8 (71-287), 9-12 (289-442)
<i>ELANE</i>	1-2 (1-48), 2 (69-75), 4-5 (123-268)
<i>ETNK1</i>	3 (228-275)
<i>ETV6</i>	1-8 (1-453)
<i>EZH2</i>	2-5 (1-158), 5-6 (160-205), 7 (209-217), 8-19 (243-732), 20 (752)
<i>FBXW7</i>	9-12 (413-708)
<i>FLT3</i>	11-20 (437-847)
<i>GATA1</i>	2-3 (1-84)
<i>GATA2</i>	2 (2-5), 2-5 (22-377), 5-6 (379-481)
<i>GFI1</i>	2 (2-39)
<i>GNAS</i>	8 (200-202), 11 (315-324)
<i>HNRNPK</i>	3-17 (1-465)
<i>HRAS</i>	2-3 (1-59), 3-4 (87-135), 4 (137-150)
<i>IDH1</i>	4 (132-133)
<i>IDH2</i>	4 (125-178)
<i>IKZF1</i>	2-8 (1-443), 8 (445-518)
<i>IL2RG</i>	1-2 (1-45), 2-8 (51-340), 8 (352-370)
<i>IL7R</i>	5-7 (180-292)
<i>JAK1</i>	3-22 (3-1023), 22-24 (1026-1123)
<i>JAK2</i>	10 (405-442), 12-14 (505-622), 16 (665-711), 18 (762-812)
<i>JAK3</i>	2-23 (1-1069)
<i>KDM6A</i>	1-29 (1-1402)
<i>KIT</i>	8-9 (411-514), 11 (550-592), 17 (788-828)

KMT2A 2 (145-168), 3-4 (176-1075), 4 (1081-1112), 5 (1117-1184), 6 (1190-1212), 7 (1224-1325),
8-13 (1338-1560), 14-15 (1566-1665),
27 (2186-2195), 27 (2201-2355), 27 (2373-3215), 27 (3223-3324), 27 (3339-3575)
KRAS 2-4 (1-150)
MAP2K1 2 (27-90), 3 (98-146)
MPL 10 (490-522), 12 (552-636)
NF1 2-5 (21-189), 6 (201-218), 8-13 (244-467), 13-24 (478-1066), 25-26 (1082-1146),
26-31 (1160-1378), 31-35 (1380-1550), 35-38 (1564-1868),
39 (1870-1884), 39-47 (1886-2322), 47-52 (2325-2555), 52-58 (2568-2840)
NOTCH1 26-28 (1529-1795), 34 (2069-2273), 34 (2290-2556), 34 (2069-2273), 34 (2290-2556)
NPM1 11 (283-295)
NRAS 2-4 (1-150)
PAX5 1-10 (14-392)
PHF6 2-10 (1-366)
PIGA 2 (1-6), 2-6 (16-485)
PML 3 (201-255)
PRPF40B 2-19 (2-609), 19-20 (611-658), 20-26 (661-893)
PTEN 7-8 (212-285), 8 (290-342)
PTPN11 3-4 (46-125), 7 (253-285), 12 (460-462), 12-13 (465-533)
RAD21 2-14 (1-632)
RARA 6-7 (211-338)
RUNX1 2-9 (1-437), 9 (456-474)
SETBP1 4 (838-885)
SF1 1-13 (1-640)
SF3A1 1-7 (1-322), 7-9 (328-424), 9-16 (427-794)
SF3B1 13-16 (574-790)
SH2B3 2 (1-118), 2 (132-164), 2-8 (211-576)
SMC1A 1-19 (1-983), 20-25 (992-1234)
SMC3 1-6 (1-110), 6-16 (113-504), 16-17 (507-580), 17-29 (591-1217)
SRSF2 1 (1-38), 1 (45-121)
STAG1 2 (1-5), 3-20 (10-703), 21-22 (718-738), 22-27 (740-953), 27-34 (955-1259)
STAG2 2-15 (1-512), 16-33 (521-1232)
STAT3 17 (521-534), 17 (489-503), 17 (506-508), 18-22 (534-715)
STAT5A 3-7 (1-214), 8-9 (264-286), 9-20 (303-795)
STAT5B 16 (636-693)
SUZ12 1-2 (20-107), 4-5 (129-169), 7-16 (198-740)
TERT 1 (1-24), 2 (80-172), 2-4 (258-630), 4-5 (633-677), 5-6 (683-749), 6-8 (753-800), 8-16 (805-1133)
TET2 3 (1-77), 3 (91-826), 3 (829-853), 3-11 (867-2003)
TP53 2 (1-25), 4-11 (80-394)
U2AF1 2 (15-44), 6 (117-161)
U2AF2 1-5 (1-161), 6-12 (163-473)
WT1 1 (122-216), 1 (2-44), 1 (56-58), 2-10 (216-518)
ZRSR2 1-4 (1-90), 5 (108-131), 6-9 (134-263), 9-11 (267-483)

Computational and study methodology. NGS, next-generation sequencing; AIC, Akaike information criterion; EM, expectation-maximization; LFS, leukemia-free survival; OS, overall survival.

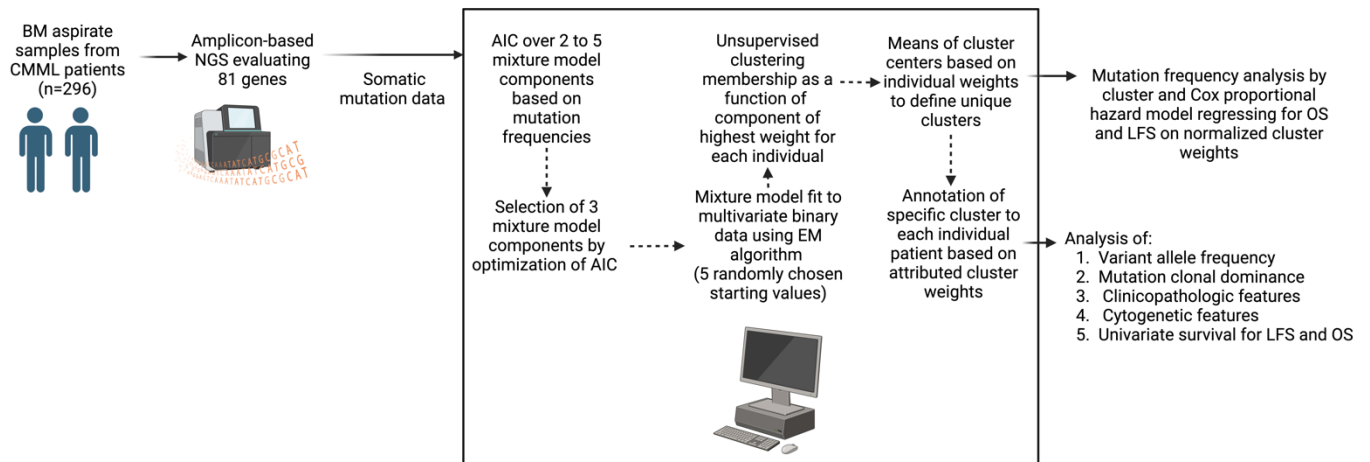


Table 1. Clinicopathologic features and response outcomes of CMML genomic clusters.

Variable	Total (n=296) n (%) / median [Range]	Cluster 1 (n=107) n (%) / median [Range]	Cluster 2 (n=135) n (%) / median [Range]	Cluster 3 (n=54) n (%) / median [Range]	P value
Age (years)	70 [30-94]	71 [34-90]	72 [36-94]	71 [30-93]	0.217
Male	210 (71)	78 (73)	91 (67)	41 (76)	0.434
MP-CMML	160 (54)	68 (64)	64 (48)	28 (52)	0.047
CMML-2 by WHO	152 (51)	60 (56)	61 (45)	31 (57)	0.149
Hgb (g/dL)	11.0 [5.3-17.3]	9.8 [5.3-16.9]	12.1 [6.6-16]	9.7 [6-17.3]	<0.001
WBC (x10 ⁹ /L)	10.7 [1.2-136.9]	14.9 [3.3-136.9]	9.6 [2.6-115.9]	10.2 [1.2-70.1]	0.001
ANC (x10 ⁹ /L)	6.1 [0.0-52.6]	8.1 [0.1-52.1]	5.3 [0-42.5]	4.9 [0.3-52.6]	0.006
AMC (x10 ⁹ /L) ¹	1.9 [0.0-73.1]	2.4 [0.4-73.1]	1.8 [0.0-47.5]	1.6 [0.0-22.3]	0.017
PB Monocyte %	19 [3-60]	19 [3-55]	20 [3-59]	18 [3-60]	0.684
PB Neutrophil %	53 [3-92]	54 [3-92]	53 [12-87]	52 [11-80]	0.606
PB Lymphocyte %	16 [2-77]	13 [2-69]	19 [4-55]	17 [3-77]	0.025
PB Blast %	0 [0-18]	0 [0-18]	0 [0-10]	0 [0-10]	<0.001
PB Promyelocyte %	0 [0-2]	0.5 [0-2]	0 [0-2]	0.5 [0-2]	0.546
PB Metamyelocyte %	4 [1-23]	6.5 [1-23]	3.5 [1-17]	2 [1-14]	0.058
Platelets (x10 ⁹ /L)	107 [4-764]	107 [9-750]	109 [10-591]	99 [4-764]	0.597
BM blast %	5 [0-18]	6 [1-18]	5 [0-18]	5 [0-18]	0.442
BM promyelocyte %	1 [0-25]	1 [0-8]	1 [0-25]	1 [1-8]	0.457
BM granulocyte %	28 [0-67]	27 [0-58]	29.2 [4-67]	24 [3-40]	0.003
BM monocyte %	11 [0-49]	10 [0-49]	11 [0-32]	9 [1-42]	0.340
Cr (mg/dL)	0.98 [0.53-2.86]	1.04 [0.54-2.59]	0.98 [0.58-2.86]	0.94 [0.53-2.46]	0.590
LDH (IU/L)	300 [126-6075]	340 [139-4464]	287 [126-6075]	254 [130-1808]	0.084
Karyotype					
Normal	184 (62)	63 (59)	99 (73)	22 (41)	<0.001
-Y	11 (4)	0 (0)	6 (4)	5 (9)	0.011
-7/del(7q)	15 (5)	12 (11)	2 (0)	3 (6)	<0.001
Trisomy 8	28 (10)	16 (15)	9 (7)	3 (6)	0.051
Inv(3)	3 (1)	0 (0)	0 (0)	3 (6)	0.001
Del(20q)	12 (4)	4 (4)	5 (4)	3 (6)	0.826
Complex	14 (5)	1 (1)	1 (1)	12 (22)	<0.001
Therapy-related	69 (23)	24 (22)	30 (22)	15 (28)	0.598
Therapy type					0.131

HMA	195 (66)	81 (76)	82 (61)	32 (59)	
Observation	80 (27)	18 (17)	44 (33)	18 (33)	
Hydroxyurea only	3 (1)	0 (0)	2 (2)	1 (2)	
LDAC-based	10 (3)	5 (5)	3 (2)	2 (4)	
Intensive	6 (2)	3 (3)	3 (2)	0 (0)	
Response²					
Overall response	109 (56)	41/82 (50)	48/82 (59)	20/31 (65)	0.313
Complete response	49 (25)	16/82 (20)	24/82 (32)	9/31 (29)	0.288

WBC: white blood cell count; MP-CMML: myeloproliferative chronic myelomonocytic leukemia; Hgb: hemoglobin; ANC: absolute neutrophil count; AMC: absolute monocyte count; PB: peripheral blood; BM: bone marrow; HMA: hypomethylating agent; LDAC: low-dose cytarabine; Cr: creatinine.

¹ Peripheral blood values at date of initial presentation. Values include those from patients with prior hydroxyurea therapy at time of presentation.

² Responses reported among patients treated with HMA therapy.

Table S2. Cox proportional hazards model for overall survival regressed on cluster weights

Variable	Log hazard ratio	Hazard ratio	95% CI	P value
Cluster 1	0.62946	1.87660	1.164-3.024	0.00974
Cluster 3	0.49413	1.63908	0.923-2.911	0.09178
Cluster 2	Reference	-	-	-
Age	0.3967	1.04046	1.016-1.066	0.00126
Sex	0.29470	1.34273	0.871-2.071	0.18244

Concordance: 0.643

Likelihood ratio test: $p=5 \times 10^{-4}$

Wald test: $p=7 \times 10^{-4}$

Score (logrank) test: $p=6 \times 10^{-4}$

Table S3. Cox proportional hazards model for leukemia-free survival regressed on cluster weights

Variable	Log hazard ratio	Hazard ratio	95% CI	P value
Cluster 1	0.71635	2.047	1.298-3.228	0.00205
Cluster 3	0.64384	1.904	1.104-3.283	0.02058
Cluster 2	Reference	-	-	-
Age	0.02768	1.028	1.006-1.051	0.01445
Sex	0.32334	1.382	0.915-2.087	0.1245

Concordance: 0.628

Likelihood ratio test: $p = 8 \times 10^{-4}$

Wald test: $p = 8 \times 10^{-4}$

Score (logrank) test: $p = 7 \times 10^{-4}$

Figure S1. Frequency of identified somatic mutations in the total cohort.

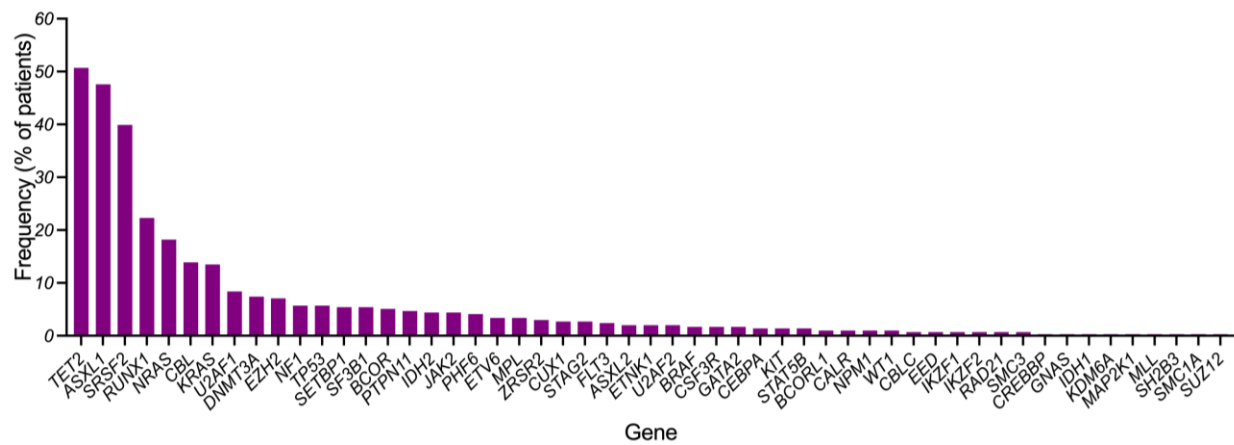


Figure S3. Variant allele frequency distributions of most common somatic mutations. Allele frequency distribution frequencies are shown for *ASXL1* (A), *TET2* (B), *SRSF2* (C), *NRAS* (D), *KRAS* (E), *CBL* (F) and *RUNX1* (G) among the three CMML genomic clusters. C: cluster.

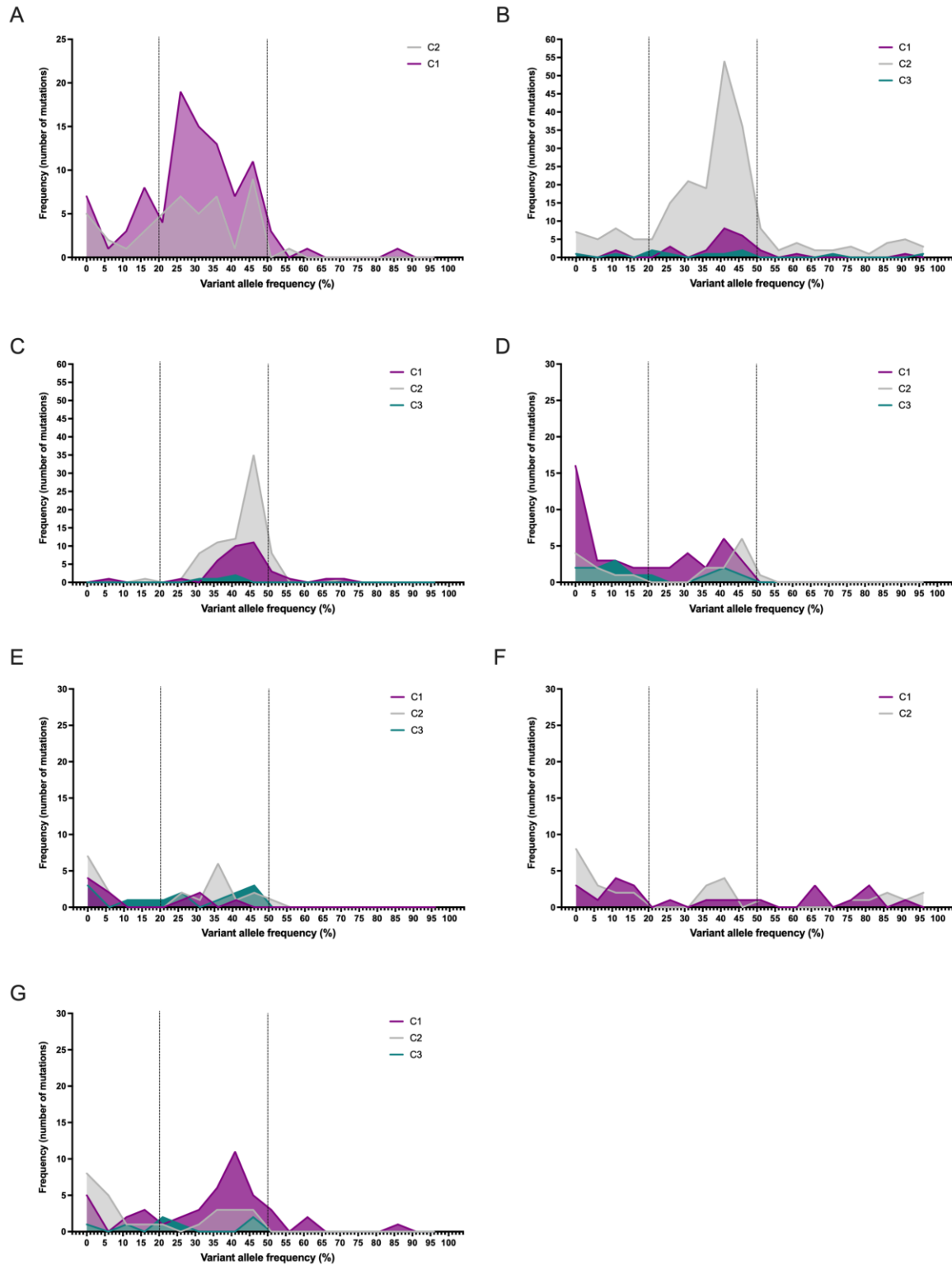


Figure S4. Mutation dominance distribution by CMML cluster. Frequencies of identified mutations as part of dominant or minor clones, in patients with 2 or more somatic mutations, among the 3 CMML genomic clusters. Clonal relationships were tested using Pearson goodness-of-fit tests with clonal heterogeneity being defined in cases with goodness-of-fit p values <0.05 suggesting significant variability of VAF distributions reflecting presence of several clones.

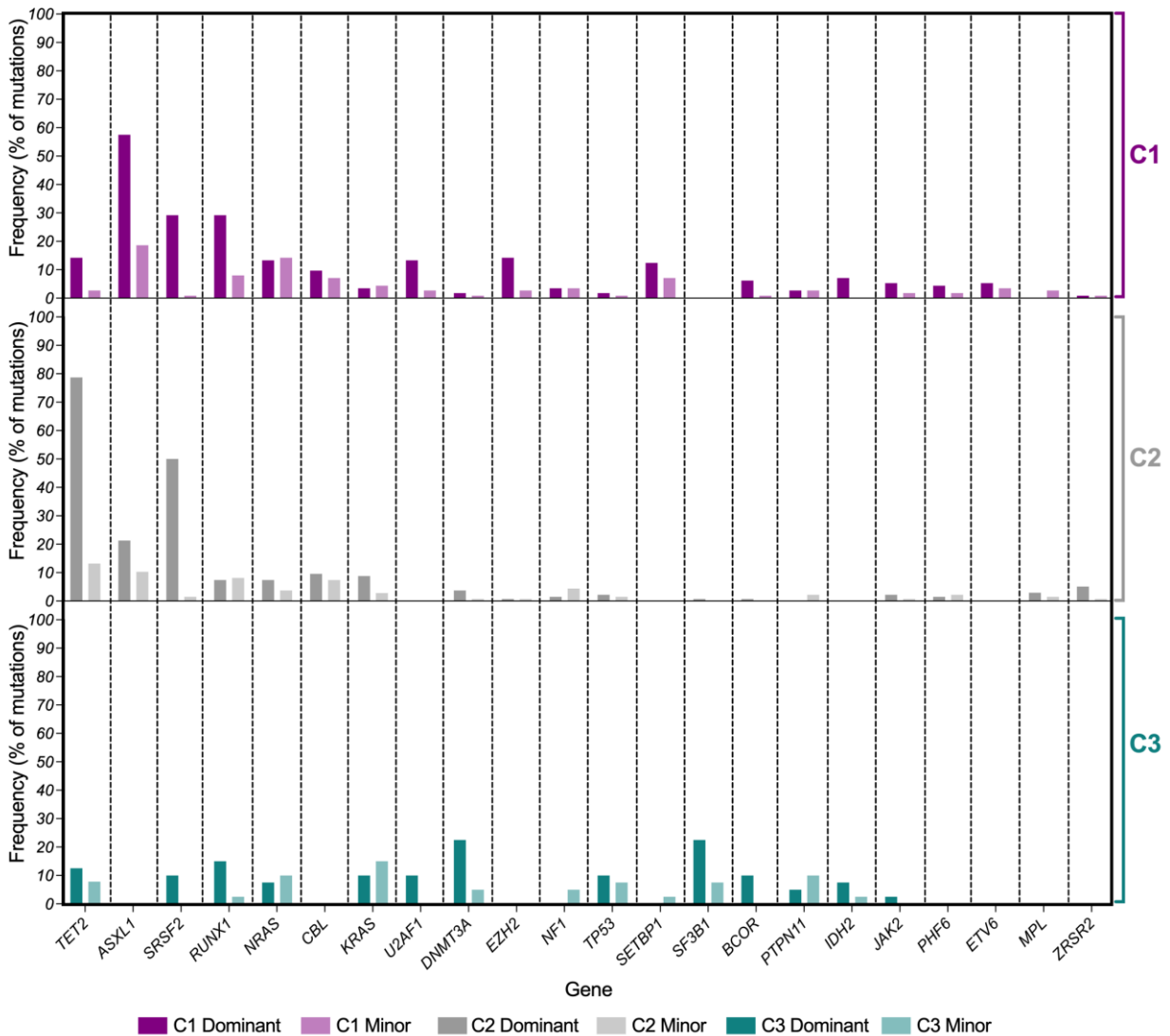


Figure S5. Clonal architecture at diagnosis and AML for each CMML cluster. Heatmap detailing frequency and clonal size of identified mutations among the 36 patients with comprehensive NGS at CMML diagnosis and at progression to AML. Mutations are color coded based on variant allele frequency (VAF) and classified among four groups: VAF <5%, 5-20%, 20-50% and >50%. Cytogenetic risk category defined according to the Revised International Prognostic Scoring System (IPSS-R) are color coded based on risk. Patients are grouped by cluster with each column representing one time point (CMML or AML diagnosis, respectively) for each individual patient. Patients are separated by thick vertical lines.

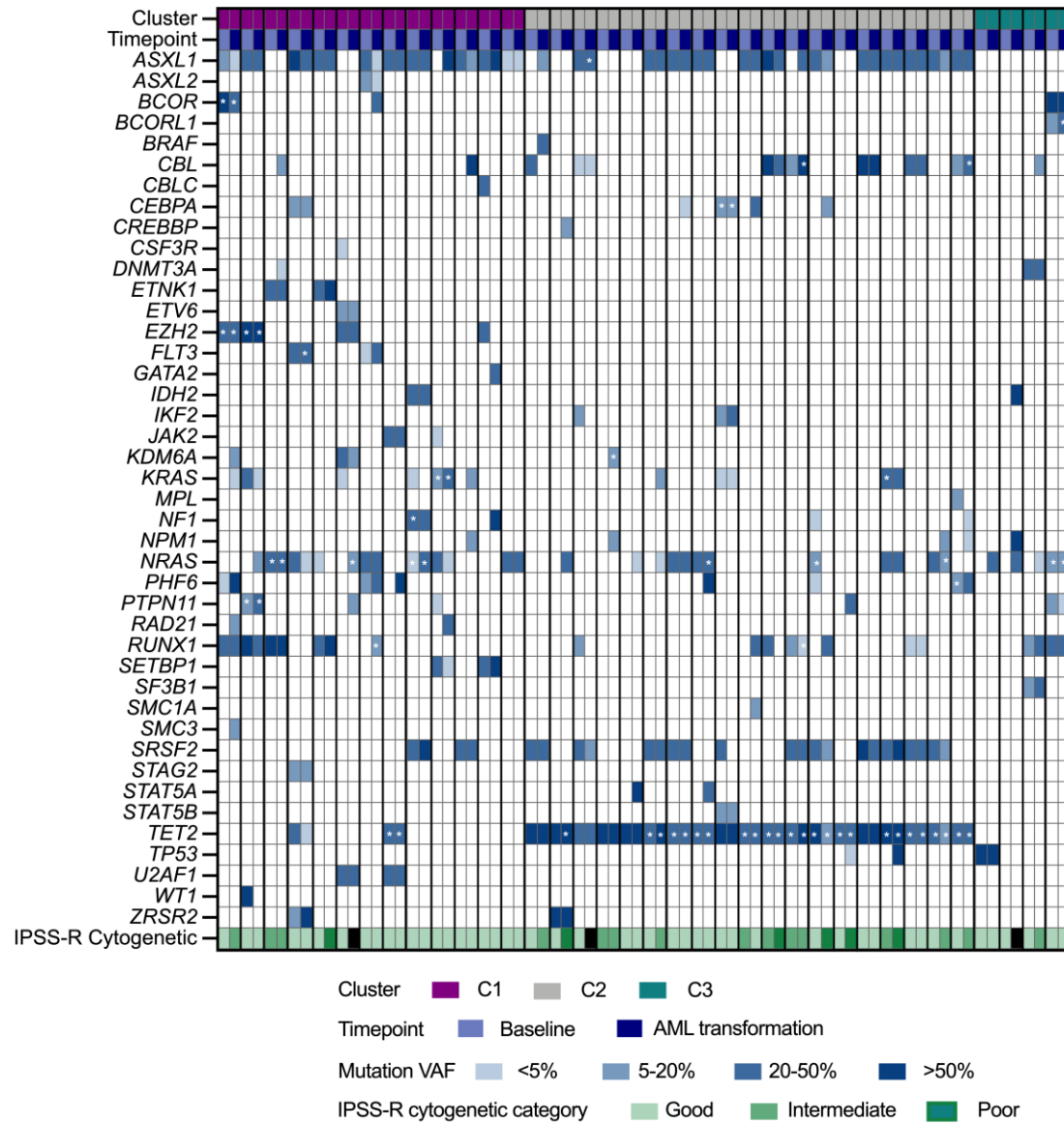


Figure S6. Frequency of emerging or expanding somatic mutations at transformation by CMML cluster. New and expanded mutations at progression among all patients (A), cluster 1 (B), cluster 2 (C) or cluster 3 (D) are shown. New mutations are shown in darker shaded color while clones with preexisting mutations that expanded at progression are shown in lighter shaded color.

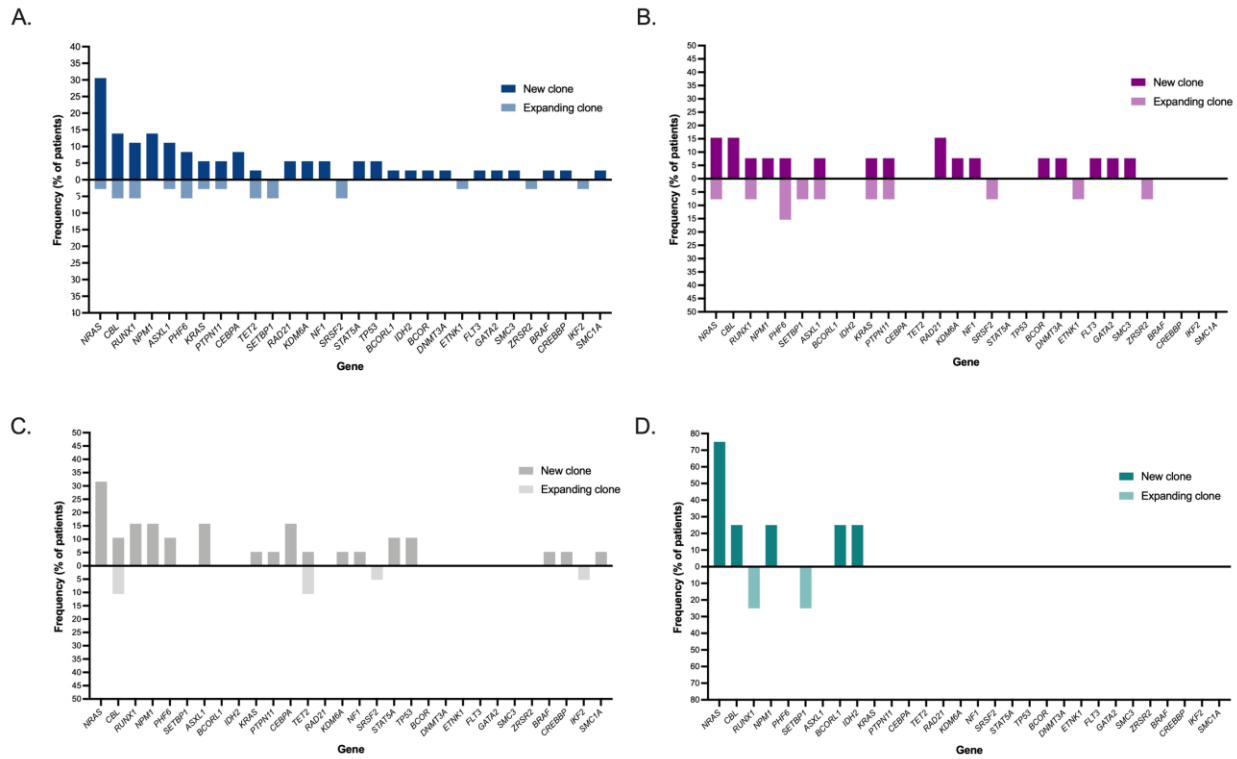
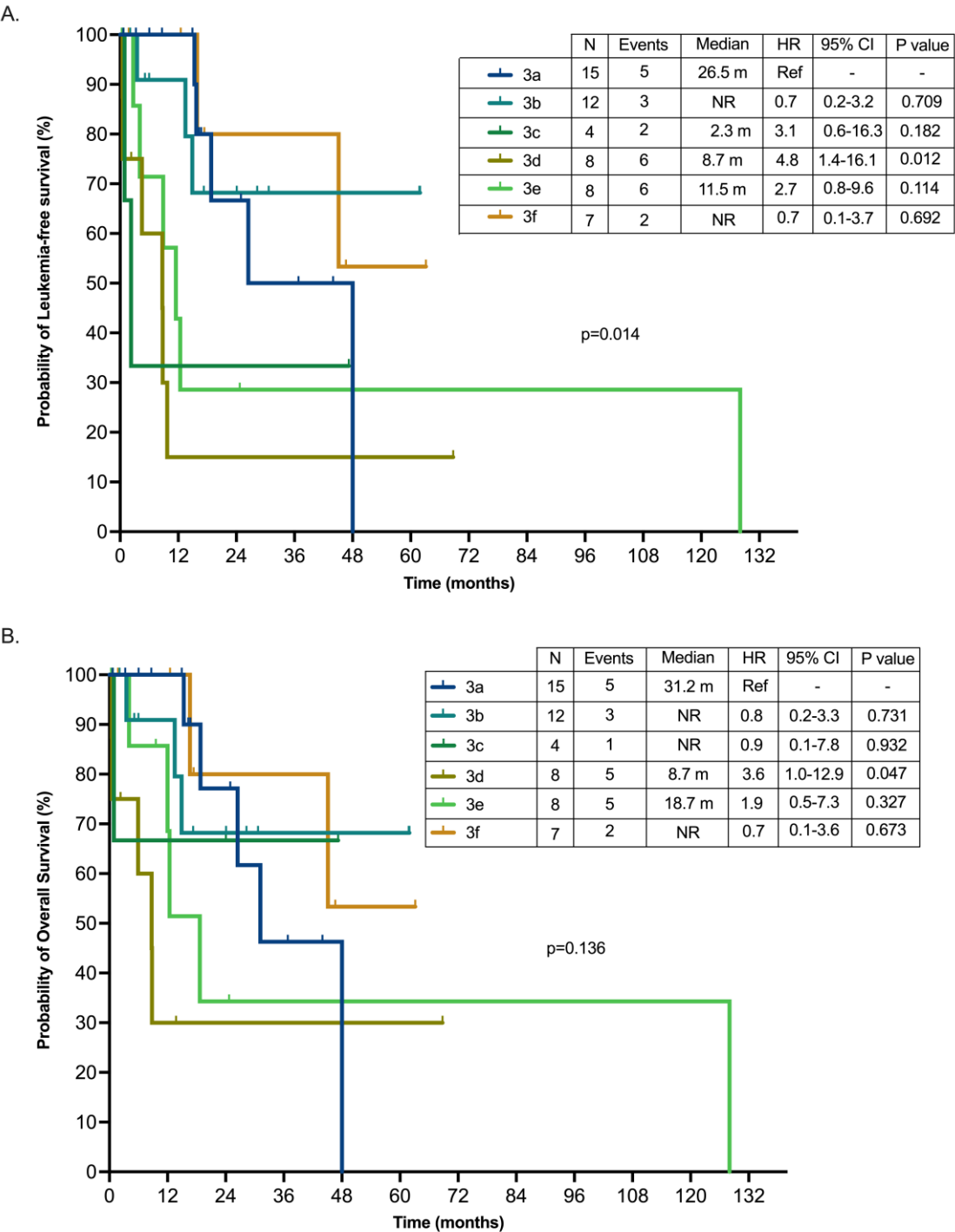


Figure S7. Survival outcomes based on cluster 3 genomic subclusters. Kaplan-Meier estimate survival curves for leukemia-free survival (A) or overall survival (B) based on genomic subcluster among patients belonging to cluster 3 based on attributable cluster weights.



DISCUSSION

The field of myeloid malignancies, particularly MDS and CMML, represents a dynamic interplay of clonal evolution, inflammatory signaling, and therapeutic resistance. The body of work presented in this thesis aims to advance our understanding of how these factors interact to drive disease progression, therapeutic failure, and potential avenues for intervention. By integrating findings across multiple studies, this discussion explores the biological underpinnings of these conditions and the challenges they pose, offering insights into innovative, targeted interventions.

Over the past two decades, no new therapeutic agents have been approved for the treatment of high-risk MDS or CMML, underscoring the persistent challenge of therapy resistance in managing these diseases (262). While the molecular and biological mechanisms driving venetoclax resistance in AML have been thoroughly explored (350, 463, 464), the reasons why patients with MDS and CMML develop secondary resistance to venetoclax following an initial response, particularly after failing HMA therapy, remain poorly understood. Venetoclax initially induces apoptosis in HSCs reliant on BCL2-mediated survival. However, adaptive mechanisms eventually emerge, enabling malignant HSCs to evade therapy. This thesis highlights how venetoclax resistance arises through transcriptional reprogramming, where granulomonocytic-biased HSCs adapt by activating NF- κ B signaling pathways. This molecular adaptation involves genetic alterations in key regulatory genes such as *STAG2* and *RUNX1*, which reshape the transcriptional milieu to favor a myeloid lineage bias and pro-survival signaling. Importantly, the interplay between *TP53* mutations and venetoclax resistance highlights an intrinsic vulnerability of the apoptotic machinery in these malignancies. *TP53*-mutated clones not only exhibit intrinsic resistance to BCL2 inhibition but also retain their transcriptional state, making them resilient to therapy-induced depletion (465). This finding aligns with previous studies identifying *TP53* mutations as mediators of poor prognosis and therapy failure. These findings exemplify a broader theme in myeloid malignancies, where HSC hierarchy and transcriptional flexibility enable survival despite therapeutic intervention (348).

Interestingly, our data suggest that *RUNX1* and *STAG2* mutations do not directly confer venetoclax resistance but instead influence hematopoiesis by promoting the myeloid differentiation of LT-HSCs and enhancing the self-renewal capacity of LMPPs and granulocytic-monocytic progenitors (GMPs), as previously shown in conditional mouse models of *RUNX1* or *STAG2* deletion (466, 467). Consistently, delicate HSC profile studies showed that MDS LMPPs and GMPs depend on NF- κ B-mediated pathways, rather than BCL2, for survival under therapy (83). Our observations emphasize that differentiation state, rather than direct molecular effects of these mutations, drives resistance. To validate these findings, we

employed the SKM-1 cell line, derived from a patient with MDS whose disease progressed to myelomonocytic leukemia (468). This cell line harbors mutations in *STAG2*, *ASXL1*, *KRAS*, and *TP53*, faithfully recapitulating the molecular complexity observed in patients with treatment-refractory MDS. To test whether *STAG2* mutation directly influenced venetoclax resistance, we restored *STAG2* expression in SKM-1 cells using lentiviral gene delivery. Interestingly, re-expression of *STAG2* did not alter BCL2 or phospho-p65 (an effector of NF- κ B signaling) levels, nor did it affect sensitivity to venetoclax alone or in combination with HMA therapy. These findings further support the hypothesis that venetoclax resistance in MDS is driven primarily by the differentiation state of malignant HSPCs rather than the direct molecular effects of specific mutations.

A pivotal finding is the role of the HSC differentiation hierarchy as a biomarker in determining therapeutic response and resistance patterns in MDS. Patients with an immunophenotypic “CMP pattern” exhibit greater initial sensitivity to venetoclax due to their reliance on BCL2. Conversely, those with a “GMP pattern” demonstrate intrinsic resistance, reflecting their dependency on NF- κ B-mediated survival mechanisms. Over time, even CMP-pattern HSCs adapt under the selective pressure of venetoclax treatment, transitioning to NF- κ B-driven pro-survival signaling pathways. This underscores the necessity of tailoring therapeutic strategies based on the differentiation states of malignant HSCs, which serve as both predictors of treatment response and mediators of resistance. Our multi-omics analyses elucidate the genetic and transcriptional reprogramming events underlying venetoclax resistance. This plasticity not only confers resistance but also creates vulnerabilities that can be therapeutically exploited. Particularly, MCL1, a pivotal downstream mediator of NF- κ B signaling, is significantly upregulated in venetoclax-resistant HSCs, promoting survival and clonal expansion under therapeutic stress. Preclinical studies suggest that targeting MCL1 could provide a promising approach to overcoming venetoclax resistance in “GMP-pattern” MDS. These findings emphasize the importance of exploring combination therapies that leverage MCL1 inhibition to disrupt the survival mechanisms of resistant HSCs, paving the way for more effective treatment strategies in venetoclax-refractory cases.

From a clinical perspective, these findings underscore the importance of early intervention strategies that preempt the emergence of resistance pathways. Monitoring the emergence or expansion of *STAG2*- or *RUNX1*-mutated clones in venetoclax-treated patients could guide the timely incorporation of combination therapies to target adaptive survival mechanisms. Such approaches may prevent disease progression and extend the duration of therapeutic response. Furthermore, understanding the differentiation states and molecular profiles of

HSCs in individual patients could guide personalized treatment strategies, aligning with the principles of precision medicine.

The complexity of resistance in myeloid malignancies is exemplified by the dependence of RAS-mutant CMML on MCL1 and NF- κ B-mediated survival pathways. This dependency underscores how distinct mechanisms of survival are activated under therapeutic pressure (365). Following the failure of HMAs, the NF- κ B pathway emerges as a central mediator of cell survival, rerouting apoptotic reliance from BCL2 to MCL1. This shift highlights the remarkable adaptability of HSCs within CMML, particularly in RAS-mutant populations, which can evade cytotoxic interventions and sustain survival. Despite significant advancements in characterizing molecular landscape of CMML, the limited understanding of how genetic alterations influence distinct transcriptional states of monocytic/myeloid differentiation has delayed progress in improving patient survival (96, 97, 469-471). RAS pathway mutations, initially found in approximately 30% of CMML patients (471), become increasingly prevalent during disease progression, reaching up to 90% of cases. These alterations are strongly linked to an elevated risk of relapse and poorer survival outcomes following venetoclax-based (472). To date, no therapies effectively extend survival in RAS-mutant CMML patients.

The mechanistic insight provided by transcriptomic and chromatin accessibility profiling elucidates how NF- κ B and MCL1 upregulation not only contribute to cell survival but also foster conditions favorable to blast transformation. RAS mutations amplify NF- κ B signaling and immune evasion mechanisms, enabling HSCs and downstream monocytic populations to thrive under HMA failure. The reliance of RAS-mutant HSCs on MCL1, rather than BCL2, for survival highlights a shared resistance mechanism across myeloid malignancies. Notably, the selective efficacy of AMG-176, an MCL1 inhibitor, underscores the therapeutic potential of targeting this pathway in CMML patients exhibiting blast progression after HMA failure. These findings mirror observations in venetoclax-resistant MDS, where GMP-pattern HSCs upregulate MCL1 to evade apoptosis.

Using single-cell multi-omics technologies, we sought to dissect the biological mechanisms behind *RAS* pathway mutation-induced CMML evolution with the overall goal of identifying cellular vulnerabilities that could be therapeutically targeted to halt disease progression. We found that at disease initiation, CMML HSPCs significantly upregulated NF- κ B pathway and IFN-mediated inflammatory transcriptional signals that drive these cells' differentiation towards the monocytic/myeloid lineage while maintaining an intact apoptotic program. This inflammatory reprogramming was exacerbated in downstream *RAS* pathway mutant monocyte populations, which expressed high levels of cytokines and cell surface receptors

involved in NF- κ B pathway activation and immune evasion. These results suggest that disease initiation and maintenance rely on the activation of cell-intrinsic and -extrinsic inflammatory networks and provide a rationale for using inhibitors of NF- κ B-associated inflammatory signaling cascades as a frontline treatment for patients with *RAS* pathway mutated CMML. These results are in agreement with earlier studies emphasizing the involvement of inflammatory cell populations in myeloid malignancies (367, 473). Importantly, they underscore the therapeutic promise of inflammation-targeting strategies, many of which are in advanced clinical development and show considerable potential for managing myeloid malignancies (438, 474, 475).

Adding to the existing discussion, the complexity of inflammation and immune dysregulation in myeloid malignancies extends beyond HSPC-driven processes, as demonstrated by the involvement of T cells and NK cells in MDS and CMML (166). Single-cell analyses reveal that interactions between CMML monocytes and immune effector cells, such as effector CD8⁺ T cells and NK cells, are significantly altered, particularly in *RAS*-mutant CMML. These interactions are characterized by immune-suppressive ligand-receptor engagements, including HLA-E-KLRC1/2 and TGFB1-TGBR1/3 pairs, which contribute to the functional exhaustion of T cells and NK cells (476-482). As a result, both CD8⁺ T cells and NK cells in the CMML microenvironment exhibit diminished activation and cytokine production, further exacerbating immune evasion and clonal expansion.

Targeting MCL1 activity with the small molecule AMG-176 only significantly depleted HSPCs from *RAS* mutant CMML but not those from *RAS* wildtype CMML, a finding that supports the selective use of MCL1 inhibitors to treat patients with *RAS* pathway mutant CMML in whom BP occurs at the time of HMA therapy failure. These results are consistent with previous findings showing that CMML monocytes rely on MCL1, but not BCL2, for survival (483), and that *NRAS*-mutant monocytic subclones that emerge at AML relapse depend on MCL1, not BCL2, for energy production (350). Consistent with this observation, our scRNA-seq analysis of BM MNCs from one representative patient with venetoclax-resistant disease confirmed that BCL2 inhibition cannot overcome the activation of NF- κ B pathway-mediated inflammatory and survival mechanisms in HSPCs and downstream My/Mo populations.

These findings integrate seamlessly with our understanding of the interplay between NF- κ B and MCL1 signaling pathways in HSPCs, underscoring the multifaceted nature of CMML progression. The immune-suppressive microenvironment, characterized by dysfunctional CD8⁺ T cells and NK cells, not only facilitates disease persistence but also intersects with the adaptive survival mechanisms of HSPCs. Specifically, the reliance of *RAS*-mutant CMML

HSPCs on MCL1 for anti-apoptotic signaling becomes more pronounced under venetoclax resistance, creating a dual axis of therapeutic opportunity. Addressing these interconnected pathways through combination therapies that target MCL1-driven survival and simultaneously rejuvenate immune effector functions holds significant potential. Such an approach could disrupt the intricate feedback loop between immune evasion and HSPC resilience, offering a more comprehensive strategy to overcoming resistance mechanisms and enhancing clinical outcomes for patients with CMML. These findings highlight the critical need for therapeutic designs that consider both the intrinsic adaptability of leukemic cells and the extrinsic influence of the tumor microenvironment.

Inflammation not only drives disease progression but also establishes a permissive environment for clonal expansion and therapeutic resistance. Pro-inflammatory cytokines, including IL-1 β , TNF- α , and IFN- γ , are key mediators in shaping the BM microenvironment. These factors contribute to a self-reinforcing cycle of immune dysregulation and hematopoietic skewing, which exacerbates ineffective erythropoiesis and promotes the persistence of aberrant HSC clones. Mutant HSCs, particularly those harboring CHIP-associated mutations in *TET2* and *DNMT3A*, exploit this inflammatory milieu, enhancing their self-renewal capacity while evading differentiation signals. Unlike their wildtype counterparts, these mutant clones exhibit an intrinsic resistance to inflammation-induced depletion, providing a competitive edge that fuels disease evolution and therapeutic resistance (185, 186). This interplay between clonal hematopoiesis, inflammatory signaling and leukemization underscores the need for therapeutic approaches that disrupt these pathogenic pathways.

Interleukin-1 β (IL-1 β) is a master-regulator pro-inflammatory cytokine that plays a pivotal role in the innate immune response to infection and tissue injury. By binding to its receptor, IL-1R1, IL-1 β activates a signaling cascade that regulates the expression of various transcription factors, cytokines, and growth factors essential for hematopoiesis (484). This signaling cascade promotes the expression of IL-1 β target genes, such as IL-6 and IL-8, which drive myeloid skewing and contribute to ineffective erythropoiesis (179). Dysregulated IL-1 β signaling has been implicated in aging (485) and a range of diseases, including hematopoietic malignancies and cardiovascular disorders (486).

The CANTOS trial provided further evidence supporting IL-1 β inhibition in inflammation-driven malignancies. Treatment with canakinumab, an IL-1 β monoclonal antibody, resulted in improved hemoglobin levels in patients with CHIP-associated mutations, especially those with *TET2* and *DNMT3A* mutations, offering a compelling rationale for exploring its application in inflammation-driven malignancies such as MDS and CMML (486-488). Recent studies using

Tet2-deficient mouse models have shown that IL-1 β enhances the self-renewal capacity of mutant HSCs by hindering the demethylation of critical transcription factor binding sites involved in terminal differentiation (489, 490). Both genetic knockout of *IL-1r1* in *Tet2*-deficient HSPCs and pharmacological inhibition of IL-1 β signaling with the IL-1R1 antagonist anakinra led to significant reductions in myeloid skewing and clonal expansion (489, 490). These results highlight the therapeutic potential of targeting the IL-1 β pathway as a strategy to address dysfunctional myeloid skewing and clonal dominance in early-stage myeloid neoplasms, such as clonal cytopenias of undetermined significance (CCUS) and lower-risk MDS. To confirm these findings in a human setting, we conducted a phase 2 trial evaluating the efficacy of the IL-1 β inhibitor canakinumab in individuals with lower-risk MDS and CMML (NCT04239157).

Canakinumab exhibited a favorable safety profile in a final cohort of 25 patients, with no dose adjustments or treatment discontinuation reported. Cytopenia, occurring in 64% of patients, was the most frequently observed grade 3 or higher adverse event associated with the treatment. This adverse effect likely reflects a combination of treatment-induced myelosuppression and the inherent clinical trajectory of patients with lower-risk MDS. Importantly, unlike prior trials conducted in the context of IL-1 β inhibition, no grade 3 or 4 infections were reported during the trial (491, 492).

The overall response rate to canakinumab was 17%, with hematologic improvements in erythroid (HI-E, 13%) and platelet (HI-P, 4%) lineages. The median response duration among responders was 8.5 months. Patient stratification according to the IPSS-M scoring system revealed that the efficacy of canakinumab was primarily confined to patients with lower-risk MDS, where the inflammatory milieu is less confounded by high genetic complexity. Patients with founder mutations in *TET2* or *DNMT3A* exhibited durable responses, including prolonged hematologic improvements and transfusion independence. In contrast, patients with *SF3B1* mutations failed to respond, likely due to distinct pathogenic mechanisms underlying ineffective erythropoiesis and the relatively lower inflammatory signatures observed in these subtypes (493).

The lack of response in *SF3B1*-mutant MDS may also be linked to reduced HLA-DR expression levels in *SF3B1*-mutant monocytes, which impairs the efficacy of canakinumab in modulating interactions with pro-inflammatory CD8⁺GZMK⁺ T cells. These interactions are believed to promote the migration of monocytes and their differentiation into pro-inflammatory macrophages

. Previous research supports that *SF3B1*-mutant MDS is characterized by lower levels of inflammatory cytokines, including IL-1 β , compared to other lower-risk MDS subtypes,

particularly those with isolated 5q deletions (493). Consistent with these findings, canakinumab produced its most prolonged response and induced transfusion independence in the only patient with MDS-5q included in this study. Resistance to canakinumab was closely linked to increased genetic complexity, suggesting that mechanisms beyond inflammation, including cooperative mutational effects and enhanced immune suppression, contribute to the persistence of cytopenias and the clonal expansion of mutant cells. These findings highlight the multifaceted pathogenesis of MDS and the need for combination therapeutic strategies.

This study is subject to limitations inherent in early-phase dose-finding trials, including the lack of a control group and the relatively small sample size. Furthermore, the enrolled patients may not fully represent the broader lower-risk MDS population, as many had received prior intensive treatments or exhibited high-risk genetic features. While Canakinumab demonstrates a strong on-target effect in reducing inflammation and improving hematologic parameters, resistance to treatment underscores the multifactorial nature of MDS pathogenesis. High genetic complexity and immune suppression exacerbate clonal expansion, highlighting the importance of integrating anti-inflammatory therapies with other targeted approaches to address both intrinsic and extrinsic disease drivers. These results emphasize the need for patient stratification based on genetic and molecular profiles to optimize treatment outcomes and identify those most likely to benefit from IL-1 β inhibition, as well as its application in pre-leukemic stages (i.e., high-risk CCUS/CMUS).

Up to this point, we have thoroughly examined the mechanisms governing the behavior of HSPCs in a disease state, particularly within a pro-inflammatory and immunocompromised environment, and how these factors contribute to both disease initiation and progression. However, these processes operate in a broader context characterized by chromosomal instability and high tumor burden, hallmarks that profoundly shape the disease's trajectory. Within this framework, the complex interplay between co-occurring mutations and disease phenotypes in CMML, as explored in the third manuscript, provides crucial insights into disease heterogeneity and progression risks.

CMML is a clonal disorder originating in mutant HSPCs (96) and is marked by a significant risk of progression to AML (337). The integration of molecular, clinical, and cytogenetic data has enabled the development of multiple prognostic models for clinical application (53, 494). However, despite these advances, predicting disease transformation and understanding the cooperative interactions of distinct genomic events remain limited. Prior studies have hinted at the cooperative effects of specific mutations (52, 267), but more comprehensive efforts to

define recurrent genomic patterns and their impact on clinical phenotypes could refine CMML classification and guide the development of novel, rationally designed combination therapies.

Our analysis sheds light on the cooperative effects of recurrent somatic mutations in CMML, identifying specific genomic patterns associated with distinct clinical phenotypes and outcomes. In order to evaluate further if distinct genomic profiles, characterized by recurrent co-occurrence of somatic mutations, define clinicopathologic subgroups of CMML with distinct outcomes, we evaluated a cohort of patients with CMML and used computational methods to identify unique clusters defined by recurrent co-mutational patterns and define their clinical features and outcomes. Our data confirms prior reports suggesting that certain mutations co-occur in CMML (52, 267) and identifies three major genomic-defined disease clusters: Using computational approaches, three major mutational clusters were defined: Cluster 1 (C1) dominated by *ASXL1* and *RUNX1* mutations with frequent co-occurrence of *SETBP1* and *EZH2* mutations, Cluster 2 (C2) characterized by multi-hit *TET2* mutations and *SRSF2* co-dominance, and Cluster 3 (C3), a heterogeneous group enriched for *SF3B1*, *KRAS*, *DNMT3A*, and *TP53* mutations.

These clusters provide a framework for understanding how mutational co-occurrence drives clinical diversity in CMML. For example, the predominance of *ASXL1* mutations in C1 correlates with aggressive phenotypes, including elevated blast counts and a higher frequency of del(7q)/-7, which are known markers of poor prognosis (495). Conversely, the universal presence of *TET2* mutations in C2, often co-occurring with *SRSF2* mutations, reflects a distinct biological subset with prolonged survival and a higher likelihood of maintaining a normal karyotype (496). Meanwhile, the genomic heterogeneity of C3 underscores its complexity, with mutations in *SF3B1* and *TP53* defining subgroups that exhibit unique vulnerabilities and clinical behaviors.

Importantly, the dynamic nature of clonal evolution further delineates these clusters. For instance, patients in C1 and C2 showed expansion of pre-existing *NRAS*, *RUNX1*, and *ASXL1*-mutant clones at the time of AML transformation. This observation highlights the role of clonal dominance and allele frequency in defining disease evolution. Notably, C2 patients with biallelic *TET2* loss exhibited unique phenotypic features, including higher hemoglobin levels and better LFS compared to those with monoallelic *TET2* alterations. These findings emphasize the significance of genomic context in modulating disease outcomes and suggest that incorporating these mutational patterns into risk stratification models could enhance their predictive power.

From a therapeutic perspective, these results highlight the potential of targeting specific pathways associated with distinct mutational clusters. For example, the dependency of *ASXL1*-mutant clones on inflammatory and anti-apoptotic signaling pathways, such as NF- κ B and MCL1, suggests that inhibitors targeting these axes may be particularly effective in C1-dominated CMML. Similarly, the enrichment of spliceosome mutations in C2 underscores the need to explore therapeutic strategies that exploit vulnerabilities in RNA splicing machinery. For patients in C3, characterized by *TP53* and *SF3B1* mutations, interventions aimed at mitigating DNA damage responses and aberrant mitochondrial function could provide novel avenues for treatment. Overall, the integration of molecular, phenotypic, and clinical data into a unified model provides a robust framework for refining CMML classification and guiding personalized therapeutic interventions. Through the identification and detailed characterization of these mutational clusters, our study enhances the understanding of CMML pathogenesis and

lays the foundation for rationally designed therapies that address the disease's underlying molecular drivers. Future studies should aim to validate these findings in larger cohorts and investigate how these mutational profiles interact with the tumor microenvironment, particularly in shaping inflammatory signaling and immune evasion. These efforts are essential for translating these findings into clinical applications, with the ultimate goal of improving outcomes for patients affected by this complex and heterogeneous disease.

In bringing together the intricate puzzle of myeloid malignancies, this discussion highlights the profound complexity of disease biology, where clonal evolution, inflammatory signaling, and therapeutic resistance converge to create formidable challenges. The work presented bridges molecular insights with clinical implications, underscoring the transformative power of precision medicine to reframe our approach to MDS and CMML. By unraveling the adaptive survival mechanisms of HSPCs, the dynamic nature of inflammatory pathways, and the co-mutational landscapes driving disease progression, this thesis paves the way for a deeper understanding of these malignancies. It calls for a paradigm shift—one that embraces the heterogeneity of disease, anticipates resistance mechanisms, and tailors interventions to the unique vulnerabilities of each patient.

At its heart, this research is a testament to the resilience of scientific inquiry and the pursuit of hope in the face of complexity. It reminds us that while the challenges are immense, so too is the potential for innovation. By integrating knowledge across molecular, cellular, and clinical dimensions, we move closer to realizing the goal of personalized and durable therapies—turning the tide of disease, one discovery at a time. This work is not just a step forward in

understanding myeloid malignancies; it is a call to action, urging continued exploration and collaboration to bring transformative therapies to patients in need.

CONCLUSIONS

1. Differentiation hierarchies in hematopoietic stem cells strongly influence therapeutic responses in myelodysplastic syndromes and chronic myelomonocytic leukemia. Patients with common myeloid progenitor patterns show greater sensitivity to venetoclax, whereas those with granulomonocytic progenitor patterns exhibit resistance driven by NF- κ B-mediated survival pathways.
2. Venetoclax resistance is driven by adaptive transcriptional reprogramming, where granulomonocytic-biased hematopoietic stem cells transition from BCL2 dependency to reliance on NF- κ B and MCL1 signaling. This shift is fueled by the expansion of pre-existing mutations such as STAG2 and RUNX1, highlighting the plasticity of clonal evolution under therapeutic pressure.
3. RAS-mutant chronic myelomonocytic leukemia amplifies inflammatory signaling through NF- κ B, driving clonal evolution and resistance under hypomethylating agent failure. Targeting MCL1 and NF- κ B pathways in this high-risk subset provides promising therapeutic opportunities.
4. Canakinumab is safe in myelodysplastic syndromes and efficiently targets IL-1 β signaling. Sequential single-cell RNA sequencing analyses of hematopoietic stem and progenitor cell and bone marrow mononuclear cells during therapy demonstrated canakinumab's on-target effects, reducing TNF-mediated inflammatory signaling in hematopoietic populations expressing the IL-1 β receptor. Importantly, the restoration of effective erythropoiesis and transfusion independence was observed only in patients with lower genetic complexity.
5. Co-occurring mutations define distinct subgroups in chronic myelomonocytic leukemia, with ASXL1-dominant, multi-hit TET2, TET2/SRSF2-enriched, and TP53/SF3B1-associated clusters correlating with unique clinical behaviors and outcomes. These genomic patterns enhance risk stratification and reveal actionable vulnerabilities.

REFERENCES

1. Shastri A, Will B, Steidl U, Verma A. Stem and progenitor cell alterations in myelodysplastic syndromes. *Blood*. 2017;129(12):1586-94.
2. Khoury JD, Solary E, Abal O, Akkari Y, Alaggio R, Apperley JF, et al. The 5th edition of the World Health Organization classification of haematolymphoid tumours: myeloid and histiocytic/dendritic neoplasms. *Leukemia*. 2022;36(7):1703-19.
3. Khoury JD, Solary E, Abal O, Akkari Y, Alaggio R, Apperley JF, et al. The 5th edition of the World Health Organization Classification of Haematolymphoid Tumours: Myeloid and Histiocytic/Dendritic Neoplasms. *Leukemia*. 2022;36(7):1703-19.
4. Hochman MJ, DeZern AE. SOHO State of the Art Updates and Next Questions: An Update on Higher Risk Myelodysplastic Syndromes. *Clinical lymphoma, myeloma & leukemia*. 2024;24(9):573-82.
5. Jaiswal S, Ebert BL. MDS is a stem cell disorder after all. *Cancer cell*. 2014;25(6):713-4.
6. Woll PS, Kjällquist U, Chowdhury O, Doolittle H, Wedge DC, Thongjuea S, et al. Myelodysplastic syndromes are propagated by rare and distinct human cancer stem cells in vivo. *Cancer cell*. 2014;25(6):794-808.
7. Bennett JM, Catovsky D, Daniel MT, Flandrin G, Galton DA, Gralnick HR, et al. Proposals for the classification of the myelodysplastic syndromes. *British journal of haematology*. 1982;51(2):189-99.
8. Cazzola M, Malcovati L. Myelodysplastic syndromes--coping with ineffective hematopoiesis. *N Engl J Med*. 2005;352(6):536-8.
9. Tefferi A, Vardiman JW. Myelodysplastic syndromes. *N Engl J Med*. 2009;361(19):1872-85.
10. Tuzuner N, Cox C, Rowe JM, Watrous D, Bennett JM. Hypocellular myelodysplastic syndromes (MDS): new proposals. *British journal of haematology*. 1995;91(3):612-7.
11. Bennett JM, Orazi A. Diagnostic criteria to distinguish hypocellular acute myeloid leukemia from hypocellular myelodysplastic syndromes and aplastic anemia: recommendations for a standardized approach. *Haematologica*. 2009;94(2):264-8.
12. Jaffe ES. World Health Organization classification of tumours. Pathology and genetics of tumours of haematopoietic and lymphoid tissues. 2001.
13. Patnaik MM, Tefferi A. Chronic myelomonocytic leukemia: 2024 update on diagnosis, risk stratification and management. *Am J Hematol*. 2024;99(6):1142-65.
14. Swerdlow SH, World Health O, International Agency for Research on C. WHO classification of tumours of haematopoietic and lymphoid tissues 2017.
15. Swerdlow SH, Campo E, Harris NL, Jaffe ES, Pileri SA, Stein H, et al. WHO classification of tumours of haematopoietic and lymphoid tissues: International agency for research on cancer Lyon; 2008.
16. Rhoads CP, Barker WH. Refractory Anemia: Analysis of One Hundred Cases. *Journal of the American Medical Association*. 1938;110(11):794-6.
17. Hamilton-Paterson JL. Pre-leukaemic anaemia. *Acta haematologica*. 1949;2(5):309-16.
18. Bjorkman SE. Chronic refractory anemia with sideroblastic bone marrow; a study of four cases. *Blood*. 1956;11(3):250-9.
19. Block M, Jacobson LO, Bethard WF. Preleukemic acute human leukemia. *J Am Med Assoc*. 1953;152(11):1018-28.
20. Rheingold JJ, Kaufman R, Adelson E, Lear A. Smoldering acute leukemia. *N Engl J Med*. 1963;268:812-5.
21. Saarni MI, Linman JW. Preleukemia. The hematologic syndrome preceding acute leukemia. *The American journal of medicine*. 1973;55(1):38-48.
22. Sexauer J, Kass L, Schnitzer B. Subacute myelomonocytic leukemia. *Clinical*,

- morphologic and ultrastructural studies of 10 cases. *The American journal of medicine*. 1974;57(6):853-61.
23. Miescher P, Farguet J, editors. Chronic myelomonocytic leukemia in adults. *Seminars in hematology*; 1974.
 24. Bennett JM, Catovsky D, Daniel MT, Flandrin G, Galton DA, Gralnick HR, et al. Proposals for the classification of the acute leukaemias. French-American-British (FAB) co-operative group. *Br J Haematol*. 1976;33(4):451-8.
 25. Swerdlow SH, Campo E, Harris NL, Jaffe ES, Pileri SA, Stein H, et al. World Health Organization classification of tumours of haematopoietic and lymphoid tissues. Lyon: IARC press; 2008.
 26. Worsley A, Oscier DG, Stevens J, Darlow S, Figs A, Mufti GJ, et al. Prognostic features of chronic myelomonocytic leukaemia: a modified Bournemouth score gives the best prediction of survival. *British journal of haematology*. 1988;68(1):17-21.
 27. Aul C, Gattermann N, Heyll A, Germing U, Derigs G, Schneider W. Primary myelodysplastic syndromes: analysis of prognostic factors in 235 patients and proposals for an improved scoring system. *Leukemia*. 1992;6(1):52-9.
 28. Onida F, Kantarjian HM, Smith TL, Ball G, Keating MJ, Estey EH, et al. Prognostic factors and scoring systems in chronic myelomonocytic leukemia: a retrospective analysis of 213 patients. *Blood*. 2002;99(3):840-9.
 29. Beran M, Wen S, Shen Y, Onida F, Jelinek J, Cortes J, et al. Prognostic factors and risk assessment in chronic myelomonocytic leukemia: validation study of the M.D. Anderson Prognostic Scoring System. *Leukemia & lymphoma*. 2007;48(6):1150-60.
 30. González-Medina I, Bueno J, Torrequebrada A, López A, Vallespí T, Massagué I. Two groups of chronic myelomonocytic leukaemia: myelodysplastic and myeloproliferative. Prognostic implications in a series of a single center. *Leukemia research*. 2002;26(9):821-4.
 31. Such E, Germing U, Malcovati L, Cervera J, Kuendgen A, Della Porta MG, et al. Development and validation of a prognostic scoring system for patients with chronic myelomonocytic leukemia. *Blood*. 2013;121(15):3005-15.
 32. Aguirre LE, Jain AG, Ball S, Ali NA, Sallman DA, Kuykendall AT, et al. Refining risk stratification in CMML: A comprehensive assessment of the IPSS-M and other molecularly informed models. *Journal of Clinical Oncology*. 2023;41(16_suppl):7020-.
 33. Bernard E, Tuechler H, Greenberg PL, Hasserjian RP, Ossa JEA, Nannya Y, et al. Molecular International Prognostic Scoring System for Myelodysplastic Syndromes. *NEJM Evidence*. 2022;0(0):EVIDoa2200008.
 34. Baer C, Huber S, Hutter S, Meggendorfer M, Nadarajah N, Walter W, et al. Risk prediction in MDS: independent validation of the IPSS-M-ready for routine? *Leukemia*. 2023;37(4):938-41.
 35. Palomo L, Morgades M, Meggendorfer M, Díaz-Beyá M, Pomares H, Ramil López G, et al. Assessment of the IPSS-M in Chronic Myelomonocytic Leukemia. *Blood*. 2024;144:3205.
 36. Rollison DE, Howlader N, Smith MT, Strom SS, Merritt WD, Ries LA, et al. Epidemiology of myelodysplastic syndromes and chronic myeloproliferative disorders in the United States, 2001-2004, using data from the NAACCR and SEER programs. *Blood*. 2008;112(1):45-52.
 37. Garcia-Manero G. Myelodysplastic syndromes: 2023 update on diagnosis, risk-stratification, and management. *American journal of hematology*. 2023;98(8):1307-25.
 38. Heibl S, Stauder R, Pfeilstöcker M. Is Myelodysplasia a Consequence of Normal Aging?

- Current Oncology Reports. 2021;23(12):142.
39. Adès L, Sekeres MA, Wolffromm A, Teichman ML, Tiu RV, Itzykson R, et al. Predictive factors of response and survival among chronic myelomonocytic leukemia patients treated with azacitidine. *Leukemia research*. 2013;37(6):609-13.
 40. Patnaik MM, Lasho TL, Finke CM, Hanson CA, Hodnefield JM, Knudson RA, et al. Spliceosome mutations involving SRSF2, SF3B1, and U2AF35 in chronic myelomonocytic leukemia: prevalence, clinical correlates, and prognostic relevance. *American journal of hematology*. 2013;88(3):201-6.
 41. Swerdlow SH, Campo E, Pileri SA, Harris NL, Stein H, Siebert R, et al. The 2016 revision of the World Health Organization classification of lymphoid neoplasms. *Blood*. 2016;127(20):2375-90.
 42. Williamson PJ, Kruger AR, Reynolds PJ, Hamblin TJ, Oscier DG. Establishing the incidence of myelodysplastic syndrome. *British journal of haematology*. 1994;87(4):743-5.
 43. Yarosh R, Roesler MA, Murray T, Cioc A, Hirsch B, Nguyen P, et al. Risk factors for de novo and therapy-related myelodysplastic syndromes (MDS). *Cancer Causes Control*. 2021;32(3):241-50.
 44. Strom SS, Gu Y, Gruschkus SK, Pierce SA, Estey EH. Risk factors of myelodysplastic syndromes: a case-control study. *Leukemia*. 2005;19(11):1912-8.
 45. Bagby GC, Meyers G. Bone marrow failure as a risk factor for clonal evolution: prospects for leukemia prevention. *Hematology American Society of Hematology Education Program*. 2007:40-6.
 46. Bagby GC, Meyers G. Myelodysplasia and acute leukemia as late complications of marrow failure: future prospects for leukemia prevention. *Hematology/oncology clinics of North America*. 2009;23(2):361-76.
 47. Poynter JN, Richardson M, Roesler M, Blair CK, Hirsch B, Nguyen P, et al. Chemical exposures and risk of acute myeloid leukemia and myelodysplastic syndromes in a population-based study. *Int J Cancer*. 2017;140(1):23-33.
 48. Wintering A, Dvorak CC, Stieglitz E, Loh ML. Juvenile myelomonocytic leukemia in the molecular era: a clinician's guide to diagnosis, risk stratification, and treatment. *Blood Adv*. 2021;5(22):4783-93.
 49. Kim HS, Lee JW, Kang D, Yu H, Kim Y, Kang H, et al. Characteristics of RAS pathway mutations in juvenile myelomonocytic leukaemia: a single-institution study from Korea. *British journal of haematology*. 2021;195(5):748-56.
 50. Stieglitz E, Taylor-Weiner AN, Chang TY, Gelston LC, Wang YD, Mazor T, et al. The genomic landscape of juvenile myelomonocytic leukemia. *Nature genetics*. 2015;47(11):1326-33.
 51. Itzykson R, Duchmann M, Lucas N, Solary E. CMML: Clinical and molecular aspects. *International journal of hematology*. 2017;105(6):711-9.
 52. Itzykson R, Kosmider O, Renneville A, Gelsi-Boyer V, Meggendorfer M, Morabito M, et al. Prognostic score including gene mutations in chronic myelomonocytic leukemia. *J Clin Oncol*. 2013;31(19):2428-36.
 53. Elena C, Galli A, Such E, Meggendorfer M, Germing U, Rizzo E, et al. Integrating clinical features and genetic lesions in the risk assessment of patients with chronic myelomonocytic leukemia. *Blood*. 2016;128(10):1408-17.
 54. Doulatov S, Notta F, Laurenti E, Dick JE. Hematopoiesis: a human perspective. *Cell Stem Cell*. 2012;10(2):120-36.
 55. Akashi K, Traver D, Miyamoto T, Weissman IL. A clonogenic common myeloid progenitor

- that gives rise to all myeloid lineages. *Nature*. 2000;404(6774):193-7.
56. Reya T, Morrison SJ, Clarke MF, Weissman IL. Stem cells, cancer, and cancer stem cells. *Nature*. 2001;414(6859):105-11.
 57. Zhang Y, Gao S, Xia J, Liu F. Hematopoietic Hierarchy - An Updated Roadmap. *Trends Cell Biol*. 2018;28(12):976-86.
 58. Pellin D, Loperfido M, Baricordi C, Wolock SL, Montepeloso A, Weinberg OK, et al. A comprehensive single cell transcriptional landscape of human hematopoietic progenitors. *Nature Communications*. 2019;10(1):2395.
 59. Paul F, Arkin Y, Giladi A, Jaitin DA, Kenigsberg E, Keren-Shaul H, et al. Transcriptional Heterogeneity and Lineage Commitment in Myeloid Progenitors. *Cell*. 2015;163(7):1663-77.
 60. Laurenti E, Göttgens B. From haematopoietic stem cells to complex differentiation landscapes. *Nature*. 2018;553(7689):418-26.
 61. Notta F, Zandi S, Takayama N, Dobson S, Gan OI, Wilson G, et al. Distinct routes of lineage development reshape the human blood hierarchy across ontogeny. *Science*. 2016;351(6269):aab2116.
 62. Laurenti E, Doulatov S, Zandi S, Plumb I, Chen J, April C, et al. The transcriptional architecture of early human hematopoiesis identifies multilevel control of lymphoid commitment. *Nature immunology*. 2013;14(7):756-63.
 63. Bonnet D, Dick JE. Human acute myeloid leukemia is organized as a hierarchy that originates from a primitive hematopoietic cell. *Nat Med*. 1997;3(7):730-7.
 64. Chen L, Kostadima M, Martens JHA, Canu G, Garcia SP, Turro E, et al. Transcriptional diversity during lineage commitment of human blood progenitors. *Science*. 2014;345(6204):1251033.
 65. Adolfsson J, Månsson R, Buza-Vidas N, Hultquist A, Liuba K, Jensen CT, et al. Identification of Flt3+ lympho-myeloid stem cells lacking erythro-megakaryocytic potential a revised road map for adult blood lineage commitment. *Cell*. 2005;121(2):295-306.
 66. Rodriguez-Fraticelli AE, Wolock SL, Weinreb CS, Panero R, Patel SH, Jankovic M, et al. Clonal analysis of lineage fate in native haematopoiesis. *Nature*. 2018;553(7687):212-6.
 67. Li JJ, Liu J, Li YE, Chen LV, Cheng H, Li Y, et al. Differentiation route determines the functional outputs of adult megakaryopoiesis. *Immunity*. 2024;57(3):478-94.e6.
 68. de Pooter RF, Dias S, Chowdhury M, Bartom ET, Okoreeh MK, Sigvardsson M, et al. Cutting Edge: Lymphomyeloid-Primed Progenitor Cell Fates Are Controlled by the Transcription Factor Tal1. *J Immunol*. 2019;202(10):2837-42.
 69. Doulatov S, Papapetrou EP. Studying clonal evolution of myeloid malignancies using induced pluripotent stem cells. *Curr Opin Hematol*. 2021;28(1):50-6.
 70. Buenrostro JD, Corces MR, Lareau CA, Wu B, Schep AN, Aryee MJ, et al. Integrated Single-Cell Analysis Maps the Continuous Regulatory Landscape of Human Hematopoietic Differentiation. *Cell*. 2018;173(6):1535-48 e16.
 71. Liggett LA, Sankaran VG. Unraveling Hematopoiesis through the Lens of Genomics. *Cell*. 2020;182(6):1384-400.
 72. Feng J, Jang G, Esteva E, Adams NM, Jin H, Reizis B. Clonal barcoding of endogenous adult hematopoietic stem cells reveals a spectrum of lineage contributions. *Proc Natl Acad Sci U S A*. 2024;121(4):e2317929121.
 73. Su T-Y, Hauenstein J, Somuncular E, Dumral Ö, Leonard E, Gustafsson C, et al. Aging is associated with functional and molecular changes in distinct hematopoietic stem cell subsets. *Nature Communications*. 2024;15(1):7966.
 74. Yamamoto R, Nakauchi H. In vivo clonal analysis of aging hematopoietic stem cells. *Mech*

Ageing Dev. 2020;192:111378.

75. Beerman I, Bhattacharya D, Zandi S, Sigvardsson M, Weissman IL, Bryder D, et al. Functionally distinct hematopoietic stem cells modulate hematopoietic lineage potential during aging by a mechanism of clonal expansion. *Proc Natl Acad Sci U S A*. 2010;107(12):5465-70.
76. Rossi DJ, Bryder D, Zahn JM, Ahlenius H, Sonu R, Wagers AJ, et al. Cell intrinsic alterations underlie hematopoietic stem cell aging. *Proc Natl Acad Sci U S A*. 2005;102(26):9194-9.
77. Pang WW, Price EA, Sahoo D, Beerman I, Maloney WJ, Rossi DJ, et al. Human bone marrow hematopoietic stem cells are increased in frequency and myeloid-biased with age. *Proc Natl Acad Sci U S A*. 2011;108(50):20012-7.
78. Ross JB, Myers LM, Noh JJ, Collins MM, Carmody AB, Messer RJ, et al. Depleting myeloid-biased haematopoietic stem cells rejuvenates aged immunity. *Nature*. 2024;628(8006):162-70.
79. Vanickova K, Milosevic M, Ribeiro Bas I, Burocziova M, Yokota A, Danek P, et al. Hematopoietic stem cells undergo a lymphoid to myeloid switch in early stages of emergency granulopoiesis. *Embo j*. 2023;42(23):e113527.
80. Pietras EM, Reynaud D, Kang YA, Carlin D, Calero-Nieto FJ, Leavitt AD, et al. Functionally Distinct Subsets of Lineage-Biased Multipotent Progenitors Control Blood Production in Normal and Regenerative Conditions. *Cell Stem Cell*. 2015;17(1):35-46.
81. Will B, Zhou L, Vogler TO, Ben-Neriah S, Schinke C, Tamari R, et al. Stem and progenitor cells in myelodysplastic syndromes show aberrant stage-specific expansion and harbor genetic and epigenetic alterations. *Blood*. 2012;120(10):2076-86.
82. Nilsson L, Edén P, Olsson E, Månsson R, Astrand-Grundström I, Strömbeck B, et al. The molecular signature of MDS stem cells supports a stem-cell origin of 5q myelodysplastic syndromes. *Blood*. 2007;110(8):3005-14.
83. Ganán-Gómez I, Yang H, Ma F, Montalbán-Bravo G, Thongon N, Marchica V, et al. Stem cell architecture drives myelodysplastic syndrome progression and predicts response to venetoclax-based therapy. *Nature medicine*. 2022.
84. Craddock C, Quek L, Goardon N, Freeman S, Siddique S, Raghavan M, et al. Azacitidine fails to eradicate leukemic stem/progenitor cell populations in patients with acute myeloid leukemia and myelodysplasia. *Leukemia*. 2013;27(5):1028-36.
85. Tehranchi R, Woll PS, Anderson K, Buza-Vidas N, Mizukami T, Mead AJ, et al. Persistent malignant stem cells in del(5q) myelodysplasia in remission. *N Engl J Med*. 2010;363(11):1025-37.
86. Pang WW, Pluvinau JV, Price EA, Sridhar K, Arber DA, Greenberg PL, et al. Hematopoietic stem cell and progenitor cell mechanisms in myelodysplastic syndromes. *Proc Natl Acad Sci U S A*. 2013;110(8):3011-6.
87. Isobe T, Kucinski I, Barile M, Wang X, Hannah R, Bastos HP, et al. Preleukemic single-cell landscapes reveal mutation-specific mechanisms and gene programs predictive of AML patient outcomes. *Cell Genom*. 2023;3(12):100426.
88. Itzykson R, Kosmider O, Renneville A, Morabito M, Preudhomme C, Berthon C, et al. Clonal architecture of chronic myelomonocytic leukemias. *Blood*. 2013;121(12):2186-98.
89. Itzykson R, Solary E. An evolutionary perspective on chronic myelomonocytic leukemia. *Leukemia*. 2013;27(7):1441-50.
90. Gurney M, Greipp PT, Gliem T, Knudson R, Al-Kali A, Gangat N, et al. TET2 somatic copy number alterations and allelic imbalances in chronic myelomonocytic leukemia. *Leukemia research*. 2023;134:107391.

91. Garcia-Gisbert N, Arenillas L, Roman-Bravo D, Rodriguez-Sevilla JJ, Fernández-Rodríguez C, Garcia-Avila S, et al. Multi-hit TET2 mutations as a differential molecular signature of oligomonocytic and overt chronic myelomonocytic leukemia. *Leukemia*. 2022;36(12):2922-6.
92. Li Z, Cai X, Cai CL, Wang J, Zhang W, Petersen BE, et al. Deletion of Tet2 in mice leads to dysregulated hematopoietic stem cells and subsequent development of myeloid malignancies. *Blood*. 2011;118(17):4509-18.
93. Calvo X, Roman-Bravo D, Garcia-Gisbert N, Rodriguez-Sevilla JJ, Garcia-Avila S, Florensa L, et al. Outcomes and molecular profile of oligomonocytic CMML support its consideration as the first stage in the CMML continuum. *Blood Adv*. 2022;6(13):3921-31.
94. Calvo X, Garcia-Gisbert N, Parraga I, Gibert J, Florensa L, Andrade-Campos M, et al. Oligomonocytic and overt chronic myelomonocytic leukemia show similar clinical, genomic, and immunophenotypic features. *Blood Adv*. 2020;4(20):5285-96.
95. Wudhikarn K, Loghavi S, Mangaonkar AA, Al-Kali A, Binder M, Carr R, et al. SF3B1-mutant CMML defines a predominantly dysplastic CMML subtype with a superior acute leukemia-free survival. *Blood Adv*. 2020;4(22):5716-21.
96. Itzykson R, Kosmider O, Renneville A, Morabito M, Preudhomme C, Berthon C, et al. Clonal architecture of chronic myelomonocytic leukemias. *Blood*. 2013;121(12):2186-98.
97. Carr RM, Vorobyev D, Lasho T, Marks DL, Tolosa EJ, Vedder A, et al. RAS mutations drive proliferative chronic myelomonocytic leukemia via a KMT2A-PLK1 axis. *Nat Commun*. 2021;12(1):2901.
98. Geissler K, Jäger E, Barna A, Alendar T, Ljubuncic E, Sliwa T, et al. Chronic myelomonocytic leukemia patients with RAS pathway mutations show high in vitro myeloid colony formation in the absence of exogenous growth factors. *Leukemia*. 2016;30(11):2280-1.
99. Hanahan D. Hallmarks of Cancer: New Dimensions. *Cancer discovery*. 2022;12(1):31-46.
100. Waldman AD, Fritz JM, Lenardo MJ. A guide to cancer immunotherapy: from T cell basic science to clinical practice. *Nature Reviews Immunology*. 2020;20(11):651-68.
101. Kumar BV, Connors TJ, Farber DL. Human T Cell Development, Localization, and Function throughout Life. *Immunity*. 2018;48(2):202-13.
102. Sun L, Su Y, Jiao A, Wang X, Zhang B. T cells in health and disease. *Signal Transduction and Targeted Therapy*. 2023;8(1):235.
103. Sumida TS, Cheru NT, Hafler DA. The regulation and differentiation of regulatory T cells and their dysfunction in autoimmune diseases. *Nat Rev Immunol*. 2024;24(7):503-17.
104. Hamann A, Syrbe U. T-cell trafficking into sites of inflammation. *Rheumatology (Oxford)*. 2000;39(7):696-9.
105. Xia A, Zhang Y, Xu J, Yin T, Lu XJ. T Cell Dysfunction in Cancer Immunity and Immunotherapy. *Frontiers in immunology*. 2019;10:1719.
106. Disis ML. Immune regulation of cancer. *Journal of clinical oncology : official journal of the American Society of Clinical Oncology*. 2010;28(29):4531-8.
107. Balandrán JC, Lasry A, Aifantis I. The Role of Inflammation in the Initiation and Progression of Myeloid Neoplasms. *Blood Cancer Discovery*. 2023;OF1-OF13.
108. Lynch OF, Calvi LM. Immune Dysfunction, Cytokine Disruption, and Stromal Changes in Myelodysplastic Syndrome: A Review. *Cells*. 2022;11(3).
109. Simoni Y, Chapuis N. Diagnosis of Myelodysplastic Syndromes: From Immunological Observations to Clinical Applications. *Diagnostics (Basel)*. 2022;12(7).
110. Chokr N, Patel R, Wattamwar K, Chokr S. The Rising Era of Immune Checkpoint

- Inhibitors in Myelodysplastic Syndromes. *Advances in hematology*. 2018;2018:2458679.
111. Tay RE, Richardson EK, Toh HC. Revisiting the role of CD4+ T cells in cancer immunotherapy—new insights into old paradigms. *Cancer Gene Therapy*. 2021;28(1):5-17.
 112. Wang R, Lan C, Benlagha K, Camara NOS, Miller H, Kubo M, et al. The interaction of innate immune and adaptive immune system. *MedComm* (2020). 2024;5(10):e714.
 113. Chatzileontiadou DSM, Sloane H, Nguyen AT, Gras S, Grant EJ. The Many Faces of CD4(+) T Cells: Immunological and Structural Characteristics. *Int J Mol Sci*. 2020;22(1).
 114. Mosmann TR, Cherwinski H, Bond MW, Giedlin MA, Coffman RL. Two types of murine helper T cell clone. I. Definition according to profiles of lymphokine activities and secreted proteins. *Journal of Immunology* (Baltimore, MD: 1950). 1986;136(7):2348-57.
 115. Tan Y, Tan Y, Li J, Hu P, Guan P, Kuang H, et al. Combined IFN- γ and IL-2 release assay for detect active pulmonary tuberculosis: a prospective multicentre diagnostic study in China. *J Transl Med*. 2021;19(1):289.
 116. Li X, Körner H, Liu X. Susceptibility to Intracellular Infections: Contributions of TNF to Immune Defense. *Front Microbiol*. 2020;11:1643.
 117. Wang X, Wu DP, He G, Miao M, Sun A. Research of Subset and Function of Th Cells in Bone Marrow of Myelodysplastic Syndrome Patients. *Blood*. 2005;106(11):4913-.
 118. Liu Z, Xu X, Zheng L, Ding K, Yang C, Huang J, et al. The value of serum IL-4 to predict the survival of MDS patients. *European Journal of Medical Research*. 2023;28(1):7.
 119. van Leeuwen-Kerkhoff N, Westers TM, Poddighe PJ, de Gruijl TD, Kordasti S, van de Loosdrecht AA. Thrombomodulin-expressing monocytes are associated with low-risk features in myelodysplastic syndromes and dampen excessive immune activation. *Haematologica*. 2020;105(4):961-71.
 120. Hamilton DH, Bretscher PA. Different immune correlates associated with tumor progression and regression: implications for prevention and treatment of cancer. *Cancer Immunol Immunother*. 2008;57(8):1125-36.
 121. Hamilton D, Ismail N, Kroeger D, Rudulier C, Bretscher P. Macroimmunology and immunotherapy of cancer. *Immunotherapy*. 2009;1(3):367-83.
 122. Martinez GJ, Nurieva RI, Yang XO, Dong C. Regulation and function of proinflammatory TH17 cells. *Ann N Y Acad Sci*. 2008;1143:188-211.
 123. Jiang Q, Yang G, Xiao F, Xie J, Wang S, Lu L, et al. Role of Th22 Cells in the Pathogenesis of Autoimmune Diseases. *Frontiers in immunology*. 2021;12:688066.
 124. Romagnani S, Maggi E, Liotta F, Cosmi L, Annunziato F. Properties and origin of human Th17 cells. *Mol Immunol*. 2009;47(1):3-7.
 125. Nistala K, Wedderburn LR. Th17 and regulatory T cells: rebalancing pro- and anti-inflammatory forces in autoimmune arthritis. *Rheumatology* (Oxford). 2009;48(6):602-6.
 126. Zhao J, Chen X, Herjan T, Li X. The role of interleukin-17 in tumor development and progression. *Journal of Experimental Medicine*. 2019;217(1).
 127. Castro G, Liu X, Ngo K, De Leon-Tabaldo A, Zhao S, Luna-Roman R, et al. ROR γ t and ROR α signature genes in human Th17 cells. *PloS one*. 2017;12(8):e0181868.
 128. Zhang Z, Li X, Guo J, Xu F, He Q, Zhao Y, et al. Interleukin-17 enhances the production of interferon- γ and tumour necrosis factor- α by bone marrow T lymphocytes from patients with lower risk myelodysplastic syndromes. *Eur J Haematol*. 2013;90(5):375-84.
 129. Kordasti SY, Afzali B, Lim Z, Ingram W, Hayden J, Barber L, et al. IL-17-producing CD4(+) T cells, pro-inflammatory cytokines and apoptosis are increased in low risk myelodysplastic syndrome. *Br J Haematol*. 2009;145(1):64-72.
 130. Hossein-Khannazer N, Zian Z, Bakkach J, Kamali AN, Hosseinzadeh R, Anka AU, et al.

- Features and roles of T helper 22 cells in immunological diseases and malignancies. *Scandinavian Journal of Immunology*. 2021;93(5):e13030.
131. Saxton RA, Henneberg LT, Calafiore M, Su L, Jude KM, Hanash AM, et al. The tissue protective functions of interleukin-22 can be decoupled from pro-inflammatory actions through structure-based design. *Immunity*. 2021;54(4):660-72.e9.
 132. Shao LL, Zhang L, Hou Y, Yu S, Liu XG, Huang XY, et al. Th22 cells as well as Th17 cells expand differentially in patients with early-stage and late-stage myelodysplastic syndrome. *PLoS One*. 2012;7(12):e51339.
 133. Zou W. Regulatory T cells, tumour immunity and immunotherapy. *Nature Reviews Immunology*. 2006;6(4):295-307.
 134. Wang C, Yang Y, Gao S, Chen J, Yu J, Zhang H, et al. Immune dysregulation in myelodysplastic syndrome: Clinical features, pathogenesis and therapeutic strategies. *Crit Rev Oncol Hematol*. 2018;122:123-32.
 135. Aggarwal S, van de Loosdrecht AA, Alhan C, Ossenkoppele GJ, Westers TM, Bontkes HJ. Role of immune responses in the pathogenesis of low-risk MDS and high-risk MDS: implications for immunotherapy. *Br J Haematol*. 2011;153(5):568-81.
 136. Nishikawa H, Koyama S. Mechanisms of regulatory T cell infiltration in tumors: implications for innovative immune precision therapies. *J Immunother Cancer*. 2021;9(7).
 137. Kordasti SY, Ingram W, Hayden J, Darling D, Barber L, Afzali B, et al. CD4+CD25high Foxp3+ regulatory T cells in myelodysplastic syndrome (MDS). *Blood*. 2007;110(3):847-50.
 138. Giovazzino A, Leone S, Rubino V, Palatucci AT, Cerciello G, Alfinito F, et al. Reduced regulatory T cells (Treg) in bone marrow preferentially associate with the expansion of cytotoxic T lymphocytes in low risk MDS patients. *British Journal of Haematology*. 2019;185(2):357-60.
 139. Kotsianidis I, Bouchliou I, Nakou E, Spanoudakis E, Margaritis D, Christophoridou AV, et al. Kinetics, function and bone marrow trafficking of CD4+CD25+FOXP3+ regulatory T cells in myelodysplastic syndromes (MDS). *Leukemia*. 2009;23(3):510-8.
 140. Lambert C, Wu Y, Aanei C. Bone Marrow Immunity and Myelodysplasia. *Frontiers in oncology*. 2016;6:172.
 141. Hamdi W, Ogawara H, Handa H, Tsukamoto N, Nojima Y, Murakami H. Clinical significance of regulatory T cells in patients with myelodysplastic syndrome. *European journal of haematology*. 2009;82(3):201-7.
 142. Raskov H, Orhan A, Christensen JP, Gögenur I. Cytotoxic CD8+ T cells in cancer and cancer immunotherapy. *British journal of cancer*. 2021;124(2):359-67.
 143. Szabo PA, Levitin HM, Miron M, Snyder ME, Senda T, Yuan J, et al. Single-cell transcriptomics of human T cells reveals tissue and activation signatures in health and disease. *Nat Commun*. 2019;10(1):4706.
 144. Philip M, Schietinger A. CD8+ T cell differentiation and dysfunction in cancer. *Nature Reviews Immunology*. 2022;22(4):209-23.
 145. Geerman S, Brasser G, Bhushal S, Salerno F, Kragten NA, Hoogenboezem M, et al. Memory CD8(+) T cells support the maintenance of hematopoietic stem cells in the bone marrow. *Haematologica*. 2018;103(6):e230-e3.
 146. Lopes MR, Traina F, Campos Pde M, Pereira JK, Machado-Neto JA, Machado Hda C, et al. IL10 inversely correlates with the percentage of CD8⁺ cells in MDS patients. *Leuk Res*. 2013;37(5):541-6.
 147. Zheng Z, Qianqiao Z, Qi H, Feng X, Chunkang C, Xiao L. In vitro deprivation of CD8+ CD57+ T cells promotes the malignant growth of bone marrow colony cells in patients

- with lower-risk myelodysplastic syndrome. *Experimental hematology*. 2010;38(8):677-84.
148. Sand K, Theorell J, Bruserud Ø, Bryceson YT, Kittang AO. Reduced potency of cytotoxic T lymphocytes from patients with high-risk myelodysplastic syndromes. *Cancer Immunol Immunother*. 2016;65(9):1135-47.
 149. Mitroulis I, Tasis A, Grigoriou M, Papaioannou N, Paschalidis N, Loukogiannaki K, et al. Phenotypic and Molecular Landscape of Bone Marrow CD8+ T Cells in Myeloid Neoplasms Predicts Response to Treatment with Hypomethylating Agents. *Blood*. 2023;142(Supplement 1):4588-.
 150. Fane M, Weeraratna AT. How the ageing microenvironment influences tumour progression. *Nat Rev Cancer*. 2020;20(2):89-106.
 151. Seidel JA, Otsuka A, Kabashima K. Anti-PD-1 and Anti-CTLA-4 Therapies in Cancer: Mechanisms of Action, Efficacy, and Limitations. *Frontiers in oncology*. 2018;8:86.
 152. Yang H, Bueso-Ramos C, DiNardo C, Estecio MR, Davanlou M, Geng QR, et al. Expression of PD-L1, PD-L2, PD-1 and CTLA4 in myelodysplastic syndromes is enhanced by treatment with hypomethylating agents. *Leukemia*. 2014;28(6):1280-8.
 153. Meng F, Li L, Lu F, Yue J, Liu Z, Zhang W, et al. Overexpression of TIGIT in NK and T Cells Contributes to Tumor Immune Escape in Myelodysplastic Syndromes. *Frontiers in oncology*. 2020;10:1595.
 154. Haroun F, Solola SA, Nassereddine S, Tabbara I. PD-1 signaling and inhibition in AML and MDS. *Annals of hematology*. 2017;96:1441-8.
 155. Coats T, Smith Ae, Mourikis TP, Irish JM, Kordasti S, Mufti GJ. Mass Cytometry Reveals PD1 Upregulation Is an Early Step in MDS Disease Progression. *Blood*. 2016;128(22):4296.
 156. Tcvetkov NY, Morozova EV, Epifanovskaya OS, Babenko EV, Barabanshikova MV, Lepik KV, et al. Profile of Checkpoint Molecules Expression on Bone Marrow Cell Populations in Patients with High-Risk Myelodysplastic Syndrome. *Blood*. 2020;136:43-4.
 157. Kitagawa M, Saito I, Kuwata T, Yoshida S, Yamaguchi S, Takahashi M, et al. Overexpression of tumor necrosis factor (TNF)-alpha and interferon (IFN)-gamma by bone marrow cells from patients with myelodysplastic syndromes. *Leukemia*. 1997;11(12):2049-54.
 158. Stifter G, Heiss S, Gastl G, Tzankov A, Stauder R. Over-expression of tumor necrosis factor-alpha in bone marrow biopsies from patients with myelodysplastic syndromes: relationship to anemia and prognosis. *European journal of haematology*. 2005;75(6):485-91.
 159. Basiorka AA, McGraw KL, Eksioglu EA, Chen X, Johnson J, Zhang L, et al. The NLRP3 inflammasome functions as a driver of the myelodysplastic syndrome phenotype. *Blood*. 2016;128(25):2960-75.
 160. Thompson CB, Allison JP. The emerging role of CTLA-4 as an immune attenuator. *Immunity*. 1997;7(4):445-50.
 161. Aref S, El Agdar M, El Sebaie A, Abouzeid T, Sabry M, Ibrahim L. Prognostic value of CD200 expression and soluble CTLA-4 concentrations in intermediate and high-risk myelodysplastic syndrome patients. *Asian Pacific Journal of Cancer Prevention: APJCP*. 2020;21(8):2225.
 162. Tao J, Li L, Wang Y, Fu R, Wang H, Shao Z. Increased TIM3+CD8+T cells in Myelodysplastic Syndrome patients displayed less perforin and granzyme B secretion and higher CD95 expression. *Leukemia research*. 2016;51:49-55.
 163. Fu R, Li L, Hu J, Wang Y, Tao J, Liu H, et al. Elevated TIM3 expression of T helper cells affects immune system in patients with myelodysplastic syndrome. *J Investig Med*.

- 2019;67(8):1125-30.
164. Zeidan AM, Giagounidis A, Sekeres MA, Xiao Z, Sanz GF, Hoef MV, et al. STIMULUS-MDS2 design and rationale: a phase III trial with the anti-TIM-3 sabatolimab (MBG453) + azacitidine in higher risk MDS and CMML-2. *Future oncology* (London, England). 2023;19(9):631-42.
 165. Peng X, Zhu X, Di T, Tang F, Guo X, Liu Y, et al. The yin-yang of immunity: Immune dysregulation in myelodysplastic syndrome with different risk stratification. *Frontiers in immunology*. 2022;13:994053.
 166. Rodriguez-Sevilla JJ, Colla S. T cell dysfunctions in myelodysplastic syndromes. *Blood*. 2024.
 167. Garcia-Manero G, Chien KS, Montalban-Bravo G. Myelodysplastic syndromes: 2021 update on diagnosis, risk stratification and management. *American journal of hematology*. 2020;95(11):1399-420.
 168. Kondo A, Yamashita T, Tamura H, Zhao W, Tsuji T, Shimizu M, et al. Interferon-gamma and tumor necrosis factor-alpha induce an immunoinhibitory molecule, B7-H1, via nuclear factor-kappaB activation in blasts in myelodysplastic syndromes. *Blood*. 2010;116(7):1124-31.
 169. Cheng P, Eksioglu EA, Chen X, Kandell W, Le Trinh T, Cen L, et al. S100A9-induced overexpression of PD-1/PD-L1 contributes to ineffective hematopoiesis in myelodysplastic syndromes. *Leukemia*. 2019;33(8):2034-46.
 170. Furman D, Campisi J, Verdin E, Carrera-Bastos P, Targ S, Franceschi C, et al. Chronic inflammation in the etiology of disease across the life span. *Nature Medicine*. 2019;25(12):1822-32.
 171. Stubbins RJ, Platzbecker U, Karsan A. Inflammation and myeloid malignancy: quenching the flame. *Blood*. 2022;140(10):1067-74.
 172. Pietras EM. Inflammation: a key regulator of hematopoietic stem cell fate in health and disease. *Blood*. 2017;130(15):1693-8.
 173. Mitroulis I, Kalafati L, Bornhäuser M, Hajishengallis G, Chavakis T. Regulation of the Bone Marrow Niche by Inflammation. *Frontiers in immunology*. 2020;11:1540.
 174. Takizawa H, Boettcher S, Manz MG. Demand-adapted regulation of early hematopoiesis in infection and inflammation. *Blood*. 2012;119(13):2991-3002.
 175. Caiado F, Pietras EM, Manz MG. Inflammation as a regulator of hematopoietic stem cell function in disease, aging, and clonal selection. *The Journal of experimental medicine*. 2021;218(7).
 176. Mejia-Ramirez E, Florian MC. Understanding intrinsic hematopoietic stem cell aging. *Haematologica*. 2020;105(1):22-37.
 177. Fulop T, Larbi A, Dupuis G, Le Page A, Frost EH, Cohen AA, et al. Immunosenescence and Inflamm-Aging As Two Sides of the Same Coin: Friends or Foes? *Frontiers in immunology*. 2017;8:1960.
 178. Matatall KA, Jeong M, Chen S, Sun D, Chen F, Mo Q, et al. Chronic Infection Depletes Hematopoietic Stem Cells through Stress-Induced Terminal Differentiation. *Cell reports*. 2016;17(10):2584-95.
 179. Pietras EM, Mirantes-Barbeito C, Fong S, Loeffler D, Kovtonyuk LV, Zhang S, et al. Chronic interleukin-1 exposure drives haematopoietic stem cells towards precocious myeloid differentiation at the expense of self-renewal. *Nat Cell Biol*. 2016;18(6):607-18.
 180. Essers MA, Offner S, Blanco-Bose WE, Waibler Z, Kalinke U, Duchosal MA, et al. IFNalpha activates dormant haematopoietic stem cells in vivo. *Nature*. 2009;458(7240):904-8.

181. Pietras EM, Lakshminarasimhan R, Techner JM, Fong S, Flach J, Binnewies M, et al. Re-entry into quiescence protects hematopoietic stem cells from the killing effect of chronic exposure to type I interferons. *The Journal of experimental medicine*. 2014;211(2):245-62.
182. Bogeska R, Mikecin AM, Kaschutnig P, Fawaz M, Büchler-Schäff M, Le D, et al. Inflammatory exposure drives long-lived impairment of hematopoietic stem cell self-renewal activity and accelerated aging. *Cell Stem Cell*. 2022;29(8):1273-84.e8.
183. Beerman I. Accumulation of DNA damage in the aged hematopoietic stem cell compartment. *Seminars in hematology*. 2017;54(1):12-8.
184. Gañán-Gómez I, Wei Y, Starczynowski DT, Colla S, Yang H, Cabrero-Calvo M, et al. Dereglulation of innate immune and inflammatory signaling in myelodysplastic syndromes. *Leukemia*. 2015;29(7):1458-69.
185. Florez MA, Tran BT, Wathan TK, DeGregori J, Pietras EM, King KY. Clonal hematopoiesis: Mutation-specific adaptation to environmental change. *Cell Stem Cell*. 2022;29(6):882-904.
186. Hormaechea-Agulla D, Matatall KA, Le DT, Kain B, Long X, Kus P, et al. Chronic infection drives Dnmt3a-loss-of-function clonal hematopoiesis via IFN γ signaling. *Cell Stem Cell*. 2021;28(8):1428-42.e6.
187. SanMiguel JM, Young K, Trowbridge JJ. Hand in hand: intrinsic and extrinsic drivers of aging and clonal hematopoiesis. *Exp Hematol*. 2020;91:1-9.
188. Jakobsen NA, Turkalj S, Zeng AGX, Stoilova B, Metzner M, Rahmig S, et al. Selective advantage of mutant stem cells in human clonal hematopoiesis is associated with attenuated response to inflammation and aging. *Cell Stem Cell*. 2024;31(8):1127-44.e17.
189. Cai Z, Kotzin JJ, Ramdas B, Chen S, Nelanuthala S, Palam LR, et al. Inhibition of Inflammatory Signaling in Tet2 Mutant Preleukemic Cells Mitigates Stress-Induced Abnormalities and Clonal Hematopoiesis. *Cell Stem Cell*. 2018;23(6):833-49.e5.
190. Kovtonyuk LV, Fritsch K, Feng X, Manz MG, Takizawa H. Inflamm-Aging of Hematopoiesis, Hematopoietic Stem Cells, and the Bone Marrow Microenvironment. *Frontiers in immunology*. 2016;7:502.
191. Meisel M, Hinterleitner R, Pacis A, Chen L, Earley ZM, Mayassi T, et al. Microbial signals drive pre-leukaemic myeloproliferation in a Tet2-deficient host. *Nature*. 2018;557(7706):580-4.
192. Caiado F, Kovtonyuk LV, Gonullu NG, Fullin J, Boettcher S, Manz MG. Aging drives Tet2 $^{+/-}$ clonal hematopoiesis via IL-1 signaling. *Blood*. 2023;141(8):886-903.
193. Zhang CRC, Nix D, Gregory M, Ciorba MA, Ostrander EL, Newberry RD, et al. Inflammatory cytokines promote clonal hematopoiesis with specific mutations in ulcerative colitis patients. *Exp Hematol*. 2019;80:36-41.e3.
194. Avagyan S, Henninger JE, Mannherz WP, Mistry M, Yoon J, Yang S, et al. Resistance to inflammation underlies enhanced fitness in clonal hematopoiesis. *Science*. 2021;374(6568):768-72.
195. Bergsbaken T, Fink SL, Cookson BT. Pyroptosis: host cell death and inflammation. *Nat Rev Microbiol*. 2009;7(2):99-109.
196. Schinke C, Gircz O, Li W, Shastri A, Gordon S, Barreyro L, et al. IL8-CXCR2 pathway inhibition as a therapeutic strategy against MDS and AML stem cells. *Blood*. 2015;125(20):3144-52.
197. Cicchese JM, Evans S, Hult C, Joslyn LR, Wessler T, Millar JA, et al. Dynamic balance of pro- and anti-inflammatory signals controls disease and limits pathology. *Immunol Rev*. 2018;285(1):147-67.

198. Joshi NS, Cui W, Chandele A, Lee HK, Urso DR, Hagman J, et al. Inflammation Directs Memory Precursor and Short-Lived Effector CD8⁺ T Cell Fates via the Graded Expression of T-bet Transcription Factor. *Immunity*. 2007;27(2):281-95.
199. Cain D, Kondo M, Chen H, Kelsoe G. Effects of Acute and Chronic Inflammation on B-Cell Development and Differentiation. *Journal of Investigative Dermatology*. 2009;129(2):266-77.
200. Chen L, Deng H, Cui H, Fang J, Zuo Z, Deng J, et al. Inflammatory responses and inflammation-associated diseases in organs. *Oncotarget*. 2018;9(6):7204-18.
201. Fraietta JA, Nobles CL, Sammons MA, Lundh S, Carty SA, Reich TJ, et al. Disruption of TET2 promotes the therapeutic efficacy of CD19-targeted T cells. *Nature*. 2018;558(7709):307-12.
202. Prinzing B, Zebley CC, Petersen CT, Fan Y, Anido AA, Yi Z, et al. Deleting DNMT3A in CAR T cells prevents exhaustion and enhances antitumor activity. *Science translational medicine*. 2021;13(620):eabh0272.
203. Dominguez PM, Ghamlouch H, Rosikiewicz W, Kumar P, Béguelin W, Fontán L, et al. TET2 Deficiency Causes Germinal Center Hyperplasia, Impairs Plasma Cell Differentiation, and Promotes B-cell Lymphomagenesis. *Cancer discovery*. 2018;8(12):1632-53.
204. Mahajan VS, Mattoo H, Sun N, Viswanadham V, Yuen GJ, Allard-Chamard H, et al. B1a and B2 cells are characterized by distinct CpG modification states at DNMT3A-maintained enhancers. *Nat Commun*. 2021;12(1):2208.
205. Biran A, Yin S, Kretzmer H, Ten Hacken E, Parvin S, Lucas F, et al. Activation of Notch and Myc Signaling via B-cell-Restricted Depletion of Dnmt3a Generates a Consistent Murine Model of Chronic Lymphocytic Leukemia. *Cancer Res*. 2021;81(24):6117-30.
206. Jaiswal S, Natarajan P, Silver AJ, Gibson CJ, Bick AG, Shvartz E, et al. Clonal Hematopoiesis and Risk of Atherosclerotic Cardiovascular Disease. *New England Journal of Medicine*. 2017;377(2):111-21.
207. Fuster JJ, MacLauchlan S, Zuriaga MA, Polackal MN, Ostriker AC, Chakraborty R, et al. Clonal hematopoiesis associated with TET2 deficiency accelerates atherosclerosis development in mice. *Science*. 2017;355(6327):842-7.
208. Zhang Q, Zhao K, Shen Q, Han Y, Gu Y, Li X, et al. Tet2 is required to resolve inflammation by recruiting Hdac2 to specifically repress IL-6. *Nature*. 2015;525(7569):389-93.
209. Huerga Encabo H, Aramburu IV, Garcia-Albornoz M, Piganeau M, Wood H, Song A, et al. Loss of TET2 in human hematopoietic stem cells alters the development and function of neutrophils. *Cell Stem Cell*. 2023;30(6):781-99.e9.
210. Cargo CA, Rowbotham N, Evans PA, Barrans SL, Bowen DT, Crouch S, et al. Targeted sequencing identifies patients with preclinical MDS at high risk of disease progression. *Blood*. 2015;126(21):2362-5.
211. Malcovati L, Galli A, Travaglino E, Ambaglio I, Rizzo E, Molteni E, et al. Clinical significance of somatic mutation in unexplained blood cytopenia. *Blood*. 2017;129(25):3371-8.
212. Bewersdorf JP, Ardasheva A, Podoltsev NA, Singh A, Biancon G, Halene S, et al. From clonal hematopoiesis to myeloid leukemia and what happens in between: Will improved understanding lead to new therapeutic and preventive opportunities? *Blood reviews*. 2019;37:100587.
213. Ganan-Gomez I, Kumar B, Rodriguez Sevilla JJ, Ma F, Kim YJ, Chien KS, et al. Mutant Natural Killer Cell Dysfunction Enables the Immune Escape of Premalignant MDS Cell

- Clones. *Blood*. 2023;142(Supplement 1):514-.
214. Boy M, Bisio V, Zhao L-P, Guidez F, Schell B, Lereclus E, et al. Myelodysplastic Syndrome associated TET2 mutations affect NK cell function and genome methylation. *Nature Communications*. 2023;14(1):588.
 215. Colla S, Ong DS, Ogoti Y, Marchesini M, Mistry NA, Clise-Dwyer K, et al. Telomere dysfunction drives aberrant hematopoietic differentiation and myelodysplastic syndrome. *Cancer cell*. 2015;27(5):644-57.
 216. Chen J, Kao YR, Sun D, Todorova TI, Reynolds D, Narayanagari SR, et al. Myelodysplastic syndrome progression to acute myeloid leukemia at the stem cell level. *Nat Med*. 2019;25(1):103-10.
 217. Bowman RL, Busque L, Levine RL. Clonal Hematopoiesis and Evolution to Hematopoietic Malignancies. *Cell Stem Cell*. 2018;22(2):157-70.
 218. Gondek LP, DeZern AE. Assessing clonal haematopoiesis: clinical burdens and benefits of diagnosing myelodysplastic syndrome precursor states. *The Lancet Haematology*. 2020;7(1):e73-e81.
 219. Walter MJ, Shen D, Ding L, Shao J, Koboldt DC, Chen K, et al. Clonal architecture of secondary acute myeloid leukemia. *N Engl J Med*. 2012;366(12):1090-8.
 220. da Silva-Coelho P, Kroeze LI, Yoshida K, Koorenhof-Scheele TN, Knops R, van de Locht LT, et al. Clonal evolution in myelodysplastic syndromes. *Nat Commun*. 2017;8:15099.
 221. Haferlach T, Nagata Y, Grossmann V, Okuno Y, Bacher U, Nagae G, et al. Landscape of genetic lesions in 944 patients with myelodysplastic syndromes. *Leukemia*. 2014;28(2):241-7.
 222. Papaemmanuil E, Gerstung M, Malcovati L, Tauro S, Gundem G, Van Loo P, et al. Clinical and biological implications of driver mutations in myelodysplastic syndromes. *Blood*. 2013;122(22):3616-27; quiz 99.
 223. Makishima H, Yoshizato T, Yoshida K, Sekeres MA, Radivoyevitch T, Suzuki H, et al. Dynamics of clonal evolution in myelodysplastic syndromes. *Nature genetics*. 2017;49(2):204-12.
 224. Choi S, Cho N, Kim KK. The implications of alternative pre-mRNA splicing in cell signal transduction. *Experimental & Molecular Medicine*. 2023;55(4):755-66.
 225. Ganguly BB, Kadam NN. Mutations of myelodysplastic syndromes (MDS): An update. *Mutat Res Rev Mutat Res*. 2016;769:47-62.
 226. Yoshida K, Sanada M, Shiraishi Y, Nowak D, Nagata Y, Yamamoto R, et al. Frequent pathway mutations of splicing machinery in myelodysplasia. *Nature*. 2011;478(7367):64-9.
 227. Papaemmanuil E, Cazzola M, Boultonwood J, Malcovati L, Vyas P, Bowen D, et al. Somatic SF3B1 mutation in myelodysplasia with ring sideroblasts. *N Engl J Med*. 2011;365(15):1384-95.
 228. Graubert TA, Shen D, Ding L, Okeyo-Owuor T, Lunn CL, Shao J, et al. Recurrent mutations in the U2AF1 splicing factor in myelodysplastic syndromes. *Nature genetics*. 2011;44(1):53-7.
 229. Kennedy JA, Ebert BL. Clinical Implications of Genetic Mutations in Myelodysplastic Syndrome. *Journal of clinical oncology : official journal of the American Society of Clinical Oncology*. 2017;35(9):968-74.
 230. Malcovati L, Karimi M, Papaemmanuil E, Ambaglio I, Jadersten M, Jansson M, et al. SF3B1 mutation identifies a distinct subset of myelodysplastic syndrome with ring sideroblasts. *Blood*. 2015;126(2):233-41.
 231. Kim E, Ilagan JO, Liang Y, Daubner GM, Lee SC, Ramakrishnan A, et al. SRSF2

- Mutations Contribute to Myelodysplasia by Mutant-Specific Effects on Exon Recognition. *Cancer cell*. 2015;27(5):617-30.
232. Heuser M, Yun H, Thol F. Epigenetics in myelodysplastic syndromes. *Semin Cancer Biol*. 2018;51:170-9.
 233. Pellagatti A, Boulton J. The molecular pathogenesis of the myelodysplastic syndromes. *European journal of haematology*. 2015;95(1):3-15.
 234. Sato H, Wheat JC, Steidl U, Ito K. DNMT3A and TET2 in the Pre-Leukemic Phase of Hematopoietic Disorders. *Frontiers in oncology*. 2016;6:187.
 235. Ogawa S. Genetics of MDS. *Blood*. 2019;133(10):1049-59.
 236. Liu R, Wu J, Guo H, Yao W, Li S, Lu Y, et al. Post-translational modifications of histones: Mechanisms, biological functions, and therapeutic targets. *MedComm* (2020). 2023;4(3):e292.
 237. Inoue D, Kitaura J, Togami K, Nishimura K, Enomoto Y, Uchida T, et al. Myelodysplastic syndromes are induced by histone methylation–altering ASXL1 mutations. *J Clin Invest*. 2013;123(11):4627-40.
 238. Nikoloski G, Langemeijer SM, Kuiper RP, Knops R, Massop M, Tönnissen ER, et al. Somatic mutations of the histone methyltransferase gene EZH2 in myelodysplastic syndromes. *Nature genetics*. 2010;42(8):665-7.
 239. Fisher JB, McNulty M, Burke MJ, Crispino JD, Rao S. Cohesin Mutations in Myeloid Malignancies. *Trends Cancer*. 2017;3(4):282-93.
 240. Thota S, Viny AD, Makishima H, Spitzer B, Radivoyevitch T, Przychodzen B, et al. Genetic alterations of the cohesin complex genes in myeloid malignancies. *Blood*. 2014;124(11):1790-8.
 241. Cook MR, Karp JE, Lai C. The spectrum of genetic mutations in myelodysplastic syndrome: Should we update prognostication? *EJHaem*. 2022;3(1):301-13.
 242. Xu H, Tomaszewski JM, McKay MJ. Can corruption of chromosome cohesion create a conduit to cancer? *Nat Rev Cancer*. 2011;11(3):199-210.
 243. Bresnick EH, Jung MM, Katsumura KR. Human GATA2 mutations and hematologic disease: how many paths to pathogenesis? *Blood Advances*. 2020;4(18):4584-92.
 244. Gurney M, Chekkaf I, Baranwal A, Basmaci R, Katamesh B, Greipp P, et al. The clinical and molecular spectrum of ETV6 mutated myeloid neoplasms. *Br J Haematol*. 2023;202(2):279-83.
 245. Kaisrlikova M, Vesela J, Kunderat D, Votavova H, Dostalova Merkerova M, Krejcik Z, et al. RUNX1 mutations contribute to the progression of MDS due to disruption of antitumor cellular defense: a study on patients with lower-risk MDS. *Leukemia*. 2022;36(7):1898-906.
 246. Yokota A, Huo L, Lan F, Wu J, Huang G. The Clinical, Molecular, and Mechanistic Basis of RUNX1 Mutations Identified in Hematological Malignancies. *Mol Cells*. 2020;43(2):145-52.
 247. Collin M, Dickinson R, Bigley V. Haematopoietic and immune defects associated with GATA2 mutation. *Br J Haematol*. 2015;169(2):173-87.
 248. Robbins DJ, Pavletich TS, Patil AT, Pahopos D, Lasarev M, Polaki US, et al. Linking GATA2 to myeloid dysplasia and complex cytogenetics in adult myelodysplastic neoplasm and acute myeloid leukemia. *Blood Adv*. 2024;8(1):80-92.
 249. Padron E, Yoder S, Kunigal S, Mesa T, Teer JK, Al Ali N, et al. ETV6 and signaling gene mutations are associated with secondary transformation of myelodysplastic syndromes to chronic myelomonocytic leukemia. *Blood*. 2014;123(23):3675-7.
 250. Valls PO, Esposito A. Signalling dynamics, cell decisions, and homeostatic control in

- health and disease. *Curr Opin Cell Biol.* 2022;75:102066.
251. Sperling AS, Gibson CJ, Ebert BL. The genetics of myelodysplastic syndrome: from clonal haematopoiesis to secondary leukaemia. *Nat Rev Cancer.* 2017;17(1):5-19.
 252. Buradkar A, Bezerra E, Coltro G, Lasho TL, Finke CM, Gangat N, et al. Landscape of RAS pathway mutations in patients with myelodysplastic syndrome/myeloproliferative neoplasm overlap syndromes: a study of 461 molecularly annotated patients. *Leukemia.* 2021;35(2):644-9.
 253. Levine AJ. p53: 800 million years of evolution and 40 years of discovery. *Nat Rev Cancer.* 2020;20(8):471-80.
 254. Vousden KH, Lu X. Live or let die: the cell's response to p53. *Nature Reviews Cancer.* 2002;2(8):594-604.
 255. Bejar R, Stevenson K, Abdel-Wahab O, Galili N, Nilsson B, Garcia-Manero G, et al. Clinical effect of point mutations in myelodysplastic syndromes. *N Engl J Med.* 2011;364(26):2496-506.
 256. Bernard E, Nannya Y, Hasserjian RP, Devlin SM, Tuechler H, Medina-Martinez JS, et al. Implications of TP53 allelic state for genome stability, clinical presentation and outcomes in myelodysplastic syndromes. *Nature Medicine.* 2020;26(10):1549-56.
 257. Ok CY, Patel KP, Garcia-Manero G, Routbort MJ, Peng J, Tang G, et al. TP53 mutation characteristics in therapy-related myelodysplastic syndromes and acute myeloid leukemia is similar to de novo diseases. *Journal of hematology & oncology.* 2015;8:45.
 258. Jädersten M, Saft L, Smith A, Kulasekararaj A, Pomplun S, Göhring G, et al. TP53 mutations in low-risk myelodysplastic syndromes with del(5q) predict disease progression. *Journal of clinical oncology : official journal of the American Society of Clinical Oncology.* 2011;29(15):1971-9.
 259. Arber DA, Orazi A, Hasserjian RP, Borowitz MJ, Calvo KR, Kvasnicka HM, et al. International Consensus Classification of Myeloid Neoplasms and Acute Leukemia: Integrating Morphological, Clinical, and Genomic Data. *Blood.* 2022.
 260. Haase D, Stevenson KE, Neuberg D, Maciejewski JP, Nazha A, Sekeres MA, et al. TP53 mutation status divides myelodysplastic syndromes with complex karyotypes into distinct prognostic subgroups. *Leukemia.* 2019;33(7):1747-58.
 261. Montalban-Bravo G, Kanagal-Shamanna R, Benton CB, Class CA, Chien KS, Sasaki K, et al. Genomic context and TP53 allele frequency define clinical outcomes in TP53-mutated myelodysplastic syndromes. *Blood Advances.* 2020;4(3):482-95.
 262. Rodriguez-Sevilla JJ, Adema V, Garcia-Manero G, Colla S. Emerging treatments for myelodysplastic syndromes: Biological rationales and clinical translation. *Cell Rep Med.* 2023;4(2):100940.
 263. Meggendorfer M, Roller A, Haferlach T, Eder C, Dicker F, Grossmann V, et al. SRSF2 mutations in 275 cases with chronic myelomonocytic leukemia (CMML). *Blood.* 2012;120(15):3080-8.
 264. Ball M, List AF, Padron E. When clinical heterogeneity exceeds genetic heterogeneity: thinking outside the genomic box in chronic myelomonocytic leukemia. *Blood.* 2016;128(20):2381-7.
 265. Itzykson R, Kosmider O, Renneville A, Gelsi-Boyer V, Meggendorfer M, Morabito M, et al. Prognostic score including gene mutations in chronic myelomonocytic leukemia. *Journal of clinical oncology : official journal of the American Society of Clinical Oncology.* 2013;31(19):2428-36.
 266. Patnaik MM, Zahid MF, Lasho TL, Finke C, Ketterling RL, Gangat N, et al. Number and type of TET2 mutations in chronic myelomonocytic leukemia and their clinical relevance.

- Blood Cancer J. 2016;6(9):e472.
267. Coltro G, Mangaonkar AA, Lasho TL, Finke CM, Pophali P, Carr R, et al. Clinical, molecular, and prognostic correlates of number, type, and functional localization of TET2 mutations in chronic myelomonocytic leukemia (CMML)-a study of 1084 patients. *Leukemia*. 2020;34(5):1407-21.
 268. Patnaik MM, Lasho TL, Vijayvargiya P, Finke CM, Hanson CA, Ketterling RP, et al. Prognostic interaction between ASXL1 and TET2 mutations in chronic myelomonocytic leukemia. *Blood Cancer J*. 2016;6(1):e385.
 269. Patnaik MM, Vallapureddy R, Lasho TL, Hoversten KP, Finke CM, Ketterling R, et al. EZH2 mutations in chronic myelomonocytic leukemia cluster with ASXL1 mutations and their co-occurrence is prognostically detrimental. *Blood Cancer J*. 2018;8(1):12.
 270. Patnaik MM, Pophali PA, Lasho TL, Finke CM, Horna P, Ketterling RP, et al. Clinical correlates, prognostic impact and survival outcomes in chronic myelomonocytic leukemia patients with the JAK2V617F mutation. *Haematologica*. 2019;104(6):e236-e9.
 271. Kohlmann A, Grossmann V, Klein HU, Schindela S, Weiss T, Kazak B, et al. Next-generation sequencing technology reveals a characteristic pattern of molecular mutations in 72.8% of chronic myelomonocytic leukemia by detecting frequent alterations in TET2, CBL, RAS, and RUNX1. *Journal of clinical oncology : official journal of the American Society of Clinical Oncology*. 2010;28(24):3858-65.
 272. Brown AL, Hahn CN, Scott HS. Secondary leukemia in patients with germline transcription factor mutations (RUNX1, GATA2, CEBPA). *Blood*. 2020;136(1):24-35.
 273. DiFilippo EC, Coltro G, Carr RM, Mangaonkar AA, Binder M, Khan SP, et al. Spectrum of abnormalities and clonal transformation in germline RUNX1 familial platelet disorder and a genomic comparative analysis with somatic RUNX1 mutations in MDS/MPN overlap neoplasms. *Leukemia*. 2020;34(9):2519-24.
 274. Kuo MC, Liang DC, Huang CF, Shih YS, Wu JH, Lin TL, et al. RUNX1 mutations are frequent in chronic myelomonocytic leukemia and mutations at the C-terminal region might predict acute myeloid leukemia transformation. *Leukemia*. 2009;23(8):1426-31.
 275. Gurney M, Mangaonkar AA, Lasho T, Finke C, Al-Kali A, Gangat N, et al. Somatic TP53 single nucleotide variants, indels and copy number alterations in chronic myelomonocytic leukemia (CMML). *Leukemia*. 2023;37(8):1753-6.
 276. Levy B, Kanagal-Shamanna R, Sahajpal NS, Neveling K, Rack K, Dewaele B, et al. A framework for the clinical implementation of optical genome mapping in hematologic malignancies. *American journal of hematology*. 2024;99(4):642-61.
 277. Lu S, Liu K, Wang D, Ye Y, Jiang Z, Gao Y. Genomic structural variants analysis in leukemia by a novel cytogenetic technique: Optical genome mapping. *Cancer Science*. 2024;115(11):3543-51.
 278. ISCN 2024 - An International System for Human Cytogenomic Nomenclature (2024). *Cytogenet Genome Res*. 2024;164(Suppl 1):1-224.
 279. Yang H, Garcia-Manero G, Sasaki K, Montalban-Bravo G, Tang Z, Wei Y, et al. High-resolution structural variant profiling of myelodysplastic syndromes by optical genome mapping uncovers cryptic aberrations of prognostic and therapeutic significance. *Leukemia*. 2022;36(9):2306-16.
 280. Ashton KA, Berry NK, Fodeades A, Billings R, Dooley S, Chan E, et al. Optical genome mapping using Bionano: A comparative study of genomic changes in haematological malignancies performed at the John Hunter hospital. *Pathology*. 2022;54:S16-S7.
 281. Larson RA. Therapy-related myeloid neoplasms. *Haematologica*. 2009;94(4):454-9.
 282. Schlegelberger B, Göhring G, Thol F, Heuser M. Update on cytogenetic and molecular

- changes in myelodysplastic syndromes. *Leuk Lymphoma*. 2012;53(4):525-36.
283. Vardiman J. The classification of MDS: from FAB to WHO and beyond. *Leuk Res*. 2012;36(12):1453-8.
 284. Haase D. Cytogenetic features in myelodysplastic syndromes. *Annals of hematology*. 2008;87(7):515-26.
 285. Haase D, Germing U, Schanz J, Pfeilstöcker M, Nösslinger T, Hildebrandt B, et al. New insights into the prognostic impact of the karyotype in MDS and correlation with subtypes: evidence from a core dataset of 2124 patients. *Blood*. 2007;110(13):4385-95.
 286. McGowan-Jordan J, Simons A, Schmid M. *ISCN 2016 : an international system for human cytogenomic nomenclature (2016)*. Basel ;: Karger; 2016.
 287. Solé F, Luño E, Sanzo C, Espinet B, Sanz GF, Cervera J, et al. Identification of novel cytogenetic markers with prognostic significance in a series of 968 patients with primary myelodysplastic syndromes. *Haematologica*. 2005;90(9):1168-78.
 288. Schanz J, Tüchler H, Solé F, Mallo M, Luño E, Cervera J, et al. New comprehensive cytogenetic scoring system for primary myelodysplastic syndromes (MDS) and oligoblastic acute myeloid leukemia after MDS derived from an international database merge. *Journal of clinical oncology : official journal of the American Society of Clinical Oncology*. 2012;30(8):820-9.
 289. Such E, Cervera J, Costa D, Solé F, Vallespi T, Luño E, et al. Cytogenetic risk stratification in chronic myelomonocytic leukemia. *Haematologica*. 2011;96(3):375-83.
 290. Wassie EA, Itzykson R, Lasho TL, Kosmider O, Finke CM, Hanson CA, et al. Molecular and prognostic correlates of cytogenetic abnormalities in chronic myelomonocytic leukemia: a Mayo Clinic-French Consortium Study. *American journal of hematology*. 2014;89(12):1111-5.
 291. Tang G, Zhang L, Fu B, Hu J, Lu X, Hu S, et al. Cytogenetic risk stratification of 417 patients with chronic myelomonocytic leukemia from a single institution. *American journal of hematology*. 2014;89(8):813-8.
 292. Itzykson R, Fenaux P, Bowen D, Cross NCP, Cortes J, De Witte T, et al. Diagnosis and Treatment of Chronic Myelomonocytic Leukemias in Adults: Recommendations From the European Hematology Association and the European LeukemiaNet. *Hemasphere*. 2018;2(6):e150.
 293. Grignano E, Jachiet V, Fenaux P, Ades L, Fain O, Mekinian A. Autoimmune manifestations associated with myelodysplastic syndromes. *Annals of hematology*. 2018;97(11):2015-23.
 294. Jachiet V, Moulis G, Hadjadj J, Segulier J, Laribi K, Schleinitz N, et al. Clinical spectrum, outcome and management of immune thrombocytopenia associated with myelodysplastic syndromes and chronic myelomonocytic leukemia. *Haematologica*. 2021;106(5):1414-22.
 295. Mufti GJ, Bennett JM, Goasguen J, Bain BJ, Baumann I, Brunning R, et al. Diagnosis and classification of myelodysplastic syndrome: International Working Group on Morphology of myelodysplastic syndrome (IWGM-MDS) consensus proposals for the definition and enumeration of myeloblasts and ring sideroblasts. *Haematologica*. 2008;93(11):1712-7.
 296. Goasguen JE, Bennett JM, Bain BJ, Brunning R, Vallespi MT, Tomonaga M, et al. Dyserythropoiesis in the diagnosis of the myelodysplastic syndromes and other myeloid neoplasms: problem areas. *British journal of haematology*. 2018;182(4):526-33.
 297. Goasguen JE, Bennett JM, Bain BJ, Brunning RD, Vallespi MT, Tomonaga M, et al. Quality control initiative on the evaluation of the dysmegakaryopoiesis in myeloid neoplasms: Difficulties in the assessment of dysplasia. *Leukemia research*. 2016;45:75-

- 81.
298. Goasguen JE, Bennett JM, Bain BJ, Brunning R, Vallespi MT, Tomonaga M, et al. Proposal for refining the definition of dysgranulopoiesis in acute myeloid leukemia and myelodysplastic syndromes. *Leukemia research*. 2014;38(4):447-53.
299. Goasguen JE, Bennett JM, Bain BJ, Vallespi T, Brunning R, Mufti GJ. Morphological evaluation of monocytes and their precursors. *Haematologica*. 2009;94(7):994-7.
300. Bejar R. CHIP, ICUS, CCUS and other four-letter words. *Leukemia*. 2017;31(9):1869-71.
301. DeZern AE, Malcovati L, Ebert BL. CHIP, CCUS, and other acronyms: definition, implications, and impact on practice. *American Society of Clinical Oncology Educational Book*. 2019;39:400-10.
302. Weeks LD, Niroula A, Neuberg D, Wong W, Lindsley RC, Luskin M, et al. Prediction of risk for myeloid malignancy in clonal hematopoiesis. *NEJM Evid*. 2023;2(5).
303. Baumgartner F, Baer C, Bamopoulos S, Ayoub E, Truger M, Meggendorfer M, et al. Comparing malignant monocytosis across the updated WHO and ICC classifications of 2022. *Blood*. 2024;143(12):1139-56.
304. Rodriguez-Sevilla JJ, Colla S. Inflammation in myelodysplastic syndrome pathogenesis. *Seminars in hematology*. 2024.
305. Sehgal T, Sharma P. Auer rods and faggot cells: A review of the history, significance and mimics of two morphological curiosities of enduring relevance. *European journal of haematology*. 2023;110(1):14-23.
306. Bennett JM, Catovsky D, Daniel MT, Flandrin G, Galton DAG, Gralnick H, et al. The chronic myeloid leukaemias: guidelines for distinguishing chronic granulocytic, atypical chronic myeloid, and chronic myelomonocytic leukaemia: Proposals by the French - American - British Cooperative Leukaemia Group. *British Journal of Haematology*. 1994;87(4):746-54.
307. Patnaik MM, Parikh SA, Hanson CA, Tefferi A. Chronic myelomonocytic leukaemia: a concise clinical and pathophysiological review. *Br J Haematol*. 2014;165(3):273-86.
308. Jaffe ES. Pathology and genetics of tumours of haematopoietic and lymphoid tissues: IARC; 2001.
309. Jaffe ES. World Health Organization classification of tumors. Pathology and genetics of tumors of hematopoietic and lymphoid tissues. 2001:185-7.
310. Germing U, Strupp C, Kuendgen A, Isa S, Knipp S, Hildebrandt B, et al. Prospective validation of the WHO proposals for the classification of myelodysplastic syndromes. *Haematologica*. 2006;91(12):1596-604.
311. Germing U, Strupp C, Knipp S, Kuendgen A, Giagounidis A, Hildebrandt B, et al. Chronic myelomonocytic leukemia in the light of the WHO proposals. *Haematologica*. 2007;92(7):974-7.
312. Grossmann V, Bacher U, Haferlach C, Schnittger S, Pötzinger F, Weissmann S, et al. Acute erythroid leukemia (AEL) can be separated into distinct prognostic subsets based on cytogenetic and molecular genetic characteristics. *Leukemia*. 2013;27(9):1940-3.
313. Hasserjian RP, Zuo Z, Garcia C, Tang G, Kasyan A, Luthra R, et al. Acute erythroid leukemia: a reassessment using criteria refined in the 2008 WHO classification. *Blood*. 2010;115(10):1985-92.
314. Mallo M, Cervera J, Schanz J, Such E, García-Manero G, Luño E, et al. Impact of adjunct cytogenetic abnormalities for prognostic stratification in patients with myelodysplastic syndrome and deletion 5q. *Leukemia*. 2011;25(1):110-20.
315. Schuler E, Schroeder M, Neukirchen J, Strupp C, Xicoy B, Kündgen A, et al. Refined medullary blast and white blood cell count based classification of chronic myelomonocytic

- leukemias. *Leukemia Research*. 2014;38(12):1413-9.
316. Loghavi S, Sui D, Wei P, Garcia-Manero G, Pierce S, Routbort MJ, et al. Validation of the 2017 revision of the WHO chronic myelomonocytic leukemia categories. *Blood Advances*. 2018;2(15):1807-16.
 317. Peker D, Padron E, Bennett JM, Zhang X, Horna P, Epling-Burnette PK, et al. A close association of autoimmune-mediated processes and autoimmune disorders with chronic myelomonocytic leukemia: observation from a single institution. *Acta haematologica*. 2015;133(2):249-56.
 318. Braun T, Fenaux P. Myelodysplastic Syndromes (MDS) and autoimmune disorders (AD): Cause or consequence? *Best Practice & Research Clinical Haematology*. 2013;26(4):327-36.
 319. Hadjadj J, Michel M, Chauveheid MP, Godeau B, Papo T, Sacre K. Immune thrombocytopenia in chronic myelomonocytic leukemia. *European journal of haematology*. 2014;93(6):521-6.
 320. Grignano E, Mekinian A, Braun T, Liozon E, Hamidou M, Decaux O, et al. Autoimmune and inflammatory diseases associated with chronic myelomonocytic leukemia: A series of 26 cases and literature review. *Leukemia research*. 2016;47:136-41.
 321. Jaiswal S, Fontanillas P, Flannick J, Manning A, Grauman PV, Mar BG, et al. Age-related clonal hematopoiesis associated with adverse outcomes. *N Engl J Med*. 2014;371(26):2488-98.
 322. Genovese G, Kähler AK, Handsaker RE, Lindberg J, Rose SA, Bakhoum SF, et al. Clonal hematopoiesis and blood-cancer risk inferred from blood DNA sequence. *N Engl J Med*. 2014;371(26):2477-87.
 323. Xie M, Lu C, Wang J, McLellan MD, Johnson KJ, Wendl MC, et al. Age-related mutations associated with clonal hematopoietic expansion and malignancies. *Nat Med*. 2014;20(12):1472-8.
 324. Selimoglu-Buet D, Wagner-Ballon O, Saada V, Bardet V, Itzykson R, Bencheikh L, et al. Characteristic repartition of monocyte subsets as a diagnostic signature of chronic myelomonocytic leukemia. *Blood*. 2015;125(23):3618-26.
 325. Zhang Y, Wu J, Qin T, Xu Z, Qu S, Pan L, et al. Comparison of the revised 4th (2016) and 5th (2022) editions of the World Health Organization classification of myelodysplastic neoplasms. *Leukemia*. 2022;36(12):2875-82.
 326. Greenberg P, Cox C, LeBeau MM, Fenaux P, Morel P, Sanz G, et al. International scoring system for evaluating prognosis in myelodysplastic syndromes. *Blood*. 1997;89(6):2079-88.
 327. Greenberg PL, Tuechler H, Schanz J, Sanz G, Garcia-Manero G, Solé F, et al. Revised international prognostic scoring system for myelodysplastic syndromes. *Blood*. 2012;120(12):2454-65.
 328. Malcovati L, Germing U, Kuendgen A, Della Porta MG, Pascutto C, Invernizzi R, et al. Time-dependent prognostic scoring system for predicting survival and leukemic evolution in myelodysplastic syndromes. *Journal of clinical oncology : official journal of the American Society of Clinical Oncology*. 2007;25(23):3503-10.
 329. Kantarjian H, O'Brien S, Ravandi F, Cortes J, Shan J, Bennett JM, et al. Proposal for a new risk model in myelodysplastic syndrome that accounts for events not considered in the original International Prognostic Scoring System. *Cancer*. 2008;113(6):1351-61.
 330. Florensa L, Ramos F, Sanz G, Arrizabalaga B, Valcarcel D, Díez-Campelo M, et al. Guías Españolas de Síndromes Mielodisplásicos y Leucemia Mielomonocítica Crónica 2020. 2020.

331. Makishima H, Yoshizato T, Yoshida K, Sekeres MA, Radivoyevitch T, Suzuki H, et al. Dynamics of clonal evolution in myelodysplastic syndromes. *Nature genetics*. 2017;49(2):204-12.
332. Maurya N, Mohanty P, Dhangar S, Panchal P, Jijina F, Mathan SLP, et al. Comprehensive analysis of genetic factors predicting overall survival in Myelodysplastic syndromes. *Scientific reports*. 2022;12(1):5925.
333. Kim T, Tyndel MS, Kim HJ, Ahn JS, Choi SH, Park HJ, et al. The clonal origins of leukemic progression of myelodysplasia. *Leukemia*. 2017;31(9):1928-35.
334. Takahashi K, Jabbour E, Wang X, Luthra R, Bueso-Ramos C, Patel K, et al. Dynamic acquisition of FLT3 or RAS alterations drive a subset of patients with lower risk MDS to secondary AML. *Leukemia*. 2013;27(10):2081-3.
335. Walter MJ, Shen D, Shao J, Ding L, White BS, Kandoth C, et al. Clonal diversity of recurrently mutated genes in myelodysplastic syndromes. *Leukemia*. 2013;27(6):1275-82.
336. Merz AMA, Sébert M, Sonntag J, Kubasch AS, Platzbecker U, Adès L. Phase to phase: Navigating drug combinations with hypomethylating agents in higher-risk MDS trials for optimal outcomes. *Cancer Treatment Reviews*. 2024;123:102673.
337. Patnaik MM, Padron E, LaBorde RR, Lasho TL, Finke CM, Hanson CA, et al. Mayo prognostic model for WHO-defined chronic myelomonocytic leukemia: ASXL1 and spliceosome component mutations and outcomes. *Leukemia*. 2013;27(7):1504-10.
338. Germing U, Strupp C, Aivado M, Gattermann N. New prognostic parameters for chronic myelomonocytic leukemia. *Blood*. 2002;100(2):731-2; author reply 2-3.
339. Patnaik MM, Itzykson R, Lasho TL, Kosmider O, Finke CM, Hanson CA, et al. ASXL1 and SETBP1 mutations and their prognostic contribution in chronic myelomonocytic leukemia: a two-center study of 466 patients. *Leukemia*. 2014;28(11):2206-12.
340. Elena C, Galli A, Such E, Meggendorfer M, Germing U, Rizzo E, et al. Integrating clinical features and genetic lesions in the risk assessment of patients with chronic myelomonocytic leukemia. *Blood*. 2016;128(10):1408-17.
341. Takahashi K, Patel K, Bueso-Ramos C, Zhang J, Gumbs C, Jabbour E, et al. Clinical implications of TP53 mutations in myelodysplastic syndromes treated with hypomethylating agents. *Oncotarget*. 2016;7(12):14172-87.
342. Corces-Zimmerman MR, Hong WJ, Weissman IL, Medeiros BC, Majeti R. Preleukemic mutations in human acute myeloid leukemia affect epigenetic regulators and persist in remission. *Proc Natl Acad Sci U S A*. 2014;111(7):2548-53.
343. Tahir SK, Smith ML, Hessler P, Rapp LR, Idler KB, Park CH, et al. Potential mechanisms of resistance to venetoclax and strategies to circumvent it. *BMC Cancer*. 2017;17(1):399.
344. Chen C, Edelstein LC, Gélinas C. The Rel/NF-kappaB family directly activates expression of the apoptosis inhibitor Bcl-x(L). *Mol Cell Biol*. 2000;20(8):2687-95.
345. Ramsey HE, Fischer MA, Lee T, Gorska AE, Arrate MP, Fuller L, et al. A Novel MCL1 Inhibitor Combined with Venetoclax Rescues Venetoclax-Resistant Acute Myelogenous Leukemia. *Cancer discovery*. 2018;8(12):1566-81.
346. Moujalled DM, Pomilio G, Ghiurau C, Ivey A, Salmon J, Rijal S, et al. Combining BH3-mimetics to target both BCL-2 and MCL1 has potent activity in pre-clinical models of acute myeloid leukemia. *Leukemia*. 2019;33(4):905-17.
347. Teh TC, Nguyen NY, Moujalled DM, Segal D, Pomilio G, Rijal S, et al. Enhancing venetoclax activity in acute myeloid leukemia by co-targeting MCL1. *Leukemia*. 2018;32(2):303-12.
348. Zeng AGX, Bansal S, Jin L, Mitchell A, Chen WC, Abbas HA, et al. A cellular hierarchy

- framework for understanding heterogeneity and predicting drug response in acute myeloid leukemia. *Nat Med.* 2022;28(6):1212-23.
349. Tyner JW, Tognon CE, Bottomly D, Wilmot B, Kurtz SE, Savage SL, et al. Functional genomic landscape of acute myeloid leukaemia. *Nature.* 2018;562(7728):526-31.
 350. Pei S, Pollyea DA, Gustafson A, Stevens BM, Minhajuddin M, Fu R, et al. Monocytic Subclones Confer Resistance to Venetoclax-Based Therapy in Patients with Acute Myeloid Leukemia. *Cancer discovery.* 2020;10(4):536-51.
 351. Pei S, Shelton IT, Gillen AE, Stevens BM, Gasparetto M, Wang Y, et al. A Novel Type of Monocytic Leukemia Stem Cell Revealed by the Clinical Use of Venetoclax-Based Therapy. *Cancer discovery.* 2023;13(9):2032-49.
 352. Bhatt S, Pioso MS, Olesinski EA, Yilma B, Ryan JA, Mashaka T, et al. Reduced Mitochondrial Apoptotic Priming Drives Resistance to BH3 Mimetics in Acute Myeloid Leukemia. *Cancer cell.* 2020;38(6):872-90.e6.
 353. Platzbecker U. Treatment of MDS. *Blood, The Journal of the American Society of Hematology.* 2019;133(10):1096-107.
 354. Garcia-Manero G, Chien KS, Montalban-Bravo G. Myelodysplastic syndromes: 2021 update on diagnosis, risk stratification and management. *American Journal of Hematology.* 2020;95(11):1399-420.
 355. Platzbecker U, Della Porta MG, Santini V, Zeidan AM, Komrokji RS, Shortt J, et al. Efficacy and safety of luspatercept versus epoetin alfa in erythropoiesis-stimulating agent-naïve, transfusion-dependent, lower-risk myelodysplastic syndromes (COMMANDS): interim analysis of a phase 3, open-label, randomised controlled trial. *The Lancet.* 2023;402(10399):373-85.
 356. Fenaux P, Platzbecker U, Mufti GJ, Garcia-Manero G, Buckstein R, Santini V, et al. Luspatercept in Patients with Lower-Risk Myelodysplastic Syndromes. *N Engl J Med.* 2020;382(2):140-51.
 357. Platzbecker U, Santini V, Fenaux P, Sekeres MA, Savona MR, Madanat YF, et al. Imetelstat in patients with lower-risk myelodysplastic syndromes who have relapsed or are refractory to erythropoiesis-stimulating agents (IMerge): a multinational, randomised, double-blind, placebo-controlled, phase 3 trial. *Lancet (London, England).* 2024;403(10423):249-60.
 358. Steensma DP, Fenaux P, Van Eygen K, Raza A, Santini V, Germing U, et al. Imetelstat Achieves Meaningful and Durable Transfusion Independence in High Transfusion-Burden Patients With Lower-Risk Myelodysplastic Syndromes in a Phase II Study. *J Clin Oncol.* 2021;39(1):48-56.
 359. Jabbour EJ, Garcia-Manero G, Strati P, Mishra A, Al Ali NH, Padron E, et al. Outcome of patients with low-risk and intermediate-1-risk myelodysplastic syndrome after hypomethylating agent failure: a report on behalf of the MDS Clinical Research Consortium. *Cancer.* 2015;121(6):876-82.
 360. Prebet T, Gore SD, Esterni B, Gardin C, Itzykson R, Thepot S, et al. Outcome of high-risk myelodysplastic syndrome after azacitidine treatment failure. *Journal of clinical oncology : official journal of the American Society of Clinical Oncology.* 2011;29(24):3322-7.
 361. de Witte T, Bowen D, Robin M, Malcovati L, Niederwieser D, Yakoub-Agha I, et al. Allogeneic hematopoietic stem cell transplantation for MDS and CMML: recommendations from an international expert panel. *Blood.* 2017;129(13):1753-62.
 362. Saber W, Horowitz MM. Transplantation for myelodysplastic syndromes: who, when, and which conditioning regimens. *Hematology American Society of Hematology Education*

- Program. 2016;2016(1):478-84.
363. Montalban-Bravo G, Kanagal-Shamanna R, Li Z, Hammond D, Chien K, Rodriguez-Sevilla JJ, et al. Phenotypic subtypes of leukaemic transformation in chronic myelomonocytic leukaemia. *Br J Haematol*. 2023;203(4):581-92.
 364. Jabbour E, Garcia-Manero G, Batty N, Shan J, O'Brien S, Cortes J, et al. Outcome of patients with myelodysplastic syndrome after failure of decitabine therapy. *Cancer*. 2010;116(16):3830-4.
 365. Montalban-Bravo G, Thongon N, Rodriguez-Sevilla JJ, Ma F, Ganan-Gomez I, Yang H, et al. Targeting MCL1-driven anti-apoptotic pathways overcomes blast progression after hypomethylating agent failure in chronic myelomonocytic leukemia. *Cell Rep Med*. 2024;101585.
 366. Wei Y, Kanagal-Shamanna R, Zheng H, Bao N, Lockyer PP, Class CA, et al. Cooperation between KDM6B overexpression and TET2 deficiency in the pathogenesis of chronic myelomonocytic leukemia. *Leukemia*. 2022;36(8):2097-107.
 367. Ferrall-Fairbanks MC, Dhawan A, Johnson B, Newman H, Volpe V, Letson C, et al. Progenitor Hierarchy of Chronic Myelomonocytic Leukemia Identifies Inflammatory Monocytic-Biased Trajectory Linked to Worse Outcomes. *Blood Cancer Discov*. 2022;3(6):536-53.
 368. Rathmell JC, Thompson CB. Pathways of apoptosis in lymphocyte development, homeostasis, and disease. *Cell*. 2002;109 Suppl:S97-107.
 369. Letai A, Bassik MC, Walensky LD, Sorcinelli MD, Weiler S, Korsmeyer SJ. Distinct BH3 domains either sensitize or activate mitochondrial apoptosis, serving as prototype cancer therapeutics. *Cancer cell*. 2002;2(3):183-92.
 370. Singh R, Letai A, Sarosiek K. Regulation of apoptosis in health and disease: the balancing act of BCL-2 family proteins. *Nature reviews Molecular cell biology*. 2019;20(3):175-93.
 371. Carneiro BA, El-Deiry WS. Targeting apoptosis in cancer therapy. *Nat Rev Clin Oncol*. 2020;17(7):395-417.
 372. Hanahan D, Weinberg RA. Hallmarks of cancer: the next generation. *cell*. 2011;144(5):646-74.
 373. Ashkenazi A, Fairbrother WJ, Levenson JD, Souers AJ. From basic apoptosis discoveries to advanced selective BCL-2 family inhibitors. *Nature reviews Drug discovery*. 2017;16(4):273-84.
 374. Fischer M, Song Y, Gbyli R, Arrate M, Villaume M, Childress M, et al. MCL1 dependence across MDS subtypes and dual inhibition of MCL1 and BCL2 in MISTRG6 mice. *bioRxiv*; 2020.
 375. Jilg S, Reidel V, Müller-Thomas C, König J, Schauwecker J, Höckendorf U, et al. Blockade of BCL-2 proteins efficiently induces apoptosis in progenitor cells of high-risk myelodysplastic syndromes patients. *Leukemia*. 2016;30(1):112-23.
 376. Reidel V, Kauschinger J, Hauch RT, Müller-Thomas C, Nadarajah N, Burgkart R, et al. Selective inhibition of BCL-2 is a promising target in patients with high-risk myelodysplastic syndromes and adverse mutational profile. *Oncotarget*. 2018;9(25):17270-81.
 377. Wei AH, Montesinos P, Ivanov V, DiNardo CD, Novak J, Laribi K, et al. Venetoclax plus LDAC for newly diagnosed AML ineligible for intensive chemotherapy: a phase 3 randomized placebo-controlled trial. *Blood*. 2020;135(24):2137-45.
 378. DiNardo CD, Jonas BA, Pullarkat V, Thirman MJ, Garcia JS, Wei AH, et al. Azacitidine and Venetoclax in Previously Untreated Acute Myeloid Leukemia. *The New England journal of medicine*. 2020;383(7):617-29.

379. Zeidan AM, Borate U, Pollyea DA, Brunner AM, Roncolato F, Garcia JS, et al. A phase 1b study of venetoclax and azacitidine combination in patients with relapsed or refractory myelodysplastic syndromes. *American journal of hematology*. 2022.
380. Bazinet A, Darbaniyan F, Jabbour E, Montalban-Bravo G, Ohanian M, Chien K, et al. Azacitidine plus venetoclax in patients with high-risk myelodysplastic syndromes or chronic myelomonocytic leukaemia: phase 1 results of a single-centre, dose-escalation, dose-expansion, phase 1-2 study. *Lancet Haematol*. 2022;9(10):e756-e65.
381. Garcia-Manero G, Odenike O, Fleming S, Roboz G, Jacoby M, Cunningham I, et al. Combination of Venetoclax and Azacitidine in Patients with Treatment-Naive, High-Risk Myelodysplastic Syndromes with Responses Leading to Stem Cell Transplantation. *Blood*. 2023;142:1868-.
382. Pratz KW, Jonas BA, Pullarkat V, Thirman MJ, Garcia JS, Döhner H, et al. Long-term follow-up of VIALE-A: Venetoclax and azacitidine in chemotherapy-ineligible untreated acute myeloid leukemia. *American journal of hematology*. 2024;99(4):615-24.
383. Fischer MA, Song Y, Arrate MP, Gbyli R, Villaume MT, Smith BN, et al. Selective inhibition of MCL1 overcomes venetoclax-resistance in a murine model of myelodysplastic syndromes. *Haematologica*. 2022.
384. Rabut G, Peter M. Function and regulation of protein neddylation. 'Protein modifications: beyond the usual suspects' review series. *EMBO reports*. 2008;9(10):969-76.
385. Duda DM, Borg LA, Scott DC, Hunt HW, Hammel M, Schulman BA. Structural insights into NEDD8 activation of cullin-RING ligases: conformational control of conjugation. *Cell*. 2008;134(6):995-1006.
386. Majidi F, Neukirchen J, Brille S, Fey I, Neumann F, Berger A, et al. Altered Expression of Neddylation Pathway Proteins in Myelodysplastic Syndromes. *Blood*. 2017;130(Supplement 1):5298-.
387. Hua S, Feng T, Yin L, Wang Q, Shao X. NEDD9 overexpression: Prognostic and guidance value in acute myeloid leukaemia. *Journal of cellular and molecular medicine*. 2021;25(19):9331-9.
388. Swords RT, Kelly KR, Smith PG, Garnsey JJ, Mahalingam D, Medina E, et al. Inhibition of NEDD8-activating enzyme: a novel approach for the treatment of acute myeloid leukemia. *Blood*. 2010;115(18):3796-800.
389. Smith PG, Traore T, Grossman S, Narayanan U, Carew JS, Lublinksky A, et al. Azacitidine/Decitabine Synergism with the NEDD8-Activating Enzyme Inhibitor MLN4924 in Pre-Clinical AML Models. *Blood*. 2011;118(21):578-.
390. Swords RT, Coutre S, Maris MB, Zeidner JF, Foran JM, Cruz J, et al. Pevonedistat, a first-in-class NEDD8-activating enzyme inhibitor, combined with azacitidine in patients with AML. *Blood*. 2018;131(13):1415-24.
391. Moyo TK, Watts JM, Skikne BS, Mendler JH, Klimek VM, Chen S-C, et al. Preliminary Results from a Phase II Study of the Combination of Pevonedistat and Azacitidine in the Treatment of MDS and MDS/MPN after Failure of DNA Methyltransferase Inhibition. *Blood*. 2019;134(Supplement_1):4236-.
392. Kolch W, Halasz M, Granovskaya M, Kholodenko BN. The dynamic control of signal transduction networks in cancer cells. *Nature Reviews Cancer*. 2015;15(9):515-27.
393. Du Z, Lovly CM. Mechanisms of receptor tyrosine kinase activation in cancer. *Molecular cancer*. 2018;17(1):1-13.
394. Lemmon MA, Schlessinger J. Cell signaling by receptor tyrosine kinases. *Cell*. 2010;141(7):1117-34.
395. Sanchez-Vega F, Mina M, Armenia J, Chatila WK, Luna A, La KC, et al. Oncogenic

- Signaling Pathways in The Cancer Genome Atlas. *Cell*. 2018;173(2):321-37 e10.
396. Simanshu DK, Nissley DV, McCormick F. RAS Proteins and Their Regulators in Human Disease. *Cell*. 2017;170(1):17-33.
 397. Gimple RC, Wang X. RAS: Striking at the Core of the Oncogenic Circuitry. *Front Oncol*. 2019;9:965.
 398. Alawieh D, Cysique-Foinlan L, Willekens C, Renneville A. RAS mutations in myeloid malignancies: revisiting old questions with novel insights and therapeutic perspectives. *Blood Cancer J*. 2024;14(1):72.
 399. Prior IA, Hood FE, Hartley JL. The Frequency of Ras Mutations in Cancer. *Cancer Research*. 2020;80(14):2969-74.
 400. Athuluri-Divakar SK, Vasquez-Del Carpio R, Dutta K, Baker SJ, Cosenza SC, Basu I, et al. A small molecule RAS-mimetic disrupts RAS association with effector proteins to block signaling. *Cell*. 2016;165(3):643-55.
 401. Chapman CM, Sun X, Roschewski M, Aue G, Farooqui M, Stennett L, et al. ON 01910.Na is selectively cytotoxic for chronic lymphocytic leukemia cells through a dual mechanism of action involving PI3K/AKT inhibition and induction of oxidative stress. *Clinical cancer research : an official journal of the American Association for Cancer Research*. 2012;18(7):1979-91.
 402. Garcia-Manero G, Fenaux P, Al-Kali A, Baer MR, Sekeres MA, Roboz GJ, et al. Rigosertib versus best supportive care for patients with high-risk myelodysplastic syndromes after failure of hypomethylating drugs (ONTIME): a randomised, controlled, phase 3 trial. *The Lancet Oncology*. 2016;17(4):496-508.
 403. Hallin J, Bowcut V, Calinisan A, Briere DM, Hargis L, Engstrom LD, et al. Anti-tumor efficacy of a potent and selective non-covalent KRAS(G12D) inhibitor. *Nature medicine*. 2022;28(10):2171-82.
 404. Kazi JU, Ronnstrand L. FMS-like Tyrosine Kinase 3/FLT3: From Basic Science to Clinical Implications. *Physiol Rev*. 2019;99(3):1433-66.
 405. Grafone T, Palmisano M, Nicci C, Storti S. An overview on the role of FLT3-tyrosine kinase receptor in acute myeloid leukemia: biology and treatment. *Oncol Rev*. 2012;6(1):e8.
 406. Levis M, Small D. FLT3: ITDoes matter in leukemia. *Leukemia*. 2003;17(9):1738-52.
 407. Daver N, Venugopal S, Ravandi F. FLT3 mutated acute myeloid leukemia: 2021 treatment algorithm. *Blood Cancer J*. 2021;11(5):104.
 408. Badar T, Patel KP, Thompson PA, DiNardo C, Takahashi K, Cabrero M, et al. Detectable FLT3-ITD or RAS mutation at the time of transformation from MDS to AML predicts for very poor outcomes. *Leukemia research*. 2015;39(12):1367-74.
 409. Antar AI, Otrrock ZK, Jabbour E, Mohty M, Bazarbachi A. FLT3 inhibitors in acute myeloid leukemia: ten frequently asked questions. *Leukemia*. 2020;34(3):682-96.
 410. Ley TJ, Miller C, Ding L, Raphael BJ, Mungall AJ, Robertson A, et al. Genomic and epigenomic landscapes of adult de novo acute myeloid leukemia. *The New England journal of medicine*. 2013;368(22):2059-74.
 411. DiNardo CD, Jabbour E, Ravandi F, Takahashi K, Daver N, Routbort M, et al. IDH1 and IDH2 mutations in myelodysplastic syndromes and role in disease progression. *Leukemia*. 2016;30(4):980-4.
 412. Mondesir J, Willekens C, Touat M, de Botton S. IDH1 and IDH2 mutations as novel therapeutic targets: current perspectives. *J Blood Med*. 2016;7:171-80.
 413. Dang L, White DW, Gross S, Bennett BD, Bittinger MA, Driggers EM, et al. Cancer-associated IDH1 mutations produce 2-hydroxyglutarate. *Nature*. 2009;462(7274):739-44.

414. Ward PS, Patel J, Wise DR, Abdel-Wahab O, Bennett BD, Collier HA, et al. The common feature of leukemia-associated IDH1 and IDH2 mutations is a neomorphic enzyme activity converting α -ketoglutarate to 2-hydroxyglutarate. *Cancer cell*. 2010;17(3):225-34.
415. Xu W, Yang H, Liu Y, Yang Y, Wang P, Kim S-H, et al. Oncometabolite 2-hydroxyglutarate is a competitive inhibitor of α -ketoglutarate-dependent dioxygenases. *Cancer cell*. 2011;19(1):17-30.
416. Figueroa ME, Abdel-Wahab O, Lu C, Ward PS, Patel J, Shih A, et al. Leukemic IDH1 and IDH2 mutations result in a hypermethylation phenotype, disrupt TET2 function, and impair hematopoietic differentiation. *Cancer cell*. 2010;18(6):553-67.
417. Testa U, Castelli G, Pelosi E. Isocitrate Dehydrogenase Mutations in Myelodysplastic Syndromes and in Acute Myeloid Leukemias. *Cancers (Basel)*. 2020;12(9).
418. Stein EM, DiNardo CD, Pollyea DA, Fathi AT, Roboz GJ, Altman JK, et al. Enasidenib in mutant IDH2 relapsed or refractory acute myeloid leukemia. *Blood*. 2017;130(6):722-31.
419. DiNardo CD, Venugopal S, Lachowicz CA, Takahashi K, Loghavi S, Montalban-Bravo G, et al. Targeted therapy with the mutant IDH2 inhibitor enasidenib for high-risk IDH2-mutant myelodysplastic syndrome. *Blood advances*. 2022.
420. DiNardo CD, Stein EM, de Botton S, Roboz GJ, Altman JK, Mims AS, et al. Durable Remissions with Ivosidenib in IDH1-Mutated Relapsed or Refractory AML. *New England Journal of Medicine*. 2018;378(25):2386-98.
421. Botton SD, Yee KWL, Recher C, Wei A, Montesinos P, Taussig D, et al. Effect of olutasidenib (FT-2102) on complete remissions in patients with relapsed/refractory (R/R) mIDH1 acute myeloid leukemia (AML): Results from a planned interim analysis of a phase 2 clinical trial. *Journal of Clinical Oncology*. 2021;39(15_suppl):7006-.
422. Papaemmanuil E, Gerstung M, Malcovati L, Tauro S, Gundem G, Van Loo P, et al. Clinical and biological implications of driver mutations in myelodysplastic syndromes. *Blood*. 2013;122(22):3616-27; quiz 99.
423. BarreYRO L, Chlon TM, Starczynowski DT. Chronic immune response dysregulation in MDS pathogenesis. *Blood*. 2018;132(15):1553-60.
424. Sallman DA, List A. The central role of inflammatory signaling in the pathogenesis of myelodysplastic syndromes. *Blood*. 2019;133(10):1039-48.
425. Greten FR, Grivennikov SI. Inflammation and Cancer: Triggers, Mechanisms, and Consequences. *Immunity*. 2019;51(1):27-41.
426. Nagai Y, Garrett KP, Ohta S, Bahrn U, Kouro T, Akira S, et al. Toll-like receptors on hematopoietic progenitor cells stimulate innate immune system replenishment. *Immunity*. 2006;24(6):801-12.
427. Wei Y, Dimicoli S, Bueso-Ramos C, Chen R, Yang H, Neuberg D, et al. Toll-like receptor alterations in myelodysplastic syndrome. *Leukemia*. 2013;27(9):1832-40.
428. Esplin BL, Shimazu T, Welner RS, Garrett KP, Nie L, Zhang Q, et al. Chronic exposure to a TLR ligand injures hematopoietic stem cells. *The Journal of Immunology*. 2011;186(9):5367-75.
429. Farooq M, Batool M, Kim MS, Choi S. Toll-Like Receptors as a Therapeutic Target in the Era of Immunotherapies. *Frontiers in cell and developmental biology*. 2021;9:756315.
430. El-Zayat SR, Sibaii H, Mannaa FA. Toll-like receptors activation, signaling, and targeting: an overview. *Bulletin of the National Research Centre*. 2019;43(1):1-12.
431. Akira S, Takeda K. Toll-like receptor signalling. *Nat Rev Immunol*. 2004;4(7):499-511.
432. Wei Y, Dimicoli S, Bueso-Ramos C, Chen R, Yang H, Neuberg D, et al. Toll-like receptor alterations in myelodysplastic syndrome. *Leukemia*. 2013;27(9):1832-40.
433. Garcia-Manero G, Jabbour EJ, Konopleva MY, Daver NG, Borthakur G, DiNardo CD, et

- al. A clinical study of tomaralimab (OPN-305), a toll-like receptor 2 (TLR-2) antibody, in heavily pre-treated transfusion dependent patients with lower risk myelodysplastic syndromes (MDS) that have received and failed on prior hypomethylating agent (HMA) therapy. *Blood*. 2018;132:798.
434. Rhyasen GW, Starczynowski DT. IRAK signalling in cancer. *British journal of cancer*. 2015;112(2):232-7.
 435. Smith MA, Choudhary GS, Pellagatti A, Choi K, Bolanos LC, Bhagat TD, et al. U2AF1 mutations induce oncogenic IRAK4 isoforms and activate innate immune pathways in myeloid malignancies. *Nat Cell Biol*. 2019;21(5):640-50.
 436. Choudhary GS, Pellagatti A, Agianian B, Smith MA, Bhagat TD, Gordon-Mitchell S, et al. Activation of targetable inflammatory immune signaling is seen in myelodysplastic syndromes with SF3B1 mutations. *eLife*. 2022;11:e78136.
 437. Bennett J, Starczynowski DT. IRAK1 and IRAK4 as emerging therapeutic targets in hematologic malignancies. *Curr Opin Hematol*. 2022;29(1):8-19.
 438. Garcia-Manero G, Winer ES, DeAngelo DJ, Tarantolo SR, Sallman DA, Dugan J, et al. Phase 1/2a study of the IRAK4 inhibitor CA-4948 as monotherapy or in combination with azacitidine or venetoclax in patients with relapsed/refractory (R/R) acute myeloid leukemia or myelodysplastic syndrome. *Journal of Clinical Oncology*. 2022;40(16_suppl):7016-.
 439. Garcia-Manero G, Gartenberg G, Steensma DP, Schipperus MR, Breems DA, de Paz R, et al. A phase 2, randomized, double-blind, multicenter study comparing siltuximab plus best supportive care (BSC) with placebo plus BSC in anemic patients with International Prognostic Scoring System low- or intermediate-1-risk myelodysplastic syndrome. *American journal of hematology*. 2014;89(9):E156-62.
 440. Rodon J, Carducci MA, Sepulveda-Sánchez JM, Azaro A, Calvo E, Seoane J, et al. First-in-human dose study of the novel transforming growth factor- β receptor I kinase inhibitor LY2157299 monohydrate in patients with advanced cancer and glioma. *Clinical cancer research : an official journal of the American Association for Cancer Research*. 2015;21(3):553-60.
 441. Komrokji R, Garcia-Manero G, Ades L, Prebet T, Steensma DP, Jurcic JG, et al. Sotatercept with long-term extension for the treatment of anaemia in patients with lower-risk myelodysplastic syndromes: a phase 2, dose-ranging trial. *The Lancet Haematology*. 2018;5(2):e63-e72.
 442. Baron F, Suciú S, Amadori S, Muus P, Zwierzina H, Denzlinger C, et al. Value of infliximab (Remicade®) in patients with low-risk myelodysplastic syndrome: final results of a randomized phase II trial (EORTC trial 06023) of the EORTC Leukemia Group. *Haematologica*. 2012;97(4):529-33.
 443. Sharma P, Siddiqui BA, Anandhan S, Yadav SS, Subudhi SK, Gao J, et al. The Next Decade of Immune Checkpoint Therapy. *Cancer discovery*. 2021;11(4):838-57.
 444. Garcia-Manero G, Ribrag V, Zhang Y, Farooqui M, Marinello P, Smith BD. Pembrolizumab for myelodysplastic syndromes after failure of hypomethylating agents in the phase 1b KEYNOTE-013 study. *Leukemia & lymphoma*. 2022:1-9.
 445. Morita K, Kantarjian HM, Montalban Bravo G, Sasaki K, Daver N, Jabbour E, et al. A Phase II Study of Double Immune Checkpoint Inhibitor Blockade with Nivolumab and Ipilimumab with or without Azacitidine in Patients with Myelodysplastic Syndrome (MDS). *Blood*. 2020;136(Supplement 1):7-9.
 446. Brunner AM, Esteve J, Porkka K, Knapper S, Traer E, Scholl S, et al. Efficacy and Safety of Sabatolimab (MBG453) in Combination with Hypomethylating Agents (HMAs) in

- Patients (Pts) with Very High/High-Risk Myelodysplastic Syndrome (vHR/HR-MDS) and Acute Myeloid Leukemia (AML): Final Analysis from a Phase Ib Study. *Blood*. 2021;138:244.
447. Zeidan AM, Ando K, Rauzy O, Turgut M, Wang MC, Cairoli R, et al. Sabatolimab plus hypomethylating agents in previously untreated patients with higher-risk myelodysplastic syndromes (STIMULUS-MDS1): a randomised, double-blind, placebo-controlled, phase 2 trial. *The Lancet Haematology*. 2023.
 448. Neelapu SS, Locke FL, Bartlett NL, Lekakis LJ, Miklos DB, Jacobson CA, et al. Axicabtagene Ciloleucel CAR T-Cell Therapy in Refractory Large B-Cell Lymphoma. *N Engl J Med*. 2017;377(26):2531-44.
 449. Schuster SJ, Bishop MR, Tam CS, Waller EK, Borchmann P, McGuirk JP, et al. Tisagenlecleucel in Adult Relapsed or Refractory Diffuse Large B-Cell Lymphoma. *N Engl J Med*. 2019;380(1):45-56.
 450. Abramson JS, Palomba ML, Gordon LI, Lunning MA, Wang M, Arnason J, et al. Lisocabtagene maraleucel for patients with relapsed or refractory large B-cell lymphomas (TRANSCEND NHL 001): a multicentre seamless design study. *Lancet (London, England)*. 2020;396(10254):839-52.
 451. Chua CC, Cheok KPL. Taking a step forward in CAR T-cell therapy for acute myeloid leukaemia and myelodysplastic syndrome. *Lancet Haematol*. 2023;10(3):e161-e2.
 452. Stevens BM, Zhang W, Pollyea DA, Winters A, Gutman J, Smith C, et al. CD123 CAR T cells for the treatment of myelodysplastic syndrome. *Experimental Hematology*. 2019;74:52-63.e3.
 453. Kenderian SS, Ruella M, Shestova O, Klichinsky M, Aikawa V, Morrisette JJ, et al. CD33-specific chimeric antigen receptor T cells exhibit potent preclinical activity against human acute myeloid leukemia. *Leukemia*. 2015;29(8):1637-47.
 454. Sallman DA, Kerre T, Havelange V, Poiré X, Lewalle P, Wang ES, et al. CYAD-01, an autologous NKG2D-based CAR T-cell therapy, in relapsed or refractory acute myeloid leukaemia and myelodysplastic syndromes or multiple myeloma (THINK): haematological cohorts of the dose escalation segment of a phase 1 trial. *The Lancet Haematology*. 2023;10(3):e191-e202.
 455. Liu H, Wang S, Xin J, Wang J, Yao C, Zhang Z. Role of NKG2D and its ligands in cancer immunotherapy. *Am J Cancer Res*. 2019;9(10):2064-78.
 456. Diermayr S, Himmelreich H, Durovic B, Mathys-Schneeberger A, Siegler U, Langenkamp U, et al. NKG2D ligand expression in AML increases in response to HDAC inhibitor valproic acid and contributes to allorecognition by NK-cell lines with single KIR-HLA class I specificities. *Blood*. 2008;111(3):1428-36.
 457. Driouk L, Gicobi J, Kamihara Y, Rutherford K, Dranoff G, Ritz J, et al. Chimeric Antigen Receptor T Cells Targeting NKG2D-Ligands Show Robust Efficacy Against Acute Myeloid Leukemia and T-Cell Acute Lymphoblastic Leukemia. *Blood*. 2019;134:1930.
 458. Depil S, Duchateau P, Grupp SA, Mufti G, Poirot L. 'Off-the-shelf' allogeneic CAR T cells: development and challenges. *Nature reviews Drug discovery*. 2020;19(3):185-99.
 459. Heine R, Thielen FW, Koopmanschap M, Kersten MJ, Einsele H, Jaeger U, et al. Health Economic Aspects of Chimeric Antigen Receptor T-cell Therapies for Hematological Cancers: Present and Future. *Hemasphere*. 2021;5(2):e524.
 460. Haber L, Olson K, Kelly MP, Crawford A, DiLillo DJ, Tavaré R, et al. Generation of T-cell-redirecting bispecific antibodies with differentiated profiles of cytokine release and biodistribution by CD3 affinity tuning. *Sci Rep*. 2021;11(1):14397.
 461. Allen C, Zeidan AM, Bewersdorf JP. BiTEs, DARTS, BiKEs and TriKEs-Are Antibody

- Based Therapies Changing the Future Treatment of AML? *Life* (Basel, Switzerland). 2021;11(6).
462. Uckun FM, Lin TL, Mims AS, Patel P, Lee C, Shahidzadeh A, et al. A Clinical Phase 1B Study of the CD3xCD123 Bispecific Antibody APVO436 in Patients with Relapsed/Refractory Acute Myeloid Leukemia or Myelodysplastic Syndrome. *Cancers*. 2021;13(16).
 463. Jones CL, Stevens BM, Pollyea DA, Culp-Hill R, Reisz JA, Nemkov T, et al. Nicotinamide Metabolism Mediates Resistance to Venetoclax in Relapsed Acute Myeloid Leukemia Stem Cells. *Cell Stem Cell*. 2020;27(5):748-64.e4.
 464. Stevens BM, Jones CL, Pollyea DA, Culp-Hill R, D'Alessandro A, Winters A, et al. Fatty acid metabolism underlies venetoclax resistance in acute myeloid leukemia stem cells. *Nat Cancer*. 2020;1(12):1176-87.
 465. Nechiporuk T, Kurtz SE, Nikolova O, Liu T, Jones CL, D'Alessandro A, et al. The TP53 Apoptotic Network Is a Primary Mediator of Resistance to BCL2 Inhibition in AML Cells. *Cancer discovery*. 2019;9(7):910-25.
 466. Behrens K, Triviari I, Schwieger M, Tekin N, Alawi M, Spohn M, et al. Runx1 downregulates stem cell and megakaryocytic transcription programs that support niche interactions. *Blood*. 2016;127(26):3369-81.
 467. Viny AD, Bowman RL, Liu Y, Lavallée VP, Eisman SE, Xiao W, et al. Cohesin Members Stag1 and Stag2 Display Distinct Roles in Chromatin Accessibility and Topological Control of HSC Self-Renewal and Differentiation. *Cell Stem Cell*. 2019;25(5):682-96.e8.
 468. Nakagawa T, Matozaki S. The SKM-1 leukemic cell line established from a patient with progression to myelomonocytic leukemia in myelodysplastic syndrome (MDS)-contribution to better understanding of MDS. *Leukemia & lymphoma*. 1995;17(3-4):335-9.
 469. Awada H, Nagata Y, Goyal A, Asad MF, Patel B, Hirsch CM, et al. Invariant phenotype and molecular association of biallelic TET2 mutant myeloid neoplasia. *Blood Adv*. 2019;3(3):339-49.
 470. Zhang Y, He L, Selimoglu-Buet D, Jegu C, Morabito M, Willekens C, et al. Engraftment of chronic myelomonocytic leukemia cells in immunocompromised mice supports disease dependency on cytokines. *Blood Adv*. 2017;1(14):972-9.
 471. Patel BJ, Przychodzen B, Thota S, Radivoyevitch T, Visconte V, Kuzmanovic T, et al. Genomic determinants of chronic myelomonocytic leukemia. *Leukemia*. 2017;31(12):2815-23.
 472. Montalban-Bravo G, Hammond D, DiNardo CD, Konopleva M, Borthakur G, Short NJ, et al. Activity of venetoclax-based therapy in chronic myelomonocytic leukemia. *Leukemia*. 2021.
 473. Chen X, Eksioglu EA, Zhou J, Zhang L, Djeu J, Fortenbery N, et al. Induction of myelodysplasia by myeloid-derived suppressor cells. *J Clin Invest*. 2013;123(11):4595-611.
 474. Hunter AM, Newman H, Dezern AE, Steensma DP, Niyongere S, Roboz GJ, et al. Integrated Human and Murine Clinical Study Establishes Clinical Efficacy of Ruxolitinib in Chronic Myelomonocytic Leukemia. *Clin Cancer Res*. 2021;27(22):6095-105.
 475. Walker AR, Byrd JC, Blachly JS, Bhatnagar B, Mims AS, Orwick S, et al. Entospletinib in Combination with Induction Chemotherapy in Previously Untreated Acute Myeloid Leukemia: Response and Predictive Significance of HOXA9 and MEIS1 Expression. *Clin Cancer Res*. 2020;26(22):5852-9.
 476. Morandi F, Airoidi I, Pistoia V. IL-27 driven upregulation of surface HLA-E expression on

- monocytes inhibits IFN- γ release by autologous NK cells. *Journal of immunology research*. 2014;2014:938561.
477. Pereira BI, Devine OP, Vukmanovic-Stejic M, Chambers ES, Subramanian P, Patel N, et al. Senescent cells evade immune clearance via HLA-E-mediated NK and CD8(+) T cell inhibition. *Nat Commun*. 2019;10(1):2387.
 478. Ramsuran V, Naranbhai V, Horowitz A, Qi Y, Martin MP, Yuki Y, et al. Elevated HLA-A expression impairs HIV control through inhibition of NKG2A-expressing cells. *Science*. 2018;359(6371):86-90.
 479. Banh C, Fugère C, Brossay L. Immunoregulatory functions of KLRG1 cadherin interactions are dependent on forward and reverse signaling. *Blood*. 2009;114(26):5299-306.
 480. Lou C, Wu K, Shi J, Dai Z, Xu Q. N-cadherin protects oral cancer cells from NK cell killing in the circulation by inducing NK cell functional exhaustion via the KLRG1 receptor. *J Immunother Cancer*. 2022;10(9).
 481. Yang R, Sun L, Li CF, Wang YH, Yao J, Li H, et al. Galectin-9 interacts with PD-1 and TIM-3 to regulate T cell death and is a target for cancer immunotherapy. *Nat Commun*. 2021;12(1):832.
 482. Slattery K, Woods E, Zaiatz-Bittencourt V, Marks S, Chew S, Conroy M, et al. TGF β drives NK cell metabolic dysfunction in human metastatic breast cancer. *J Immunother Cancer*. 2021;9(2).
 483. Sevin M, Debeurme F, Laplane L, Badel S, Morabito M, Newman HL, et al. Cytokine-like protein 1-induced survival of monocytes suggests a combined strategy targeting MCL1 and MAPK in CMML. *Blood*. 2021;137(24):3390-402.
 484. Martín-Sánchez F, Diamond C, Zeitler M, Gomez AI, Baroja-Mazo A, Bagnall J, et al. Inflammasome-dependent IL-1 β release depends upon membrane permeabilisation. *Cell death and differentiation*. 2016;23(7):1219-31.
 485. Mitchell CA, Verovskaya EV, Calero-Nieto FJ, Olson OC, Swann JW, Wang X, et al. Stromal niche inflammation mediated by IL-1 signalling is a targetable driver of haematopoietic ageing. *Nature Cell Biology*. 2023;25(1):30-41.
 486. Svensson EC, Madar A, Campbell CD, He Y, Sultan M, Healey ML, et al. TET2-Driven Clonal Hematopoiesis and Response to Canakinumab: An Exploratory Analysis of the CANTOS Randomized Clinical Trial. *JAMA Cardiol*. 2022;7(5):521-8.
 487. Woo J, Lu D, Lewandowski A, Ridker PM, Ebert BL, Steensma D. Canakinumab Effects on Erythropoiesis, Cardiovascular Risk, and Clonal Hematopoiesis: Proteogenomic Analysis of the Cantos Randomized Clinical Trial. *Blood*. 2022;140(Supplement 1):2236-7.
 488. Woo J, Lu D, Lewandowski A, Xu H, Serrano P, Healey M, et al. Effects of IL-1 β inhibition on anemia and clonal hematopoiesis in the randomized CANTOS trial. *Blood Advances*. 2023;7(24):7471-84.
 489. McClatchy J, Strogantsev R, Wolfe E, Lin HY, Mohammadhosseini M, Davis BA, et al. Clonal hematopoiesis related TET2 loss-of-function impedes IL1 β -mediated epigenetic reprogramming in hematopoietic stem and progenitor cells. *Nat Commun*. 2023;14(1):8102.
 490. Burns SS, Kumar R, Pasupuleti SK, So K, Zhang C, Kapur R. Il-1r1 drives leukemogenesis induced by Tet2 loss. *Leukemia*. 2022;36(10):2531-4.
 491. Ridker PM, Everett BM, Thuren T, MacFadyen JG, Chang WH, Ballantyne C, et al. Antiinflammatory Therapy with Canakinumab for Atherosclerotic Disease. *New England Journal of Medicine*. 2017;377(12):1119-31.

492. Ridker PM, MacFadyen JG, Thuren T, Everett BM, Libby P, Glynn RJ. Effect of interleukin-1 β inhibition with canakinumab on incident lung cancer in patients with atherosclerosis: exploratory results from a randomised, double-blind, placebo-controlled trial. *Lancet* (London, England). 2017;390(10105):1833-42.
493. Schneider M, Rolfs C, Trumpp M, Winter S, Fischer L, Richter M, et al. Activation of distinct inflammatory pathways in subgroups of LR-MDS. *Leukemia*. 2023;37(8):1709-18.
494. Padron E, Garcia-Manero G, Patnaik MM, Itzykson R, Lasho T, Nazha A, et al. An international data set for CMML validates prognostic scoring systems and demonstrates a need for novel prognostication strategies. *Blood Cancer J*. 2015;5:e333.
495. Jerez A, Sugimoto Y, Makishima H, Verma A, Jankowska AM, Przychodzen B, et al. Loss of heterozygosity in 7q myeloid disorders: clinical associations and genomic pathogenesis. *Blood*. 2012;119(25):6109-17.
496. Cockey SG, Zhang H, Hussaini MO, Zhang L, Moscinski LC, Yang E, et al. A Large Cohort Study of 412 Patients with SRSF2/TET2 Co-Mutated Myeloid Neoplasms: The Molecular Landscape and Clinical Outcomes. *Blood*. 2023;142(Supplement 1):1882-.